19. Validation for C_4H_{10}

Shock tube ignition delay time

19.1) Healy, D., Donato, N. S., Aul, C. J., Petersen, E. L., Zinner, C. M., Bourque, G., & Curran, H. J., Combustion and Flame, 157(8) (2010) 1526-1539.

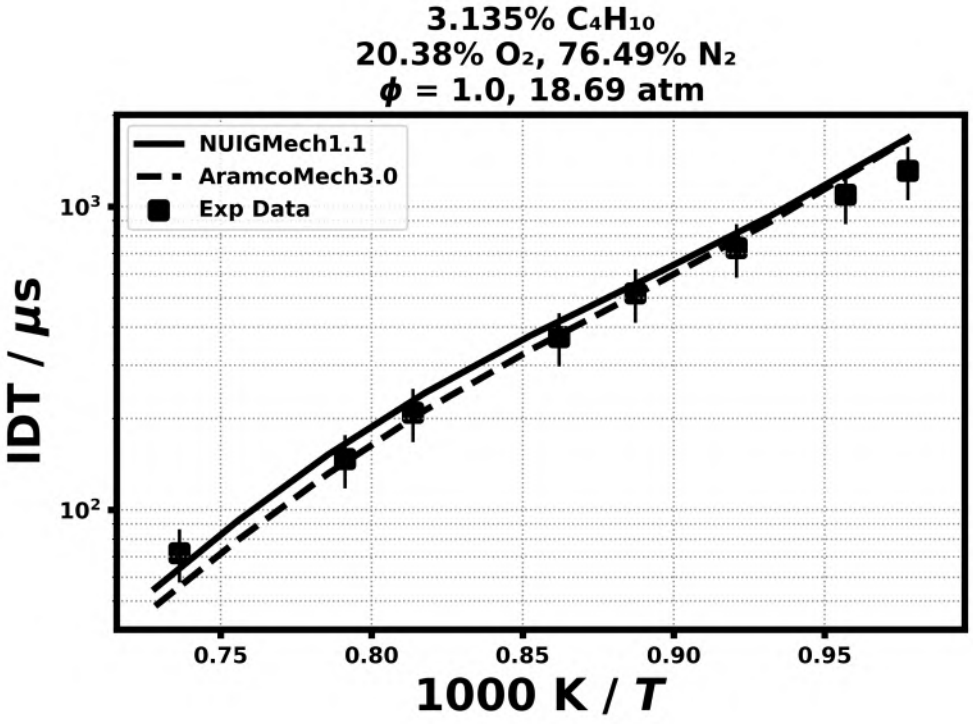

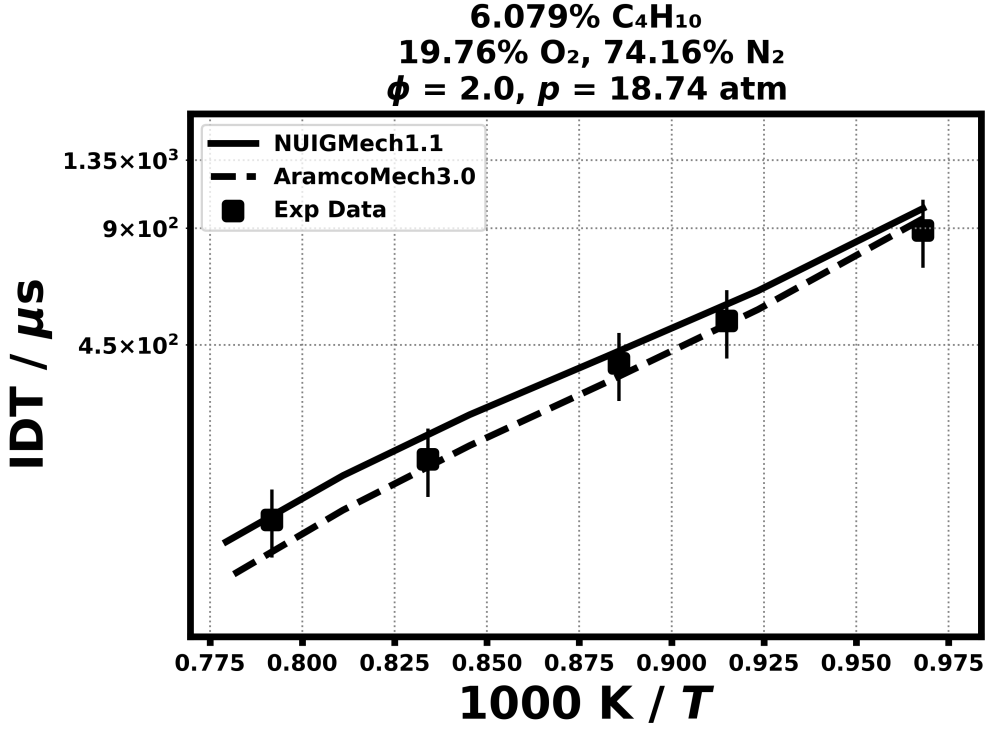

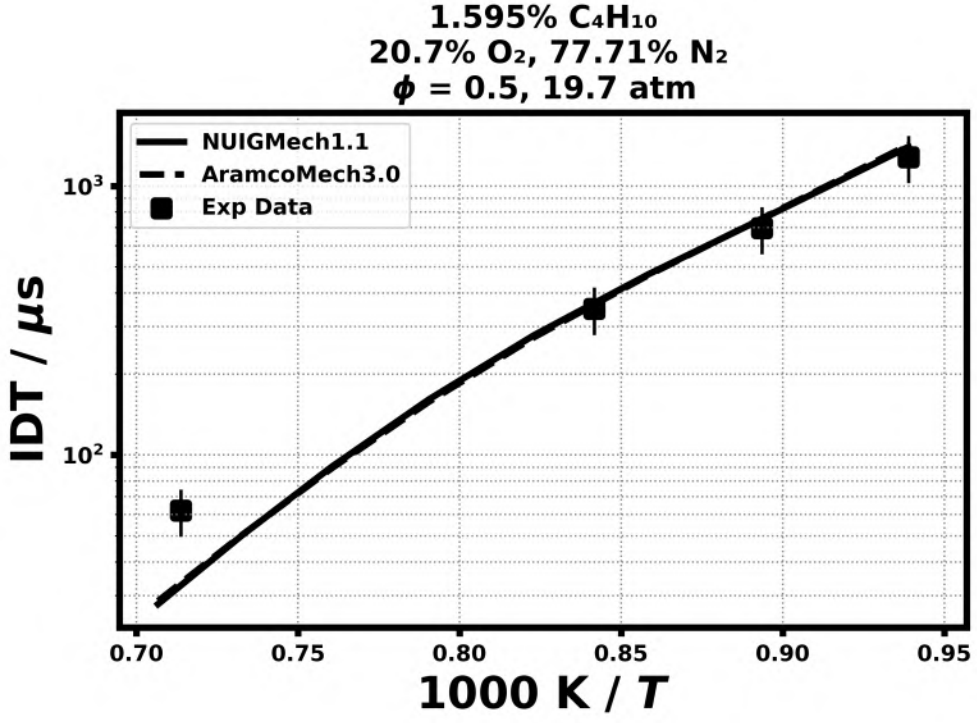
1.595% C4H10
20.7% O2, 77.71% N2
ϕ = 0.5, 19.7 atm
NUIGMech1.1
AramcoMech3.0
Exp Data
IDT / μs
10³
10²
0.70
0.75
0.80
0.85
0.90
0.95
1000 K / T

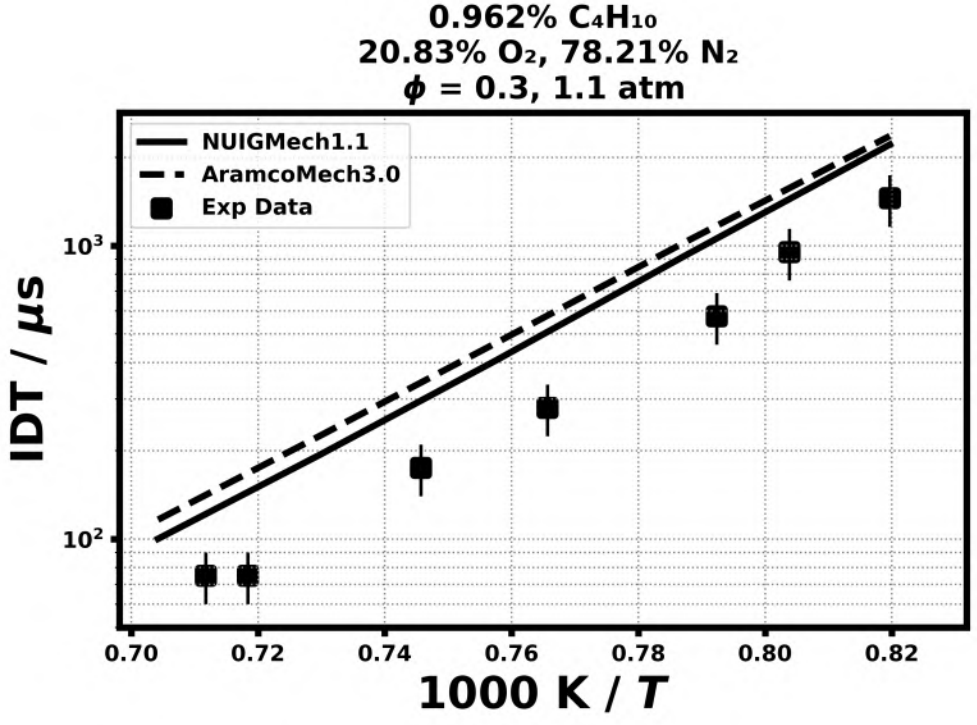
0.962% C4H10
20.83% O2, 78.21% N2
ϕ = 0.3, 1.1 atm
NUIGMech1.1
AramcoMech3.0
Exp Data
IDT / μs
10³
10²
0.70
0.72
0.74
0.76
0.78
0.80
0.82
1000 K / T

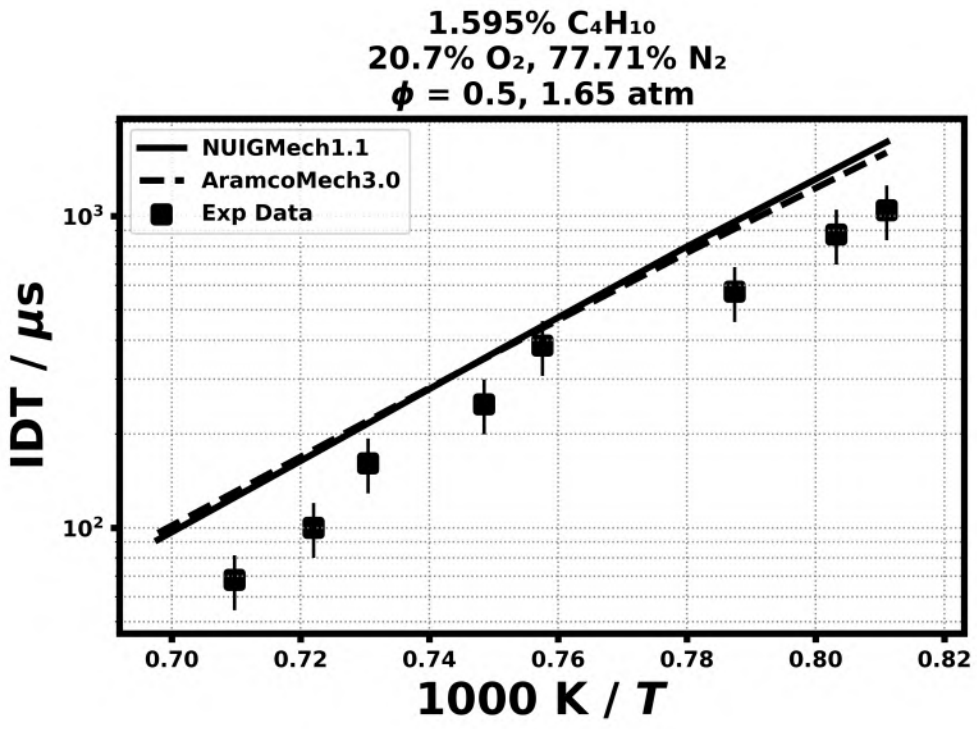
1.595% C4H10
20.7% O2, 77.71% N2
ϕ = 0.5, 1.65 atm
NUIGMech1.1
AramcoMech3.0
Exp Data
IDT / μs
10^3
10^2
0.70
0.72
0.74
0.76
0.78
0.80
0.82
1000 K / T

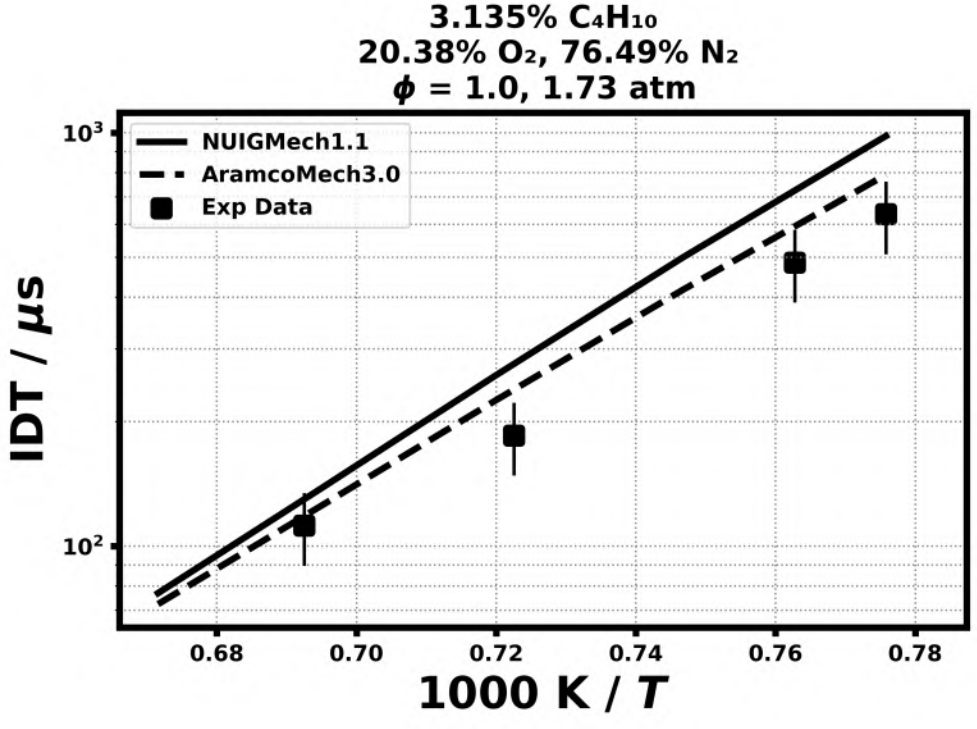
3.135% C4H10
20.38% O2, 76.49% N2
ϕ = 1.0, 1.73 atm
NUIGMech1.1
AramcoMech3.0
Exp Data
IDT / μs
10^3
10^2
0.68
0.70
0.72
0.74
0.76
0.78
1000 K / T

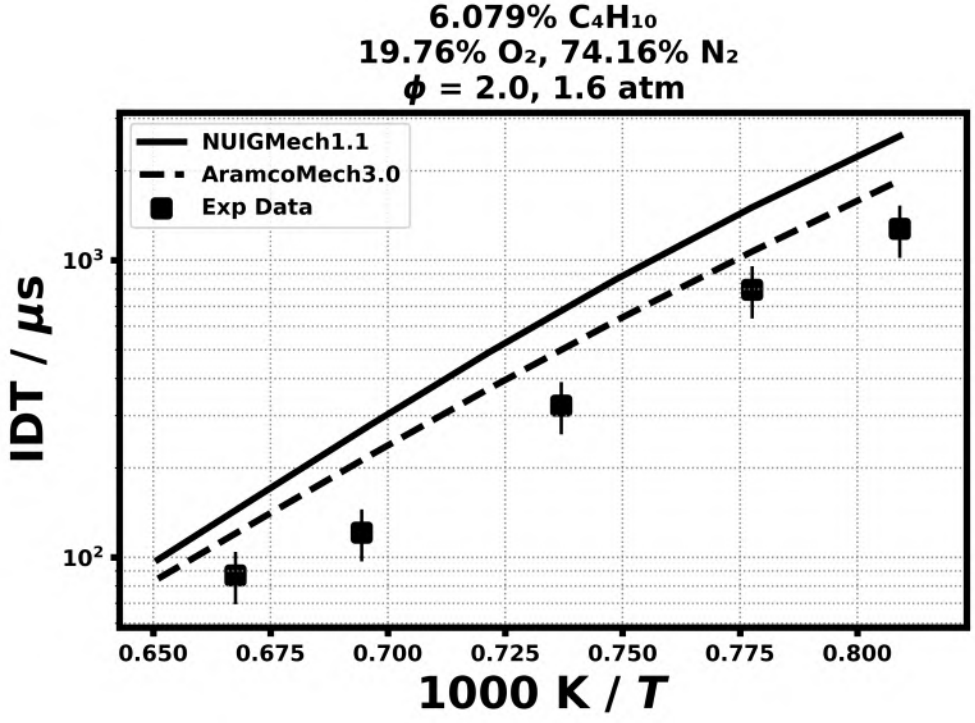
6.079% C4H10
19.76% O2, 74.16% N2
ϕ = 2.0, 1.6 atm
NUIGMech1.1
AramcoMech3.0
Exp Data
IDT / μs
10^3
10^2
0.650
0.675
0.700
0.725
0.750
0.775
0.800
1000 K / T

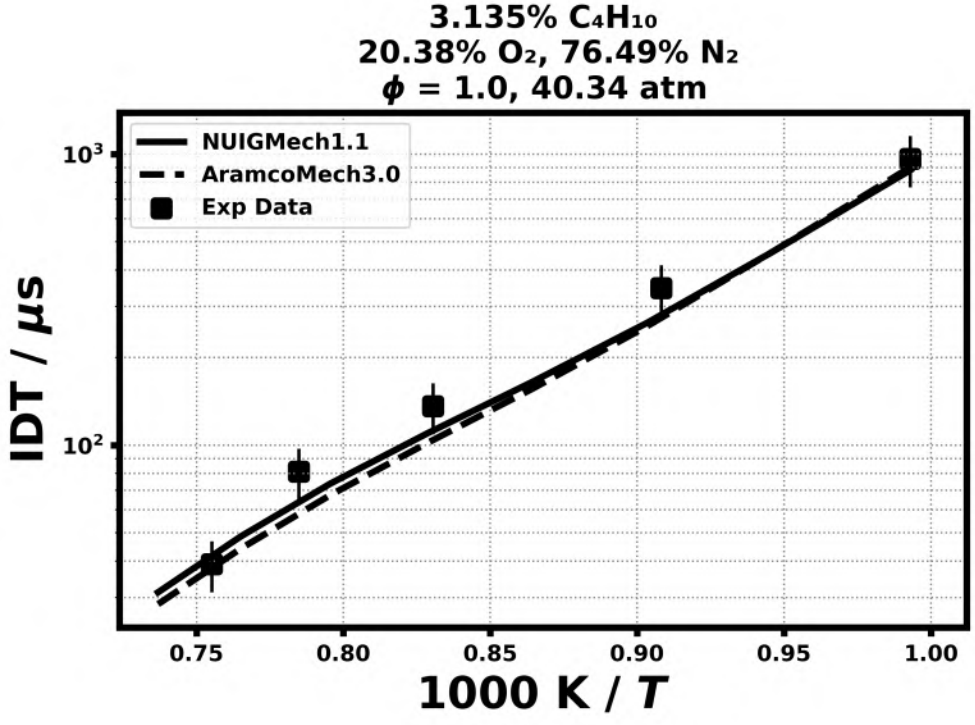
3.135% C4H10
20.38% O2, 76.49% N2
ϕ = 1.0, 40.34 atm
NUIGMech1.1
AramcoMech3.0
Exp Data
IDT / μs
10^3
10^2
0.75
0.80
0.85
0.90
0.95
1.00
1000 K / T

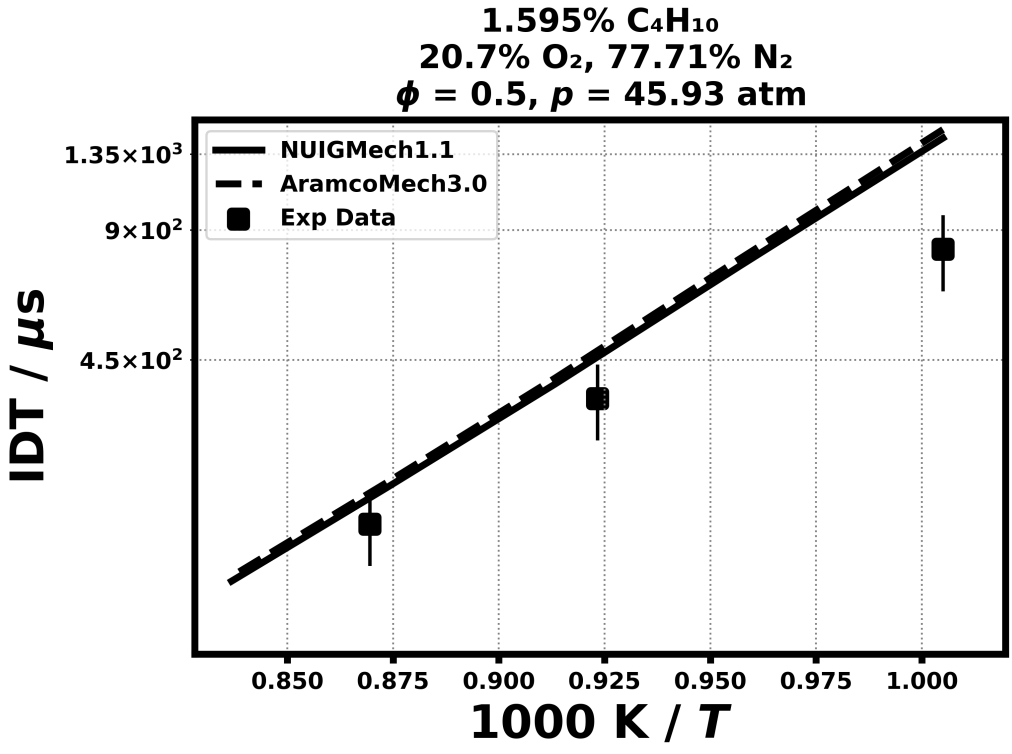
1.595% C4H10
20.7% O2, 77.71% N2
ϕ = 0.5, p = 45.93 atm
NUIGMech1.1
AramcoMech3.0
Exp Data
1.35×10³
9×10²
4.5×10²
IDT / μs
0.850
0.875
0.900
0.925
0.950
0.975
1.000
1000 K / T

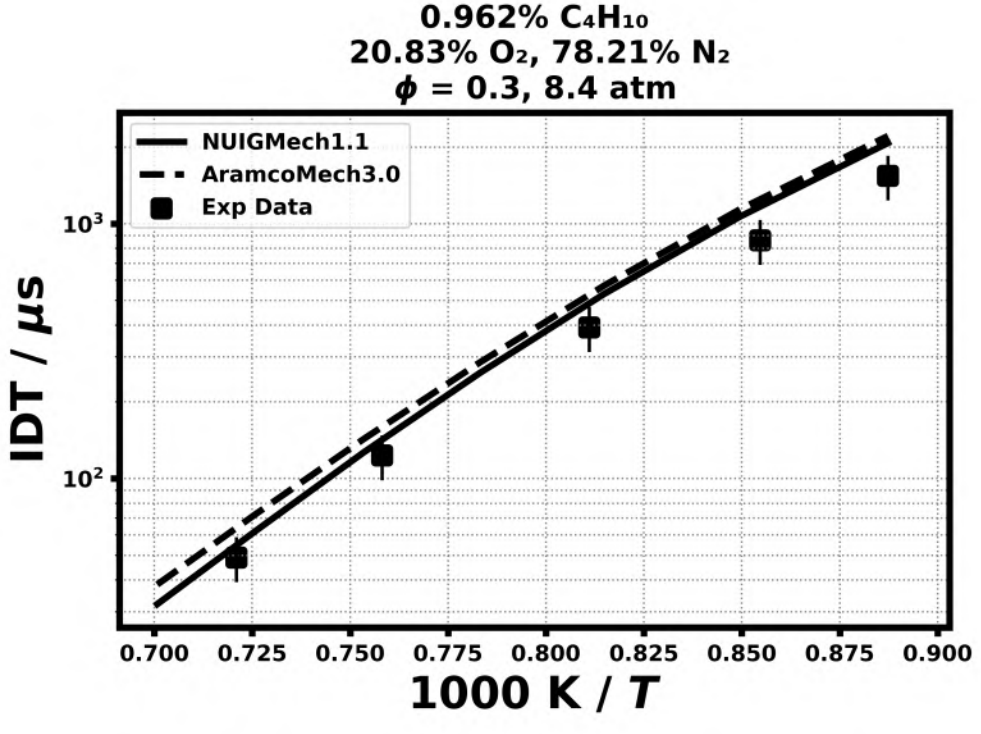
0.962% C4H10
20.83% O2, 78.21% N2
ϕ = 0.3, 8.4 atm
NUIGMech1.1
AramcoMech3.0
Exp Data
10³
10²
IDT / μs
0.700
0.725
0.750
0.775
0.800
0.825
0.850
0.875
0.900
1000 K / T

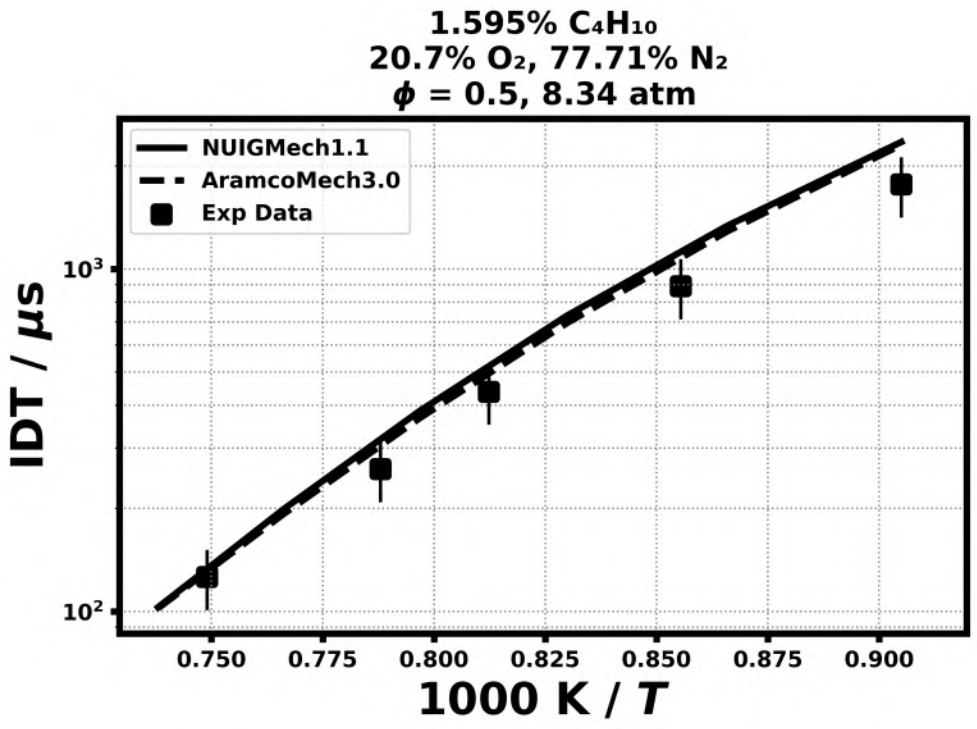
1.595% C4H10
20.7% O2, 77.71% N2
ϕ = 0.5, 8.34 atm
NUIGMech1.1
AramcoMech3.0
Exp Data
IDT / μs
10^3
10^2
0.750
0.775
0.800
0.825
0.850
0.875
0.900
1000 K / T

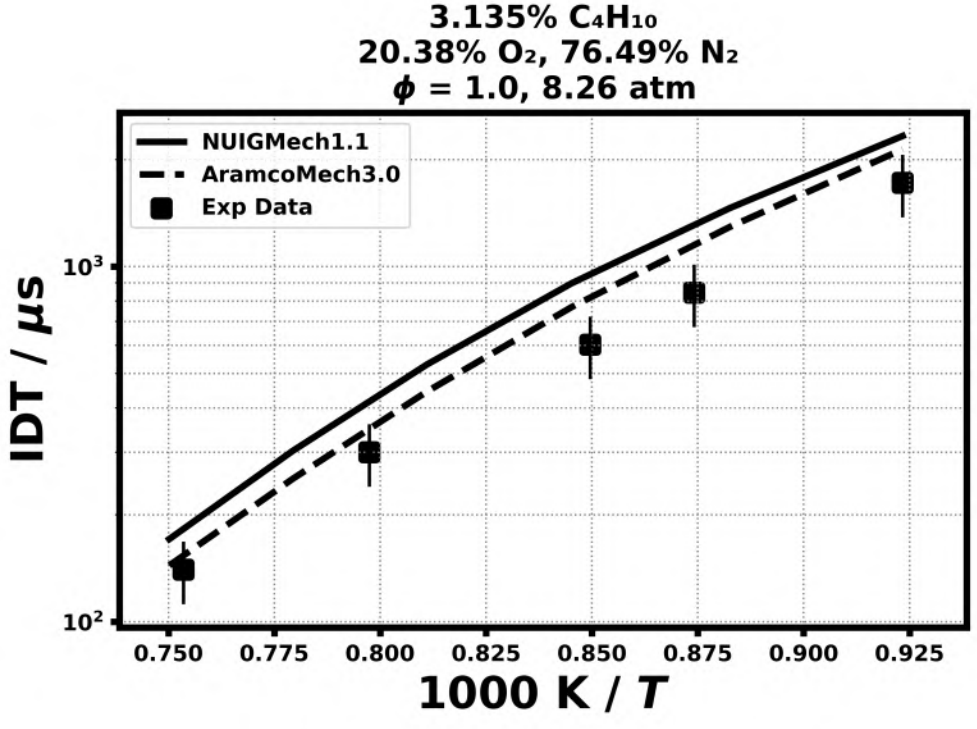
3.135% C4H10
20.38% O2, 76.49% N2
ϕ = 1.0, 8.26 atm
NUIGMech1.1
AramcoMech3.0
Exp Data
IDT / μs
10^3
10^2
0.750
0.775
0.800
0.825
0.850
0.875
0.900
0.925
1000 K / T

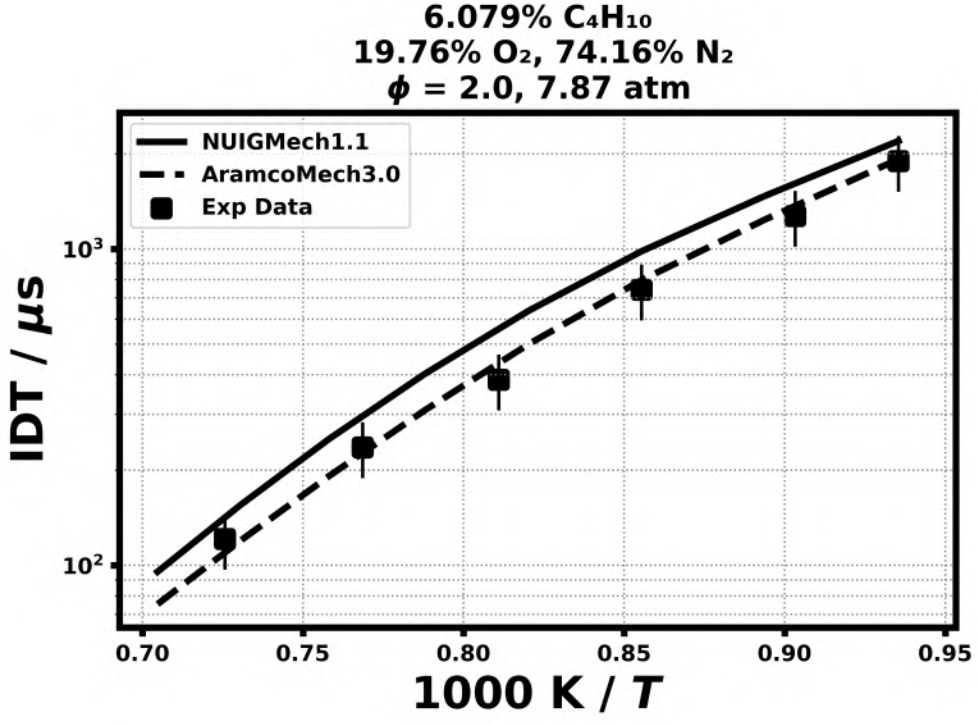
6.079% C4H10
19.76% O2, 74.16% N2
ϕ = 2.0, 7.87 atm
NUIGMech1.1
AramcoMech3.0
Exp Data
IDT / μs
10^3
10^2
0.70
0.75
0.80
0.85
0.90
0.95
1000 K / T

Laminar flame speed

19.1) Hirasawa, T., Sung, C. J., Joshi, A., Yang, Z., Wang, H., Law, C. K, Proceedings of the Combustion Institute 29 (2002) 1427-1434.
19.2) Davis, S.G., Law, C.K., Combustion Science and Technology 140 (1998) 427-449.
19.3) Bosschaart, K.J., de Goey, L.P.H., Combustion and Flame 136 (2004) 261–269.

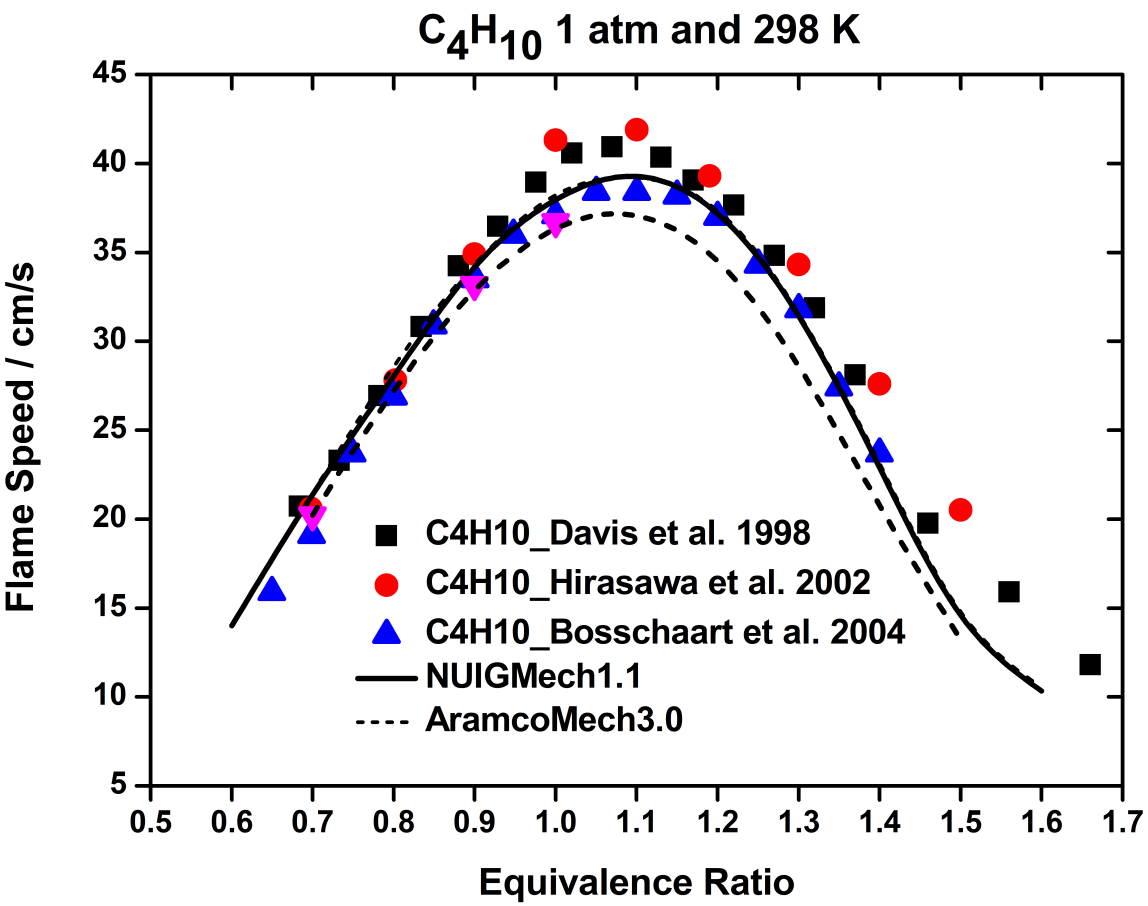

20. Validation for C_4H_8-1

Shock tube ignition delay time

20.1) Li, Y., Zhou, C. W., Somers, K. P., Zhang, K., & Curran, H. J., Proceedings of the Combustion Institute, 36(1) (2017) 403-411.

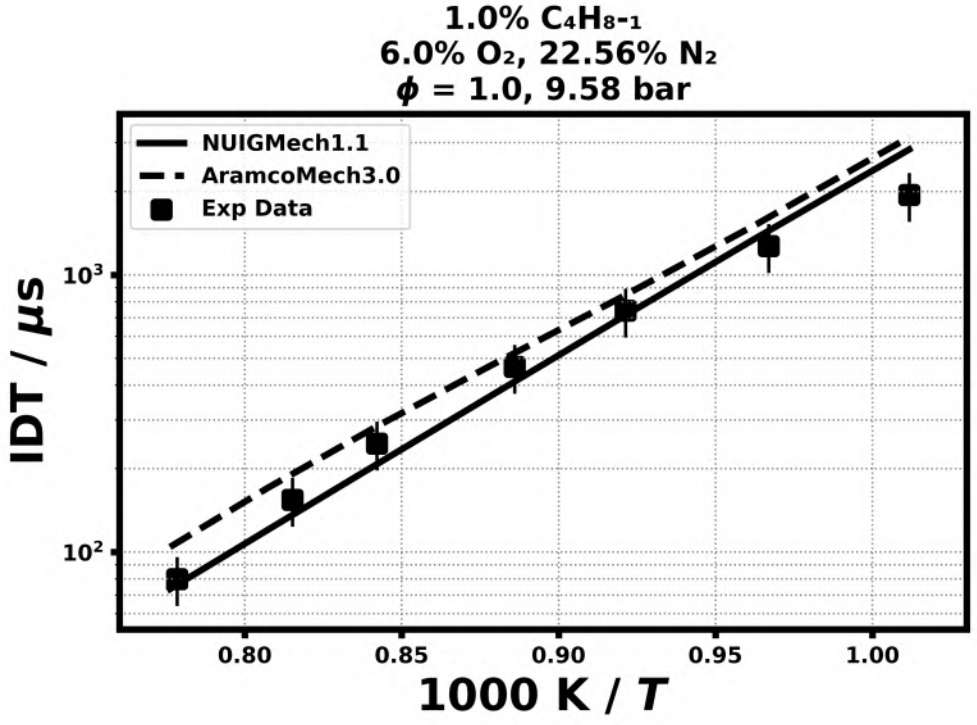

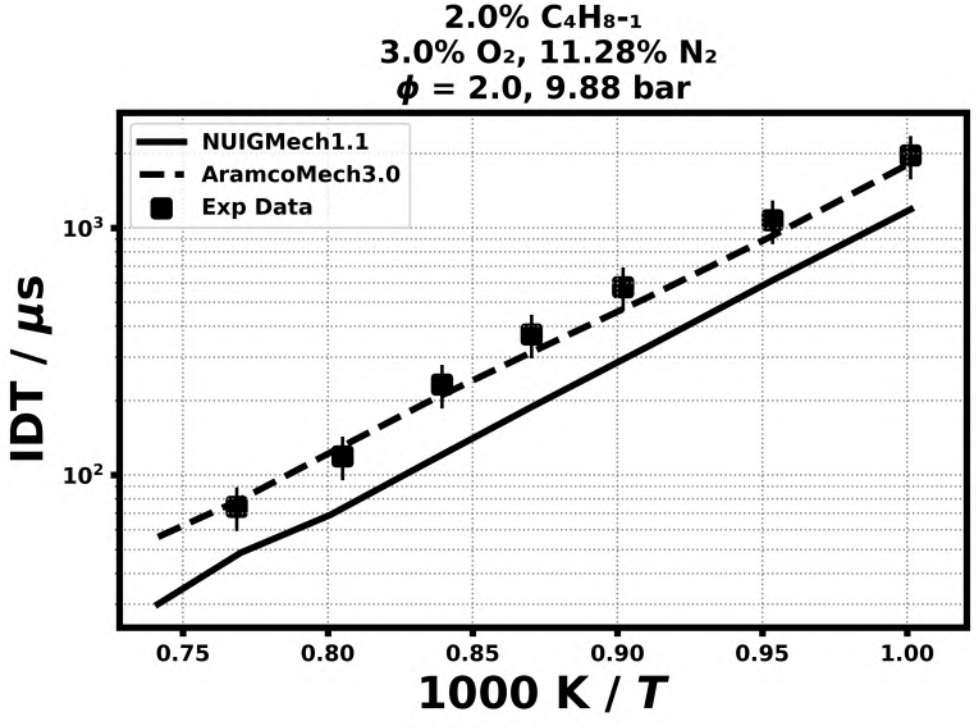

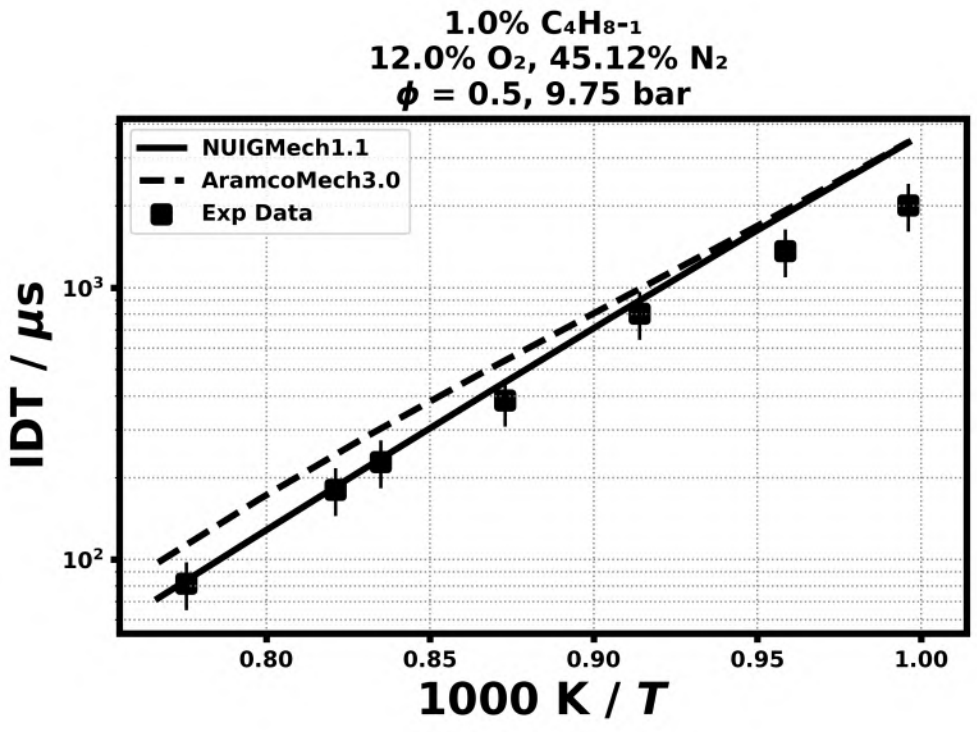
1.0% C4H8-1
12.0% O2, 45.12% N2
ϕ = 0.5, 9.75 bar
NUIGMech1.1
AramcoMech3.0
Exp Data
IDT / μs
10^3
10^2
0.80
0.85
0.90
0.95
1.00
1000 K / T

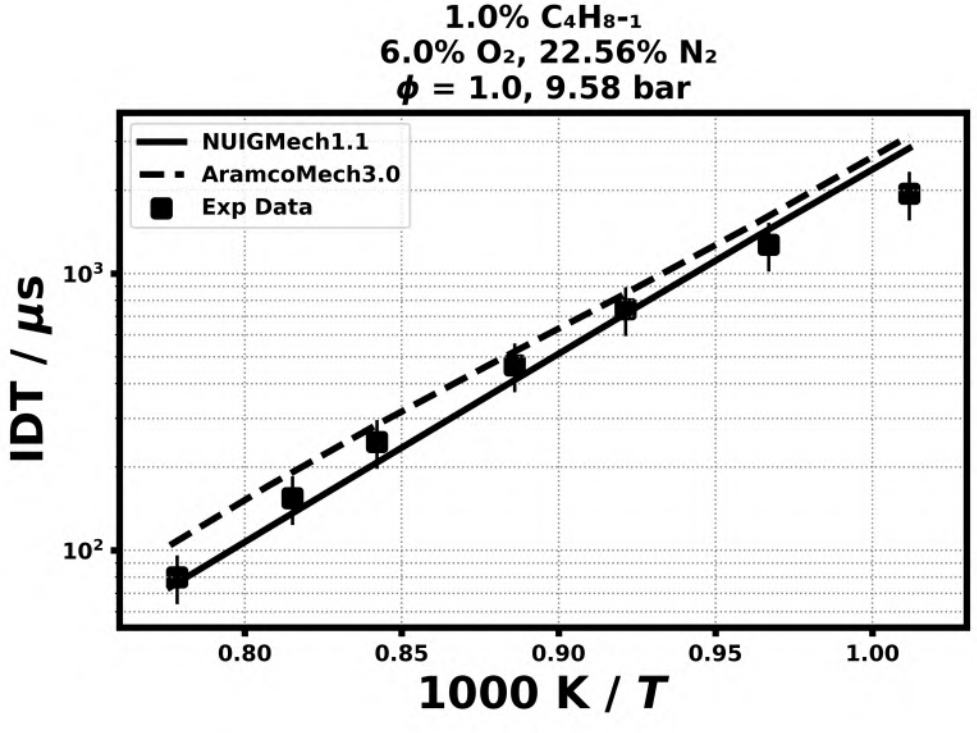
1.0% C4H8-1
6.0% O2, 22.56% N2
ϕ = 1.0, 9.58 bar
NUIGMech1.1
AramcoMech3.0
Exp Data
IDT / μs
10^3
10^2
0.80
0.85
0.90
0.95
1.00
1000 K / T

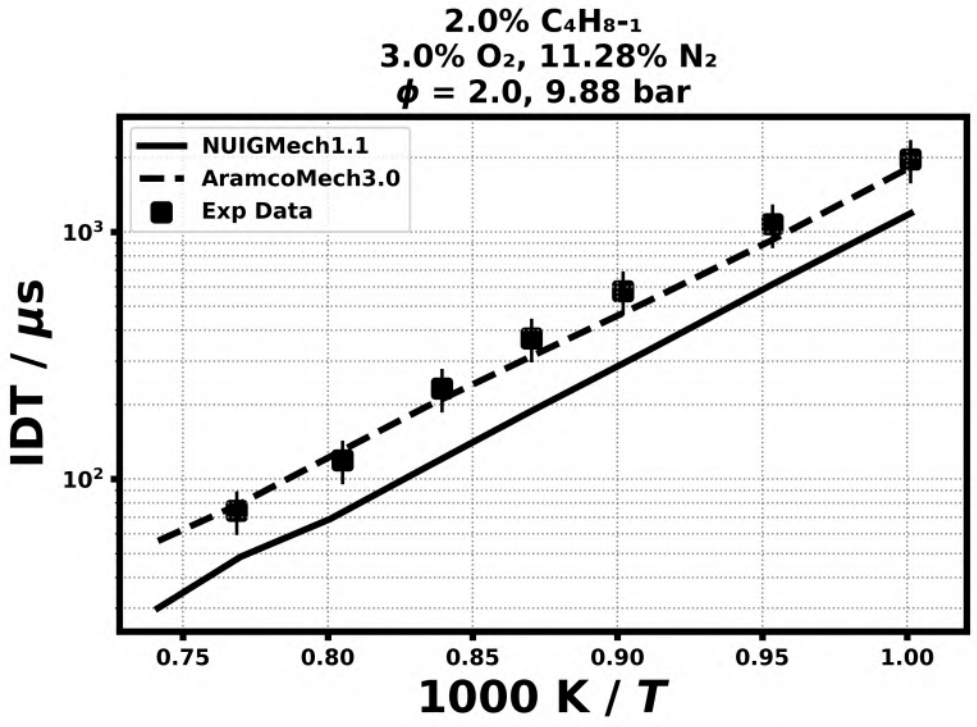
2.0% C4H8-1
3.0% O2, 11.28% N2
ϕ = 2.0, 9.88 bar
NUIGMech1.1
AramcoMech3.0
Exp Data
IDT / μs
10^3
10^2
0.75
0.80
0.85
0.90
0.95
1.00
1000 K / T

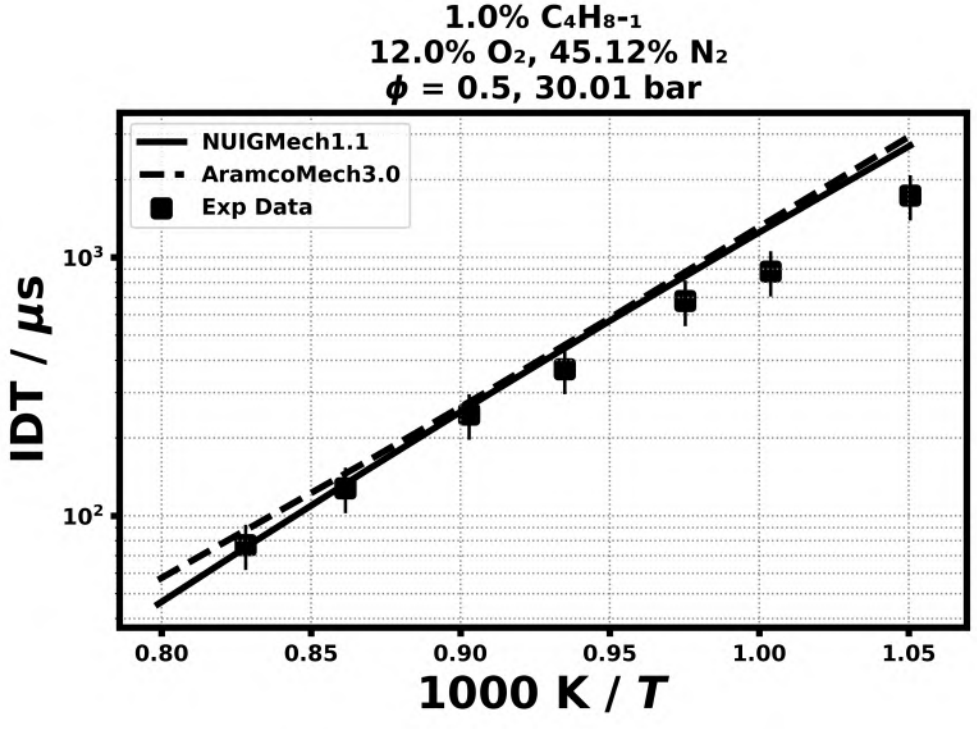
1.0% C4H8-1
12.0% O2, 45.12% N2
ϕ = 0.5, 30.01 bar
NUIGMech1.1
AramcoMech3.0
Exp Data
IDT / μs
10^3
10^2
0.80
0.85
0.90
0.95
1.00
1.05
1000 K / T

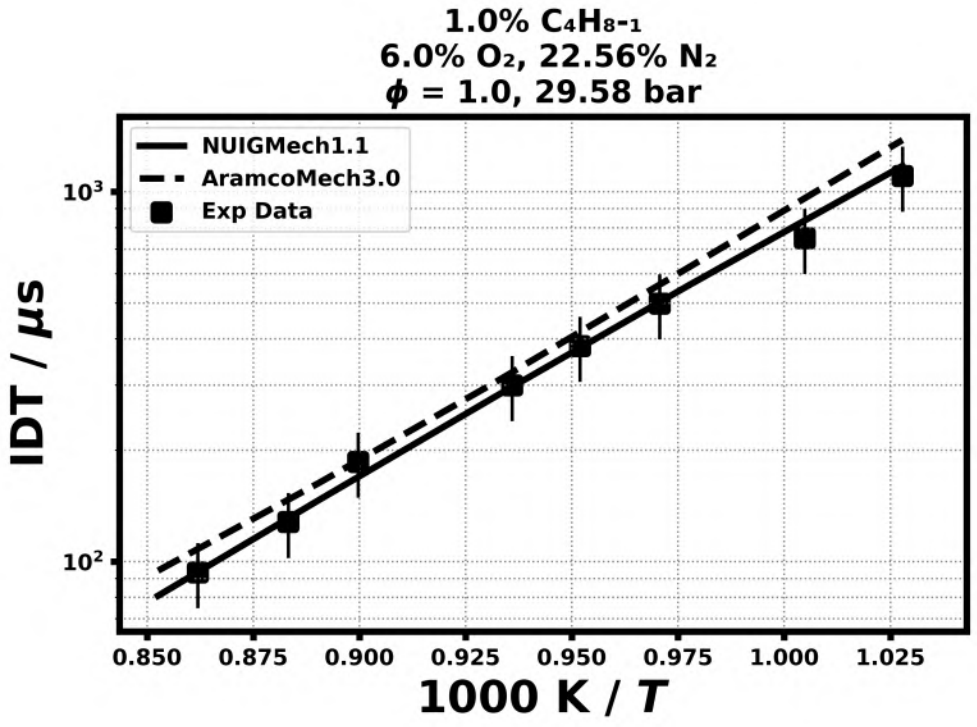
1.0% C4H8-1
6.0% O2, 22.56% N2
ϕ = 1.0, 29.58 bar
NUIGMech1.1
AramcoMech3.0
Exp Data
IDT / μs
10^3
10^2
0.850
0.875
0.900
0.925
0.950
0.975
1.000
1.025
1000 K / T

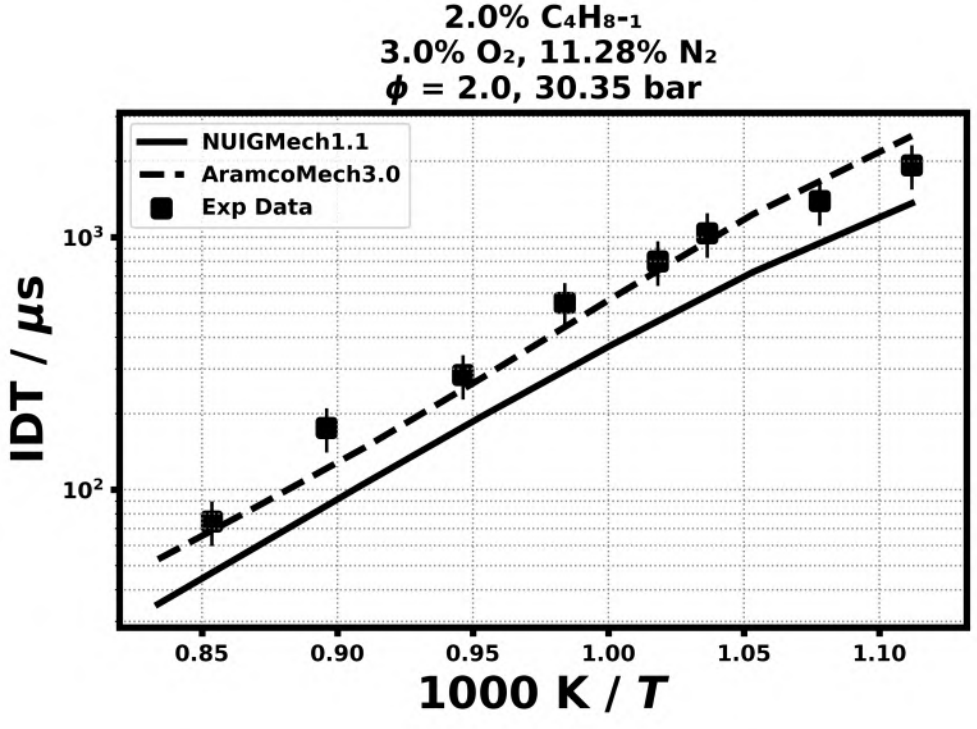
2.0% C4H8-1
3.0% O2, 11.28% N2
ϕ = 2.0, 30.35 bar
NUIGMech1.1
AramcoMech3.0
Exp Data
IDT / μs
10^3
10^2
0.85
0.90
0.95
1.00
1.05
1.10
1000 K / T

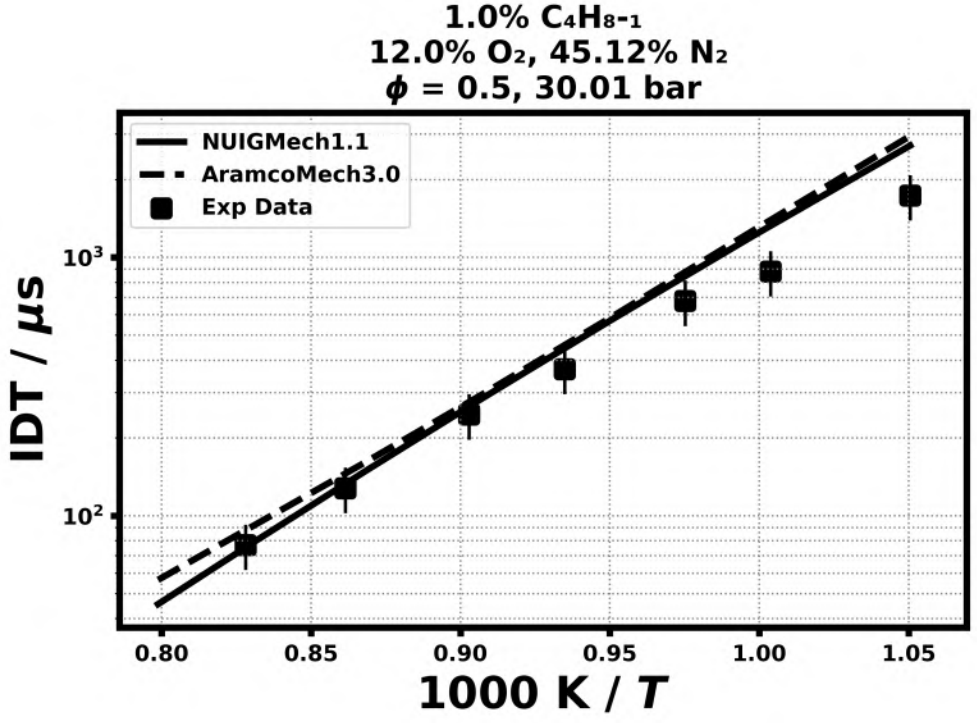
1.0% C4H8-1
12.0% O2, 45.12% N2
ϕ = 0.5, 30.01 bar
NUIGMech1.1
AramcoMech3.0
Exp Data
IDT / μs
10^3
10^2
0.80
0.85
0.90
0.95
1.00
1.05
1000 K / T

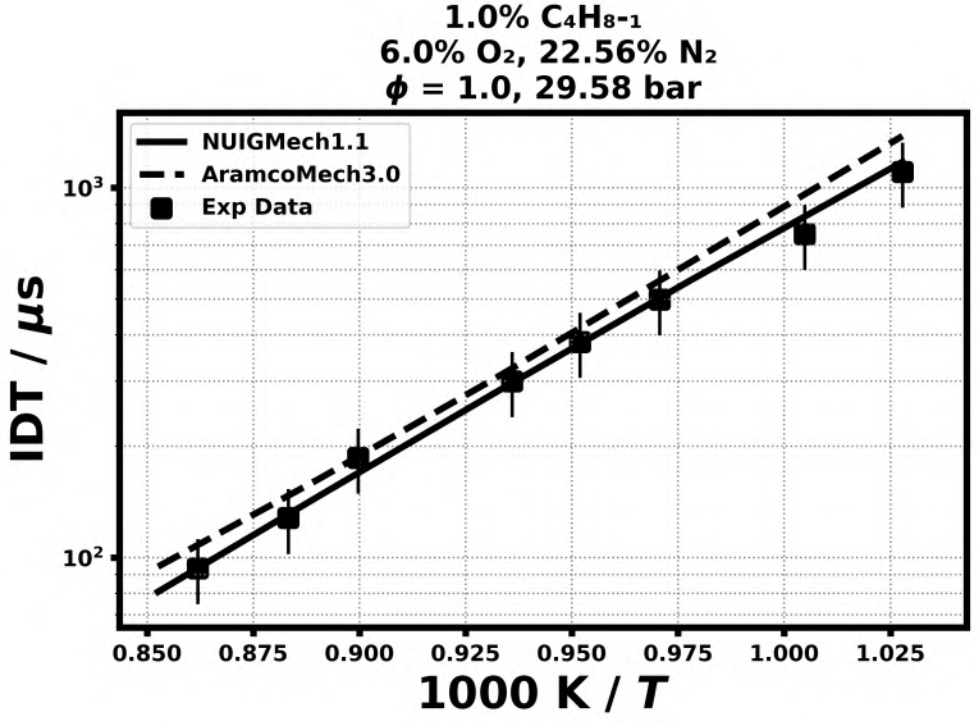
1.0% C4H8-1
6.0% O2, 22.56% N2
ϕ = 1.0, 29.58 bar
NUIGMech1.1
AramcoMech3.0
Exp Data
IDT / μs
10^3
10^2
0.850
0.875
0.900
0.925
0.950
0.975
1.000
1.025
1000 K / T

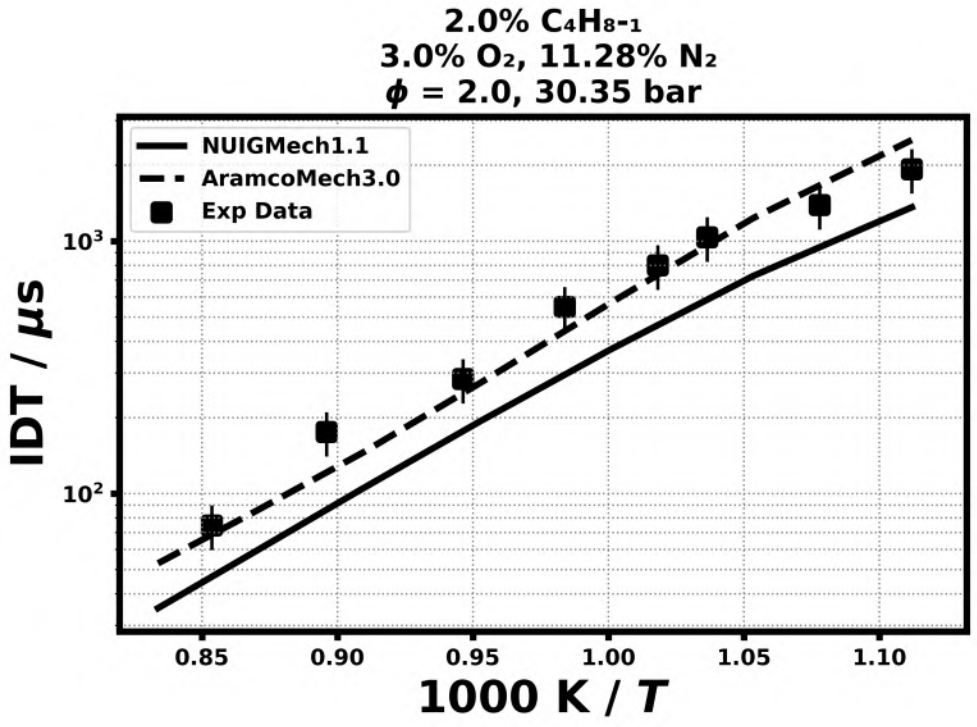
2.0% C4H8-1
3.0% O2, 11.28% N2
ϕ = 2.0, 30.35 bar
NUIGMech1.1
AramcoMech3.0
Exp Data
IDT / μs
10^3
10^2
0.85
0.90
0.95
1.00
1.05
1.10
1000 K / T

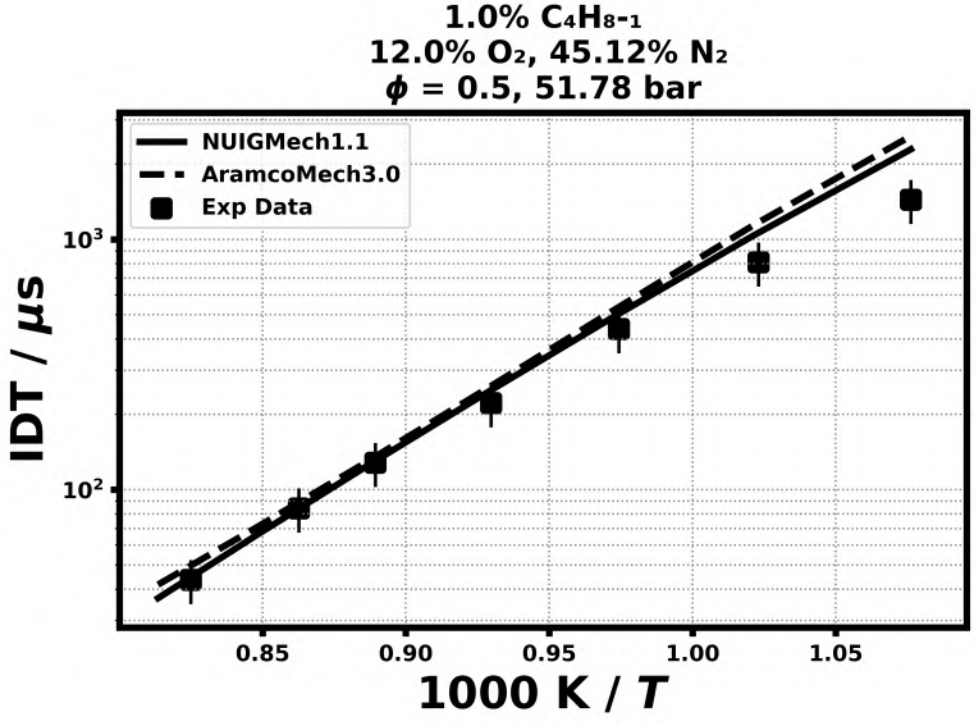
1.0% C4H8-1
12.0% O2, 45.12% N2
ϕ = 0.5, 51.78 bar
NUIGMech1.1
AramcoMech3.0
Exp Data
IDT / μs
10^3
10^2
0.85
0.90
0.95
1.00
1.05
1000 K / T

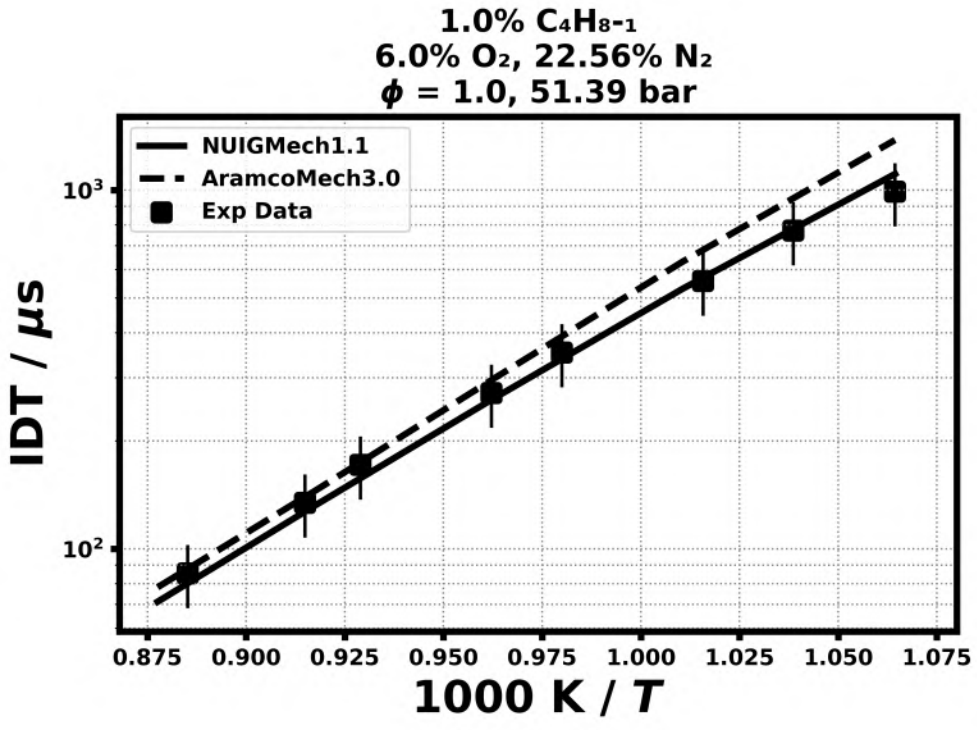
1.0% C4H8-1
6.0% O2, 22.56% N2
ϕ = 1.0, 51.39 bar
NUIGMech1.1
AramcoMech3.0
Exp Data
IDT / μs
10³
10²
0.875
0.900
0.925
0.950
0.975
1.000
1.025
1.050
1.075
1000 K / T

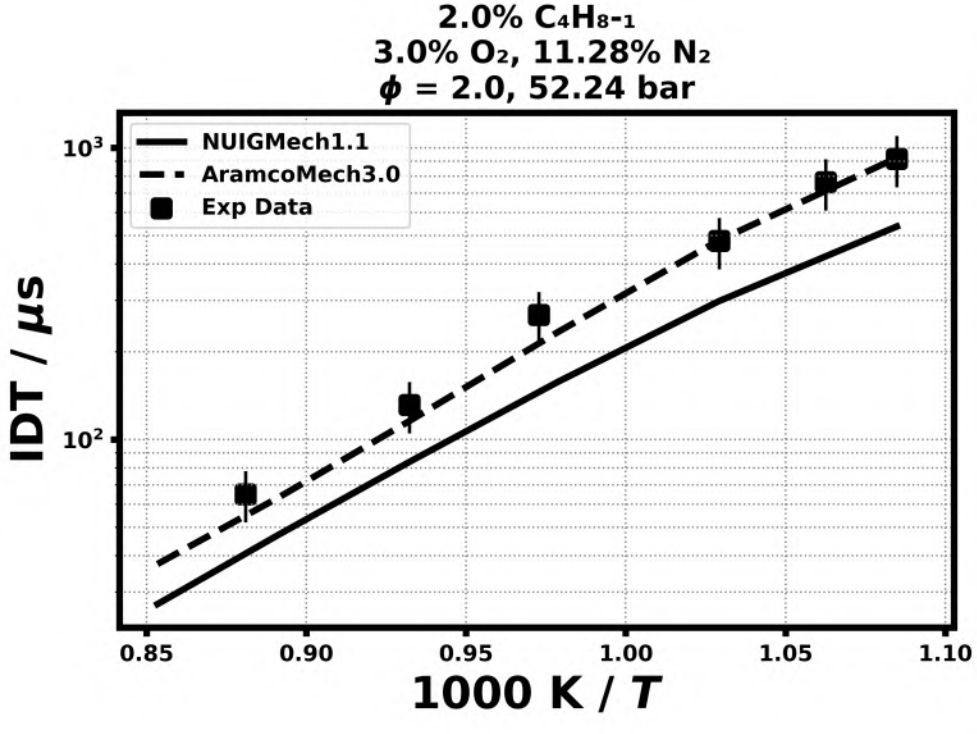
2.0% C4H8-1
3.0% O2, 11.28% N2
ϕ = 2.0, 52.24 bar
NUIGMech1.1
AramcoMech3.0
Exp Data
IDT / μs
10³
10²
0.85
0.90
0.95
1.00
1.05
1.10
1000 K / T

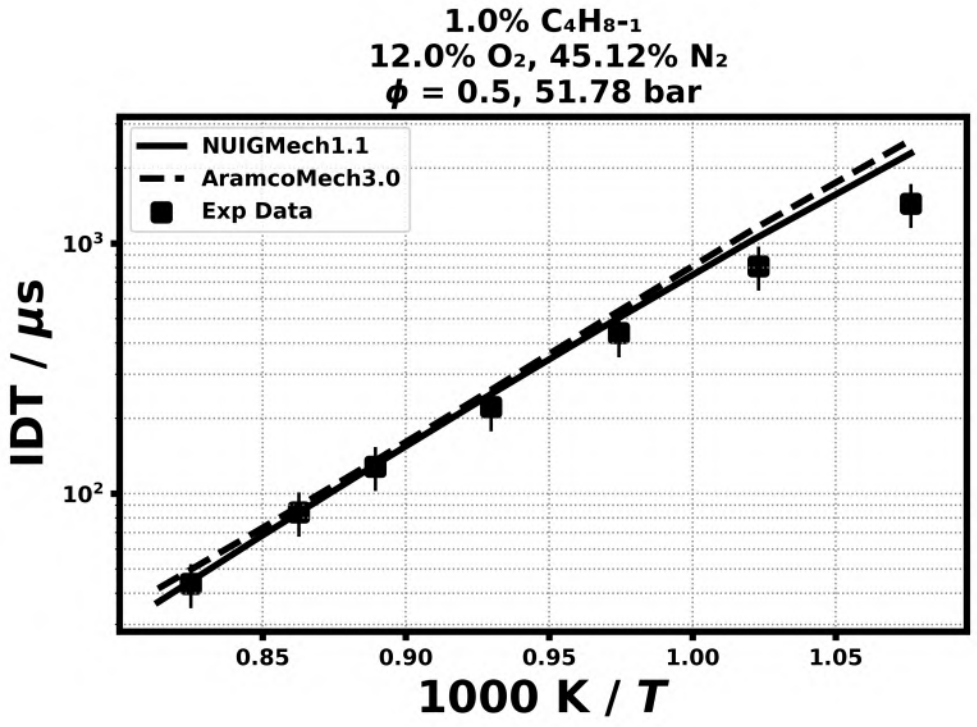
1.0% C4H8-1
12.0% O2, 45.12% N2
ϕ = 0.5, 51.78 bar
NUIGMech1.1
AramcoMech3.0
Exp Data
IDT / μs
10^3
10^2
0.85
0.90
0.95
1.00
1.05
1000 K / T

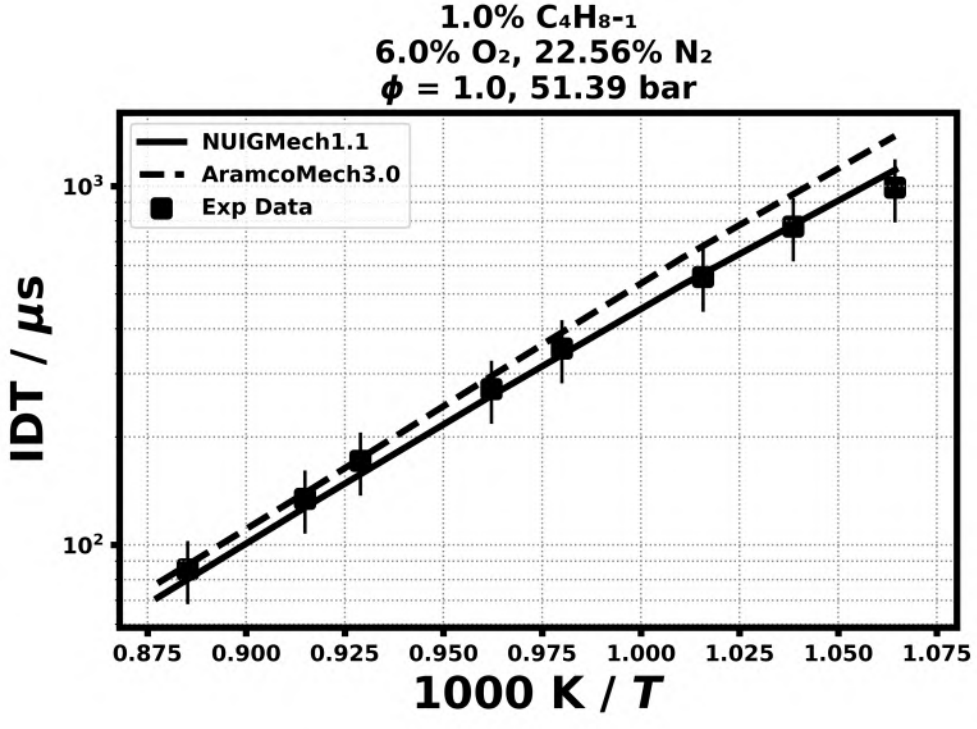
1.0% C4H8-1
6.0% O2, 22.56% N2
ϕ = 1.0, 51.39 bar
NUIGMech1.1
AramcoMech3.0
Exp Data
IDT / μs
10^3
10^2
0.875
0.900
0.925
0.950
0.975
1.000
1.025
1.050
1.075
1000 K / T

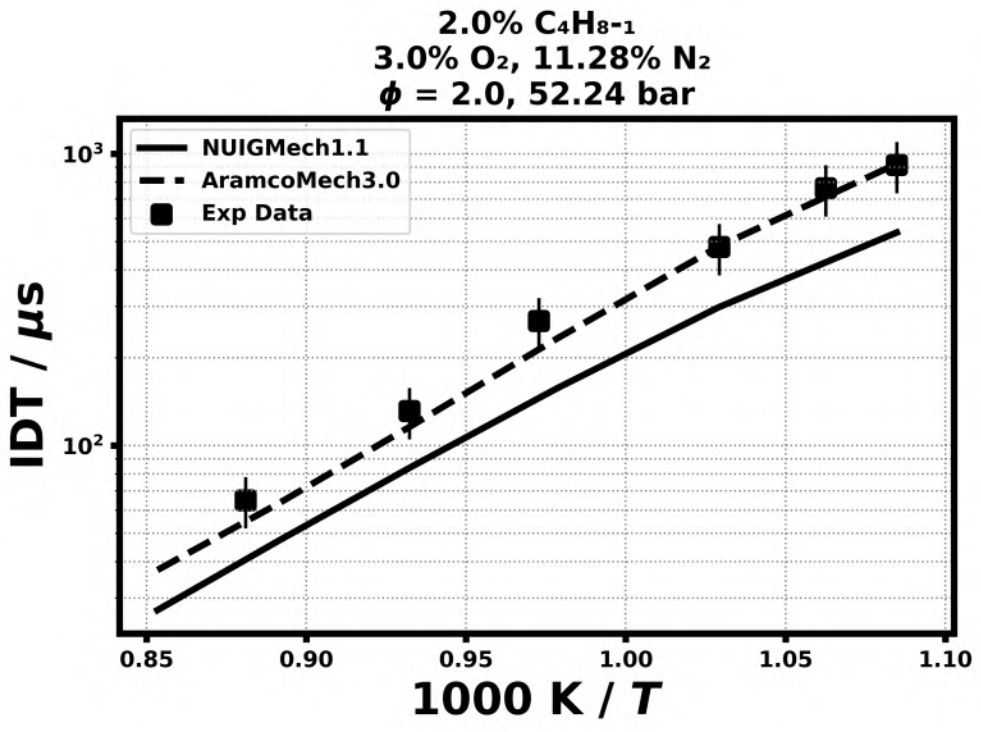
2.0% C4H8-1
3.0% O2, 11.28% N2
ϕ = 2.0, 52.24 bar
NUIGMech1.1
AramcoMech3.0
Exp Data
IDT / μs
10^3
10^2
0.85
0.90
0.95
1.00
1.05
1.10
1000 K / T

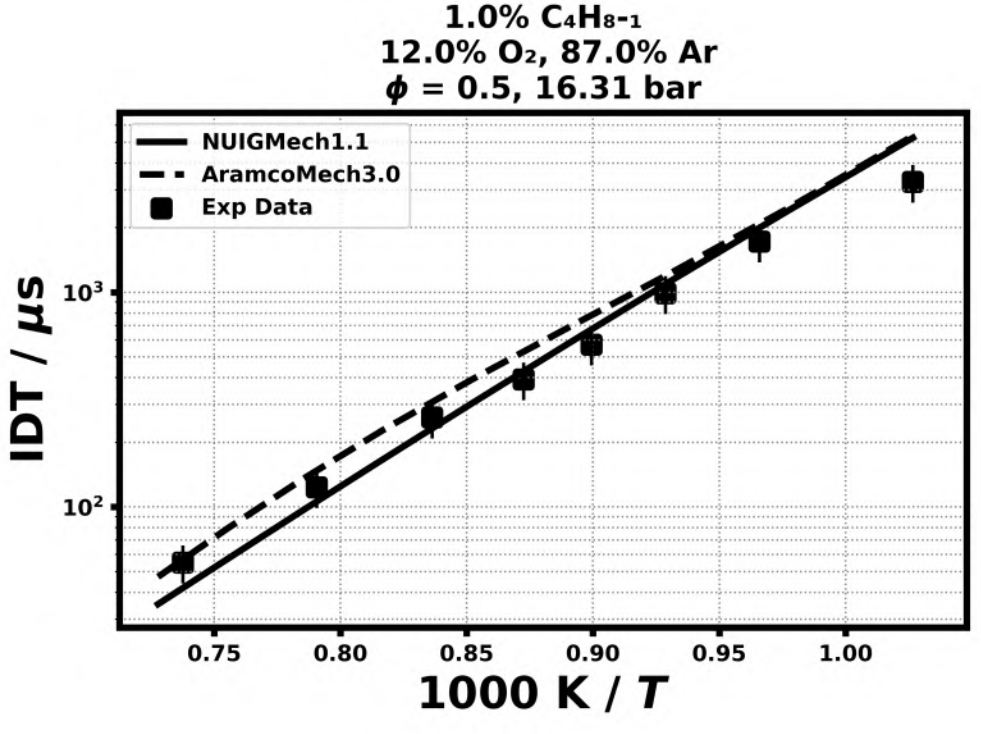
1.0% C4H8-1
12.0% O2, 87.0% Ar
ϕ = 0.5, 16.31 bar
NUIGMech1.1
AramcoMech3.0
Exp Data
IDT / μs
10^3
10^2
0.75
0.80
0.85
0.90
0.95
1.00
1000 K / T

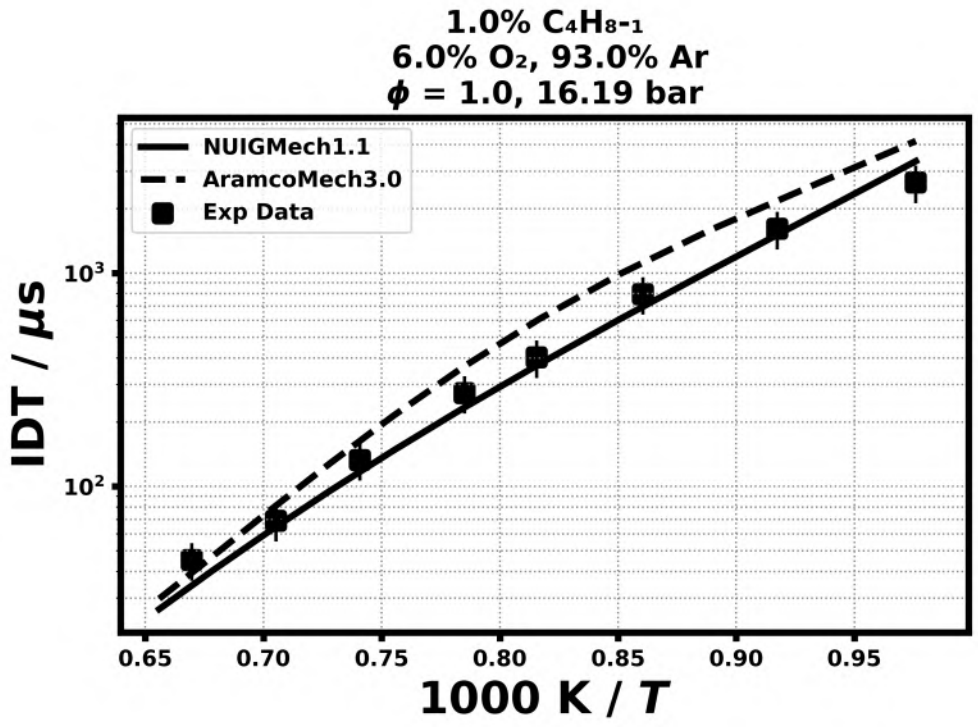

20.2) Pan, L., Hu, E., Zhang, J., Tian, Z., Li, X., & Huang, Z., Fuel, 157 (2015) 21-27.

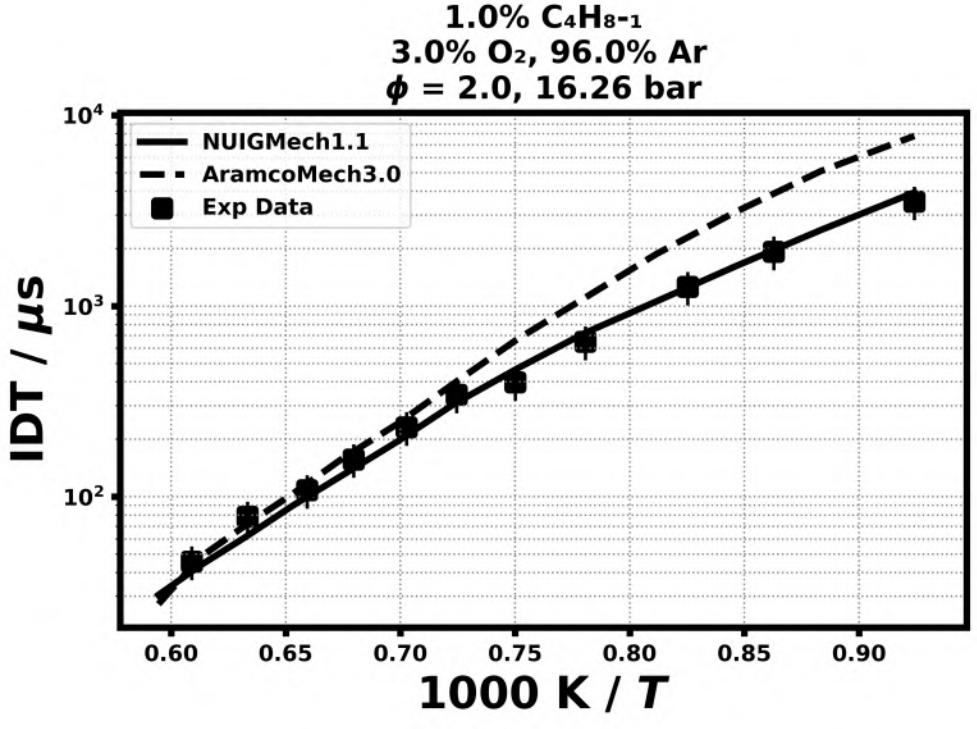

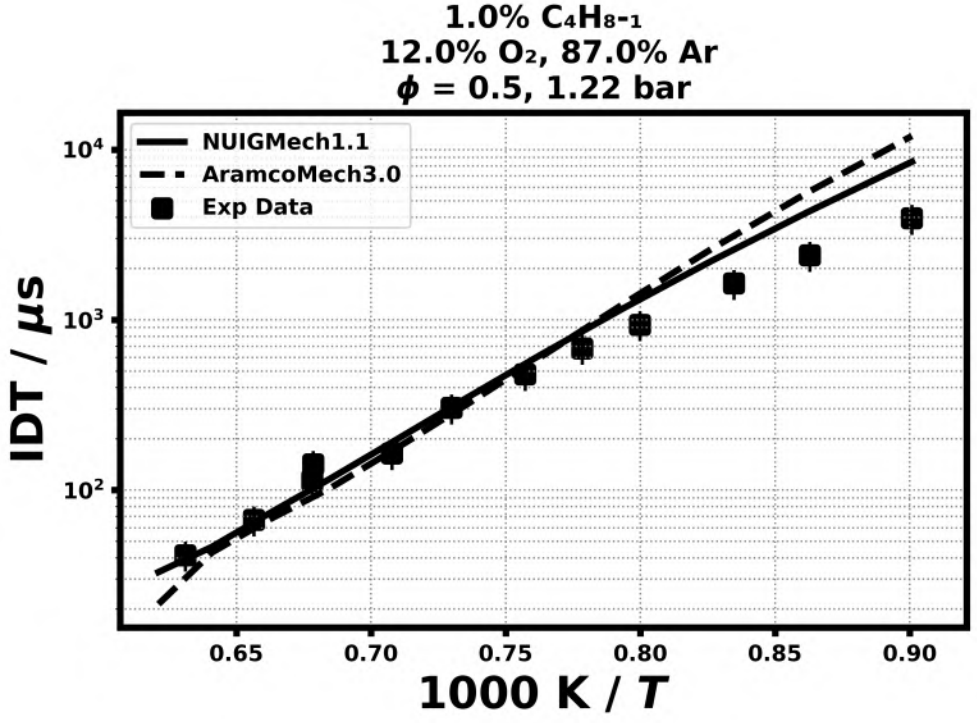
1.0% C4H8-1
12.0% O2, 87.0% Ar
ϕ = 0.5, 1.22 bar
NUIGMech1.1
AramcoMech3.0
Exp Data
IDT / μs
10^4
10^3
10^2
0.65
0.70
0.75
0.80
0.85
0.90
1000 K / T

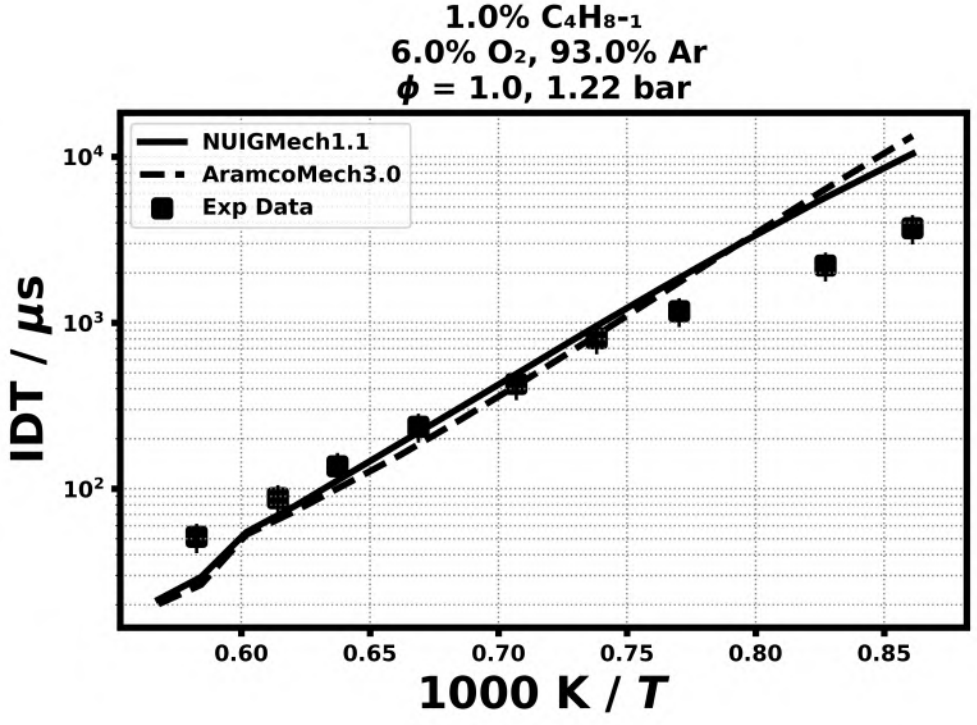
1.0% C4H8-1
6.0% O2, 93.0% Ar
ϕ = 1.0, 1.22 bar
NUIGMech1.1
AramcoMech3.0
Exp Data
IDT / μs
10^4
10^3
10^2
0.60
0.65
0.70
0.75
0.80
0.85
1000 K / T

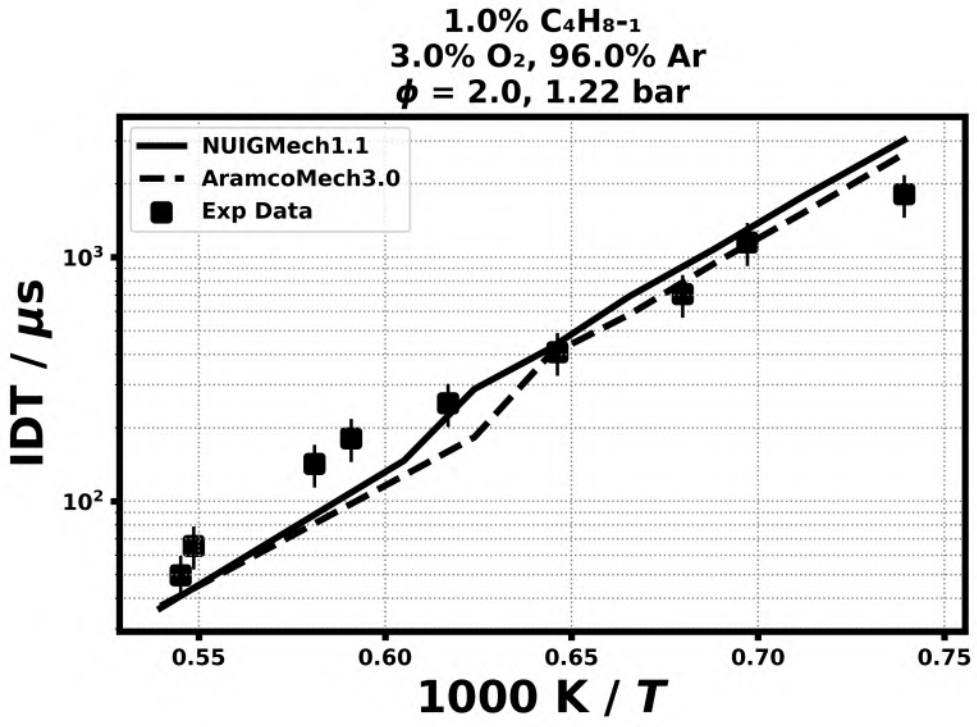
1.0% C4H8-1
3.0% O2, 96.0% Ar
ϕ = 2.0, 1.22 bar
NUIGMech1.1
AramcoMech3.0
Exp Data
IDT / μs
10^3
10^2
0.55
0.60
0.65
0.70
0.75
1000 K / T

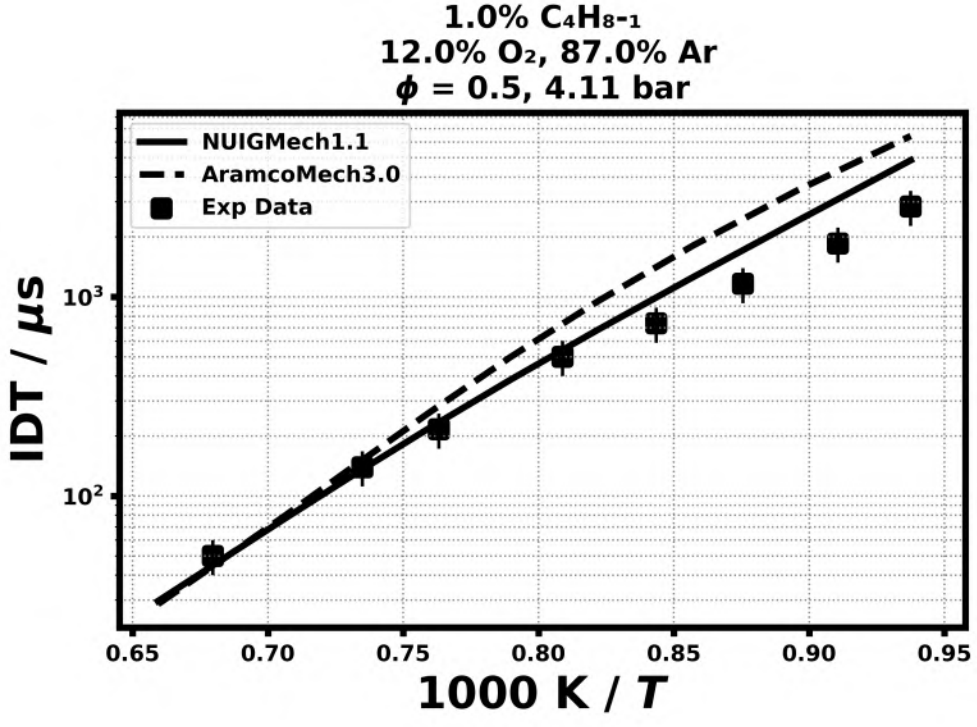
1.0% C4H8-1
12.0% O2, 87.0% Ar
ϕ = 0.5, 4.11 bar
NUIGMech1.1
AramcoMech3.0
Exp Data
IDT / μs
10^3
10^2
0.65
0.70
0.75
0.80
0.85
0.90
0.95
1000 K / T

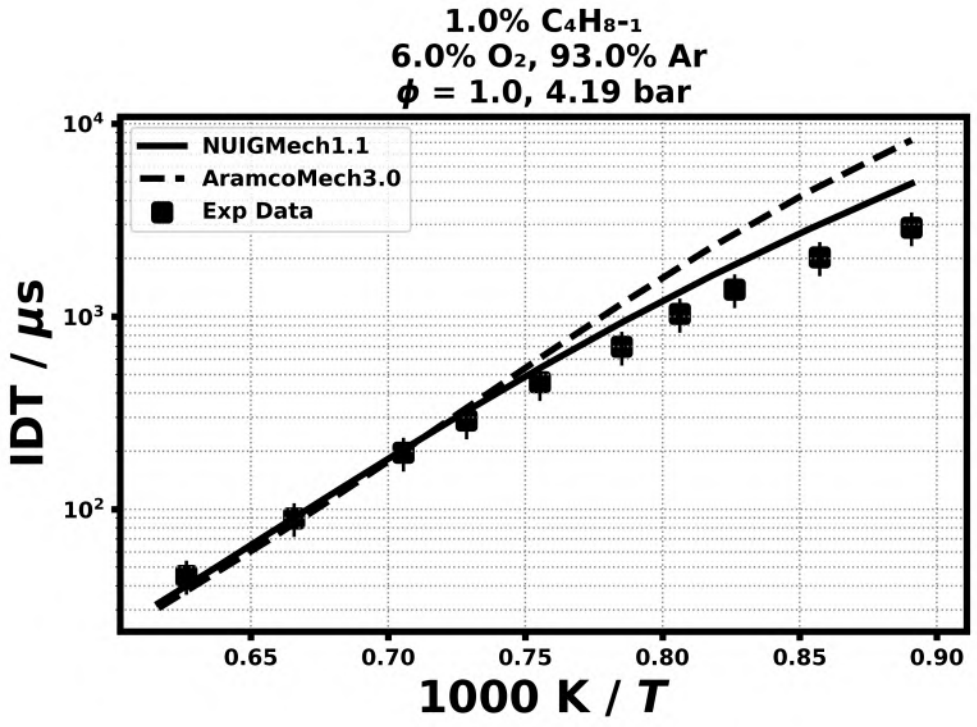
1.0% C4H8-1
6.0% O2, 93.0% Ar
ϕ = 1.0, 4.19 bar
NUIGMech1.1
AramcoMech3.0
Exp Data
IDT / μs
10^4
10^3
10^2
0.65
0.70
0.75
0.80
0.85
0.90
1000 K / T

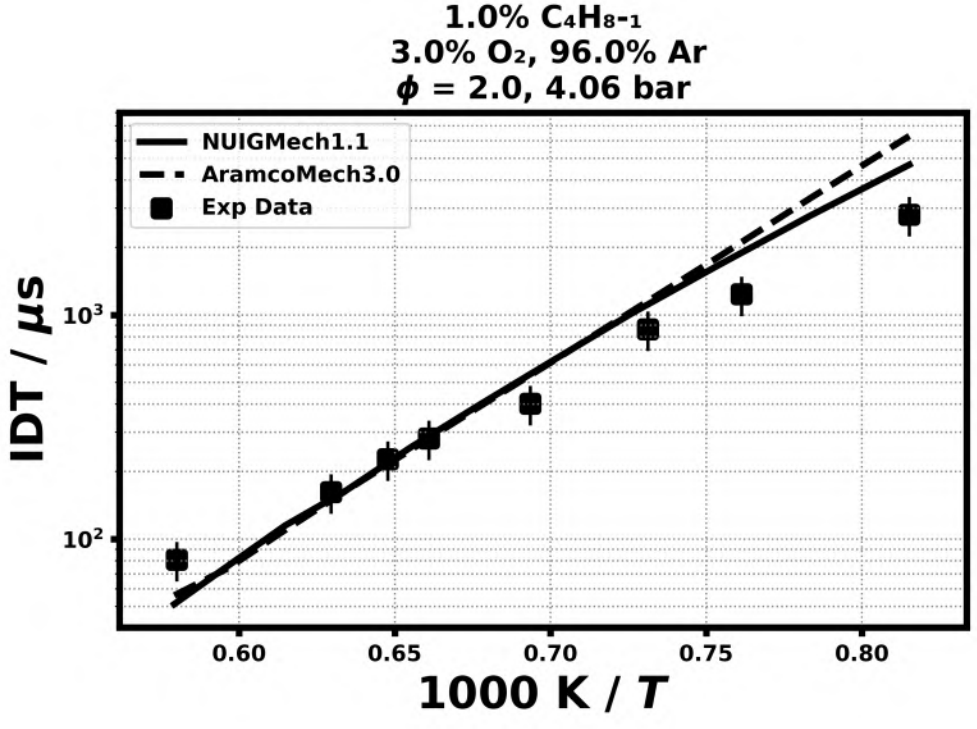
1.0% C4H8-1
3.0% O2, 96.0% Ar
ϕ = 2.0, 4.06 bar
NUIGMech1.1
AramcoMech3.0
Exp Data
IDT / μs
10^3
10^2
0.60
0.65
0.70
0.75
0.80
1000 K / T

RCM Ignition delay time

20.3) Li, Y., Zhou, C. W., Somers, K. P., Zhang, K., & Curran, H. J., Proceedings of the Combustion Institute, 36(1) (2017) 403-411.

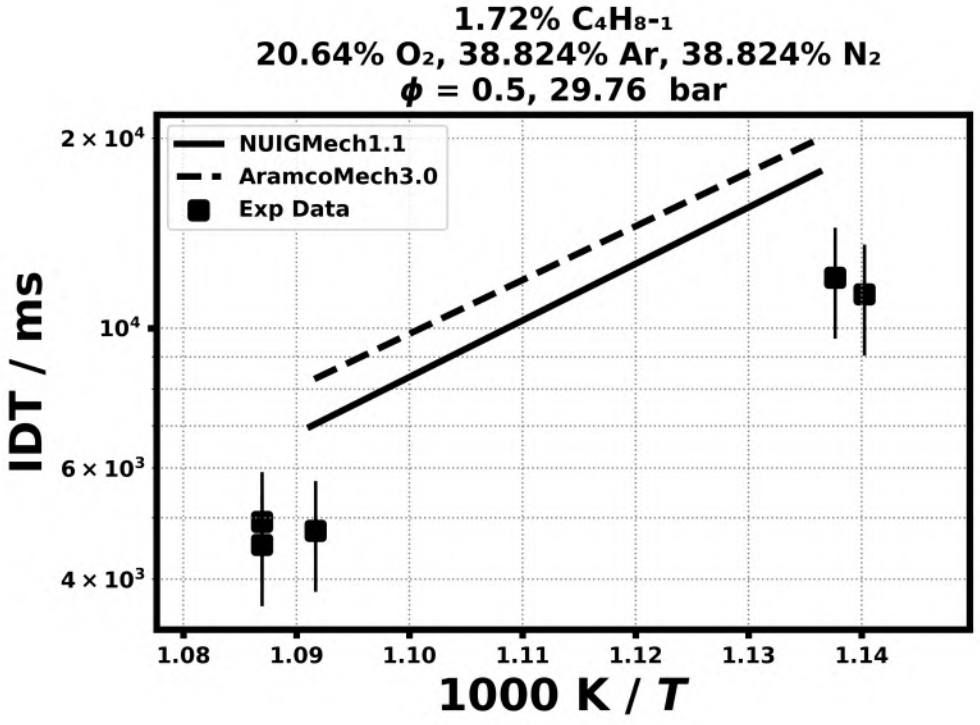

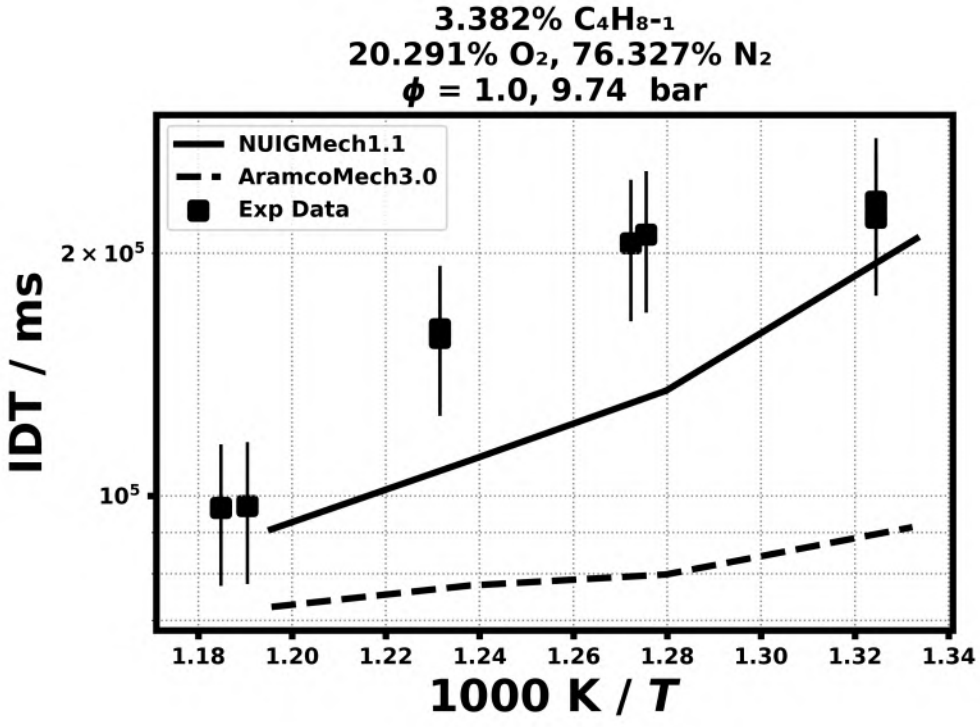

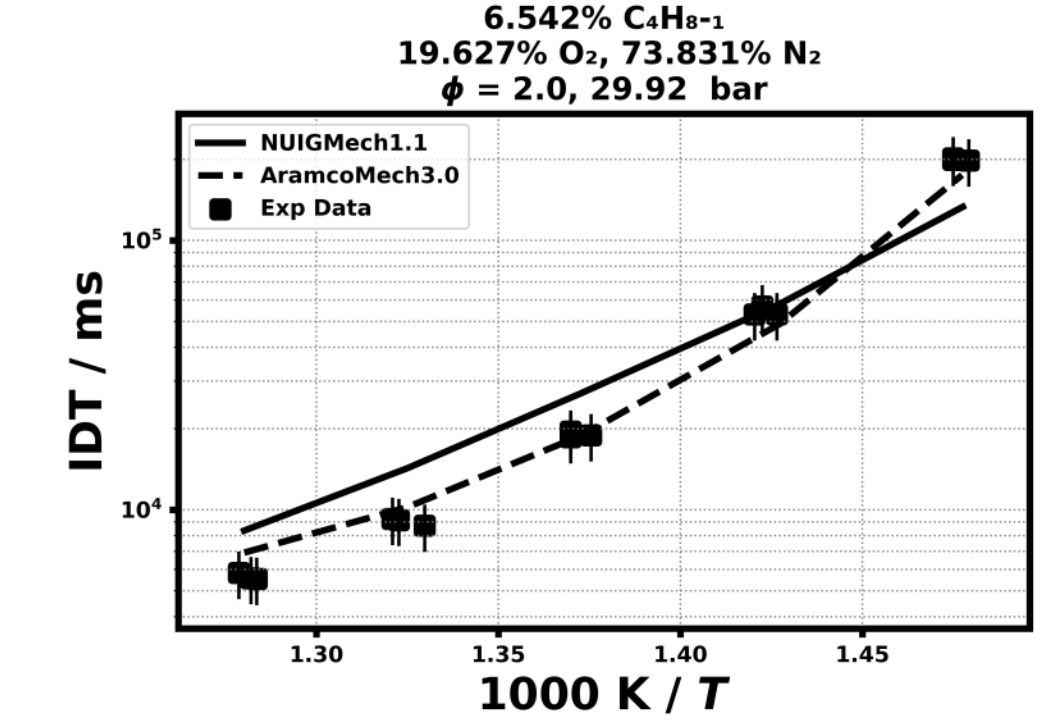
6.542% C4H8-1
19.627% O2, 73.831% N2
ϕ = 2.0, 29.92 bar
NUIGMech1.1
AramcoMech3.0
Exp Data
IDT / ms
10^5
10^4
1.30
1.35
1.40
1.45
1000 K / T

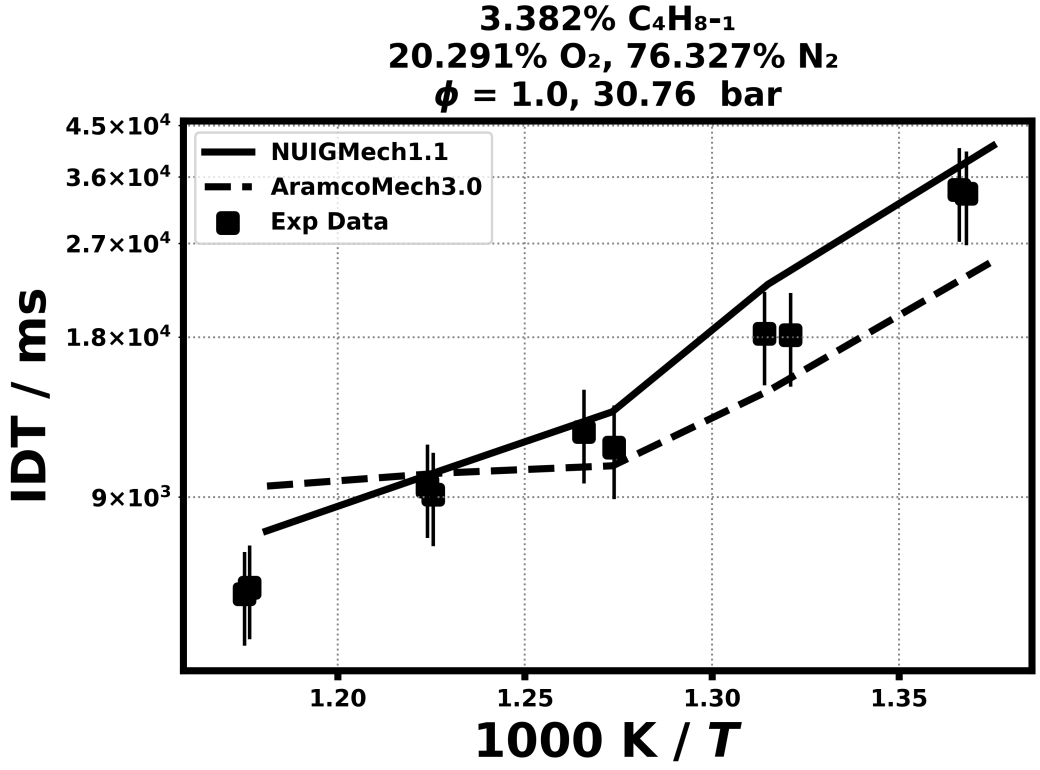
3.382% C4H8-1
20.291% O2, 76.327% N2
ϕ = 1.0, 30.76 bar
NUIGMech1.1
AramcoMech3.0
Exp Data
IDT / ms
4.5×10^4
3.6×10^4
2.7×10^4
1.8×10^4
9×10^3
1.20
1.25
1.30
1.35
1000 K / T

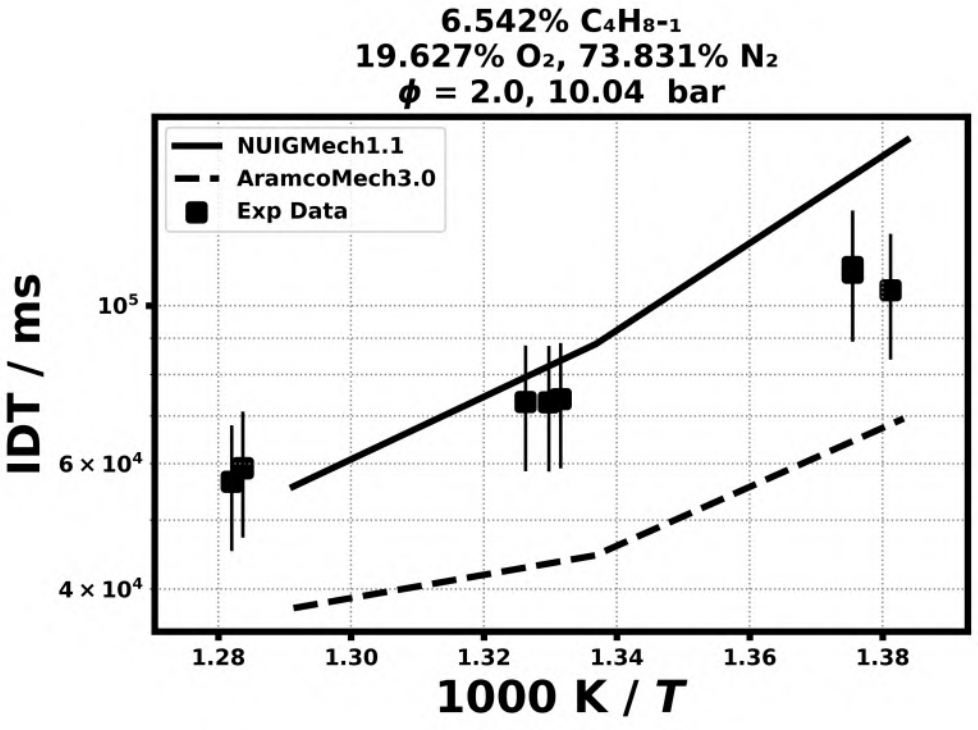
6.542% C4H8-1
19.627% O2, 73.831% N2
ϕ = 2.0, 10.04 bar
NUIGMech1.1
AramcoMech3.0
Exp Data
IDT / ms
10^5
6 × 10^4
4 × 10^4
1.28
1.30
1.32
1.34
1.36
1.38
1000 K / T

Laminar flame speed

20.3) Davis, S.G., Law, C.K., Combustion Science and Technology 140 (1998) 427-449.
20.4) Zhao, P., Yuan, W., Sun, H., Li, Y., Kelley, A. P., Zheng, X., & Law, C. K. Proceedings of the Combustion Institute, 35(1) (2015) 309-316.
20.5) Fenard, Y., Dayma, G., Halter, F., Foucher, F., Serinyel, Z., & Dagaut, P. Energy & Fuels, 29(2) (2015) 1107-1118.
20.6) Li, Y., Zhou, C. W., Somers, K. P., Zhang, K., & Curran, H. J., Proceedings of the Combustion Institute, 36(1) (2017) 403-411.

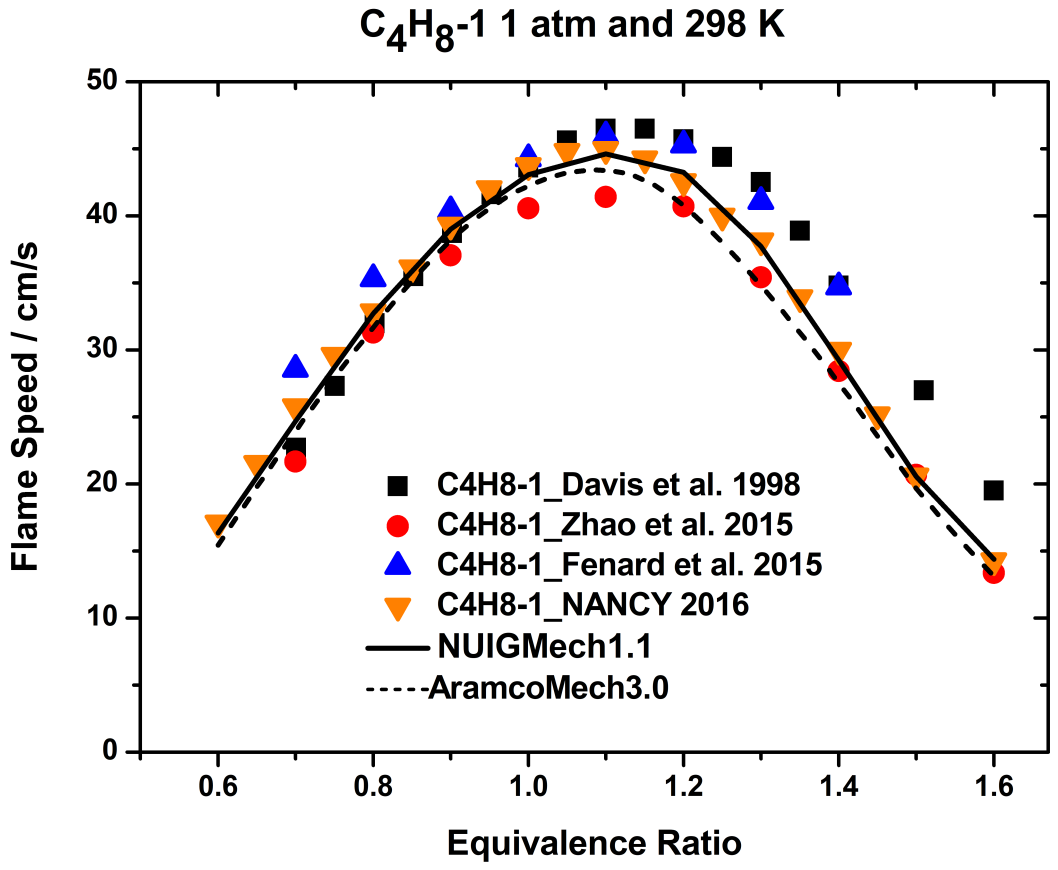

21. Validation for iC_4H_8

Shock tube ignition delay time

21.1) Li, Y., Zhou, C. W., Somers, K. P., Zhang, K., & Curran, H. J., Proceedings of the Combustion Institute, 36(1) (2017) 403-411.

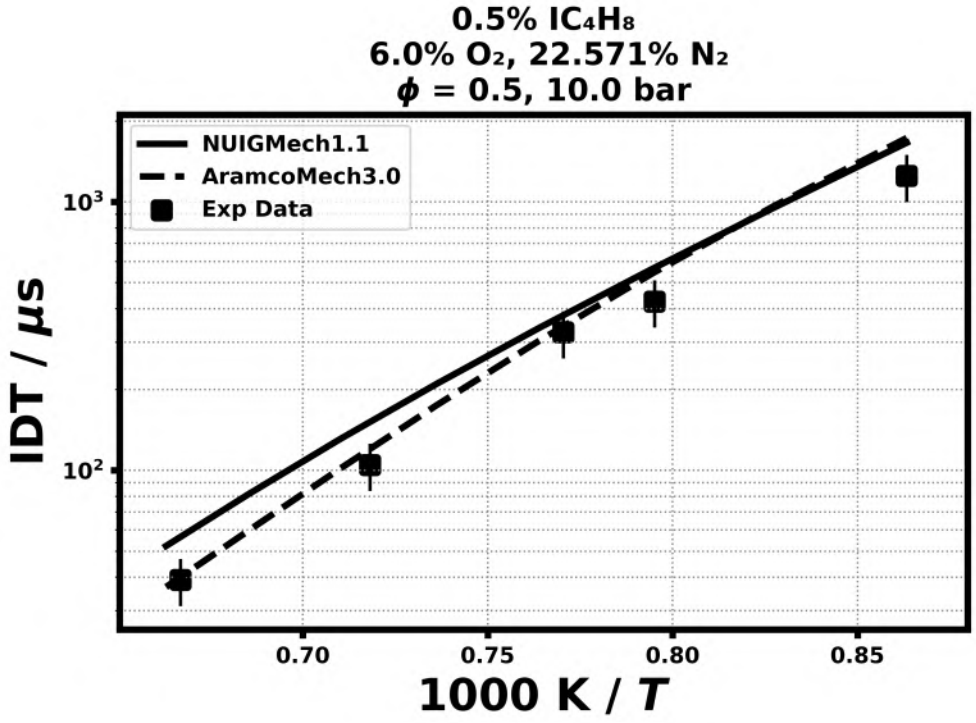

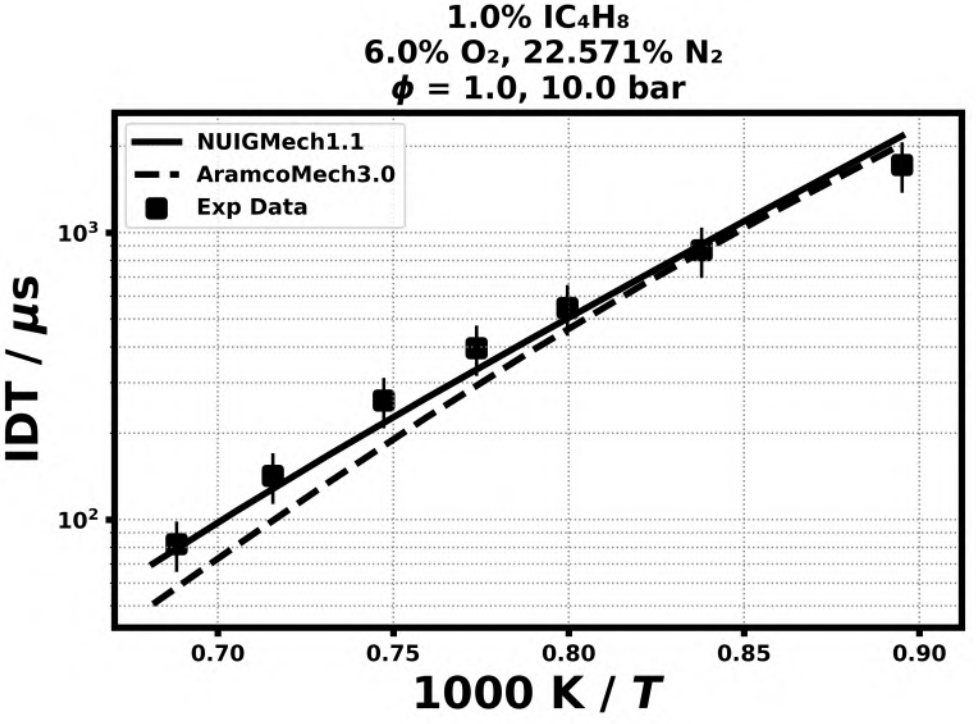

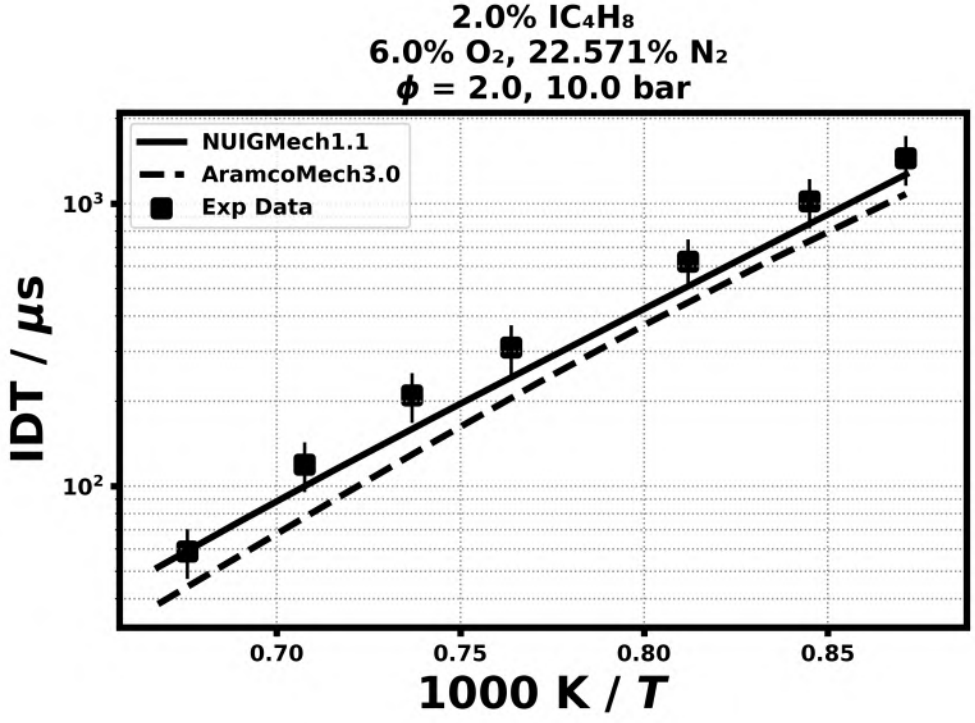
2.0% IC4H8
6.0% O2, 22.571% N2
ϕ = 2.0, 10.0 bar
NUIGMech1.1
AramcoMech3.0
Exp Data
IDT / μs
10^3
10^2
0.70
0.75
0.80
0.85
1000 K / T

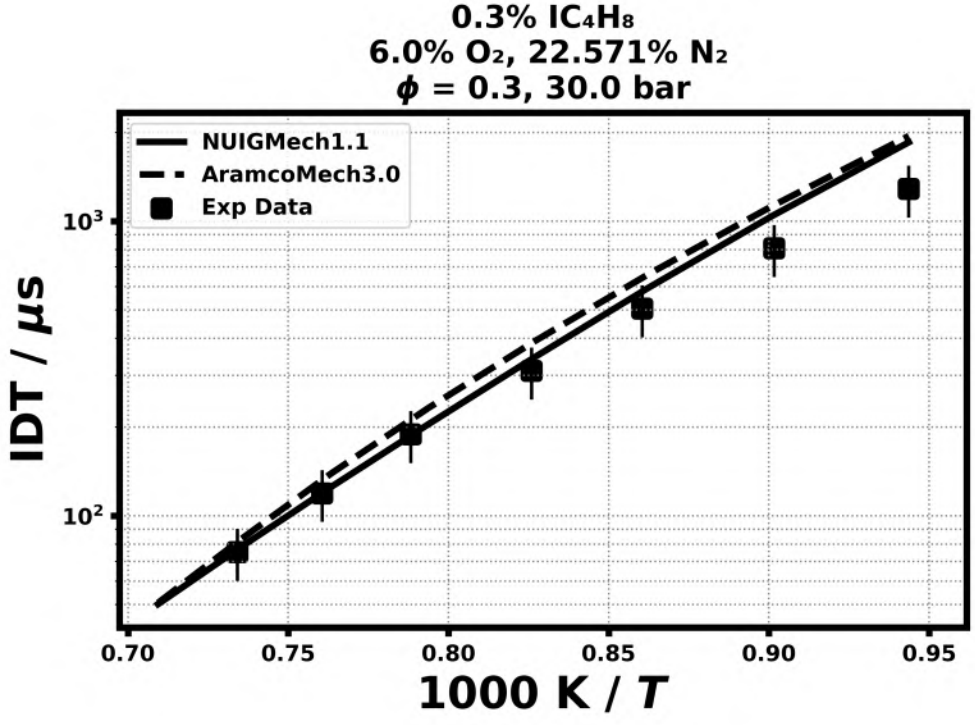
0.3% IC4H8
6.0% O2, 22.571% N2
ϕ = 0.3, 30.0 bar
NUIGMech1.1
AramcoMech3.0
Exp Data
IDT / μs
10^3
10^2
0.70
0.75
0.80
0.85
0.90
0.95
1000 K / T

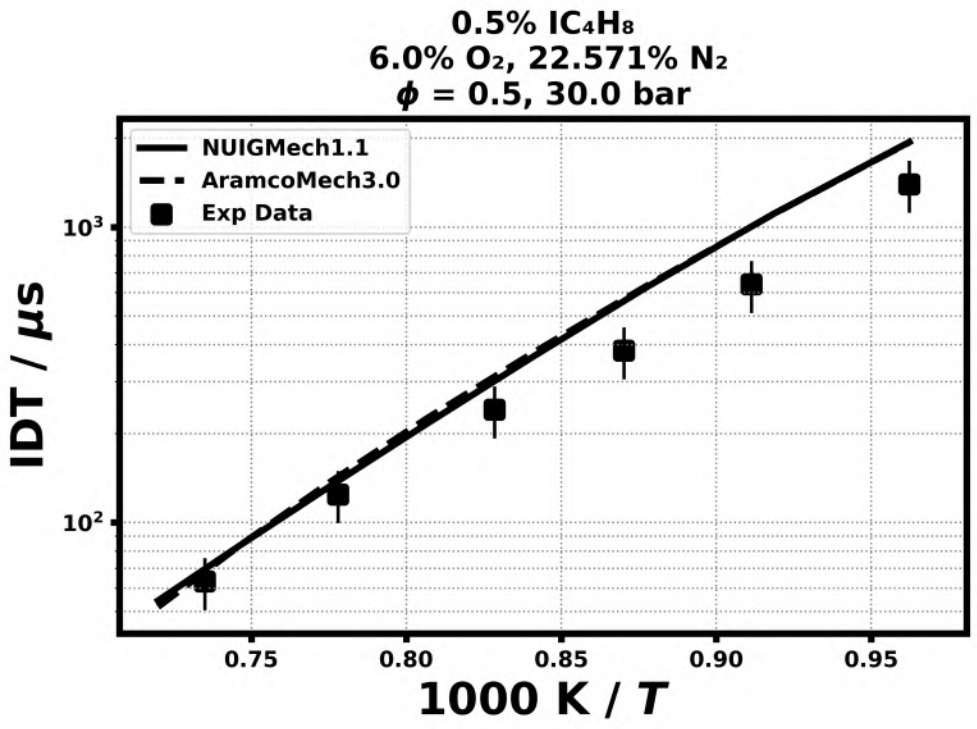
0.5% IC4H8
6.0% O2, 22.571% N2
ϕ = 0.5, 30.0 bar
NUIGMech1.1
AramcoMech3.0
Exp Data
IDT / μs
10^3
10^2
0.75
0.80
0.85
0.90
0.95
1000 K / T

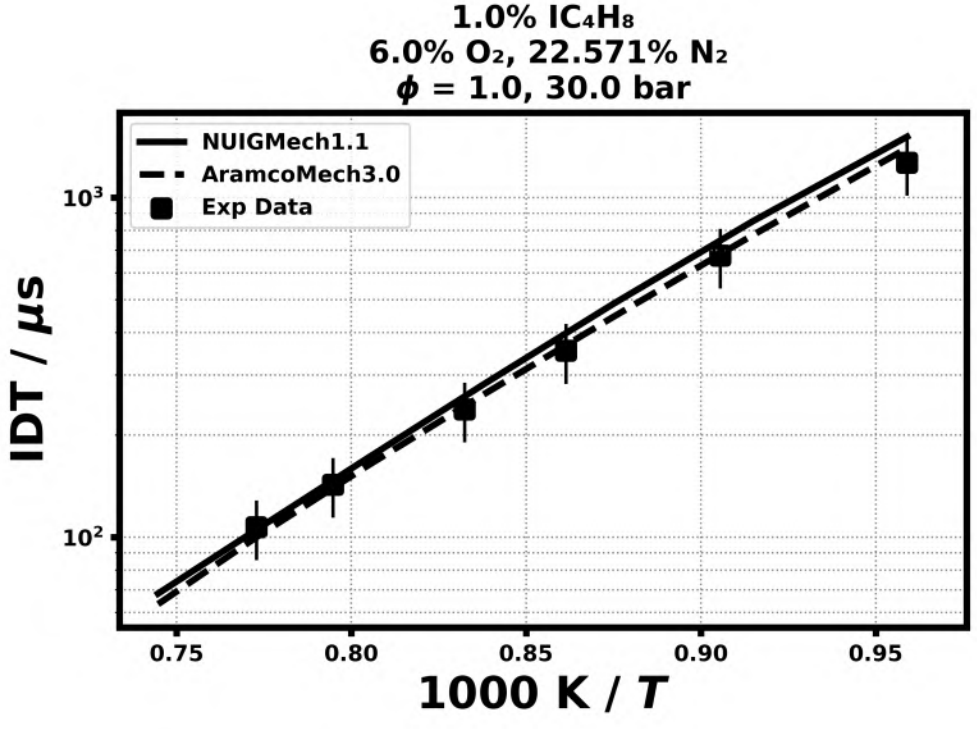
1.0% IC4H8
6.0% O2, 22.571% N2
ϕ = 1.0, 30.0 bar
NUIGMech1.1
AramcoMech3.0
Exp Data
IDT / μs
10^3
10^2
0.75
0.80
0.85
0.90
0.95
1000 K / T

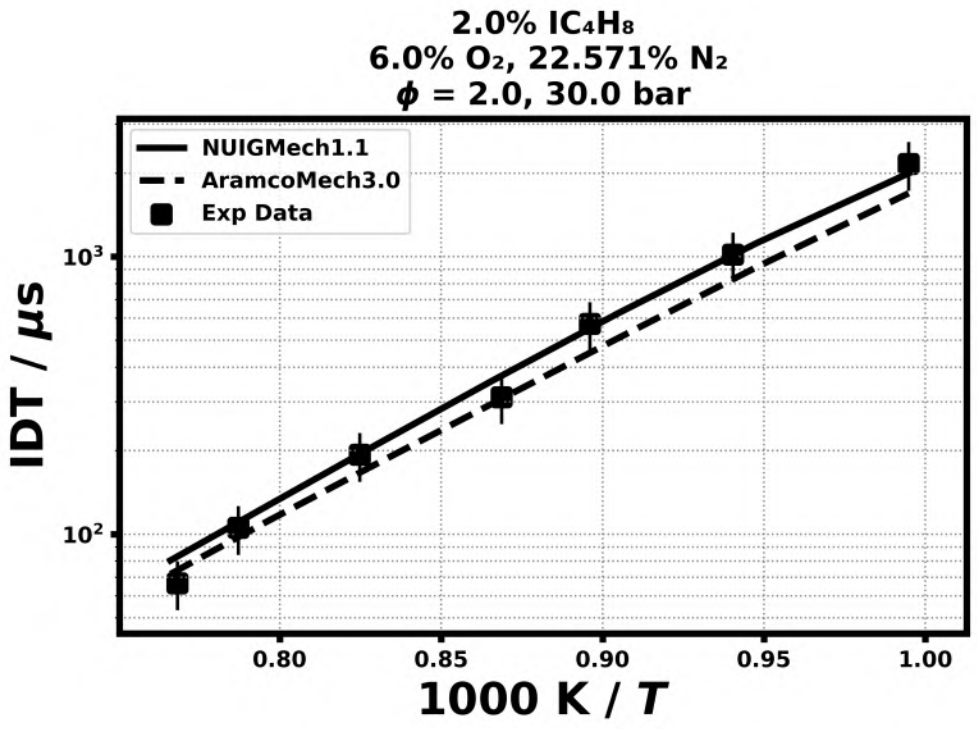
2.0% IC4H8
6.0% O2, 22.571% N2
ϕ = 2.0, 30.0 bar
NUIGMech1.1
AramcoMech3.0
Exp Data
IDT / μs
10^3
10^2
0.80
0.85
0.90
0.95
1.00
1000 K / T

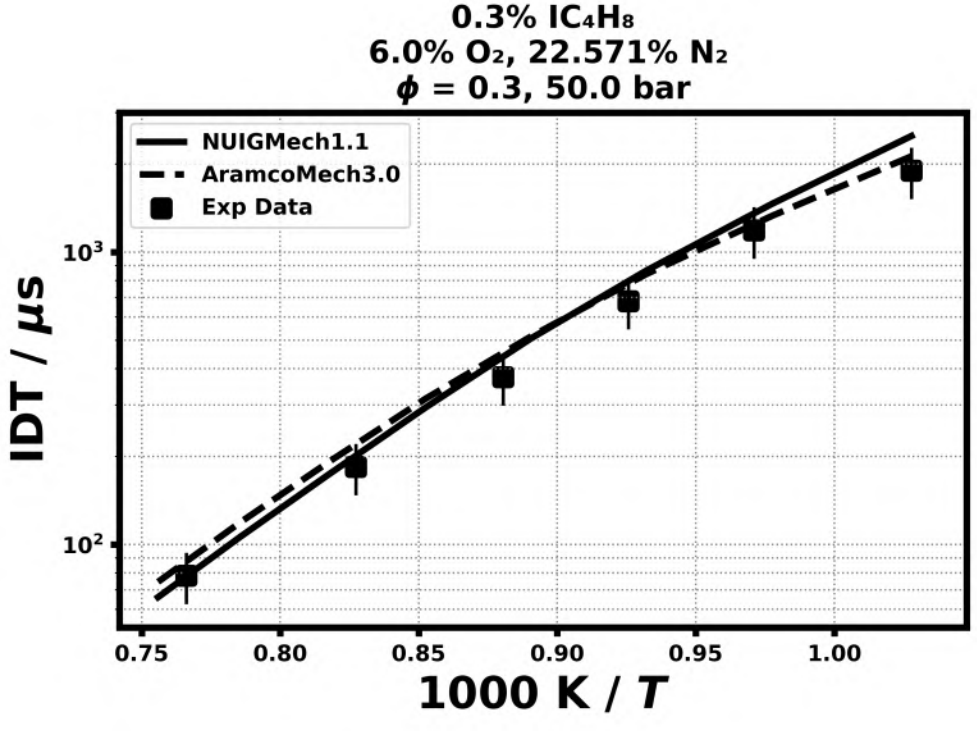
0.3% IC4H8
6.0% O2, 22.571% N2
ϕ = 0.3, 50.0 bar
NUIGMech1.1
AramcoMech3.0
Exp Data
IDT / μs
10^3
10^2
0.75
0.80
0.85
0.90
0.95
1.00
1000 K / T

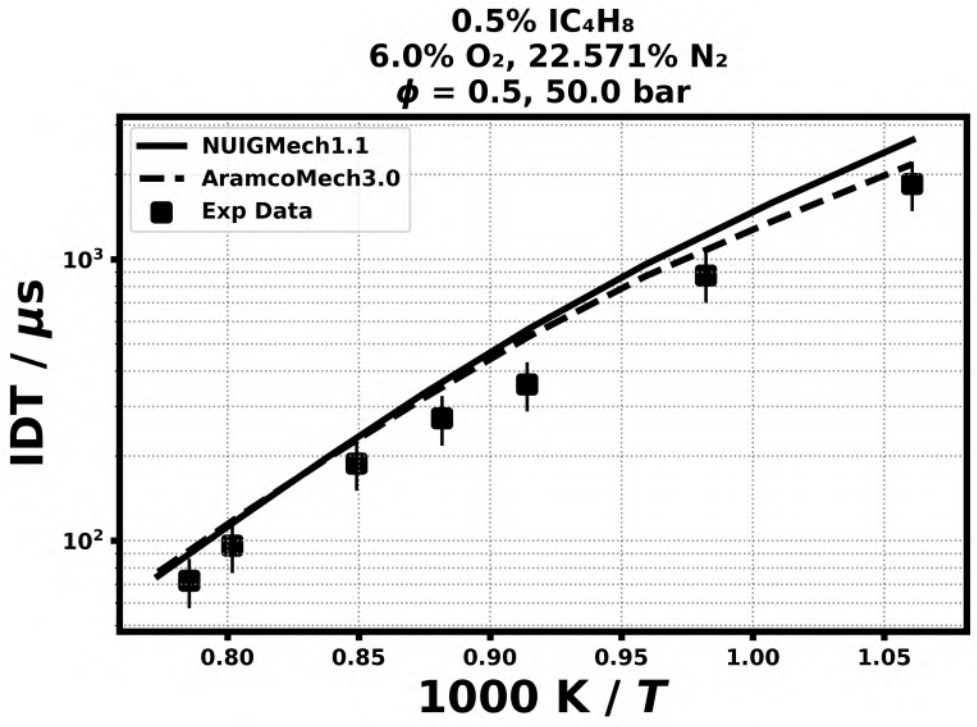
0.5% IC4H8
6.0% O2, 22.571% N2
ϕ = 0.5, 50.0 bar
NUIGMech1.1
AramcoMech3.0
Exp Data
IDT / μs
10³
10²
0.80
0.85
0.90
0.95
1.00
1.05
1000 K / T

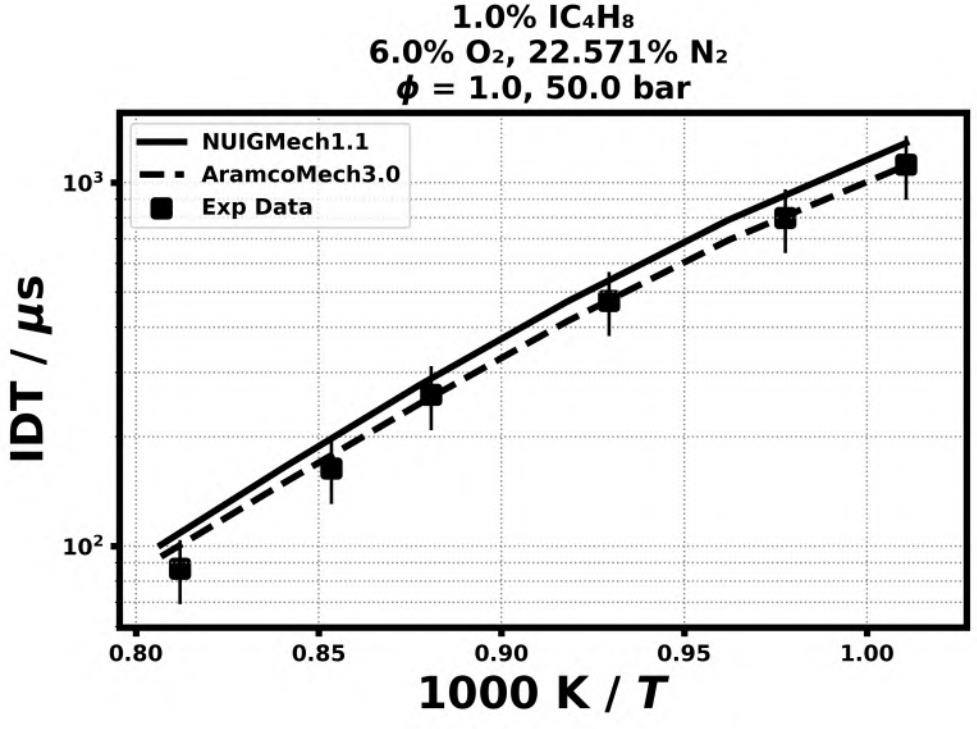
1.0% IC4H8
6.0% O2, 22.571% N2
ϕ = 1.0, 50.0 bar
NUIGMech1.1
AramcoMech3.0
Exp Data
IDT / μs
10³
10²
0.80
0.85
0.90
0.95
1.00
1000 K / T

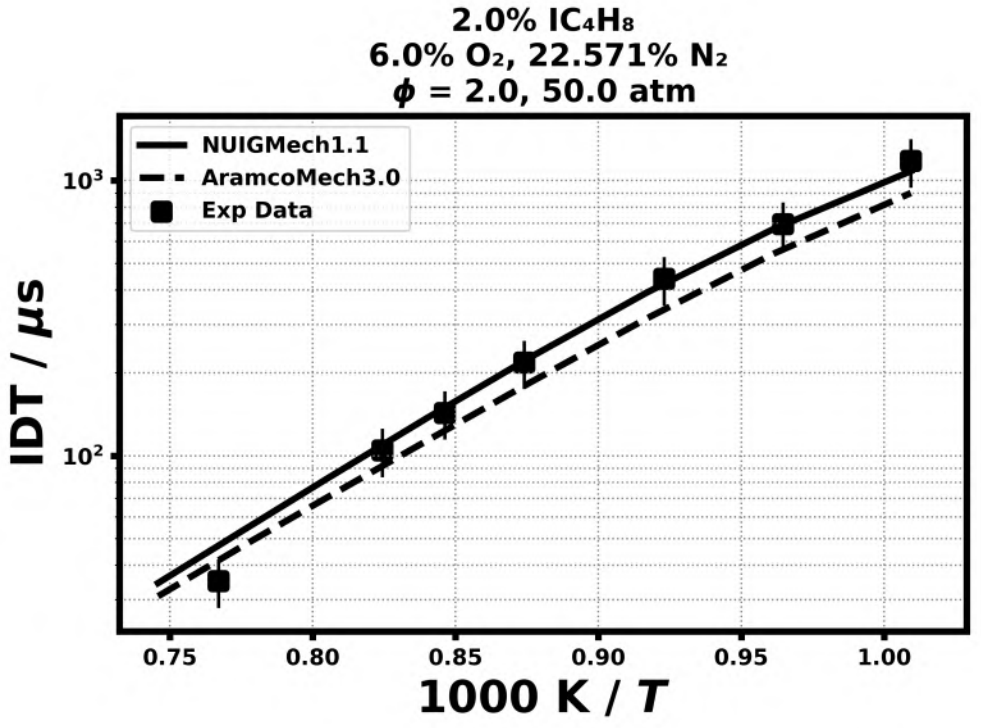

RCM Ignition delay time

21.2) Li, Y., Zhou, C. W., Somers, K. P., Zhang, K., & Curran, H. J., Proceedings of the Combustion Institute, 36(1) (2017) 403-411.

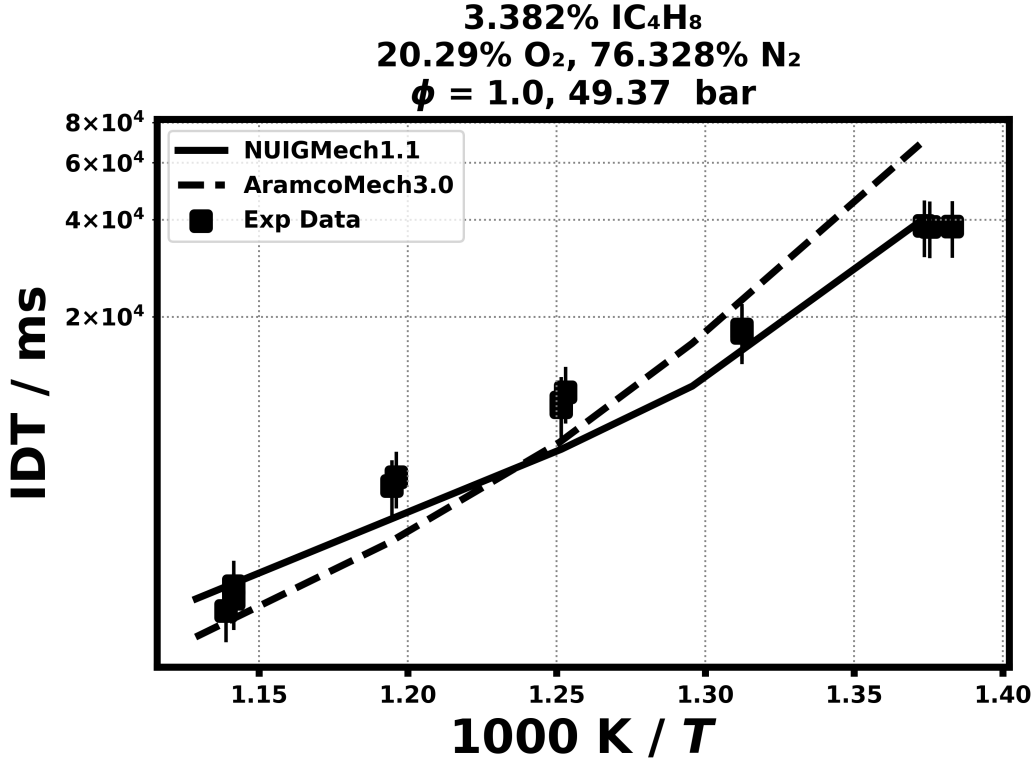

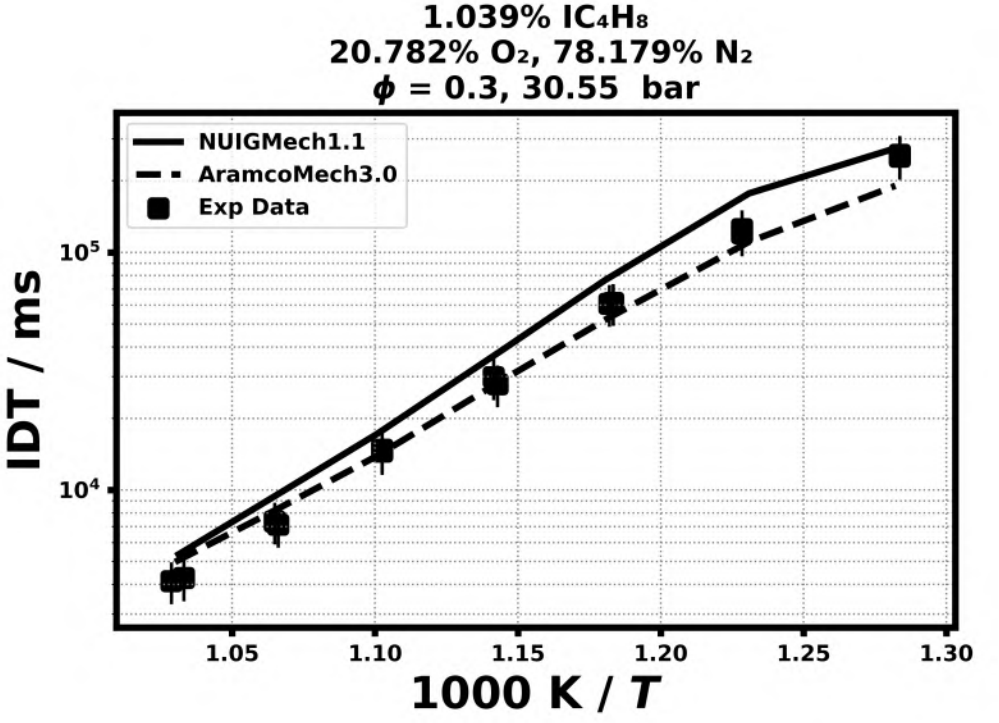
1.039% IC4H8
20.782% O2, 78.179% N2
ϕ = 0.3, 30.55 bar
NUIGMech1.1
AramcoMech3.0
Exp Data
IDT / ms
10^5
10^4
1.05
1.10
1.15
1.20
1.25
1.30
1000 K / T

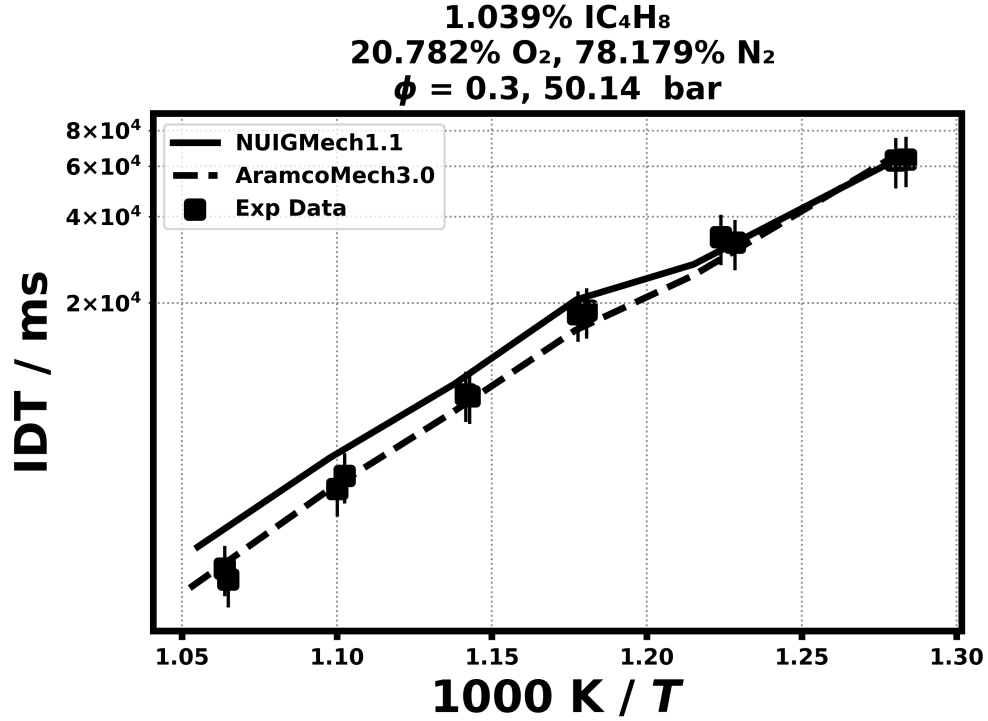
1.039% IC4H8
20.782% O2, 78.179% N2
ϕ = 0.3, 50.14 bar
NUIGMech1.1
AramcoMech3.0
Exp Data
IDT / ms
8×10^4
6×10^4
4×10^4
2×10^4
1.05
1.10
1.15
1.20
1.25
1.30
1000 K / T

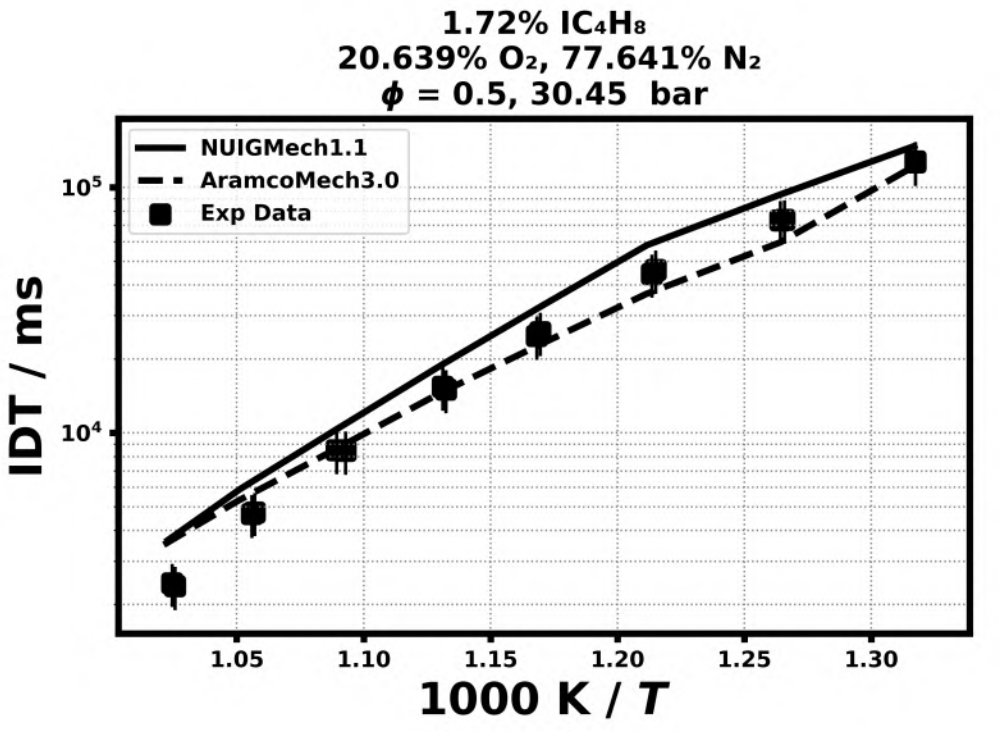
1.72% IC4H8
20.639% O2, 77.641% N2
ϕ = 0.5, 30.45 bar
NUIGMech1.1
AramcoMech3.0
Exp Data
10^5
10^4
IDT / ms
1.05
1.10
1.15
1.20
1.25
1.30
1000 K / T

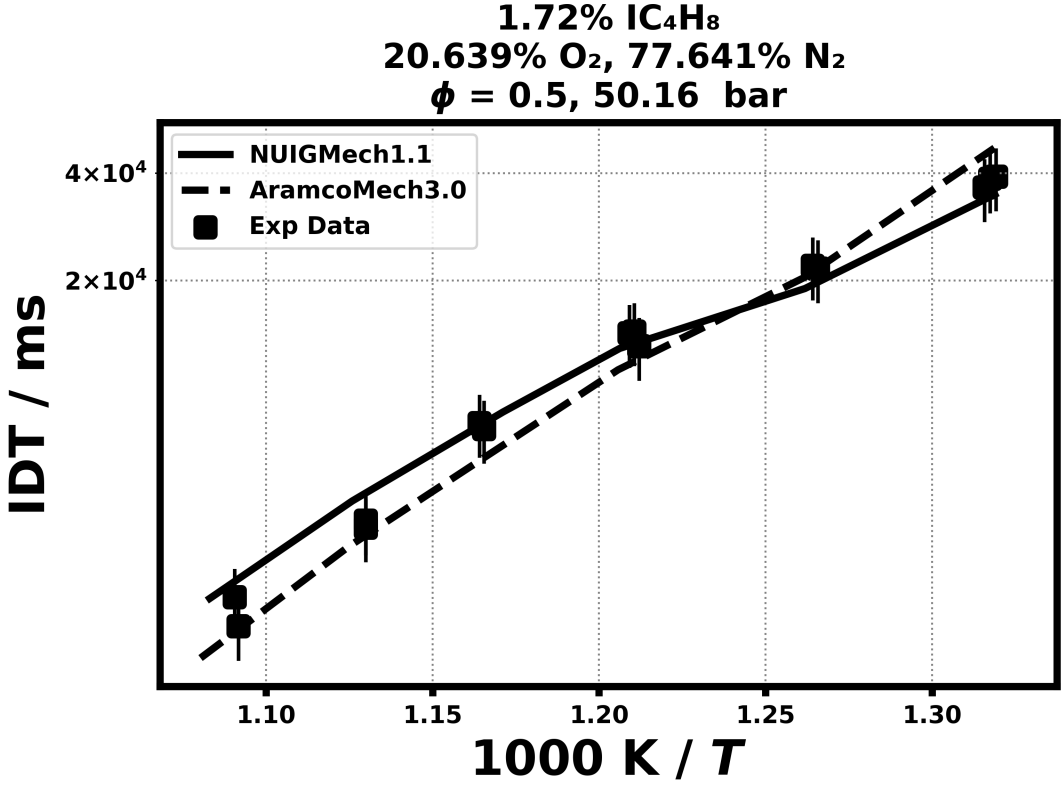
1.72% IC4H8
20.639% O2, 77.641% N2
ϕ = 0.5, 50.16 bar
NUIGMech1.1
AramcoMech3.0
Exp Data
4×10^4
2×10^4
IDT / ms
1.10
1.15
1.20
1.25
1.30
1000 K / T

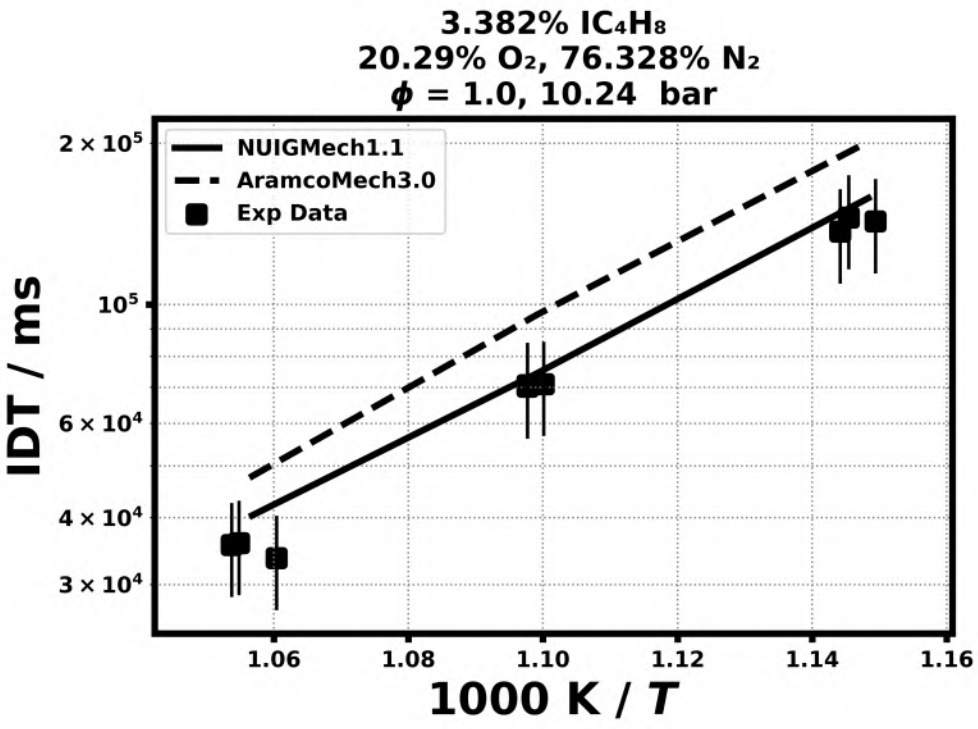
3.382% IC4H8
20.29% O2, 76.328% N2
ϕ = 1.0, 10.24 bar
NUIGMech1.1
AramcoMech3.0
Exp Data
IDT / ms
2 × 10^5
10^5
6 × 10^4
4 × 10^4
3 × 10^4
1.06
1.08
1.10
1.12
1.14
1.16
1000 K / T

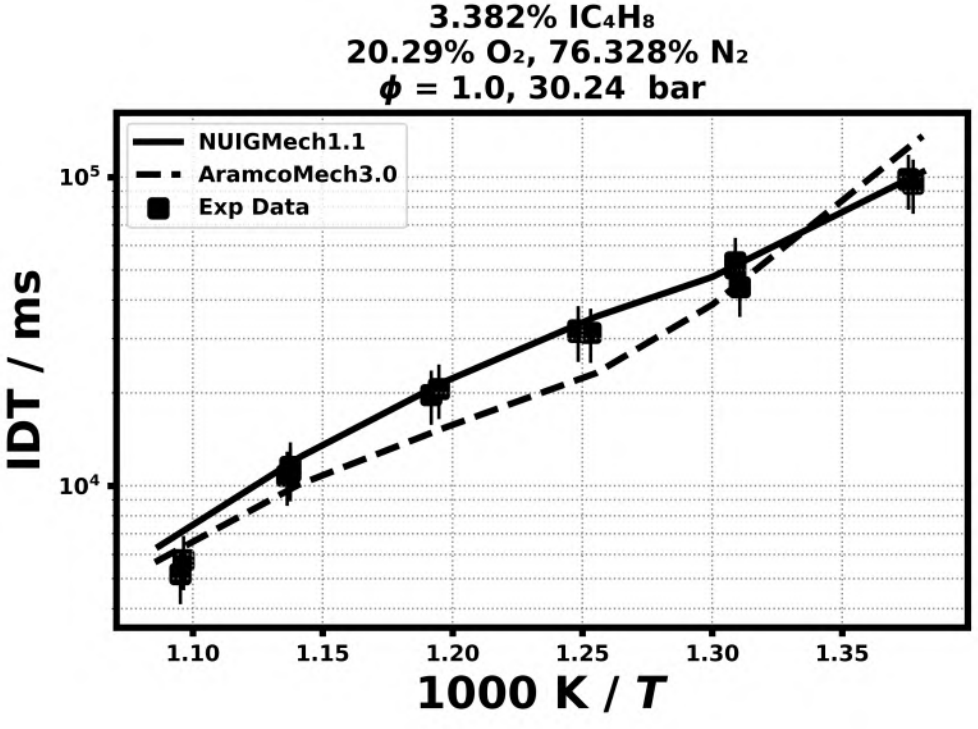
3.382% IC4H8
20.29% O2, 76.328% N2
ϕ = 1.0, 30.24 bar
NUIGMech1.1
AramcoMech3.0
Exp Data
IDT / ms
10^5
10^4
1.10
1.15
1.20
1.25
1.30
1.35
1000 K / T

Laminar flame speed

21.3) Zhou, C. W., Li, Y., O'Connor, E., Somers, K. P., Thion, S., Keesee, C., ... & Kukkadapu, G., Combustion and Flame, 167 (2016) 353-379.

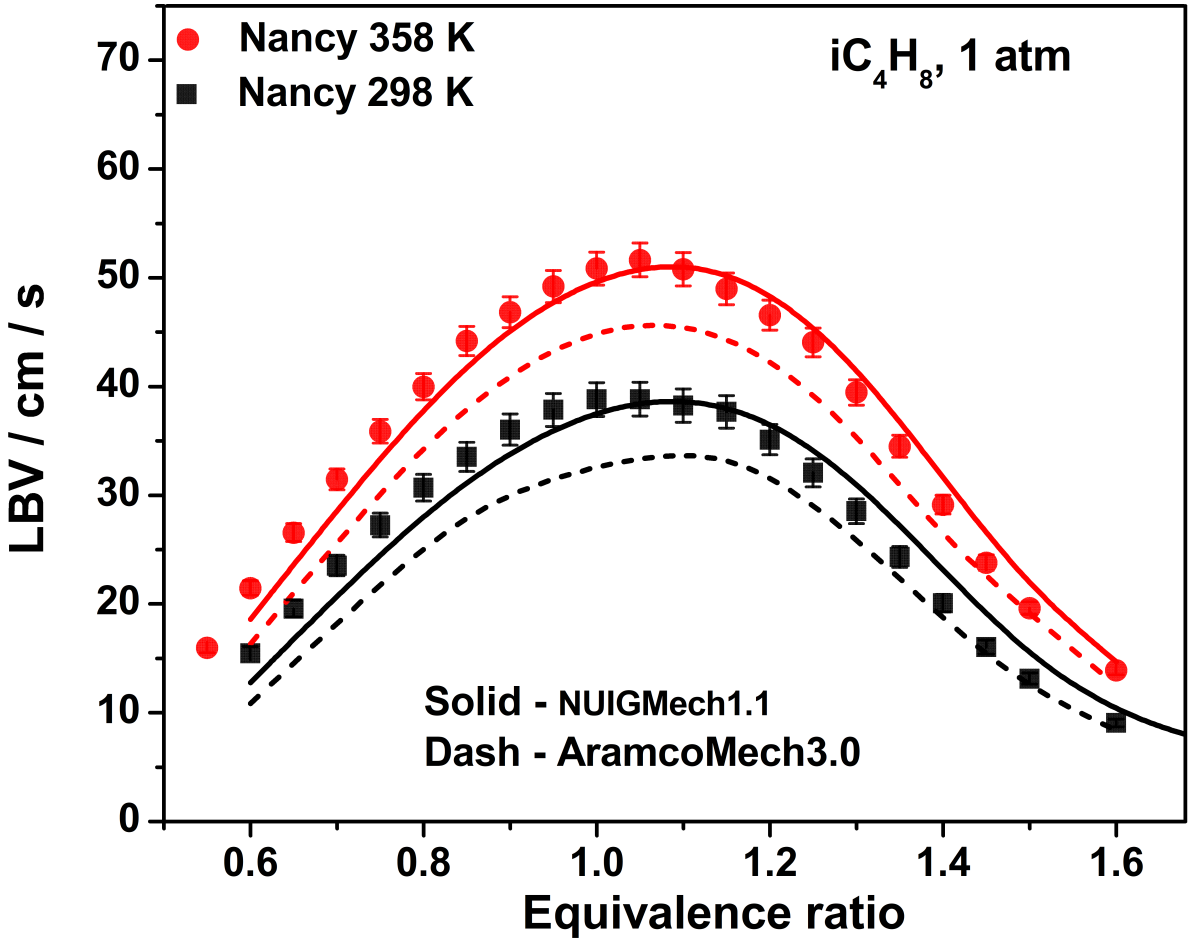

22. Validation for 1,3-C_4H_6

Shock tube ignition delay time

21.1) Zhou, C. W., Li, Y., Burke, U., Banyon, C., Somers, K. P., Ding, S., ... & Petersen, E. L., Combustion and Flame, 197 (2018) 423-438.

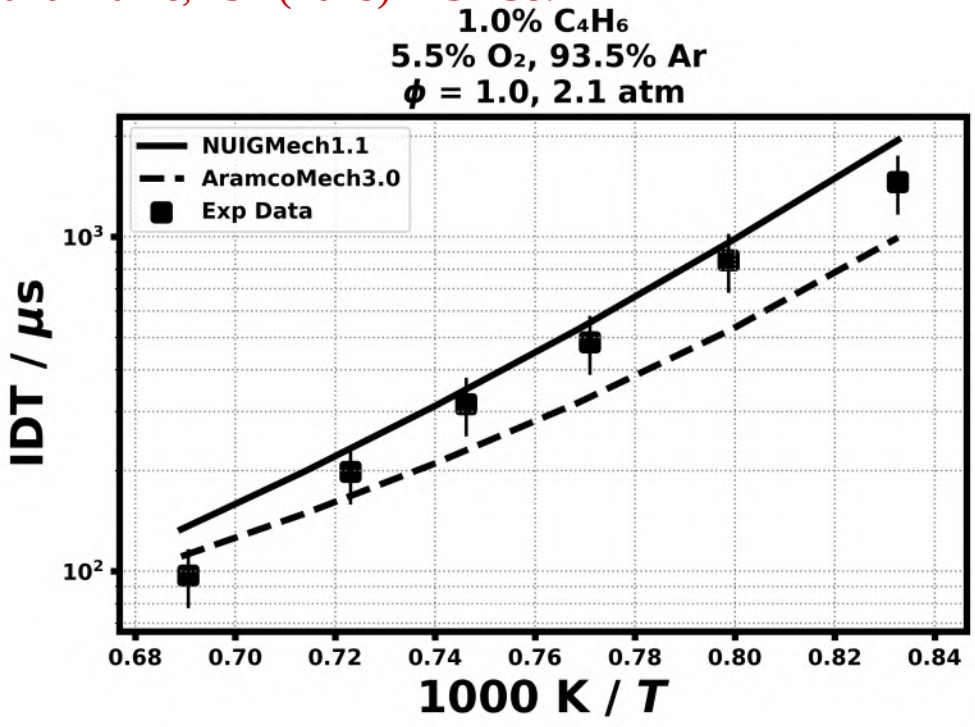

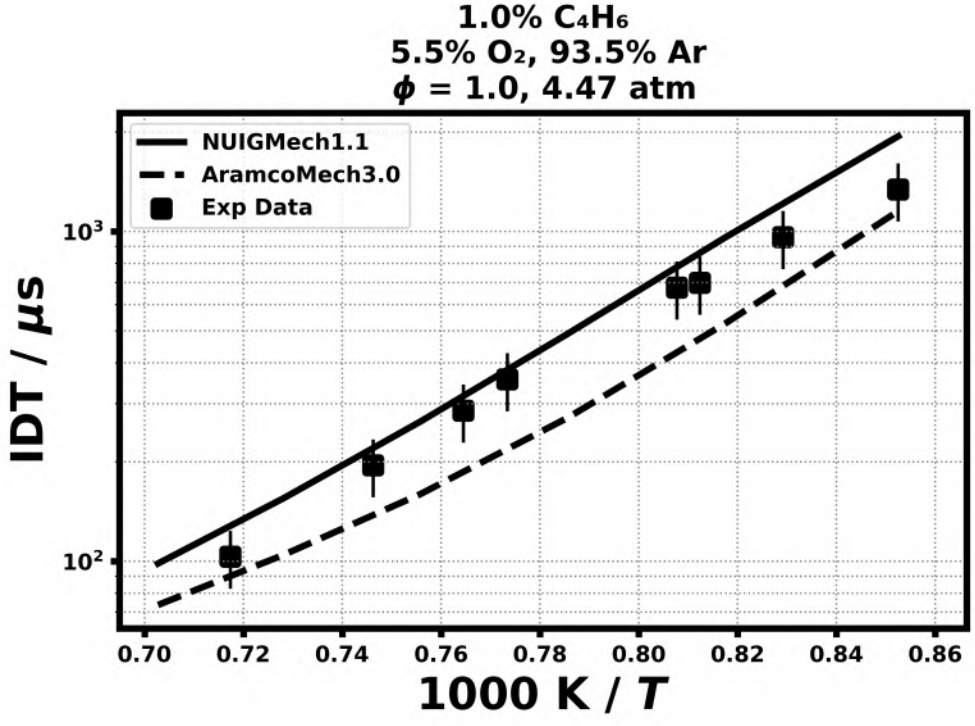

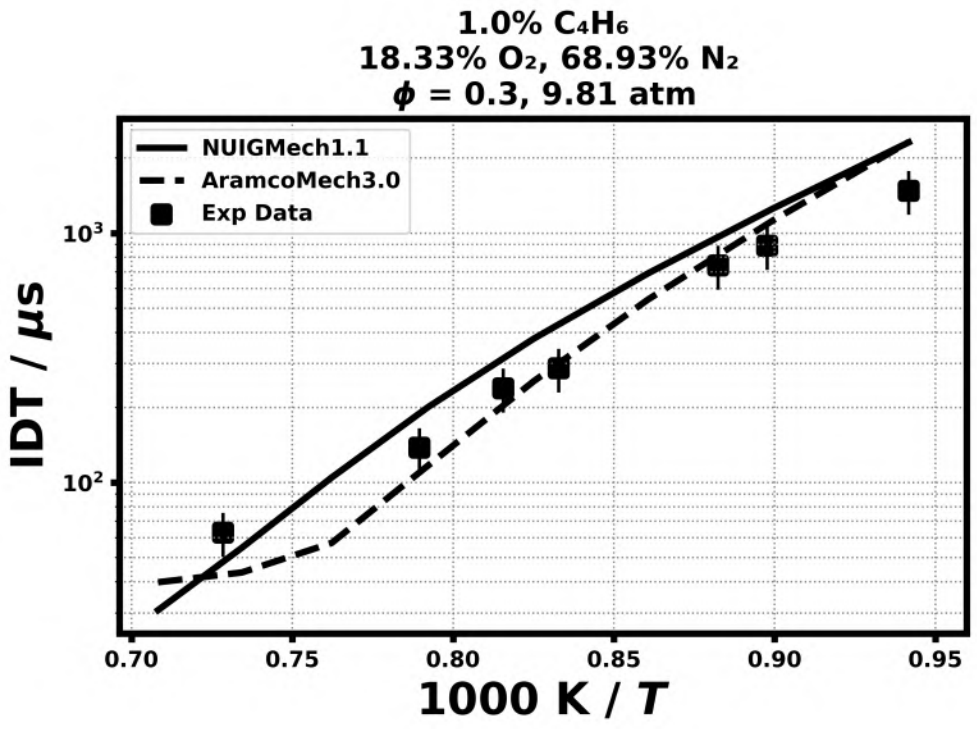
1.0% C4H6
18.33% O2, 68.93% N2
ϕ = 0.3, 9.81 atm
NUIGMech1.1
AramcoMech3.0
Exp Data
IDT / μs
10^3
10^2
0.70
0.75
0.80
0.85
0.90
0.95
1000 K / T

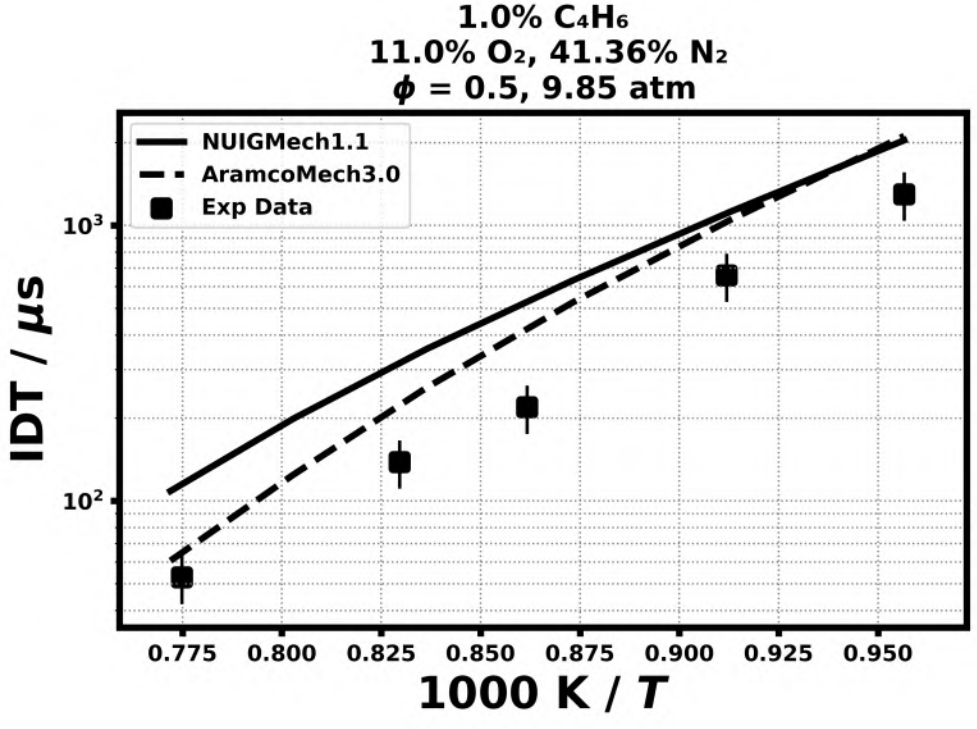
1.0% C4H6
11.0% O2, 41.36% N2
ϕ = 0.5, 9.85 atm
NUIGMech1.1
AramcoMech3.0
Exp Data
IDT / μs
10^3
10^2
0.775
0.800
0.825
0.850
0.875
0.900
0.925
0.950
1000 K / T

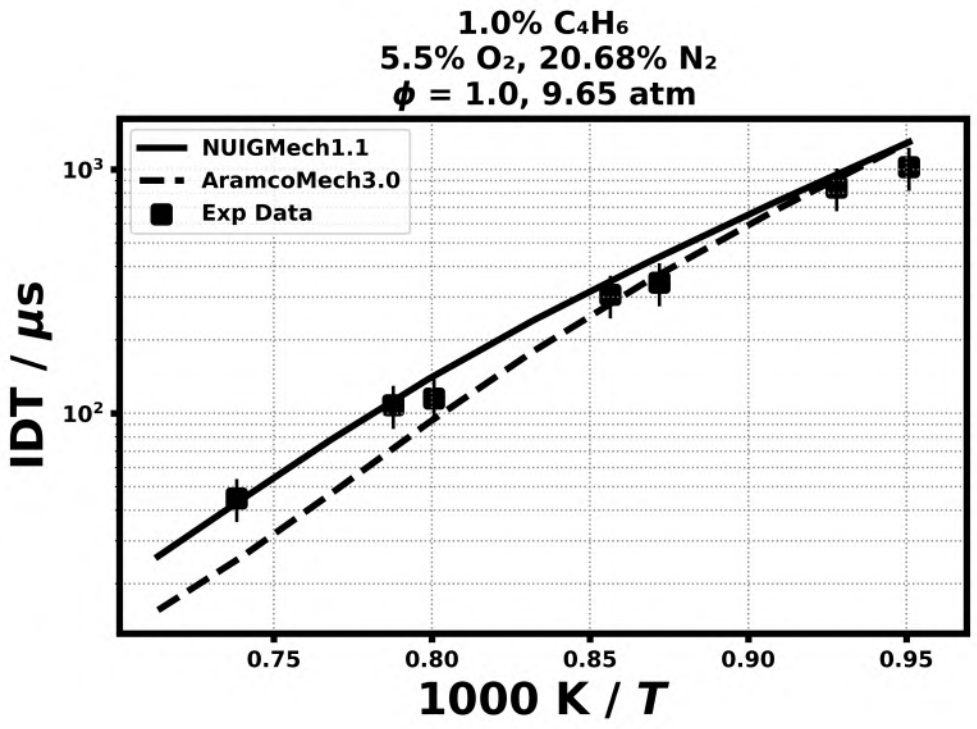
1.0% C4H6
5.5% O2, 20.68% N2
ϕ = 1.0, 9.65 atm
NUIGMech1.1
AramcoMech3.0
Exp Data
IDT / μs
10^3
10^2
0.75
0.80
0.85
0.90
0.95
1000 K / T

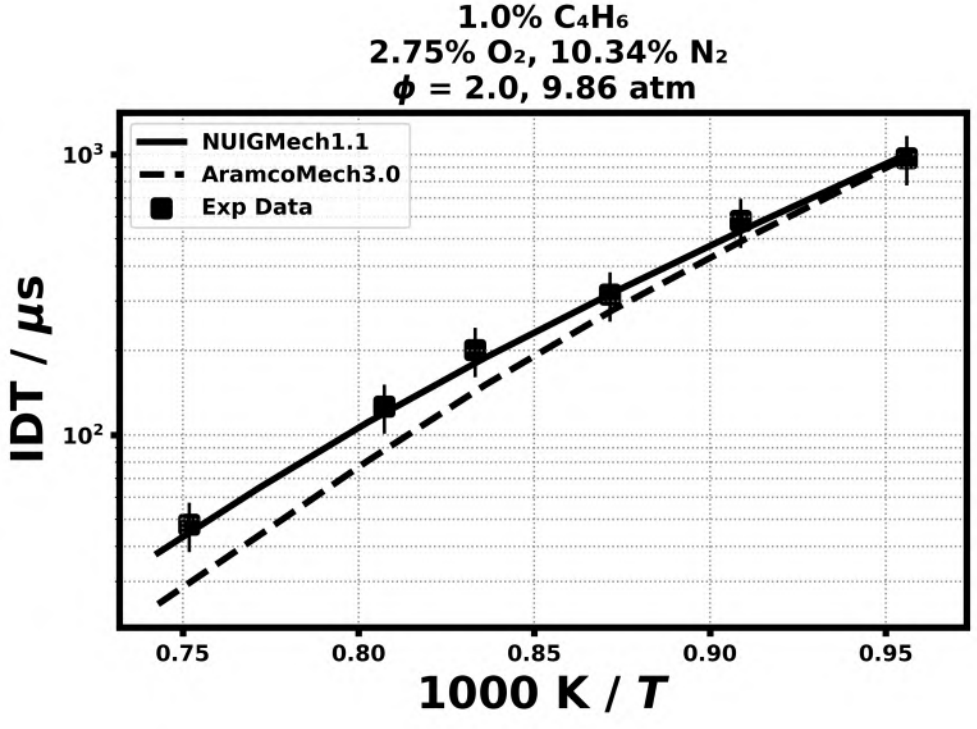
1.0% C4H6
2.75% O2, 10.34% N2
ϕ = 2.0, 9.86 atm
NUIGMech1.1
AramcoMech3.0
Exp Data
IDT / μs
10^3
10^2
0.75
0.80
0.85
0.90
0.95
1000 K / T

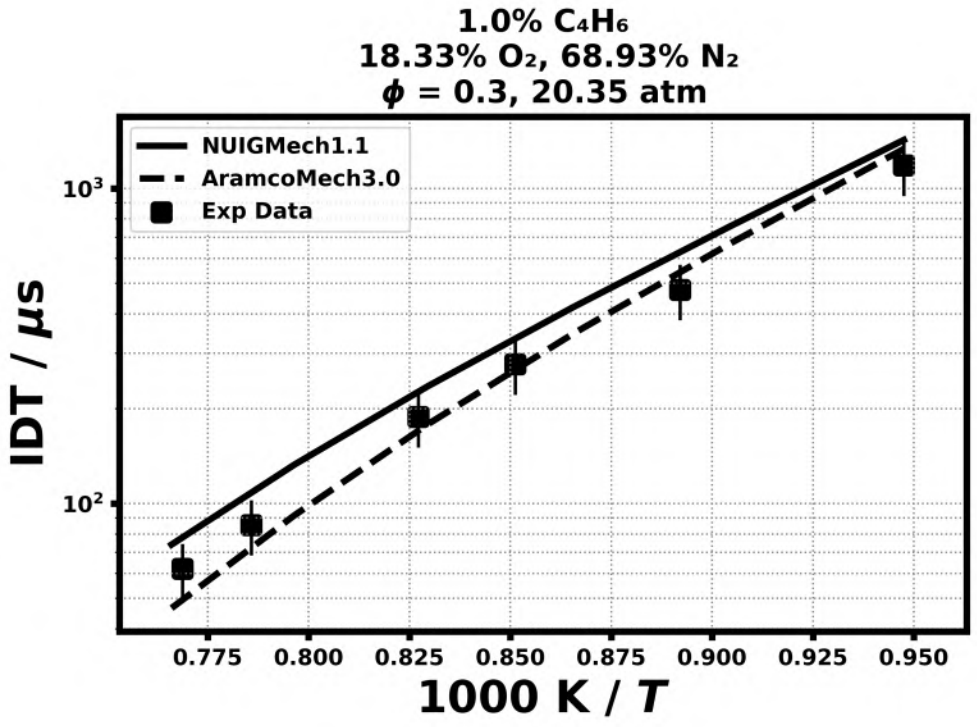
1.0% C4H6
18.33% O2, 68.93% N2
ϕ = 0.3, 20.35 atm
NUIGMech1.1
AramcoMech3.0
Exp Data
IDT / μs
10^3
10^2
0.775
0.800
0.825
0.850
0.875
0.900
0.925
0.950
1000 K / T

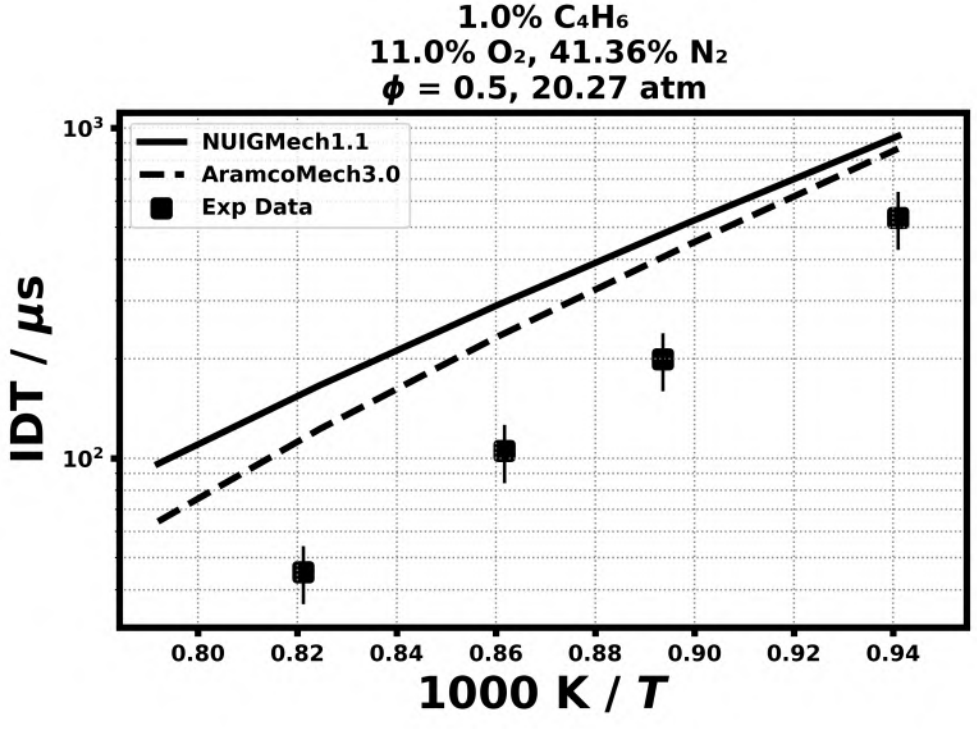
1.0% C4H6
11.0% O2, 41.36% N2
ϕ = 0.5, 20.27 atm
NUIGMech1.1
AramcoMech3.0
Exp Data
IDT / μs
10^3
10^2
0.80
0.82
0.84
0.86
0.88
0.90
0.92
0.94
1000 K / T

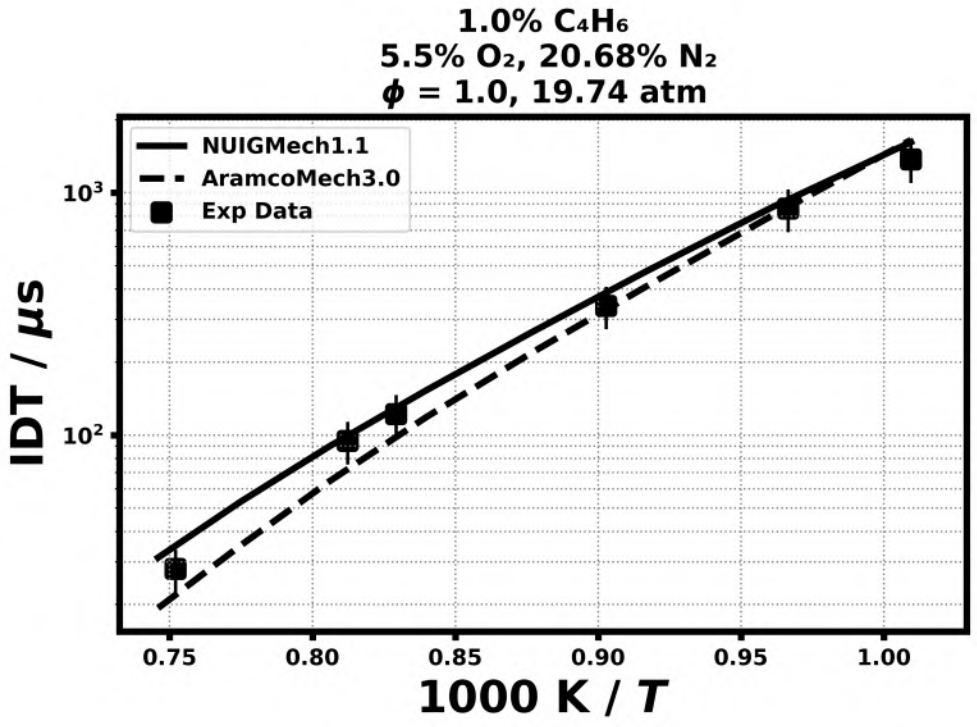
1.0% C4H6
5.5% O2, 20.68% N2
ϕ = 1.0, 19.74 atm
NUIGMech1.1
AramcoMech3.0
Exp Data
IDT / μs
10^3
10^2
0.75
0.80
0.85
0.90
0.95
1.00
1000 K / T

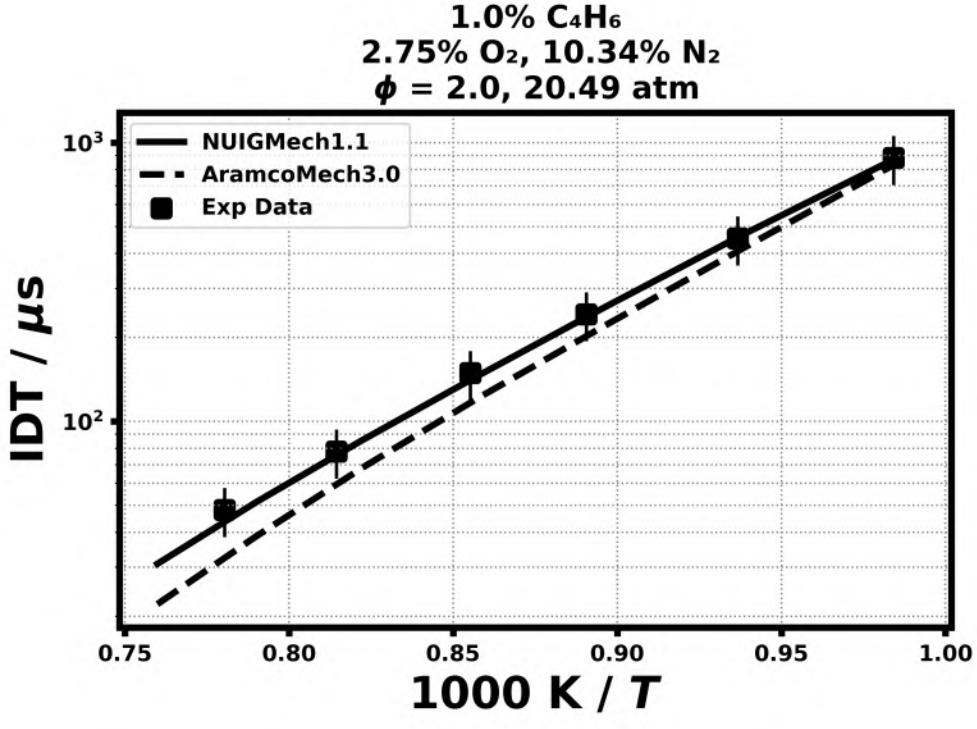
1.0% C4H6
2.75% O2, 10.34% N2
ϕ = 2.0, 20.49 atm
NUIGMech1.1
AramcoMech3.0
Exp Data
IDT / μs
10^3
10^2
0.75
0.80
0.85
0.90
0.95
1.00
1000 K / T

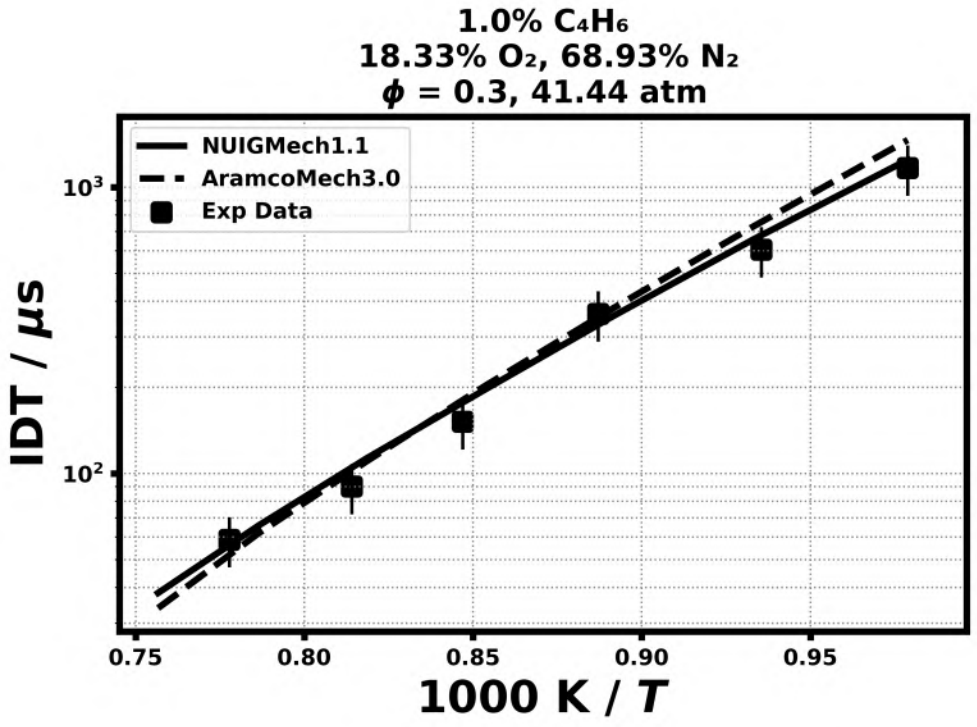
1.0% C4H6
18.33% O2, 68.93% N2
ϕ = 0.3, 41.44 atm
NUIGMech1.1
AramcoMech3.0
Exp Data
IDT / μs
10³
10²
0.75
0.80
0.85
0.90
0.95
1000 K / T

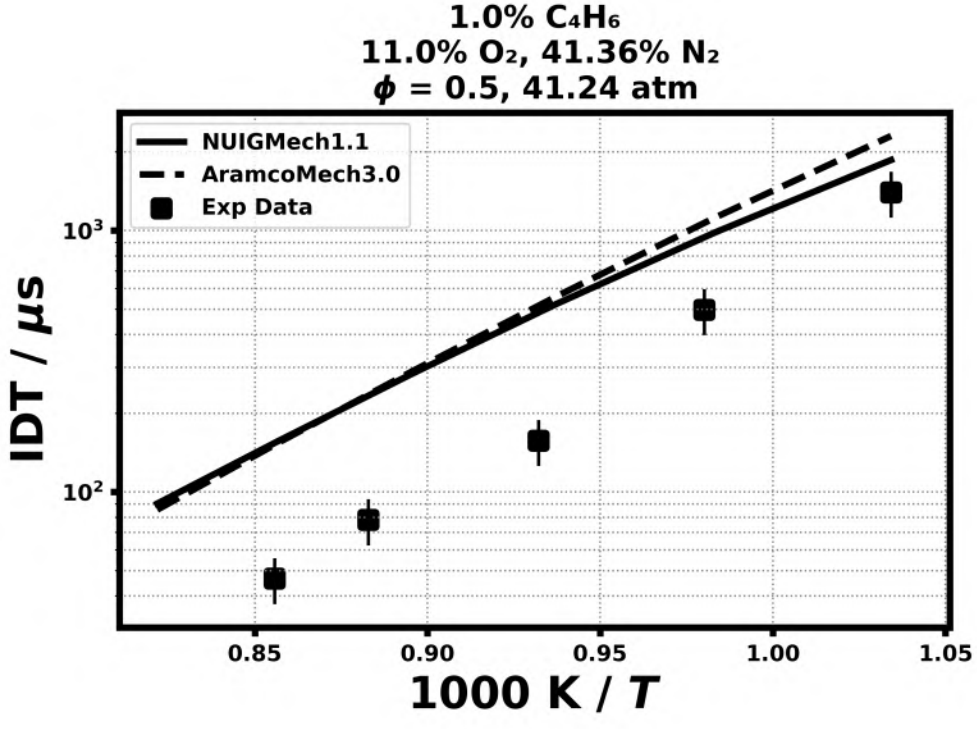
1.0% C4H6
11.0% O2, 41.36% N2
ϕ = 0.5, 41.24 atm
NUIGMech1.1
AramcoMech3.0
Exp Data
IDT / μs
10³
10²
0.85
0.90
0.95
1.00
1.05
1000 K / T

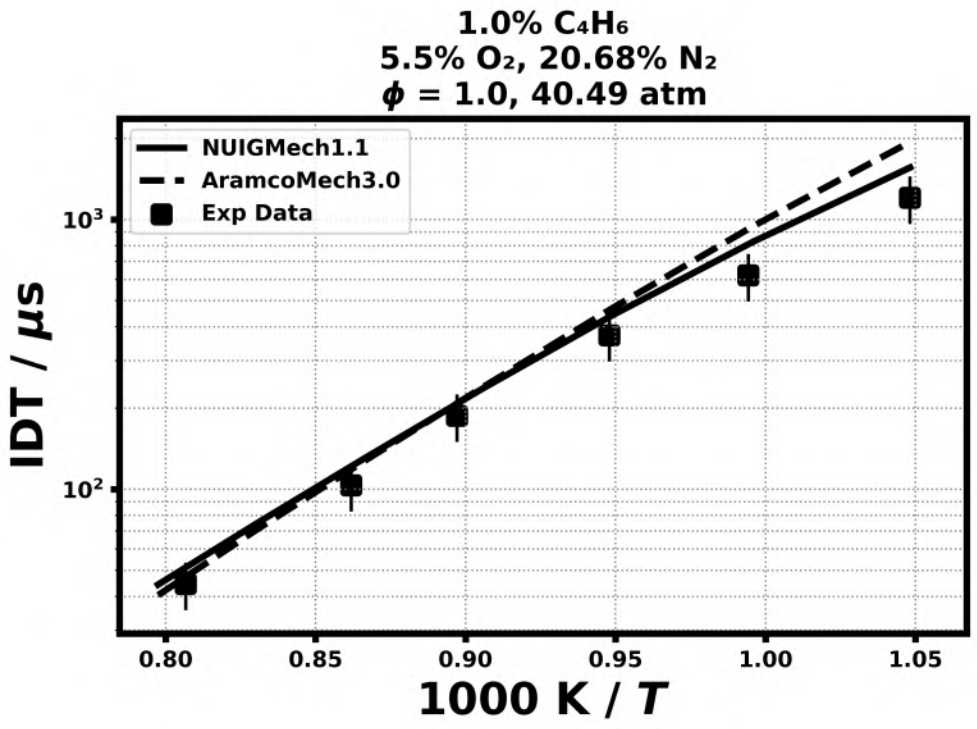
1.0% C4H6
5.5% O2, 20.68% N2
ϕ = 1.0, 40.49 atm
NUIGMech1.1
AramcoMech3.0
Exp Data
IDT / μs
10³
10²
0.80
0.85
0.90
0.95
1.00
1.05
1000 K / T

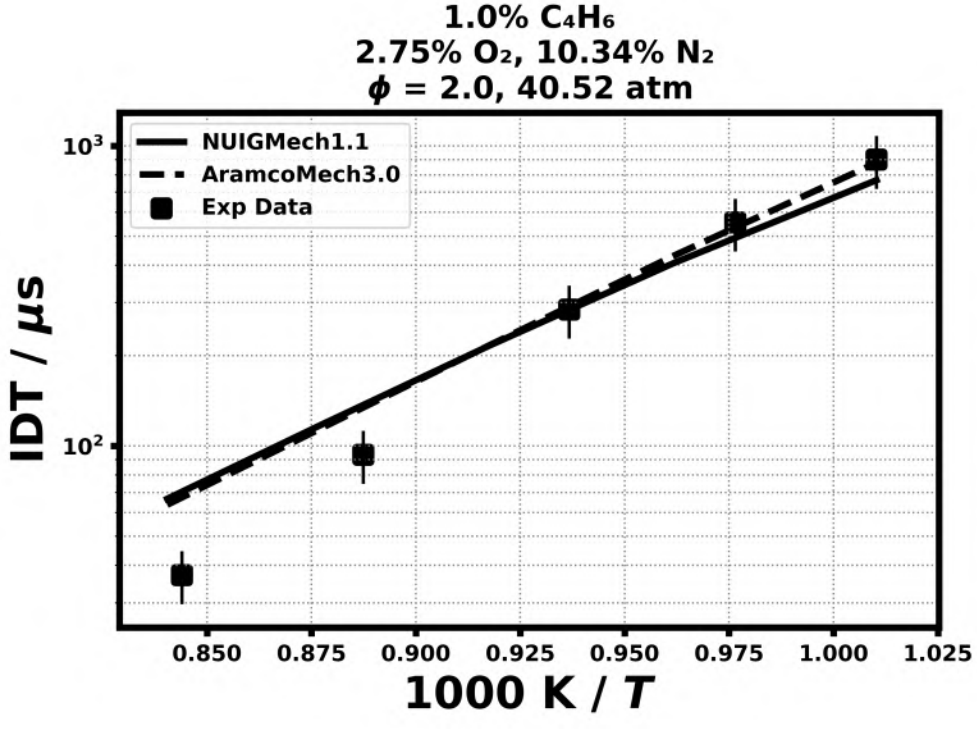
1.0% C4H6
2.75% O2, 10.34% N2
ϕ = 2.0, 40.52 atm
NUIGMech1.1
AramcoMech3.0
Exp Data
IDT / μs
10³
10²
0.850
0.875
0.900
0.925
0.950
0.975
1.000
1.025
1000 K / T

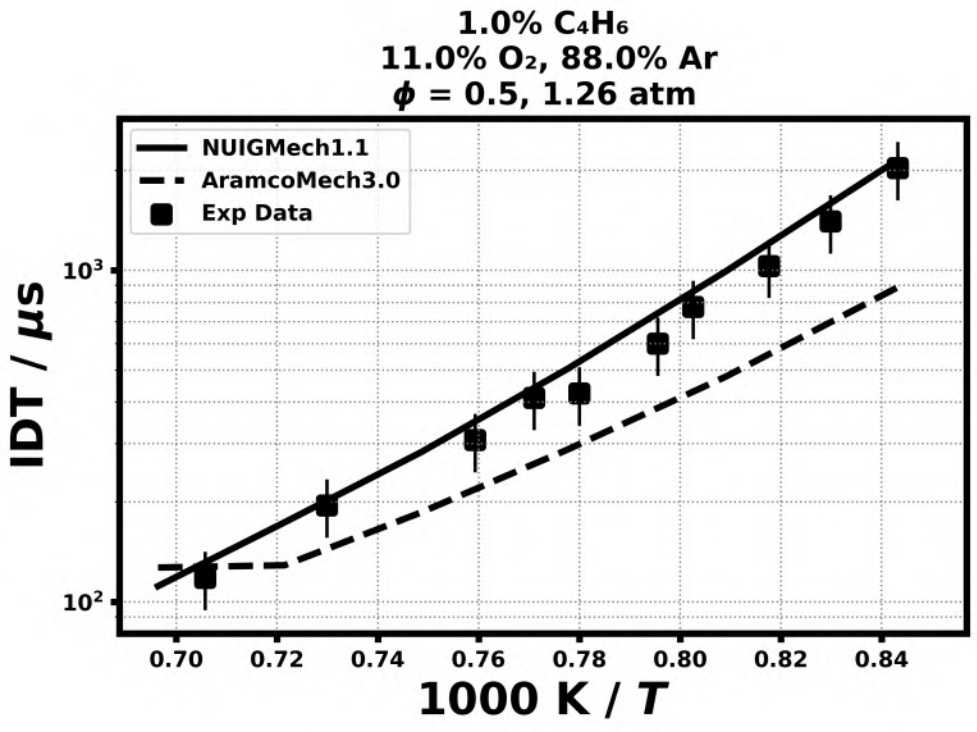
1.0% C4H6
11.0% O2, 88.0% Ar
ϕ = 0.5, 1.26 atm
NUIGMech1.1
AramcoMech3.0
Exp Data
IDT / μs
10^3
10^2
0.70
0.72
0.74
0.76
0.78
0.80
0.82
0.84
1000 K / T

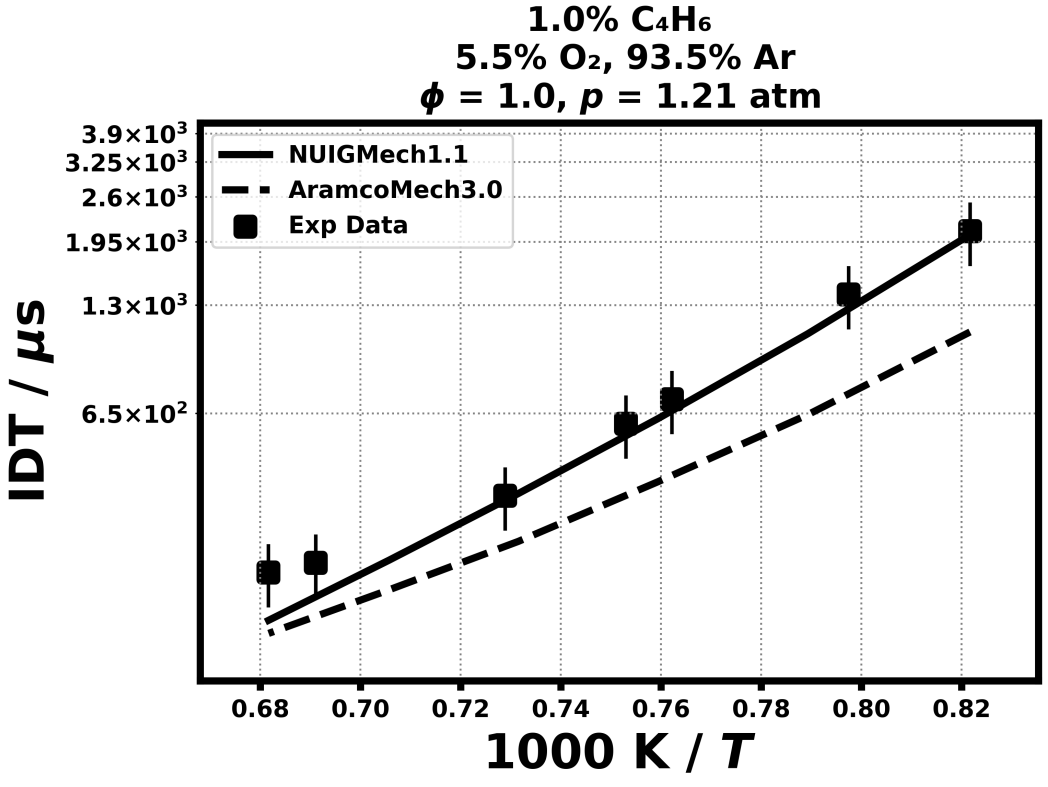
1.0% C4H6
5.5% O2, 93.5% Ar
ϕ = 1.0, p = 1.21 atm
NUIGMech1.1
AramcoMech3.0
Exp Data
IDT / μs
3.9×10^3
3.25×10^3
2.6×10^3
1.95×10^3
1.3×10^3
6.5×10^2
0.68
0.70
0.72
0.74
0.76
0.78
0.80
0.82
1000 K / T

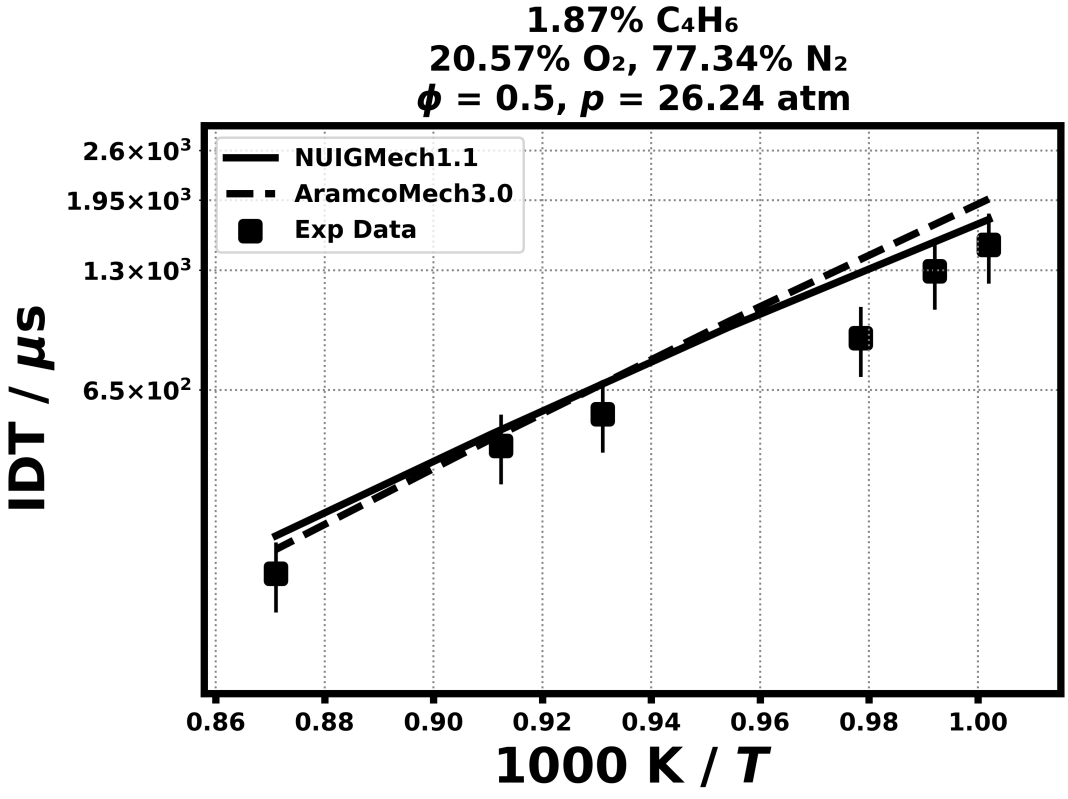
1.87% C4H6
20.57% O2, 77.34% N2
ϕ = 0.5, p = 26.24 atm
NUIGMech1.1
AramcoMech3.0
Exp Data
2.6×10³
1.95×10³
1.3×10³
6.5×10²
IDT / μs
0.86
0.88
0.90
0.92
0.94
0.96
0.98
1.00
1000 K / T

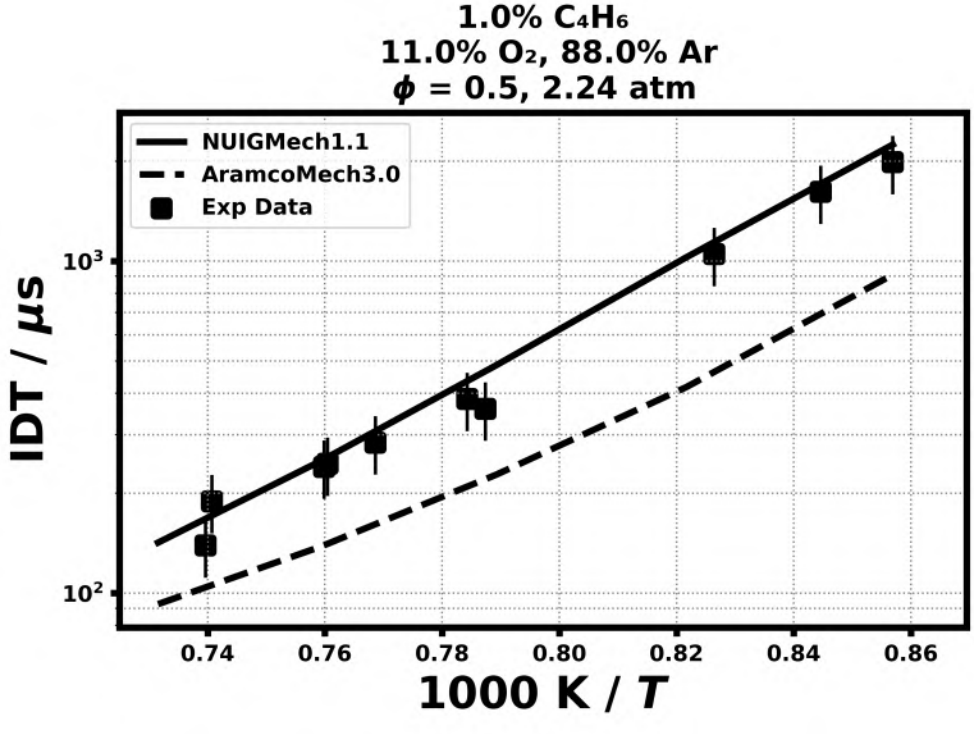
1.0% C4H6
11.0% O2, 88.0% Ar
ϕ = 0.5, 2.24 atm
NUIGMech1.1
AramcoMech3.0
Exp Data
10³
10²
IDT / μs
0.74
0.76
0.78
0.80
0.82
0.84
0.86
1000 K / T

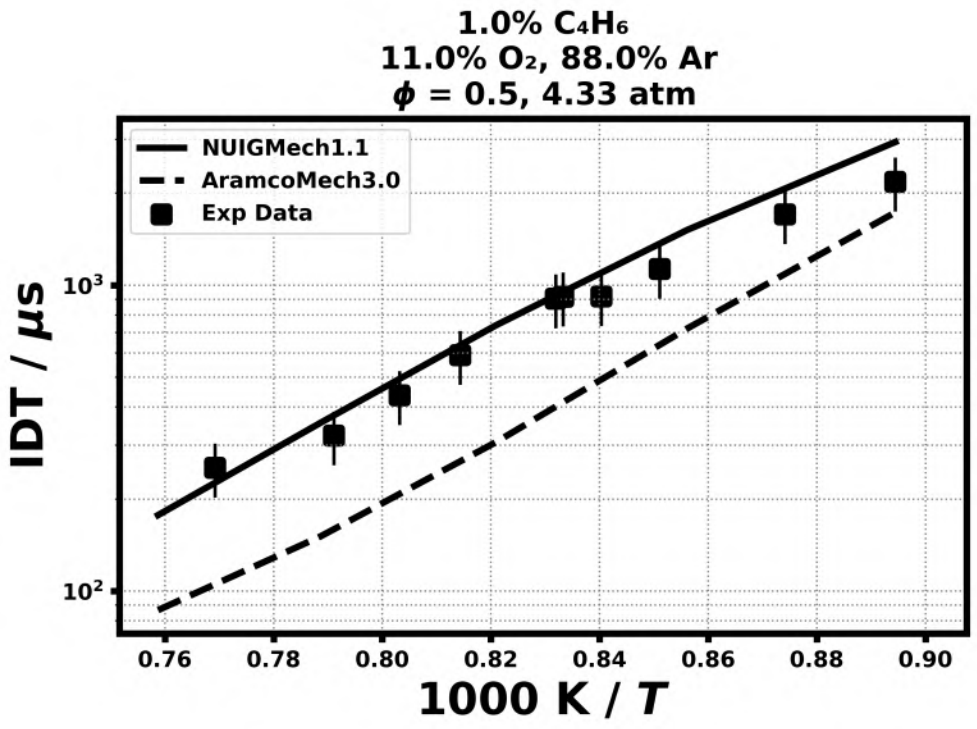
1.0% C4H6
11.0% O2, 88.0% Ar
ϕ = 0.5, 4.33 atm
NUIGMech1.1
AramcoMech3.0
Exp Data
IDT / μs
10^3
10^2
0.76
0.78
0.80
0.82
0.84
0.86
0.88
0.90
1000 K / T

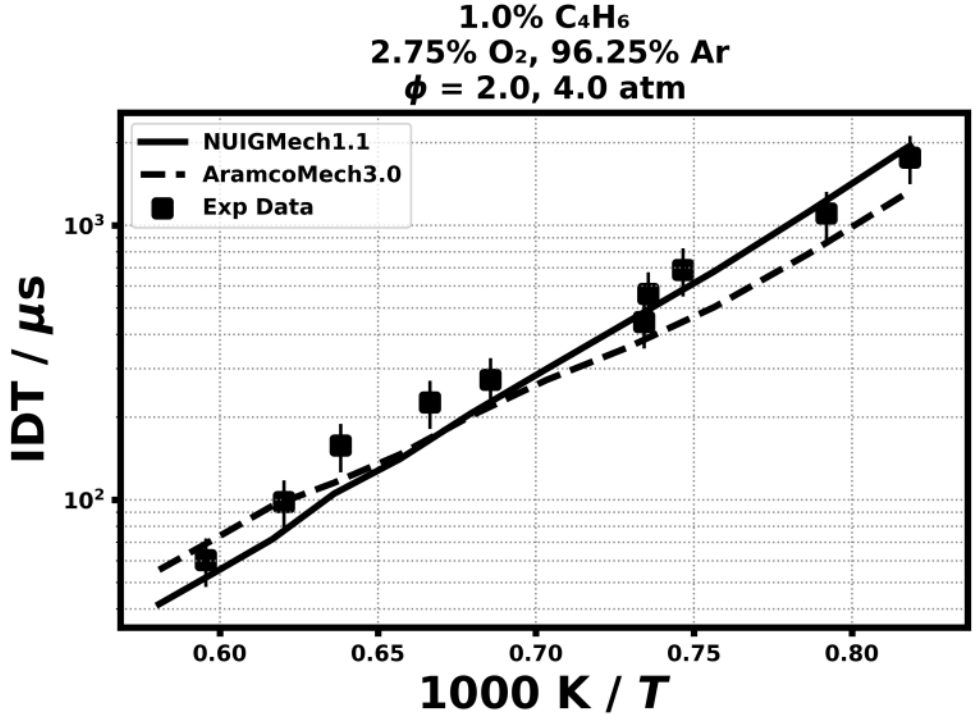
1.0% C4H6
2.75% O2, 96.25% Ar
ϕ = 2.0, 4.0 atm
NUIGMech1.1
AramcoMech3.0
Exp Data
IDT / μs
10^3
10^2
0.60
0.65
0.70
0.75
0.80
1000 K / T

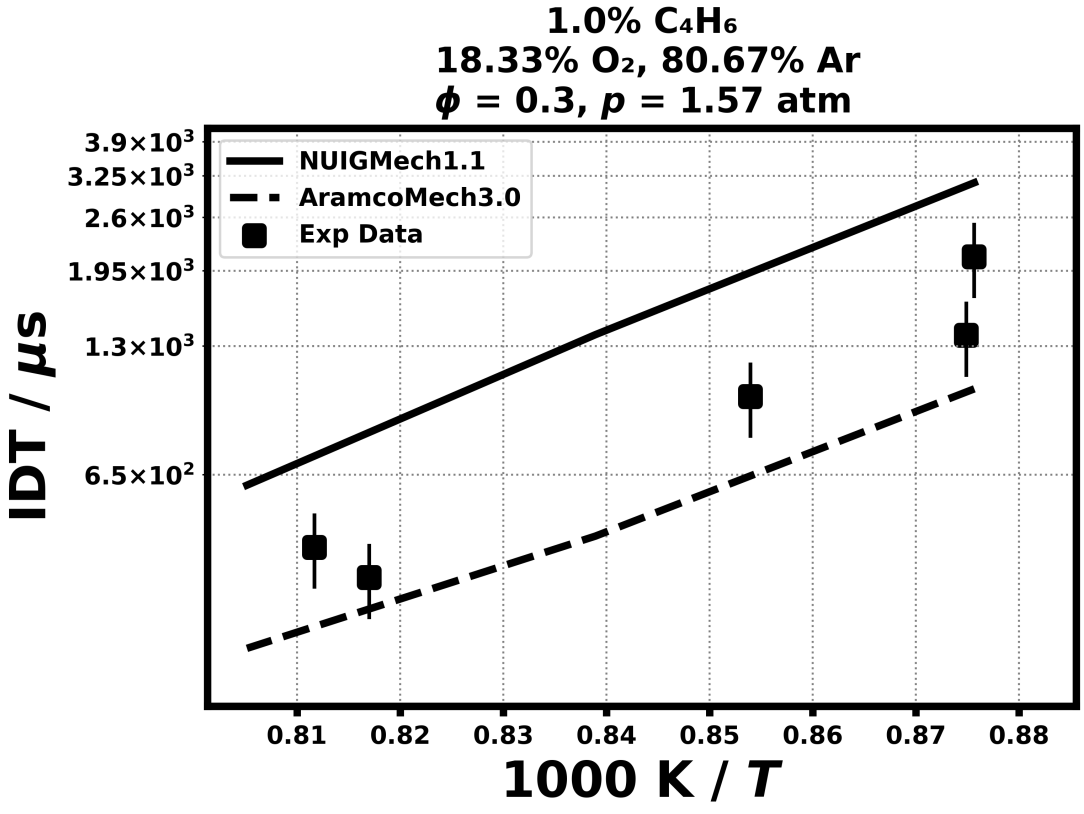
1.0% C4H6
18.33% O2, 80.67% Ar
ϕ = 0.3, p = 1.57 atm
NUIGMech1.1
AramcoMech3.0
Exp Data
IDT / μs
3.9×10³
3.25×10³
2.6×10³
1.95×10³
1.3×10³
6.5×10²
0.81
0.82
0.83
0.84
0.85
0.86
0.87
0.88
1000 K / T

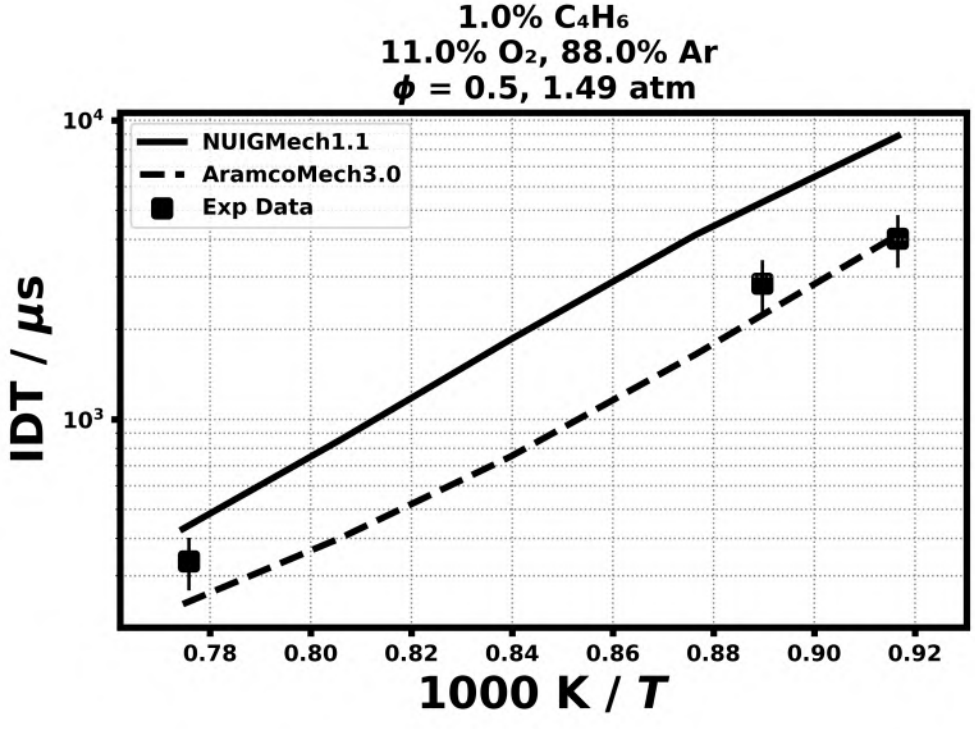
1.0% C4H6
11.0% O2, 88.0% Ar
ϕ = 0.5, 1.49 atm
NUIGMech1.1
AramcoMech3.0
Exp Data
IDT / μs
10⁴
10³
0.78
0.80
0.82
0.84
0.86
0.88
0.90
0.92
1000 K / T

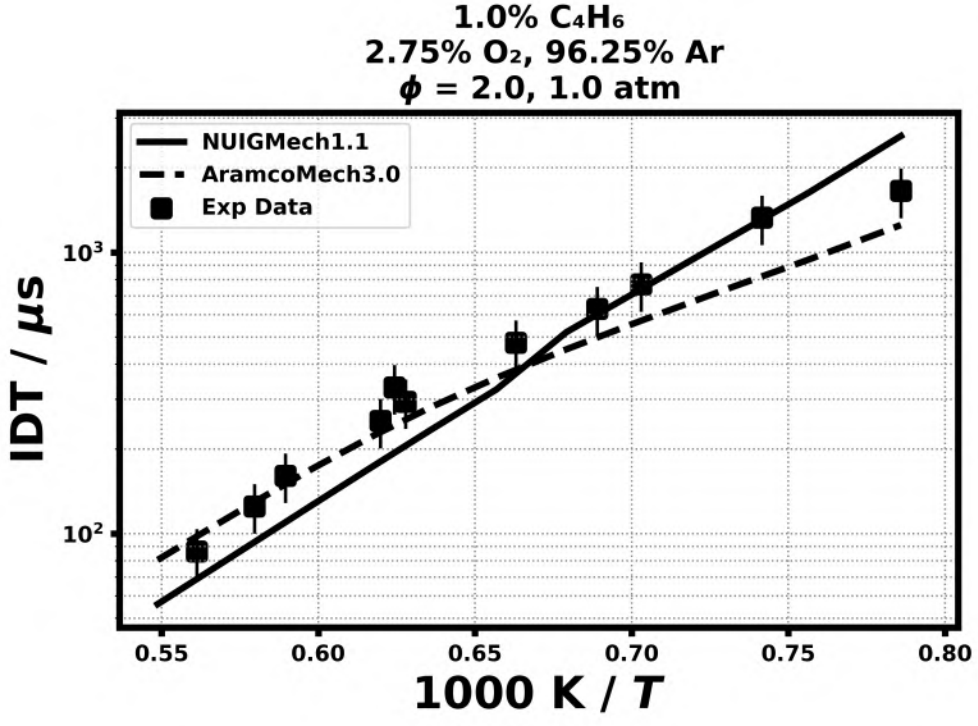
1.0% C4H6
2.75% O2, 96.25% Ar
ϕ = 2.0, 1.0 atm
NUIGMech1.1
AramcoMech3.0
Exp Data
IDT / μs
10³
10²
0.55
0.60
0.65
0.70
0.75
0.80
1000 K / T

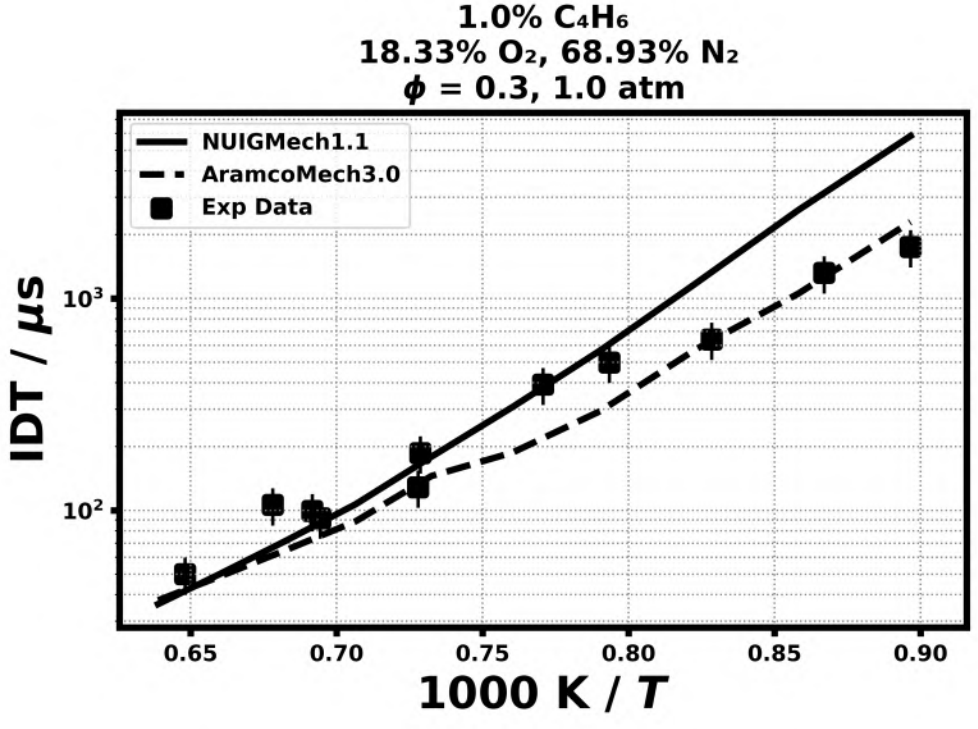
1.0% C4H6
18.33% O2, 68.93% N2
ϕ = 0.3, 1.0 atm
NUIGMech1.1
AramcoMech3.0
Exp Data
IDT / μs
10³
10²
0.65
0.70
0.75
0.80
0.85
0.90
1000 K / T

Laminar flame speed of 1,3-C_4H_6

21.2) Zhou, C. W., Li, Y., Burke, U., Banyon, C., Somers, K. P., Ding, S., ... & Petersen, E. L., Combustion and Flame, 197 (2018) 423-438.

21.3) Davis, S. G., & Law, C. K., Combustion science and technology, 140(1-6) (1998) 427-449.

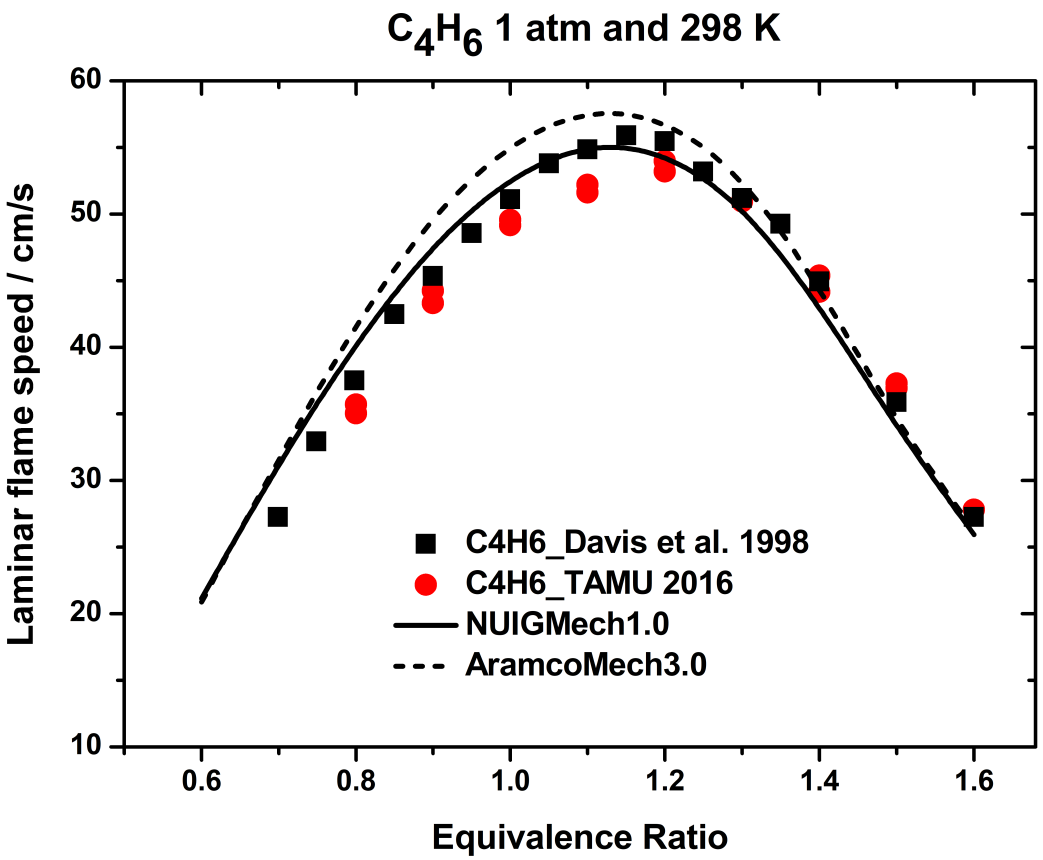

Bugler, John, et al. "An ignition delay time and chemical kinetic modeling study of the pentane isomers." Combustion and Flame 163 (2016): 138-156.

23. Validation for C_5H_{12}

Shock tube ignition delay time

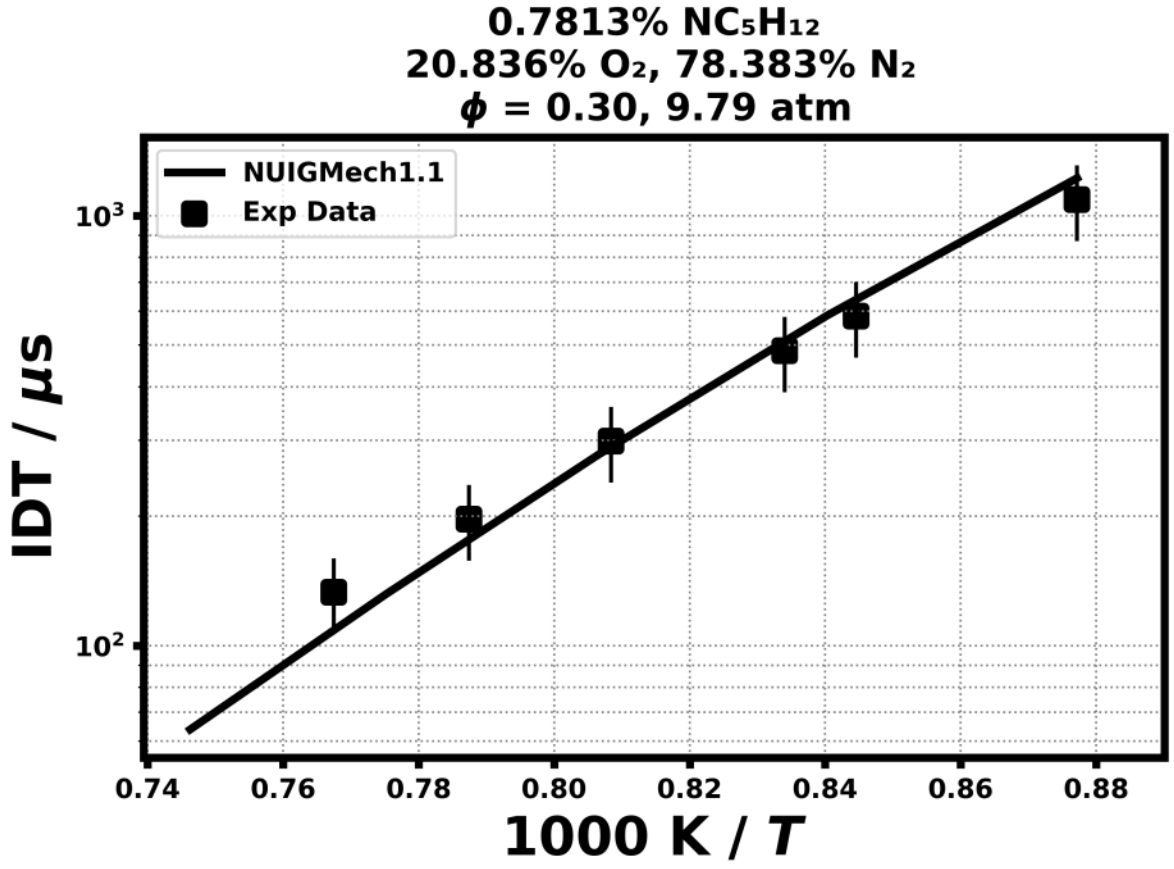

Figure 2: Dataset: 10_ATM_0.8_NC5H12_PHI_0.3

1.1.3 Case: n-C5H12/ST/BUGLER/10_ATM_1.3_NC5H12_PHI_0.5

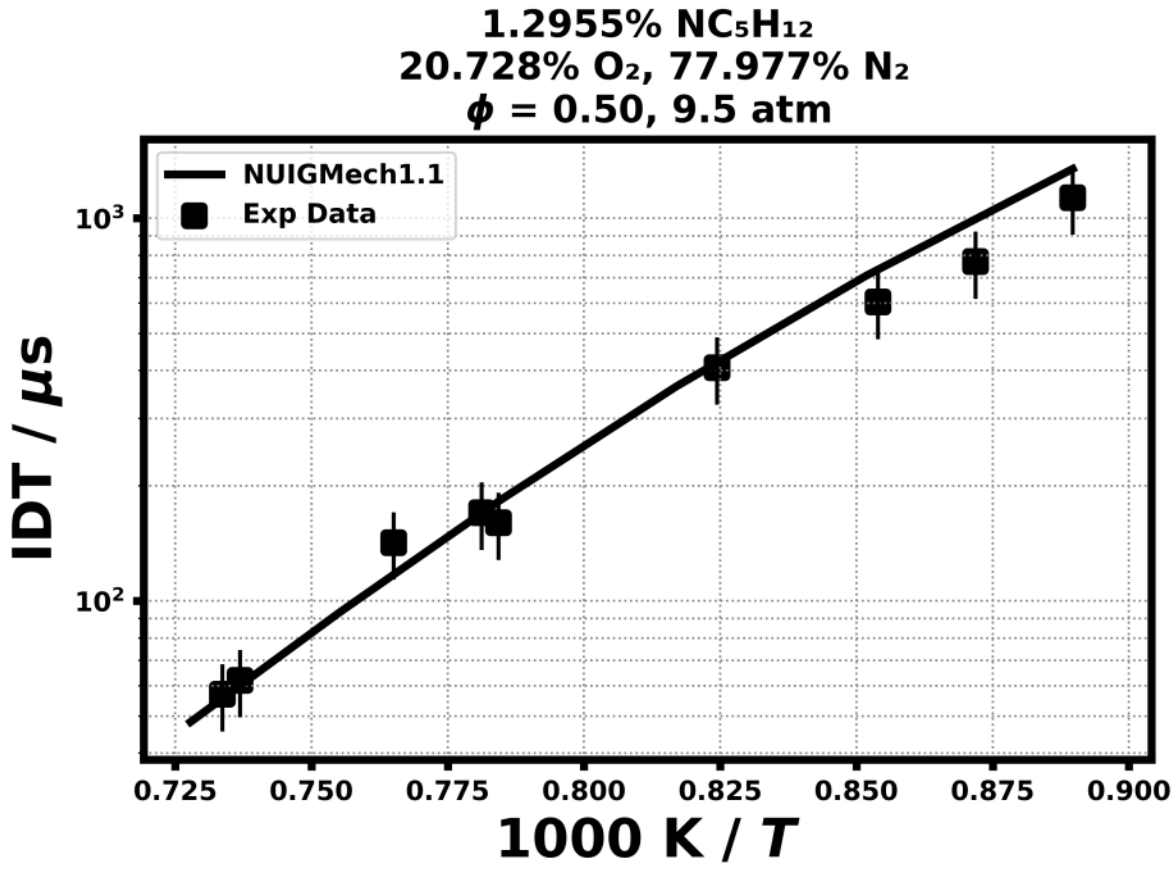

Figure 3: Dataset: 10_ATM_1.3_NC5H12_PHI_0.5

1.1.4 Case: n-C5H12/ST/BUGLER/10_ATM_2.6_NC5H12_PHI_1.0

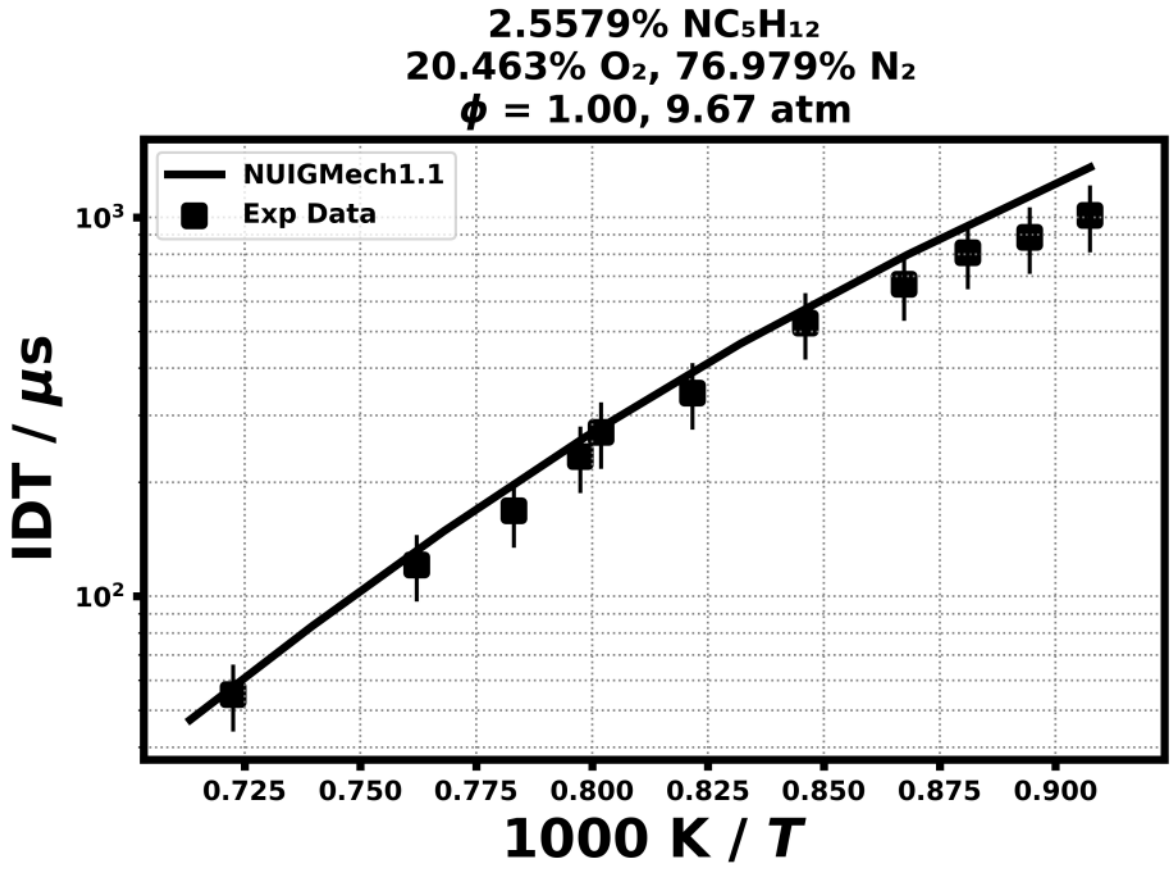

Figure 4: Dataset: 10_ATM_2.6_NC5H12_PHI_1.0

1.1.5 Case: n-C5H12/ST/BUGLER/10_ATM_5.0_NC5H12_PHI_2.0

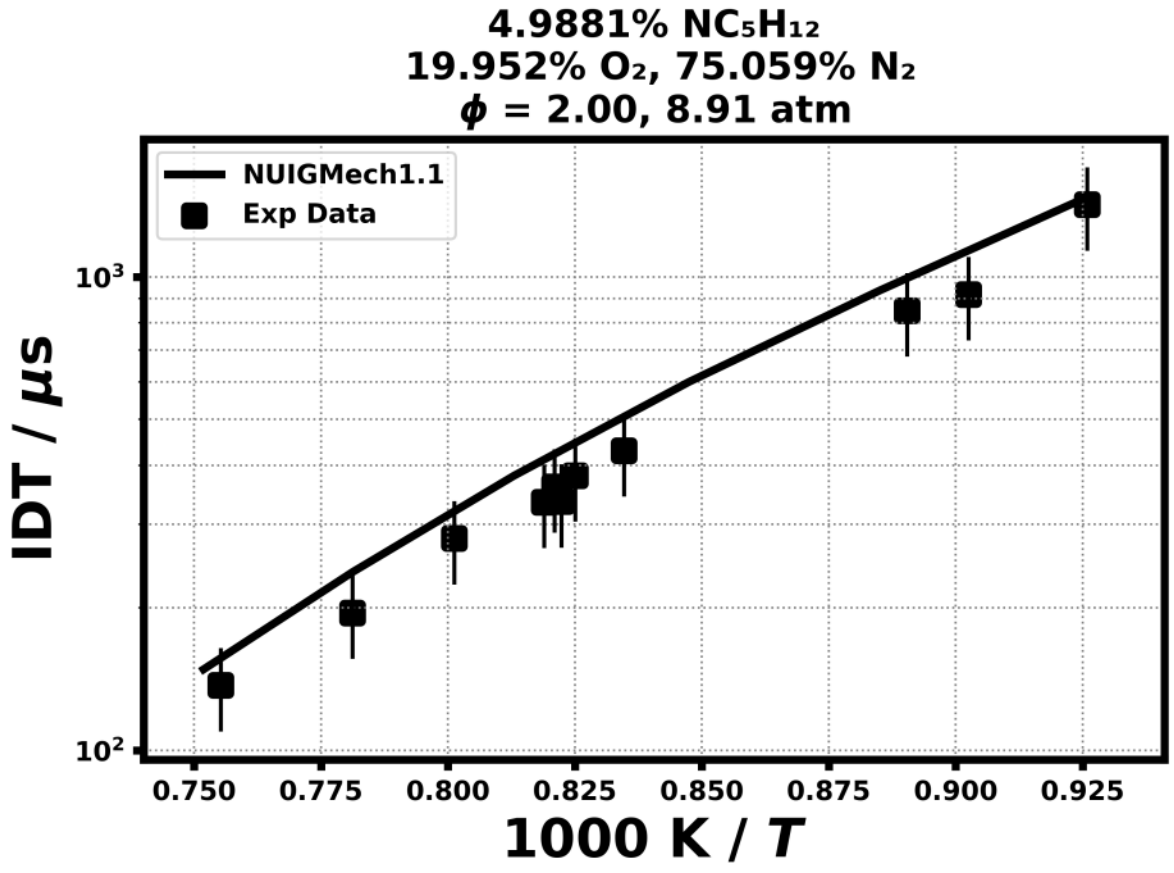

Figure 5: Dataset: 10_ATM_5.0_NC5H12_PHI_2.0

1.1.6 Case: n-C5H12/ST/BUGLER/1_ATM_0.8_NC5H12_PHI_0.3

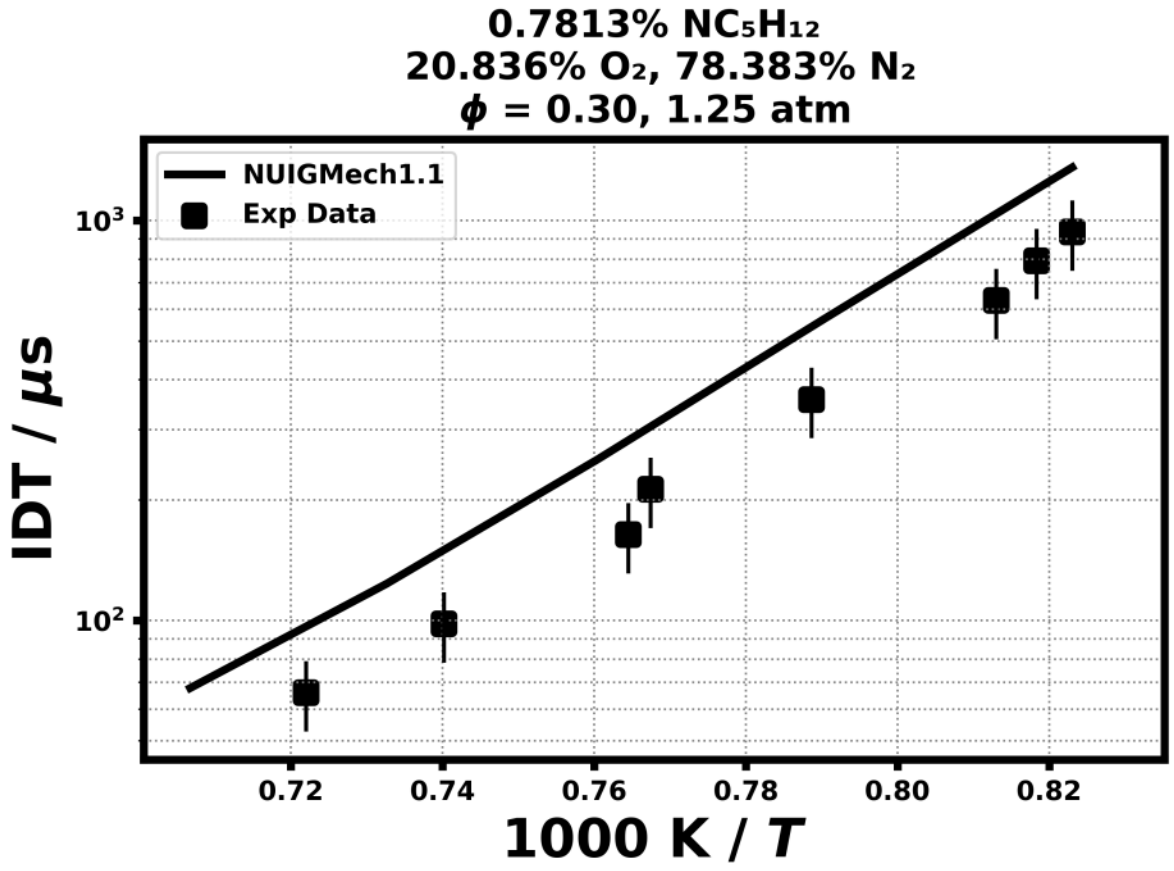

Figure 6: Dataset: 1_ATM_0.8_NC5H12_PHI_0.3

1.1.7 Case: n-C5H12/ST/BUGLER/1_ATM_1.3_NC5H12_PHI_0.5

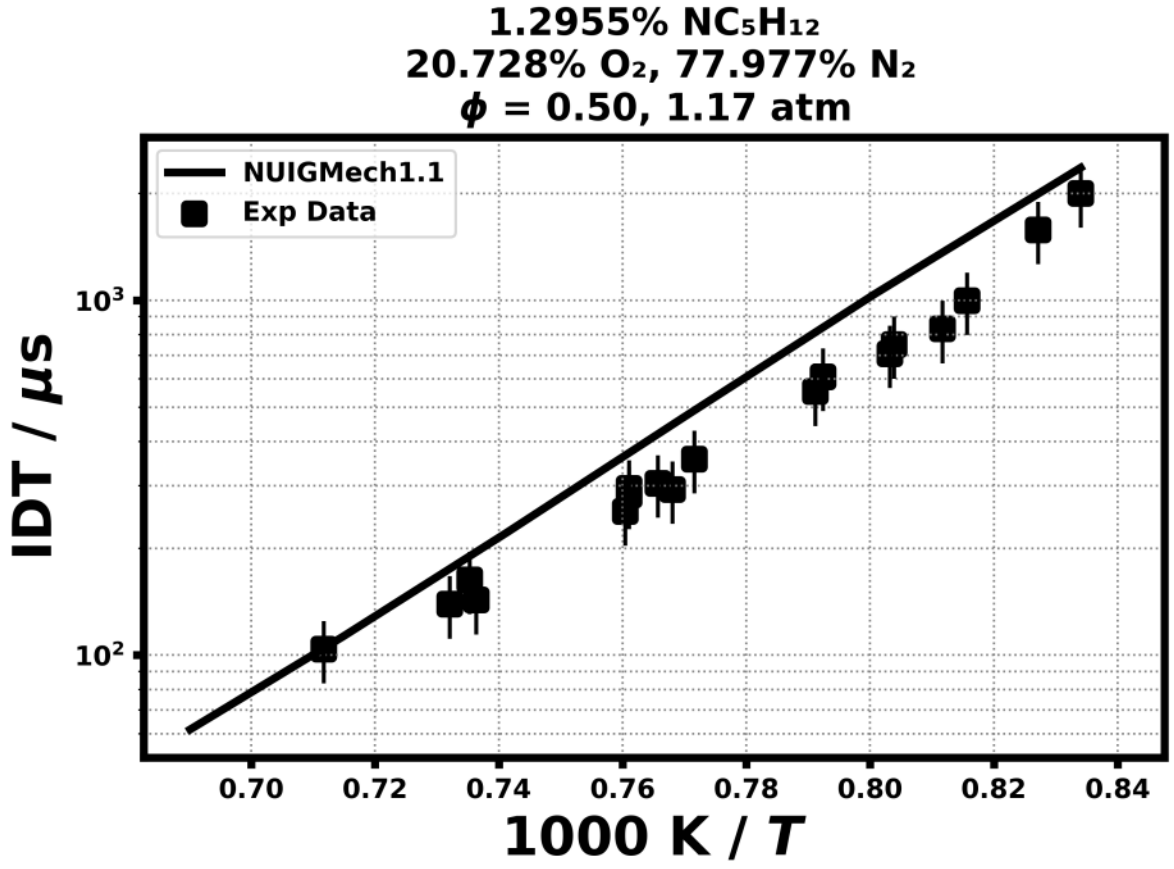

Figure 7: Dataset: 1_ATM_1.3_NC5H12_PHI_0.5

1.1.8 Case: n-C5H12/ST/BUGLER/1_ATM_2.6_NC5H12_PHI_1.0

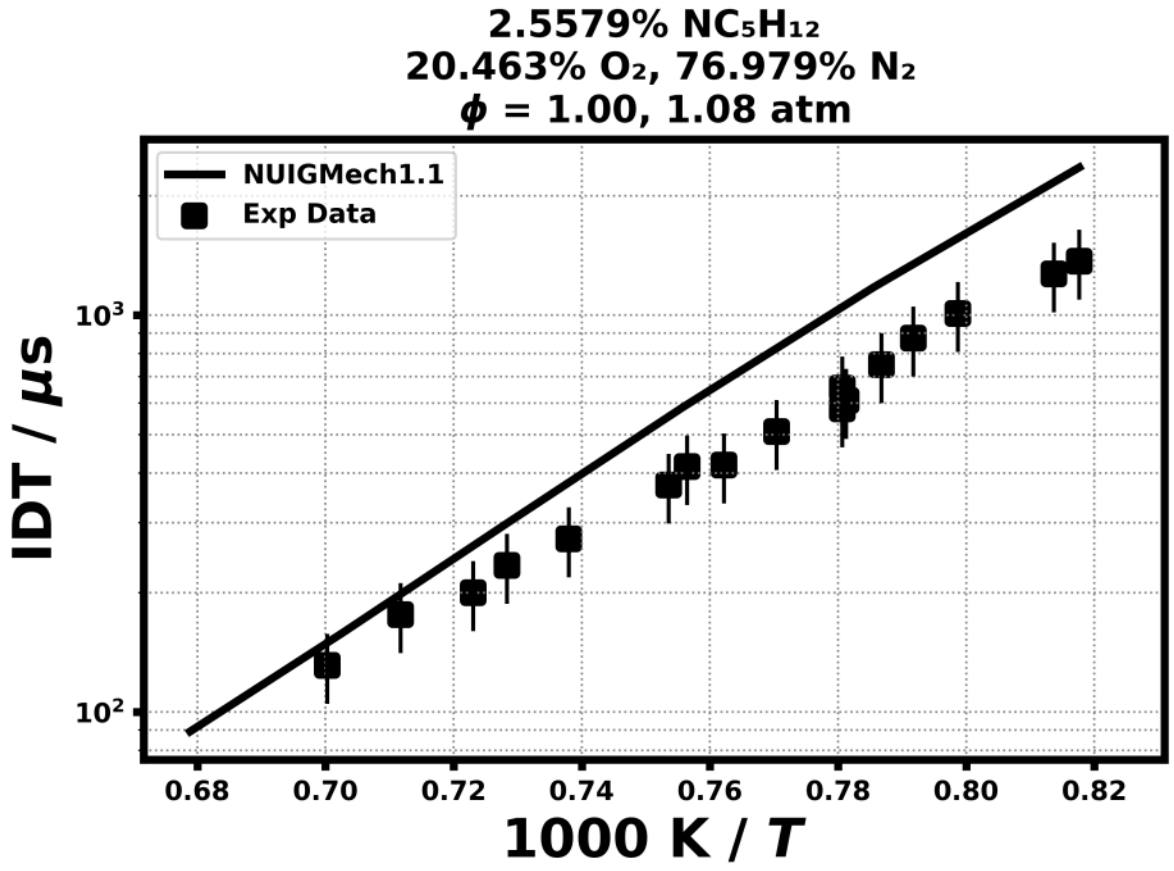

Figure 8: Dataset: 1_ATM_2.6_NC5H12_PHI_1.0

1.1.9 Case: n-C5H12/ST/BUGLER/1_ATM_5.0_NC5H12_PHI_2.0

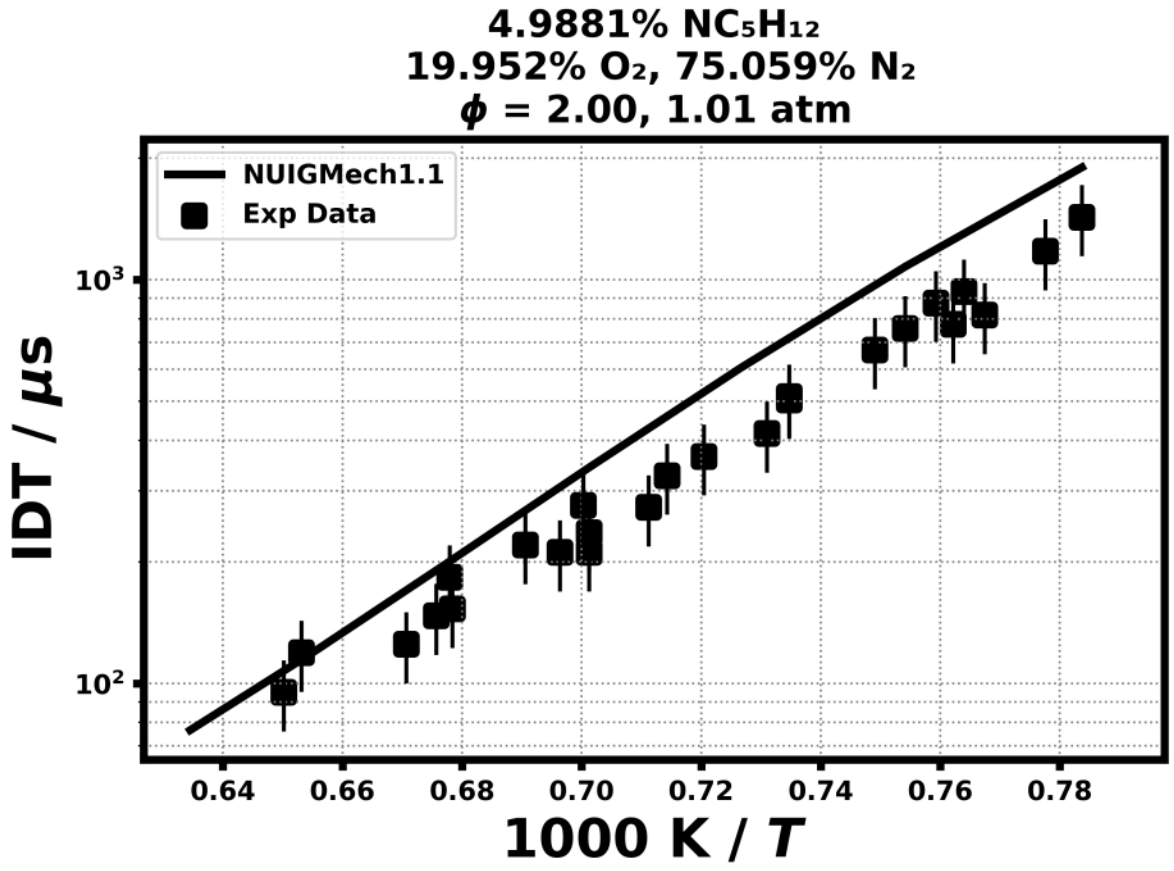

Figure 9: Dataset: 1_ATM_5.0_NC5H12_PHI_2.0

1.1.10 Case: n-C5H12/ST/BUGLER/20_ATM_1.3_NC5H12_PHI_0.5

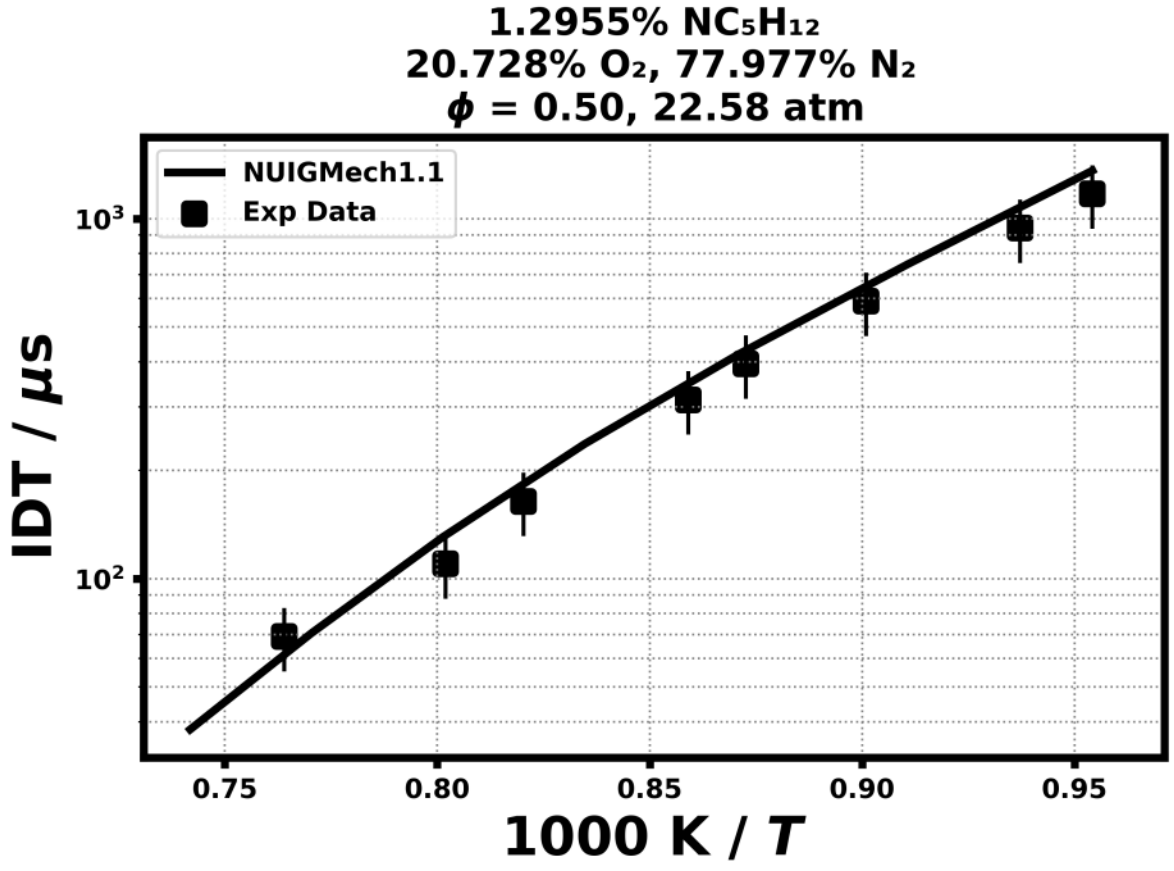

Figure 10: Dataset: 20_ATM_1.3_NC5H12_PHI_0.5

1.1.11 Case: n-C5H12/ST/BUGLER/20_ATM_2.6_NC5H12_PHI_1.0

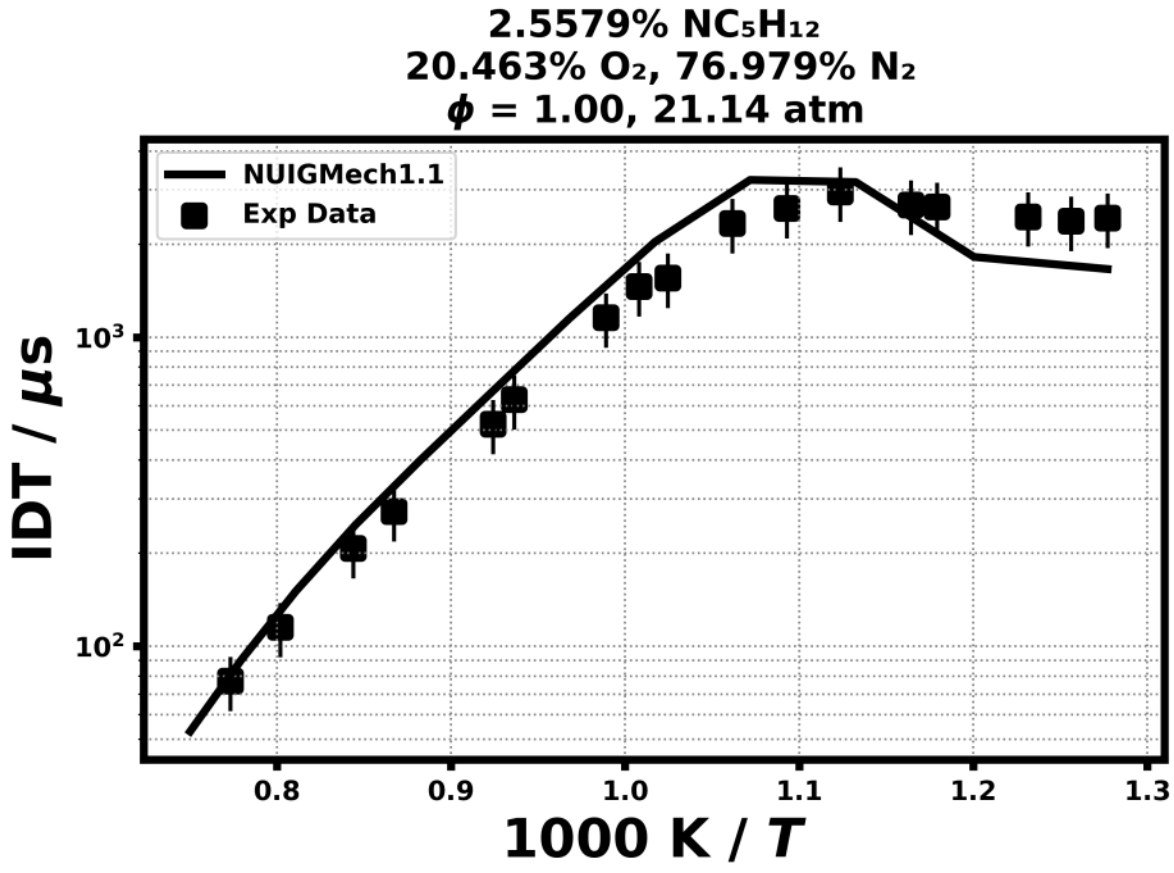

Figure 11: Dataset: 20_ATM_2.6_NC5H12_PHI_1.0

1.1.12 Case: n-C5H12/ST/BUGLER/25_ATM_0.8_NC5H12_PHI_0.3

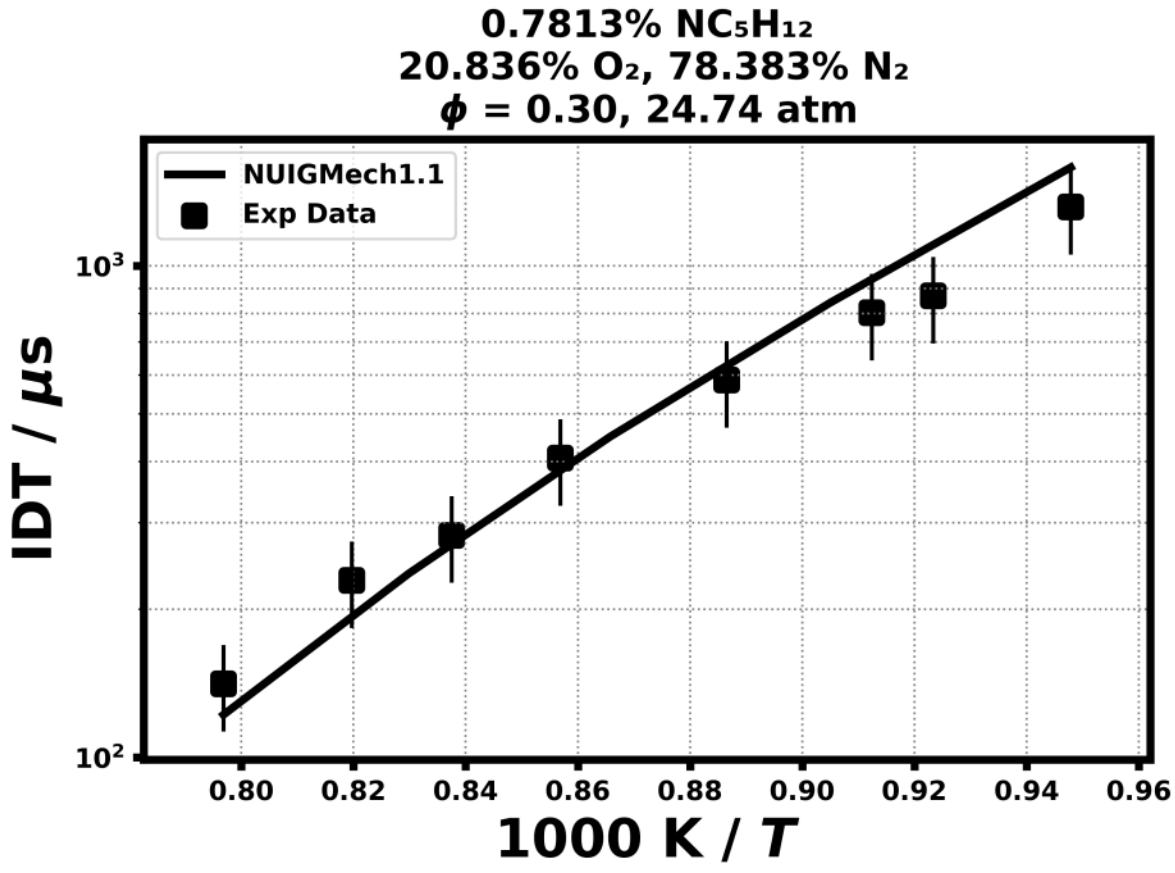

Figure 12: Dataset: 25_ATM_0.8_NC5H12_PHI_0.3

1.1.13 Case: n-C5H12/ST/BUGLER/25_ATM_5.0_NC5H12_PHI_2.0

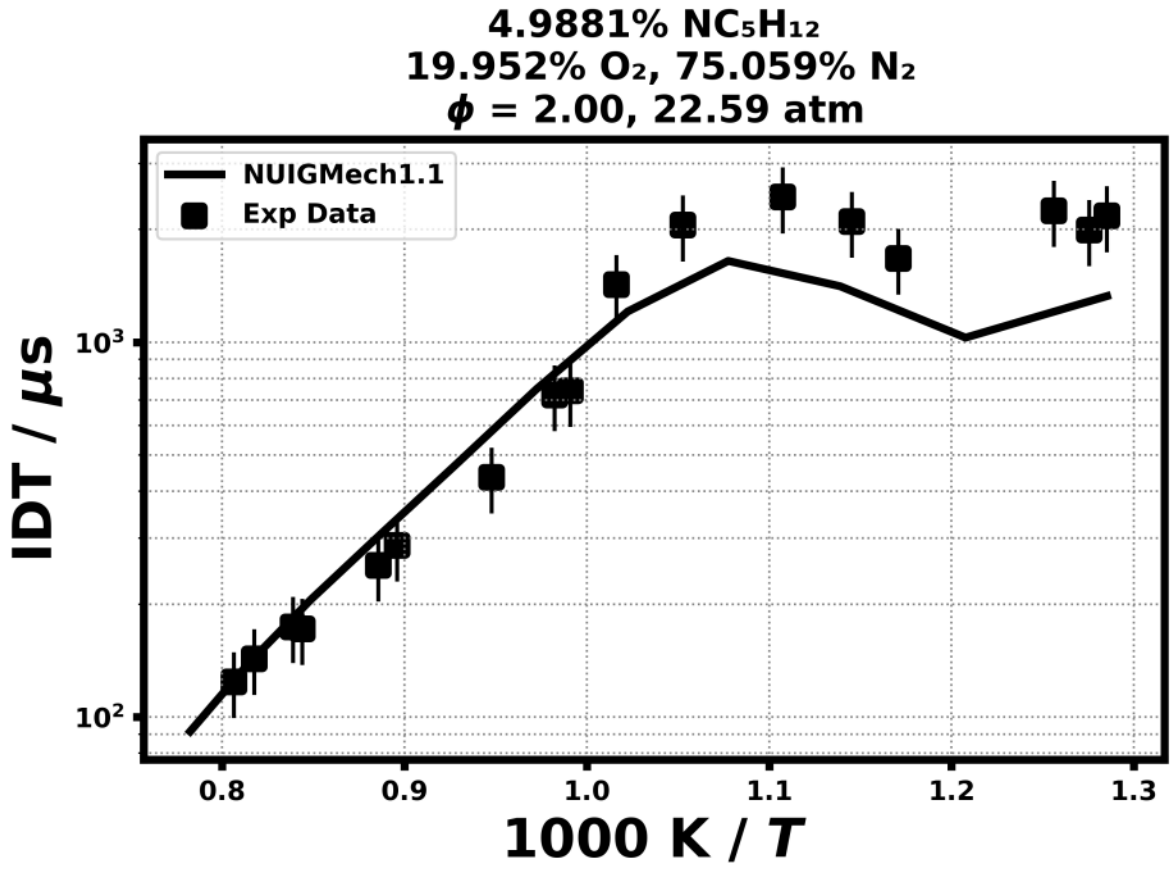

Figure 13: Dataset: 25_ATM_5.0_NC5H12_PHI_2.0

Zhukov, V. P., V. A. Sechenov, and A. Yu Starikovskii. "Self-ignition of a lean mixture of n-pentane and air over a wide range of pressures." Combustion and flame 140.3 (2005): 196-203.

1.1.14 Case: n-C5H12/ST/ZHUKOV/10_ATM_1.6_NC5H12_PHI_0.5

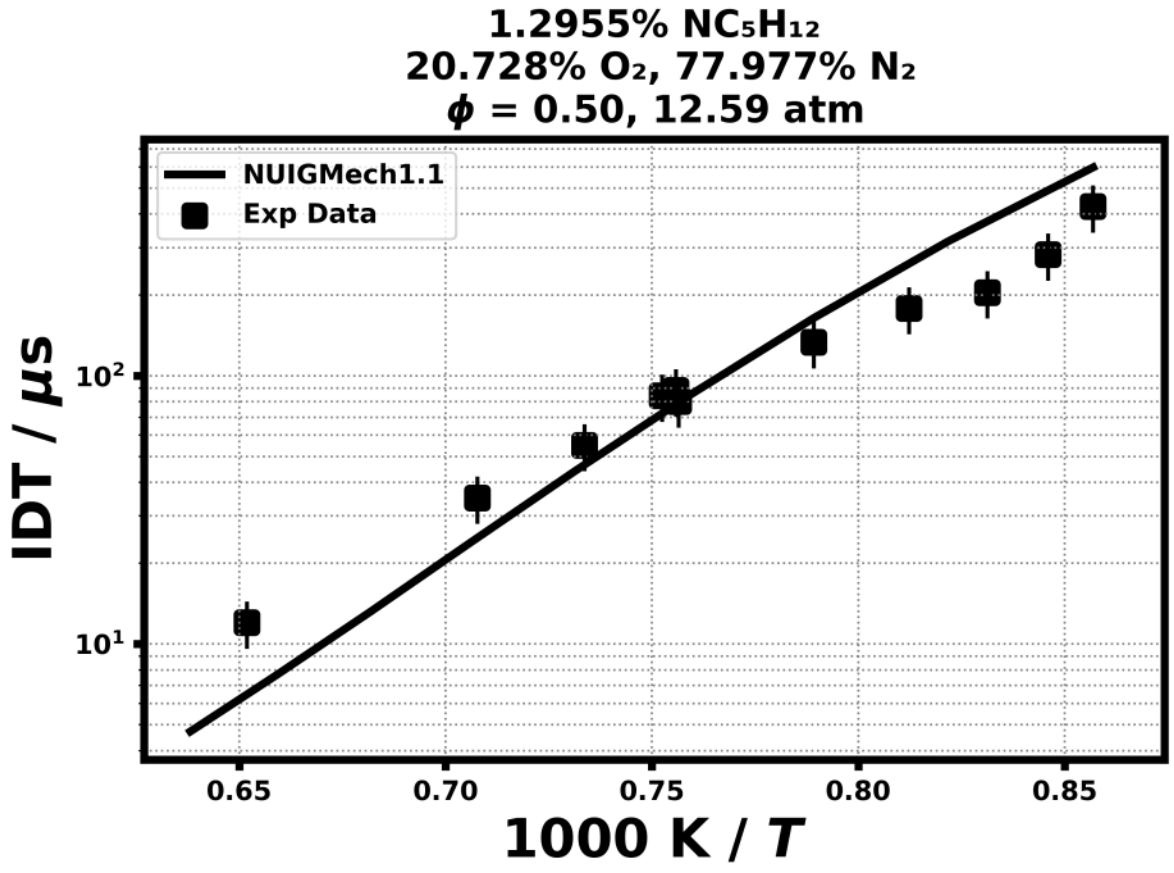

Figure 14: Dataset: 10_ATM_1.6_NC5H12_PHI_0.5

1.1.15 Case: n-C5H12/ST/ZHUKOV/250_ATM_1.6_NC5H12_PHI_0.5

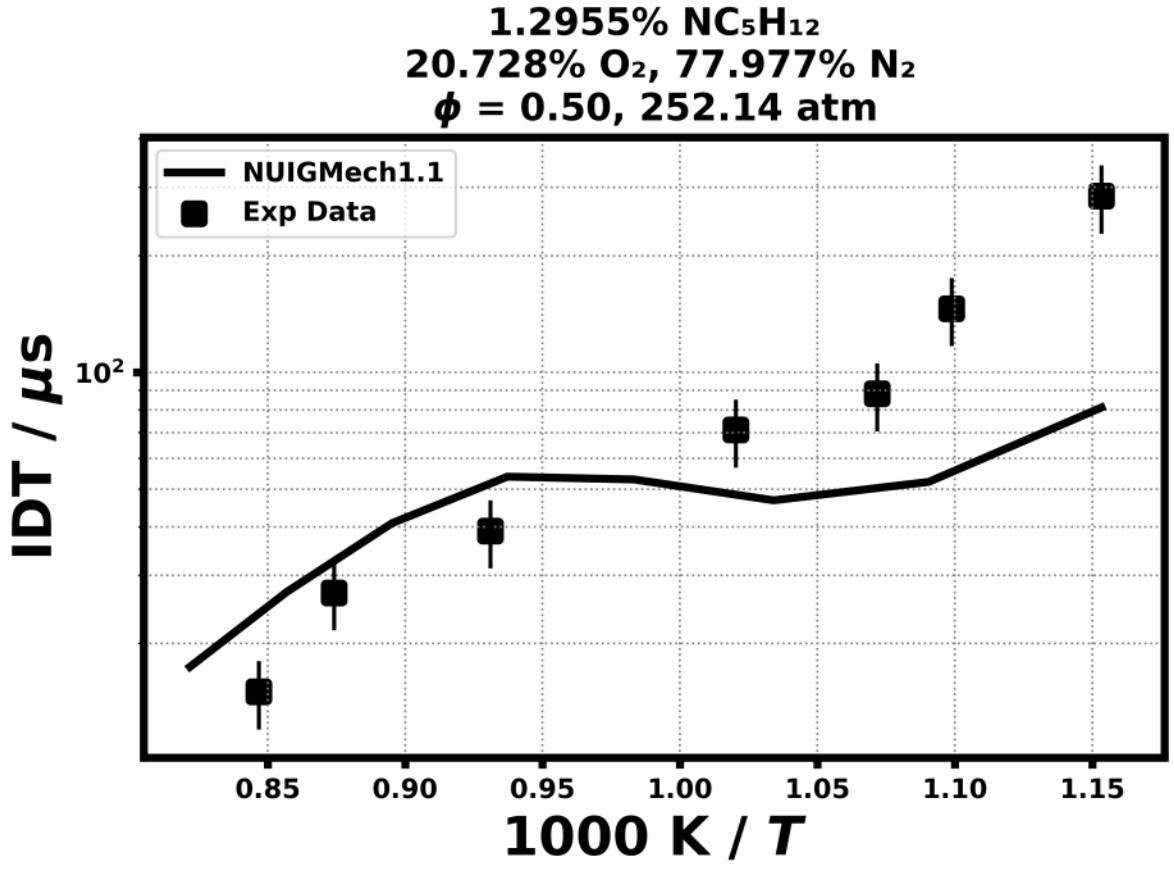

Figure 15: Dataset: 250_ATM_1.6_NC5H12_PHI_0.5

1.1.16 Case: n-C5H12/ST/ZHUKOV/520_ATM_1.6_NC5H12_PHI_0.5

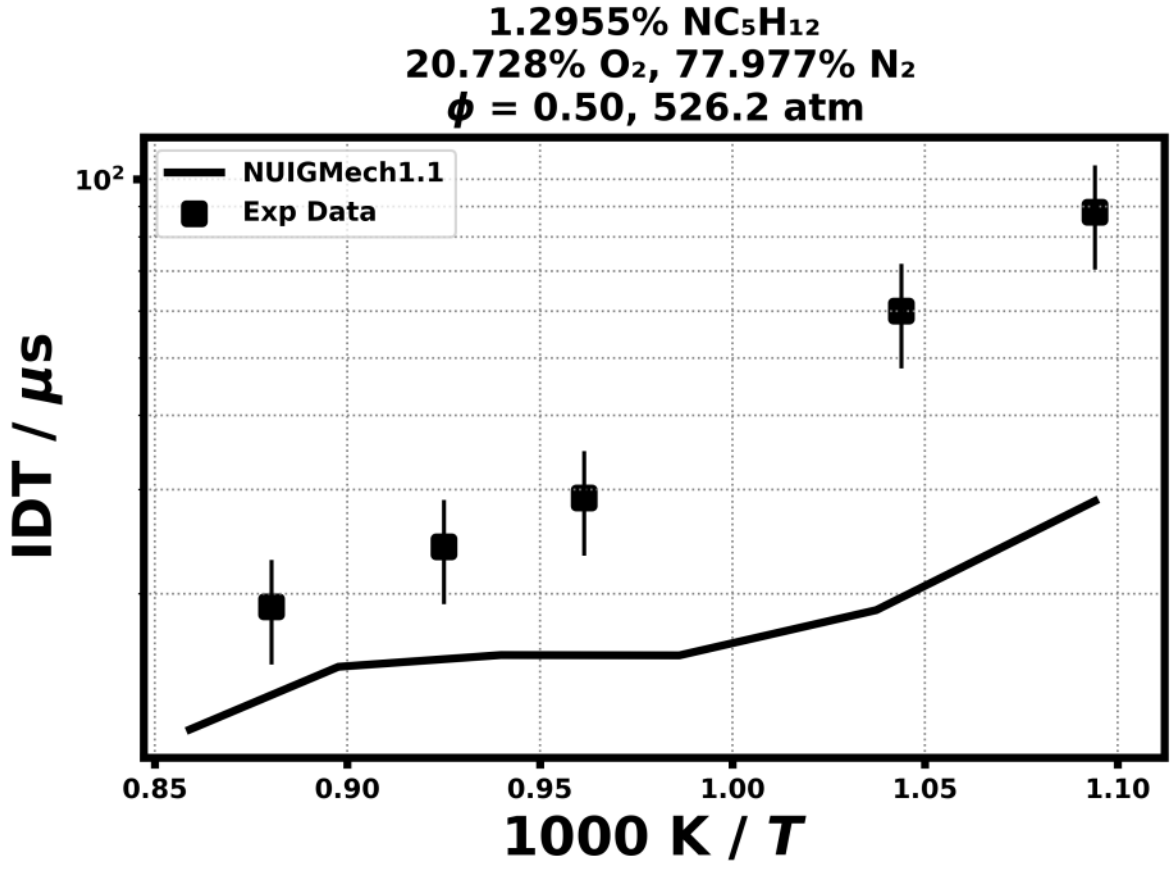

Figure 16: Dataset: 520_ATM_1.6_NC5H12_PHI_0.5

1.1.17 Case: n-C5H12/ST/ZHUKOV/60_ATM_1.6_NC5H12_PHI_0.5

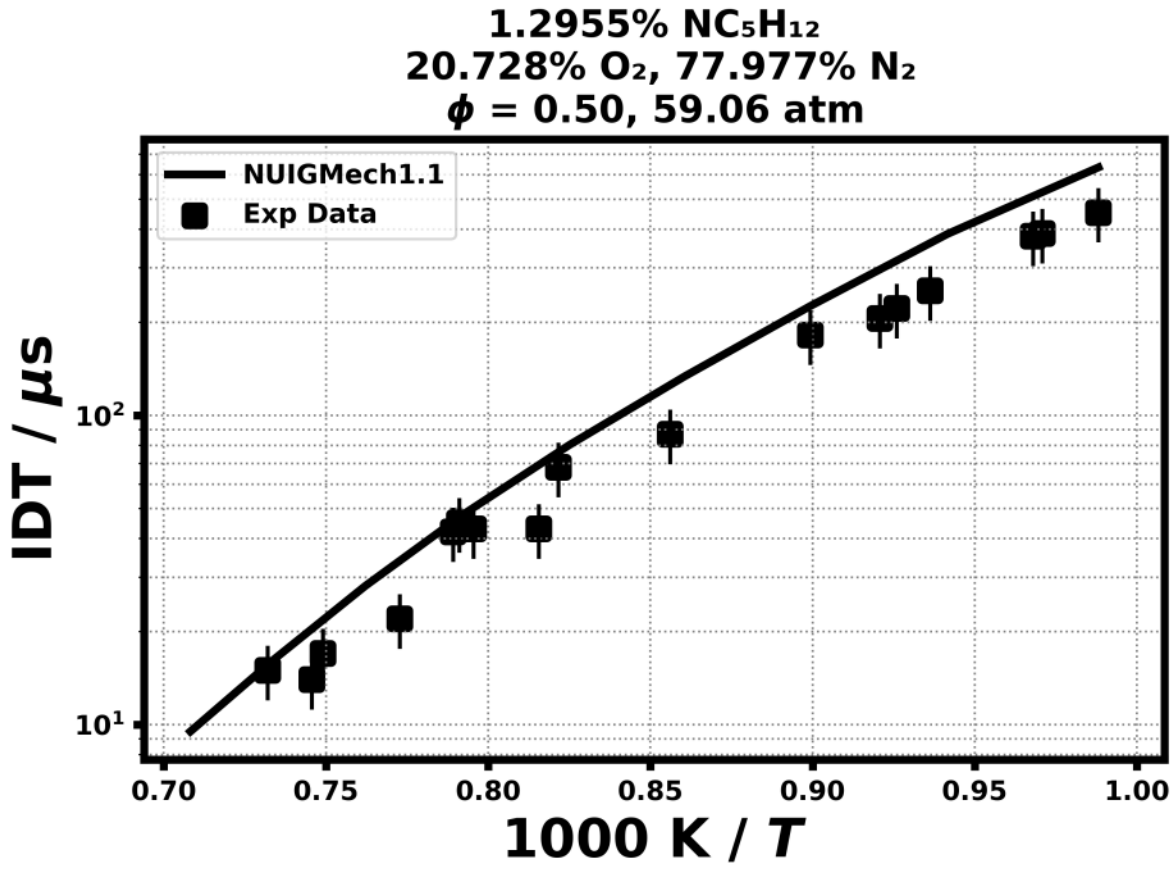

Figure 17: Dataset: 60_ATM_1.6_NC5H12_PHI_0.5

Bugler, John, et al. "An ignition delay time and chemical kinetic modeling study of the pentane isomers." Combustion and Flame 163 (2016): 138-156.

RCM Ignition delay times

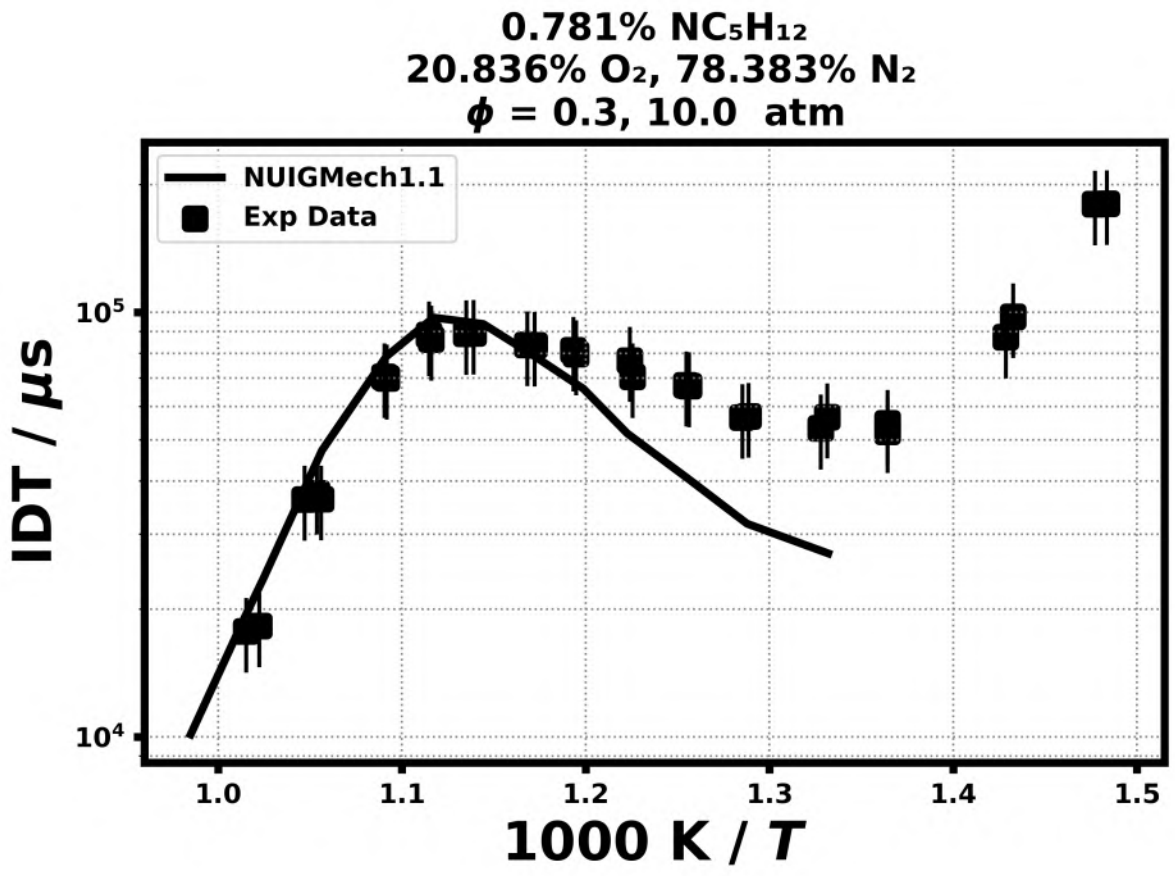

Figure 18: Dataset: F030_10ATM_100_N2

1.2.2 Case: n-C5H12/RCM/BUGLER/F030_20ATM_100_N2

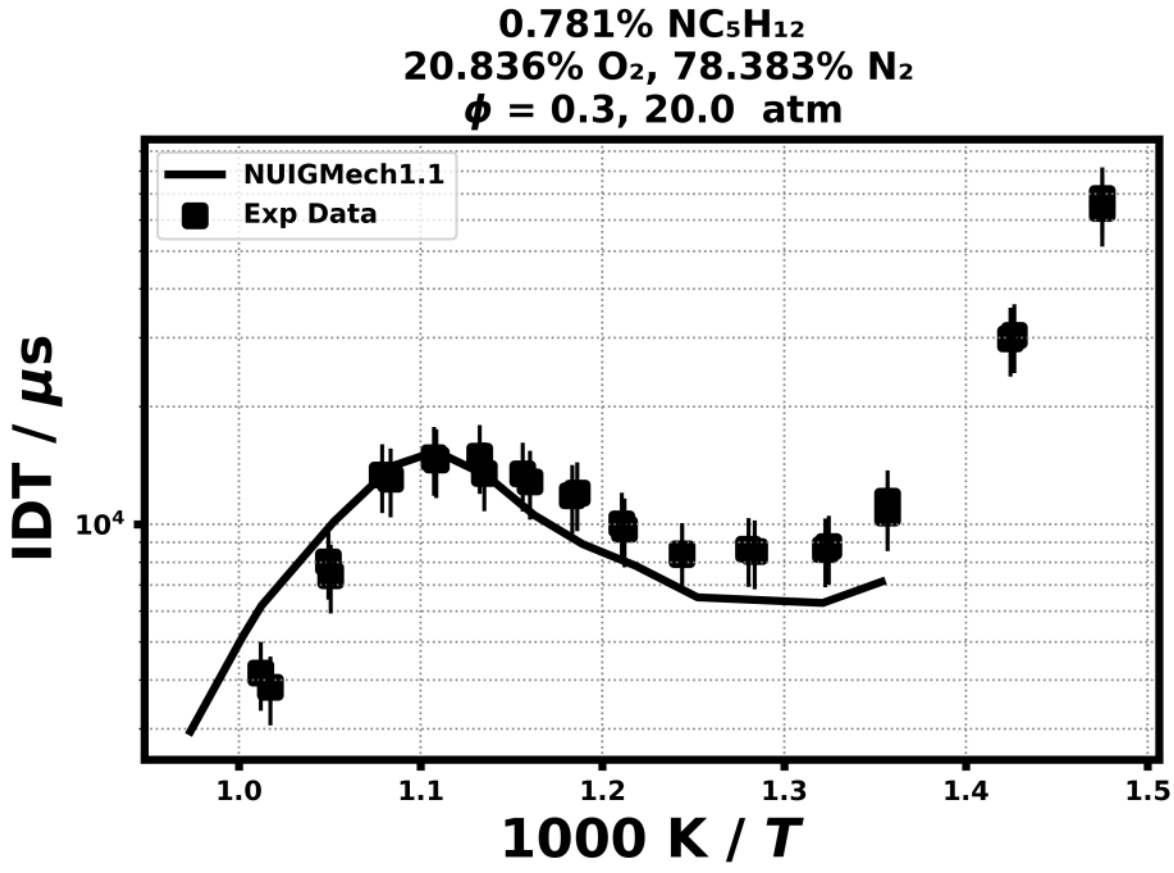

Figure 19: Dataset: F030_20ATM_100_N2

1.2.10 Case: n-C5H12/RCM/BUGLER/F100_20ATM_100_N2

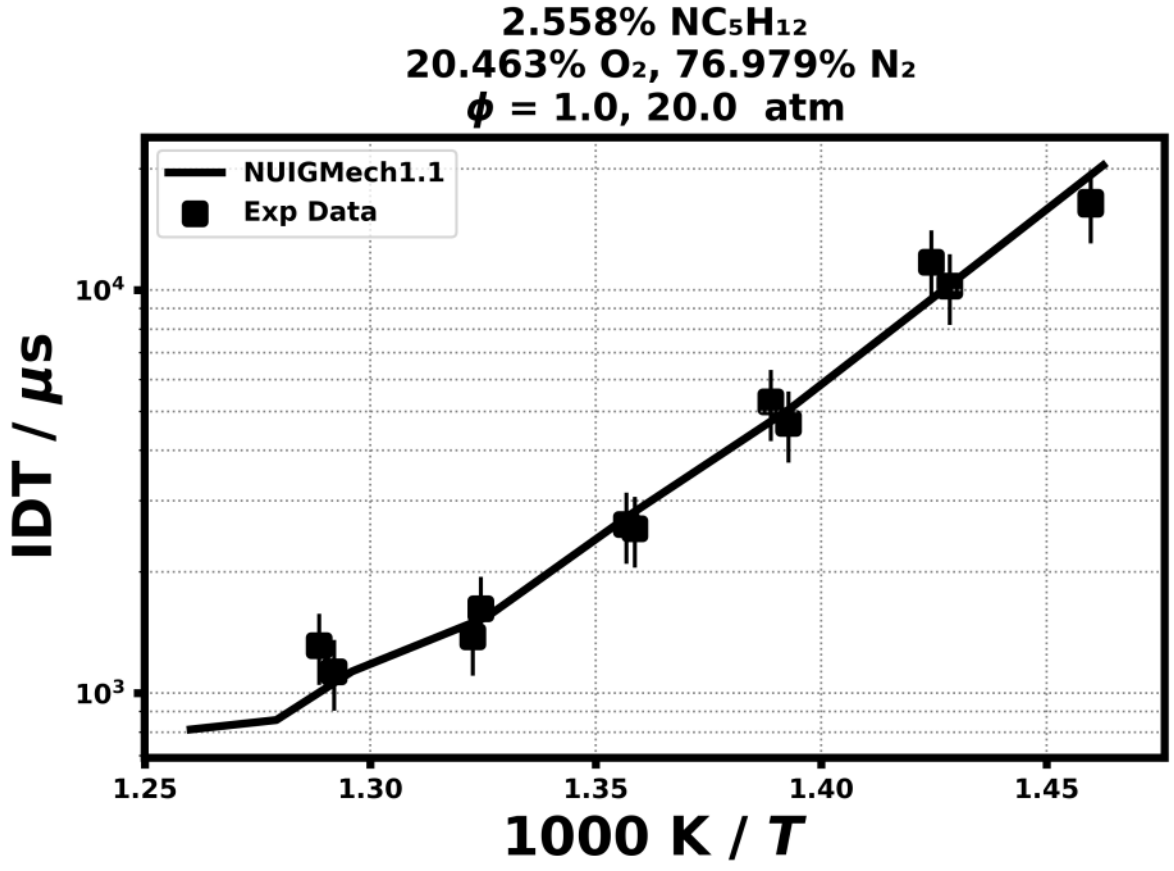

Figure 27: Dataset: F100_20ATM_100_N2

1.2.13 Case: n-C5H12/RCM/BUGLER/F200_20ATM_100_N2

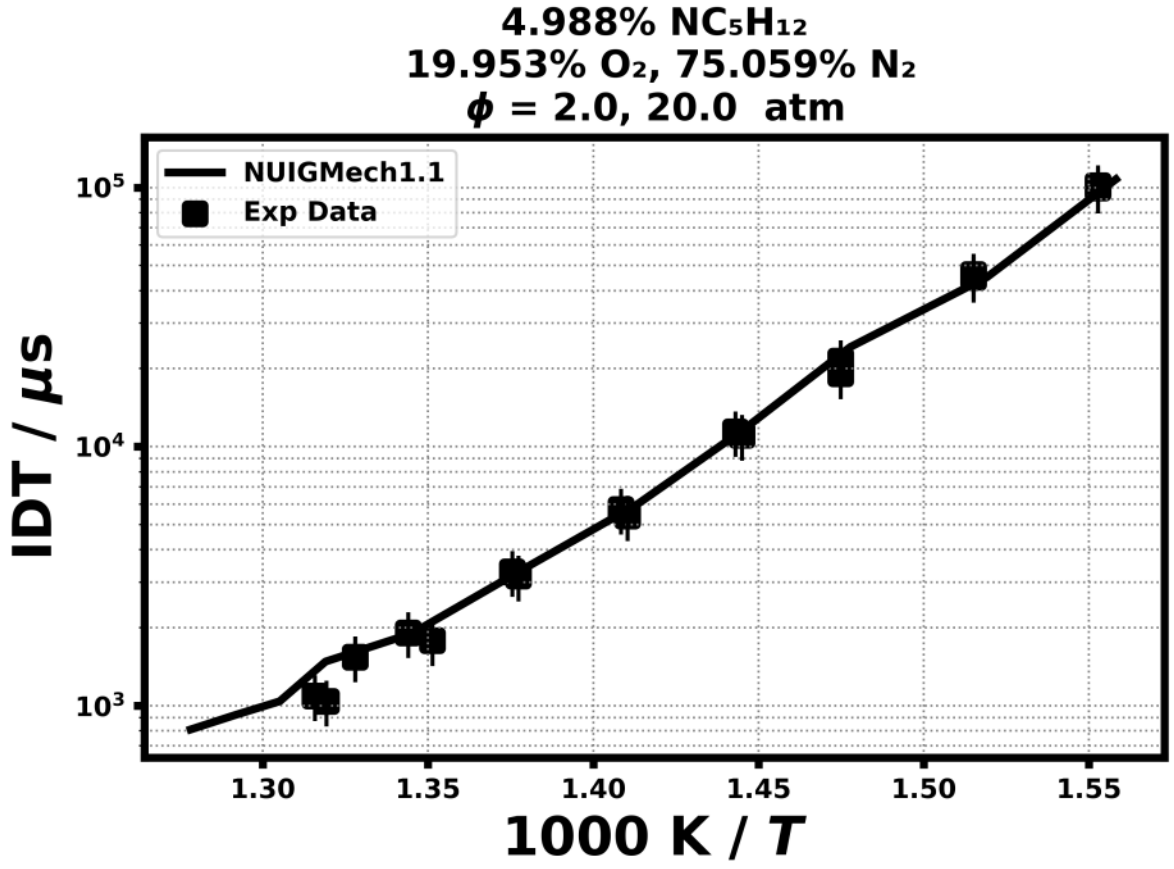

Figure 30: Dataset: F200_20ATM_100_N2

Bugler, John, et al. "An experimental and modelling study of n-pentane oxidation in two jet-stirred reactors: The importance of pressure-dependent kinetics and new reaction pathways." Proceedings of the Combustion Institute 36.1 (2017): 441-448.

Speciation in Jet-stirred reactor

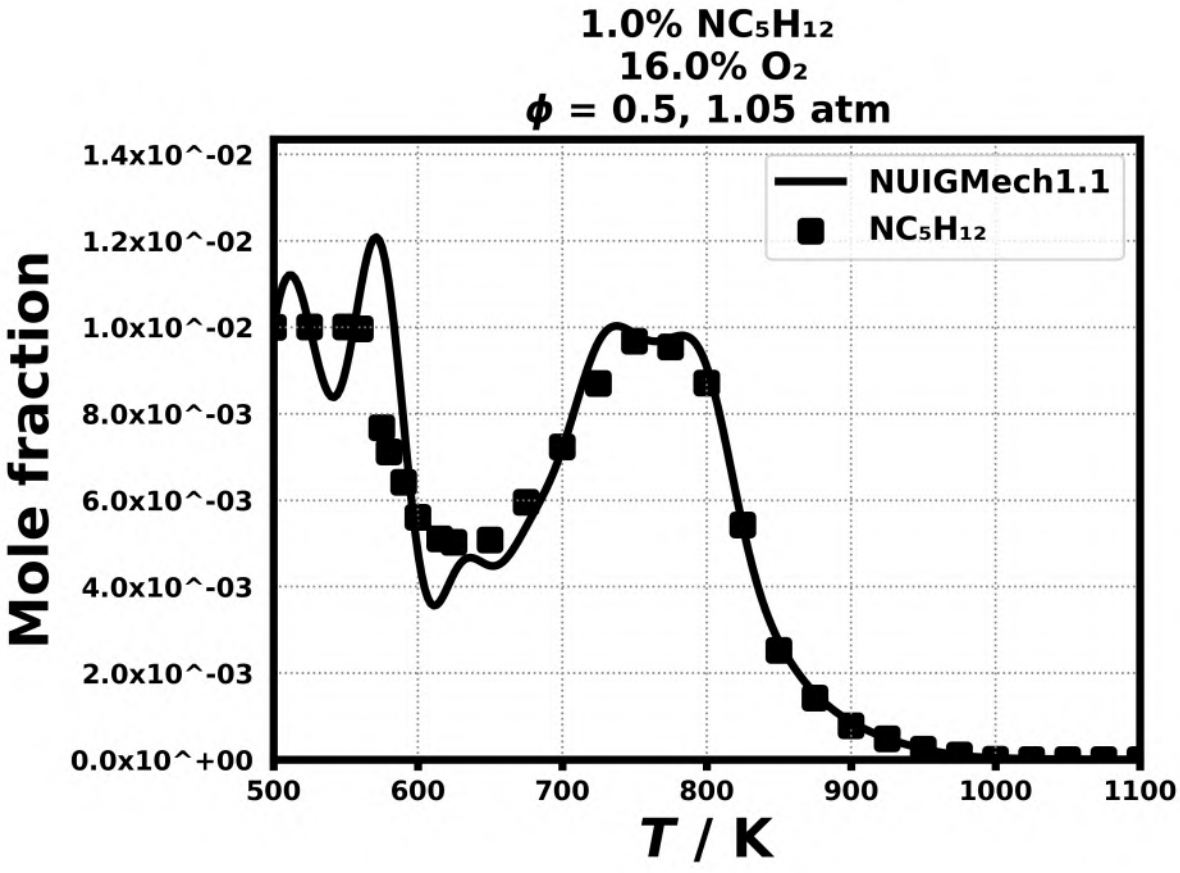

Figure 31: Dataset: 1.05_ATM_PHI_0.5

1.3.3 Case: n-C5H12/JSR/BUGLER/1.05_ATM_PHI_0.5

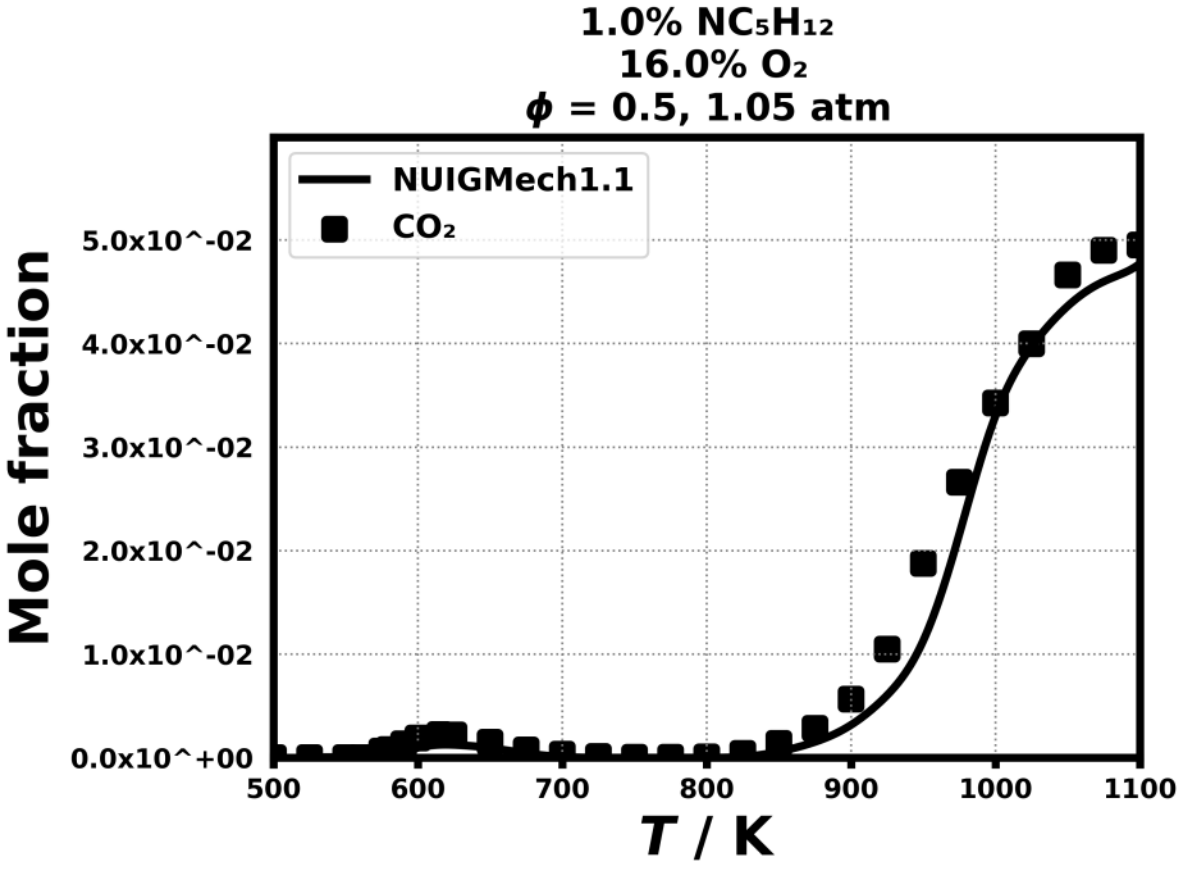

Figure 33: Dataset: 1.05_ATM_PHI_0.5

1.3.4 Case: n-C5H12/JSR/BUGLER/1.05_ATM_PHI_0.5

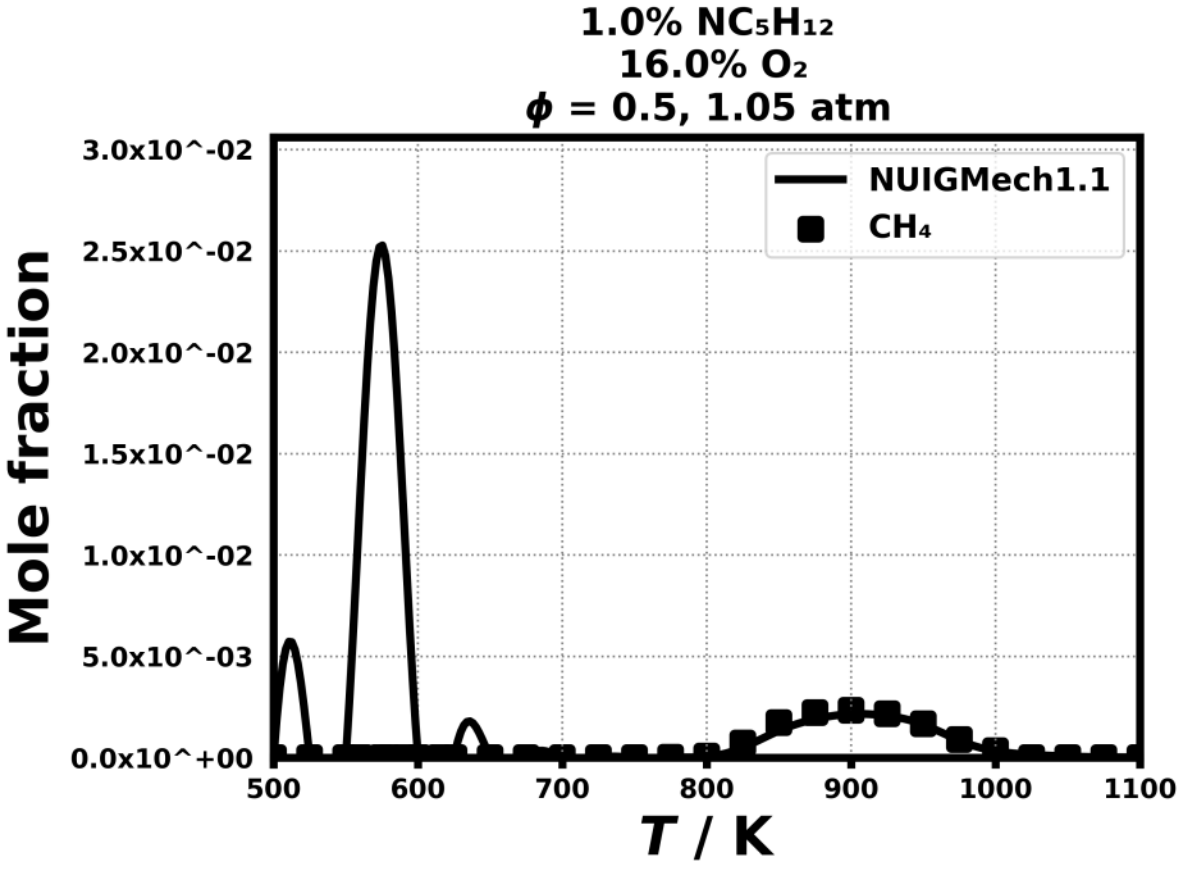

Figure 34: Dataset: 1.05_ATM_PHI_0.5

1.3.5 Case: n-C5H12/JSR/BUGLER/1.05_ATM_PHI_0.5

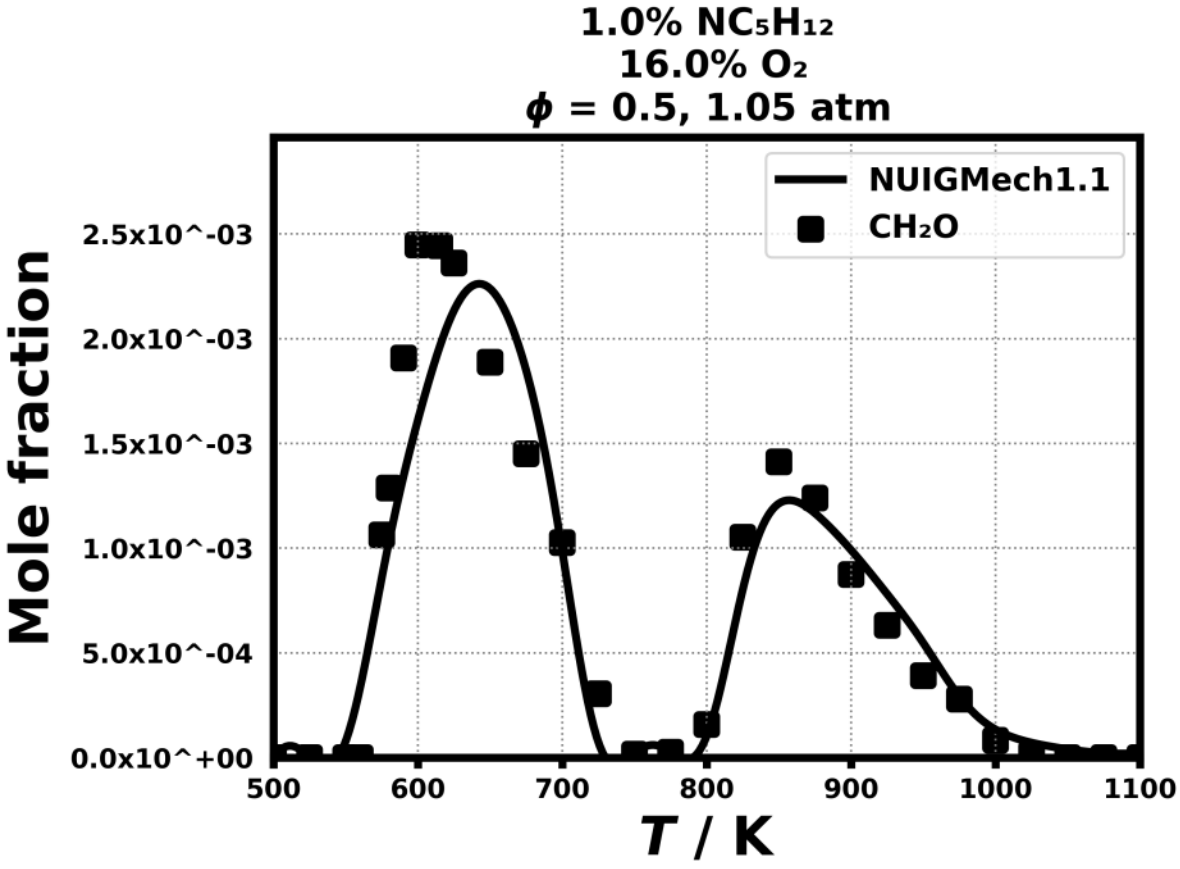

Figure 35: Dataset: 1.05_ATM_PHI_0.5

1.3.6 Case: n-C5H12/JSR/BUGLER/1.05_ATM_PHI_0.5

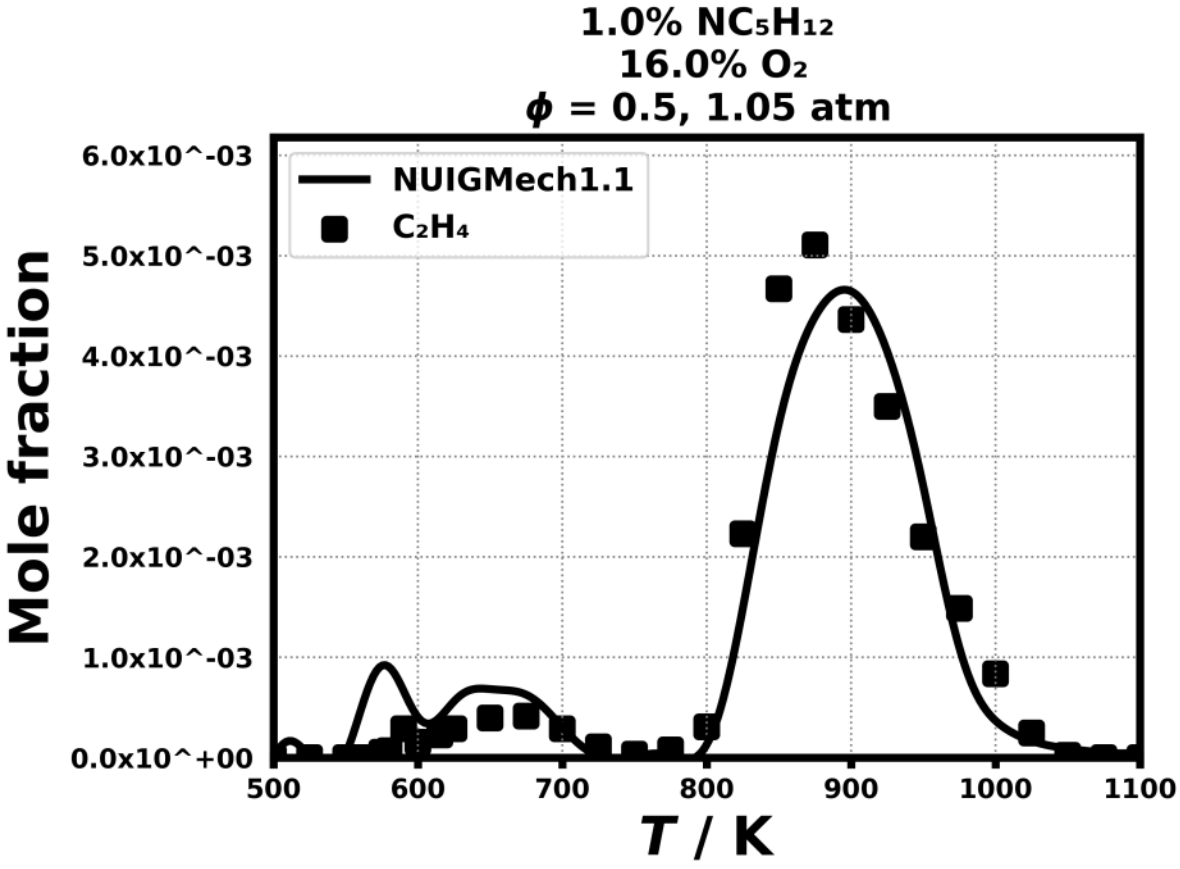

Figure 36: Dataset: 1.05_ATM_PHI_0.5

1.3.8 Case: n-C5H12/JSR/BUGLER/1.05_ATM_PHI_0.5

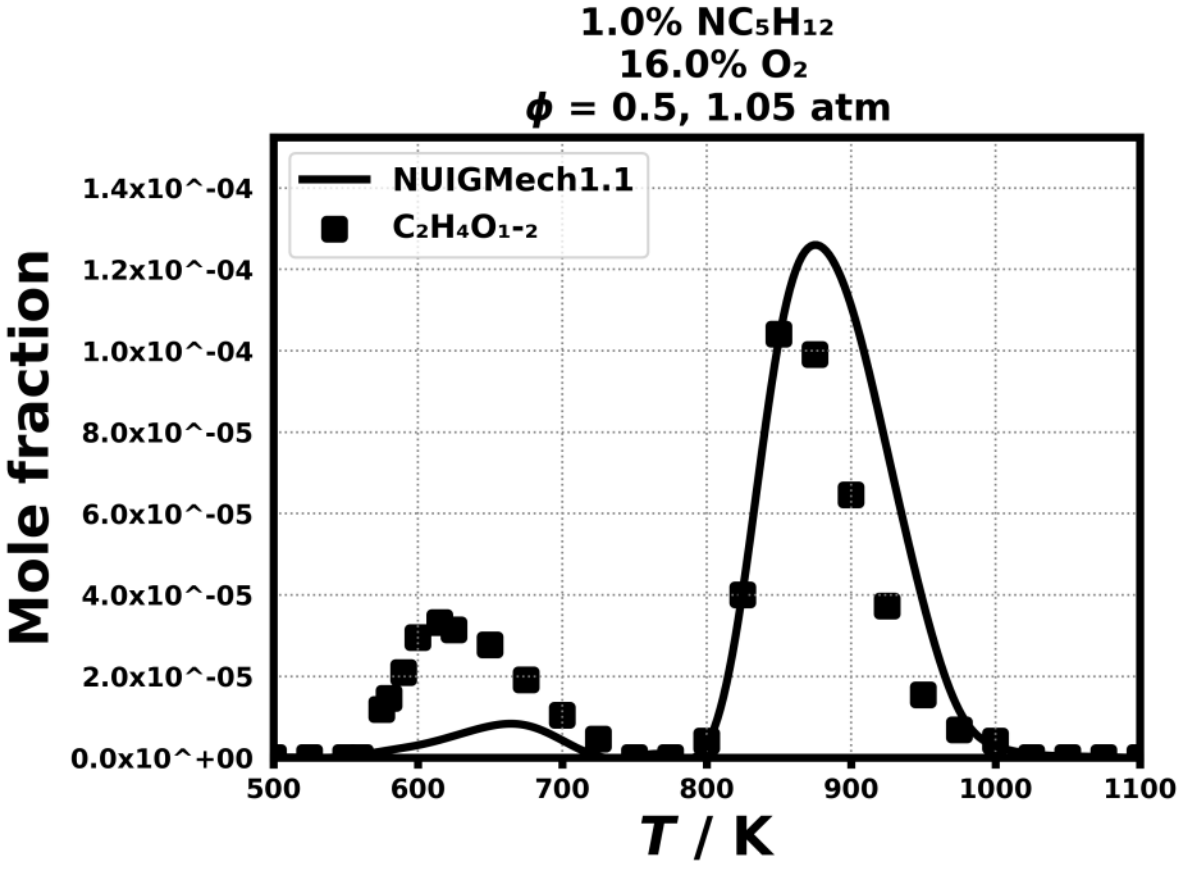

Figure 38: Dataset: 1.05_ATM_PHI_0.5

1.3.10 Case: n-C5H12/JSR/BUGLER/1.05_ATM_PHI_0.5

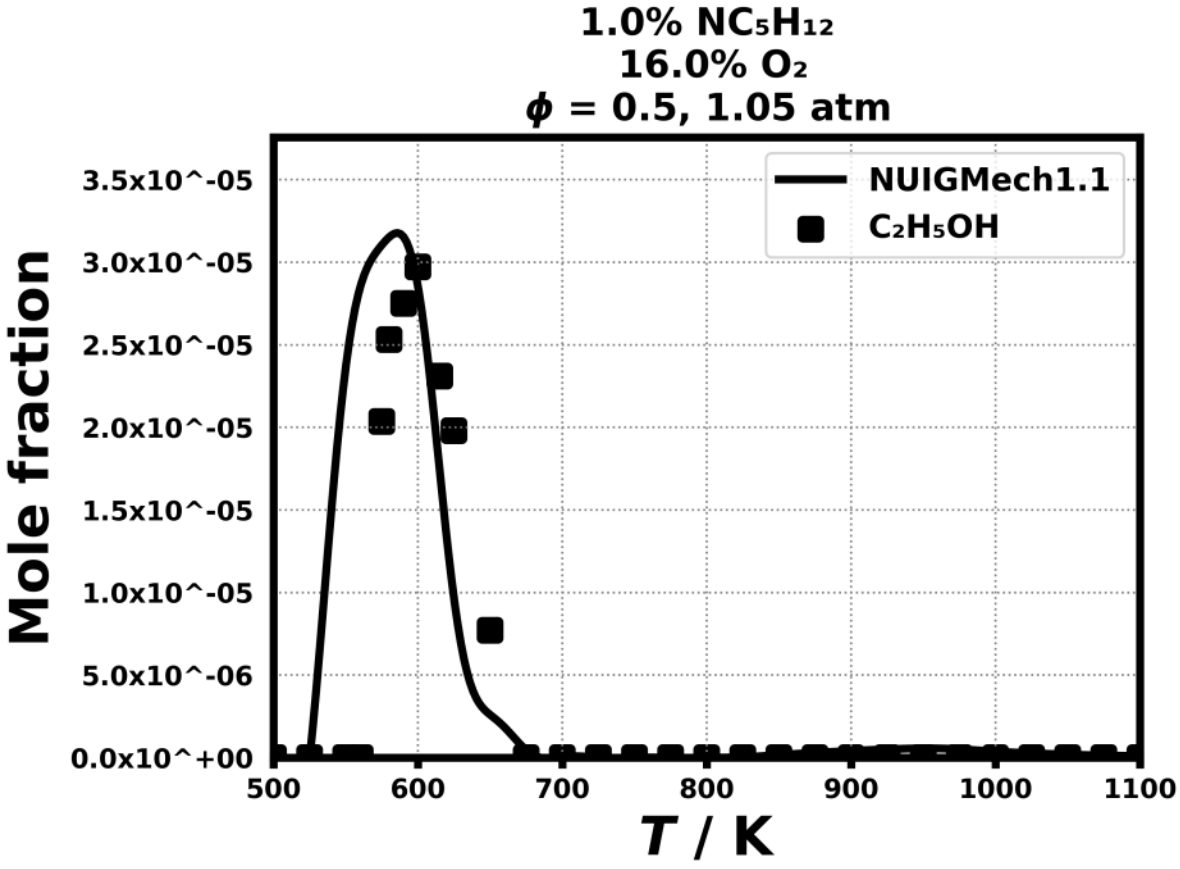

Figure 40: Dataset: 1.05_ATM_PHI_0.5

1.3.12 Case: n-C5H12/JSR/BUGLER/1.05_ATM_PHI_0.5

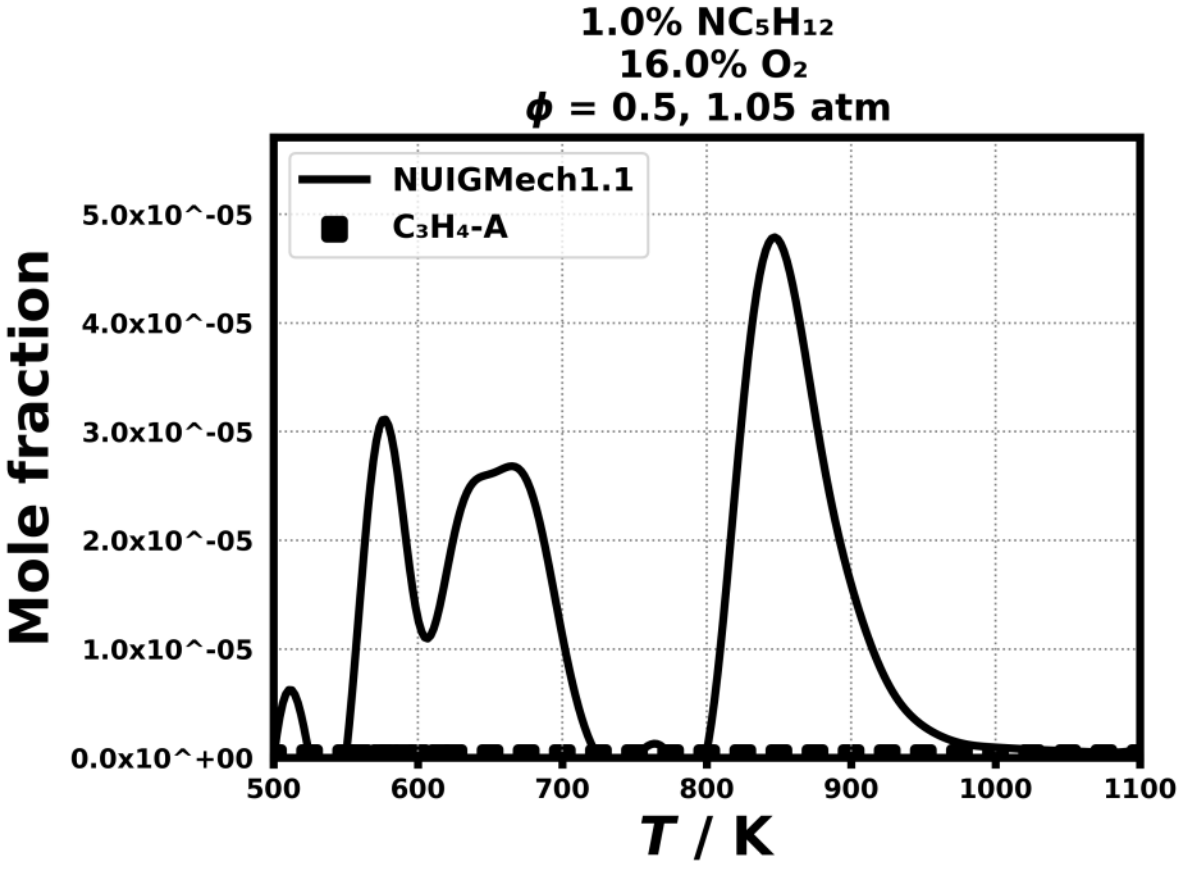

Figure 42: Dataset: 1.05_ATM_PHI_0.5

1.3.13 Case: n-C5H12/JSR/BUGLER/1.05_ATM_PHI_0.5

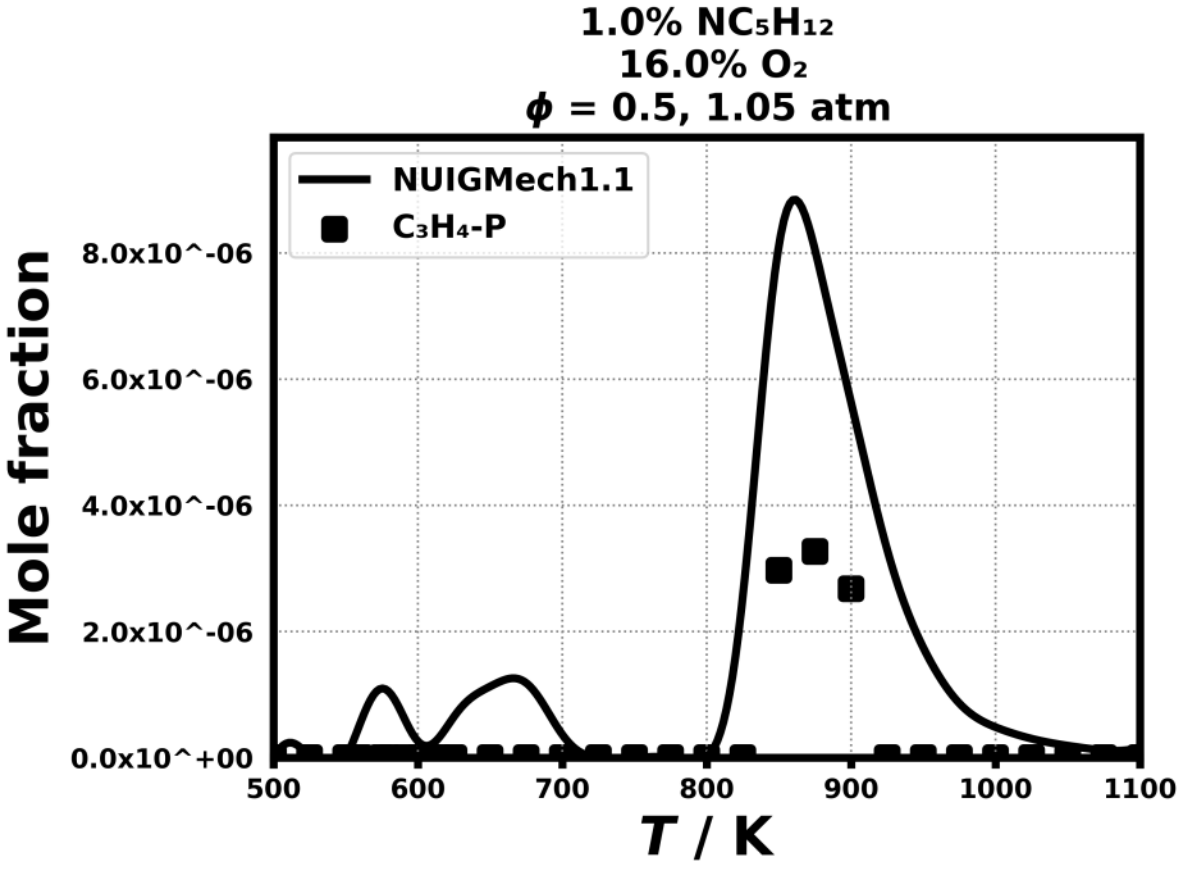

Figure 43: Dataset: 1.05_ATM_PHI_0.5

1.3.14 Case: n-C5H12/JSR/BUGLER/1.05_ATM_PHI_0.5

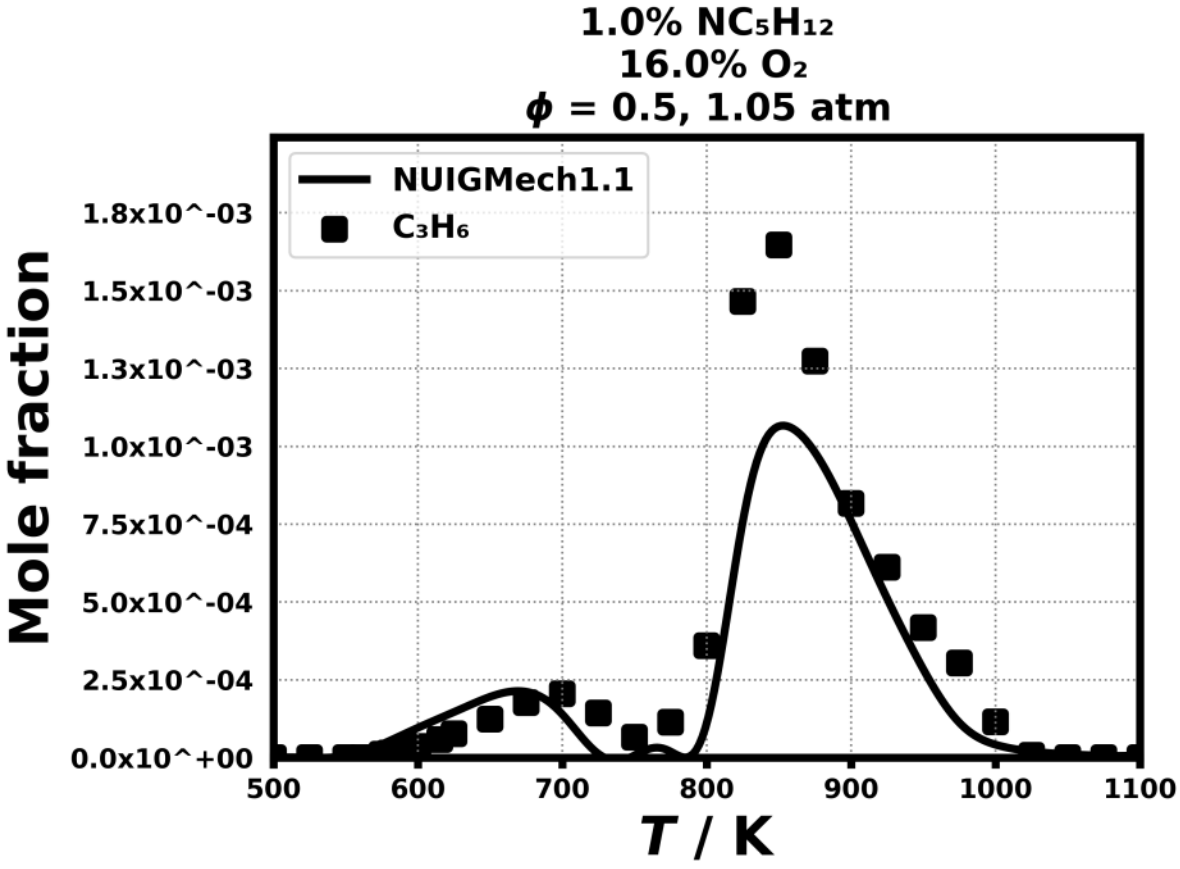

Figure 44: Dataset: 1.05_ATM_PHI_0.5

1.3.15 Case: n-C5H12/JSR/BUGLER/1.05_ATM_PHI_0.5

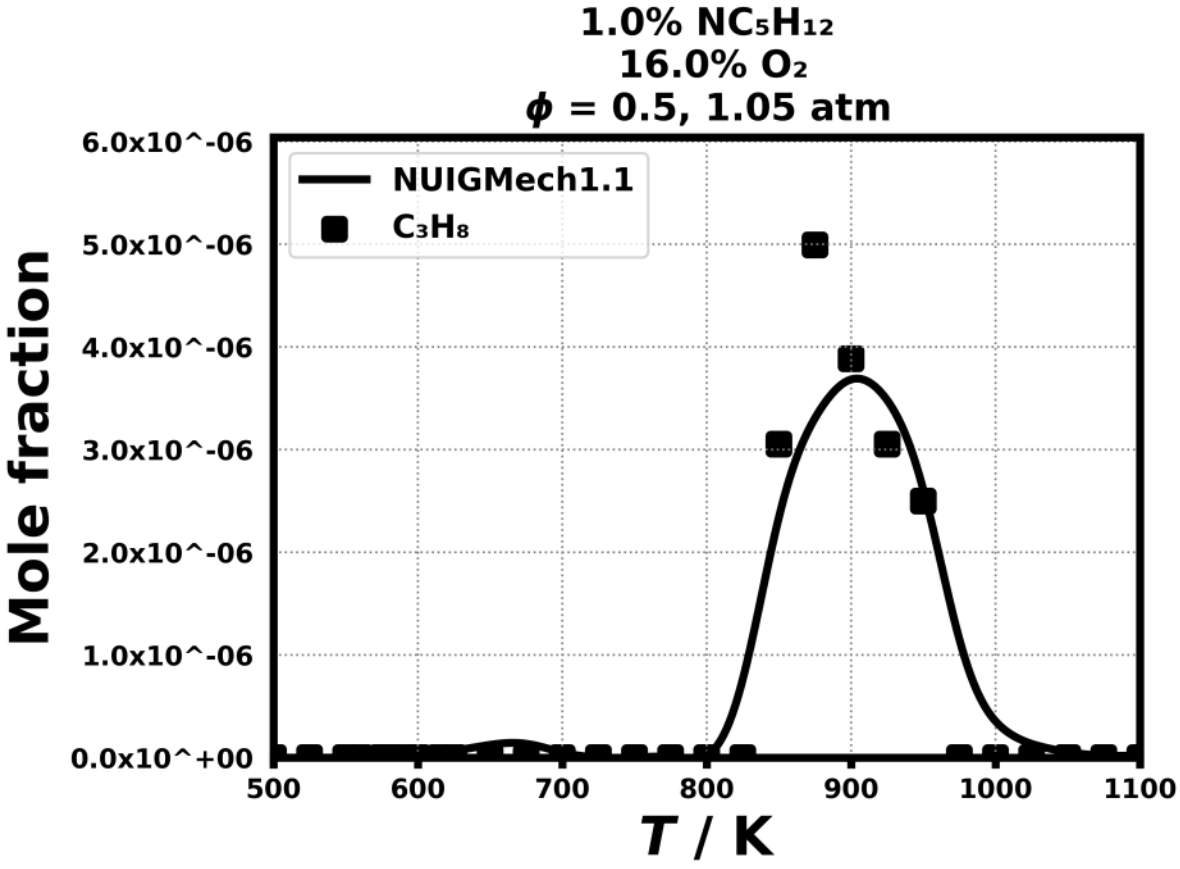

Figure 45: Dataset: 1.05_ATM_PHI_0.5

1.3.16 Case: n-C5H12/JSR/BUGLER/1.05_ATM_PHI_0.5

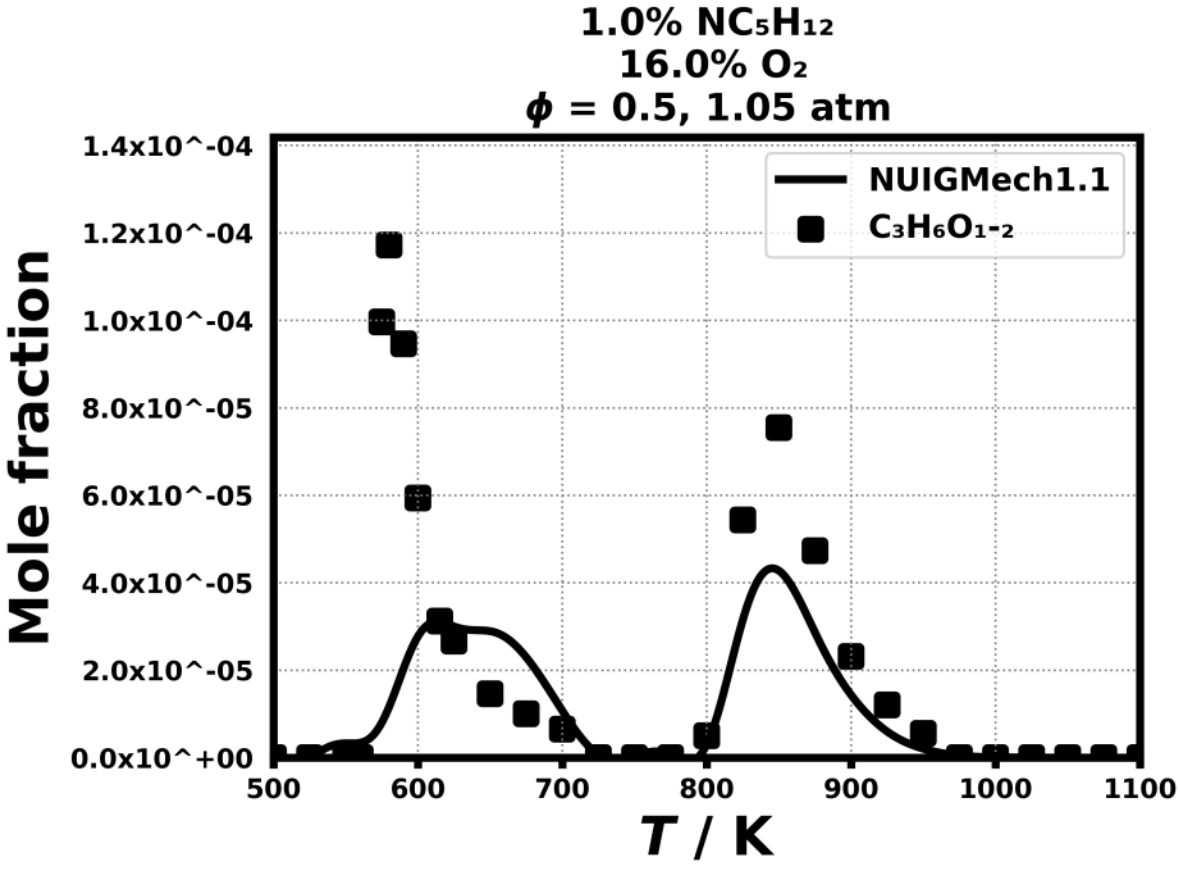

Figure 46: Dataset: 1.05_ATM_PHI_0.5

1.3.19 Case: n-C5H12/JSR/BUGLER/1.05_ATM_PHI_0.5

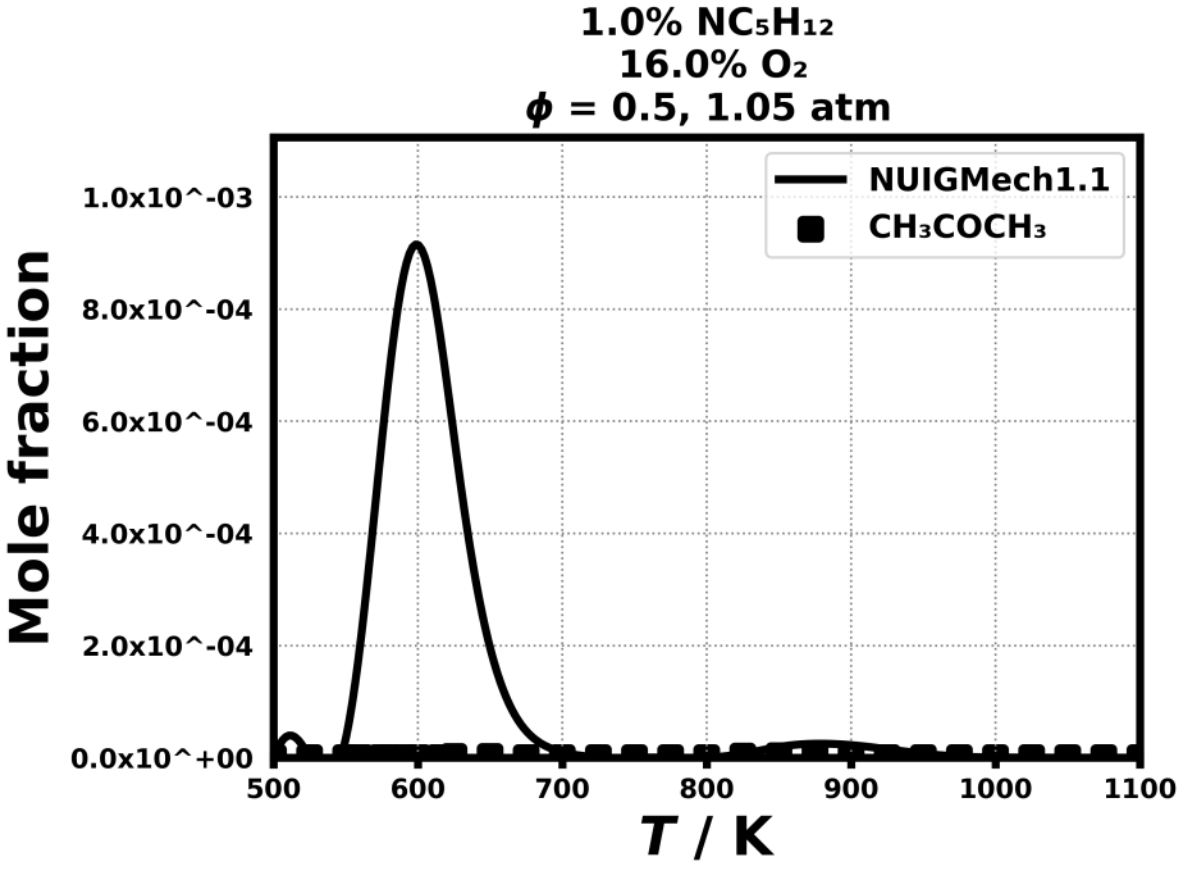

Figure 49: Dataset: 1.05_ATM_PHI_0.5

1.3.21 Case: n-C5H12/JSR/BUGLER/1.05_ATM_PHI_0.5

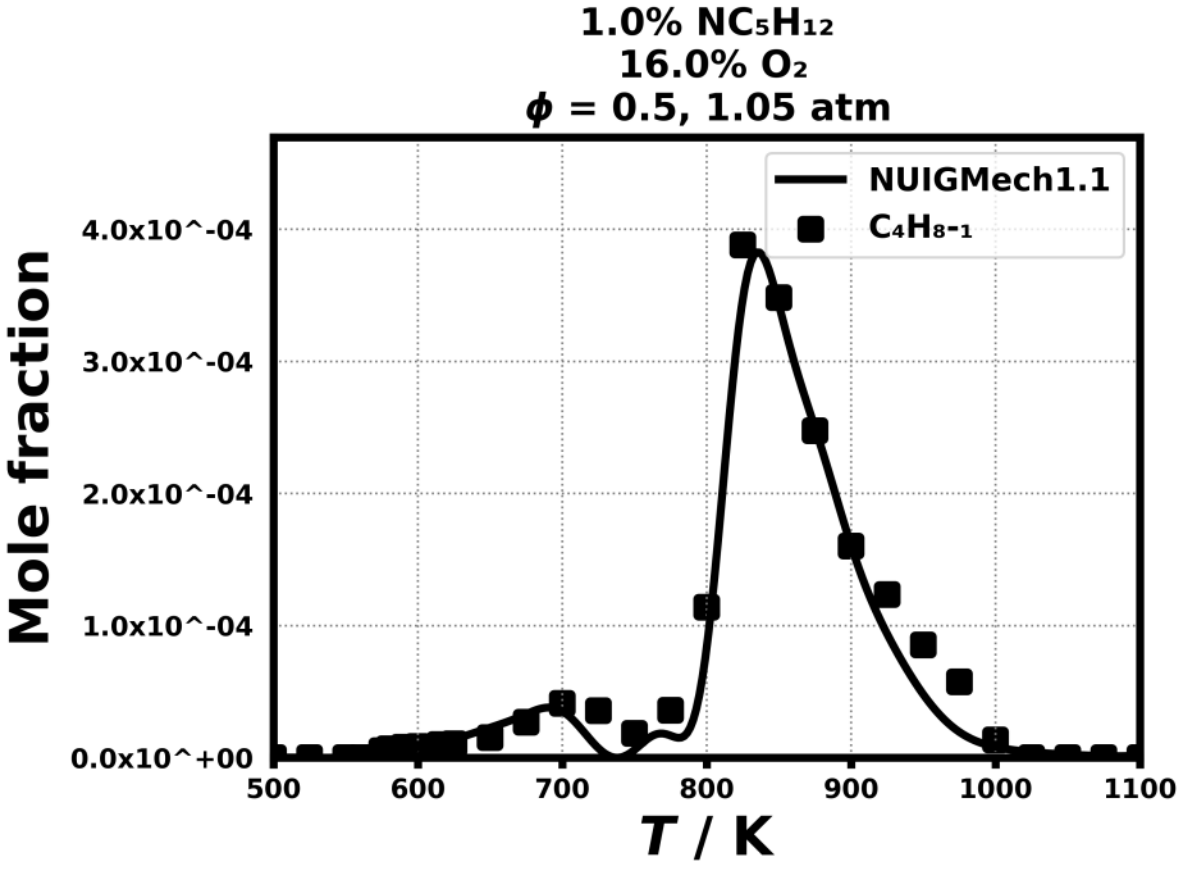

Figure 51: Dataset: 1.05_ATM_PHI_0.5

1.3.22 Case: n-C5H12/JSR/BUGLER/1.05_ATM_PHI_0.5

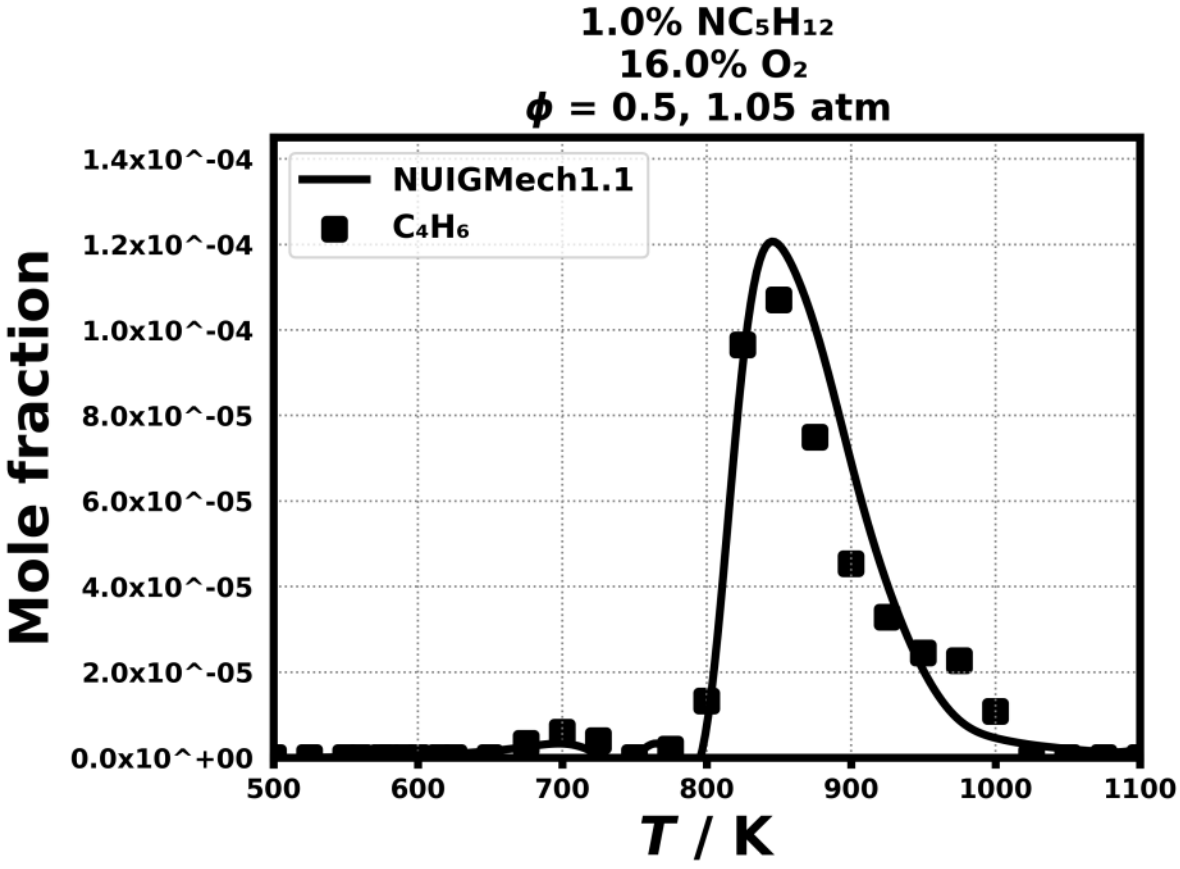

Figure 52: Dataset: 1.05_ATM_PHI_0.5

1.3.24 Case: n-C5H12/JSR/BUGLER/1.05_ATM_PHI_0.5

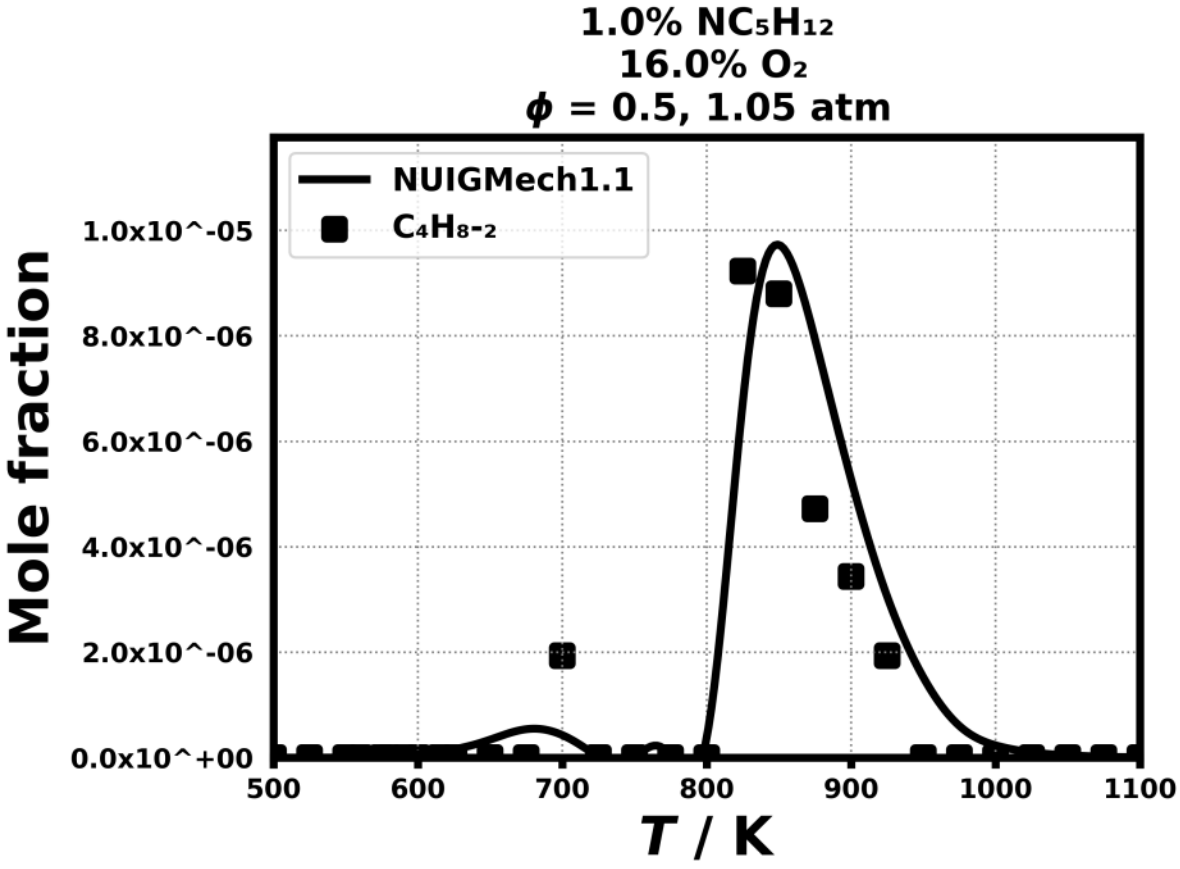

Figure 54: Dataset: 1.05_ATM_PHI_0.5

1.3.26 Case: n-C5H12/JSR/BUGLER/1.05_ATM_PHI_0.5

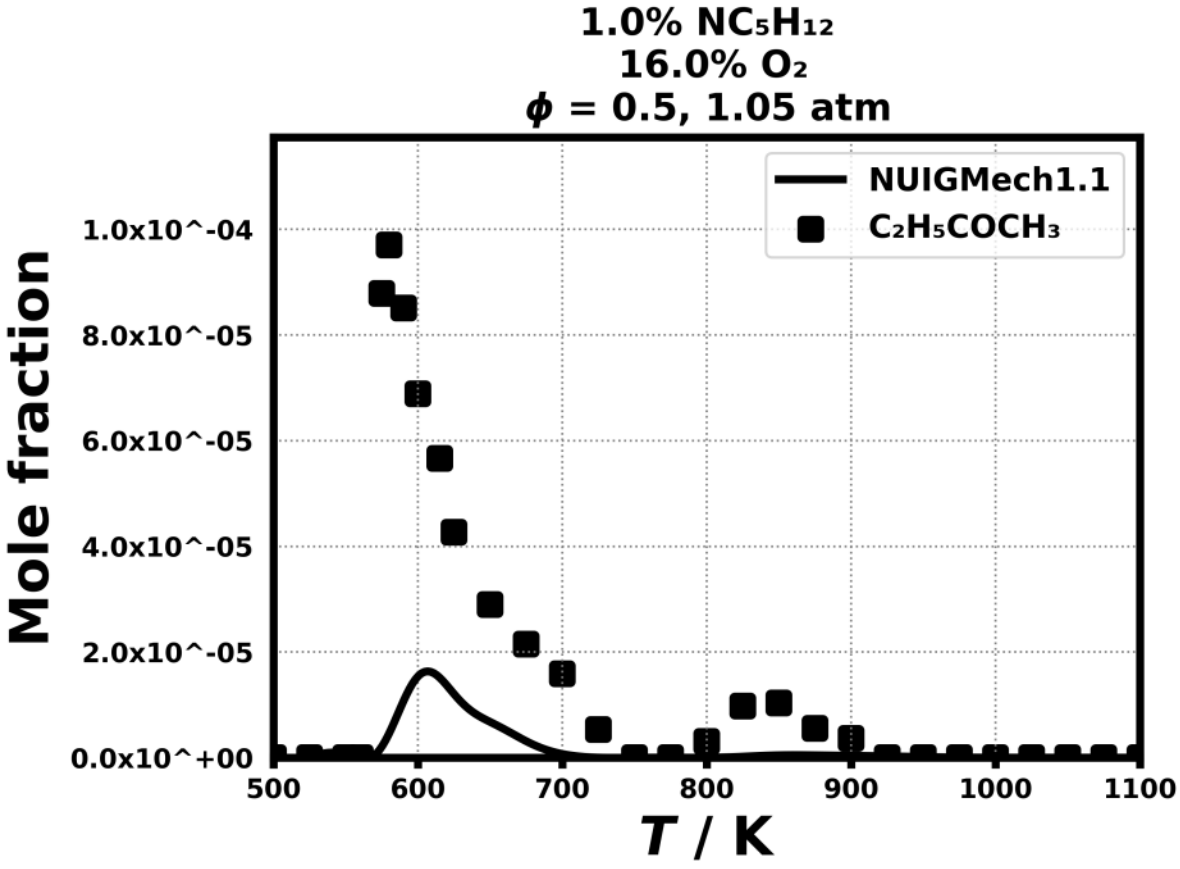

Figure 56: Dataset: 1.05_ATM_PHI_0.5

1.3.27 Case: n-C5H12/JSR/BUGLER/1.05_ATM_PHI_0.5

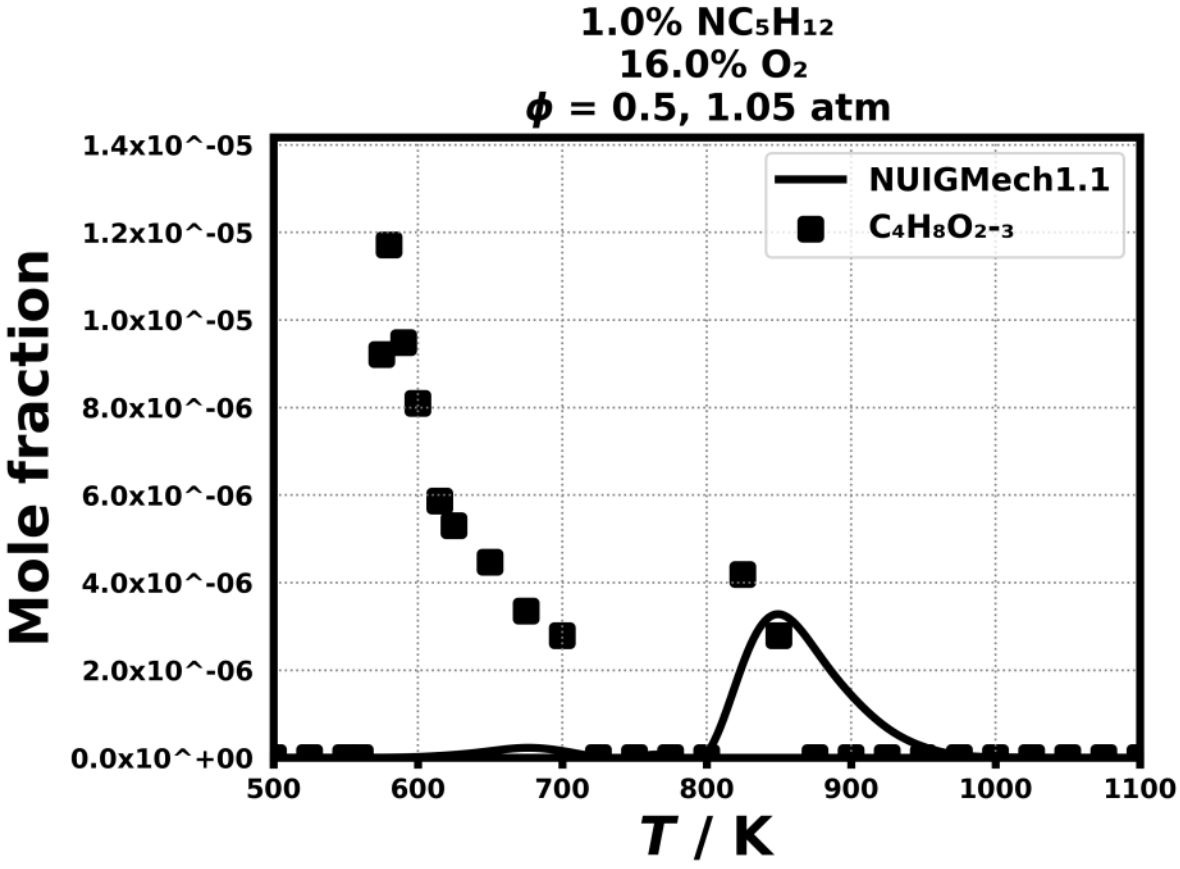

Figure 57: Dataset: 1.05_ATM_PHI_0.5

1.3.28 Case: n-C5H12/JSR/BUGLER/1.05_ATM_PHI_0.5

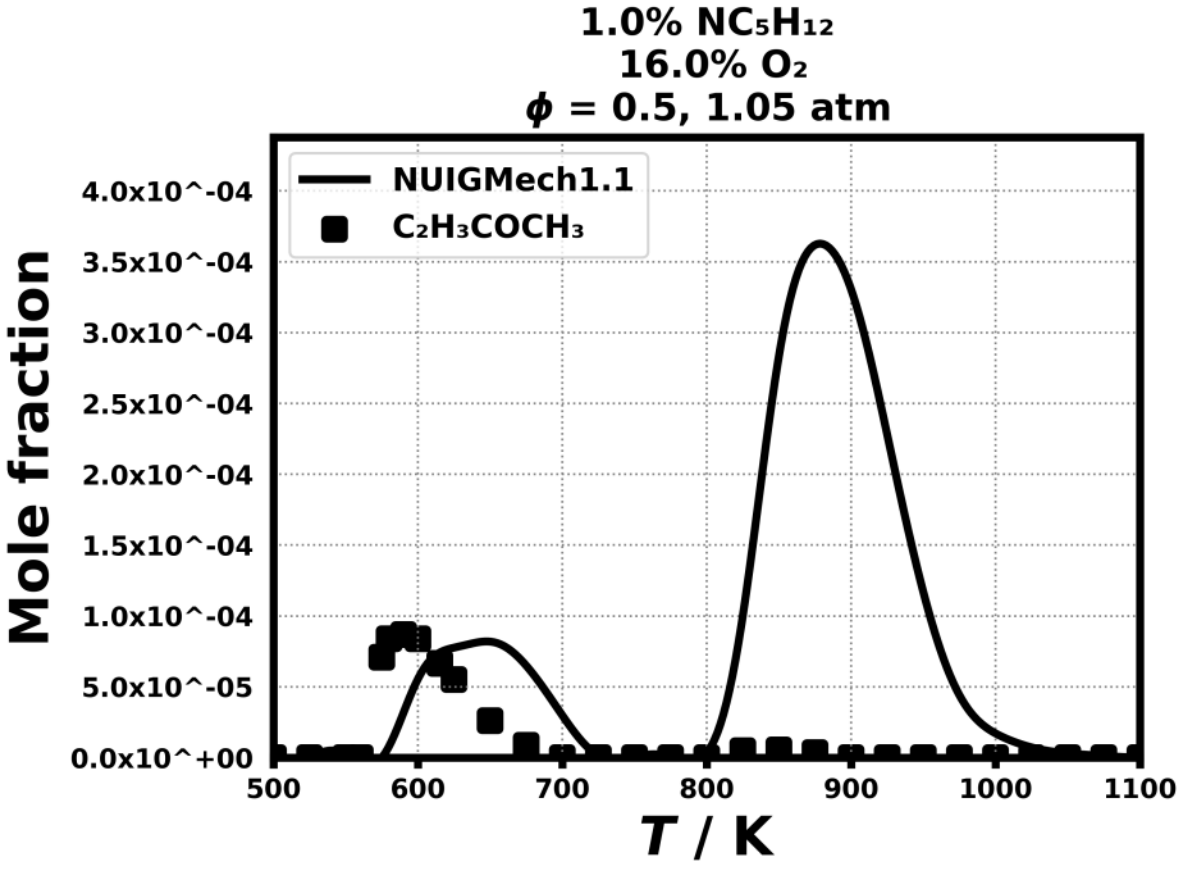

Figure 58: Dataset: 1.05_ATM_PHI_0.5

1.3.29 Case: n-C5H12/JSR/BUGLER/1.05_ATM_PHI_0.5

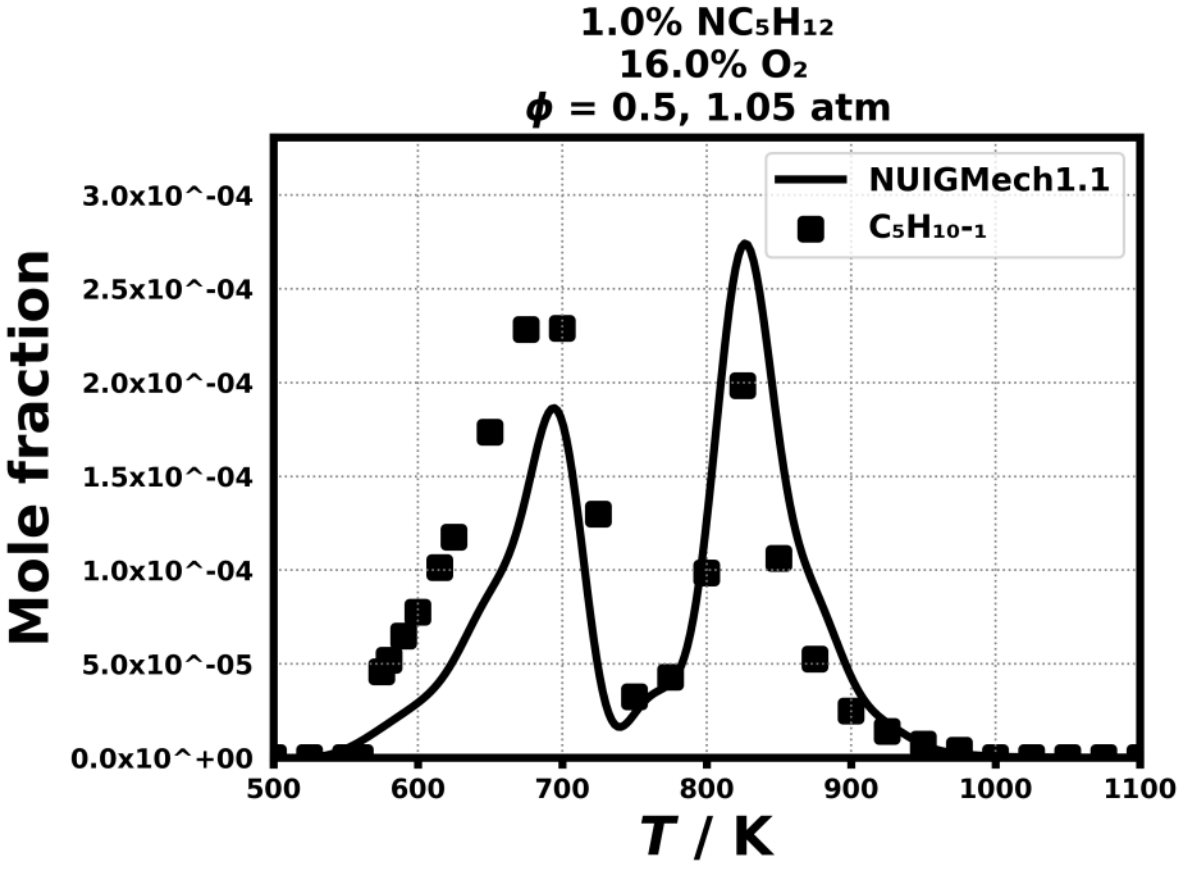

Figure 59: Dataset: 1.05_ATM_PHI_0.5

1.3.30 Case: n-C5H12/JSR/BUGLER/1.05_ATM_PHI_0.5

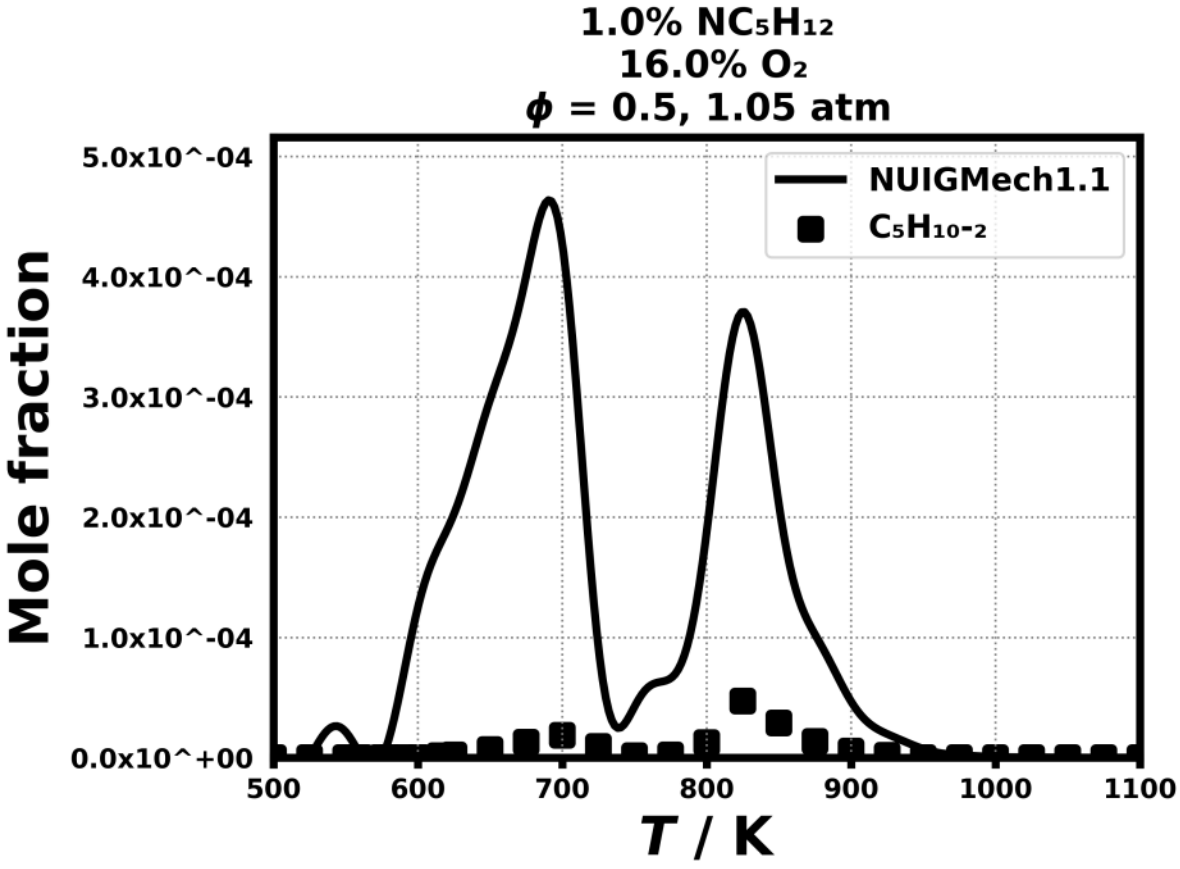

Figure 60: Dataset: 1.05_ATM_PHI_0.5

1.3.31 Case: n-C5H12/JSR/BUGLER/1.05_ATM_PHI_0.5

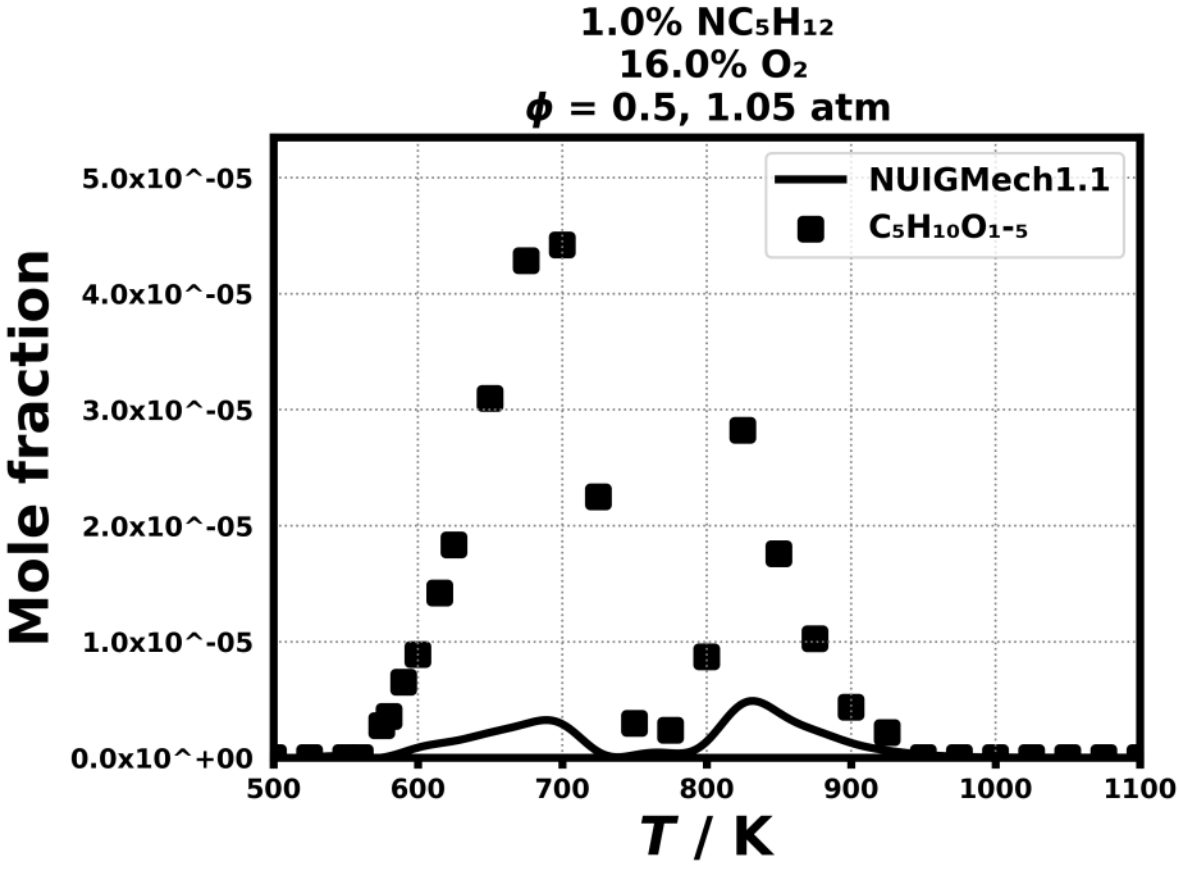

Figure 61: Dataset: 1.05_ATM_PHI_0.5

1.3.32 Case: n-C5H12/JSR/BUGLER/1.05_ATM_PHI_0.5

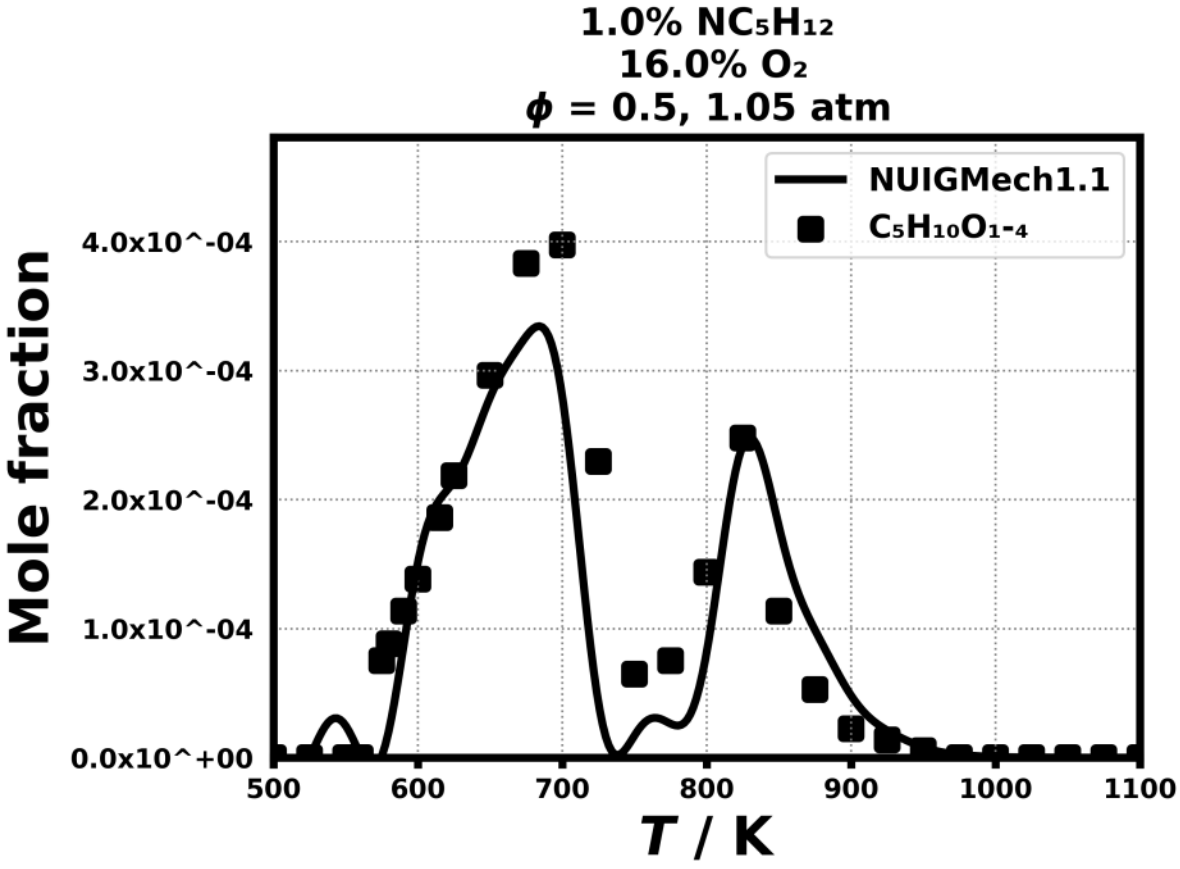

Figure 62: Dataset: 1.05_ATM_PHI_0.5

1.3.33 Case: n-C5H12/JSR/BUGLER/1.05_ATM_PHI_0.5

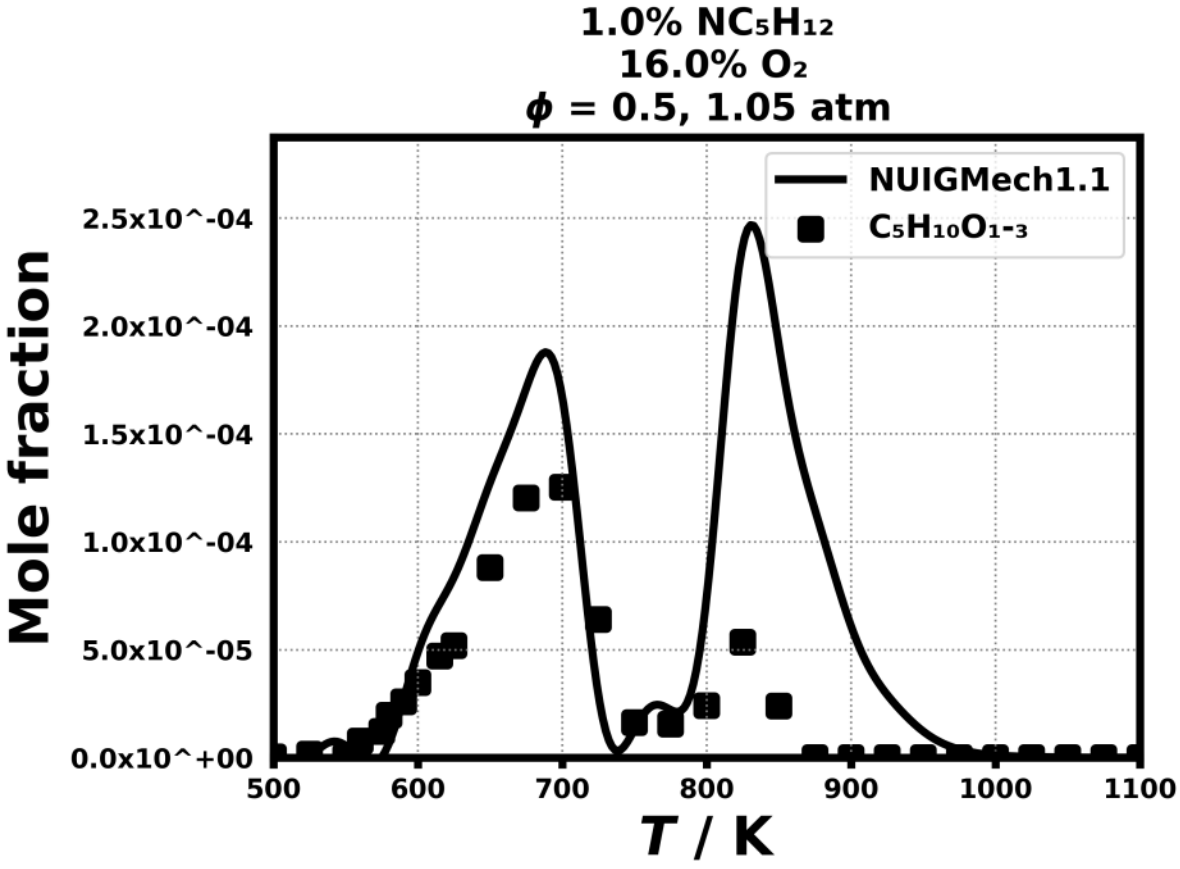

Figure 63: Dataset: 1.05_ATM_PHI_0.5

1.3.34 Case: n-C5H12/JSR/BUGLER/1.05_ATM_PHI_0.5

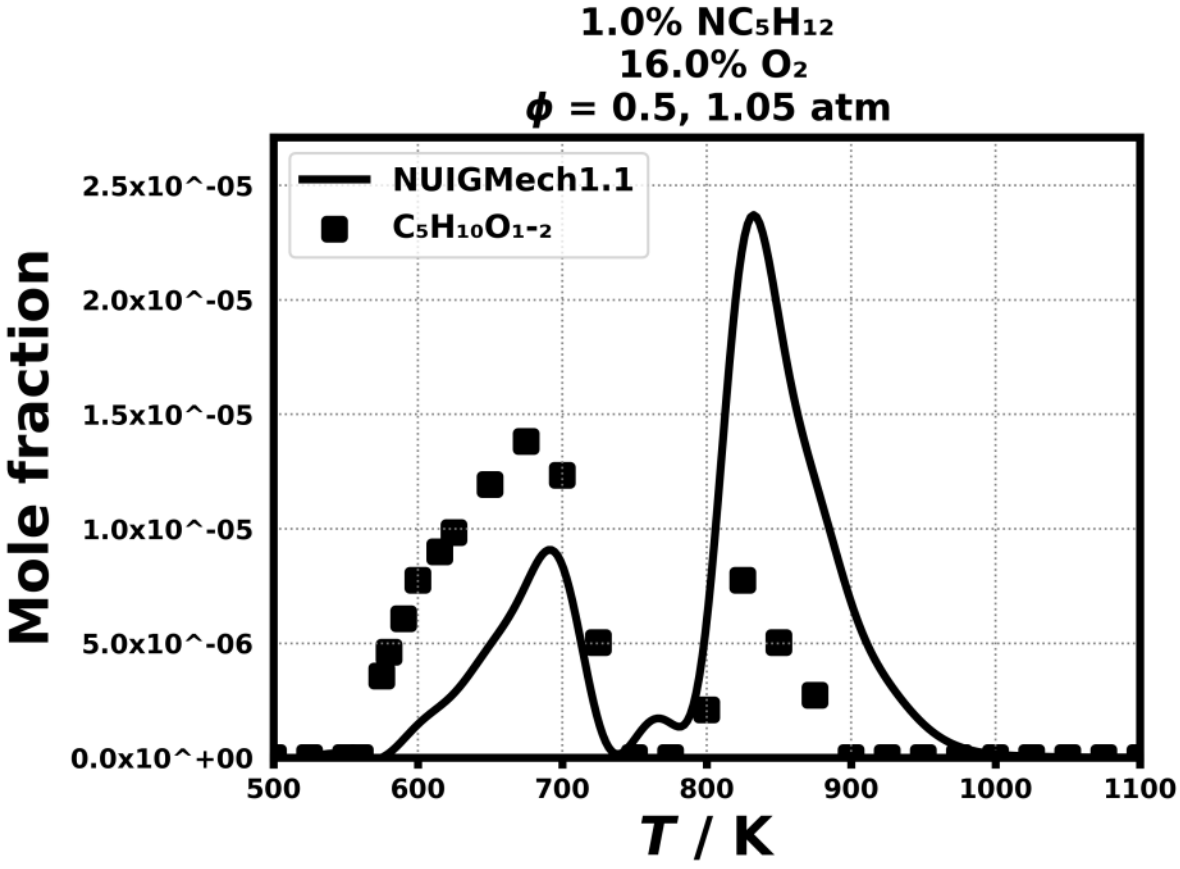

Figure 64: Dataset: 1.05_ATM_PHI_0.5

1.3.35 Case: n-C5H12/JSR/BUGLER/1.05_ATM_PHI_0.5

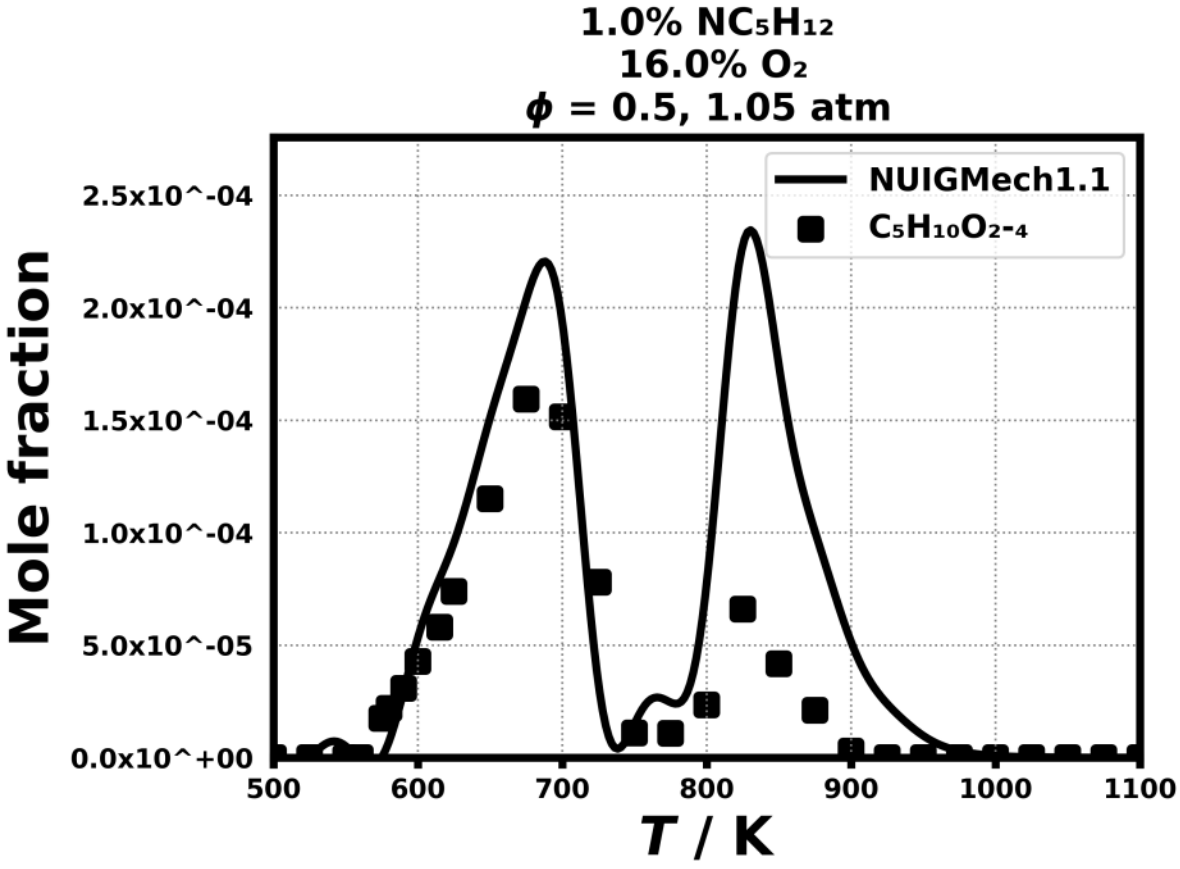

Figure 65: Dataset: 1.05_ATM_PHI_0.5

1.3.36 Case: n-C5H12/JSR/BUGLER/1.05_ATM_PHI_0.5

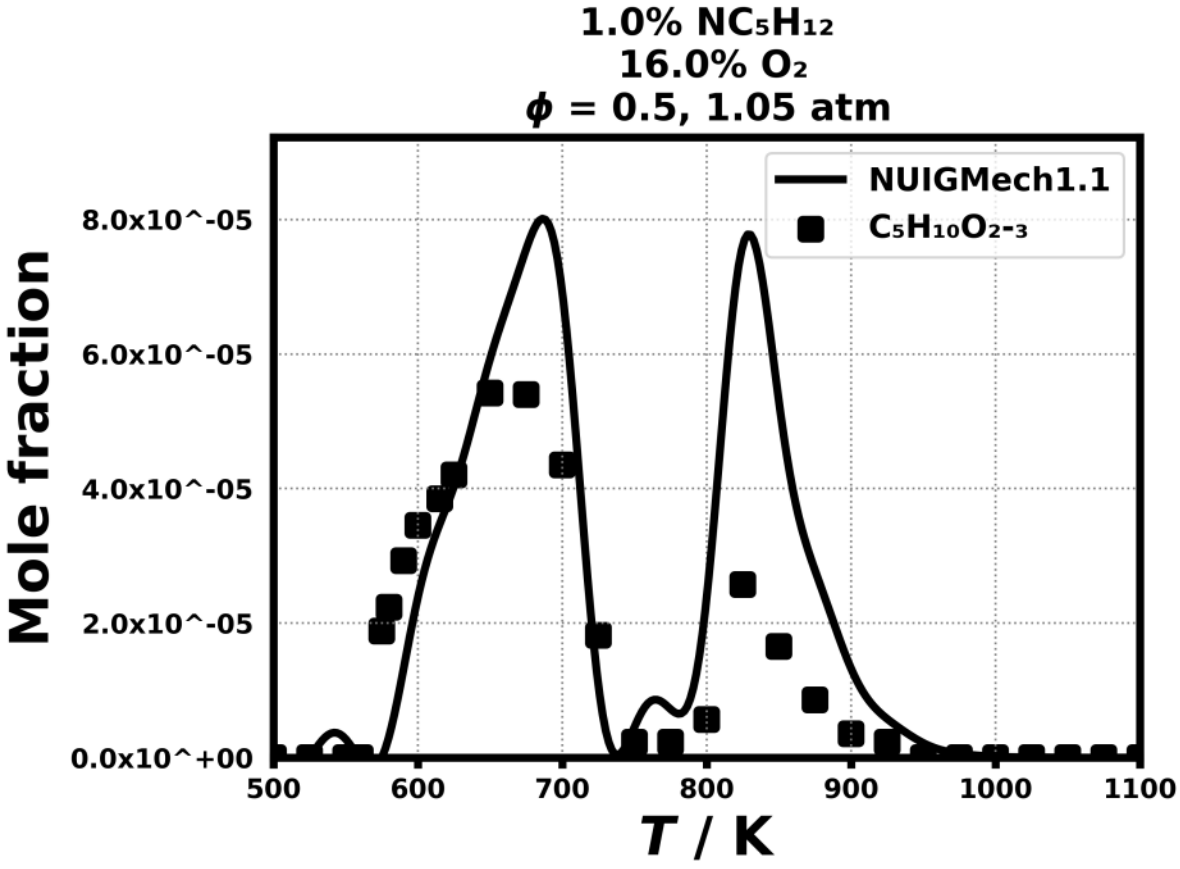

Figure 66: Dataset: 1.05_ATM_PHI_0.5

1.3.37 Case: n-C5H12/JSR/BUGLER/1.05_ATM_PHI_0.5

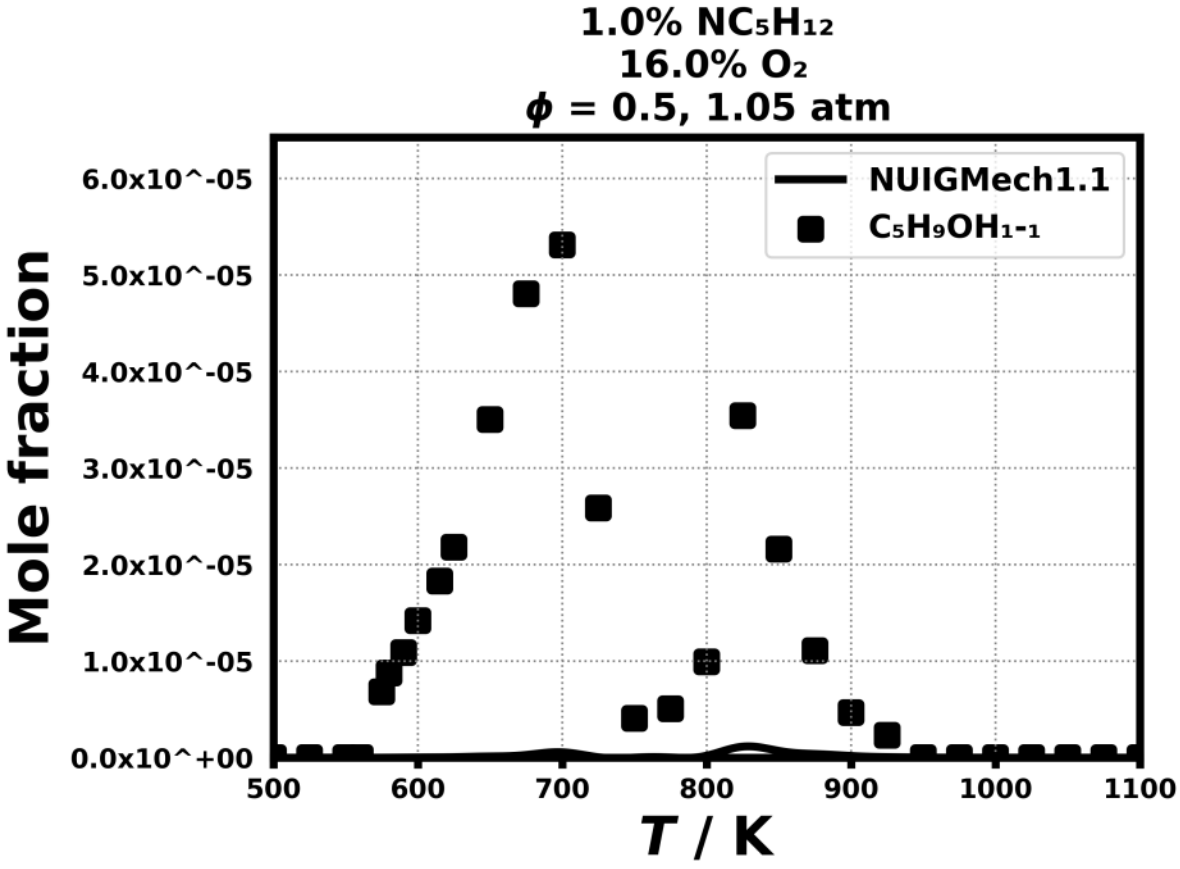

Figure 67: Dataset: 1.05_ATM_PHI_0.5

1.3.38 Case: n-C5H12/JSR/BUGLER/1.05_ATM_PHI_0.5

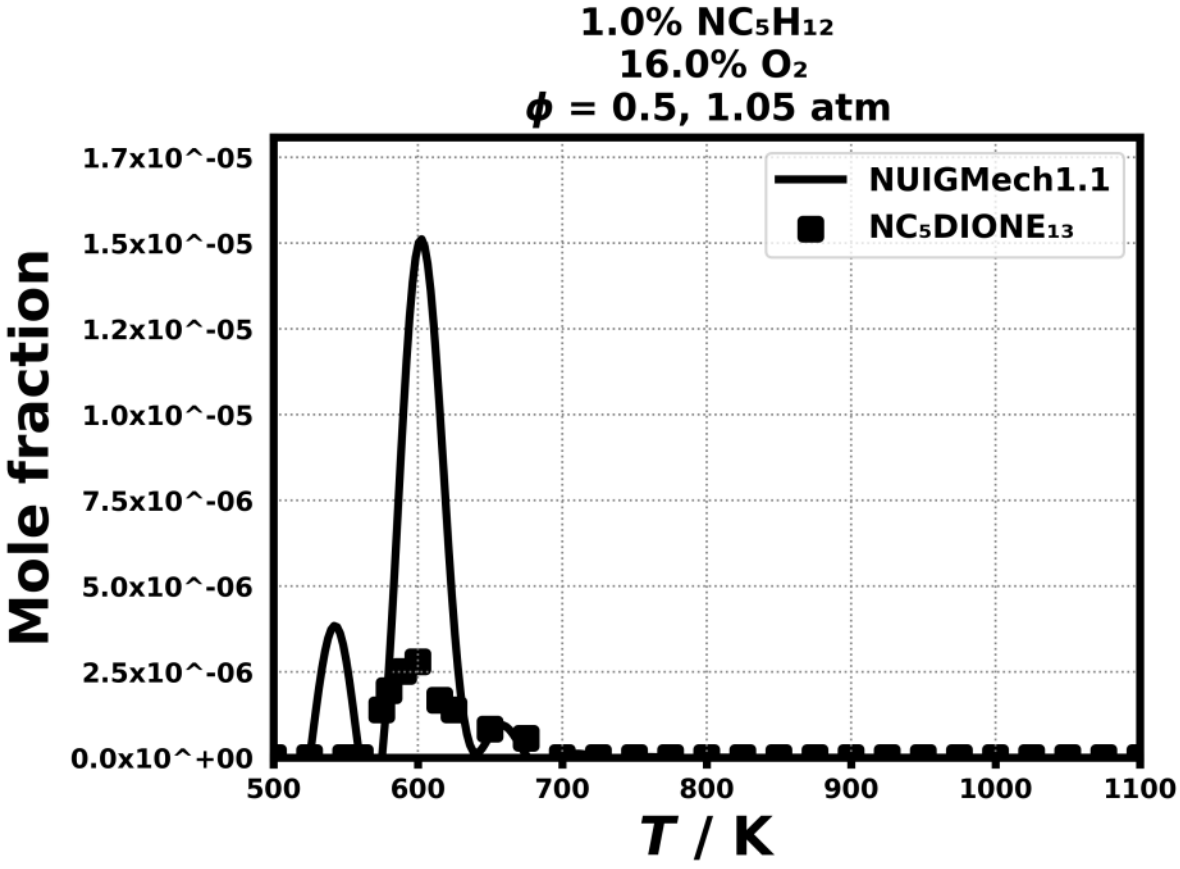

Figure 68: Dataset: 1.05_ATM_PHI_0.5

1.3.39 Case: n-C5H12/JSR/BUGLER/1.05_ATM_PHI_0.5

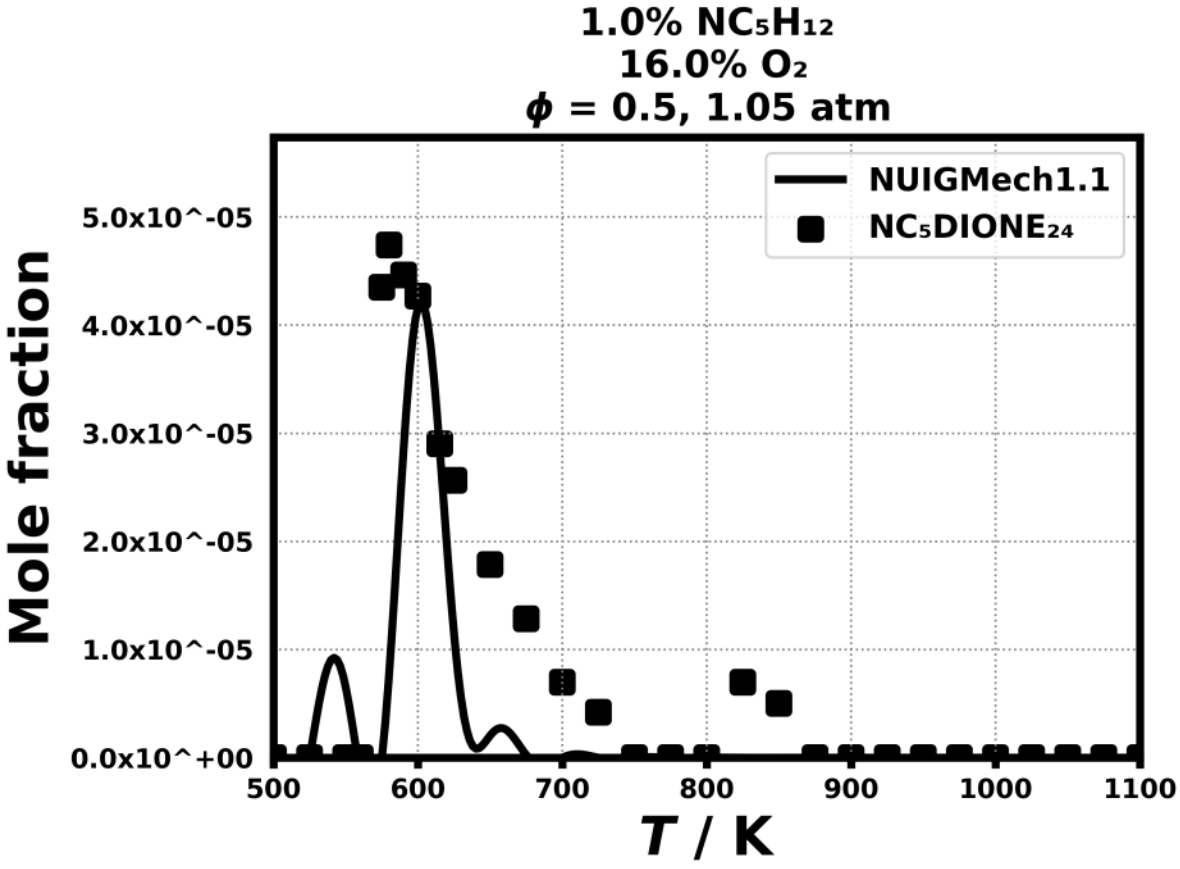

Figure 69: Dataset: 1.05_ATM_PHI_0.5

1.3.40 Case: n-C5H12/JSR/BUGLER/1.05_ATM_PHI_1.0

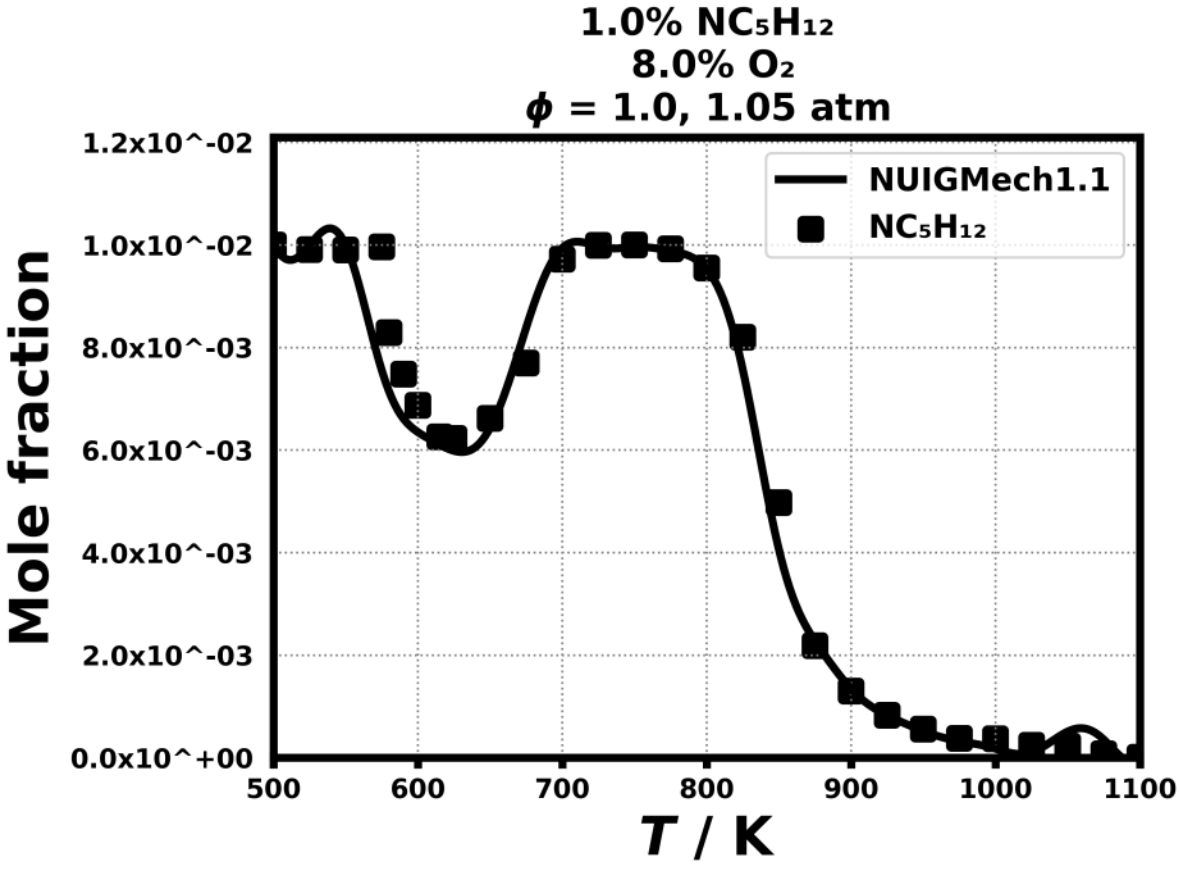

Figure 70: Dataset: 1.05_ATM_PHI_1.0

1.3.41 Case: n-C5H12/JSR/BUGLER/1.05_ATM_PHI_1.0

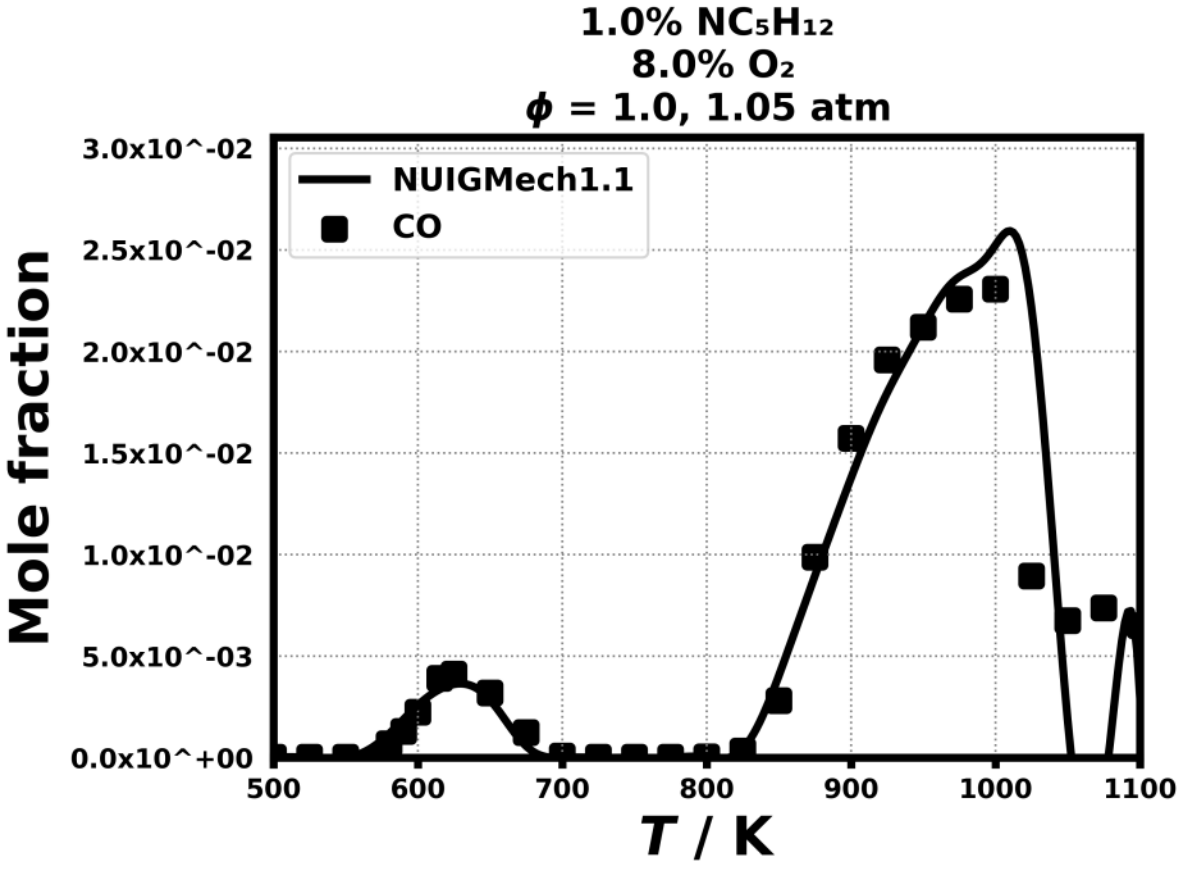

Figure 71: Dataset: 1.05_ATM_PHI_1.0

1.3.42 Case: n-C5H12/JSR/BUGLER/1.05_ATM_PHI_1.0

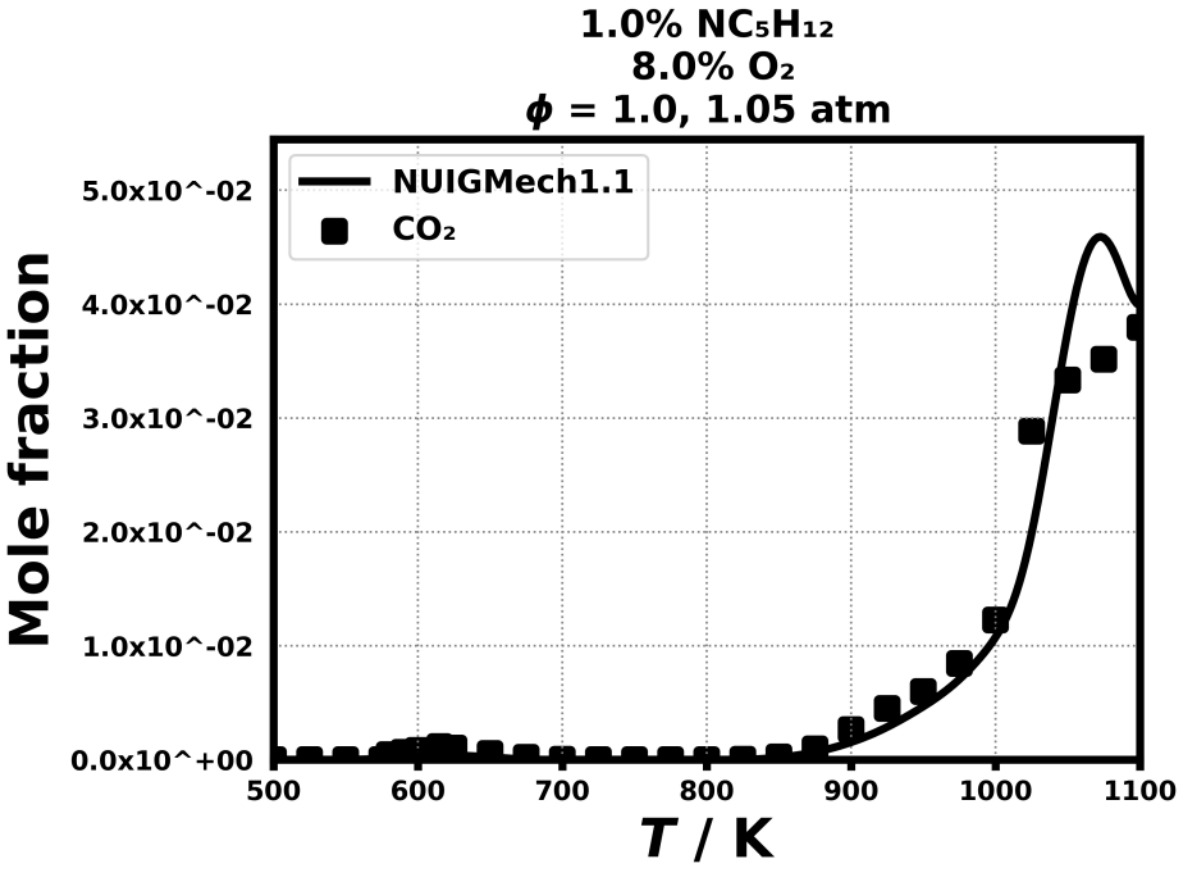

Figure 72: Dataset: 1.05_ATM_PHI_1.0

1.3.43 Case: n-C5H12/JSR/BUGLER/1.05_ATM_PHI_1.0

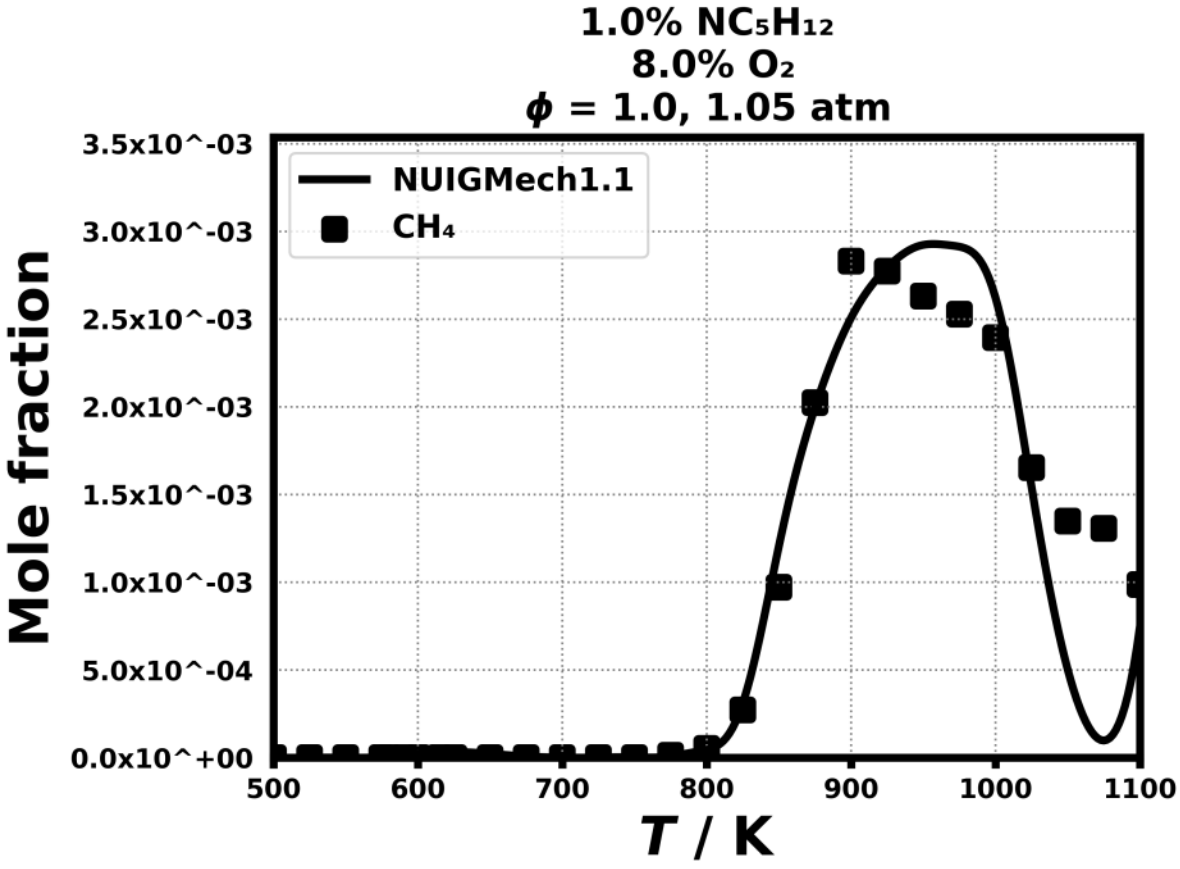

Figure 73: Dataset: 1.05_ATM_PHI_1.0

1.3.44 Case: n-C5H12/JSR/BUGLER/1.05_ATM_PHI_1.0

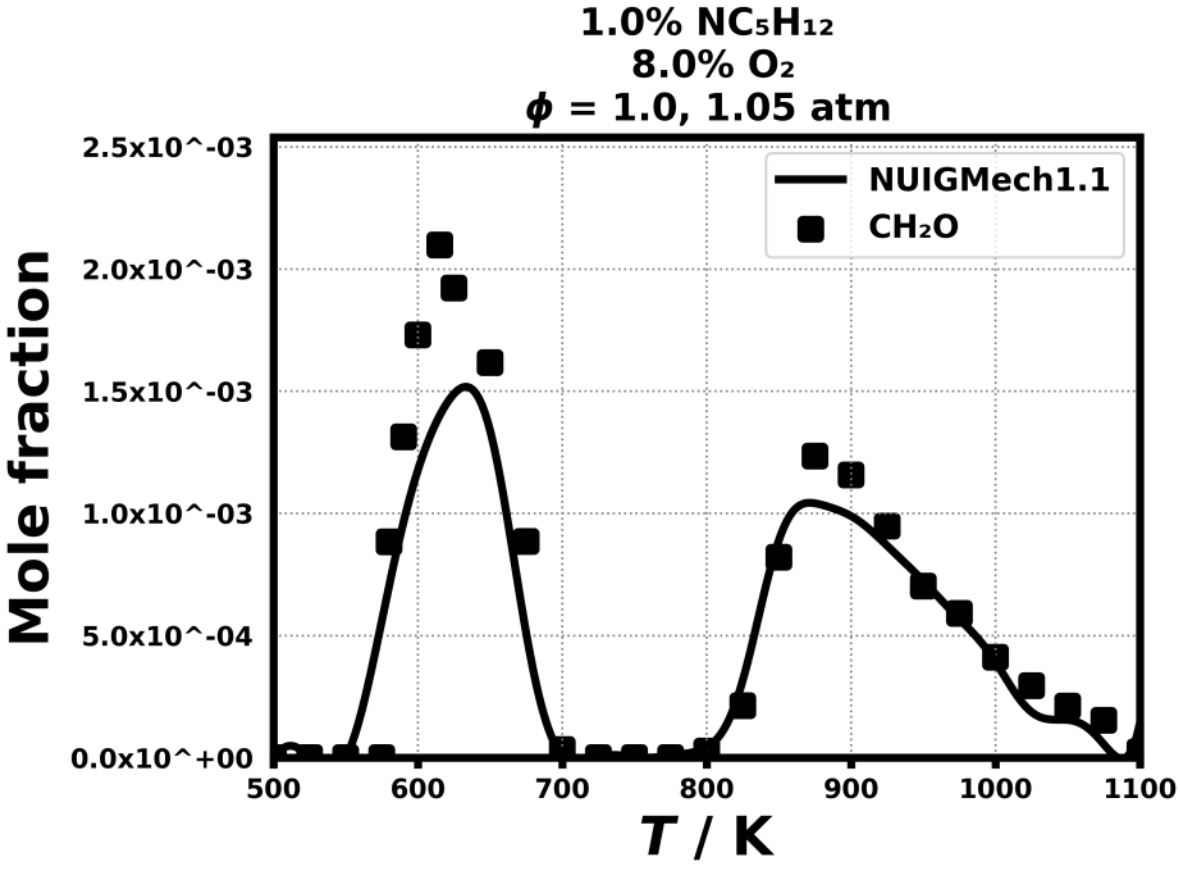

Figure 74: Dataset: 1.05_ATM_PHI_1.0

1.3.45 Case: n-C5H12/JSR/BUGLER/1.05_ATM_PHI_1.0

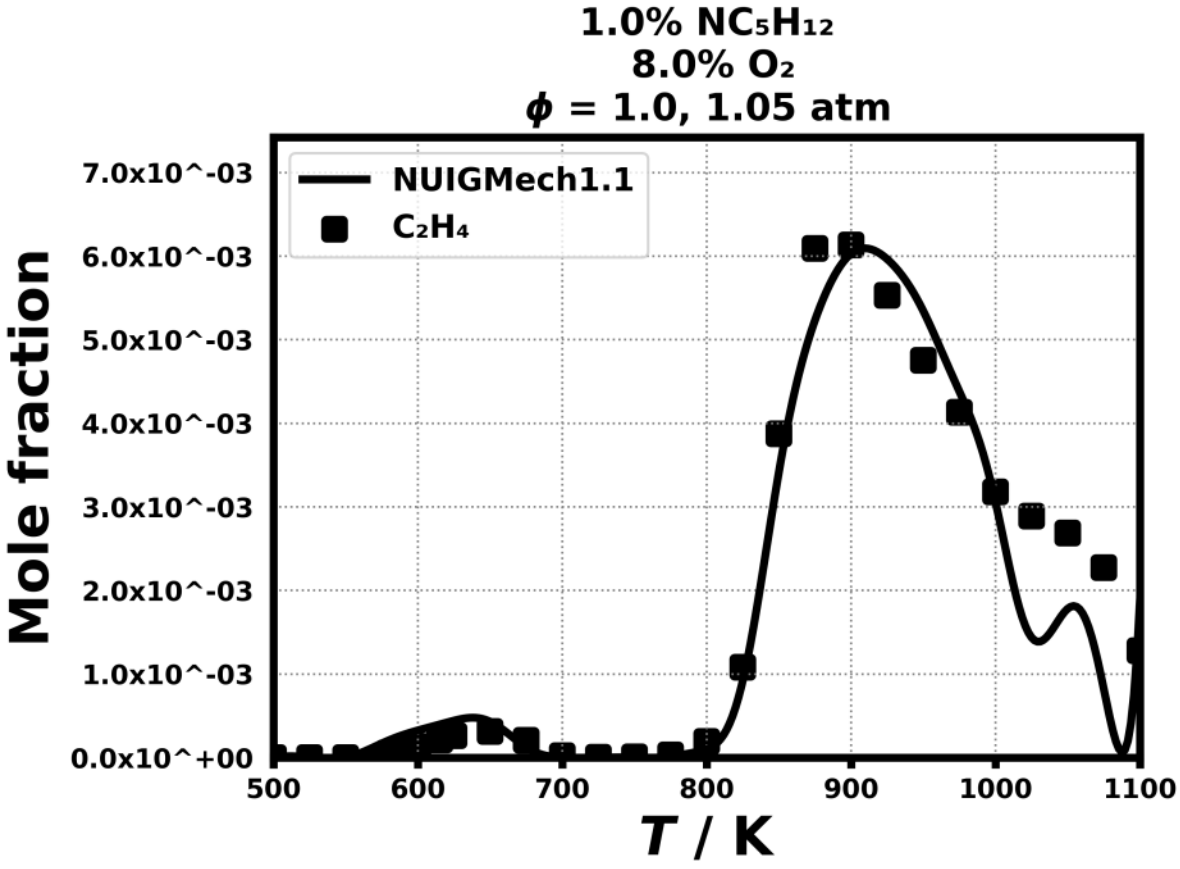

Figure 75: Dataset: 1.05_ATM_PHI_1.0

1.3.46 Case: n-C5H12/JSR/BUGLER/1.05_ATM_PHI_1.0

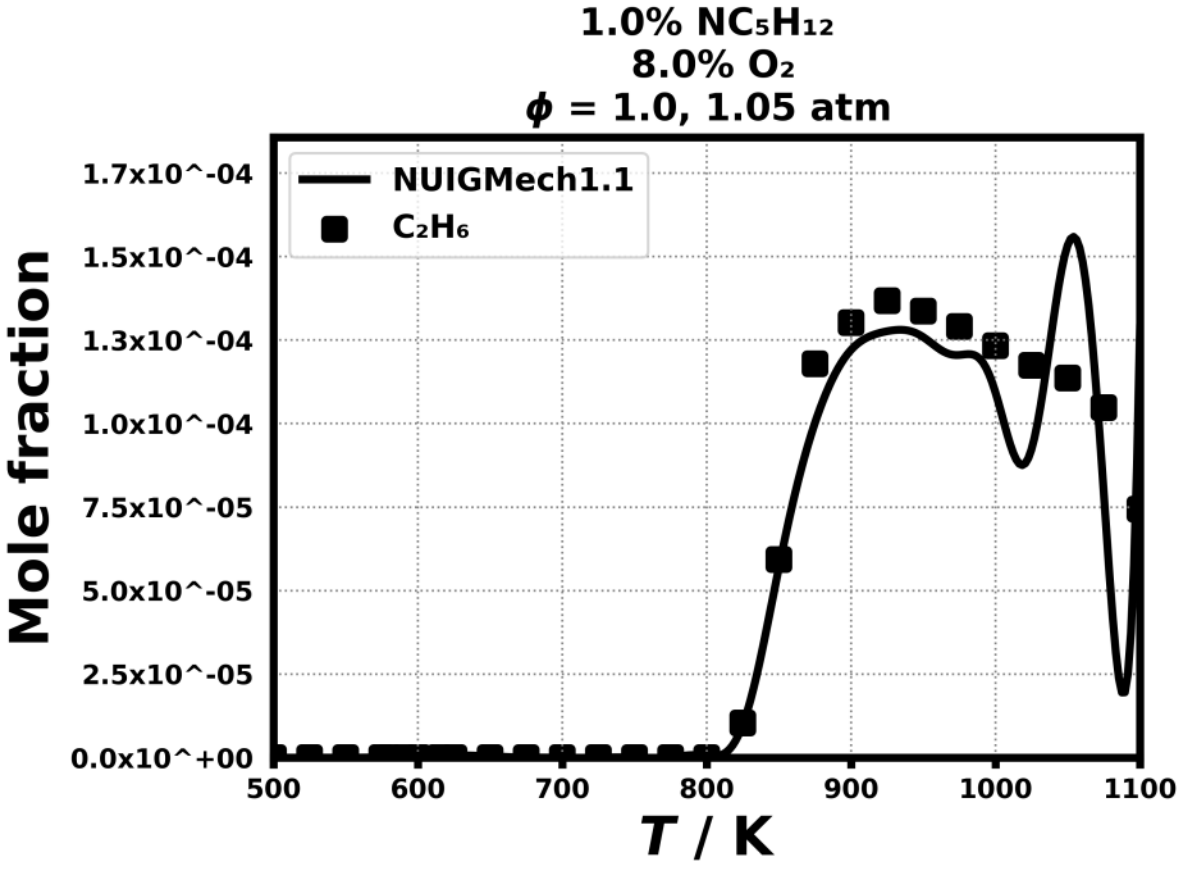

Figure 76: Dataset: 1.05_ATM_PHI_1.0

1.3.47 Case: n-C5H12/JSR/BUGLER/1.05_ATM_PHI_1.0

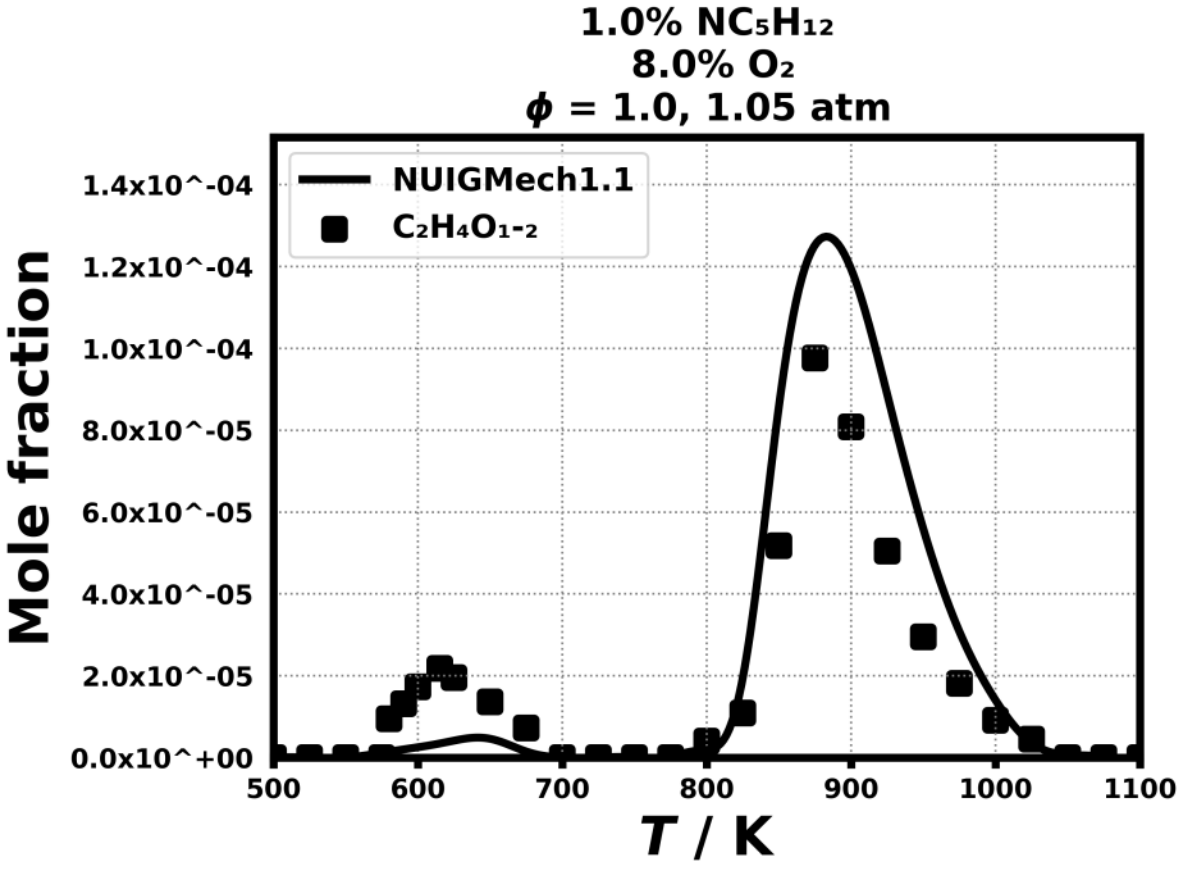

Figure 77: Dataset: 1.05_ATM_PHI_1.0

1.3.48 Case: n-C5H12/JSR/BUGLER/1.05_ATM_PHI_1.0

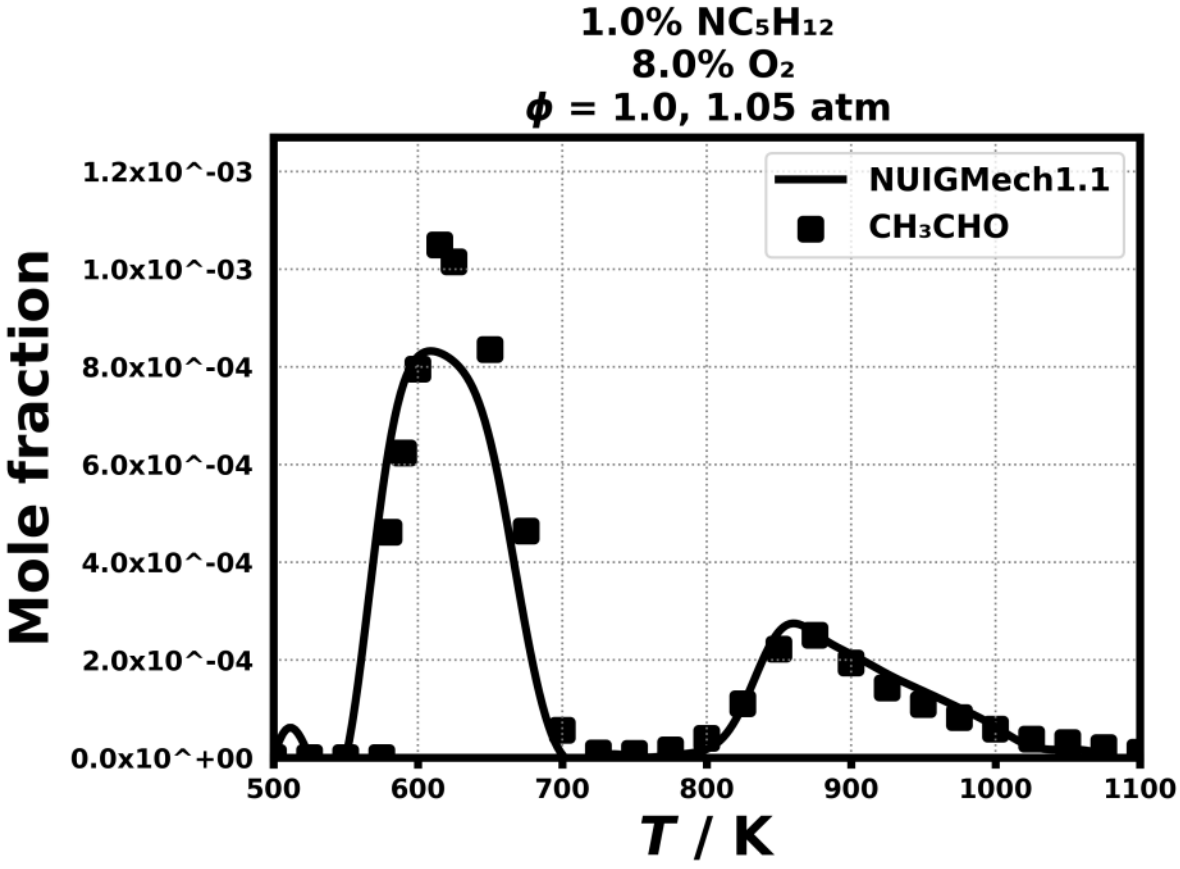

Figure 78: Dataset: 1.05_ATM_PHI_1.0

1.3.49 Case: n-C5H12/JSR/BUGLER/1.05_ATM_PHI_1.0

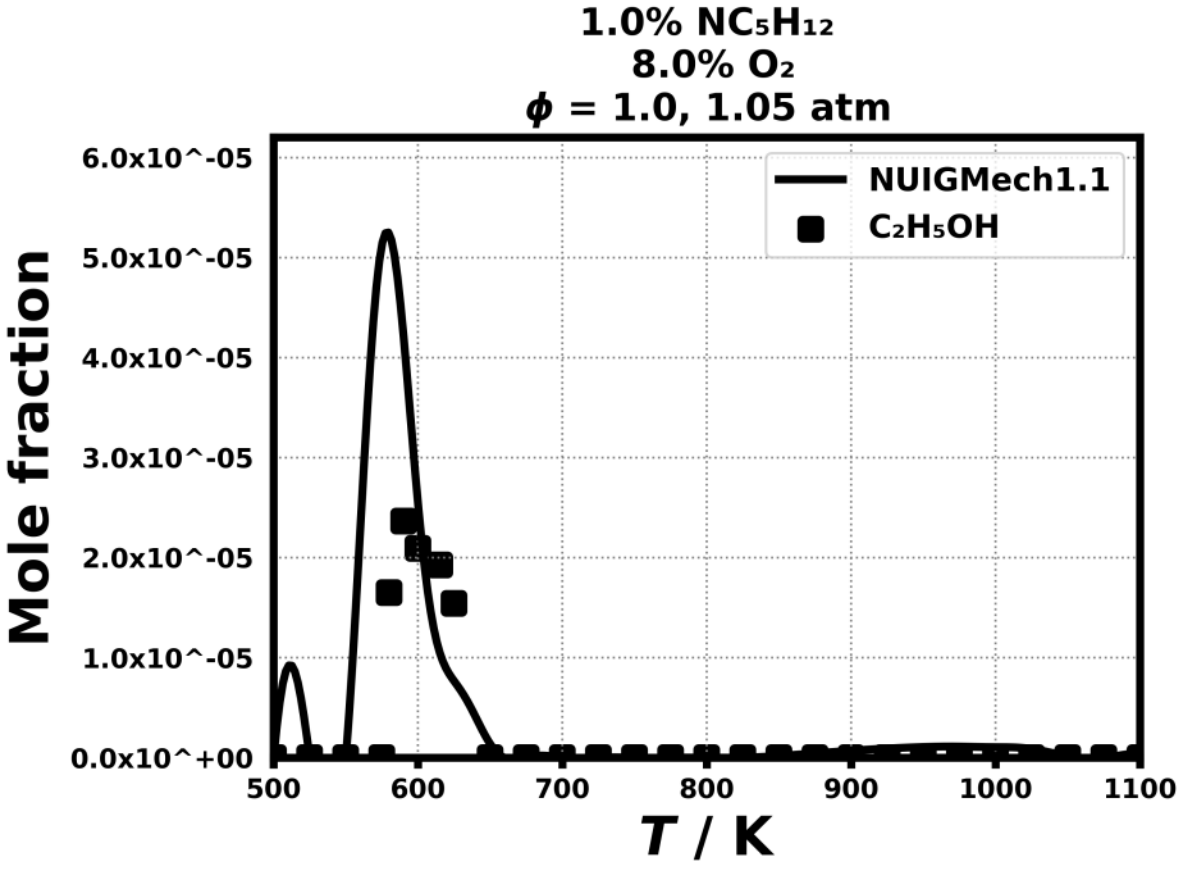

Figure 79: Dataset: 1.05_ATM_PHI_1.0

1.3.50 Case: n-C5H12/JSR/BUGLER/1.05_ATM_PHI_1.0

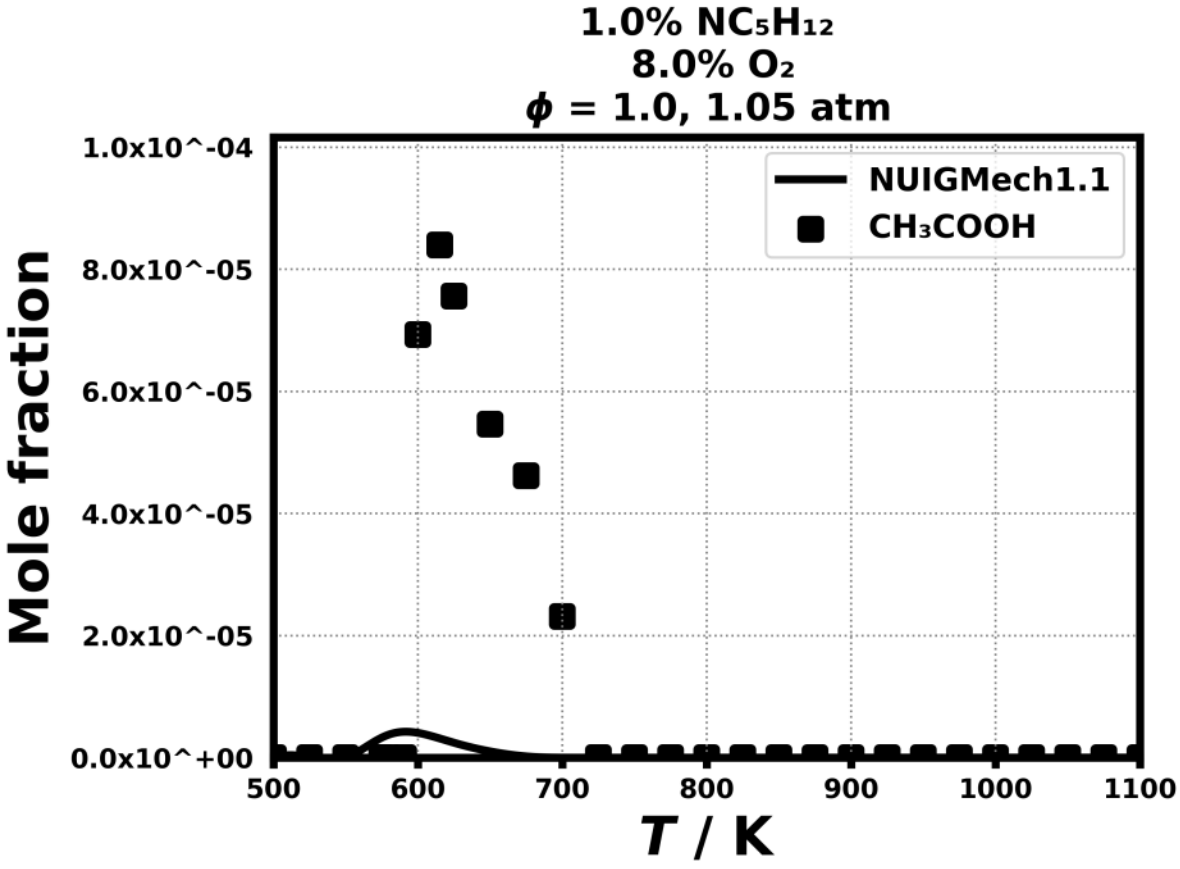

Figure 80: Dataset: 1.05_ATM_PHI_1.0

1.3.51 Case: n-C5H12/JSR/BUGLER/1.05_ATM_PHI_1.0

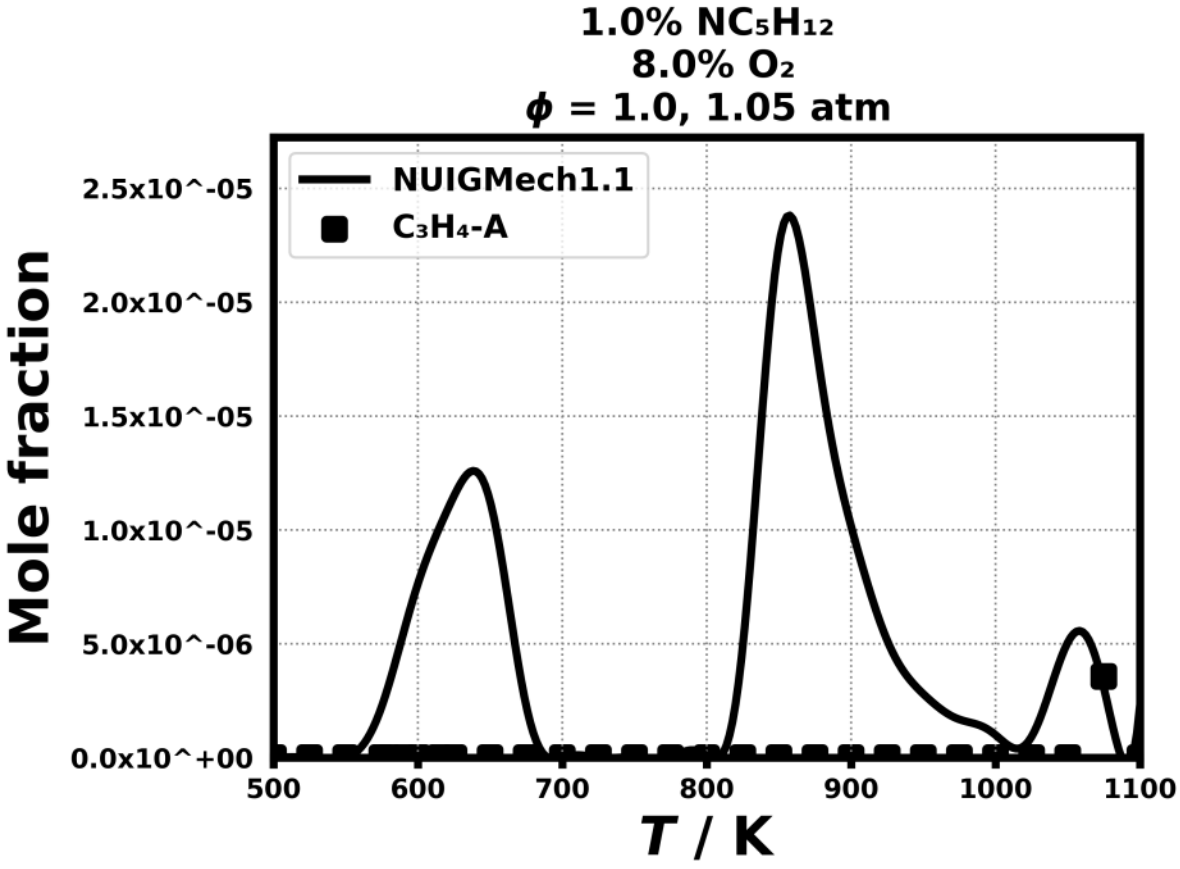

Figure 81: Dataset: 1.05_ATM_PHI_1.0

1.3.52 Case: n-C5H12/JSR/BUGLER/1.05_ATM_PHI_1.0

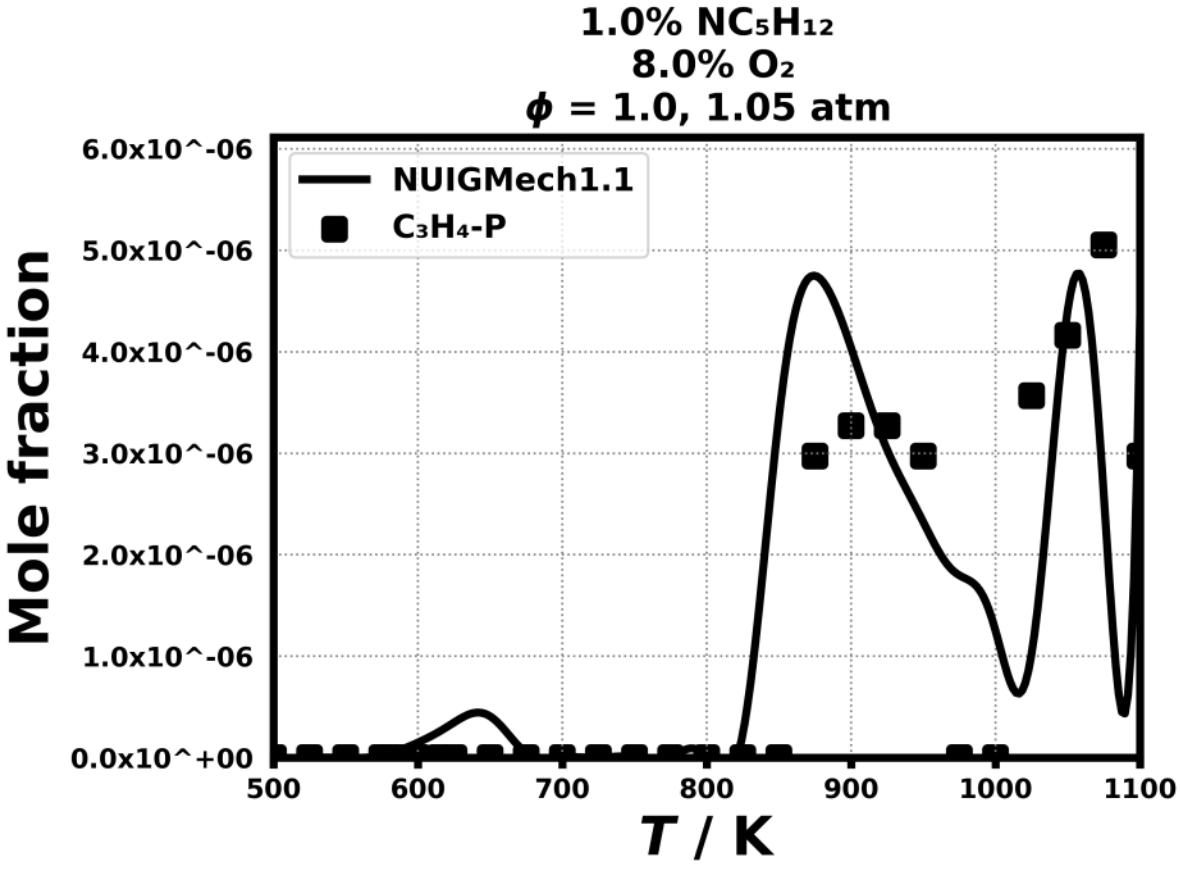

Figure 82: Dataset: 1.05_ATM_PHI_1.0

1.3.53 Case: n-C5H12/JSR/BUGLER/1.05_ATM_PHI_1.0

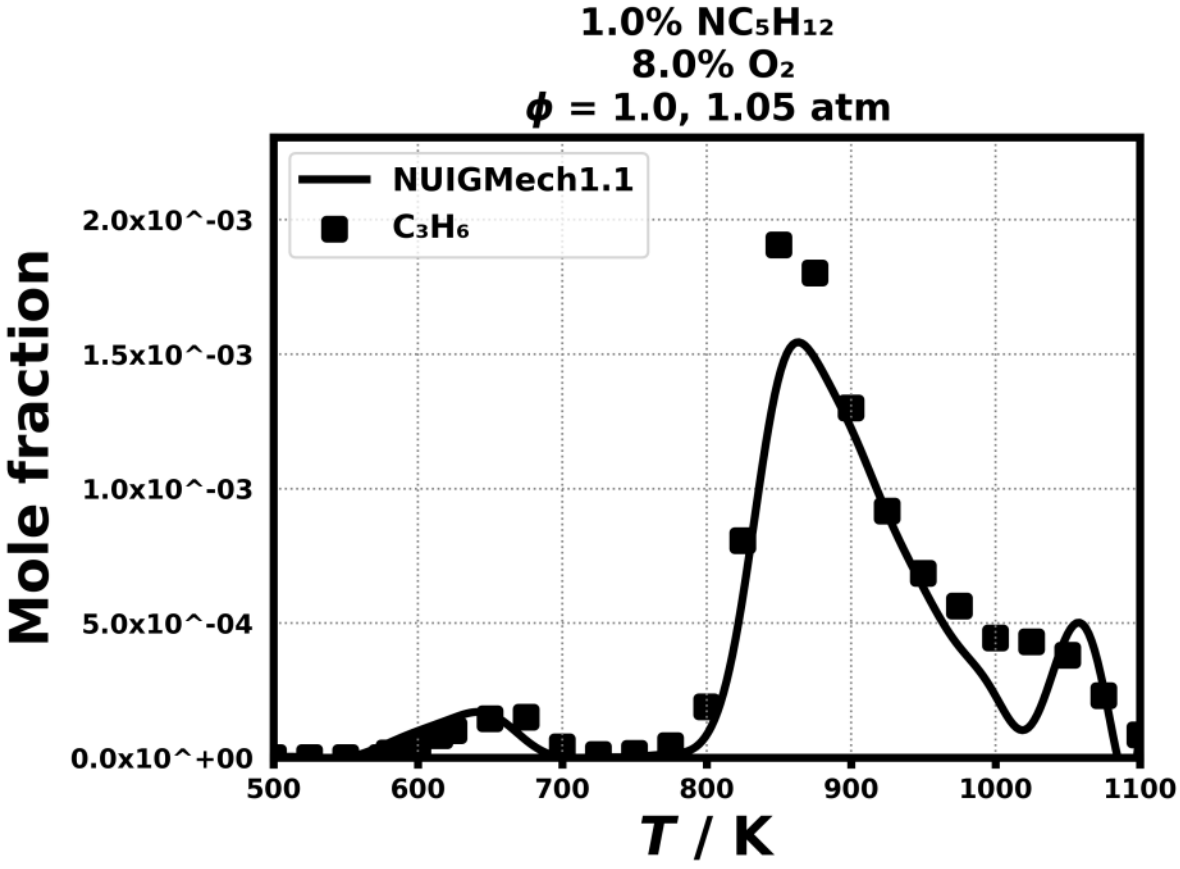

Figure 83: Dataset: 1.05_ATM_PHI_1.0

1.3.54 Case: n-C5H12/JSR/BUGLER/1.05_ATM_PHI_1.0

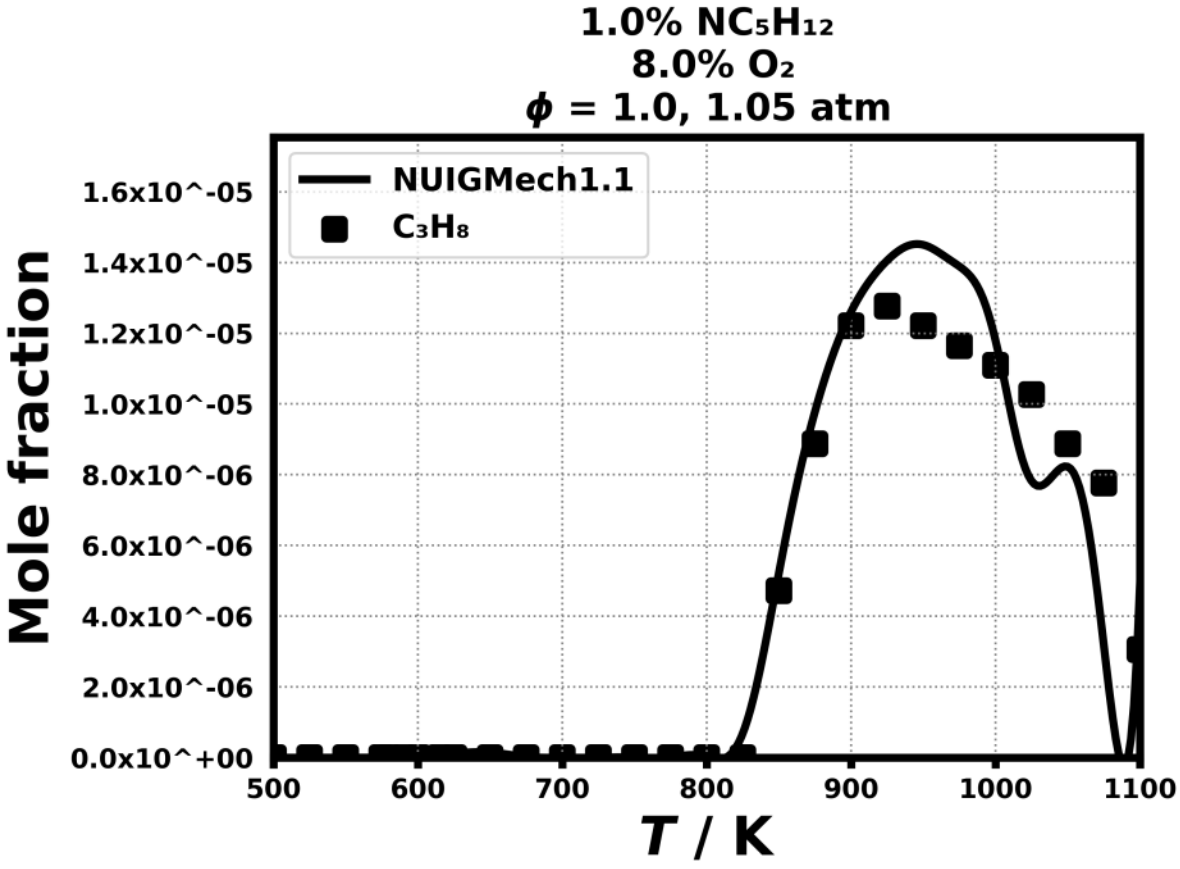

Figure 84: Dataset: 1.05_ATM_PHI_1.0

1.3.55 Case: n-C5H12/JSR/BUGLER/1.05_ATM_PHI_1.0

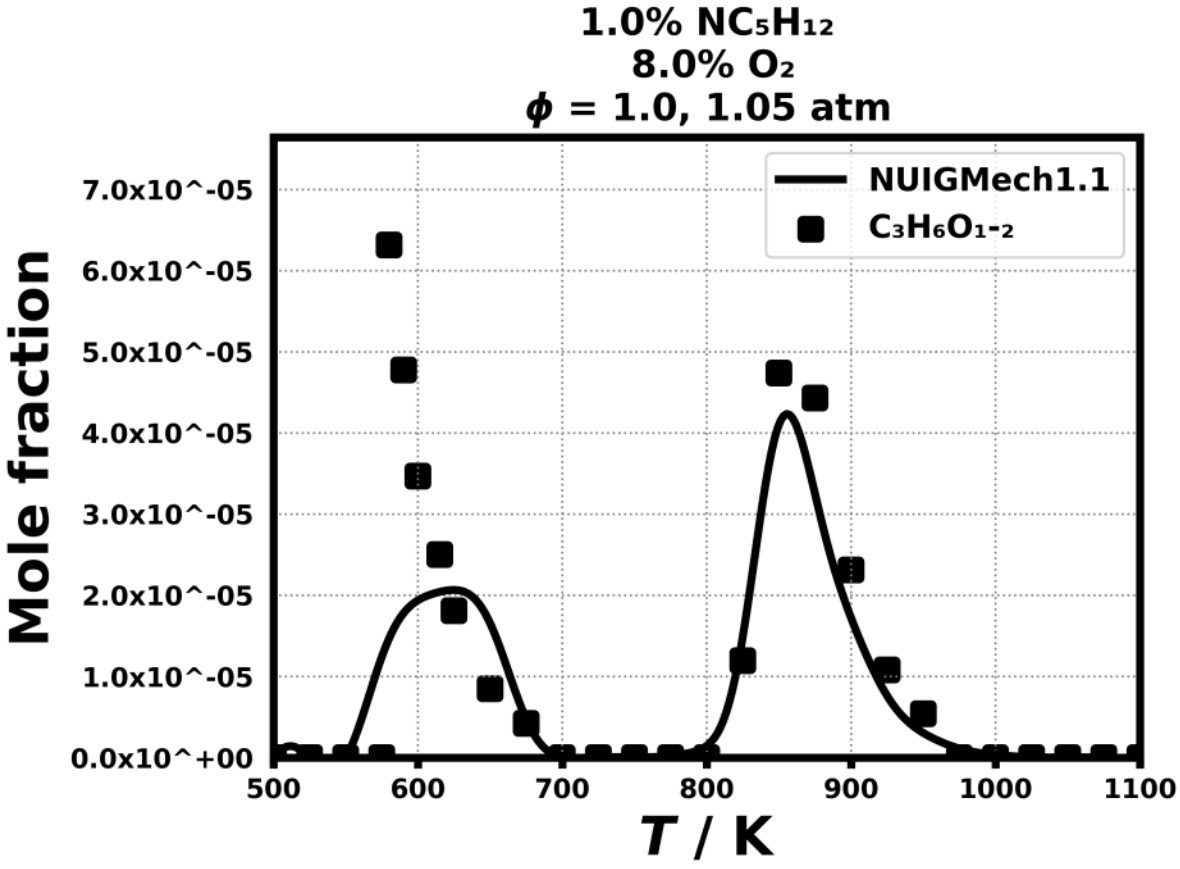

Figure 85: Dataset: 1.05_ATM_PHI_1.0

1.3.56 Case: n-C5H12/JSR/BUGLER/1.05_ATM_PHI_1.0

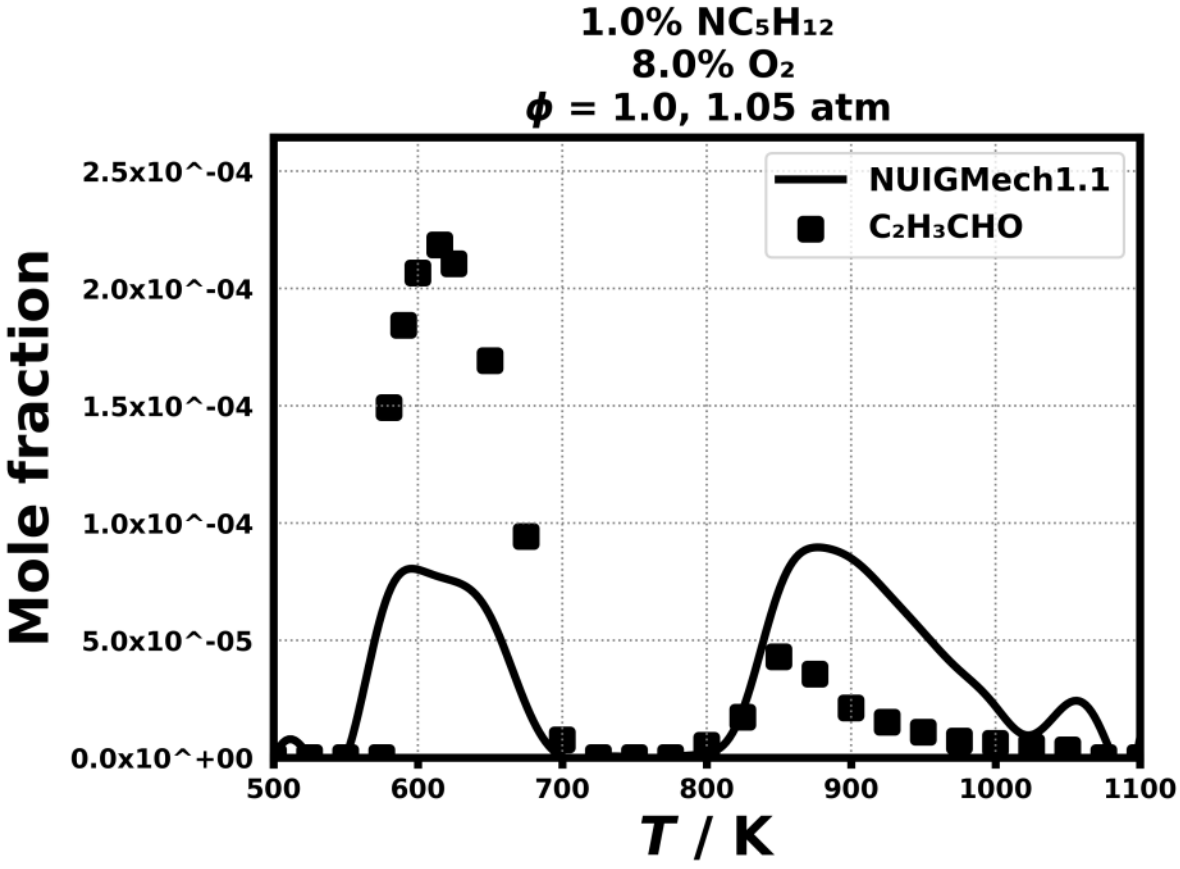

Figure 86: Dataset: 1.05_ATM_PHI_1.0

1.3.57 Case: n-C5H12/JSR/BUGLER/1.05_ATM_PHI_1.0

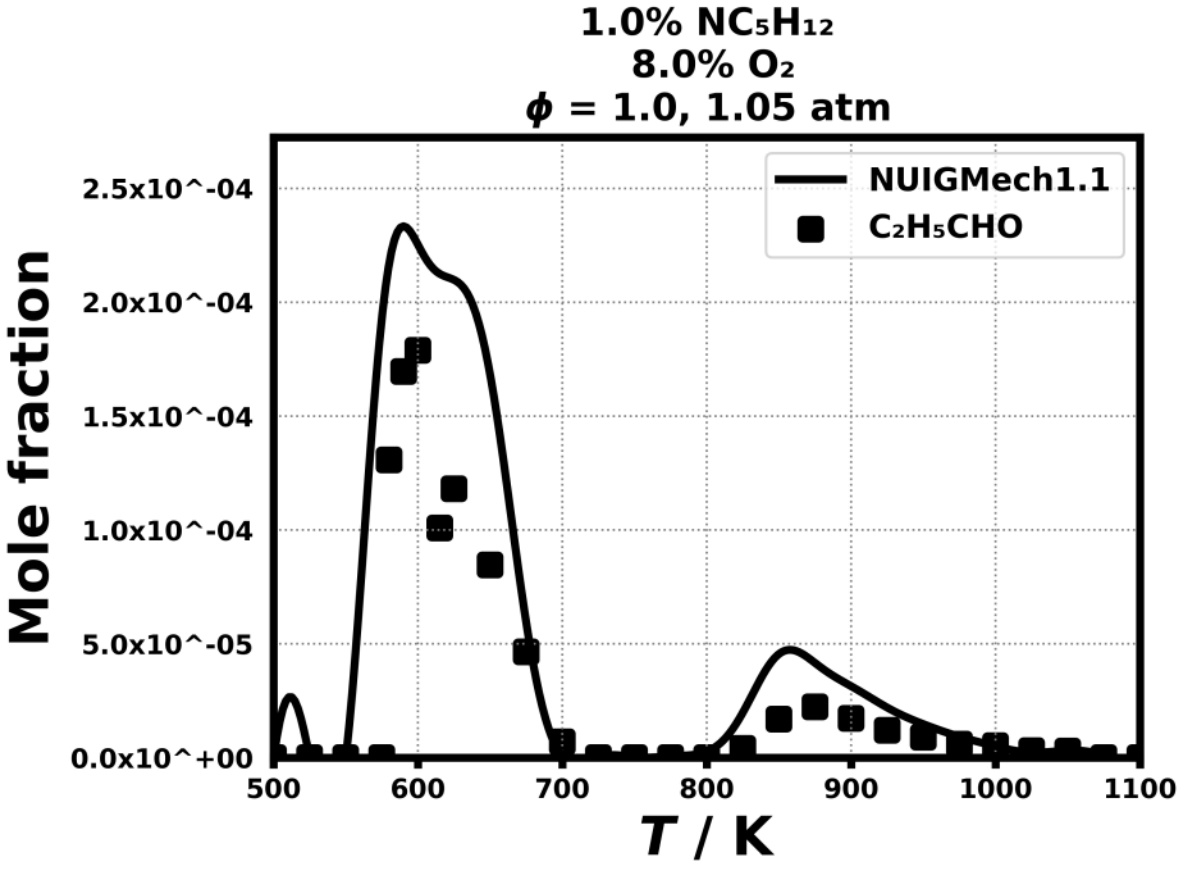

Figure 87: Dataset: 1.05_ATM_PHI_1.0

1.3.58 Case: n-C5H12/JSR/BUGLER/1.05_ATM_PHI_1.0

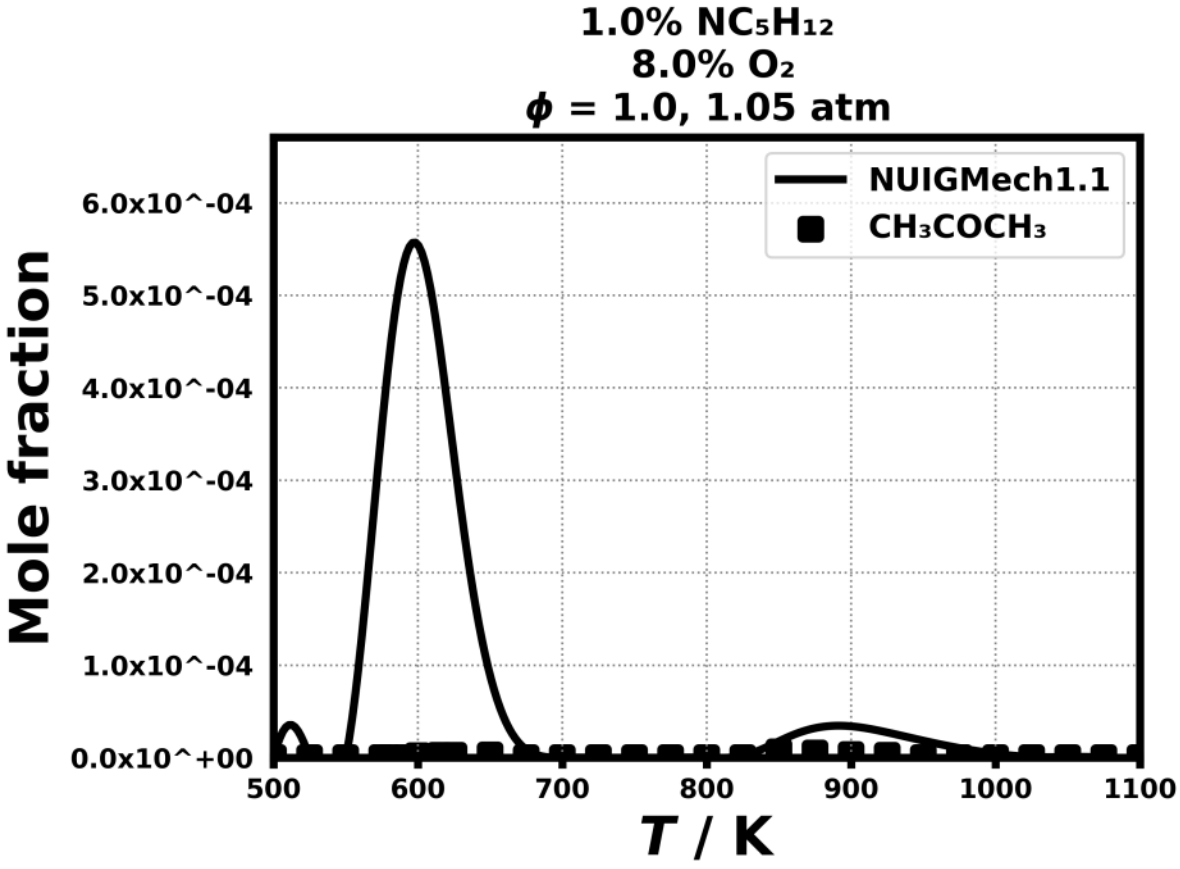

Figure 88: Dataset: 1.05_ATM_PHI_1.0

1.3.59 Case: n-C5H12/JSR/BUGLER/1.05_ATM_PHI_1.0

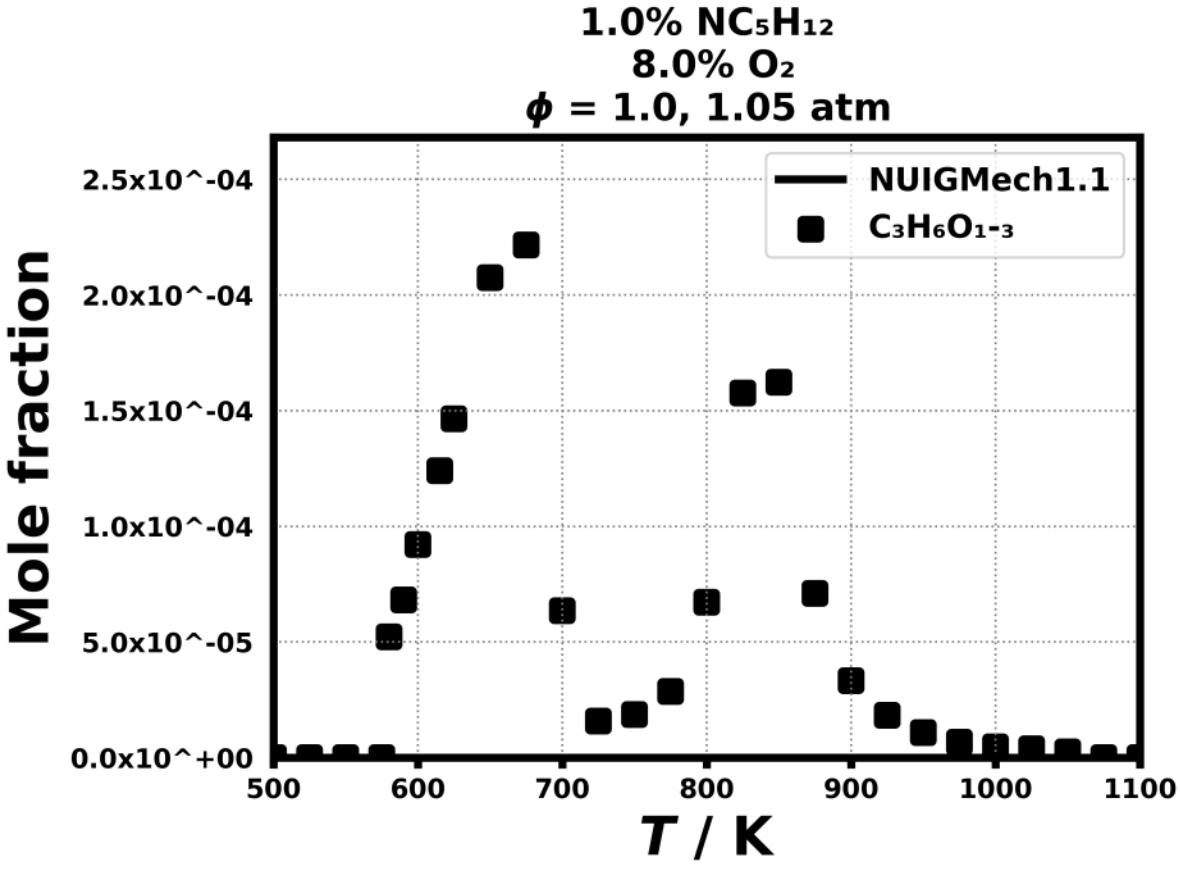

Figure 89: Dataset: 1.05_ATM_PHI_1.0

1.3.60 Case: n-C5H12/JSR/BUGLER/1.05_ATM_PHI_1.0

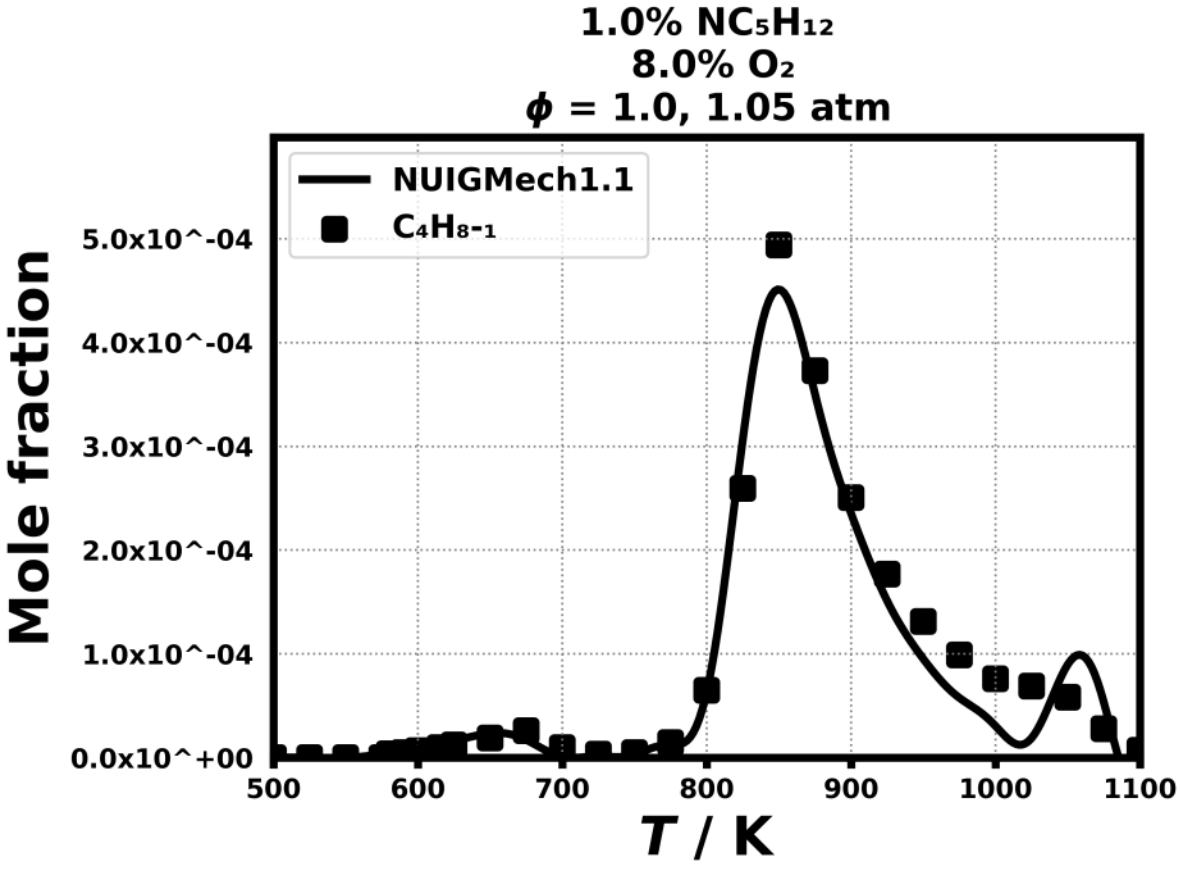

Figure 90: Dataset: 1.05_ATM_PHI_1.0

1.3.61 Case: n-C5H12/JSR/BUGLER/1.05_ATM_PHI_1.0

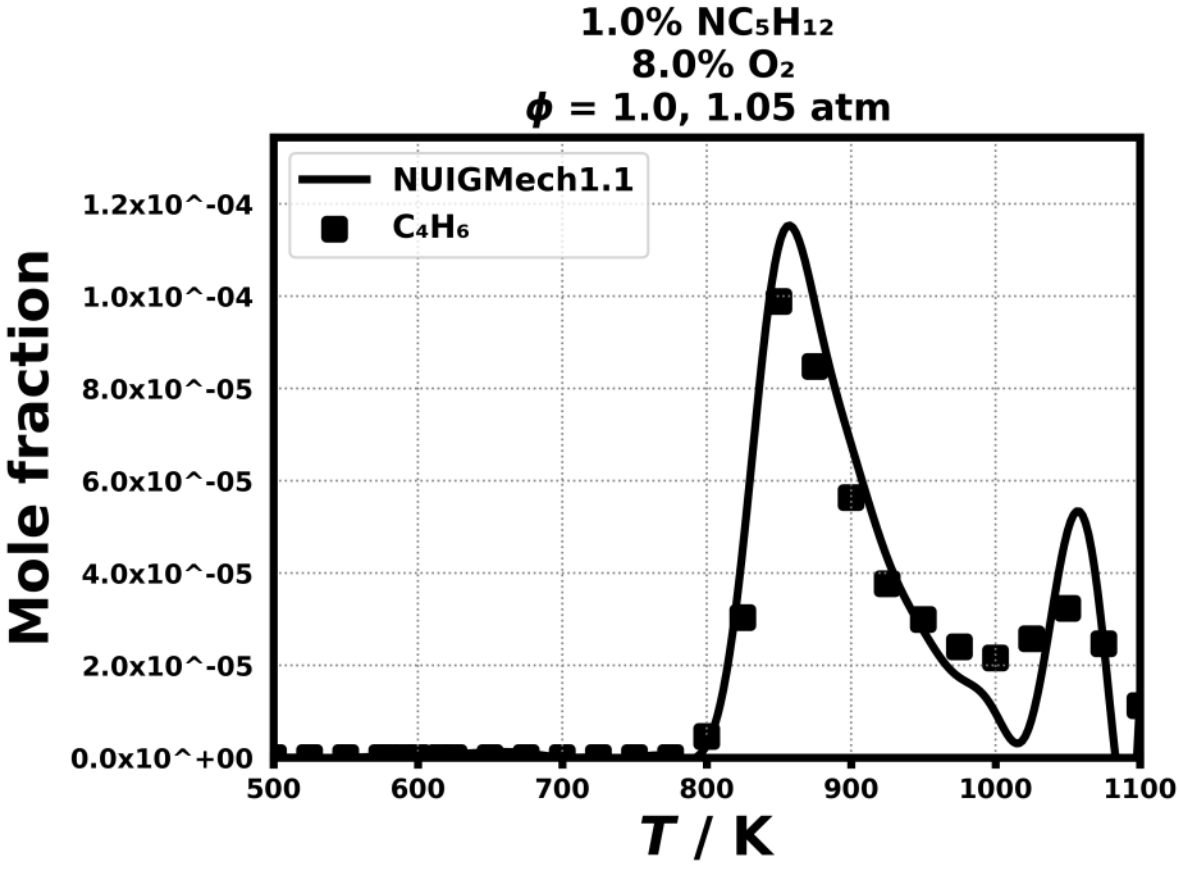

Figure 91: Dataset: 1.05_ATM_PHI_1.0

1.3.62 Case: n-C5H12/JSR/BUGLER/1.05_ATM_PHI_1.0

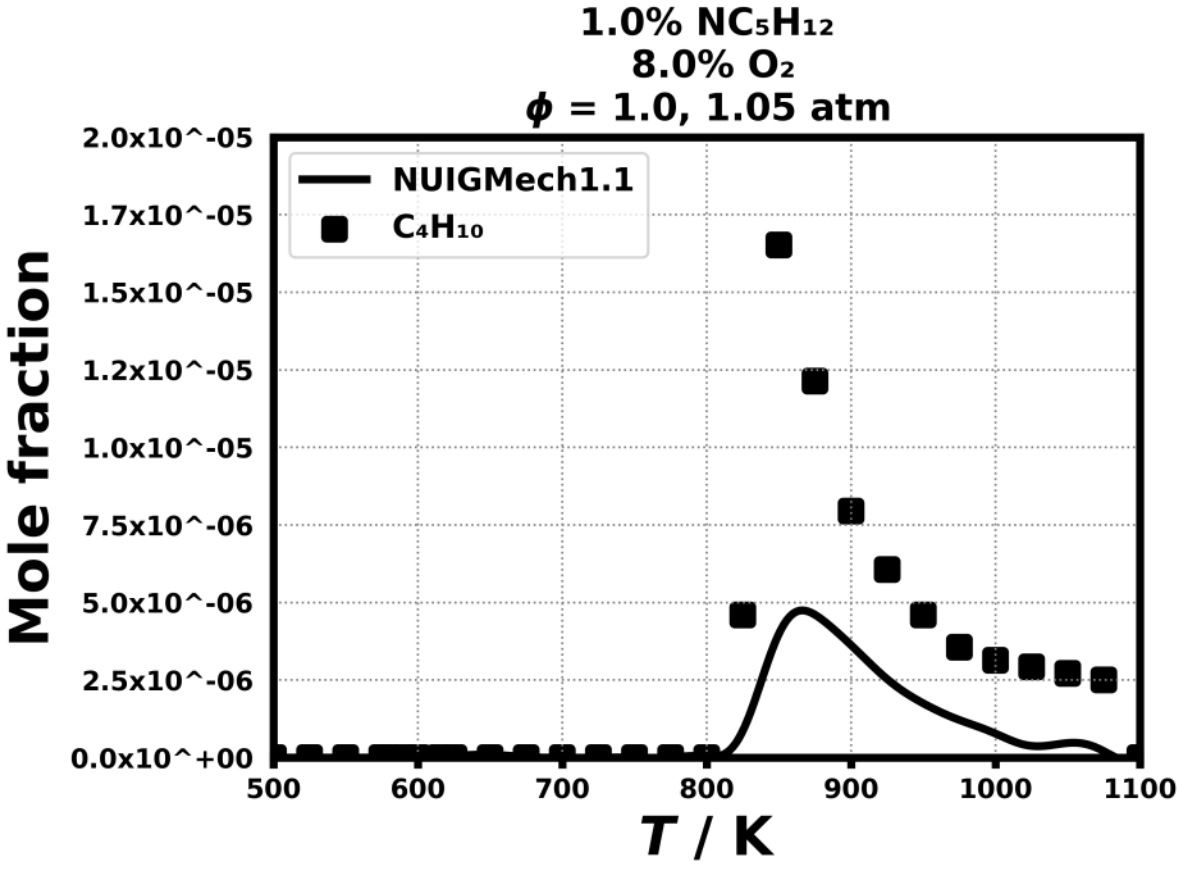

Figure 92: Dataset: 1.05_ATM_PHI_1.0

1.3.63 Case: n-C5H12/JSR/BUGLER/1.05_ATM_PHI_1.0

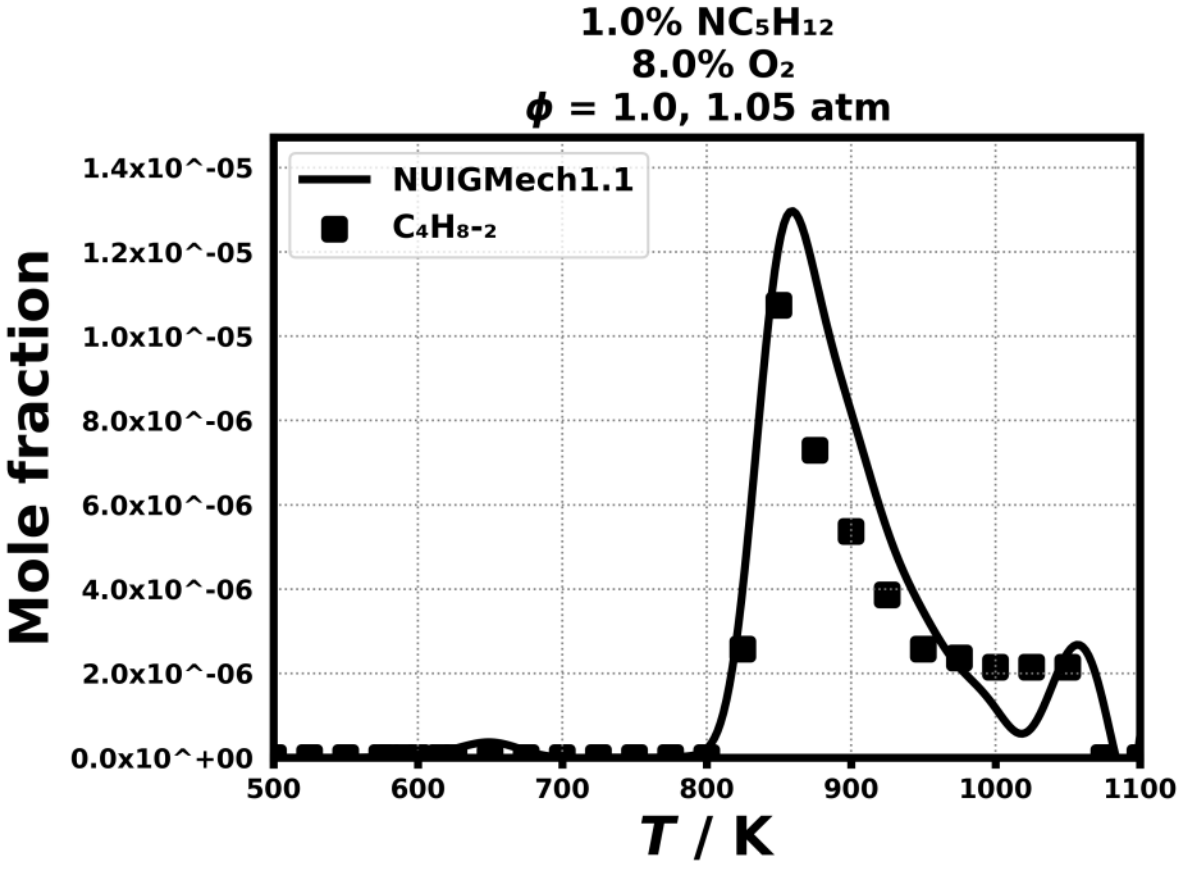

Figure 93: Dataset: 1.05_ATM_PHI_1.0

1.3.64 Case: n-C5H12/JSR/BUGLER/1.05_ATM_PHI_1.0

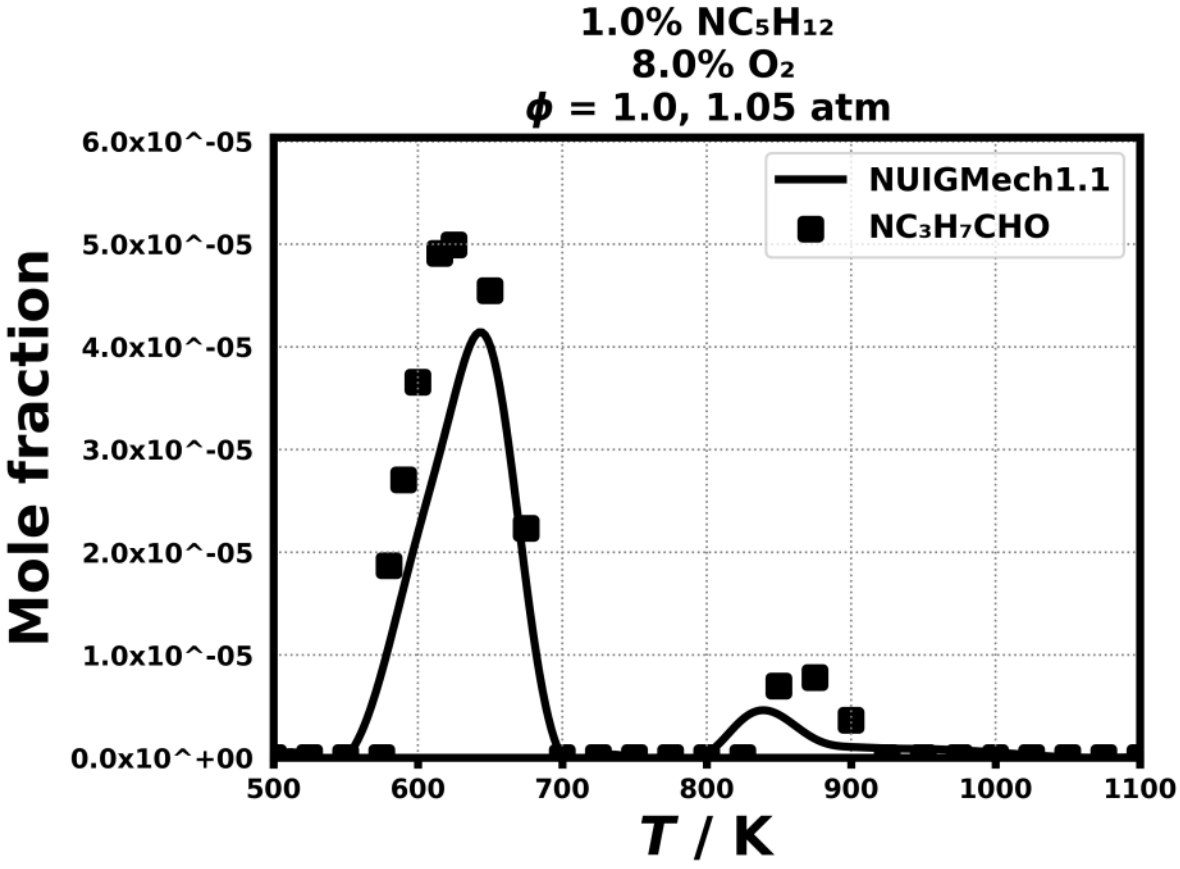

Figure 94: Dataset: 1.05_ATM_PHI_1.0

1.3.65 Case: n-C5H12/JSR/BUGLER/1.05_ATM_PHI_1.0

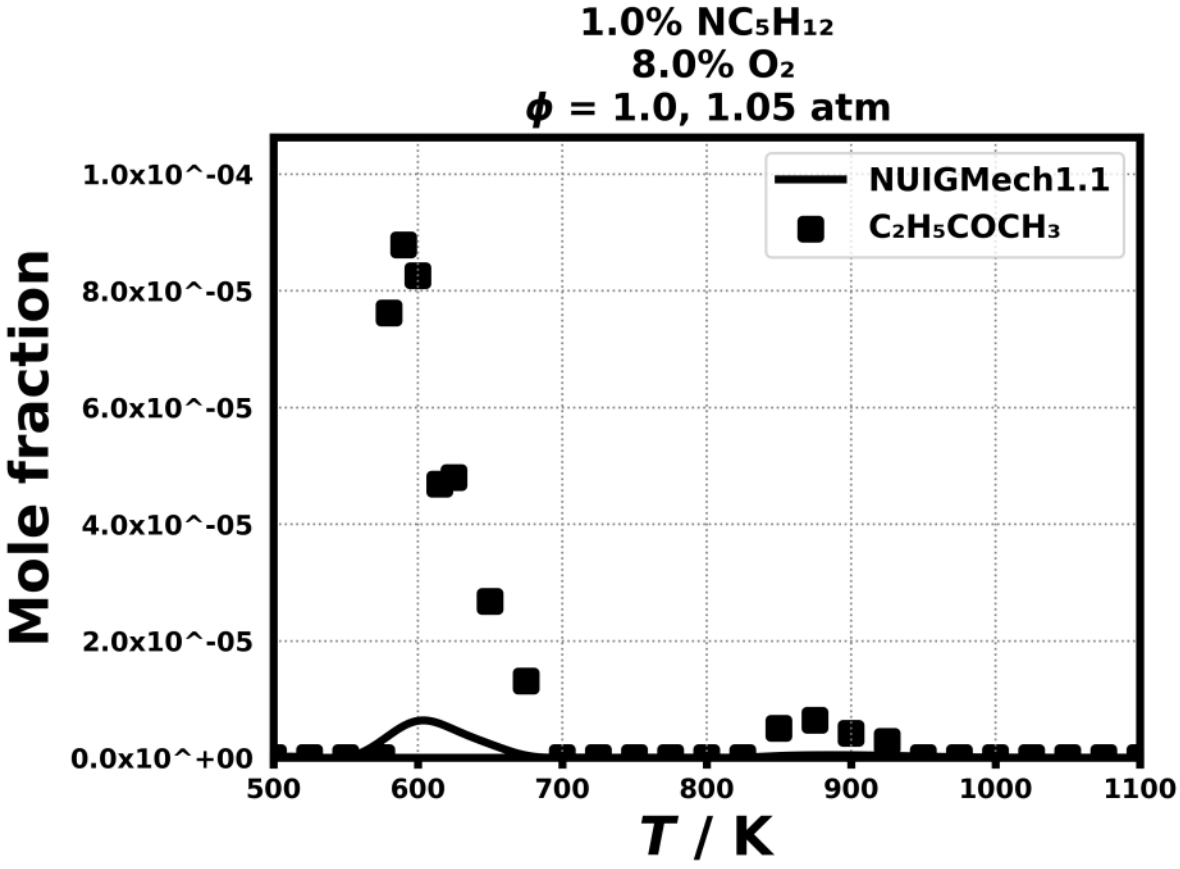

Figure 95: Dataset: 1.05_ATM_PHI_1.0

1.3.66 Case: n-C5H12/JSR/BUGLER/1.05_ATM_PHI_1.0

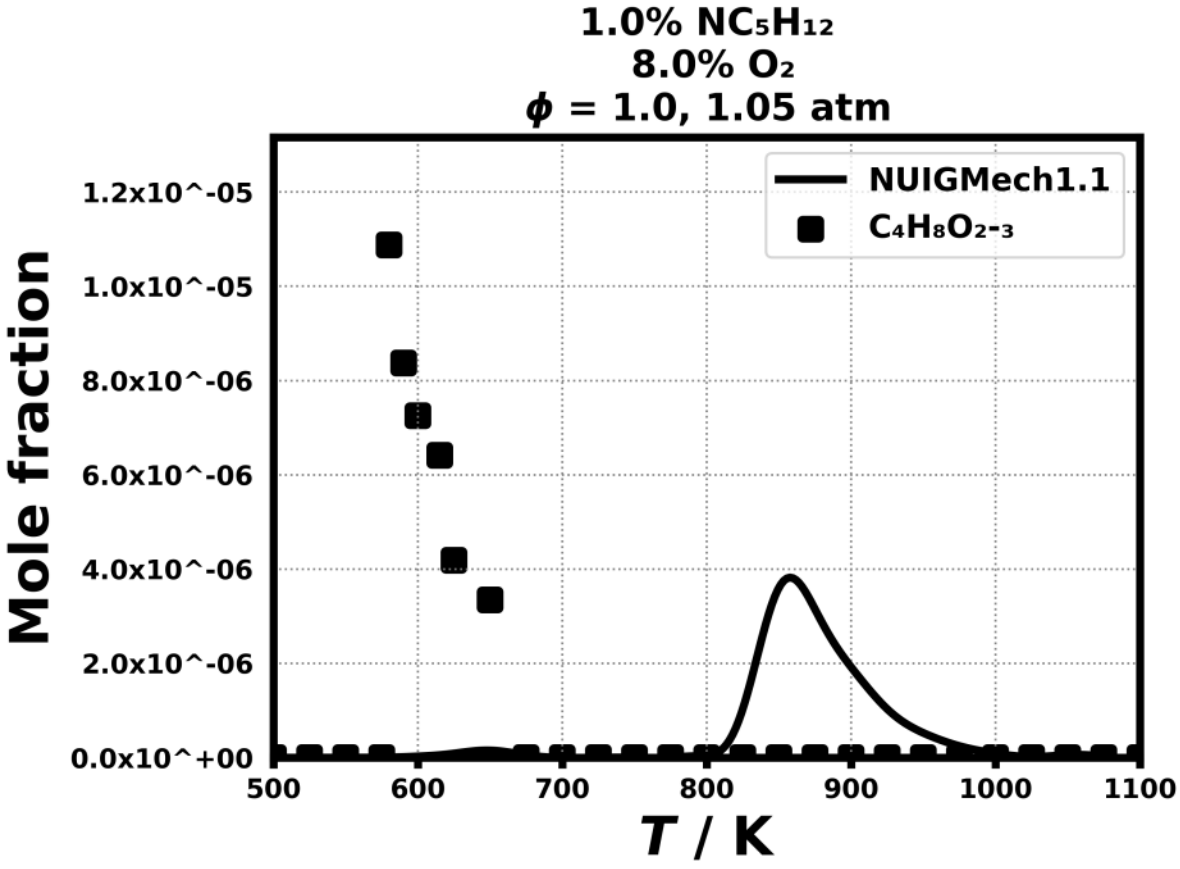

Figure 96: Dataset: 1.05_ATM_PHI_1.0

1.3.67 Case: n-C5H12/JSR/BUGLER/1.05_ATM_PHI_1.0

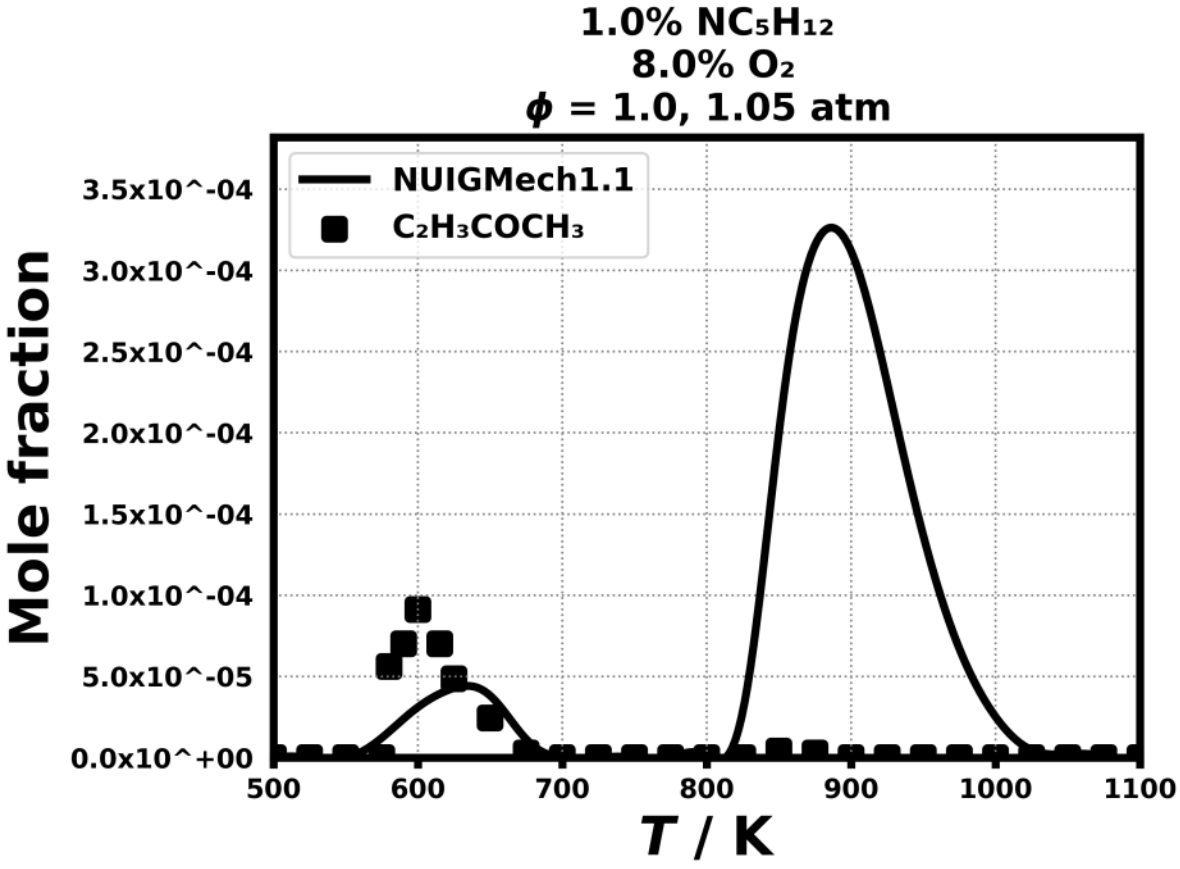

Figure 97: Dataset: 1.05_ATM_PHI_1.0

1.3.68 Case: n-C5H12/JSR/BUGLER/1.05_ATM_PHI_1.0

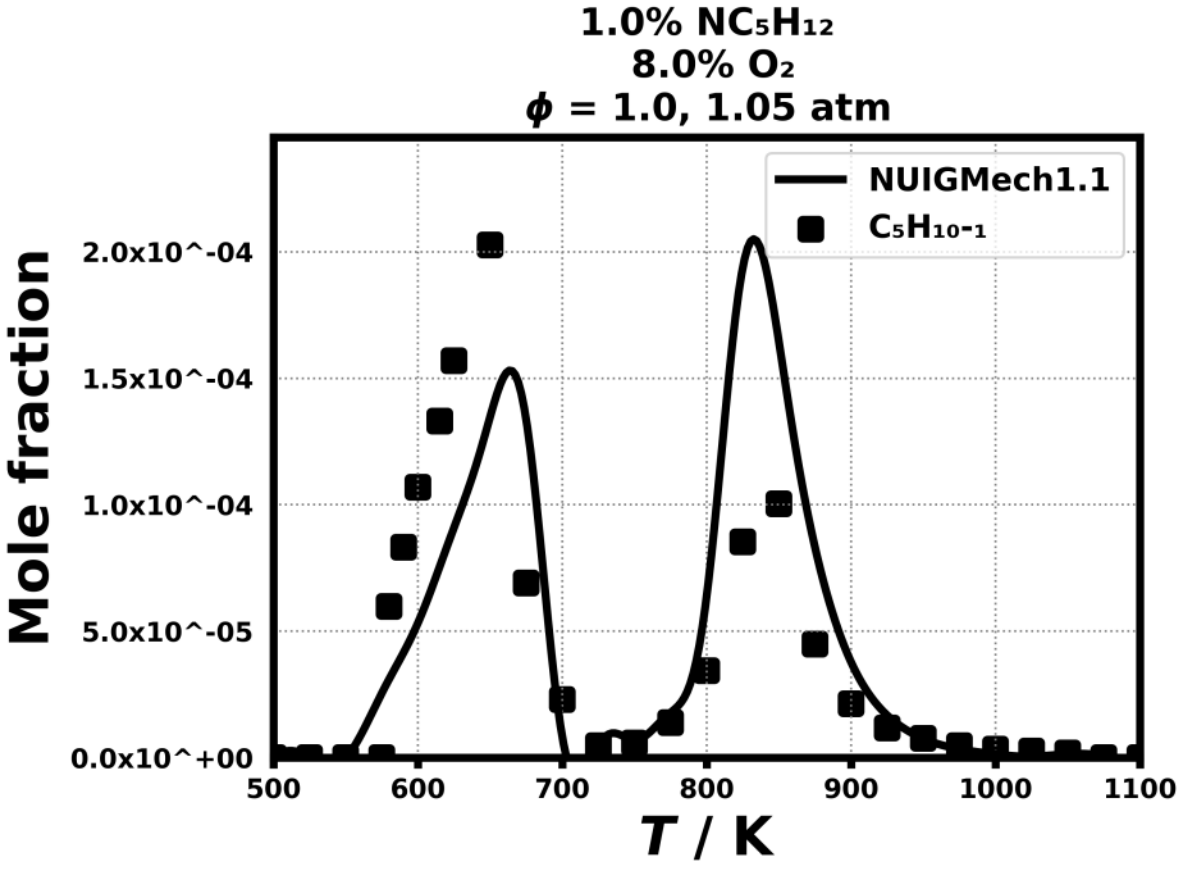

Figure 98: Dataset: 1.05_ATM_PHI_1.0

1.3.69 Case: n-C5H12/JSR/BUGLER/1.05_ATM_PHI_1.0

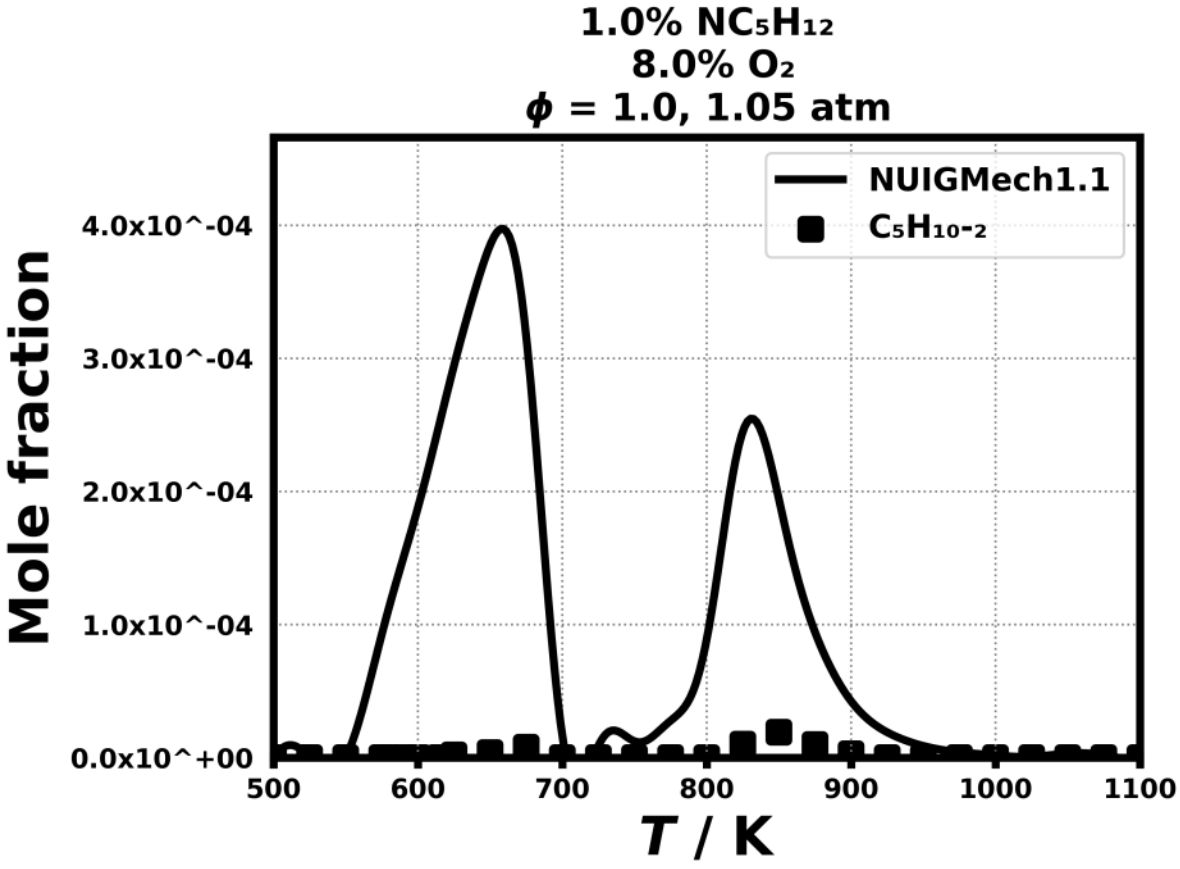

Figure 99: Dataset: 1.05_ATM_PHI_1.0

1.3.70 Case: n-C5H12/JSR/BUGLER/1.05_ATM_PHI_1.0

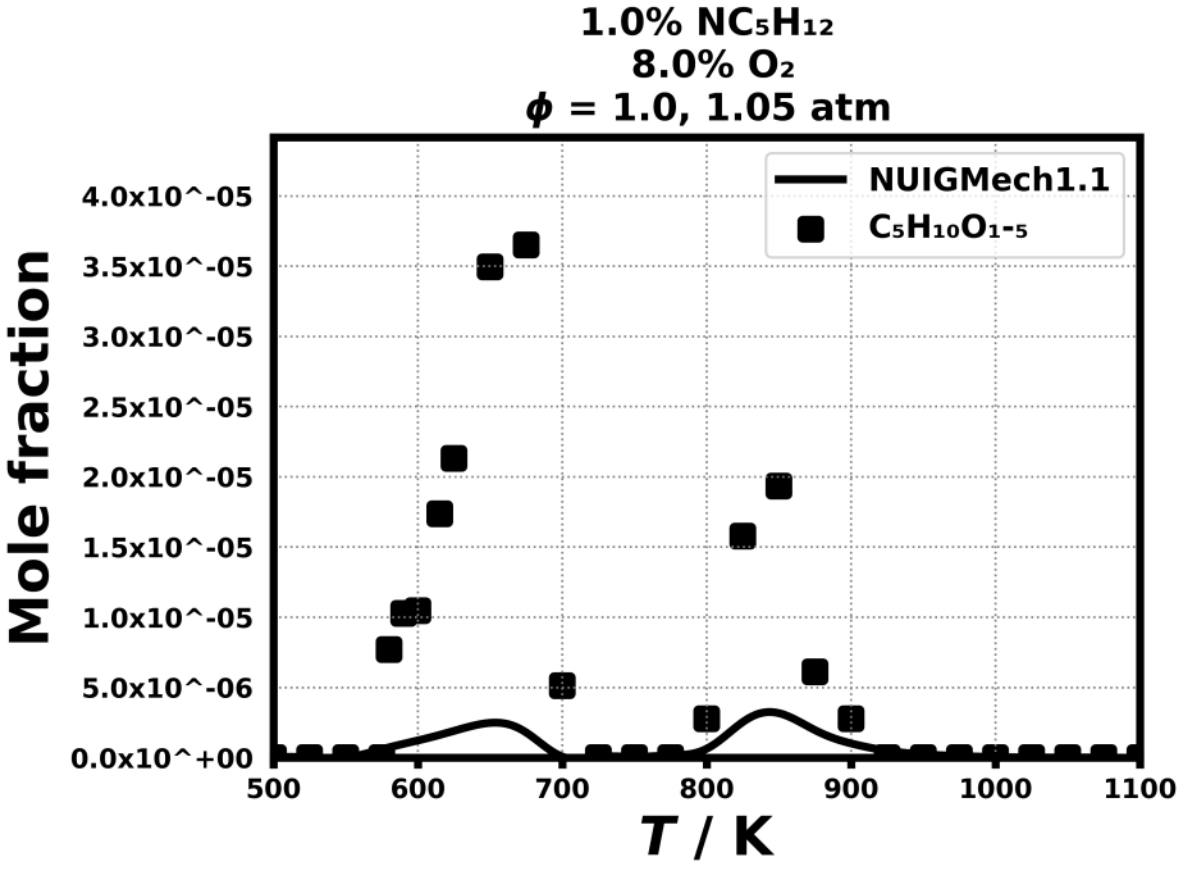

Figure 100: Dataset: 1.05_ATM_PHI_1.0

1.3.71 Case: n-C5H12/JSR/BUGLER/1.05_ATM_PHI_1.0

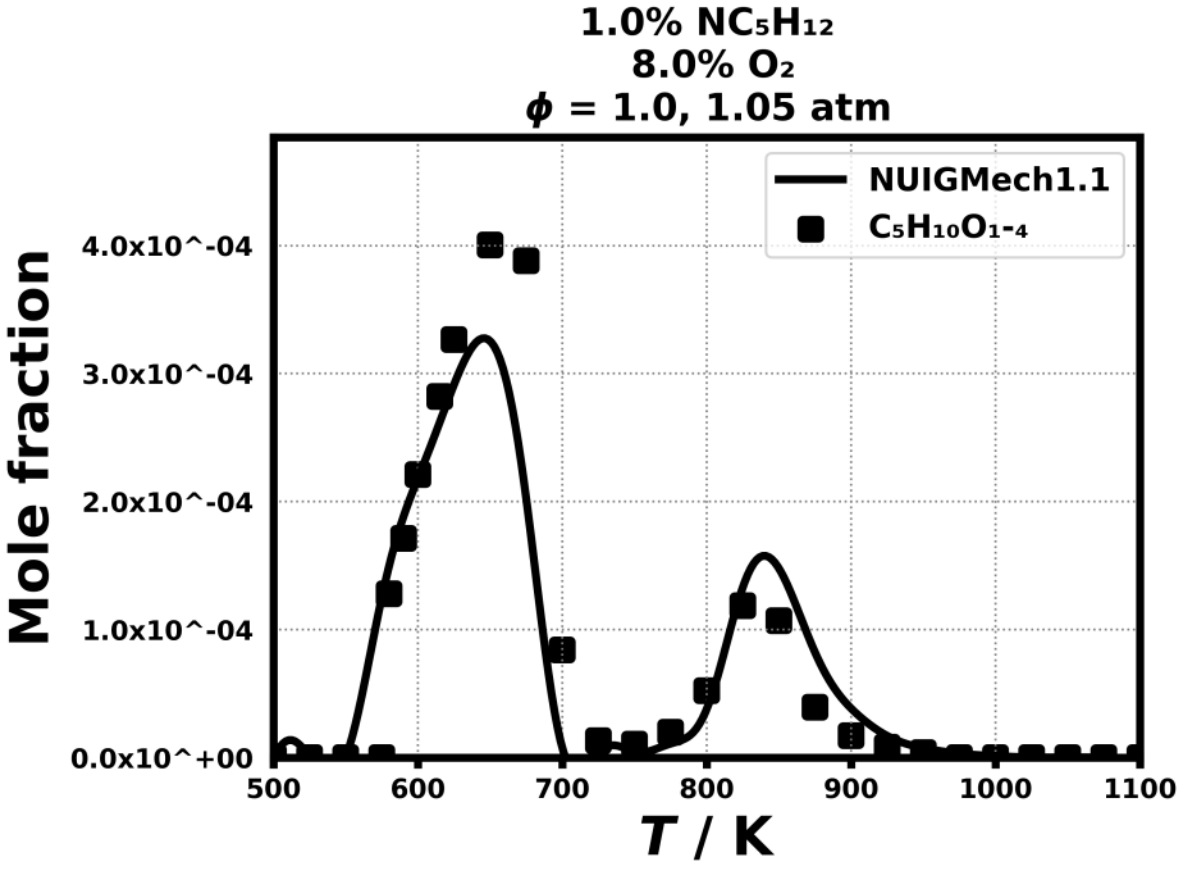

Figure 101: Dataset: 1.05_ATM_PHI_1.0

1.3.72 Case: n-C5H12/JSR/BUGLER/1.05_ATM_PHI_1.0

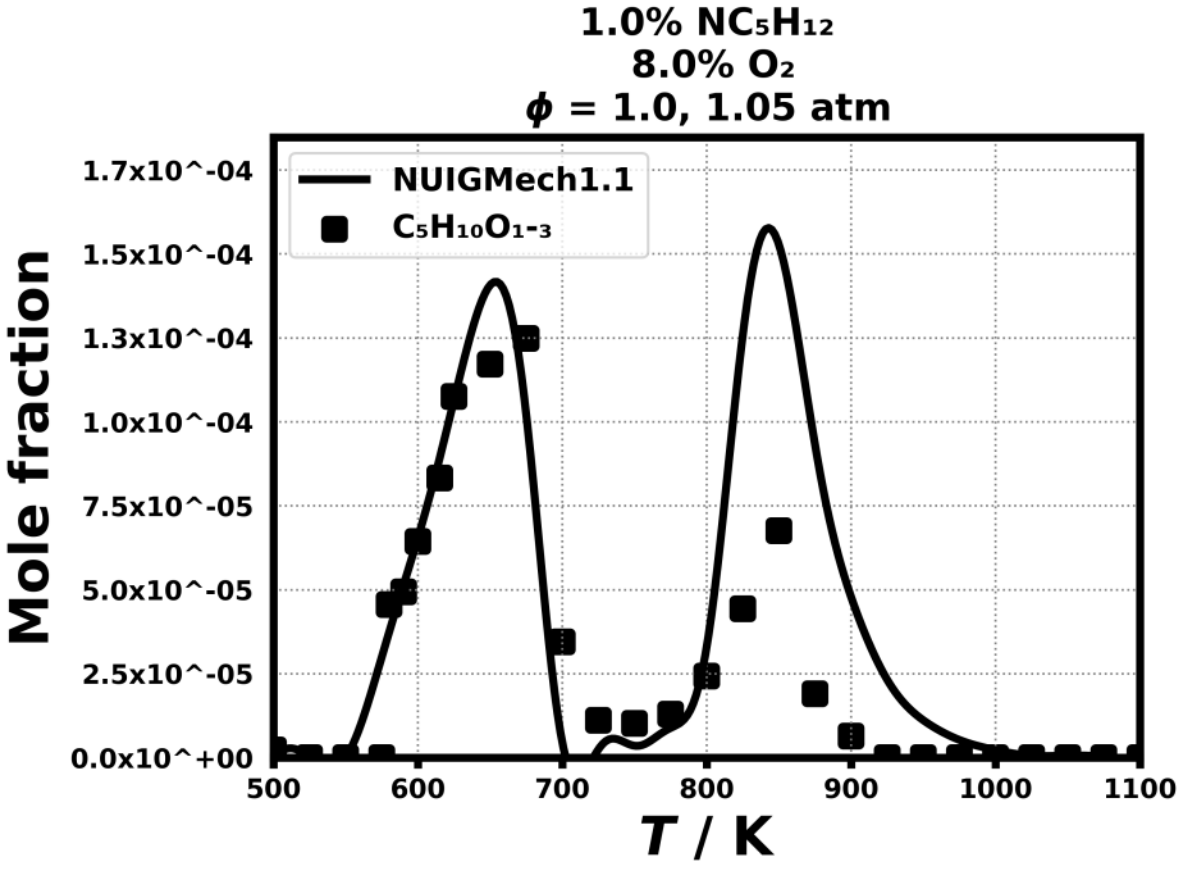

Figure 102: Dataset: 1.05_ATM_PHI_1.0

1.3.73 Case: n-C5H12/JSR/BUGLER/1.05_ATM_PHI_1.0

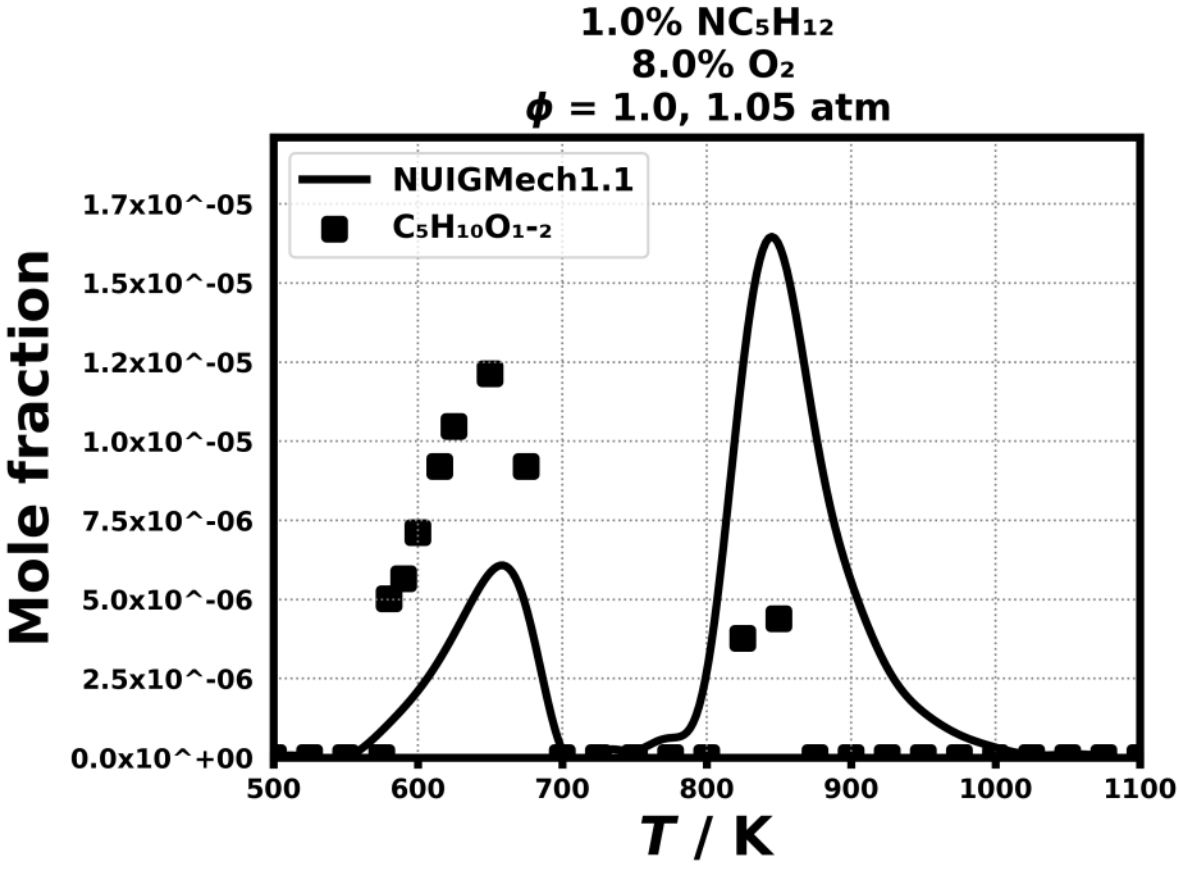

Figure 103: Dataset: 1.05_ATM_PHI_1.0

1.3.74 Case: n-C5H12/JSR/BUGLER/1.05_ATM_PHI_1.0

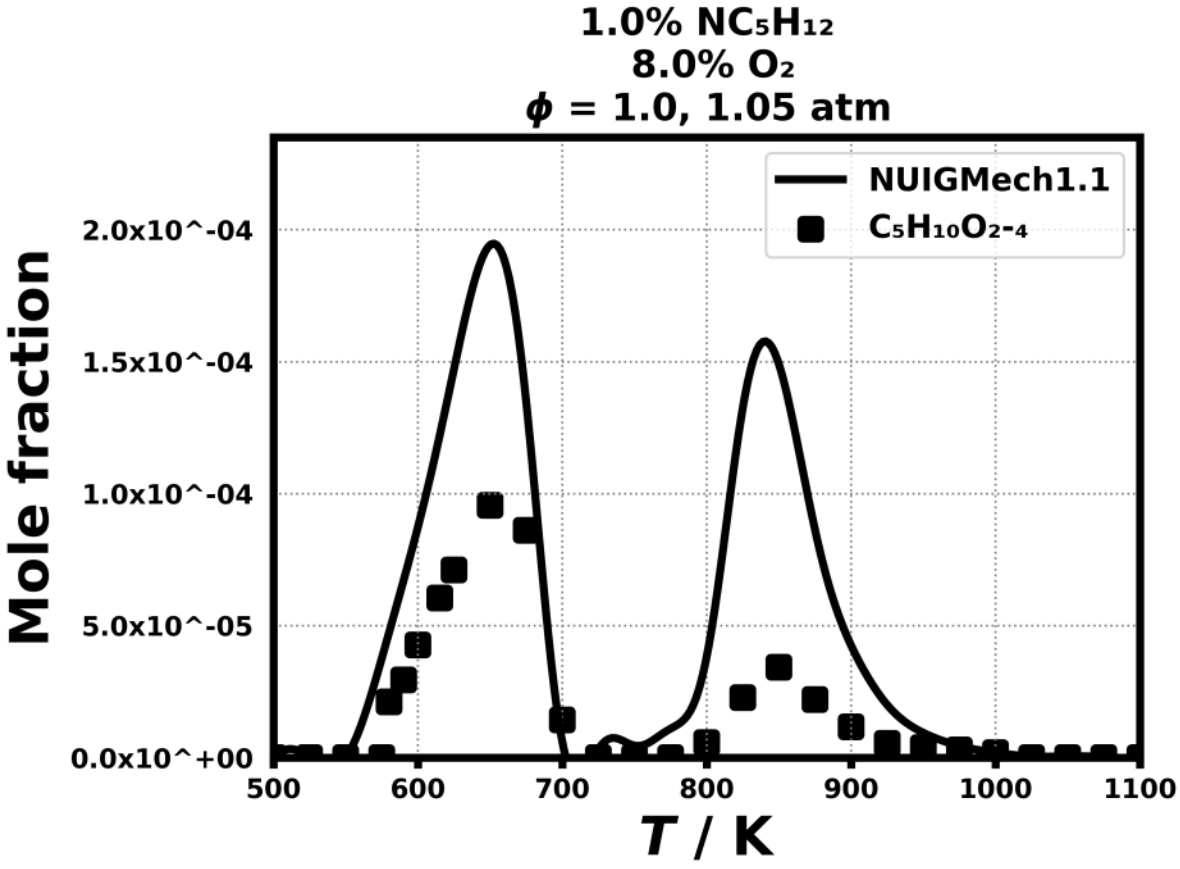

Figure 104: Dataset: 1.05_ATM_PHI_1.0

1.3.75 Case: n-C5H12/JSR/BUGLER/1.05_ATM_PHI_1.0

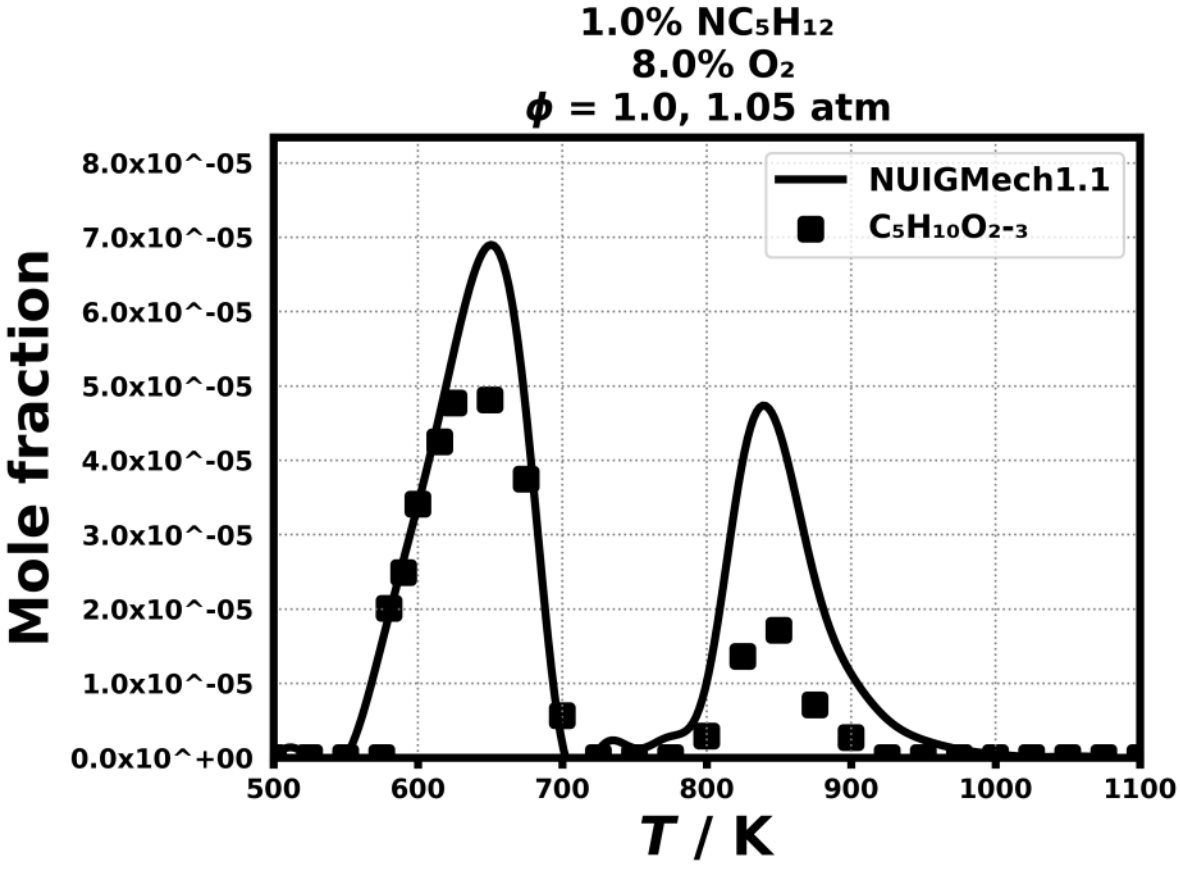

Figure 105: Dataset: 1.05_ATM_PHI_1.0

1.3.77 Case: n-C5H12/JSR/BUGLER/1.05_ATM_PHI_1.0

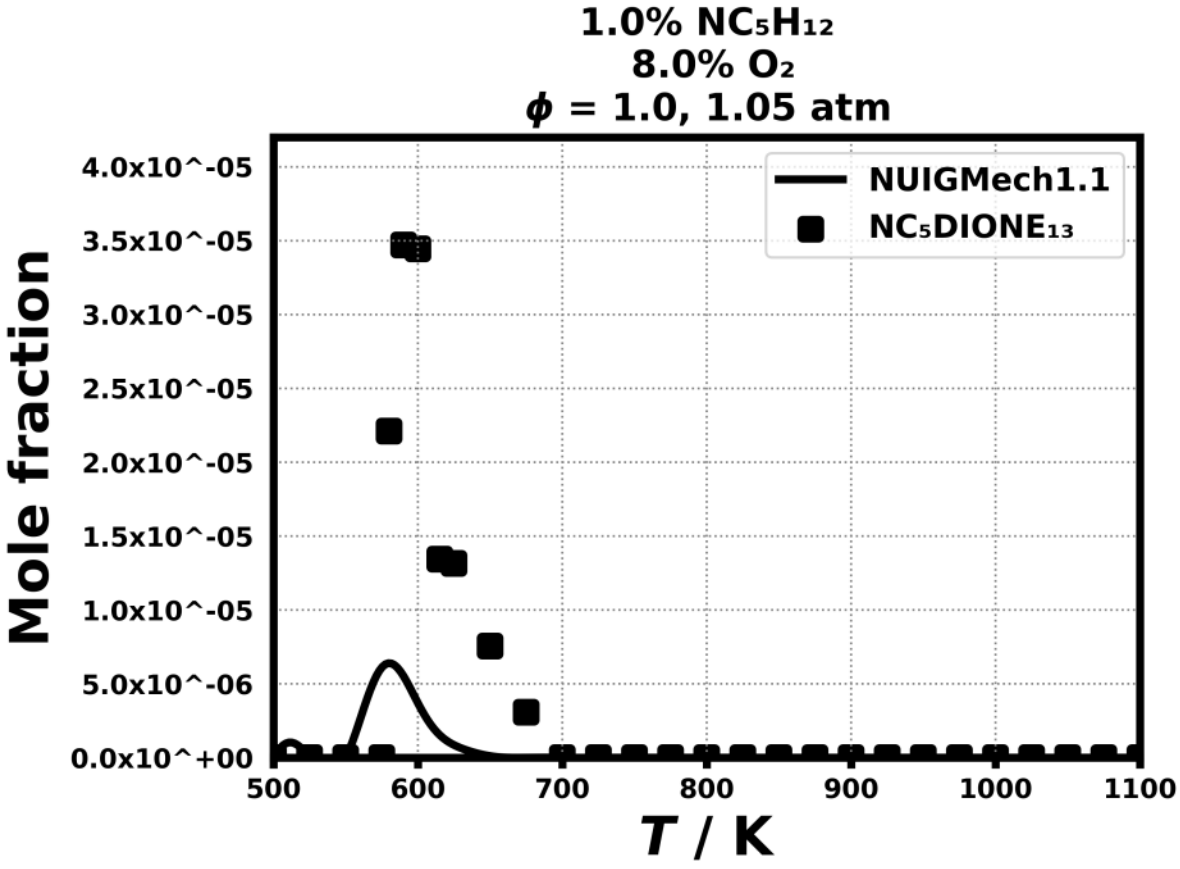

Figure 107: Dataset: 1.05_ATM_PHI_1.0

1.3.78 Case: n-C5H12/JSR/BUGLER/1.05_ATM_PHI_1.0

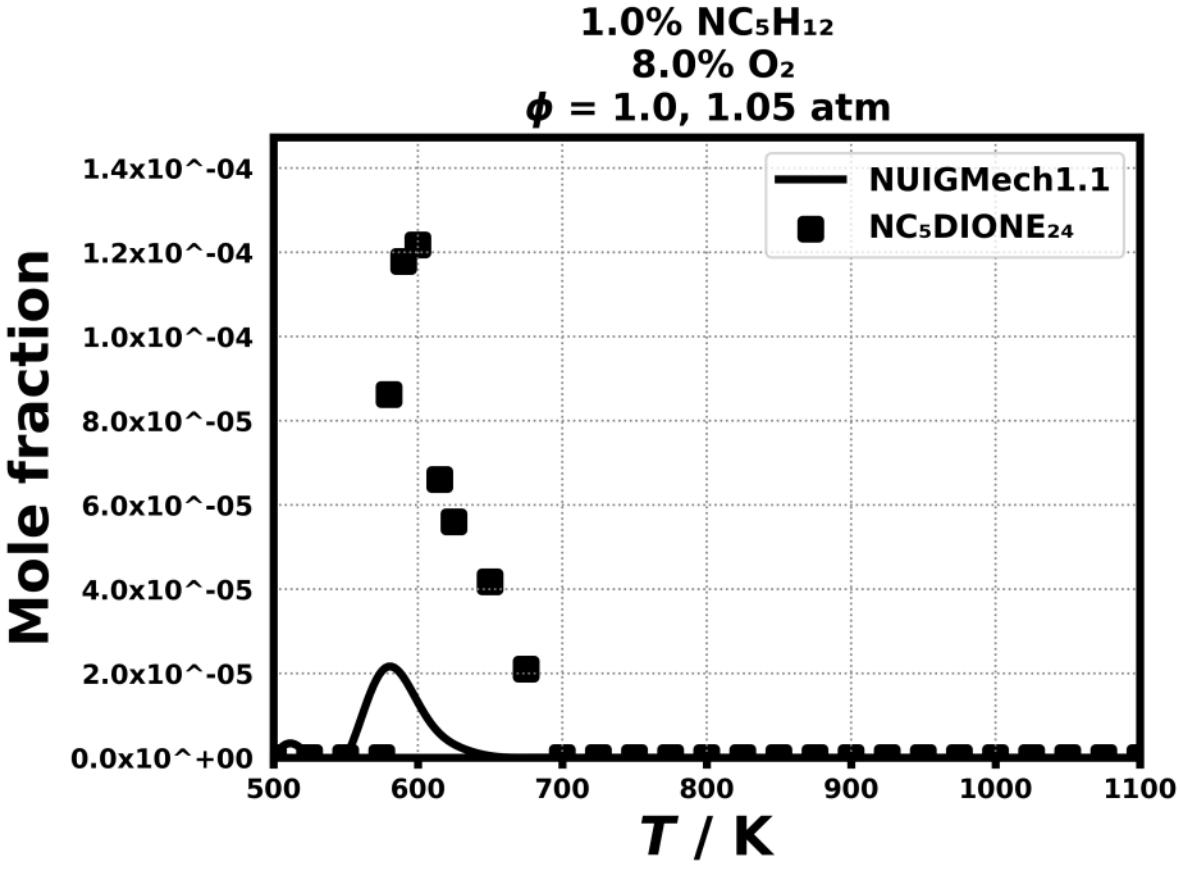

Figure 108: Dataset: 1.05_ATM_PHI_1.0

1.3.79 Case: n-C5H12/JSR/BUGLER/1.05_ATM_PHI_2.0

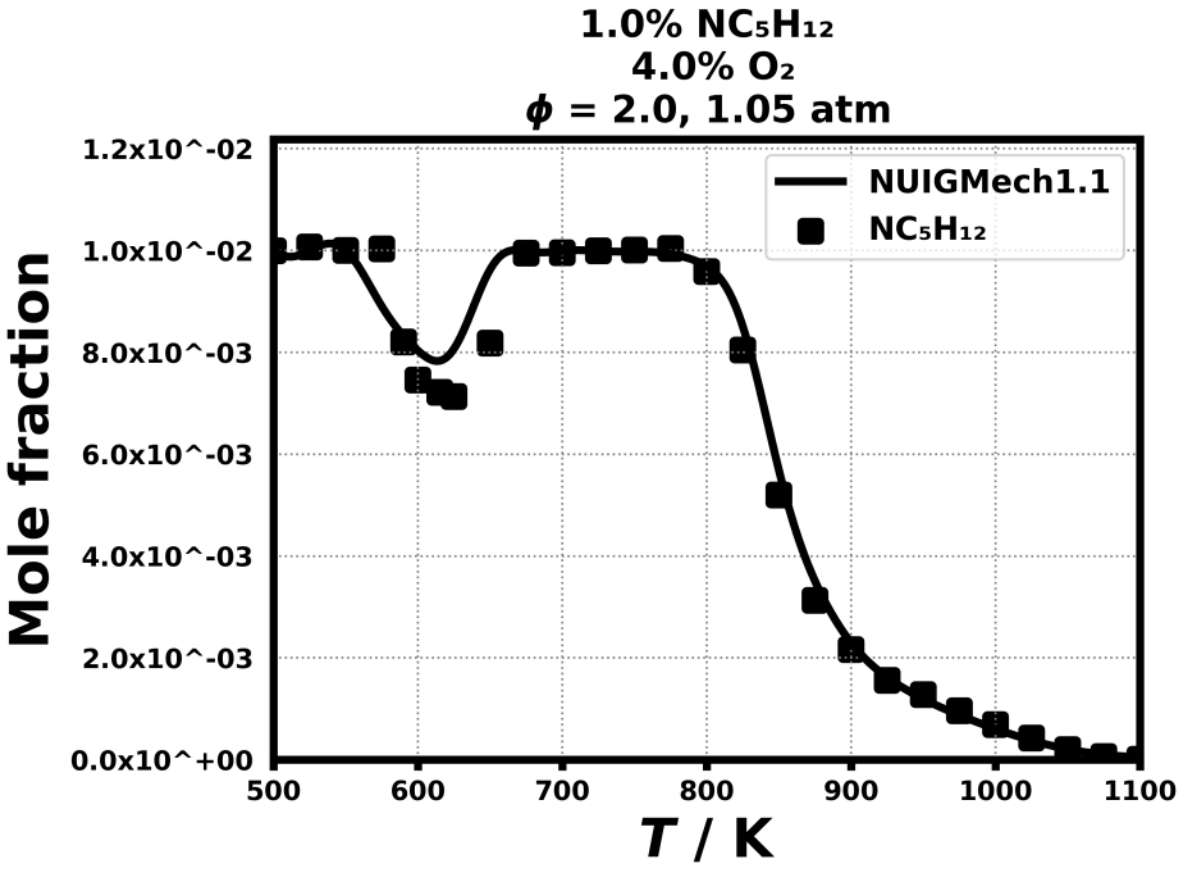

Figure 109: Dataset: 1.05_ATM_PHI_2.0

1.3.80 Case: n-C5H12/JSR/BUGLER/1.05_ATM_PHI_2.0

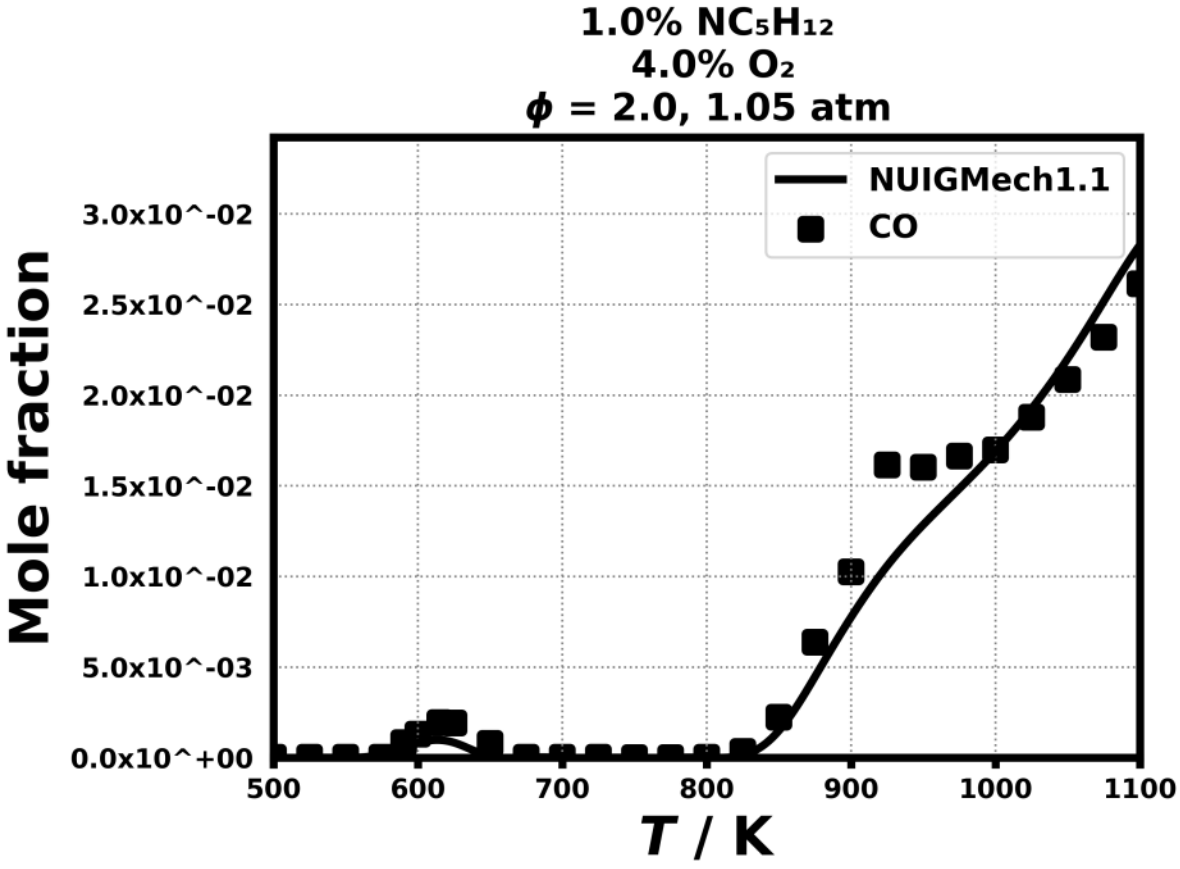

Figure 110: Dataset: 1.05_ATM_PHI_2.0

1.3.81 Case: n-C5H12/JSR/BUGLER/1.05_ATM_PHI_2.0

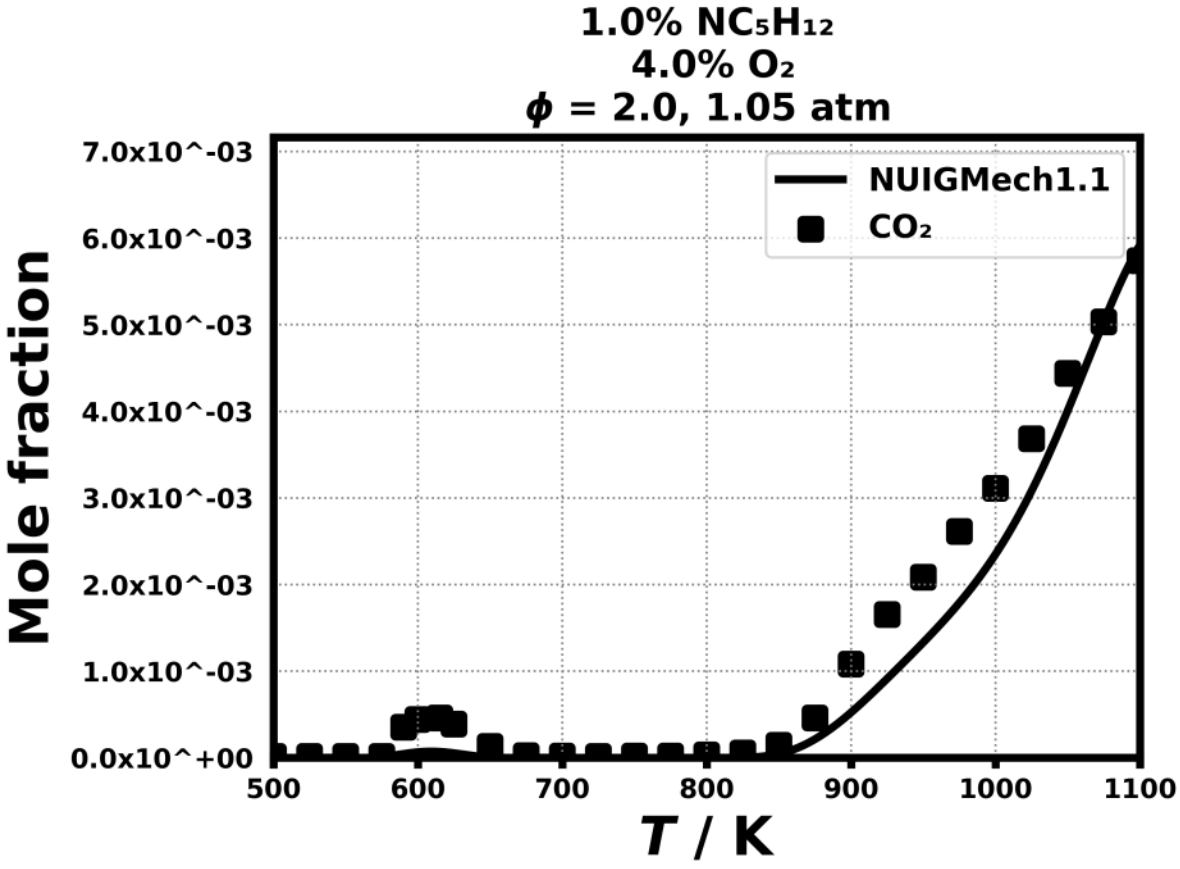

Figure 111: Dataset: 1.05_ATM_PHI_2.0

1.3.82 Case: n-C5H12/JSR/BUGLER/1.05_ATM_PHI_2.0

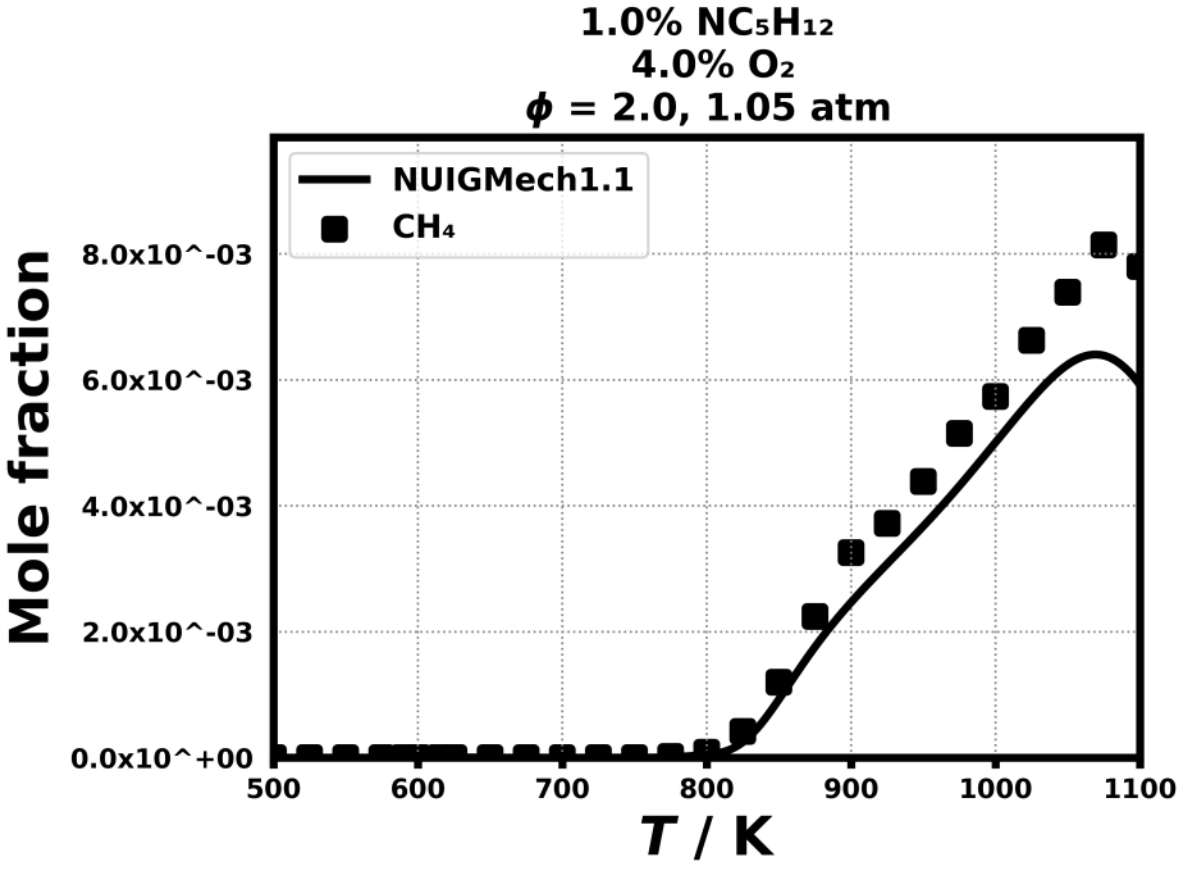

Figure 112: Dataset: 1.05_ATM_PHI_2.0

1.3.83 Case: n-C5H12/JSR/BUGLER/1.05_ATM_PHI_2.0

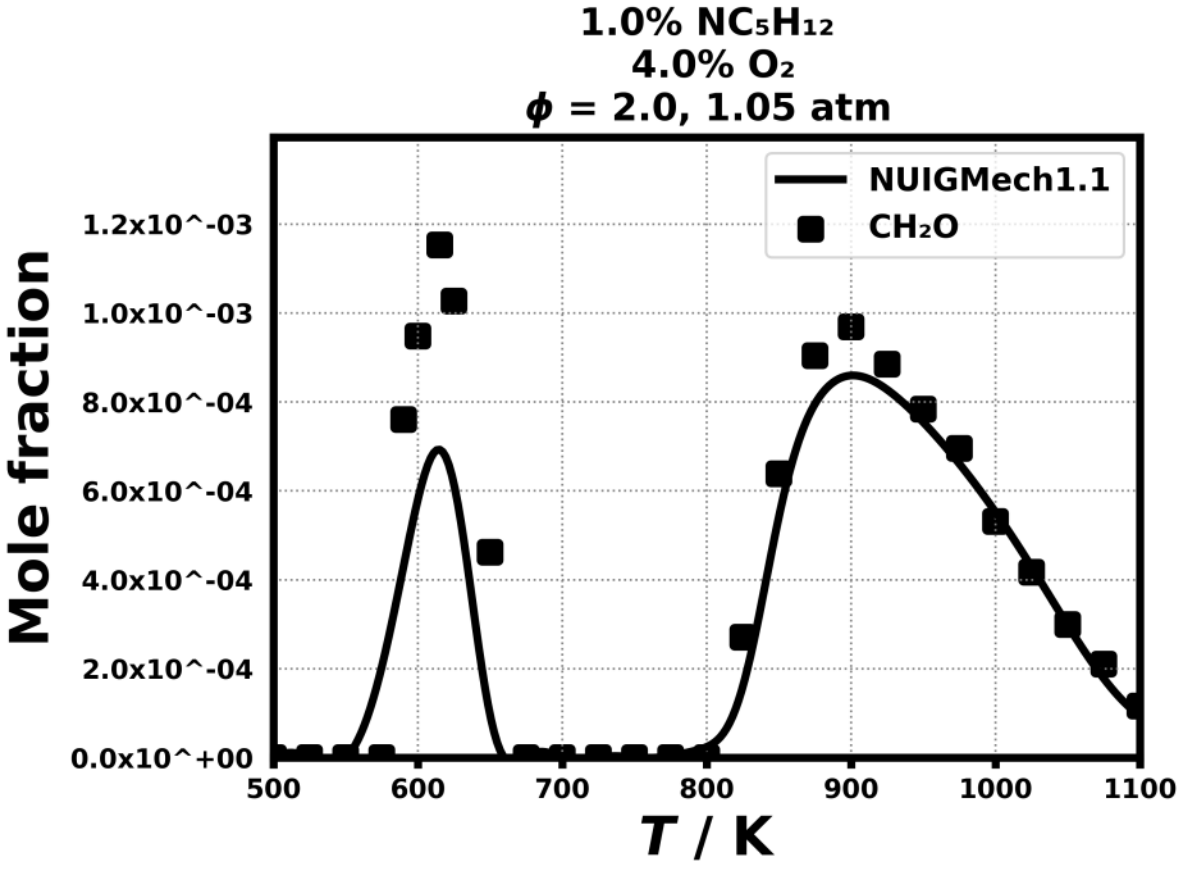

Figure 113: Dataset: 1.05_ATM_PHI_2.0

1.3.84 Case: n-C5H12/JSR/BUGLER/1.05_ATM_PHI_2.0

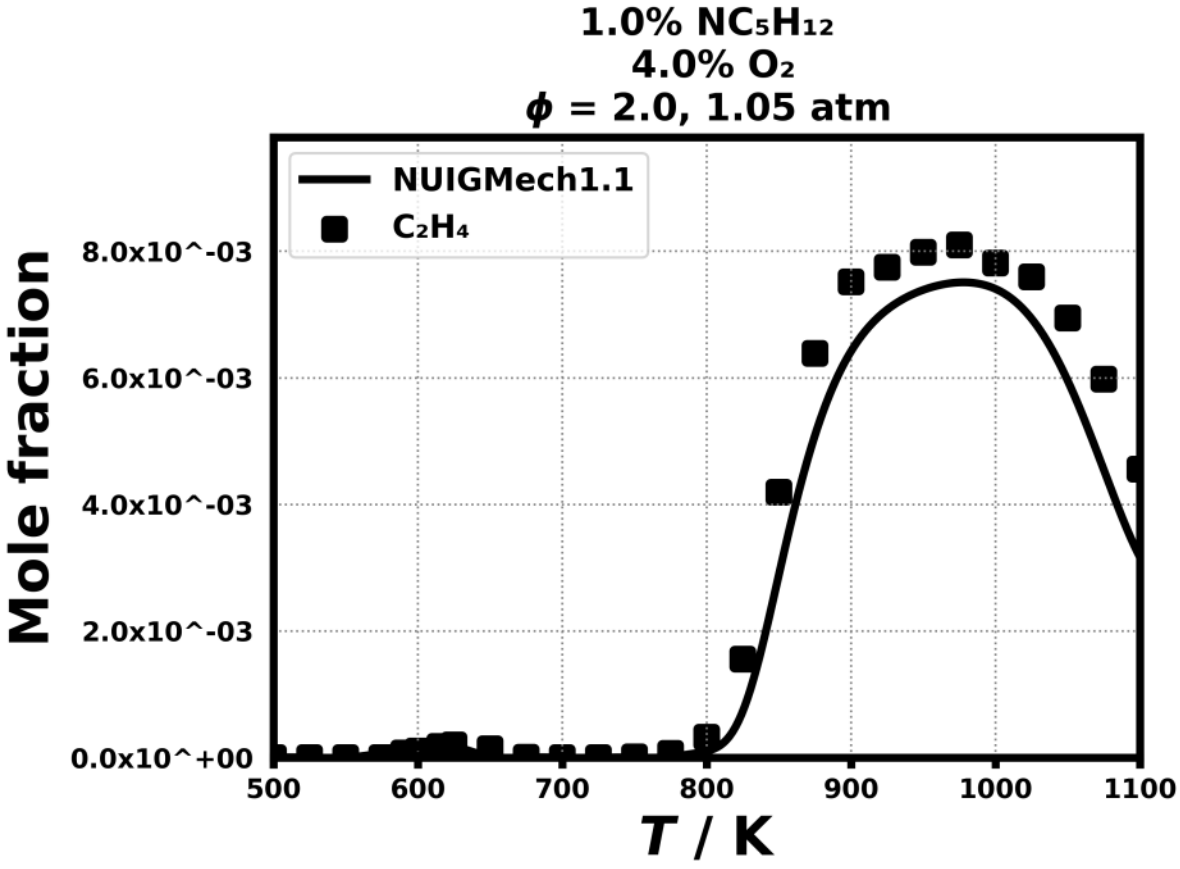

Figure 114: Dataset: 1.05_ATM_PHI_2.0

1.3.85 Case: n-C5H12/JSR/BUGLER/1.05_ATM_PHI_2.0

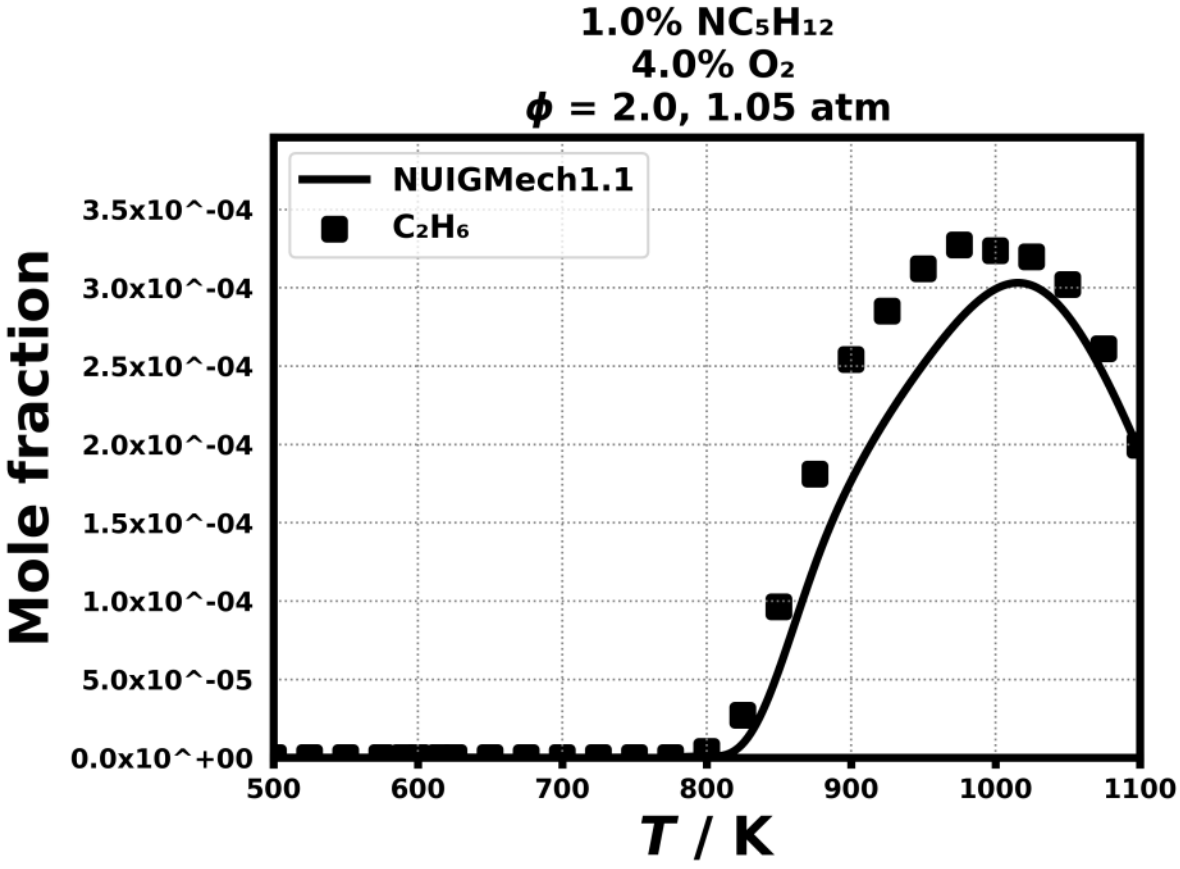

Figure 115: Dataset: 1.05_ATM_PHI_2.0

1.3.86 Case: n-C5H12/JSR/BUGLER/1.05_ATM_PHI_2.0

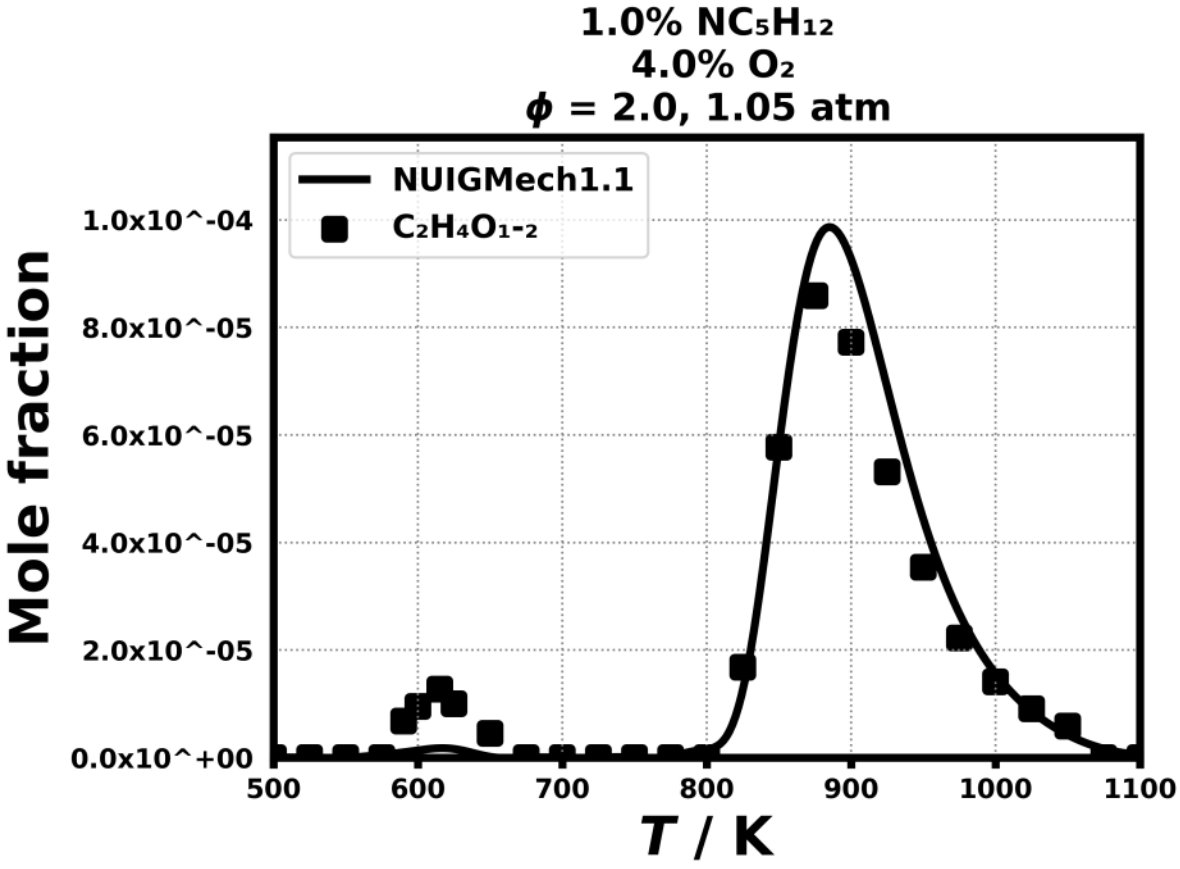

Figure 116: Dataset: 1.05_ATM_PHI_2.0

1.3.87 Case: n-C5H12/JSR/BUGLER/1.05_ATM_PHI_2.0

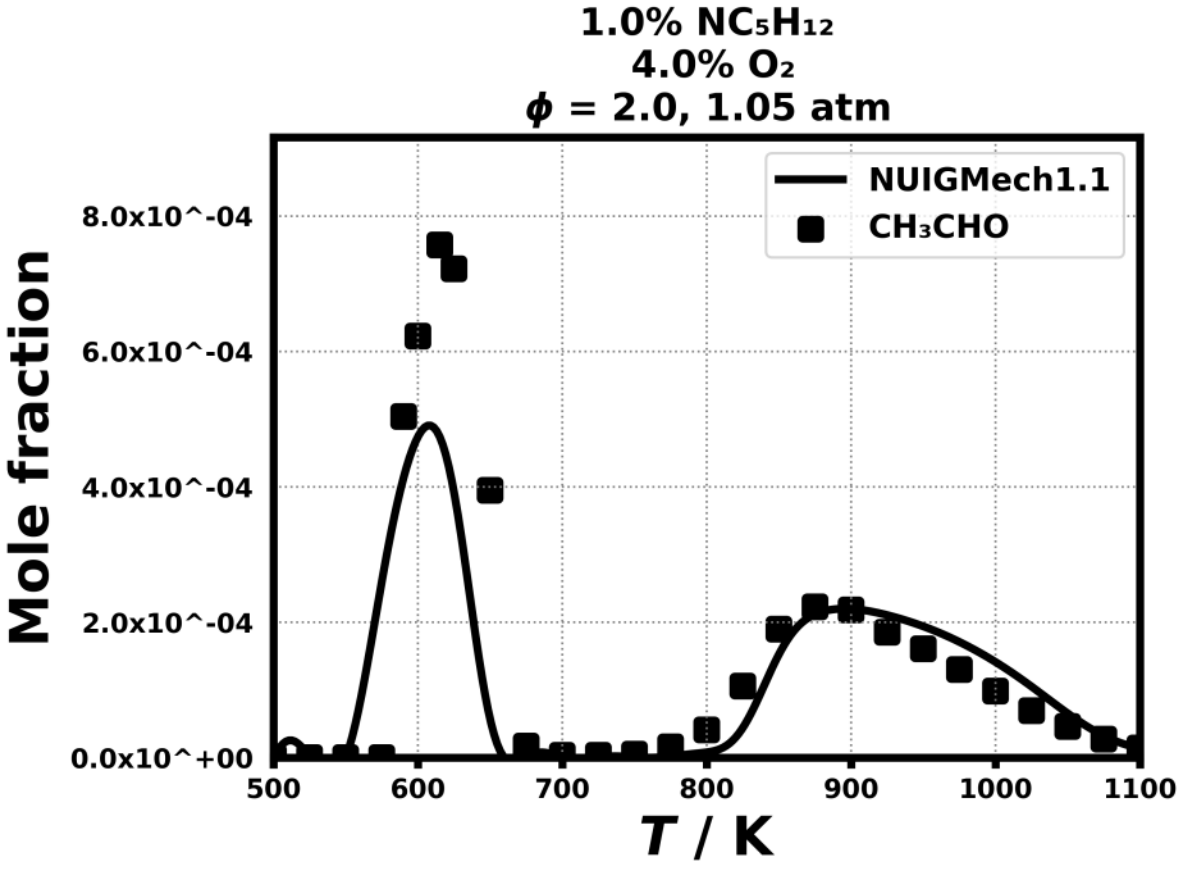

Figure 117: Dataset: 1.05_ATM_PHI_2.0

1.3.88 Case: n-C5H12/JSR/BUGLER/1.05_ATM_PHI_2.0

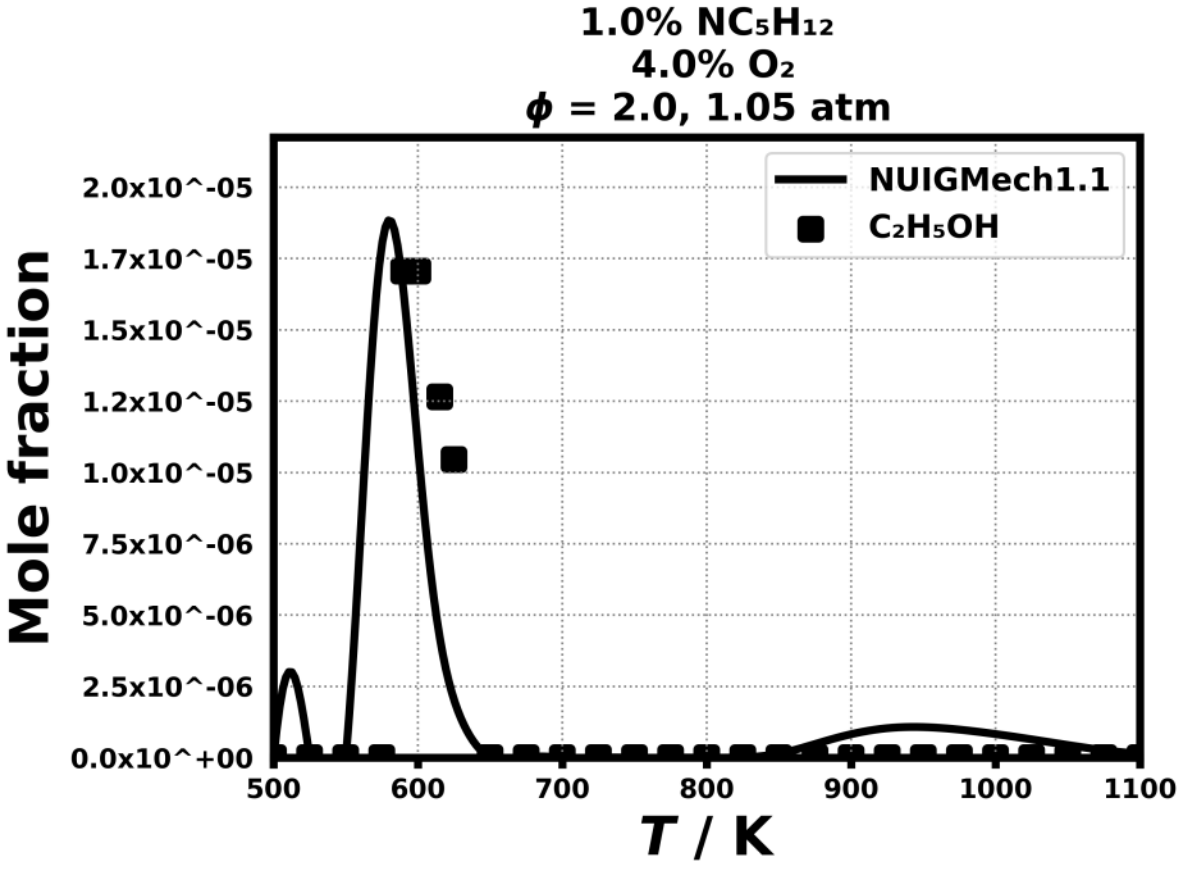

Figure 118: Dataset: 1.05_ATM_PHI_2.0

1.3.89 Case: n-C5H12/JSR/BUGLER/1.05_ATM_PHI_2.0

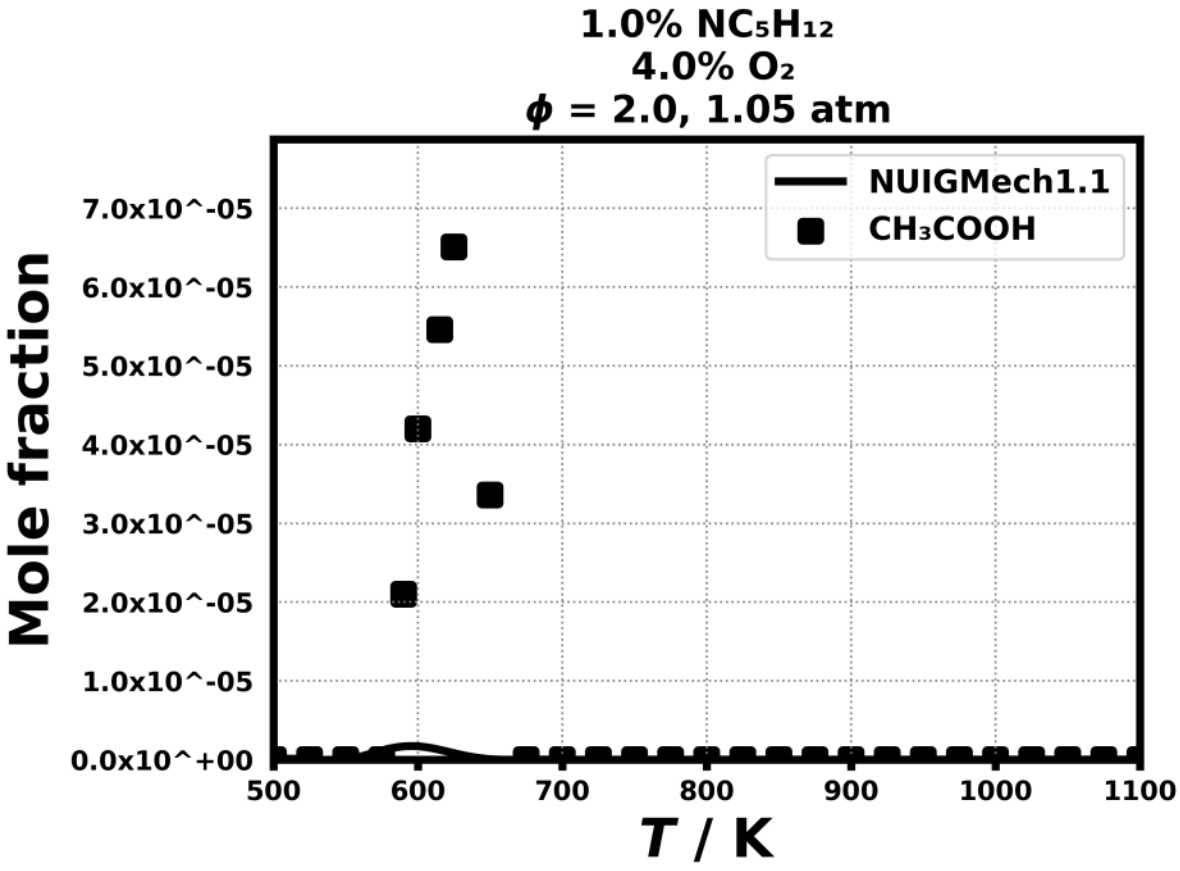

Figure 119: Dataset: 1.05_ATM_PHI_2.0

1.3.90 Case: n-C5H12/JSR/BUGLER/1.05_ATM_PHI_2.0

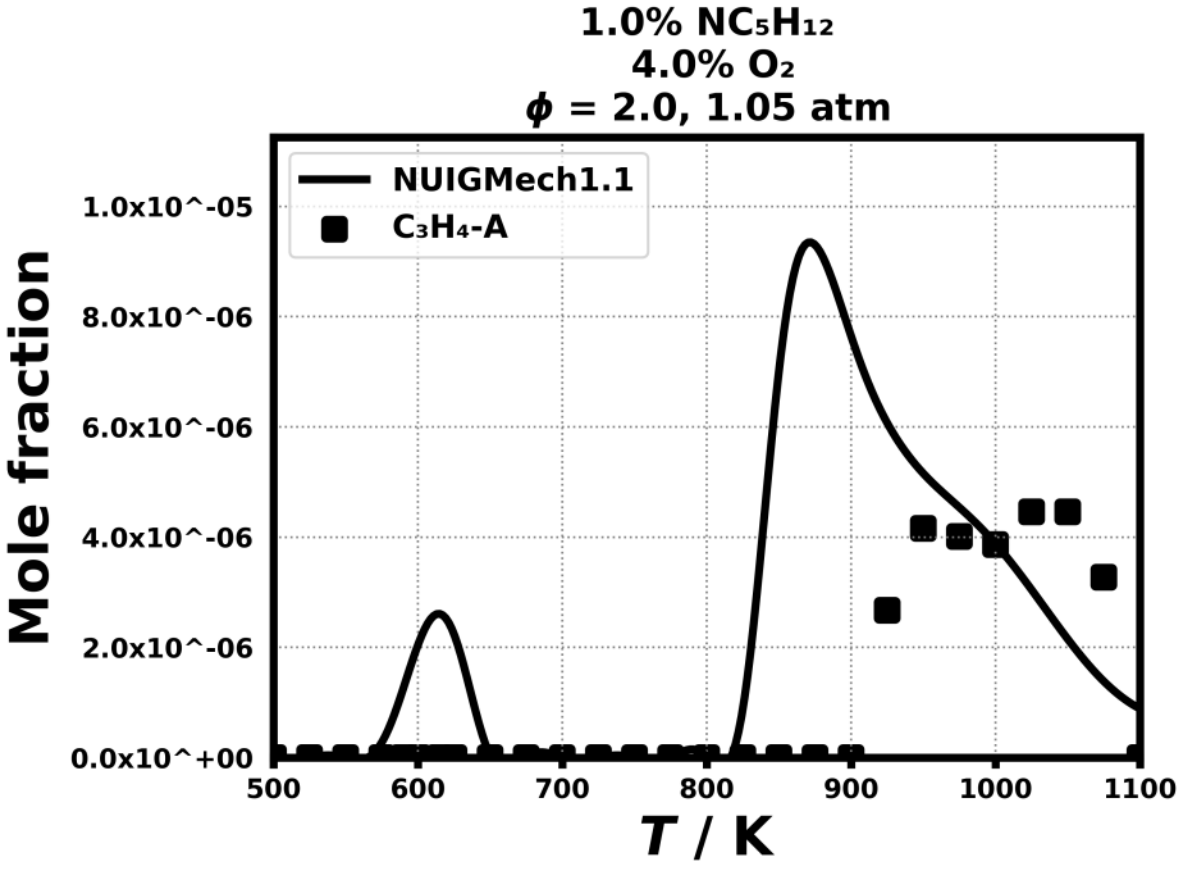

Figure 120: Dataset: 1.05_ATM_PHI_2.0

1.3.91 Case: n-C5H12/JSR/BUGLER/1.05_ATM_PHI_2.0

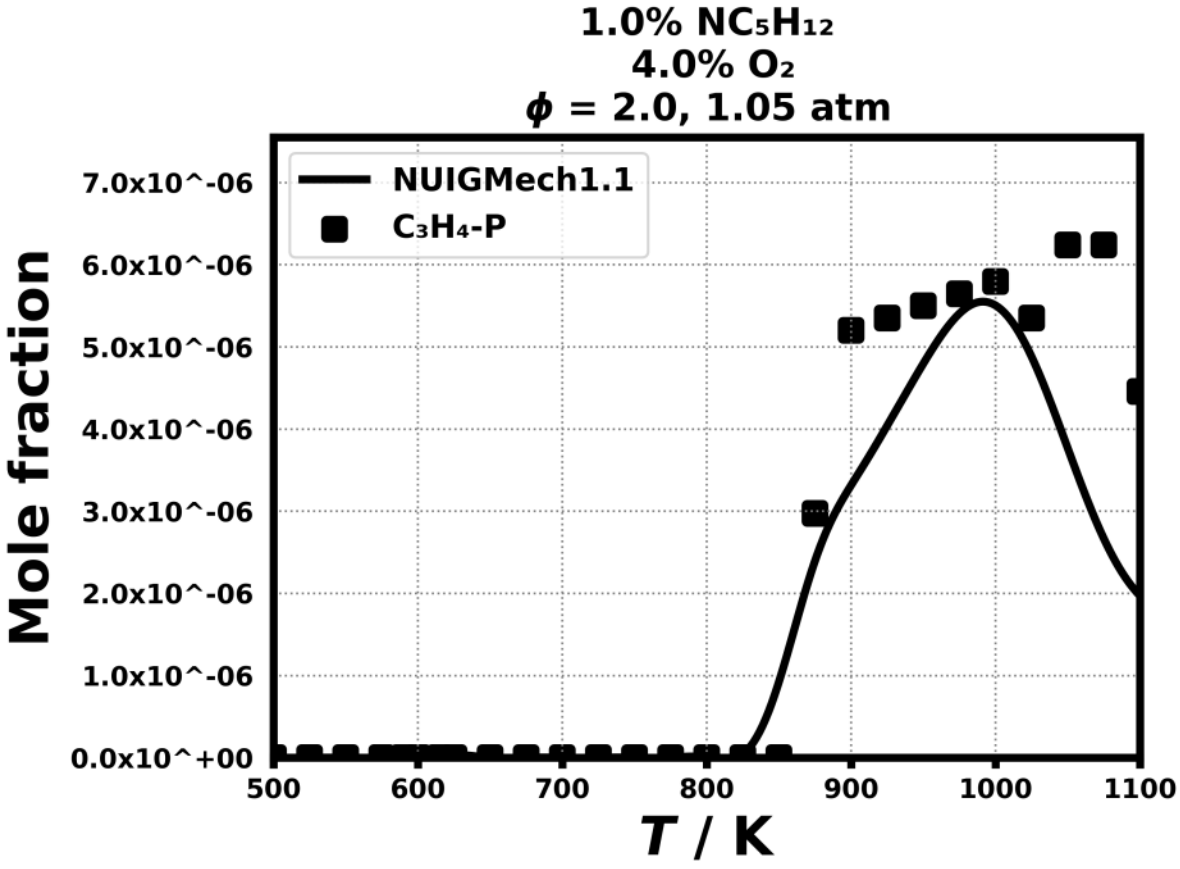

Figure 121: Dataset: 1.05_ATM_PHI_2.0

1.3.92 Case: n-C5H12/JSR/BUGLER/1.05_ATM_PHI_2.0

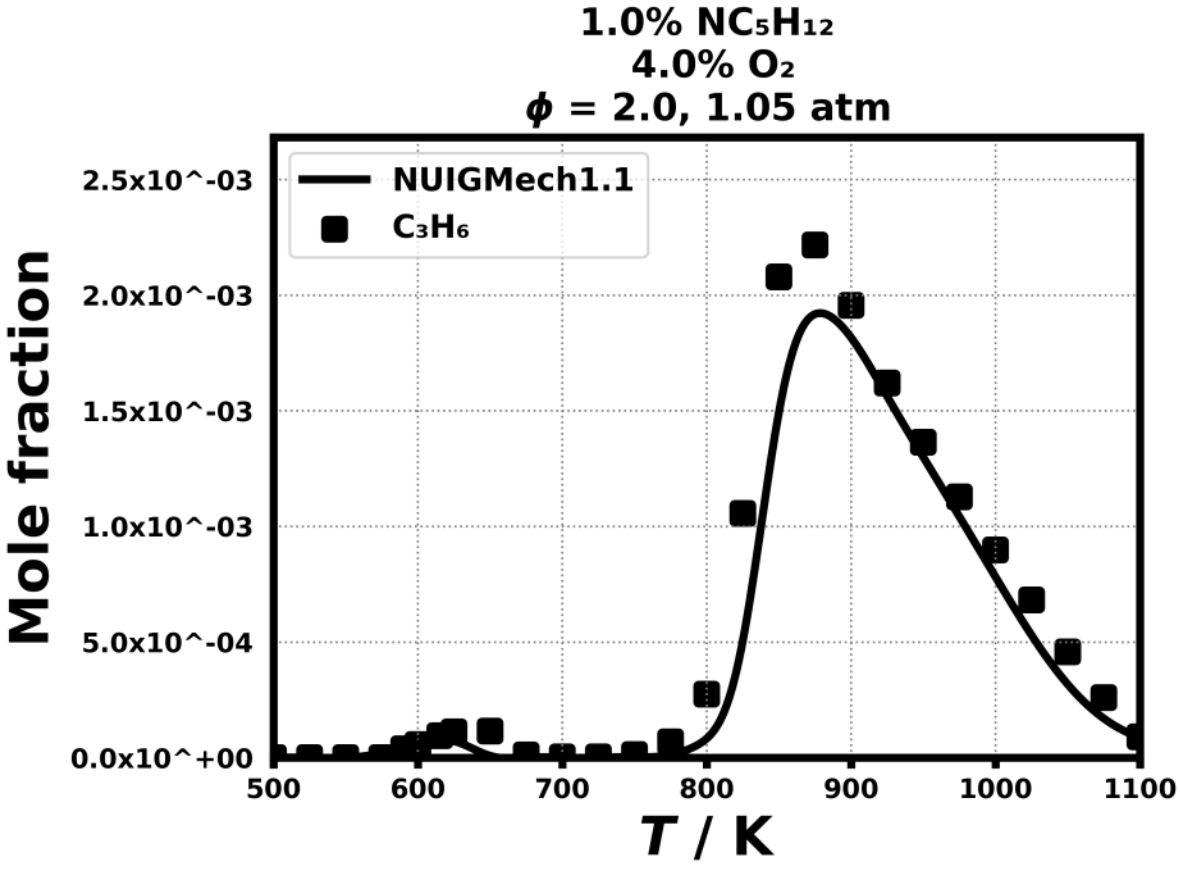

Figure 122: Dataset: 1.05_ATM_PHI_2.0

1.3.93 Case: n-C5H12/JSR/BUGLER/1.05_ATM_PHI_2.0

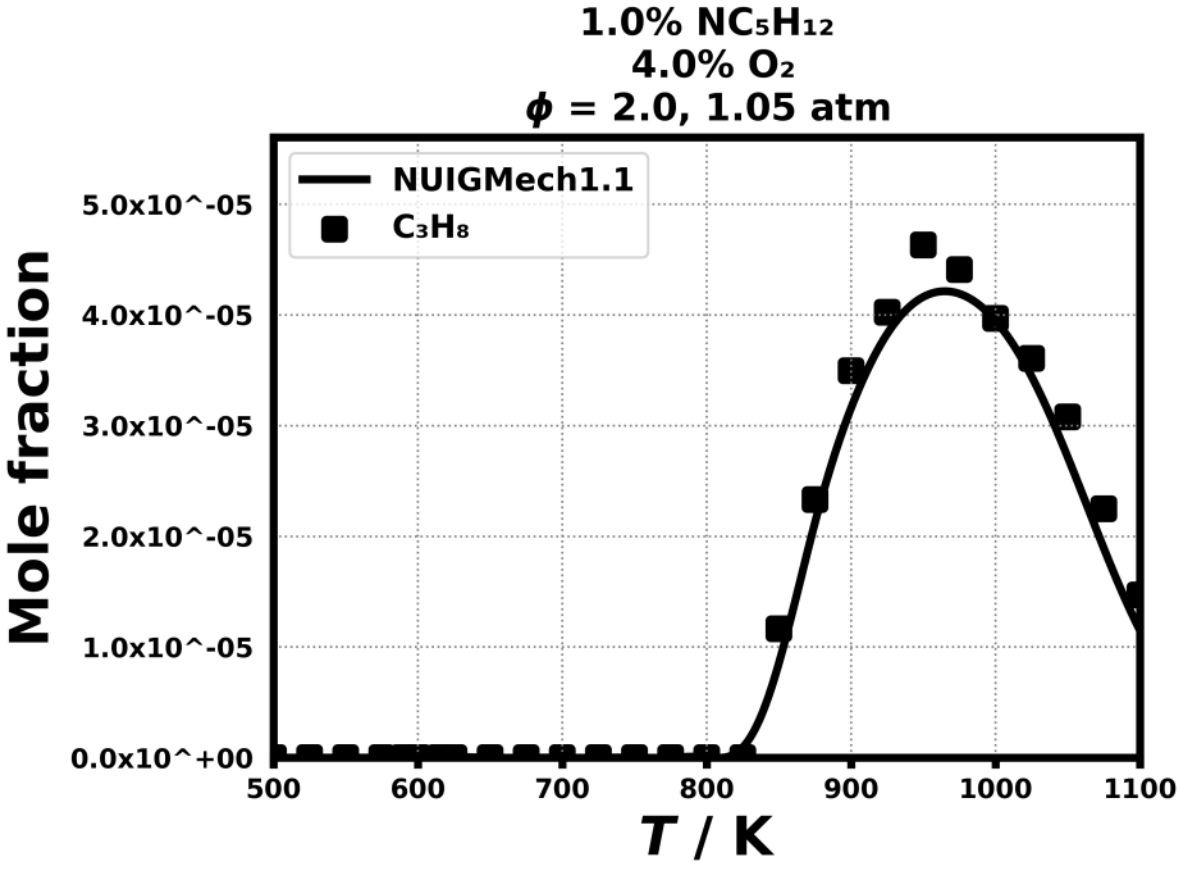

Figure 123: Dataset: 1.05_ATM_PHI_2.0

1.3.94 Case: n-C5H12/JSR/BUGLER/1.05_ATM_PHI_2.0

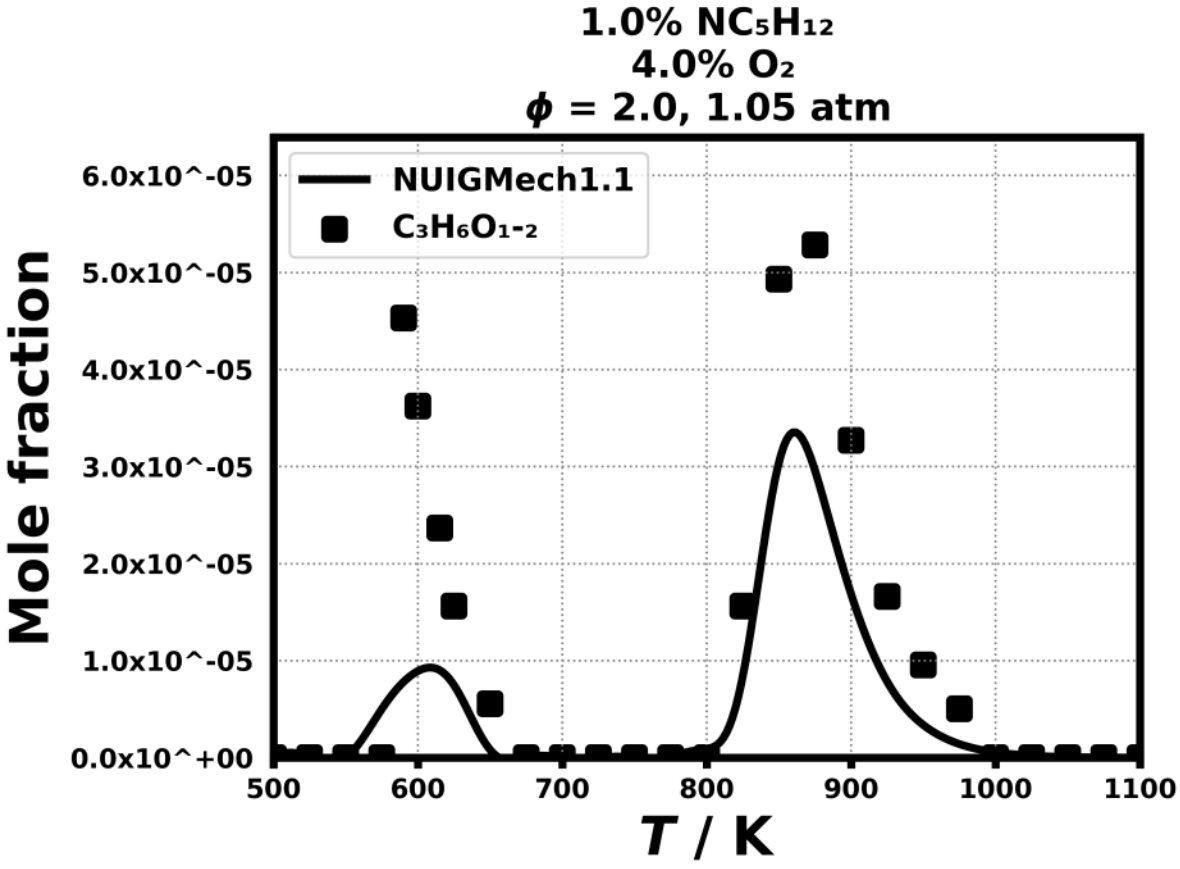

Figure 124: Dataset: 1.05_ATM_PHI_2.0

1.3.95 Case: n-C5H12/JSR/BUGLER/1.05_ATM_PHI_2.0

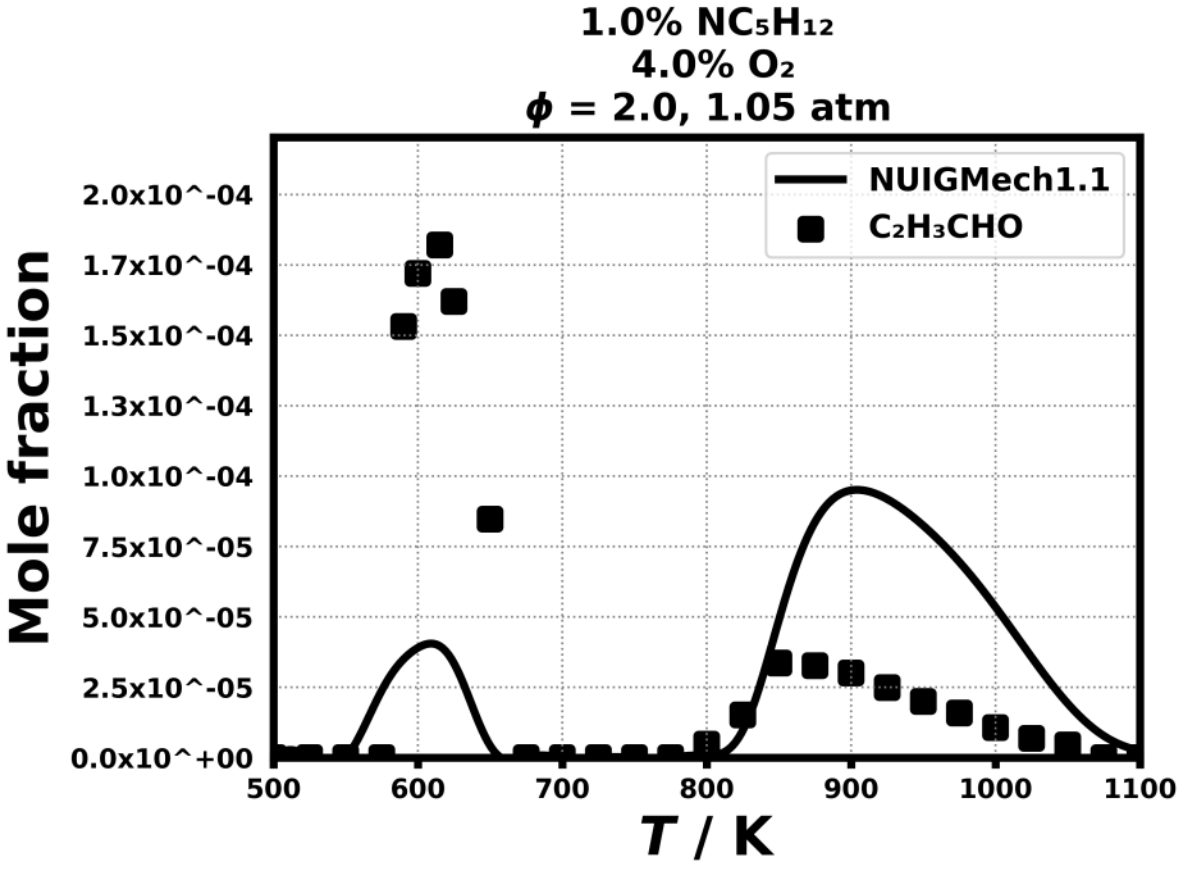

Figure 125: Dataset: 1.05_ATM_PHI_2.0

1.3.96 Case: n-C5H12/JSR/BUGLER/1.05_ATM_PHI_2.0

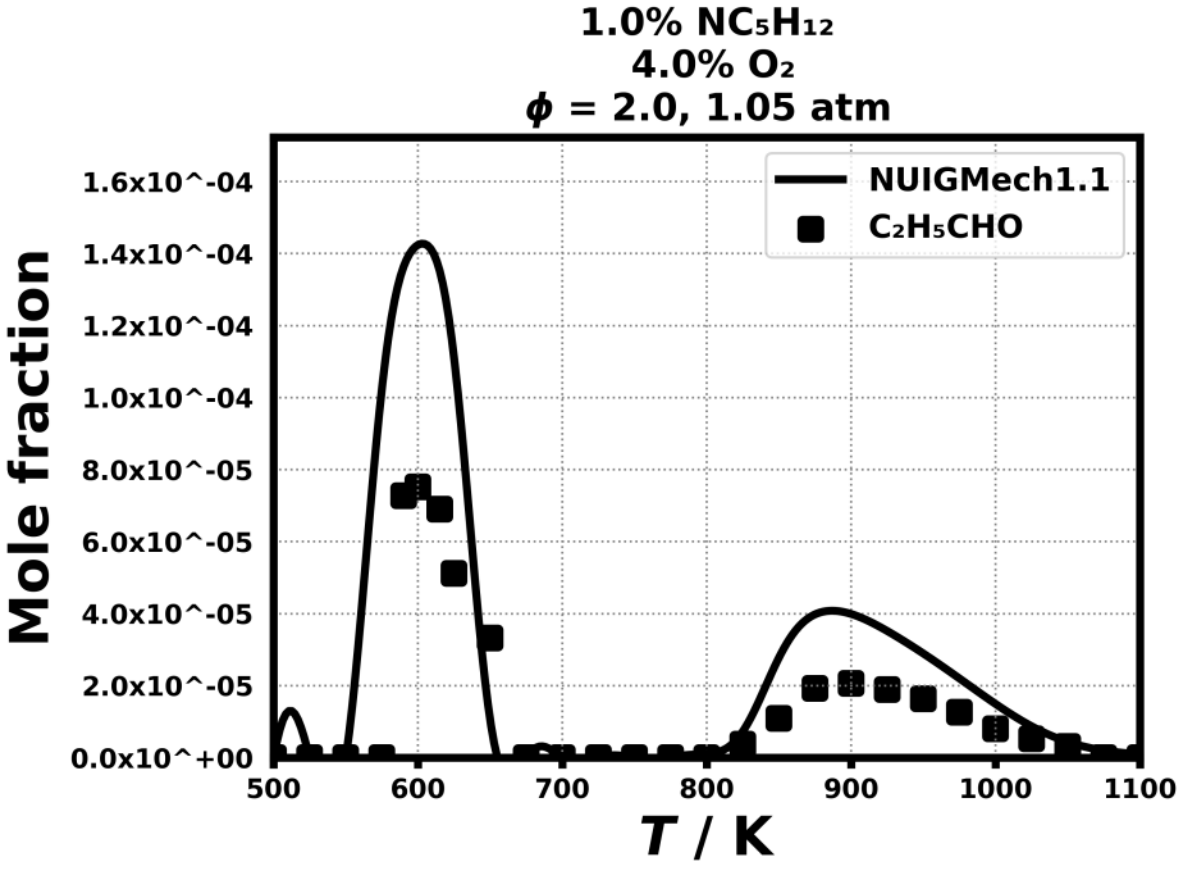

Figure 126: Dataset: 1.05_ATM_PHI_2.0

1.3.97 Case: n-C5H12/JSR/BUGLER/1.05_ATM_PHI_2.0

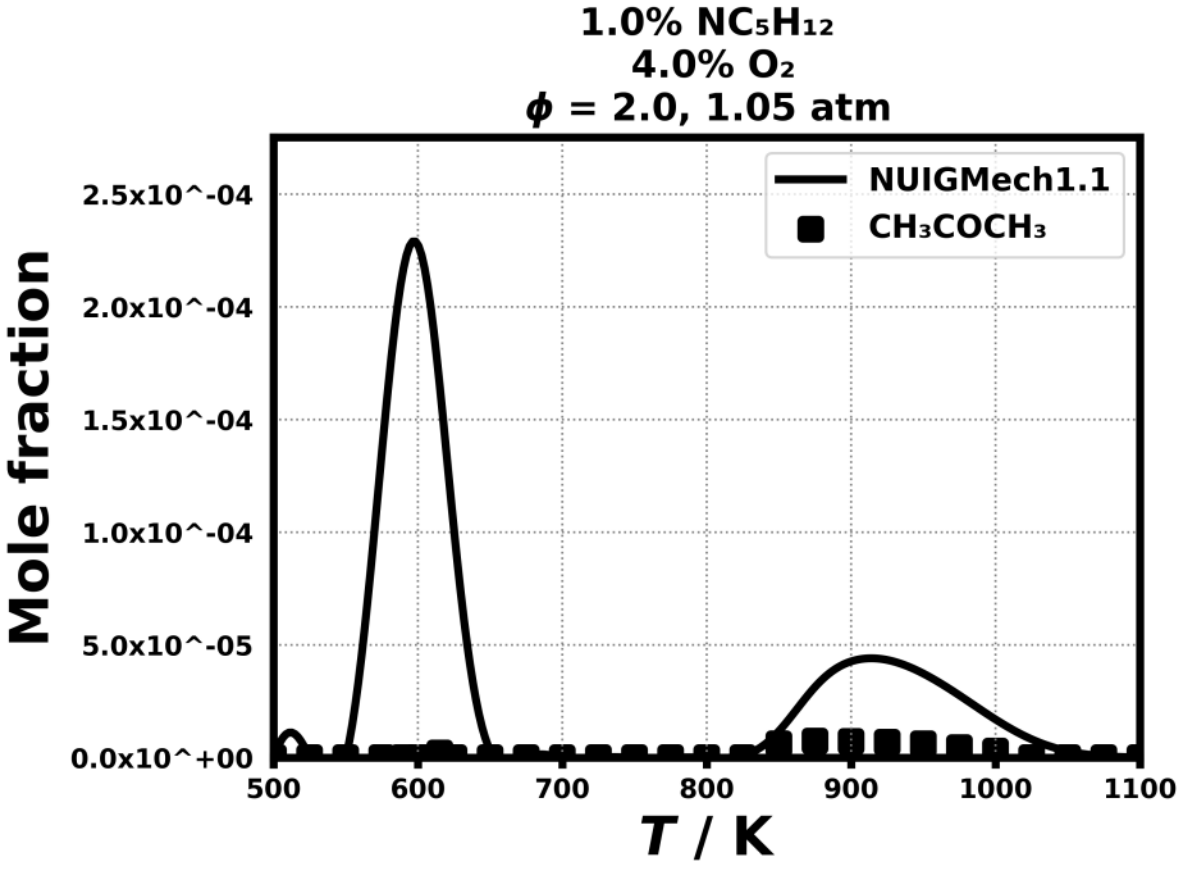

Figure 127: Dataset: 1.05_ATM_PHI_2.0

1.3.98 Case: n-C5H12/JSR/BUGLER/1.05_ATM_PHI_2.0

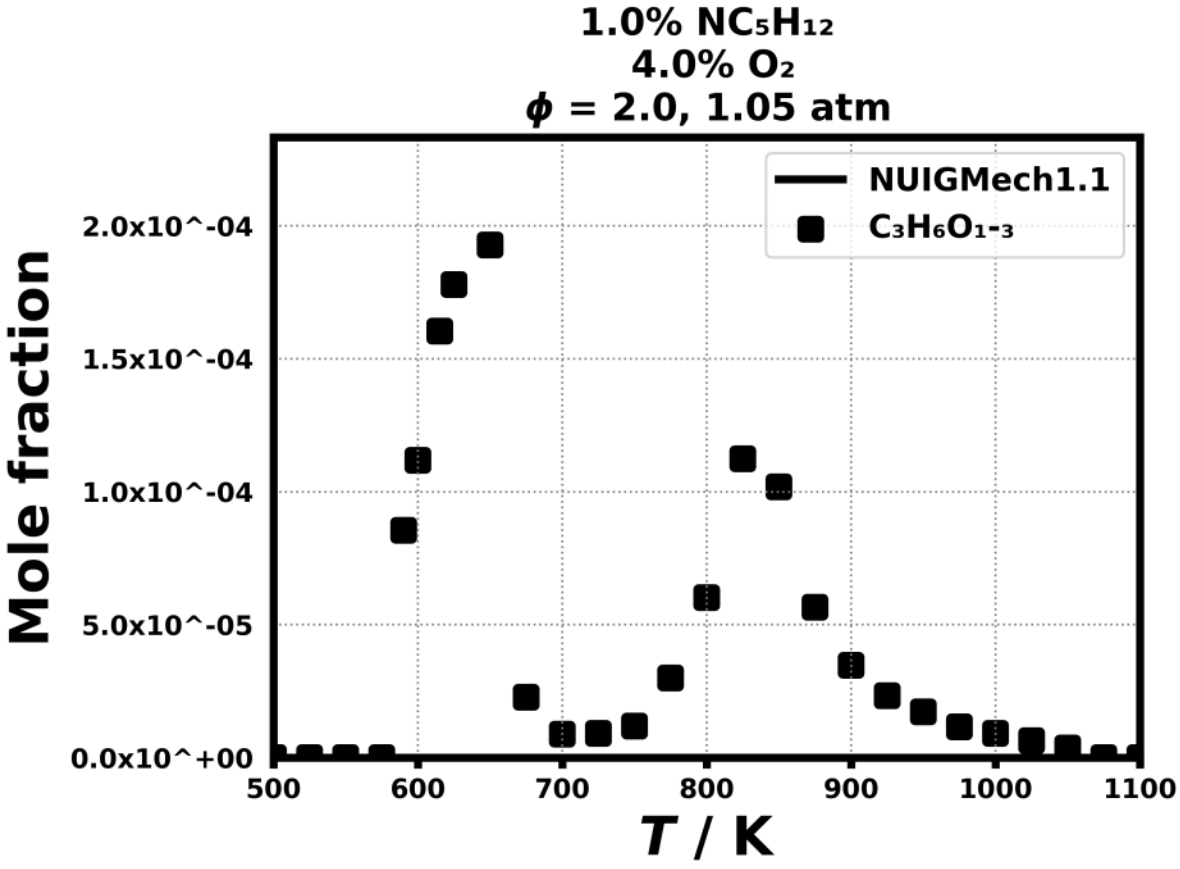

Figure 128: Dataset: 1.05_ATM_PHI_2.0

1.3.99 Case: n-C5H12/JSR/BUGLER/1.05_ATM_PHI_2.0

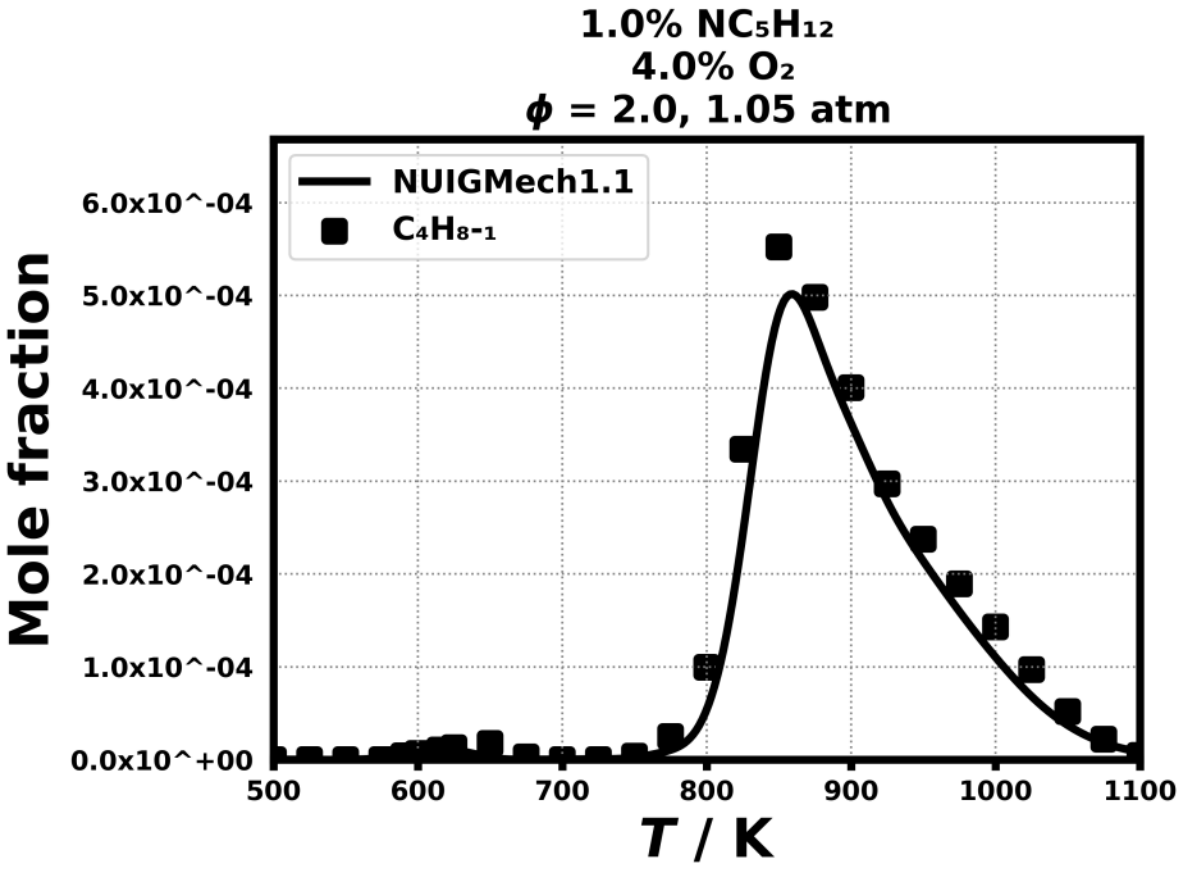

Figure 129: Dataset: 1.05_ATM_PHI_2.0

1.3.100 Case: n-C5H12/JSR/BUGLER/1.05_ATM_PHI_2.0

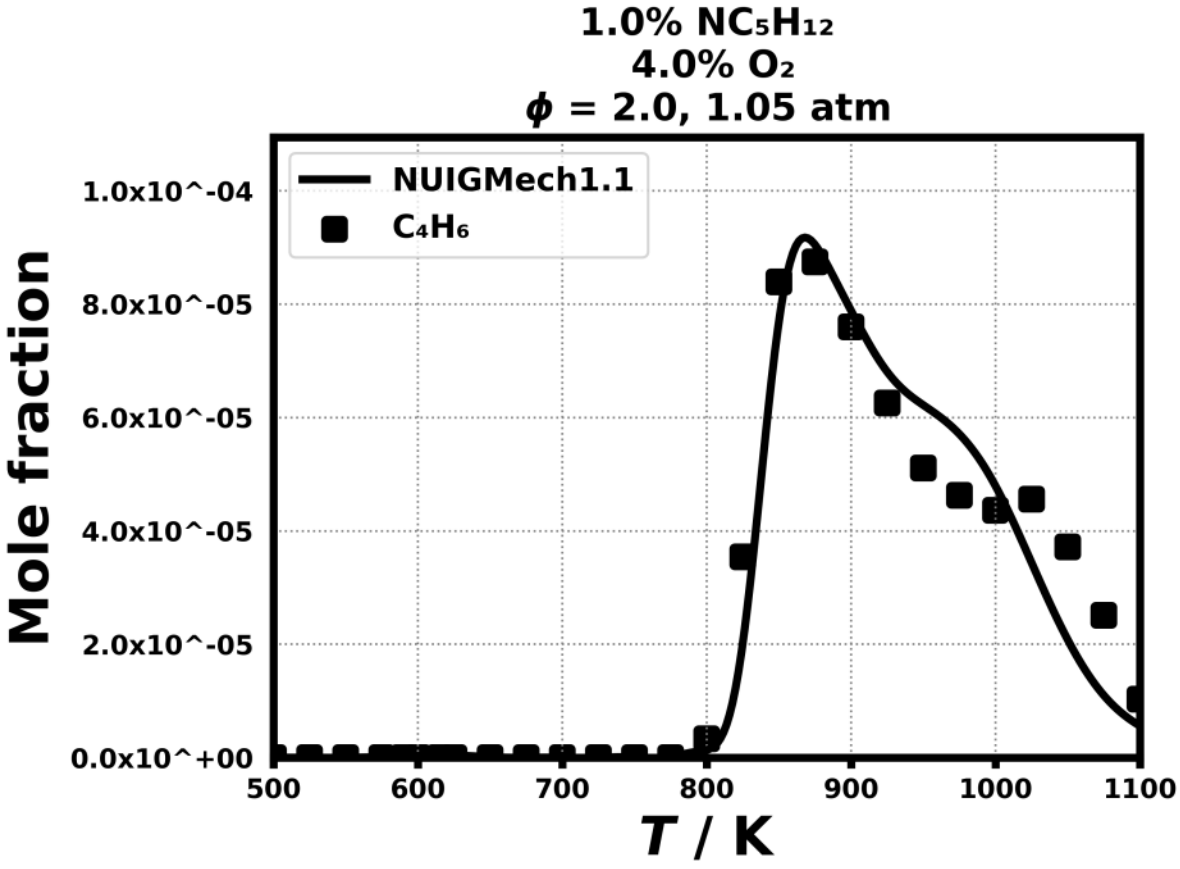

Figure 130: Dataset: 1.05_ATM_PHI_2.0

1.3.101 Case: n-C5H12/JSR/BUGLER/1.05_ATM_PHI_2.0

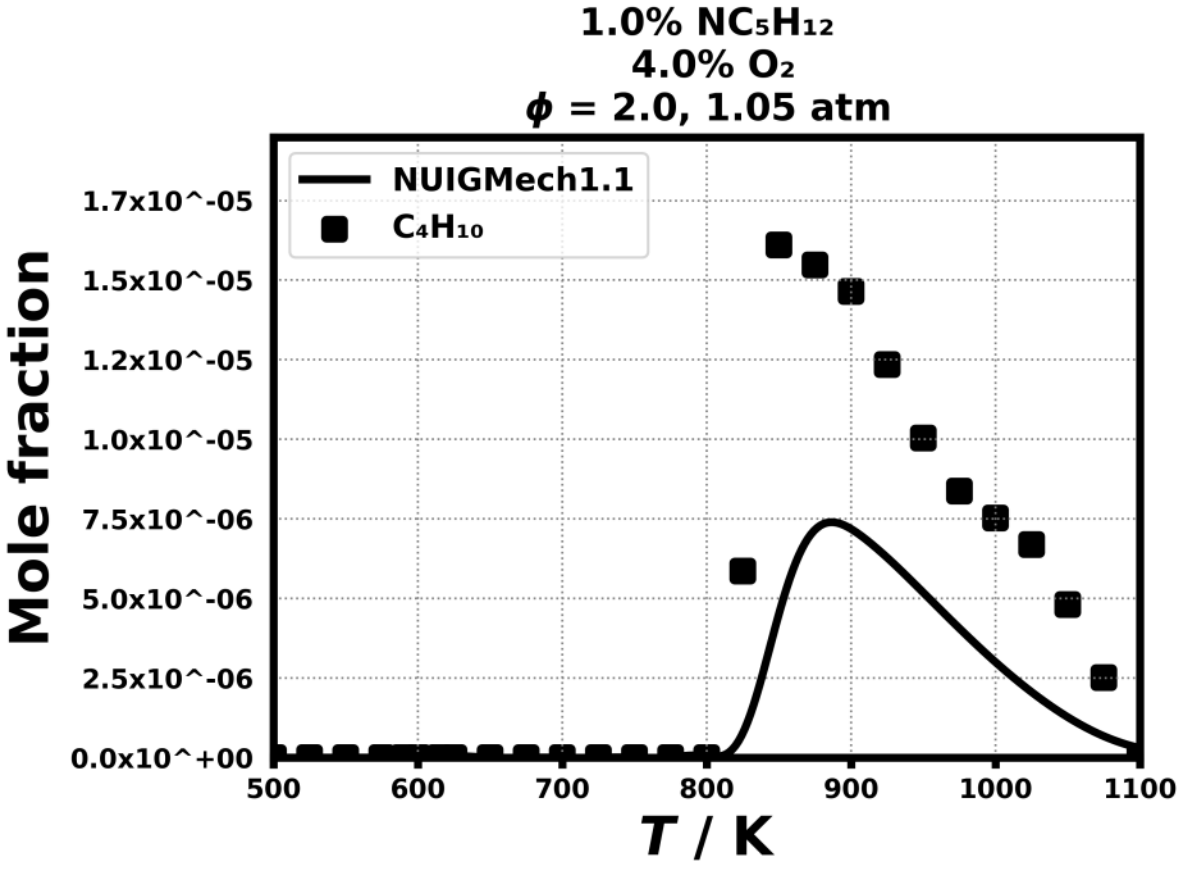

Figure 131: Dataset: 1.05_ATM_PHI_2.0

1.3.102 Case: n-C5H12/JSR/BUGLER/1.05_ATM_PHI_2.0

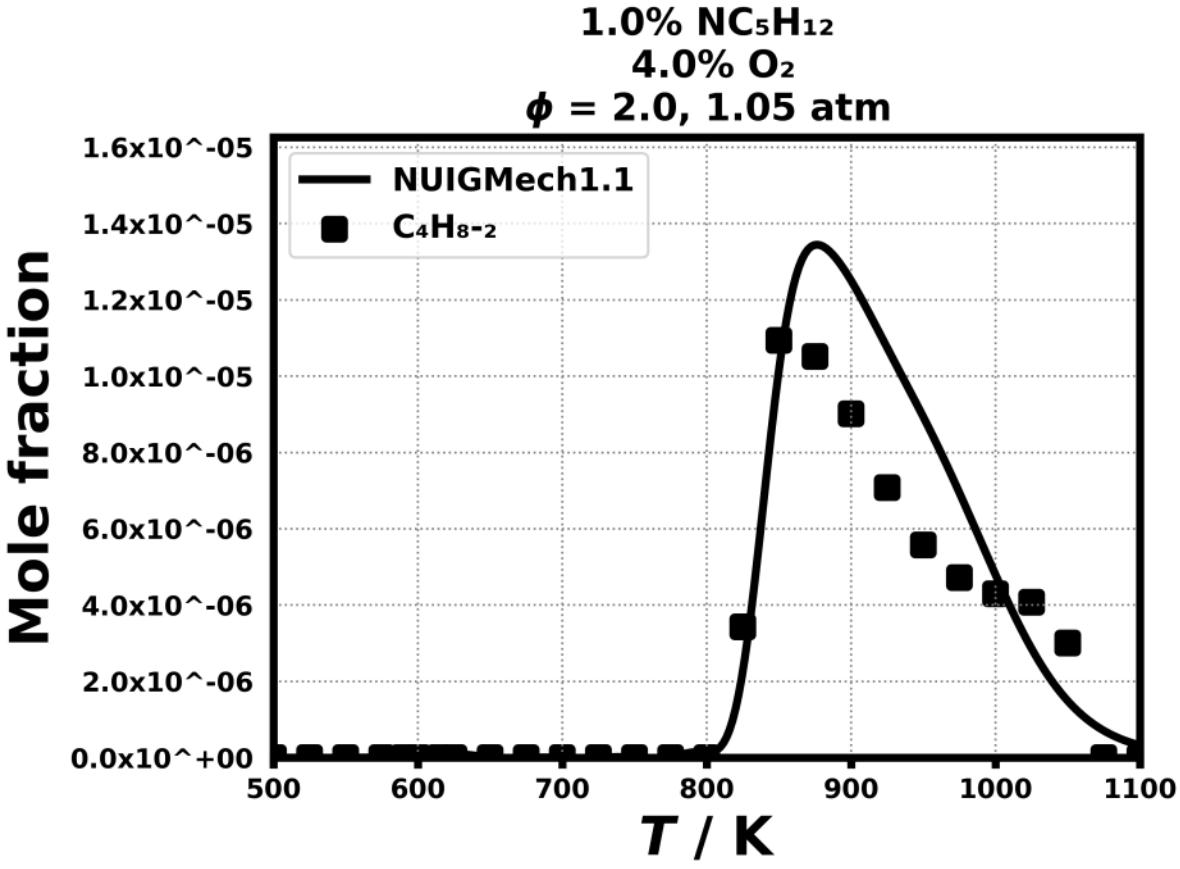

Figure 132: Dataset: 1.05_ATM_PHI_2.0

1.3.103 Case: n-C5H12/JSR/BUGLER/1.05_ATM_PHI_2.0

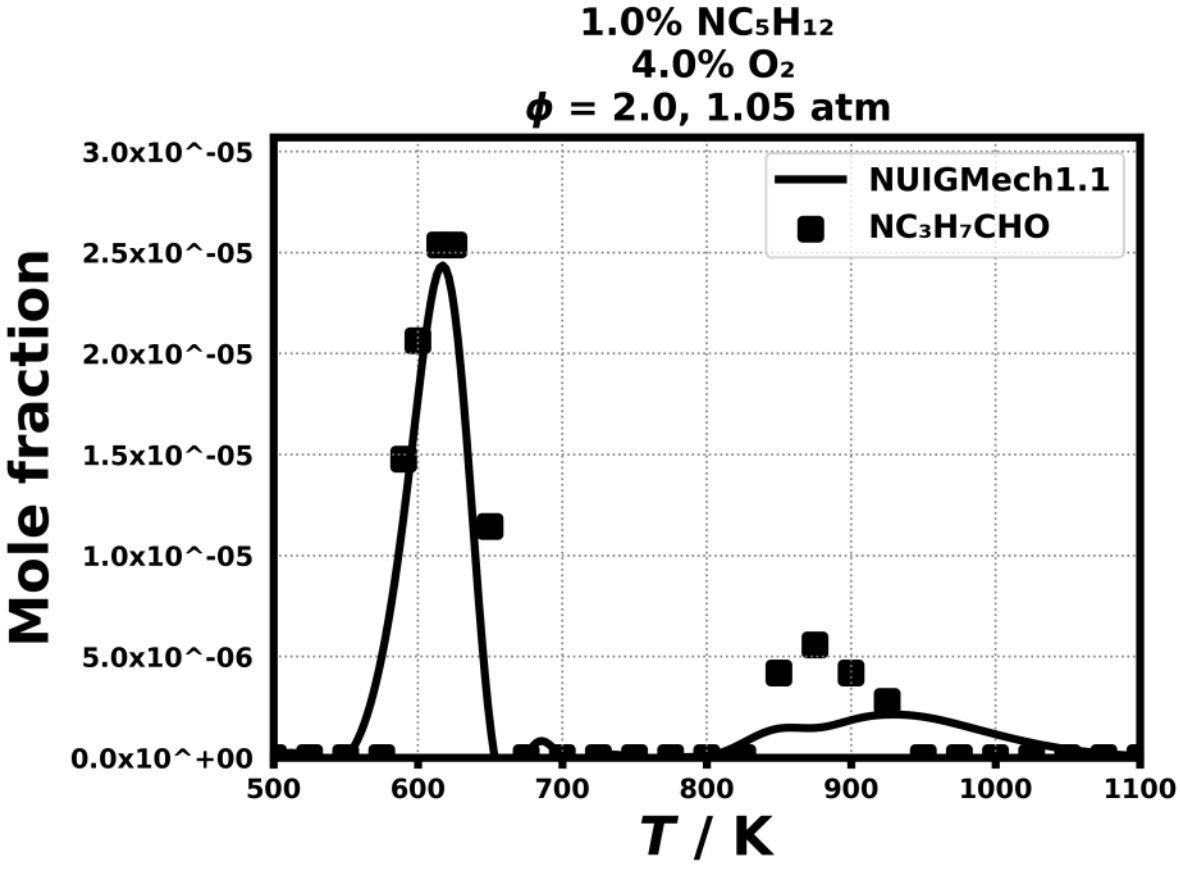

Figure 133: Dataset: 1.05_ATM_PHI_2.0

1.3.104 Case: n-C5H12/JSR/BUGLER/1.05_ATM_PHI_2.0

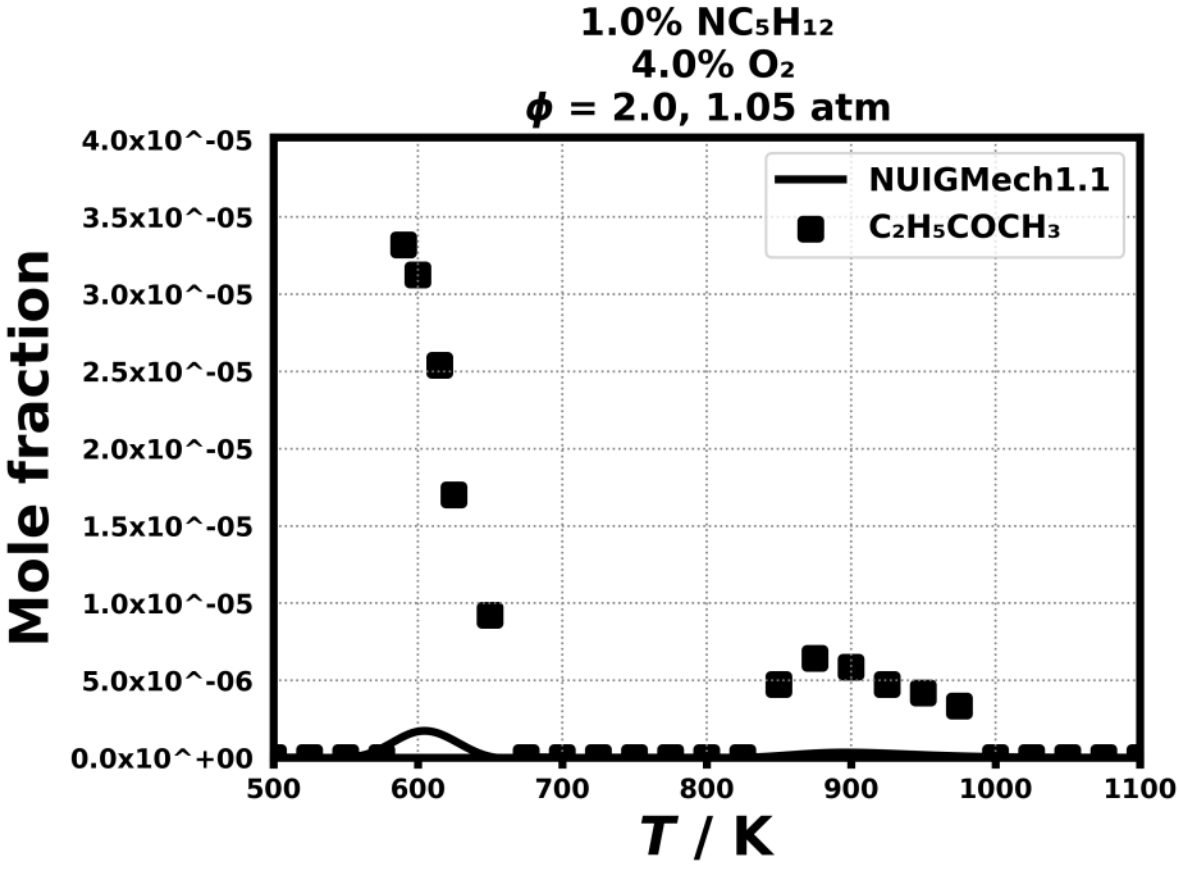

Figure 134: Dataset: 1.05_ATM_PHI_2.0

1.3.105 Case: n-C5H12/JSR/BUGLER/1.05_ATM_PHI_2.0

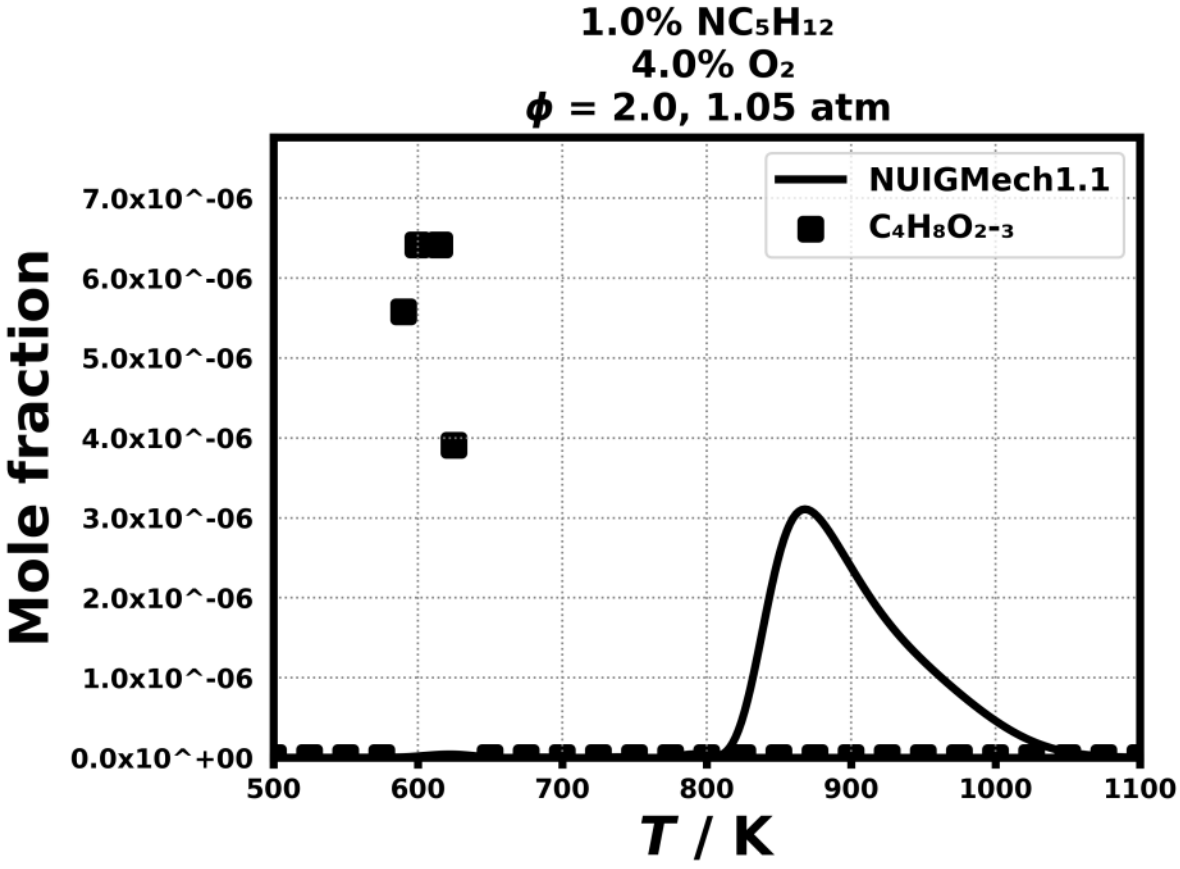

Figure 135: Dataset: 1.05_ATM_PHI_2.0

1.3.106 Case: n-C5H12/JSR/BUGLER/1.05_ATM_PHI_2.0

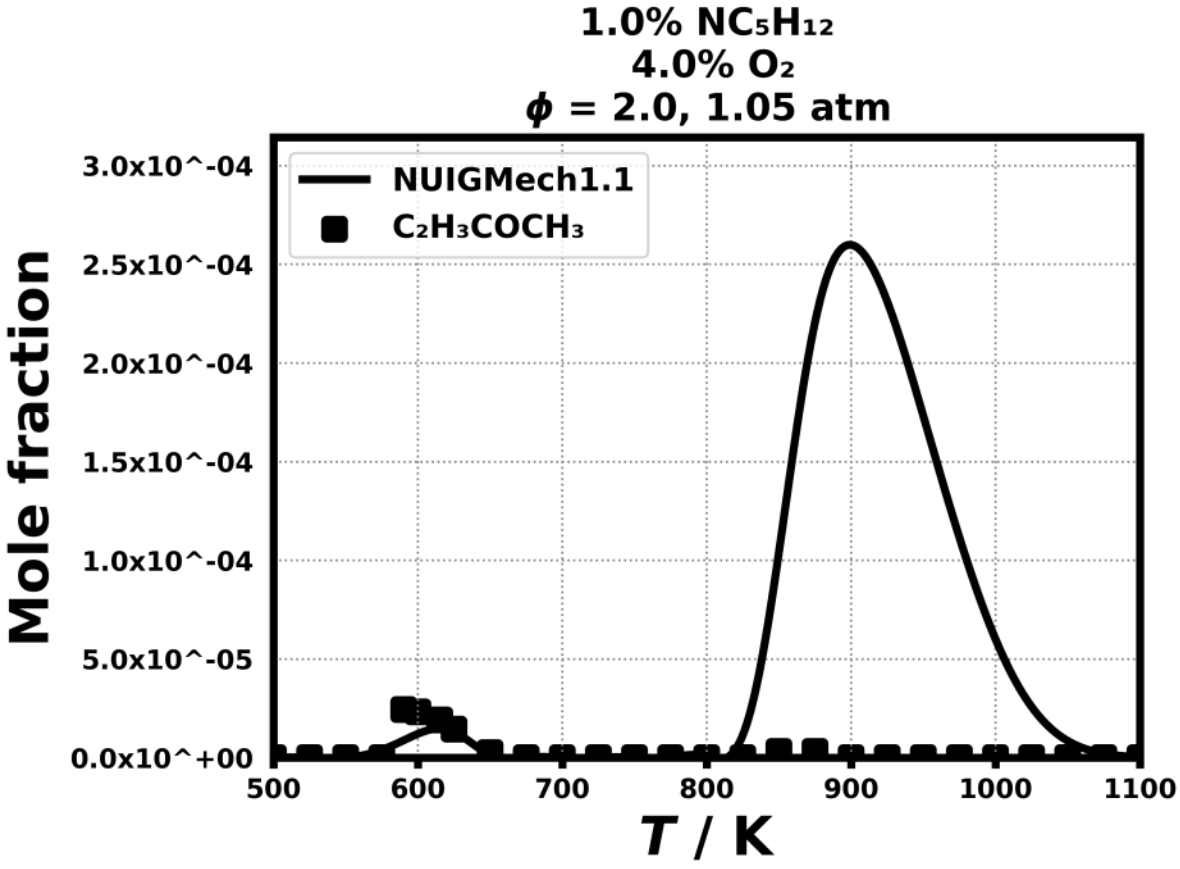

Figure 136: Dataset: 1.05_ATM_PHI_2.0

1.3.107 Case: n-C5H12/JSR/BUGLER/1.05_ATM_PHI_2.0

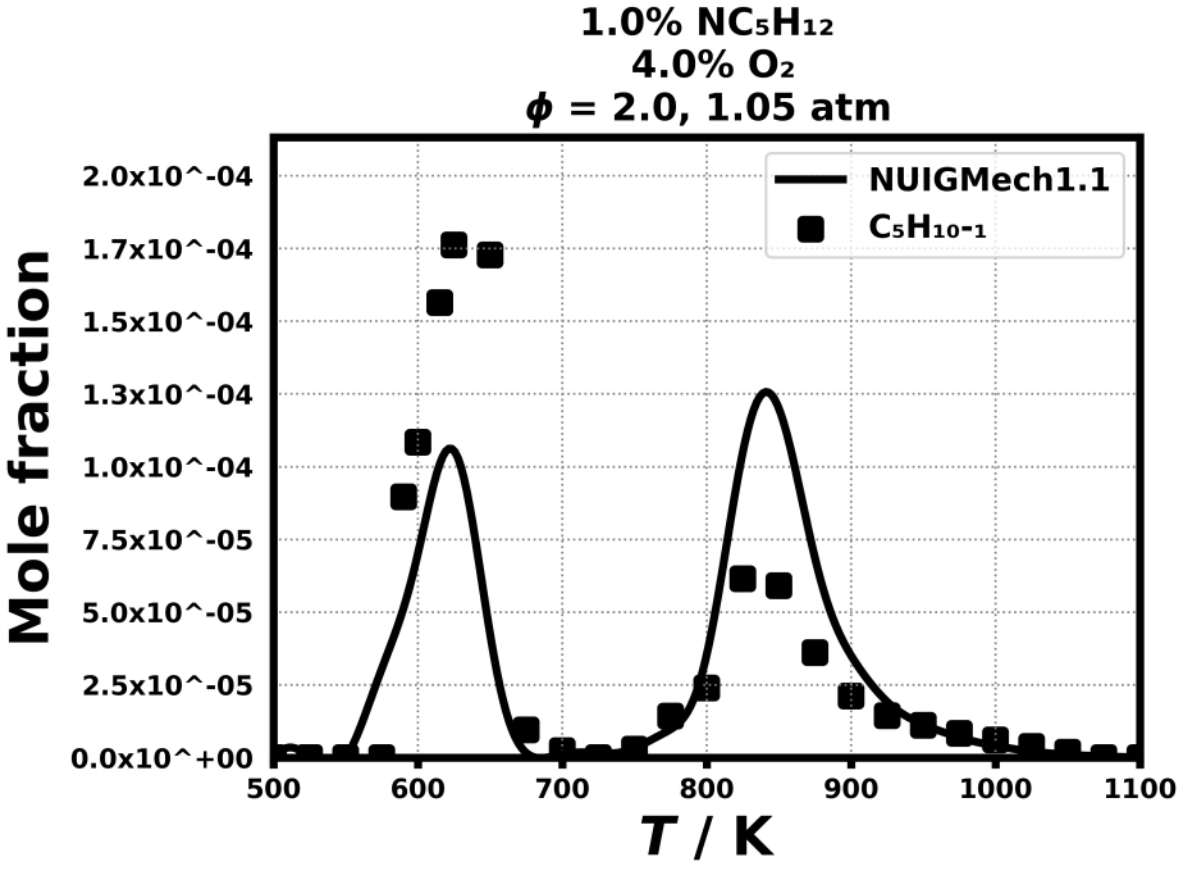

Figure 137: Dataset: 1.05_ATM_PHI_2.0

1.3.108 Case: n-C5H12/JSR/BUGLER/1.05_ATM_PHI_2.0

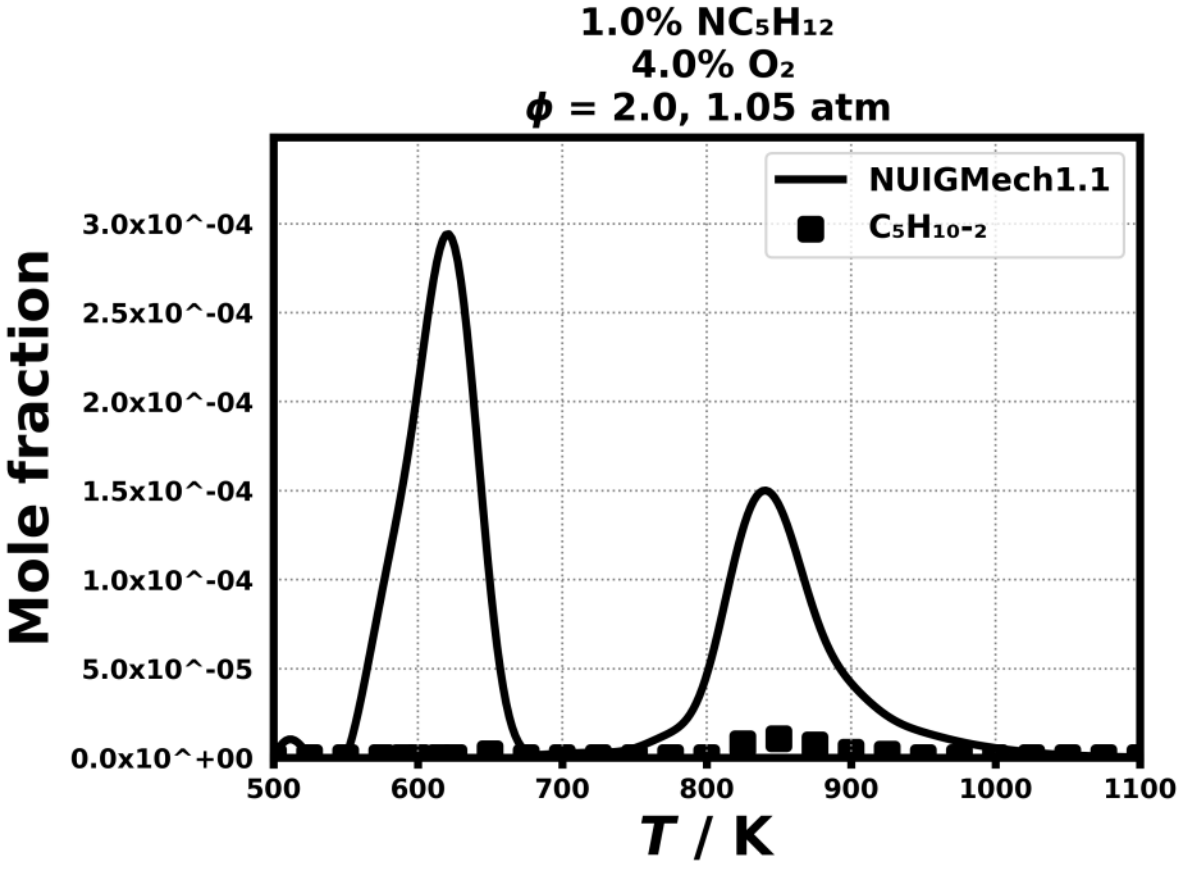

Figure 138: Dataset: 1.05_ATM_PHI_2.0

1.3.109 Case: n-C5H12/JSR/BUGLER/1.05_ATM_PHI_2.0

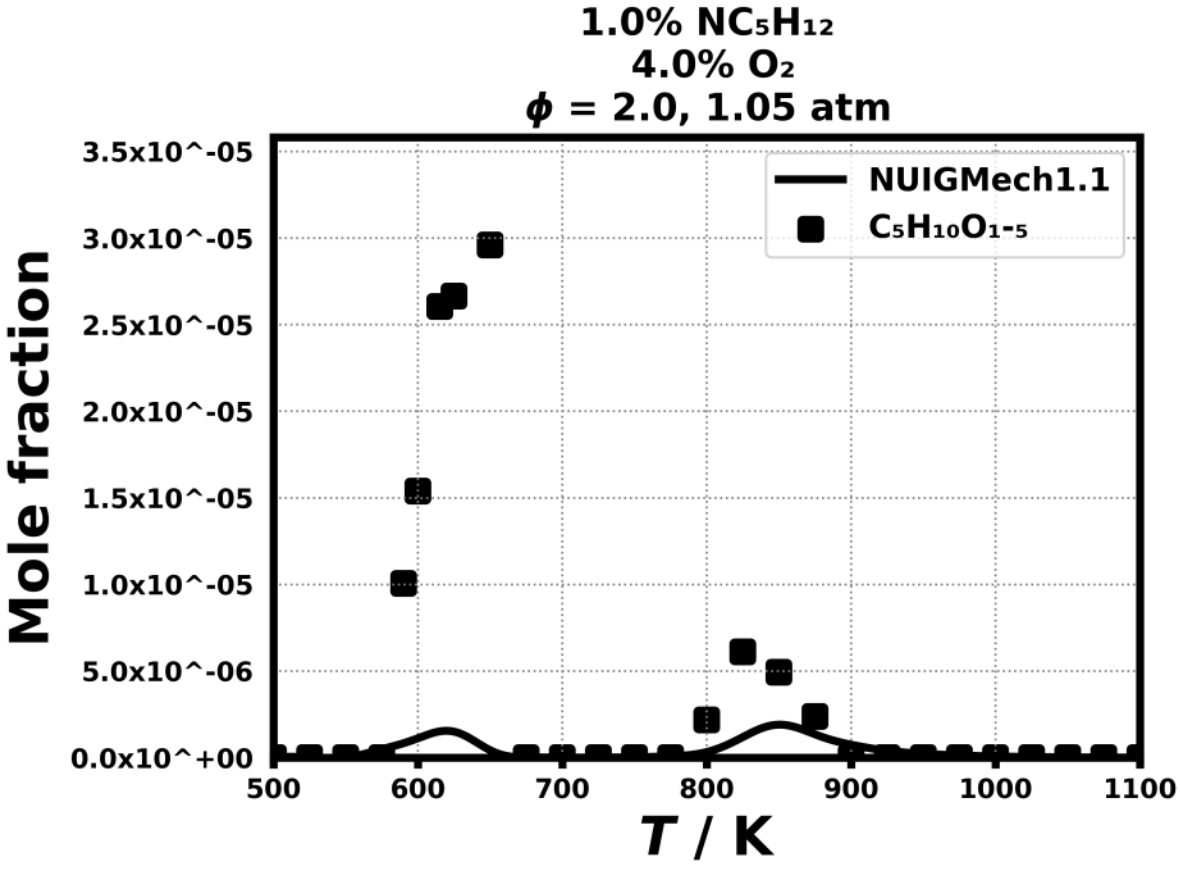

Figure 139: Dataset: 1.05_ATM_PHI_2.0

1.3.110 Case: n-C5H12/JSR/BUGLER/1.05_ATM_PHI_2.0

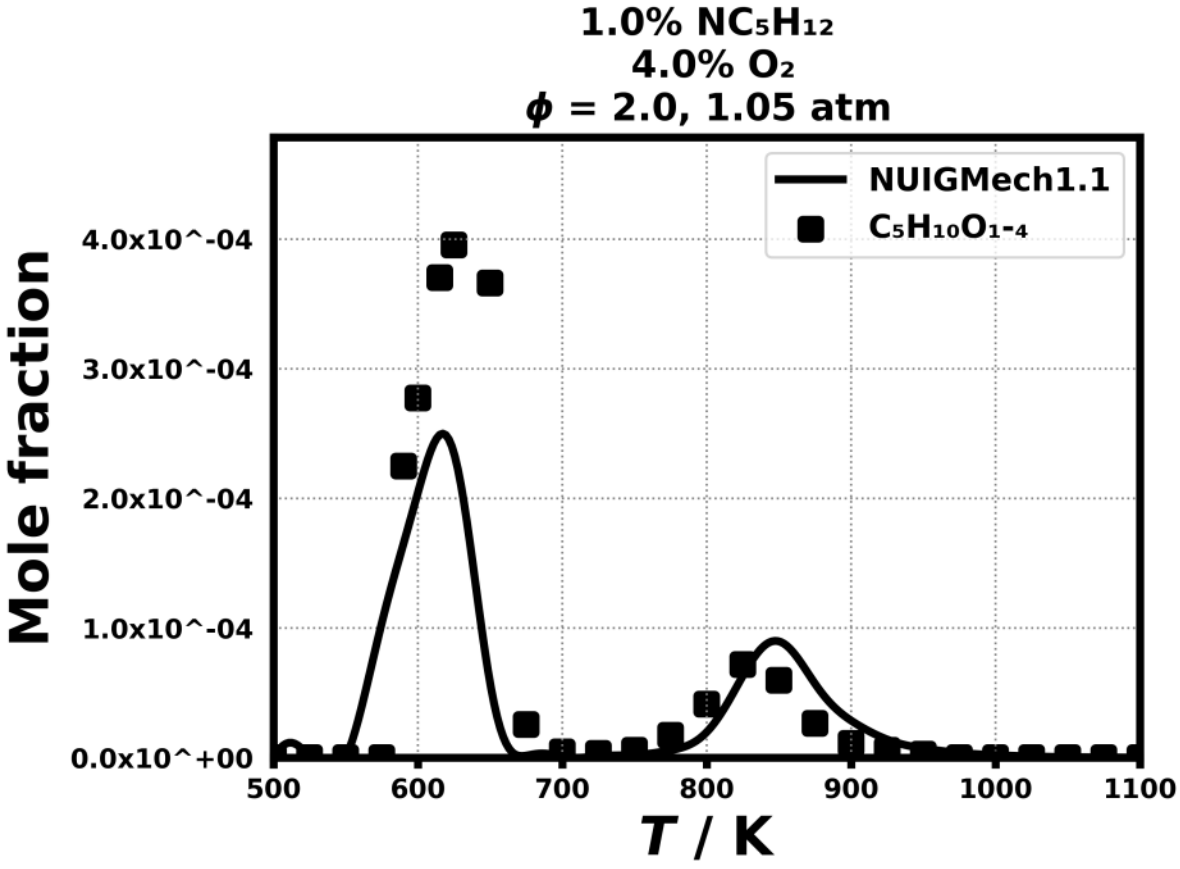

Figure 140: Dataset: 1.05_ATM_PHI_2.0

1.3.111 Case: n-C5H12/JSR/BUGLER/1.05_ATM_PHI_2.0

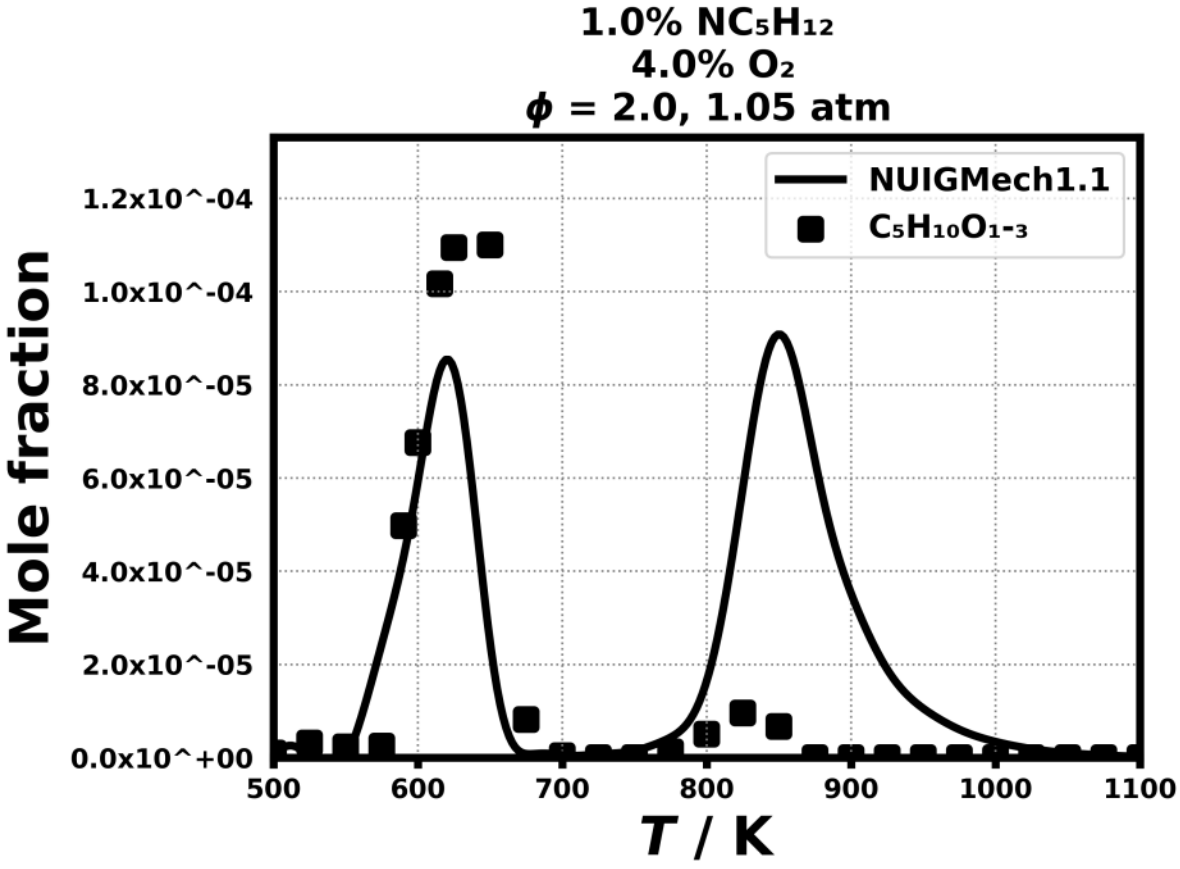

Figure 141: Dataset: 1.05_ATM_PHI_2.0

1.3.112 Case: n-C5H12/JSR/BUGLER/1.05_ATM_PHI_2.0

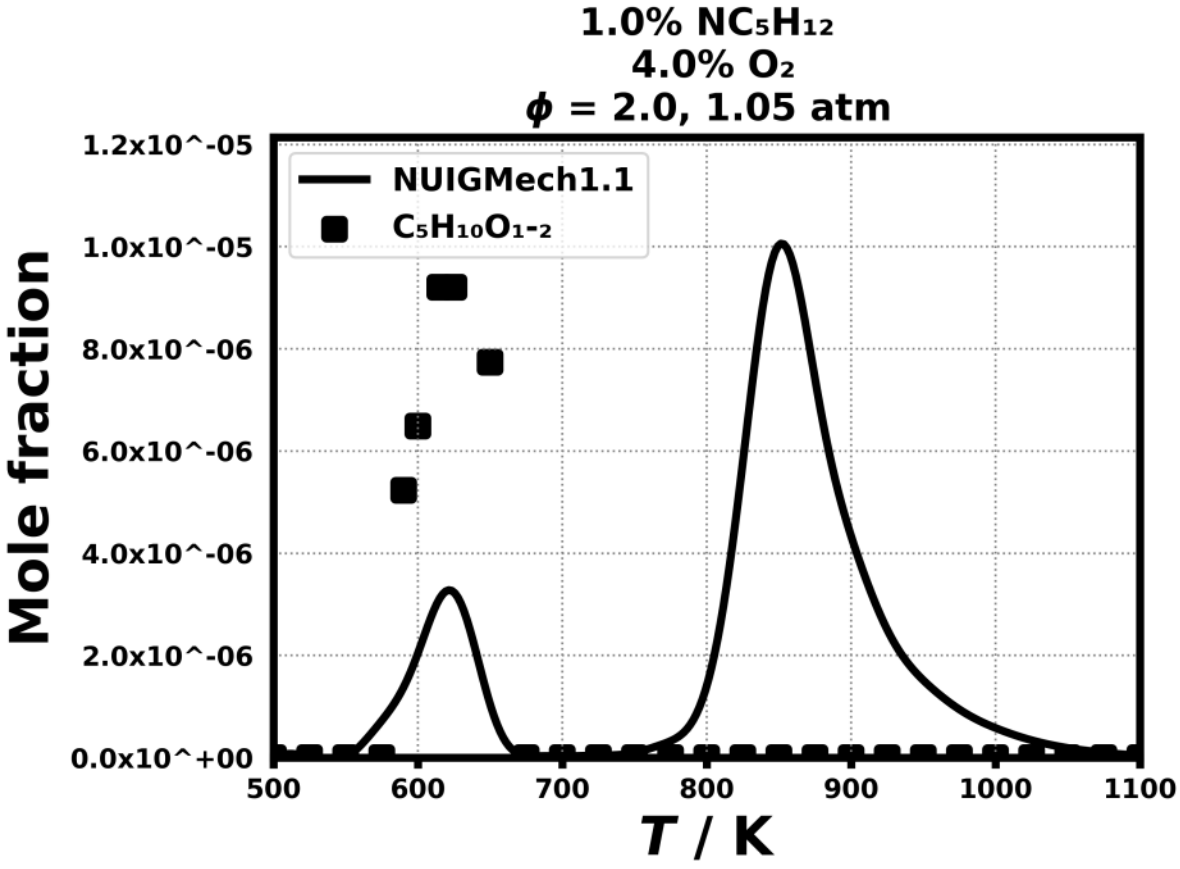

Figure 142: Dataset: 1.05_ATM_PHI_2.0

1.3.113 Case: n-C5H12/JSR/BUGLER/1.05_ATM_PHI_2.0

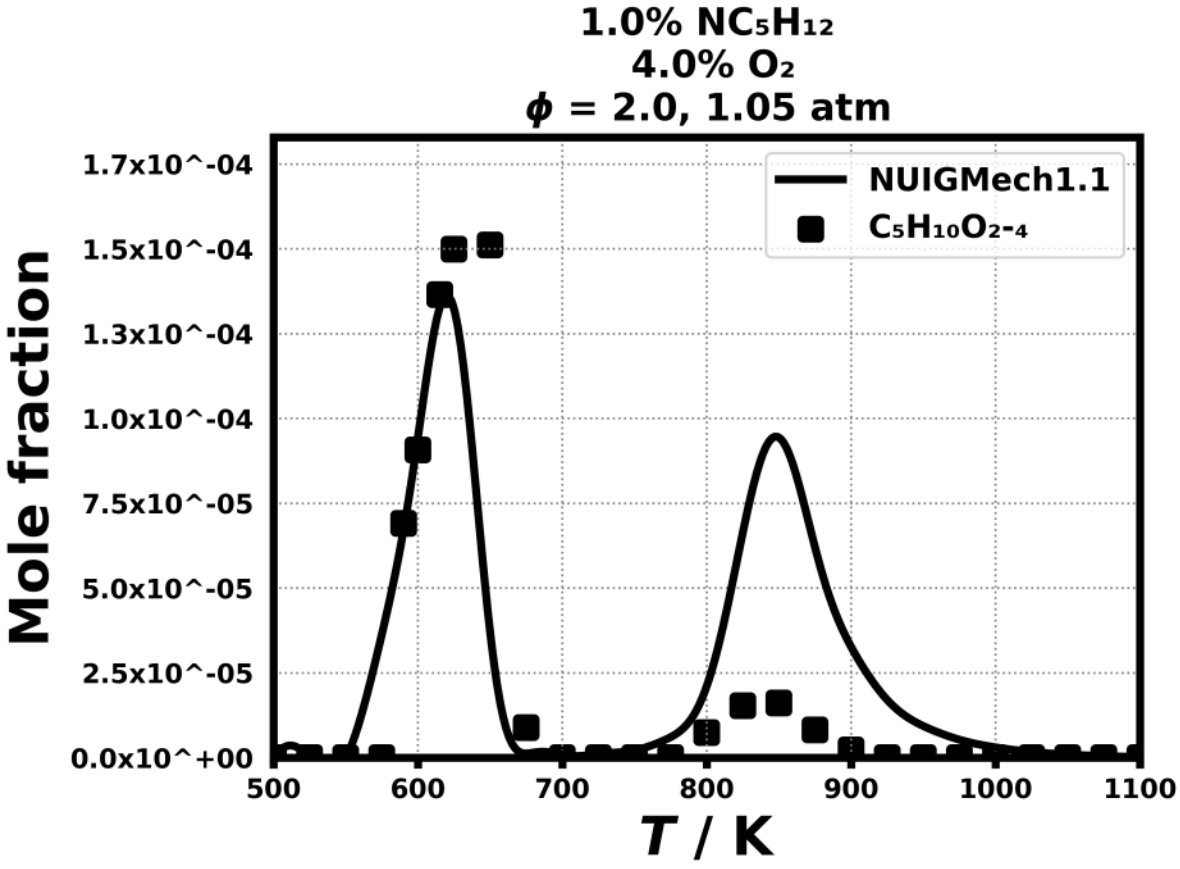

Figure 143: Dataset: 1.05_ATM_PHI_2.0

1.3.114 Case: n-C5H12/JSR/BUGLER/1.05_ATM_PHI_2.0

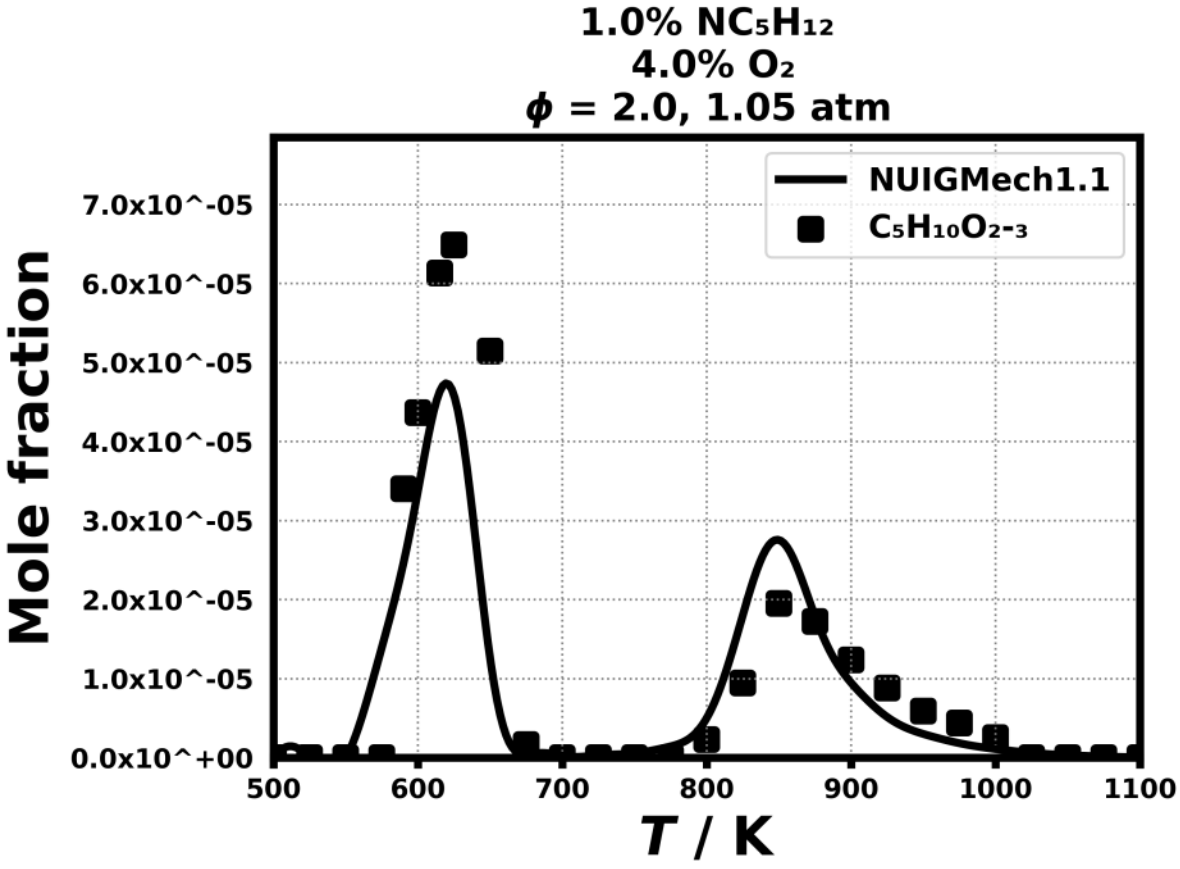

Figure 144: Dataset: 1.05_ATM_PHI_2.0

1.3.115 Case: n-C5H12/JSR/BUGLER/1.05_ATM_PHI_2.0

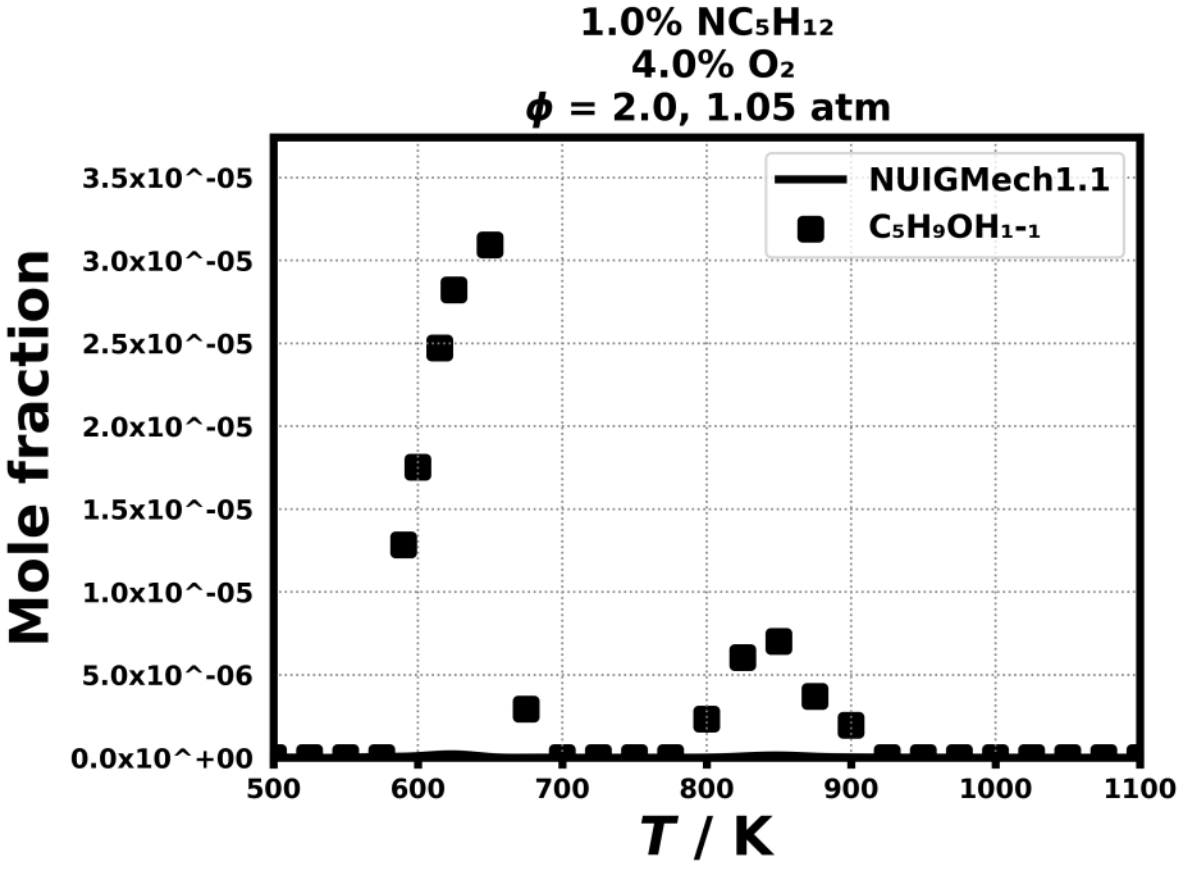

Figure 145: Dataset: 1.05_ATM_PHI_2.0

1.3.116 Case: n-C5H12/JSR/BUGLER/1.05_ATM_PHI_2.0

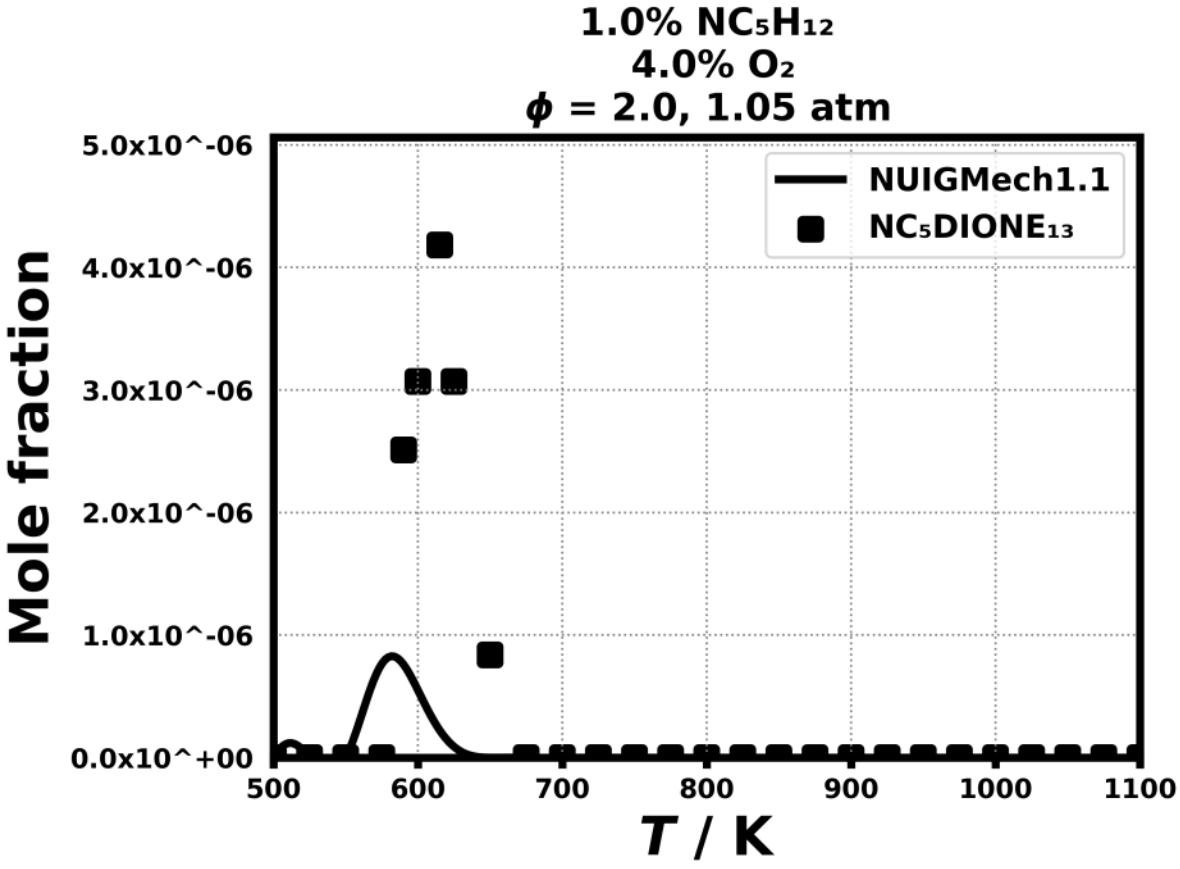

Figure 146: Dataset: 1.05_ATM_PHI_2.0

1.3.117 Case: n-C5H12/JSR/BUGLER/1.05_ATM_PHI_2.0

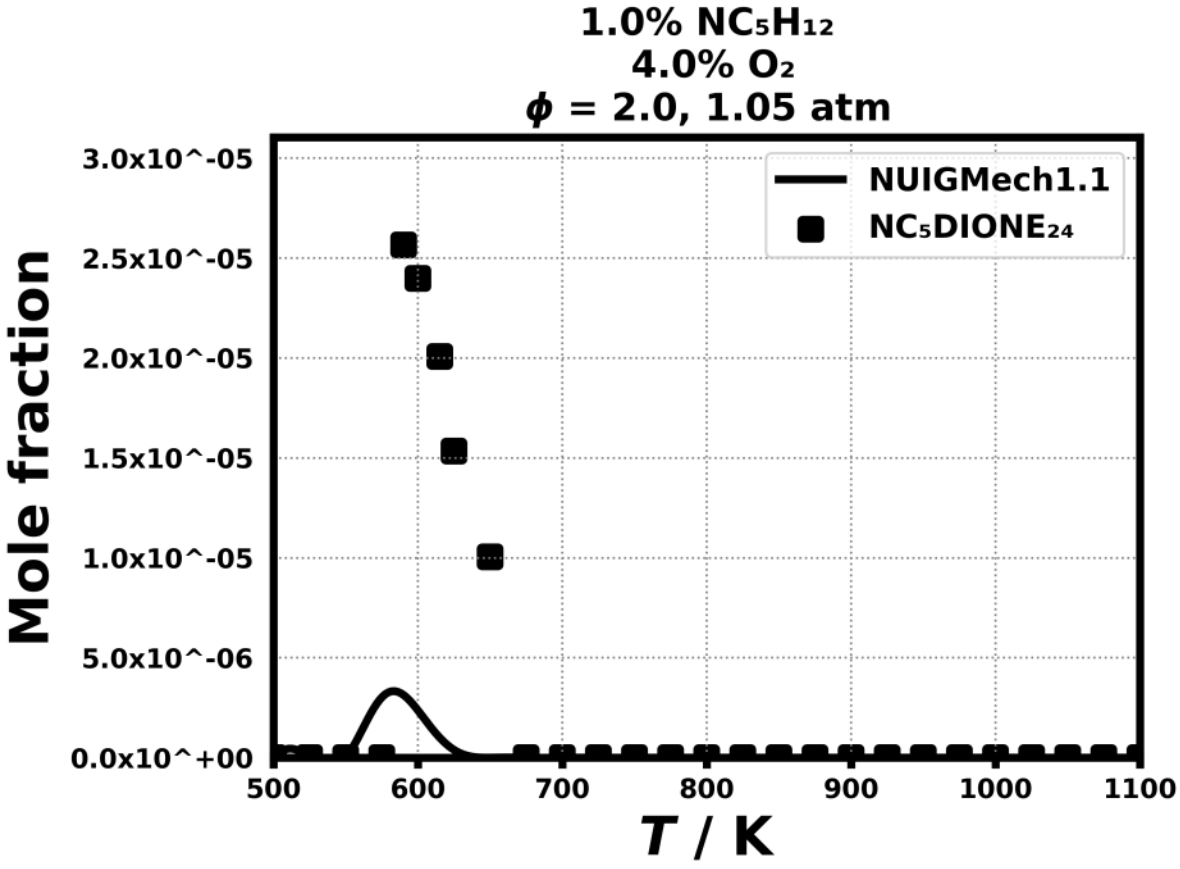

Figure 147: Dataset: 1.05_ATM_PHI_2.0

1.3.118 Case: n-C5H12/JSR/BUGLER/10_ATM_PHI_0.3

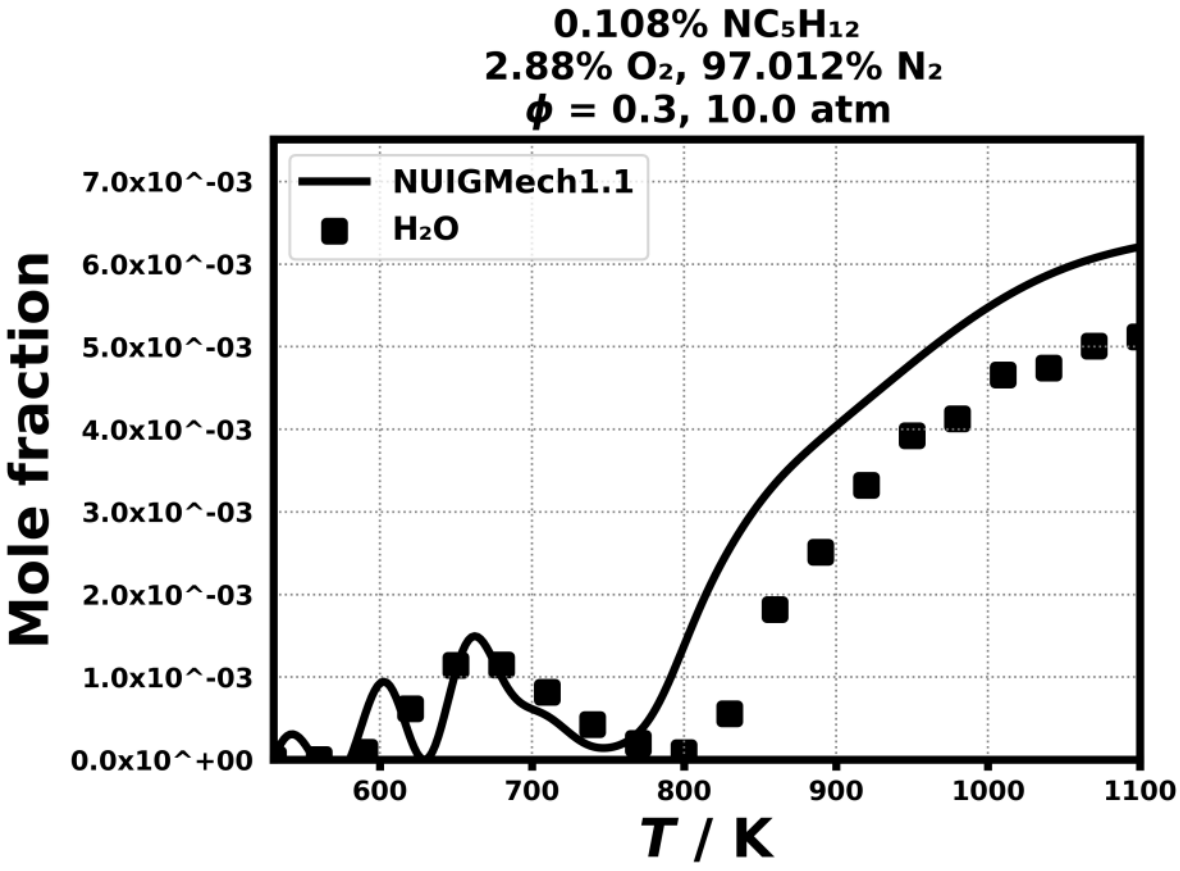

Figure 148: Dataset: 10_ATM_PHI_0.3

1.3.119 Case: n-C5H12/JSR/BUGLER/10_ATM_PHI_0.3

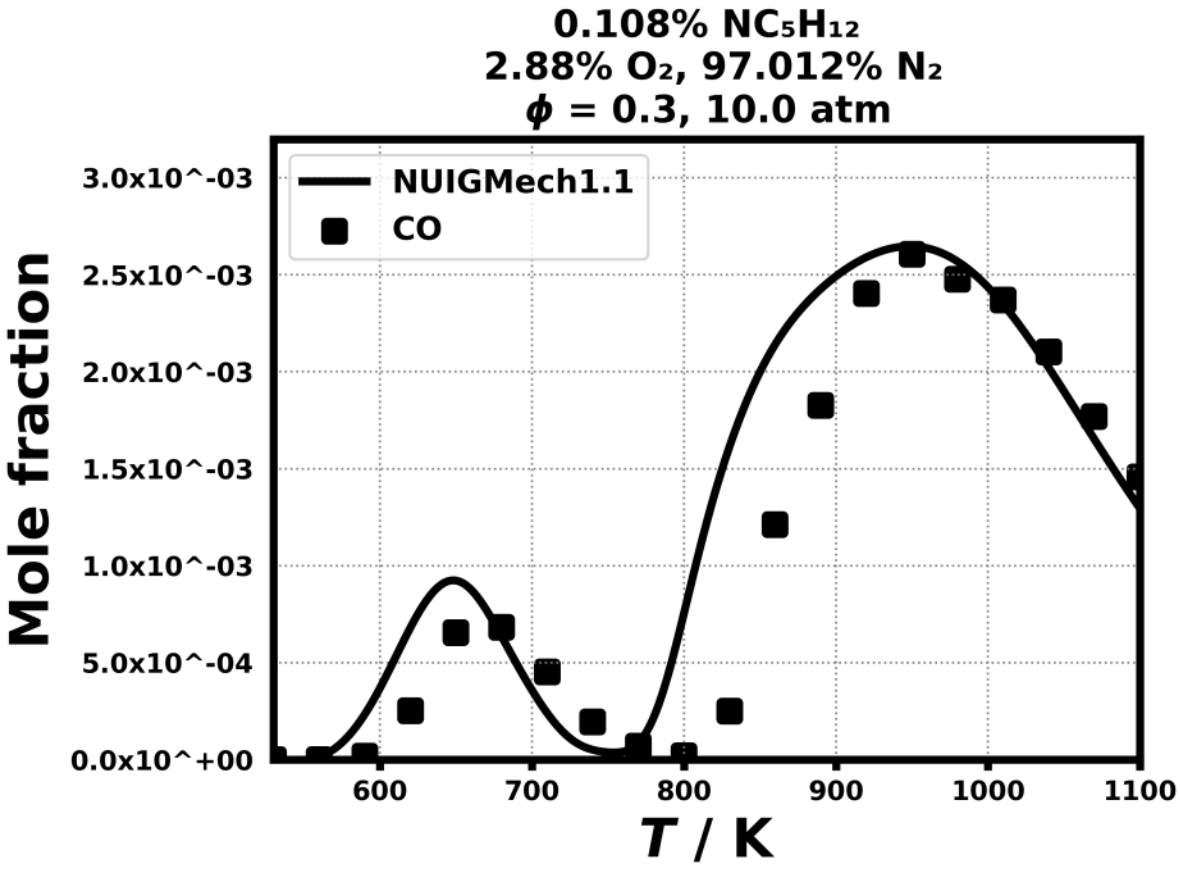

Figure 149: Dataset: 10_ATM_PHI_0.3

1.3.120 Case: n-C5H12/JSR/BUGLER/10_ATM_PHI_0.3

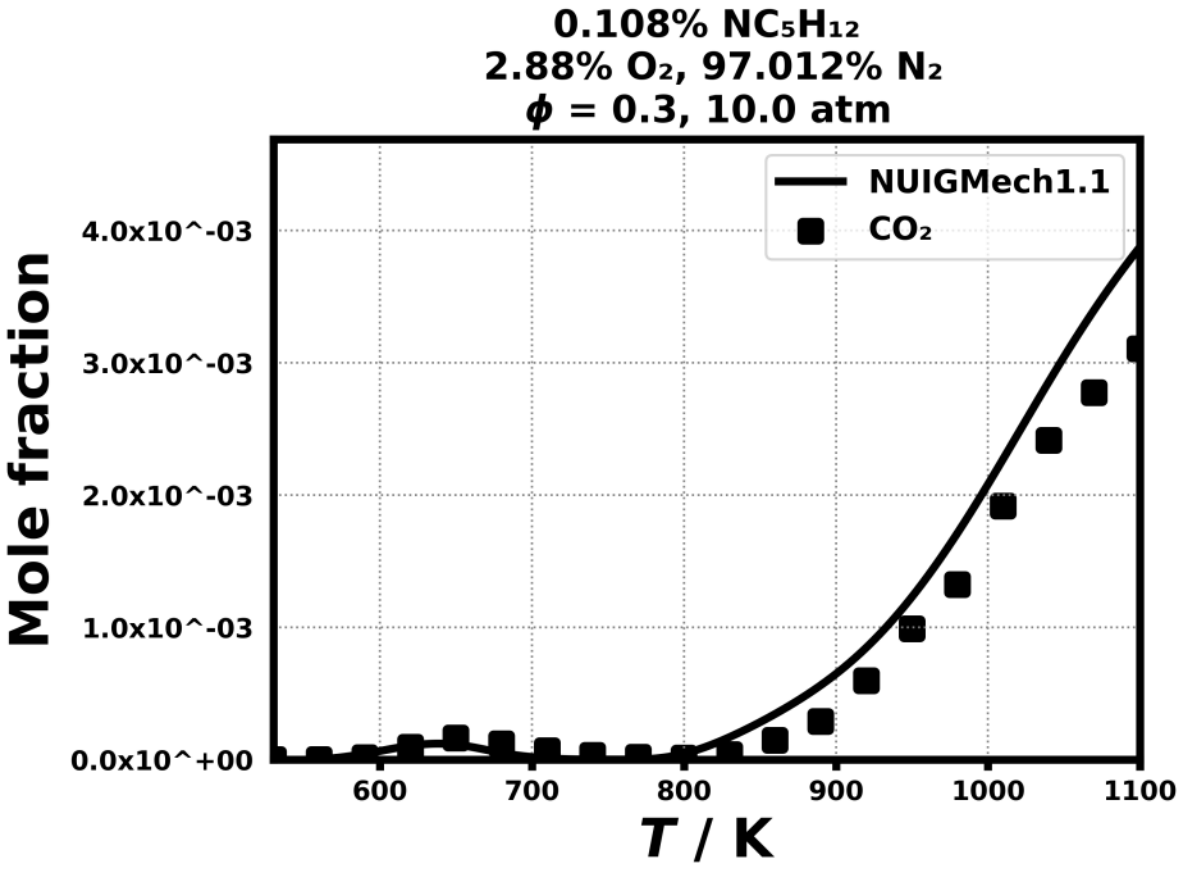

Figure 150: Dataset: 10_ATM_PHI_0.3

1.3.121 Case: n-C5H12/JSR/BUGLER/10_ATM_PHI_0.3

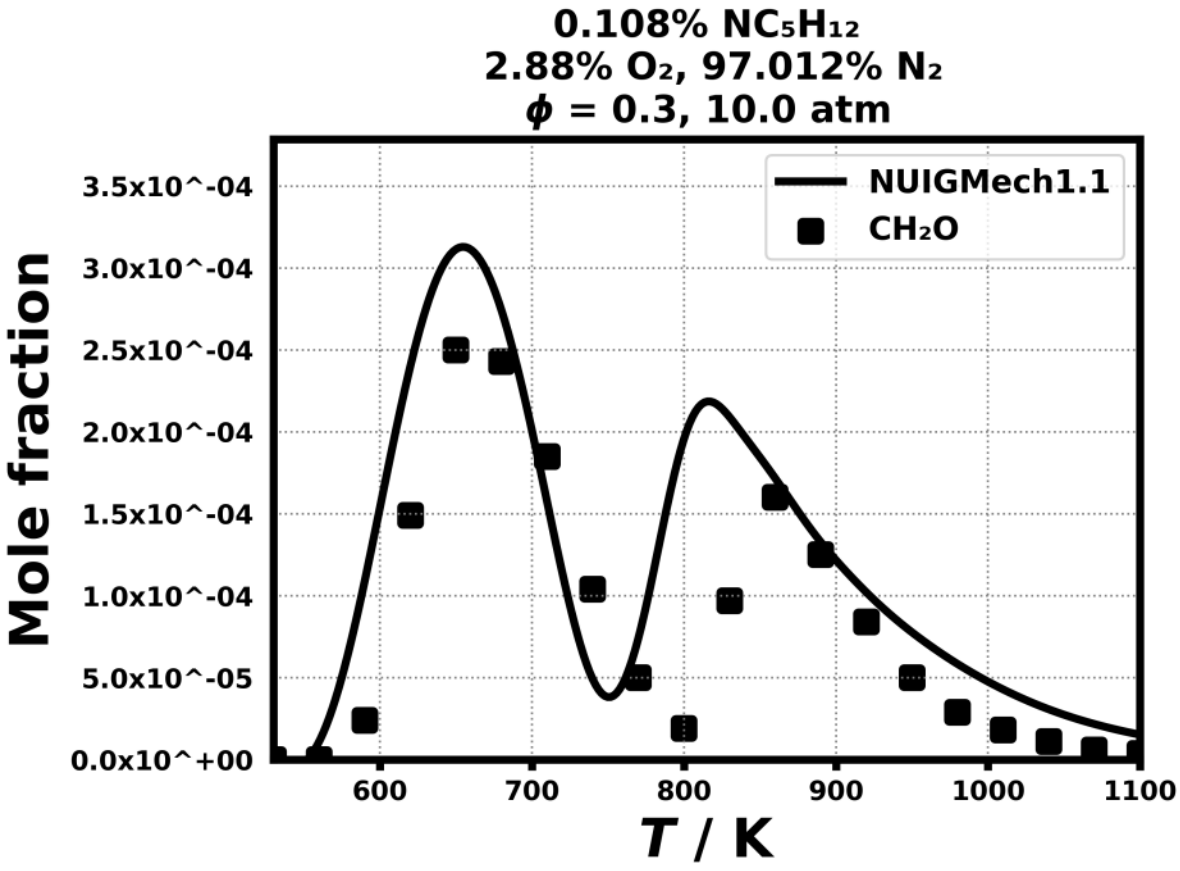

Figure 151: Dataset: 10_ATM_PHI_0.3

1.3.122 Case: n-C5H12/JSR/BUGLER/10_ATM_PHI_0.3

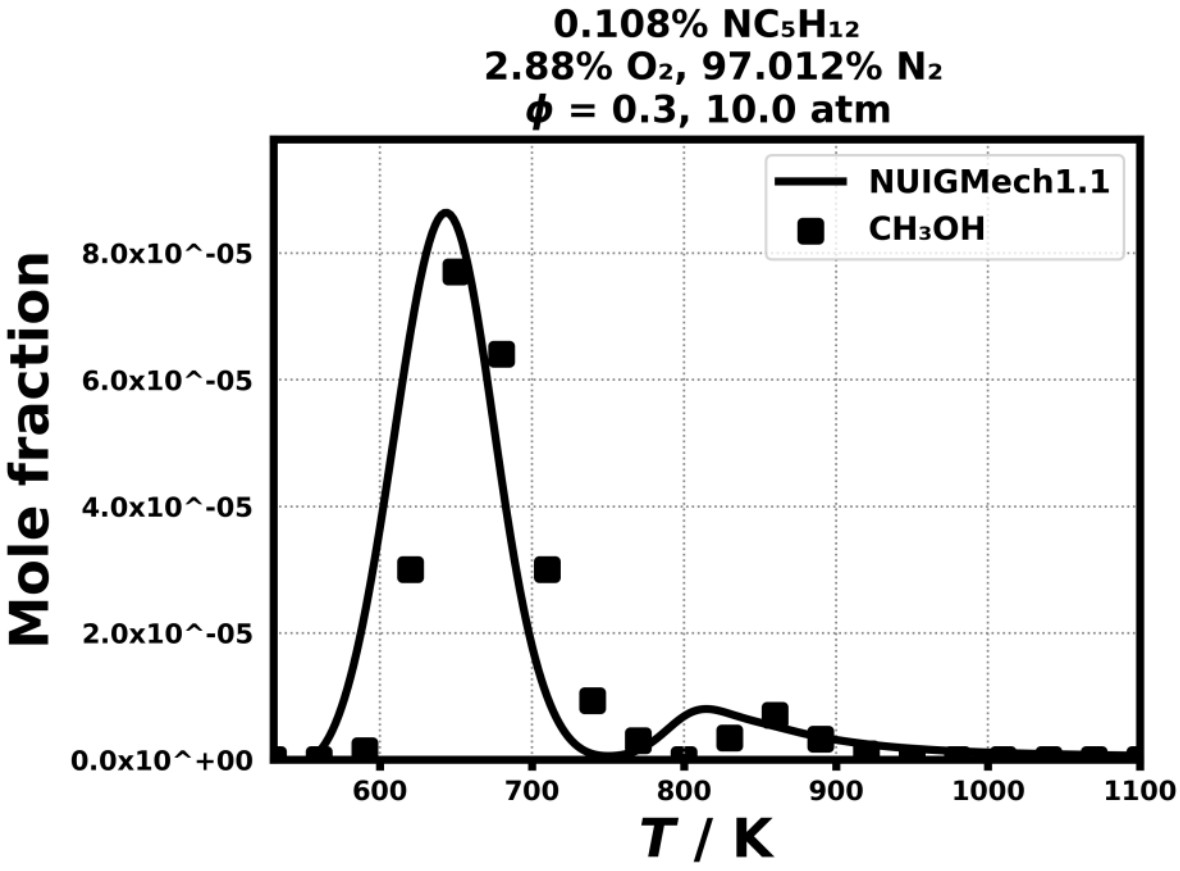

Figure 152: Dataset: 10_ATM_PHI_0.3

1.3.123 Case: n-C5H12/JSR/BUGLER/10_ATM_PHI_0.3

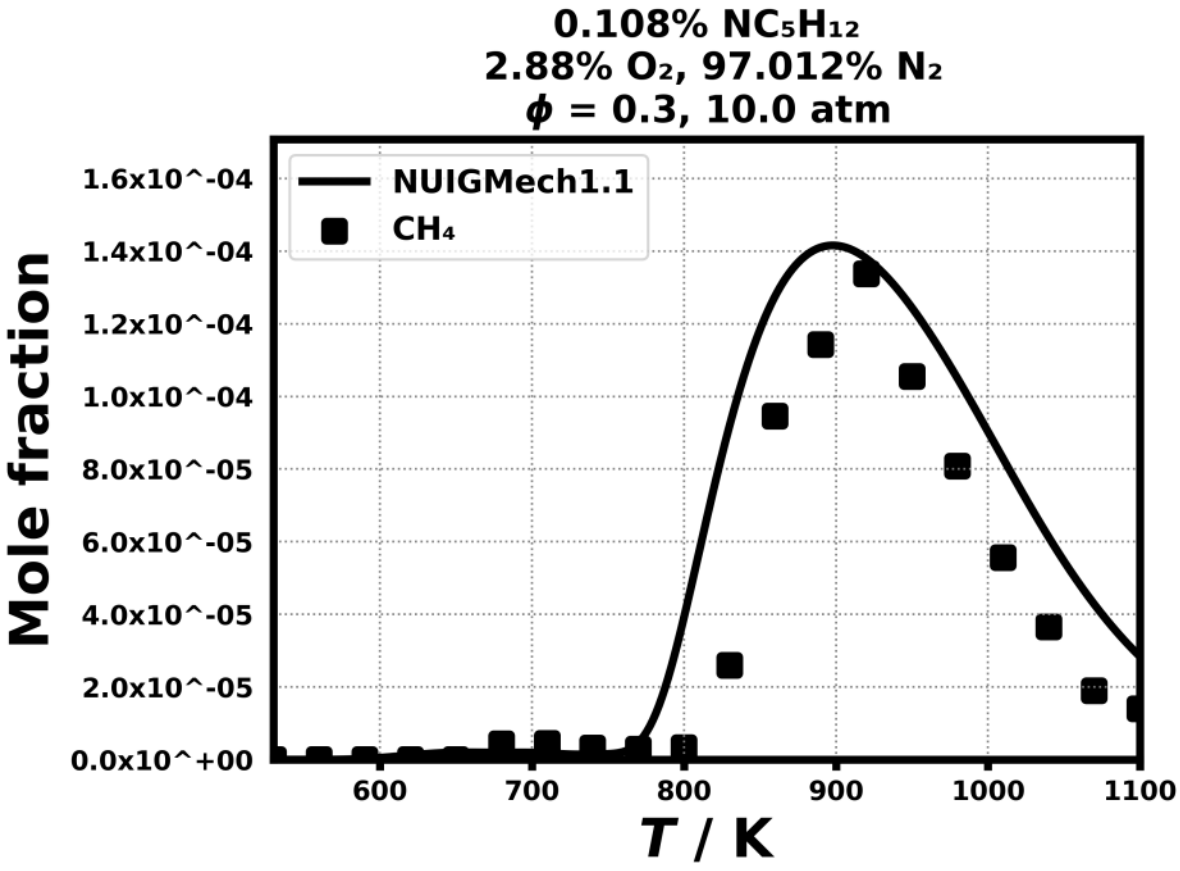

Figure 153: Dataset: 10_ATM_PHI_0.3

1.3.124 Case: n-C5H12/JSR/BUGLER/10_ATM_PHI_0.3

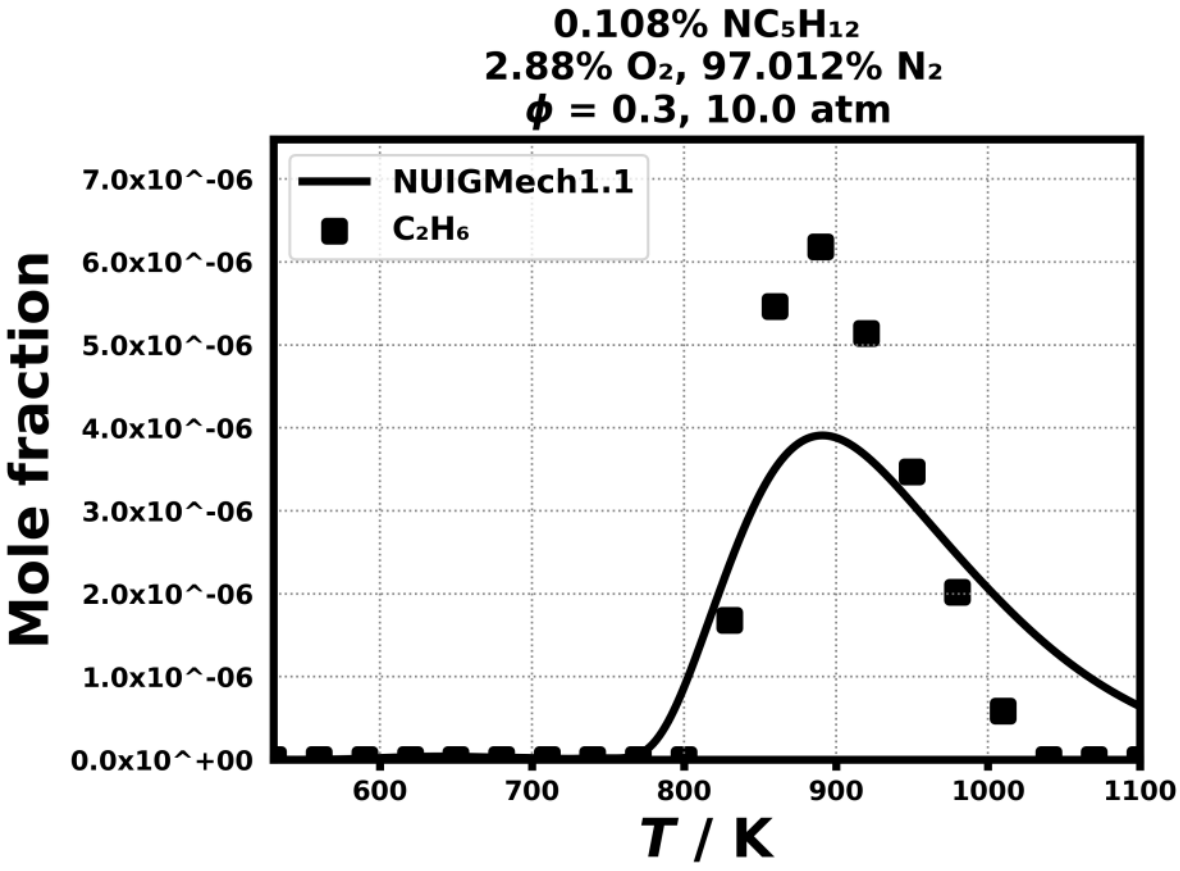

Figure 154: Dataset: 10_ATM_PHI_0.3

1.3.125 Case: n-C5H12/JSR/BUGLER/10_ATM_PHI_0.3

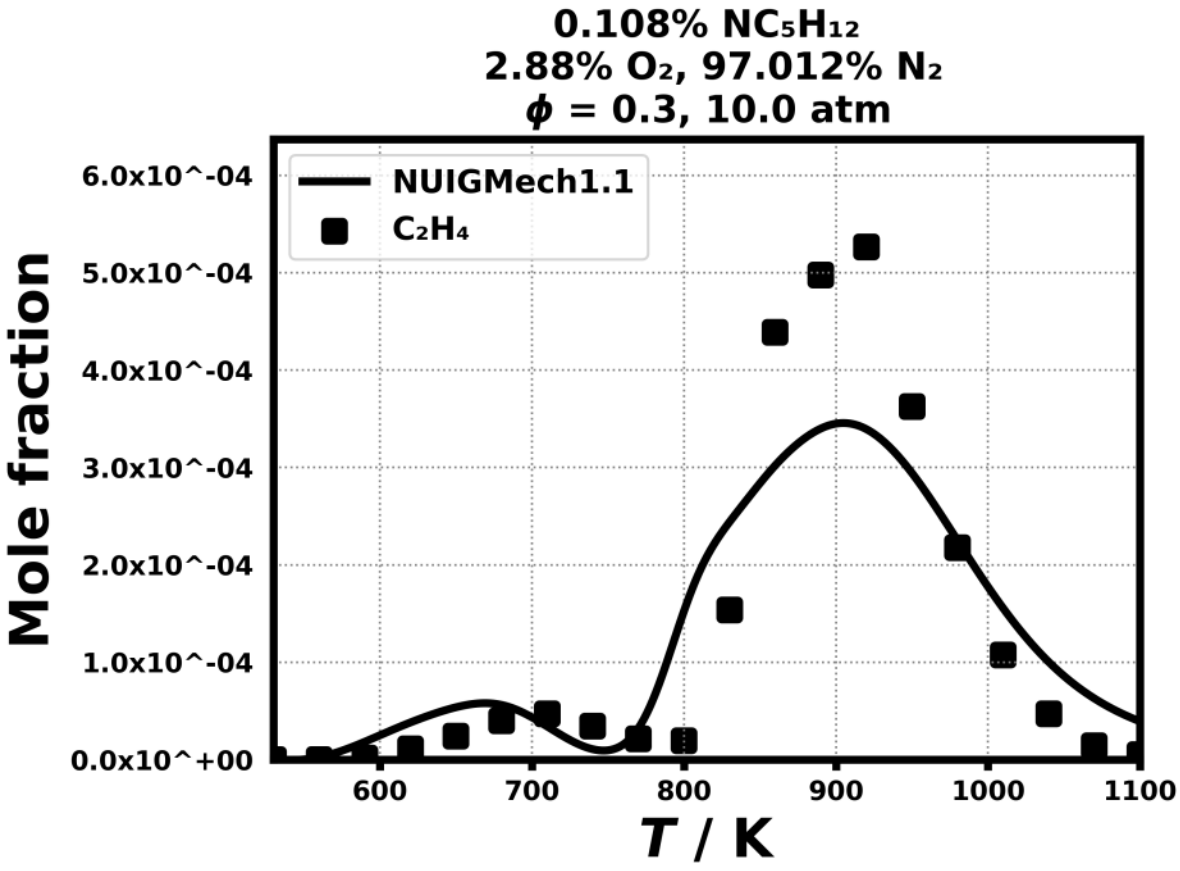

Figure 155: Dataset: 10_ATM_PHI_0.3

1.3.126 Case: n-C5H12/JSR/BUGLER/10_ATM_PHI_0.3

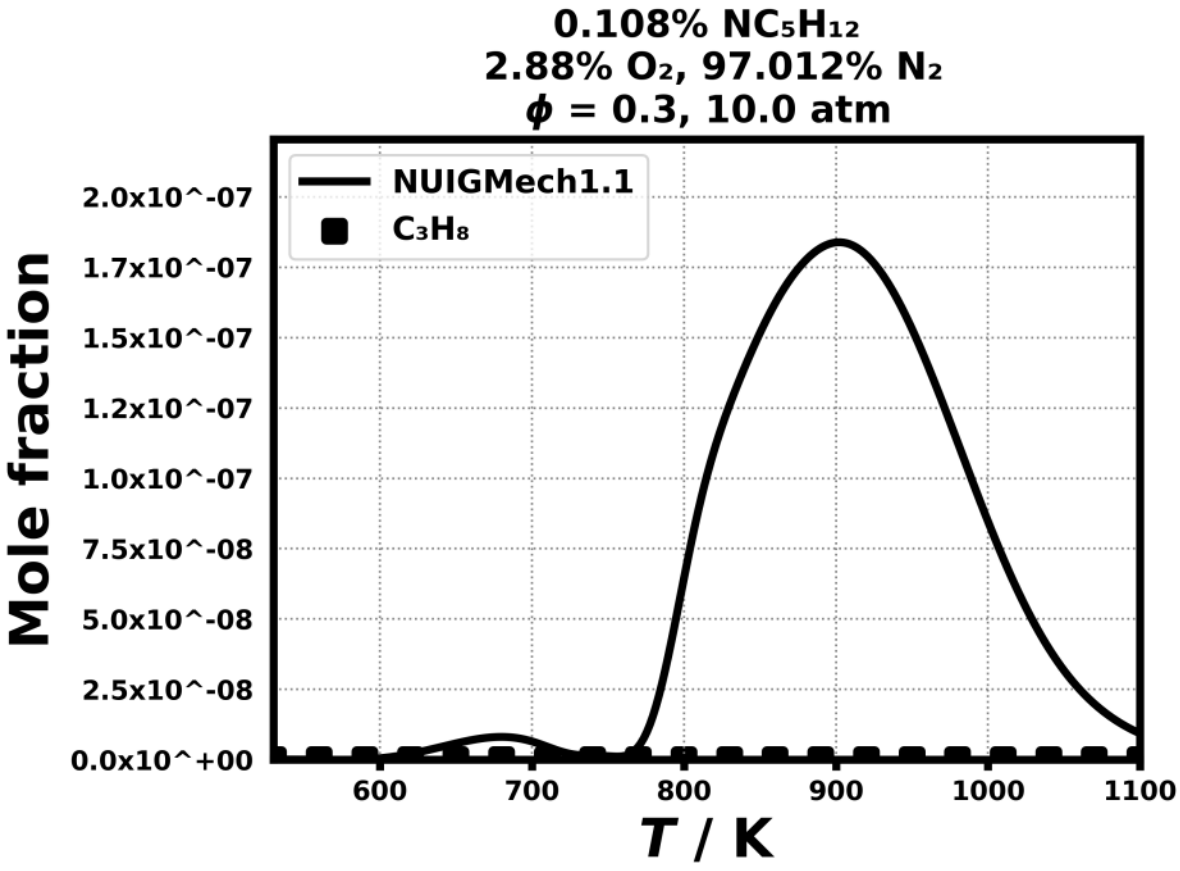

Figure 156: Dataset: 10_ATM_PHI_0.3

1.3.127 Case: n-C5H12/JSR/BUGLER/10_ATM_PHI_0.3

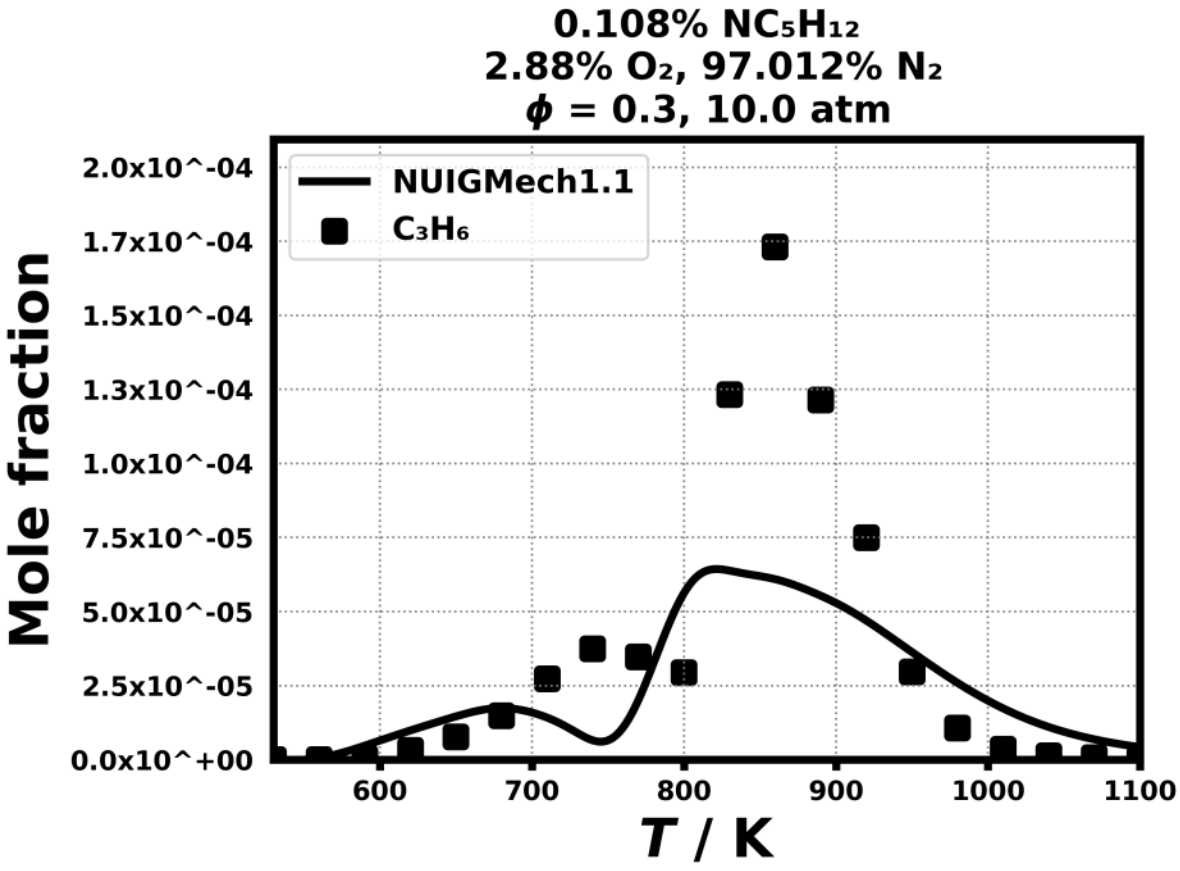

Figure 157: Dataset: 10_ATM_PHI_0.3

1.3.128 Case: n-C5H12/JSR/BUGLER/10_ATM_PHI_0.3

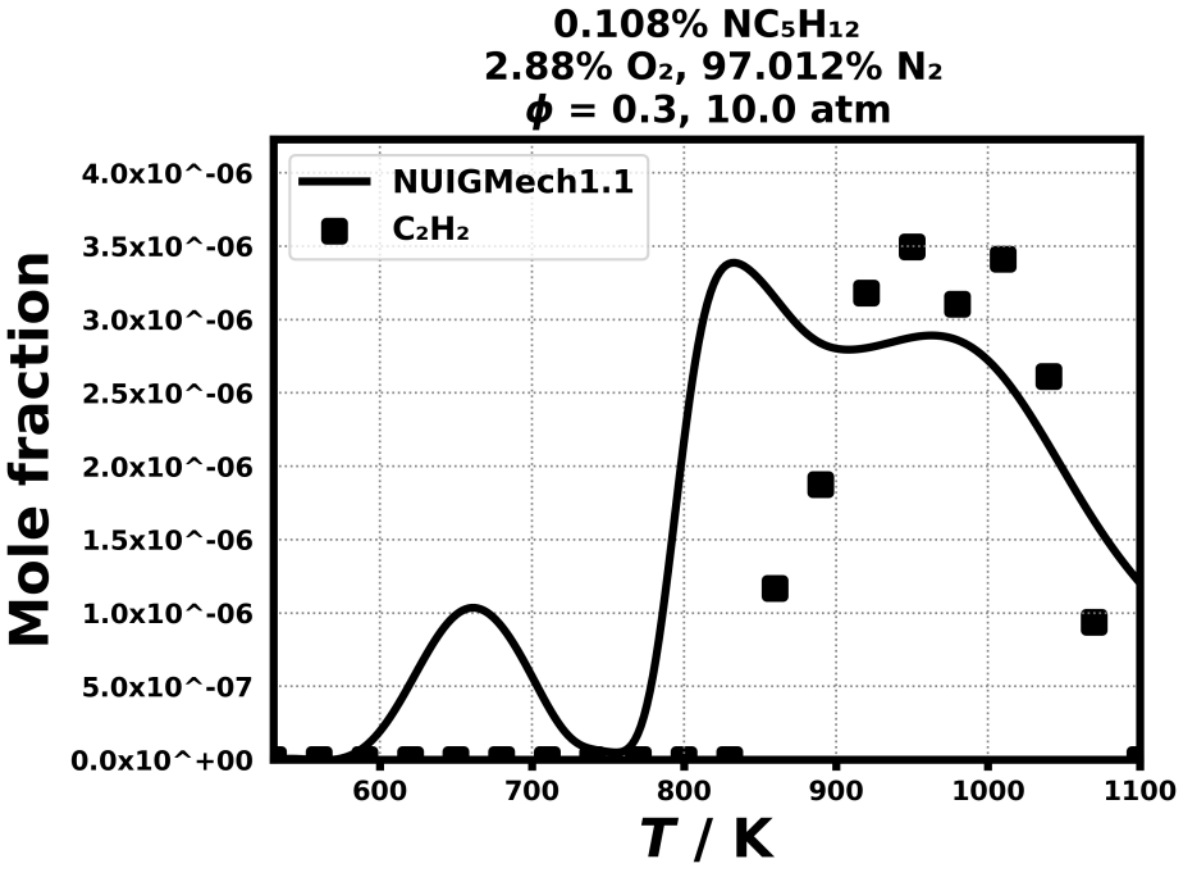

Figure 158: Dataset: 10_ATM_PHI_0.3

1.3.129 Case: n-C5H12/JSR/BUGLER/10_ATM_PHI_0.3

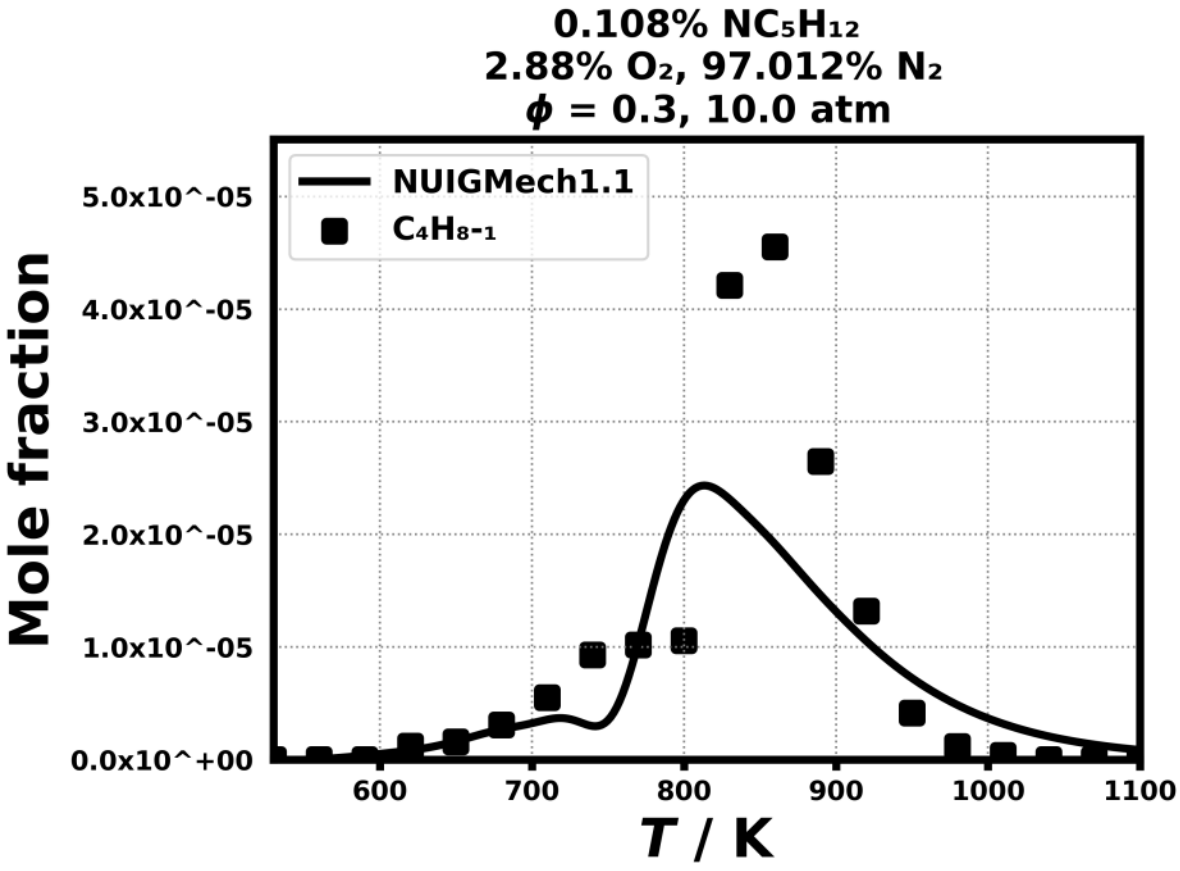

Figure 159: Dataset: 10_ATM_PHI_0.3

1.3.130 Case: n-C5H12/JSR/BUGLER/10_ATM_PHI_0.3

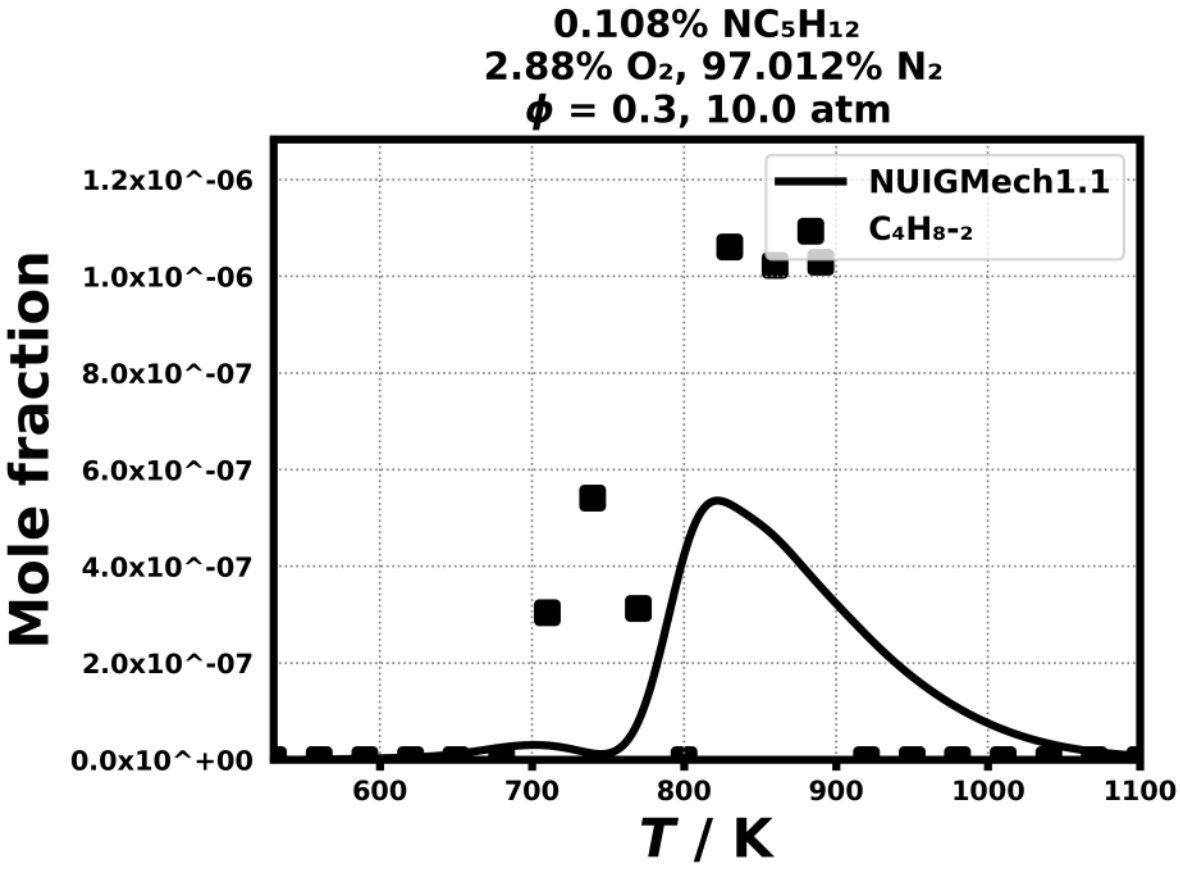

Figure 160: Dataset: 10_ATM_PHI_0.3

1.3.131 Case: n-C5H12/JSR/BUGLER/10_ATM_PHI_0.3

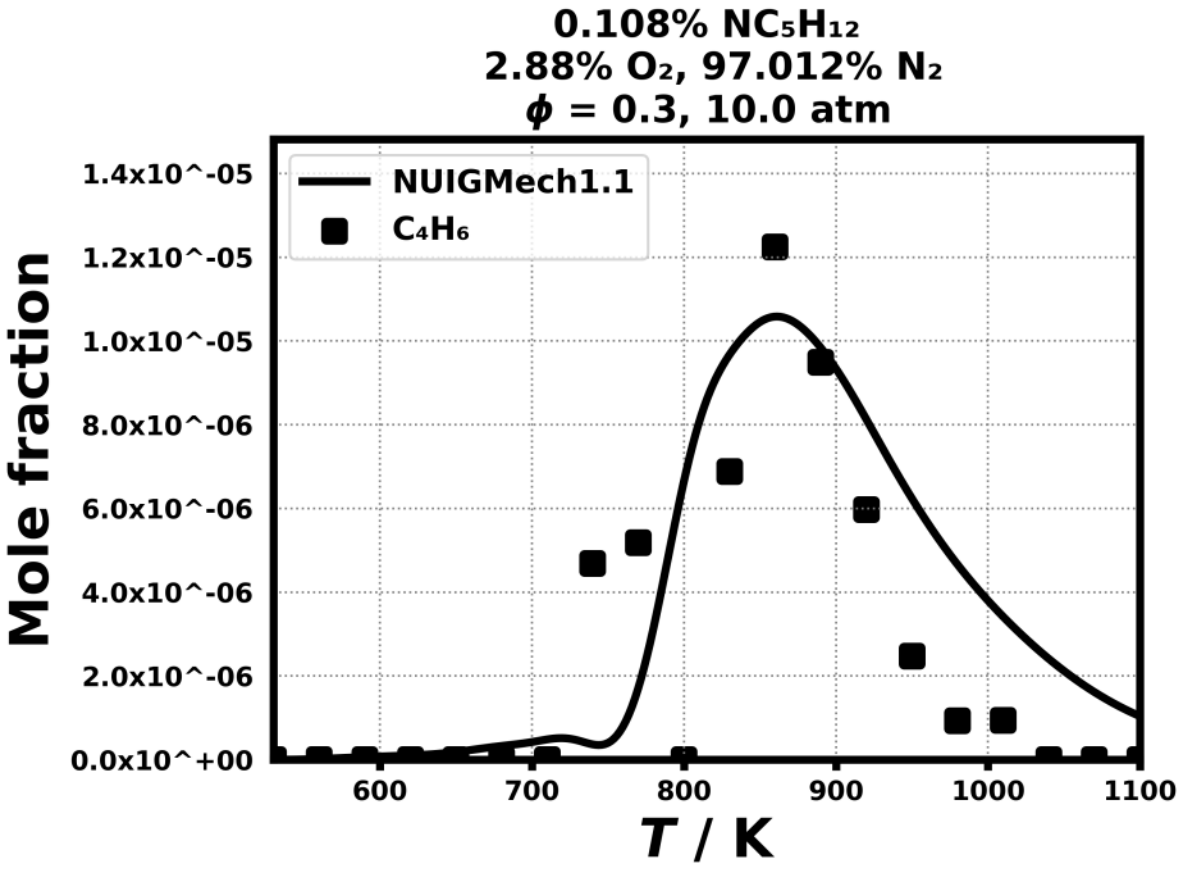

Figure 161: Dataset: 10_ATM_PHI_0.3

1.3.132 Case: n-C5H12/JSR/BUGLER/10_ATM_PHI_0.3

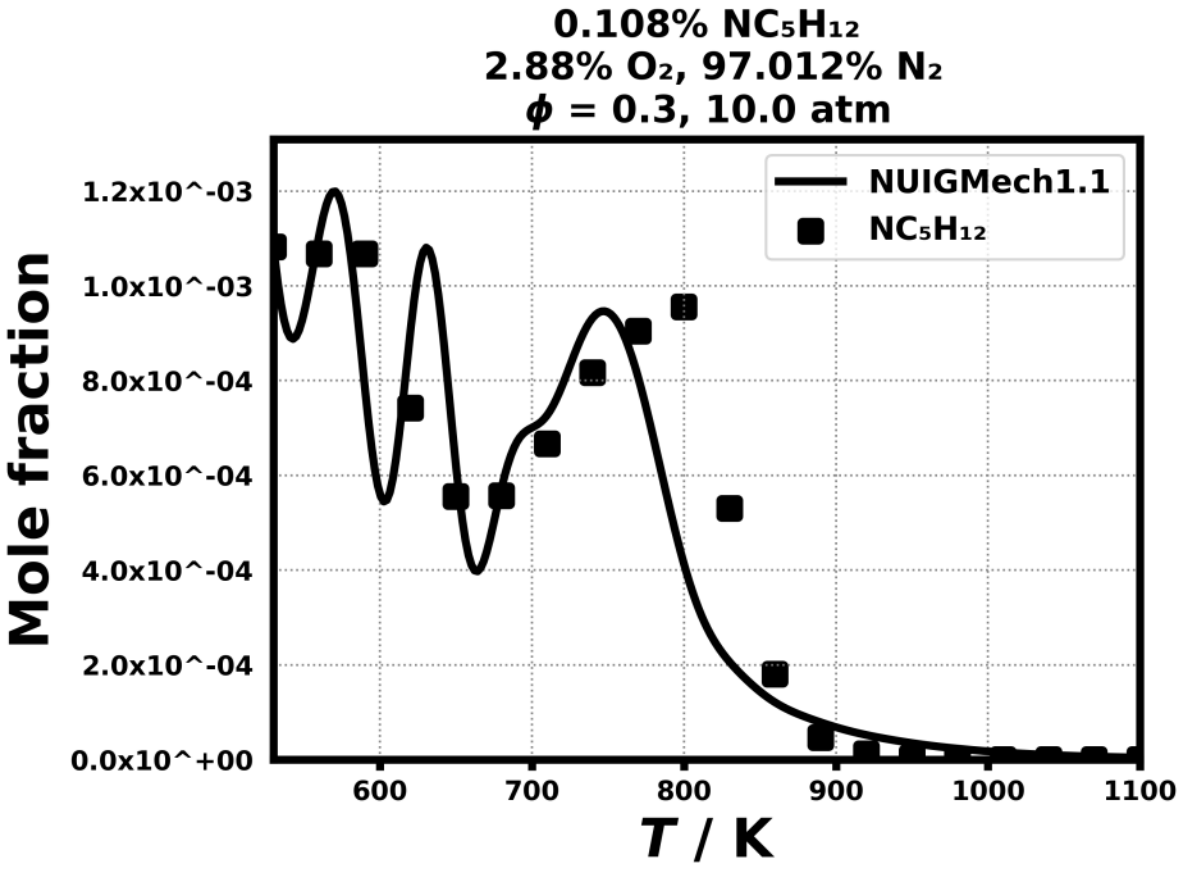

Figure 162: Dataset: 10_ATM_PHI_0.3

1.3.133 Case: n-C5H12/JSR/BUGLER/10_ATM_PHI_0.3

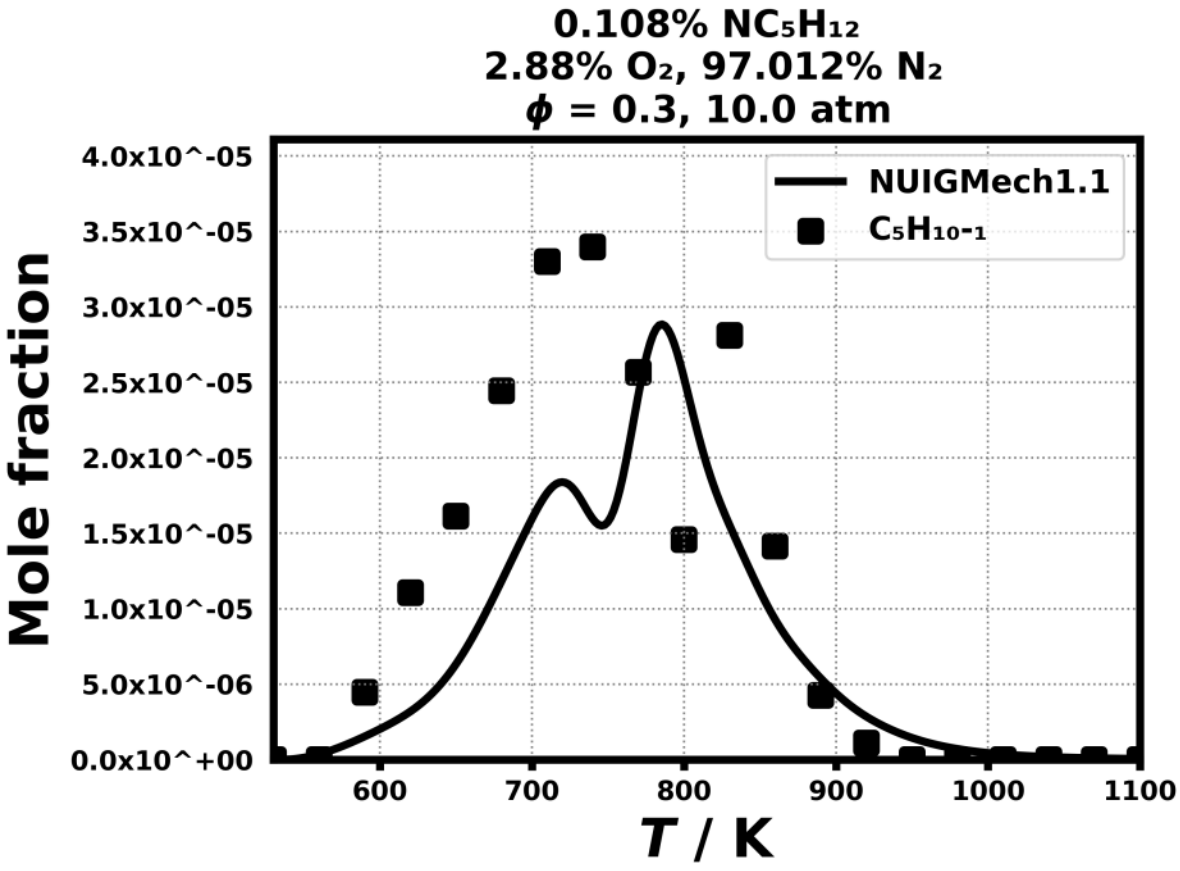

Figure 163: Dataset: 10_ATM_PHI_0.3

1.3.134 Case: n-C5H12/JSR/BUGLER/10_ATM_PHI_0.3

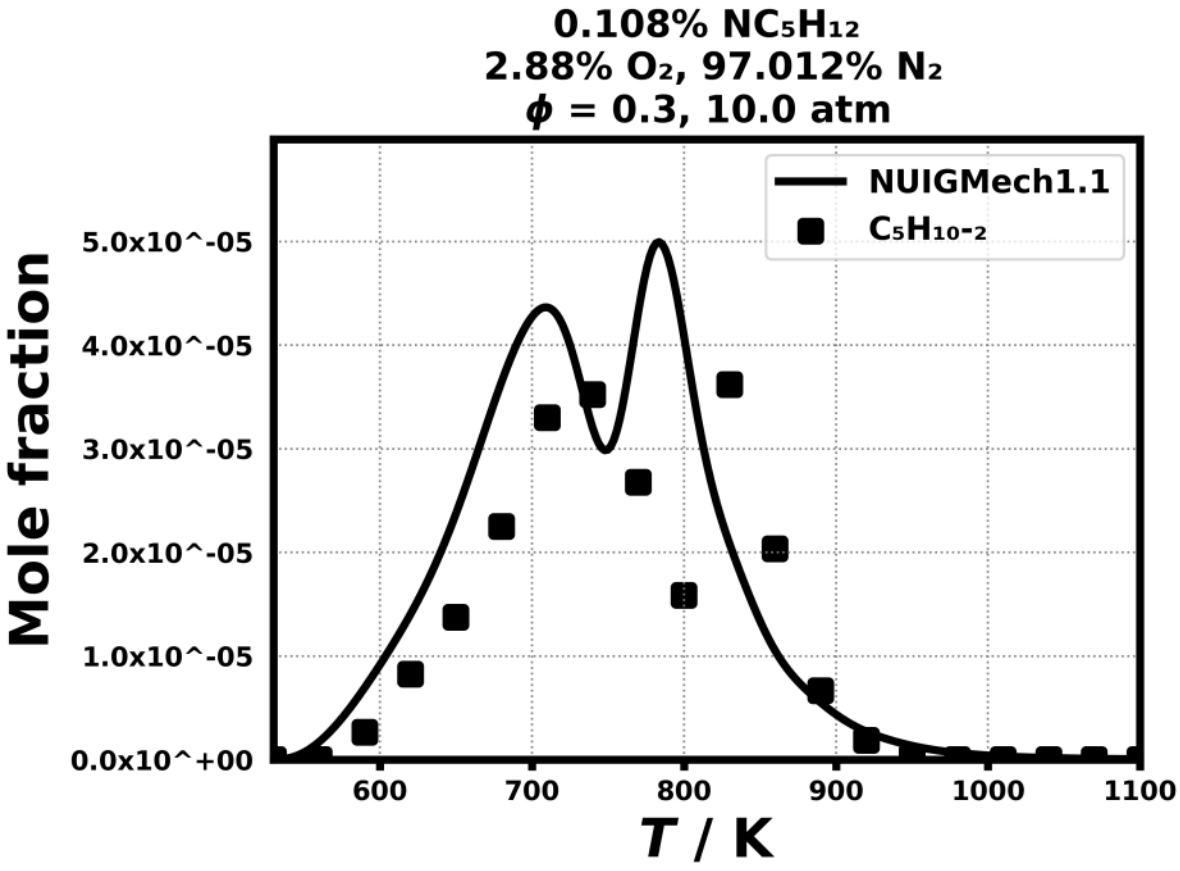

Figure 164: Dataset: 10_ATM_PHI_0.3

1.3.135 Case: n-C5H12/JSR/BUGLER/10_ATM_PHI_0.3

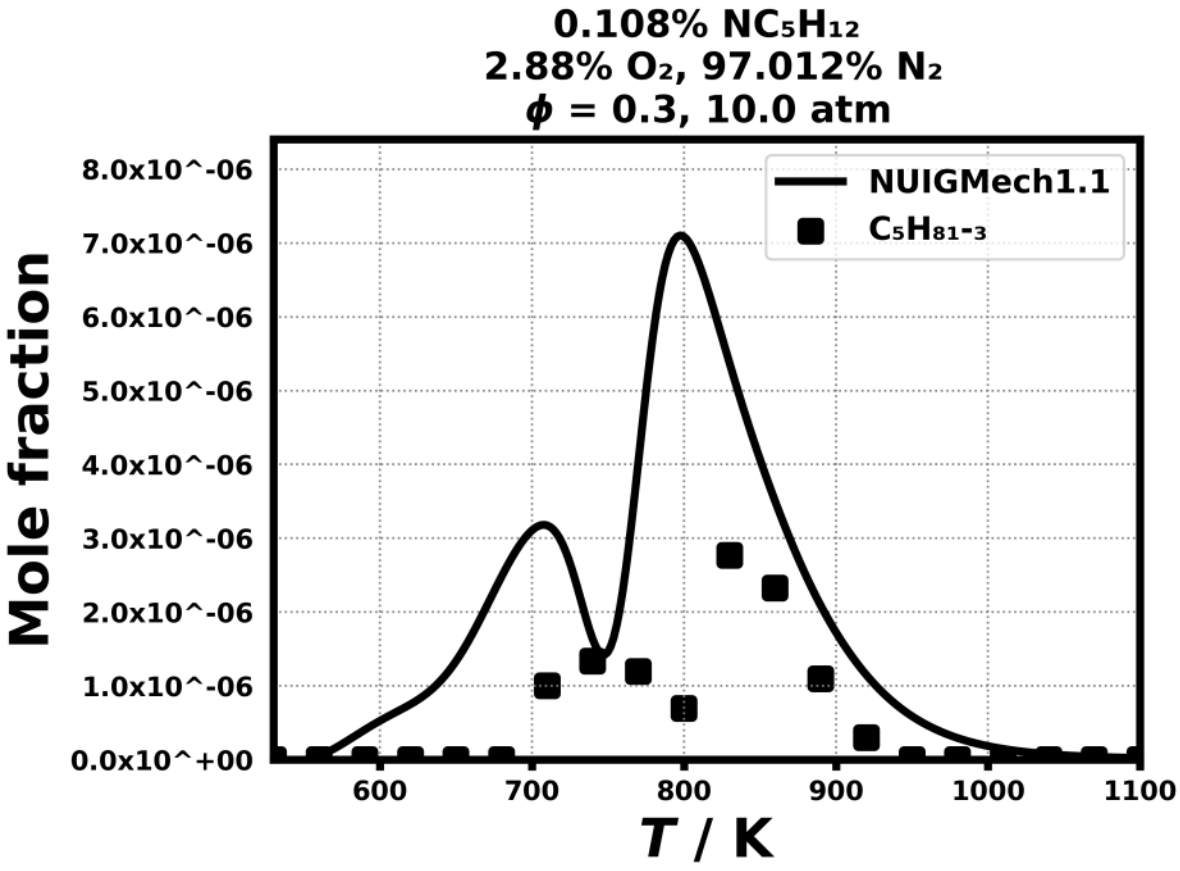

Figure 165: Dataset: 10_ATM_PHI_0.3

1.3.136 Case: n-C5H12/JSR/BUGLER/10_ATM_PHI_0.3

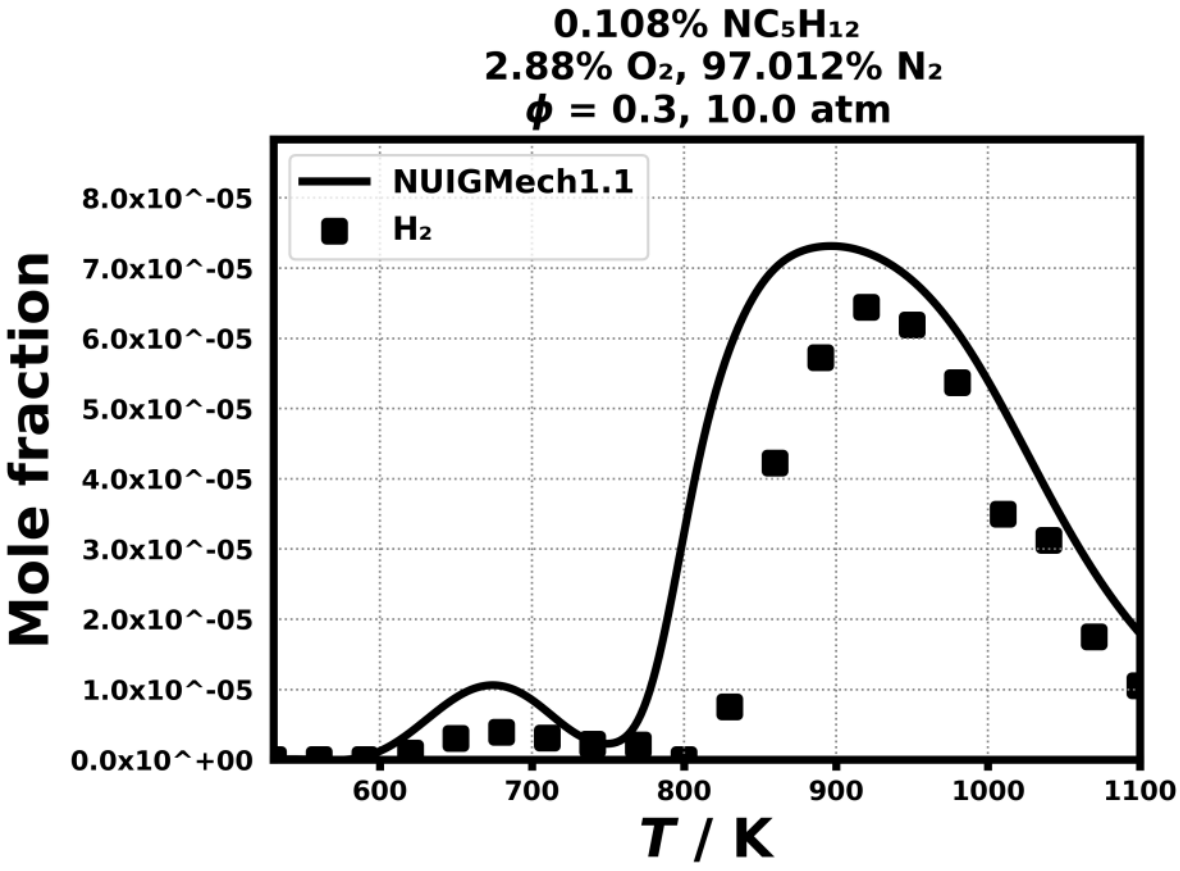

Figure 166: Dataset: 10_ATM_PHI_0.3

1.3.137 Case: n-C5H12/JSR/BUGLER/10_ATM_PHI_0.3

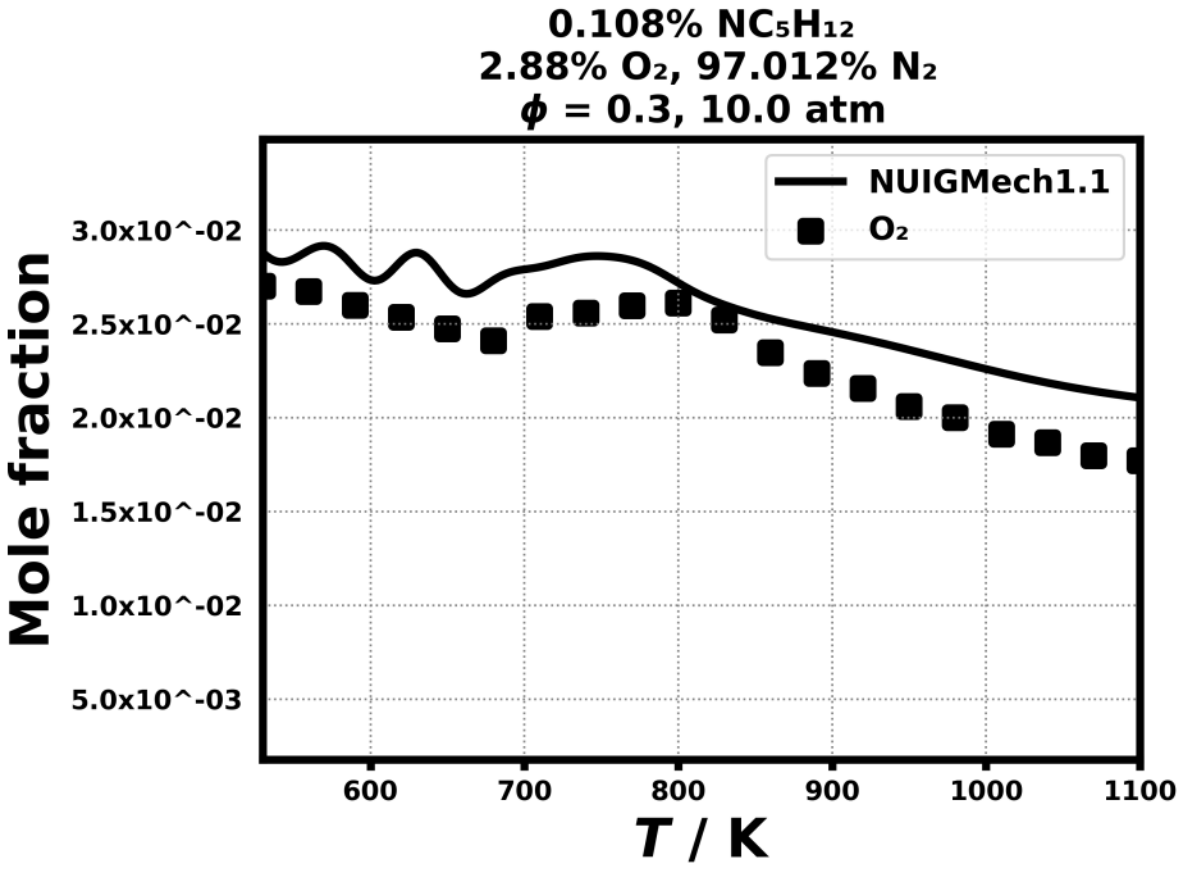

Figure 167: Dataset: 10_ATM_PHI_0.3

1.3.138 Case: n-C5H12/JSR/BUGLER/10_ATM_PHI_0.3

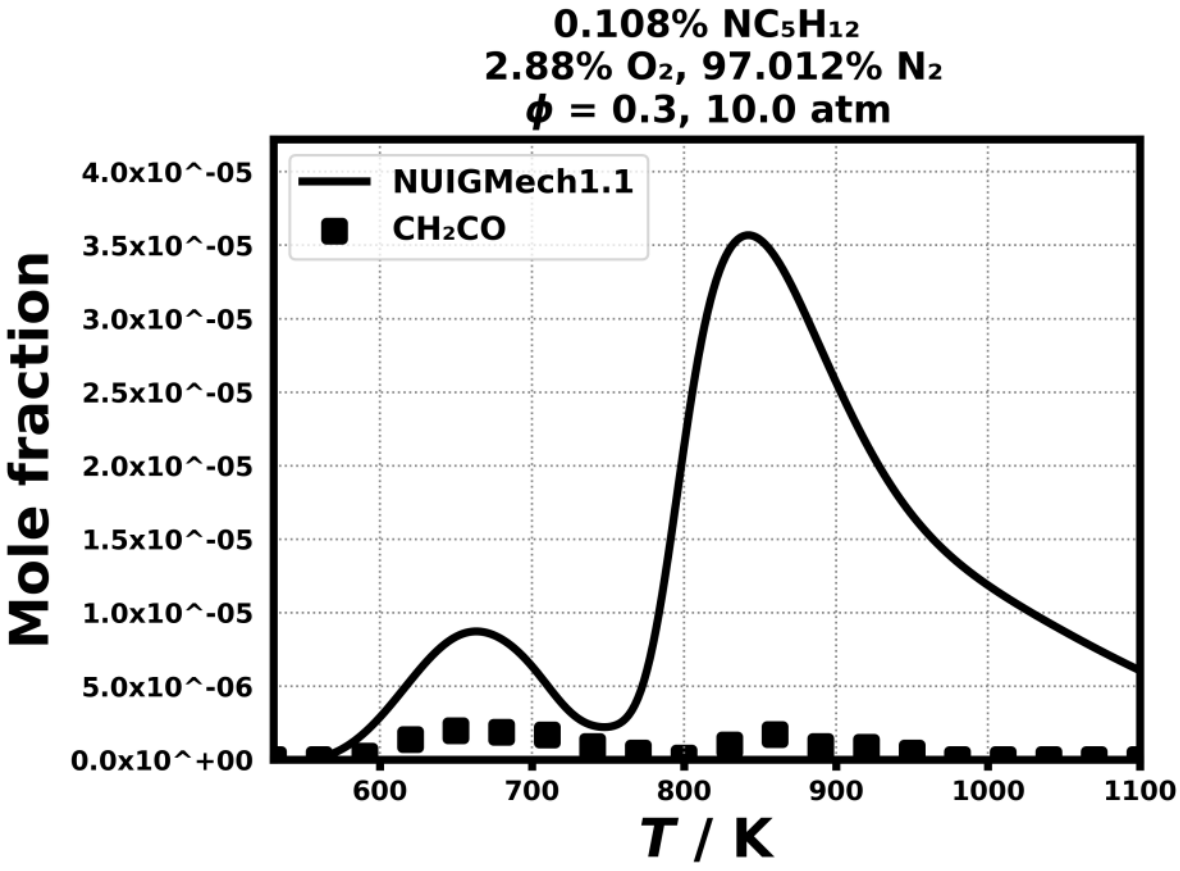

Figure 168: Dataset: 10_ATM_PHI_0.3

1.3.139 Case: n-C5H12/JSR/BUGLER/10_ATM_PHI_0.3

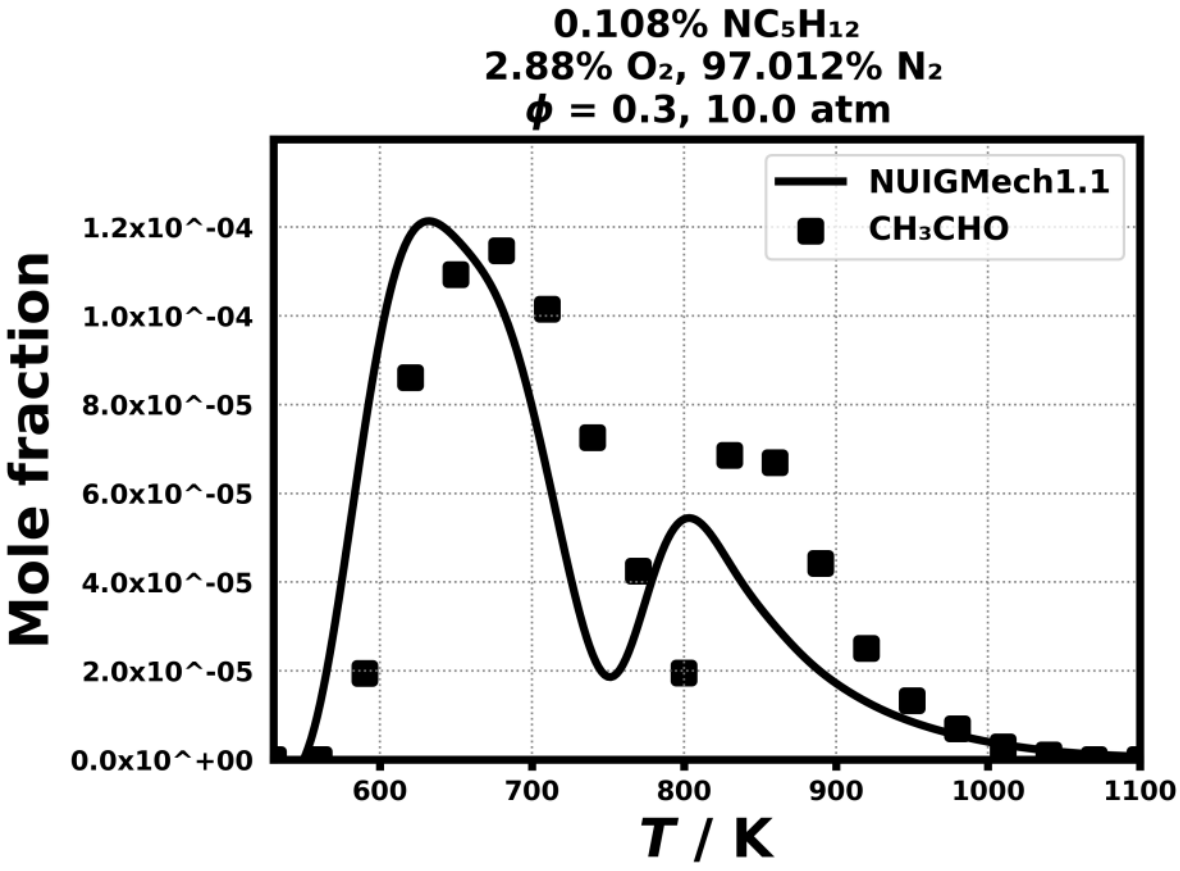

Figure 169: Dataset: 10_ATM_PHI_0.3

1.3.140 Case: n-C5H12/JSR/BUGLER/10_ATM_PHI_0.3

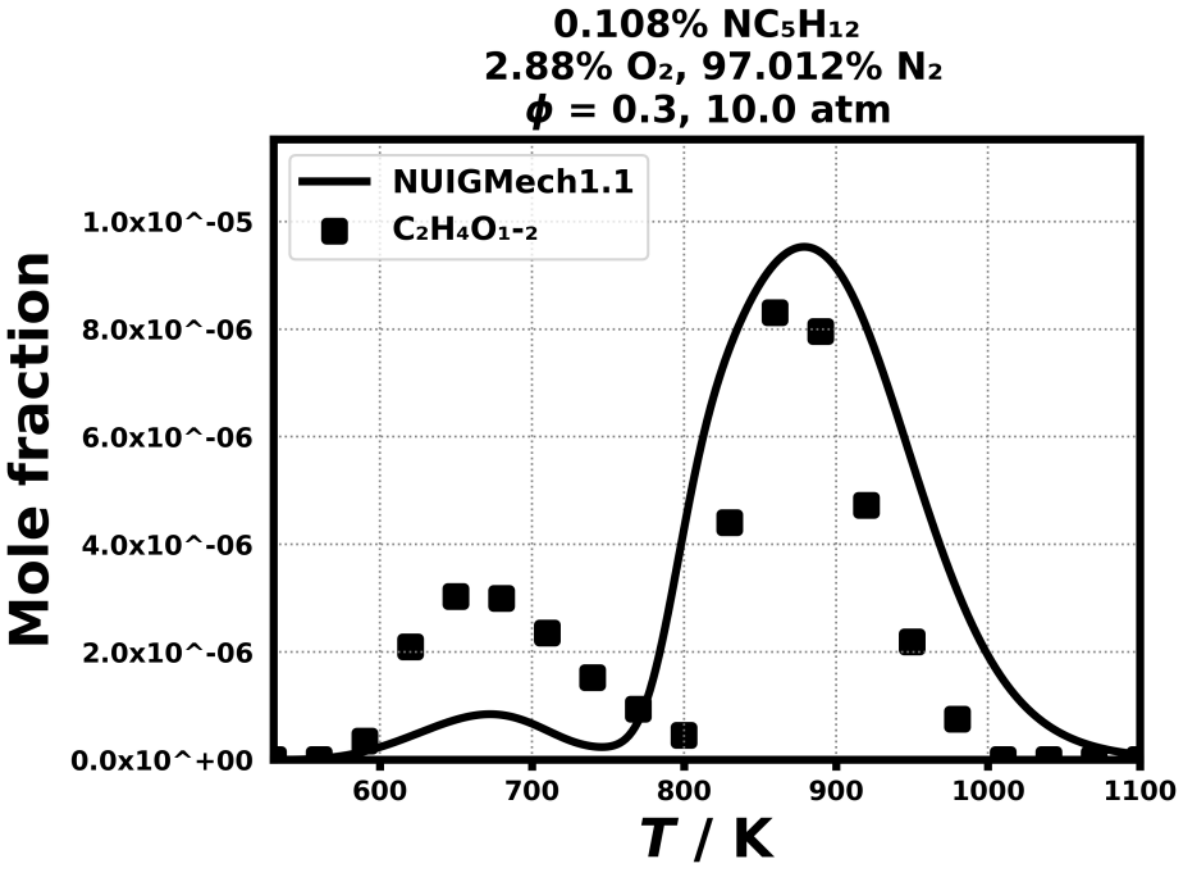

Figure 170: Dataset: 10_ATM_PHI_0.3

1.3.141 Case: n-C5H12/JSR/BUGLER/10_ATM_PHI_0.3

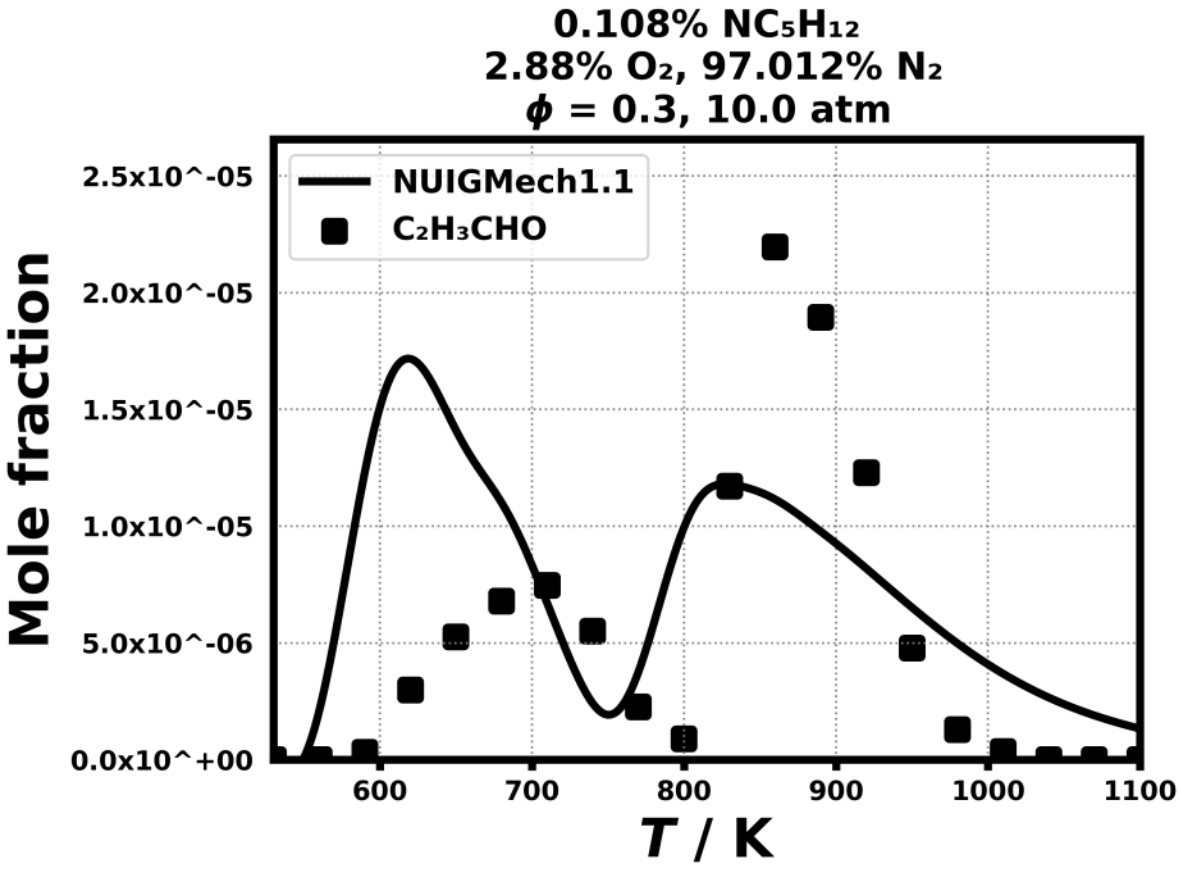

Figure 171: Dataset: 10_ATM_PHI_0.3

1.3.142 Case: n-C5H12/JSR/BUGLER/10_ATM_PHI_0.3

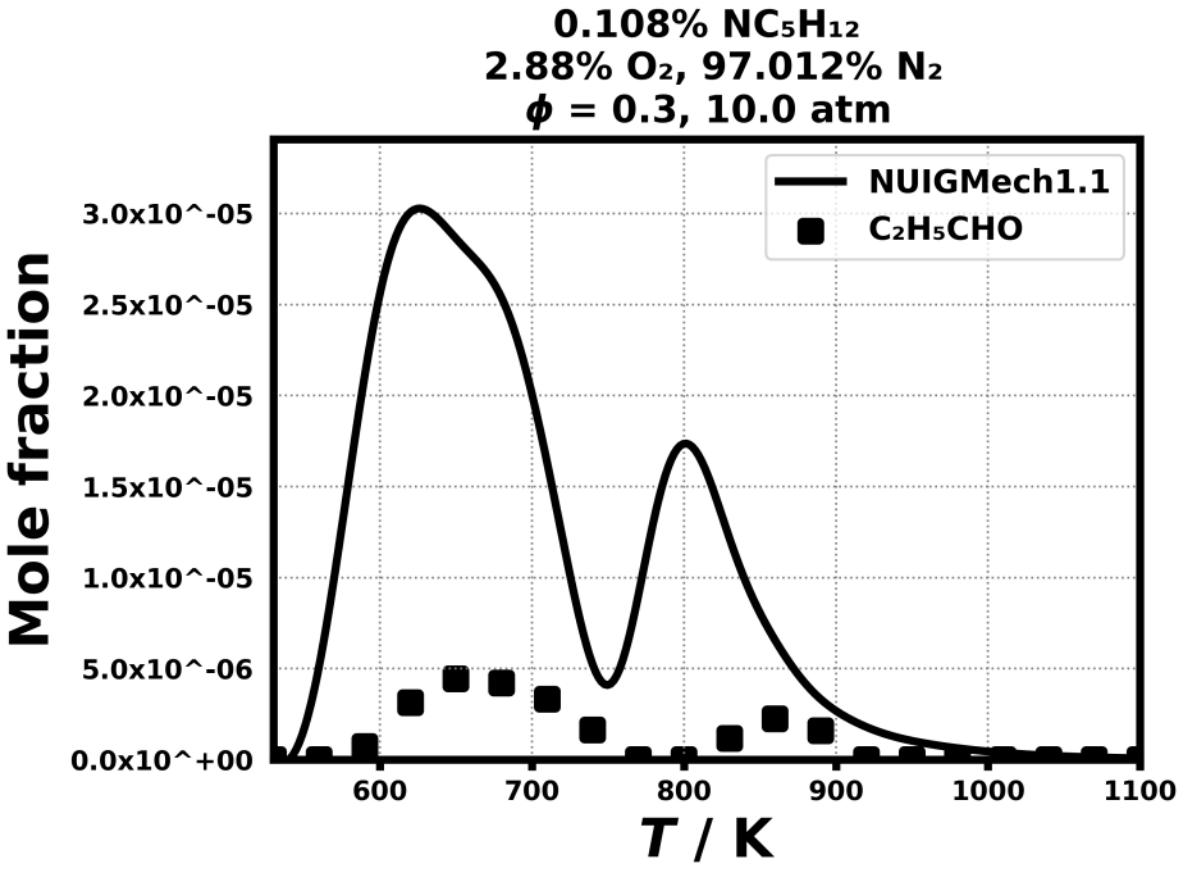

Figure 172: Dataset: 10_ATM_PHI_0.3

1.3.143 Case: n-C5H12/JSR/BUGLER/10_ATM_PHI_0.3

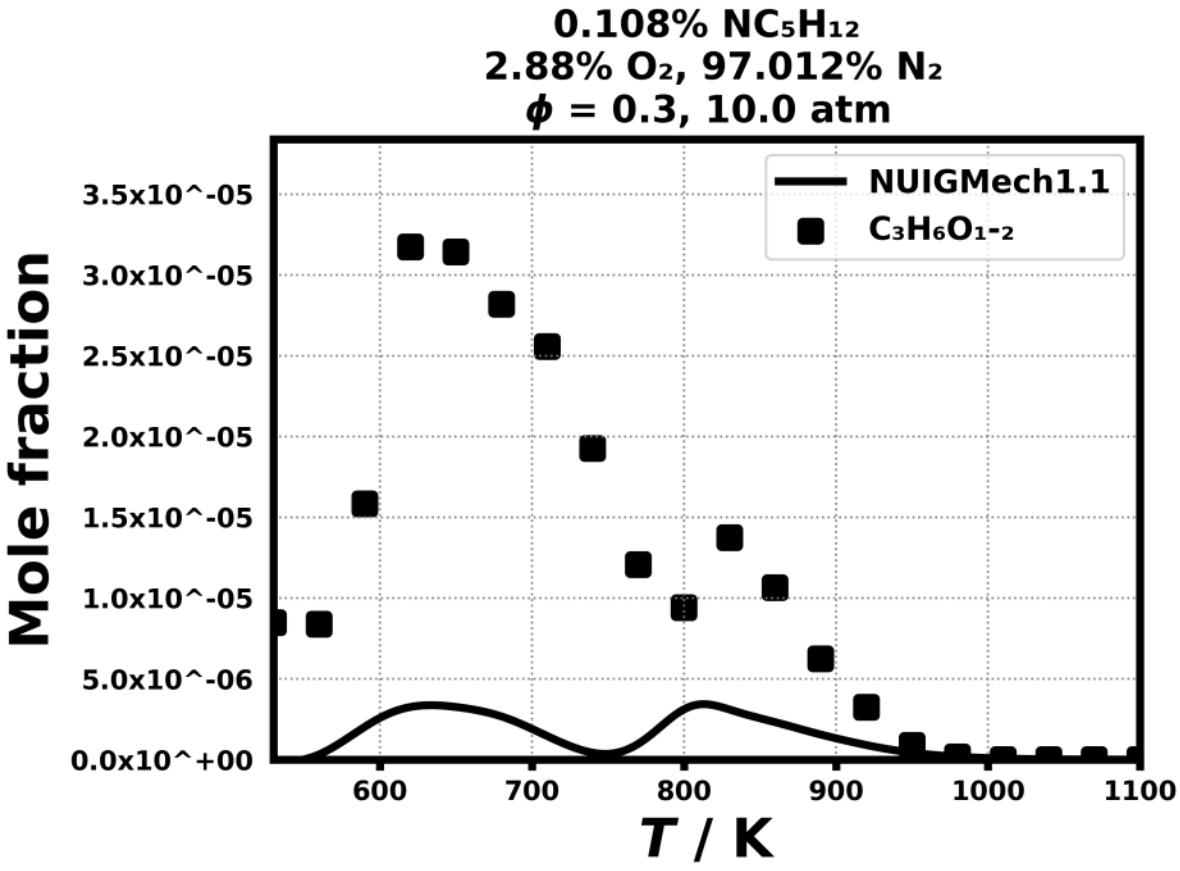

Figure 173: Dataset: 10_ATM_PHI_0.3

1.3.144 Case: n-C5H12/JSR/BUGLER/10_ATM_PHI_0.3

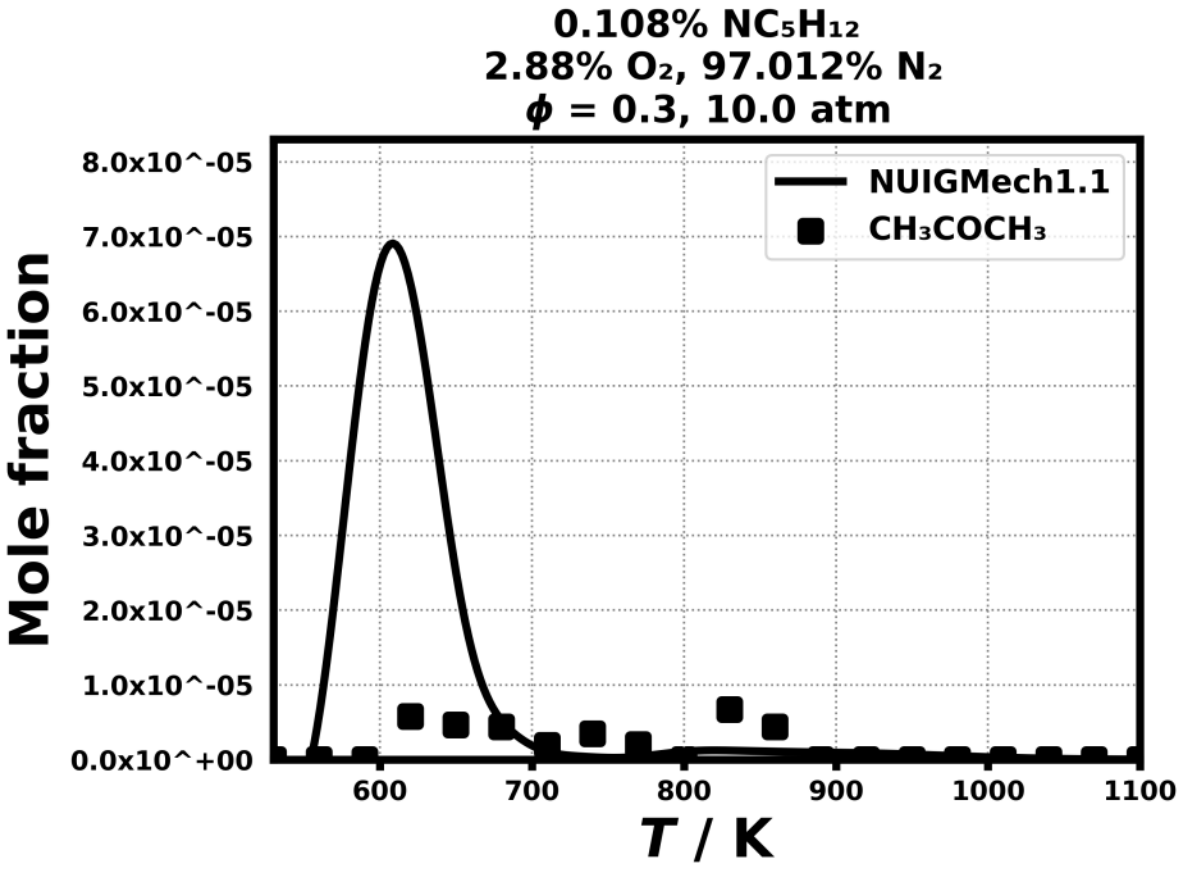

Figure 174: Dataset: 10_ATM_PHI_0.3

1.3.145 Case: n-C5H12/JSR/BUGLER/10_ATM_PHI_0.3

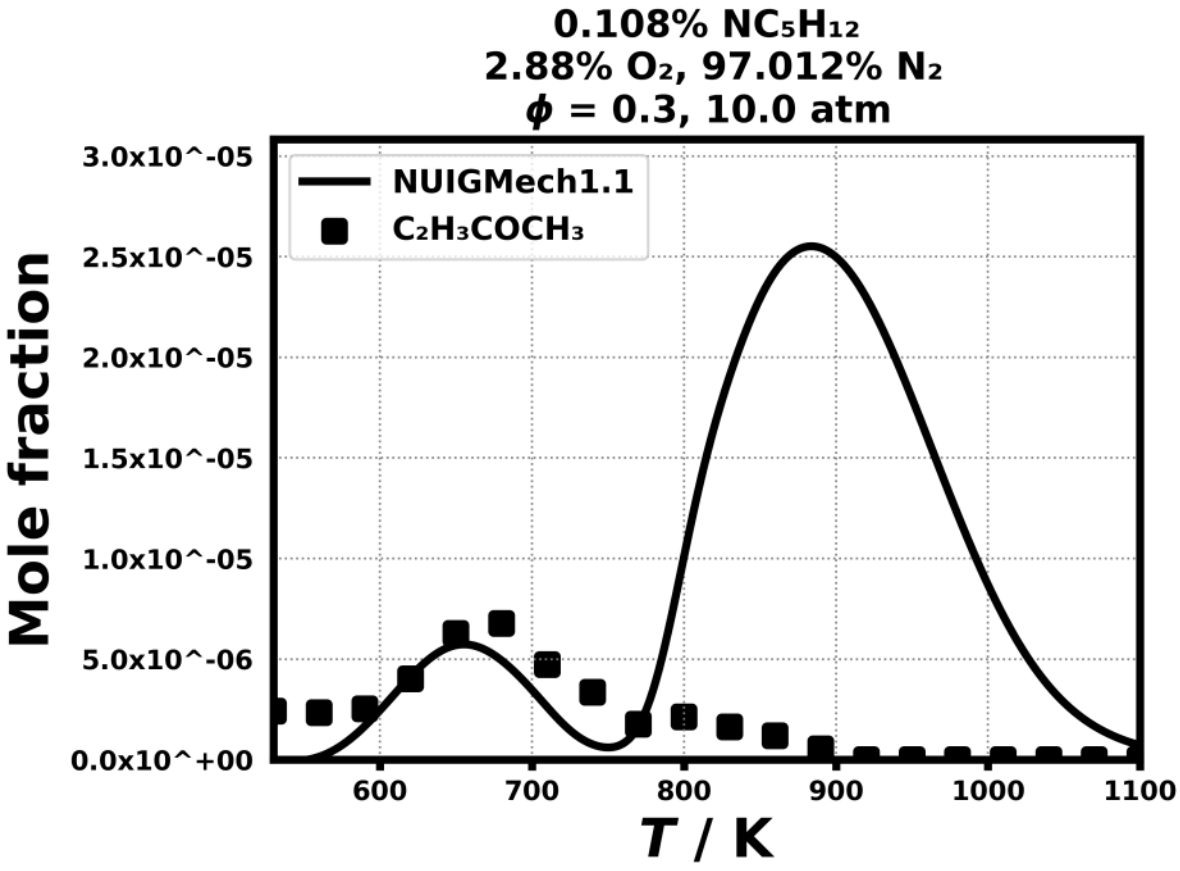

Figure 175: Dataset: 10_ATM_PHI_0.3

1.3.146 Case: n-C5H12/JSR/BUGLER/10_ATM_PHI_0.3

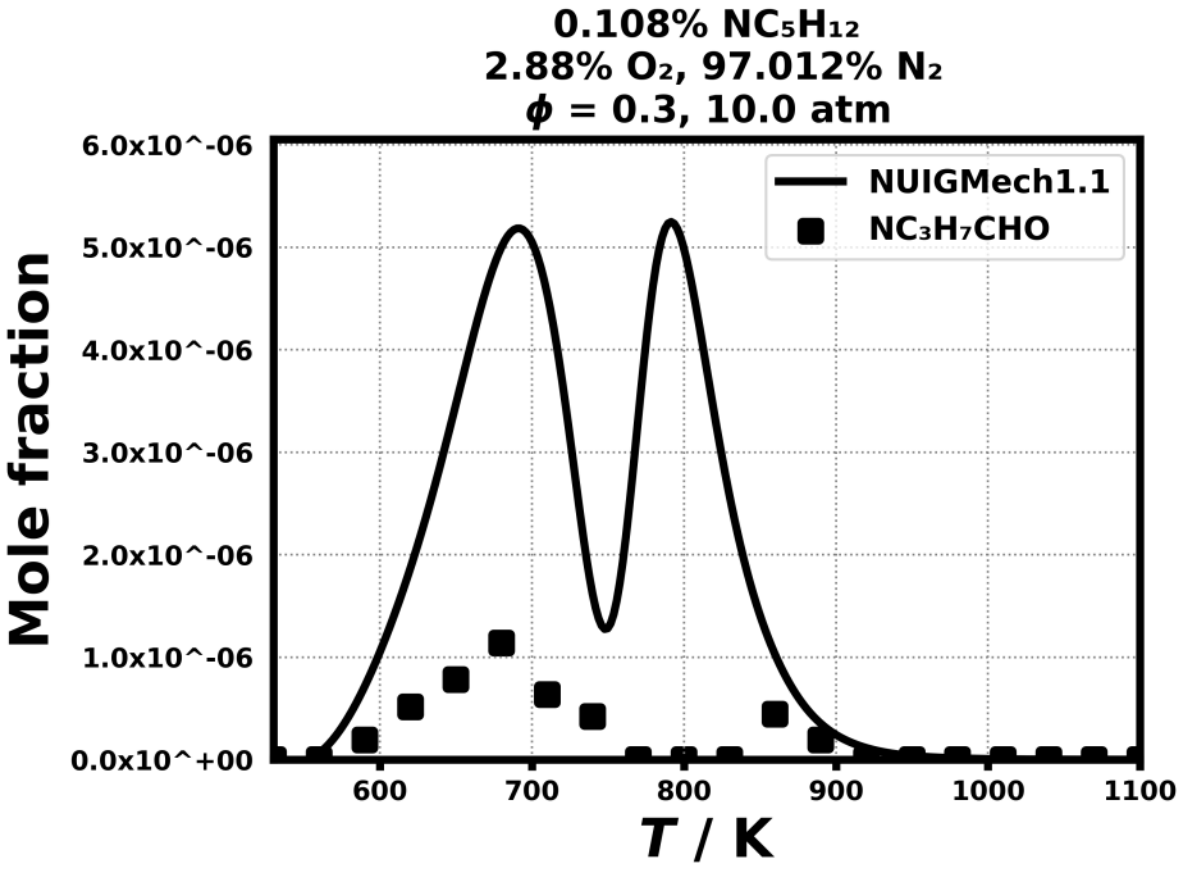

Figure 176: Dataset: 10_ATM_PHI_0.3

1.3.147 Case: n-C5H12/JSR/BUGLER/10_ATM_PHI_0.3

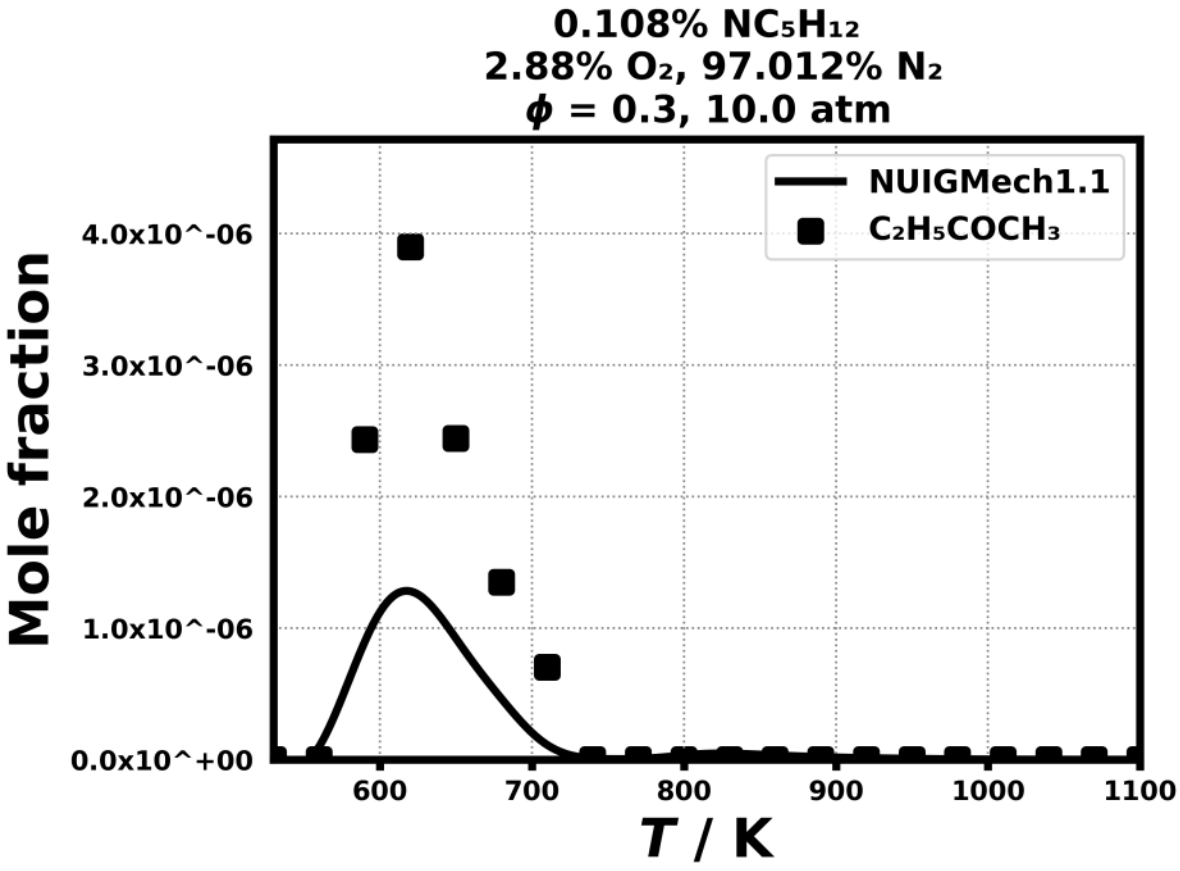

Figure 177: Dataset: 10_ATM_PHI_0.3

1.3.148 Case: n-C5H12/JSR/BUGLER/10_ATM_PHI_0.3

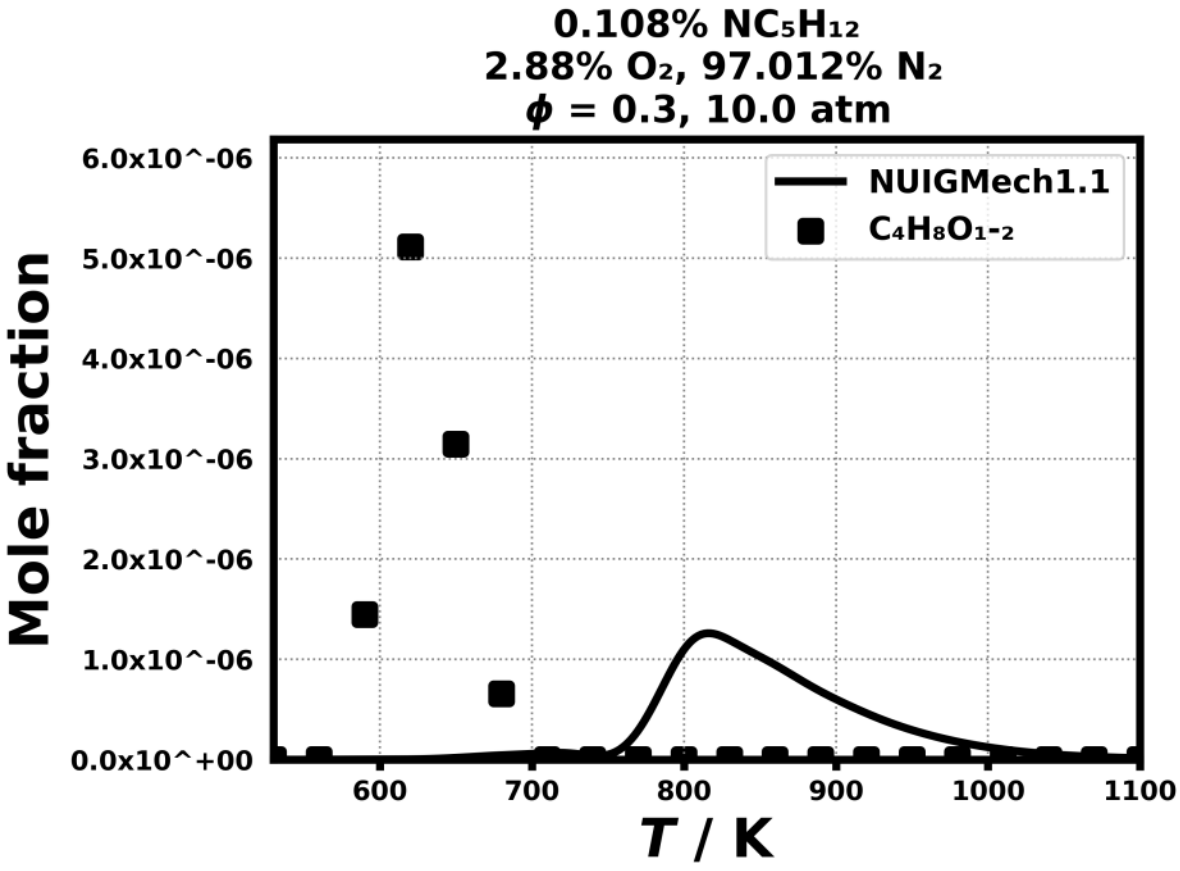

Figure 178: Dataset: 10_ATM_PHI_0.3

1.3.149 Case: n-C5H12/JSR/BUGLER/10_ATM_PHI_0.3

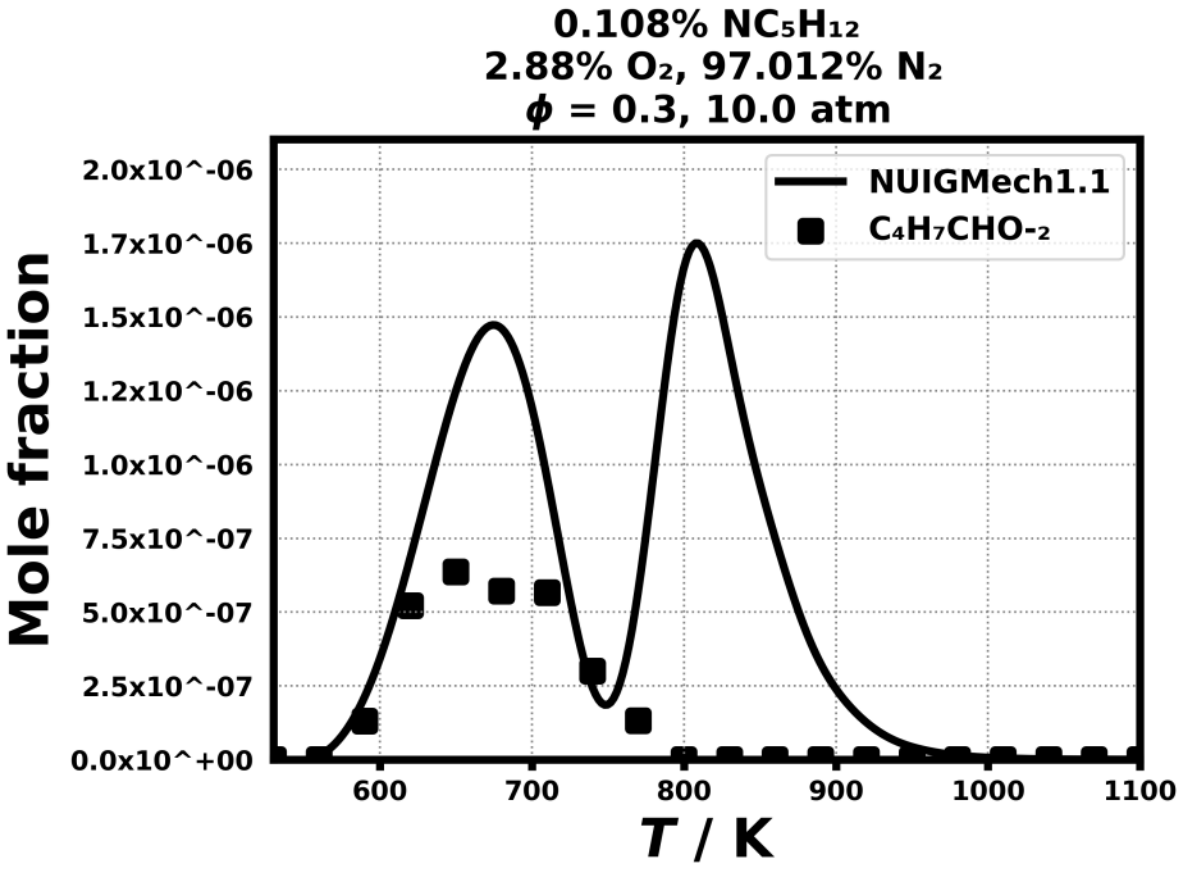

Figure 179: Dataset: 10_ATM_PHI_0.3

1.3.150 Case: n-C5H12/JSR/BUGLER/10_ATM_PHI_0.3

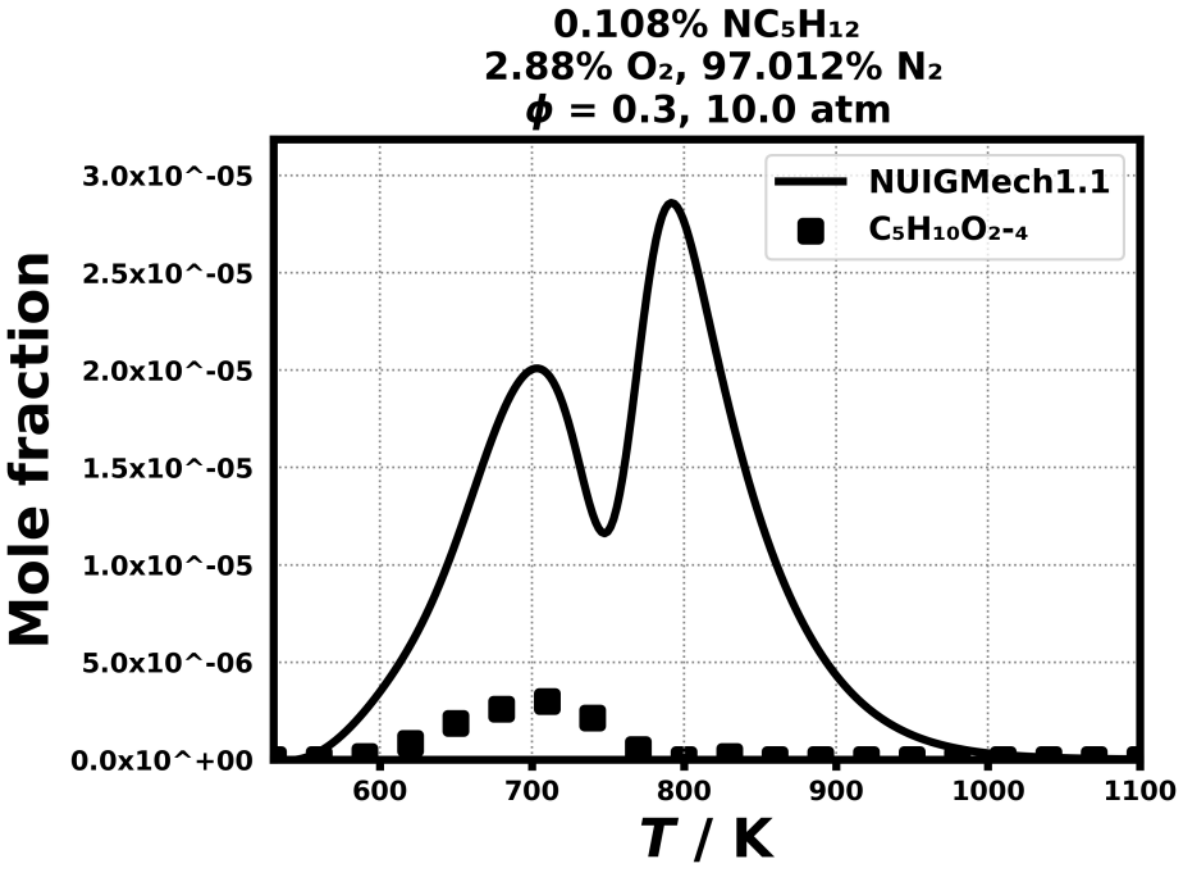

Figure 180: Dataset: 10_ATM_PHI_0.3

1.3.151 Case: n-C5H12/JSR/BUGLER/10_ATM_PHI_0.3

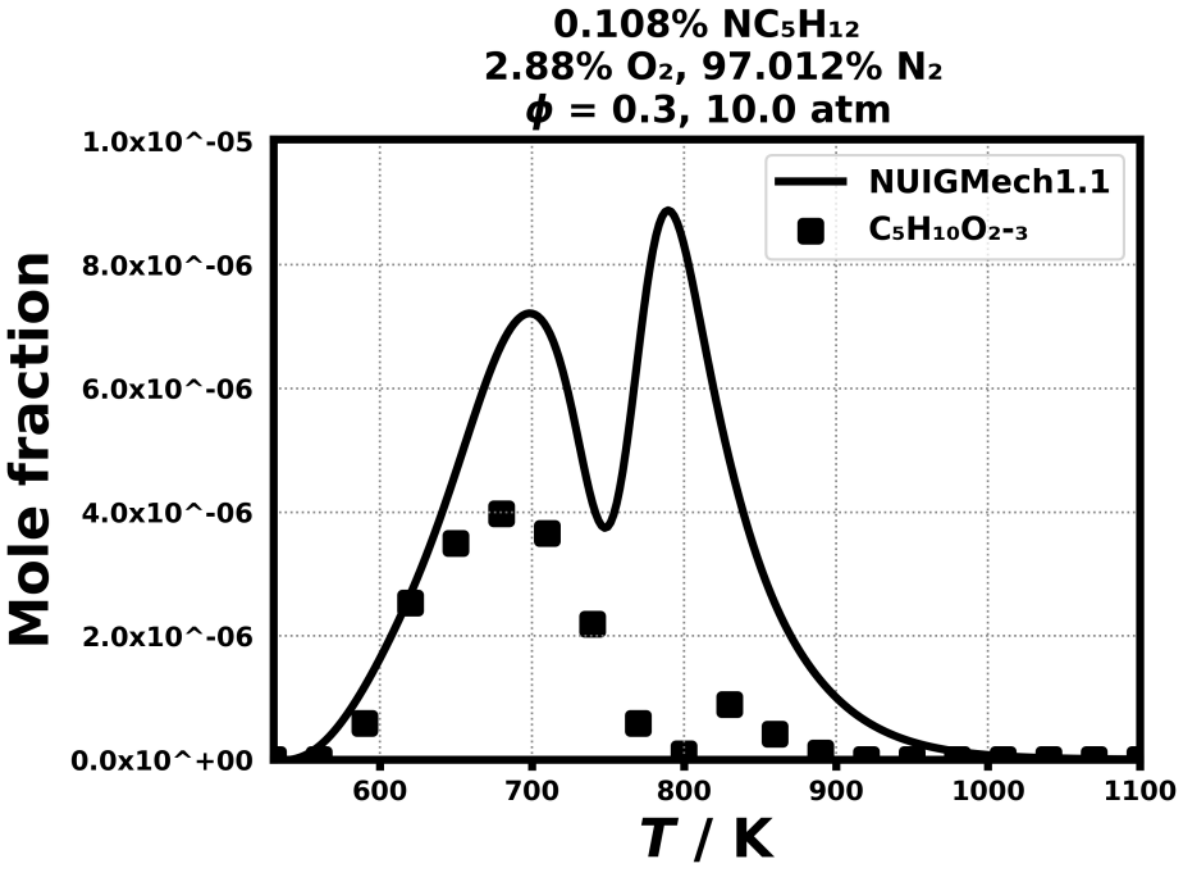

Figure 181: Dataset: 10_ATM_PHI_0.3

1.3.152 Case: n-C5H12/JSR/BUGLER/10_ATM_PHI_0.3

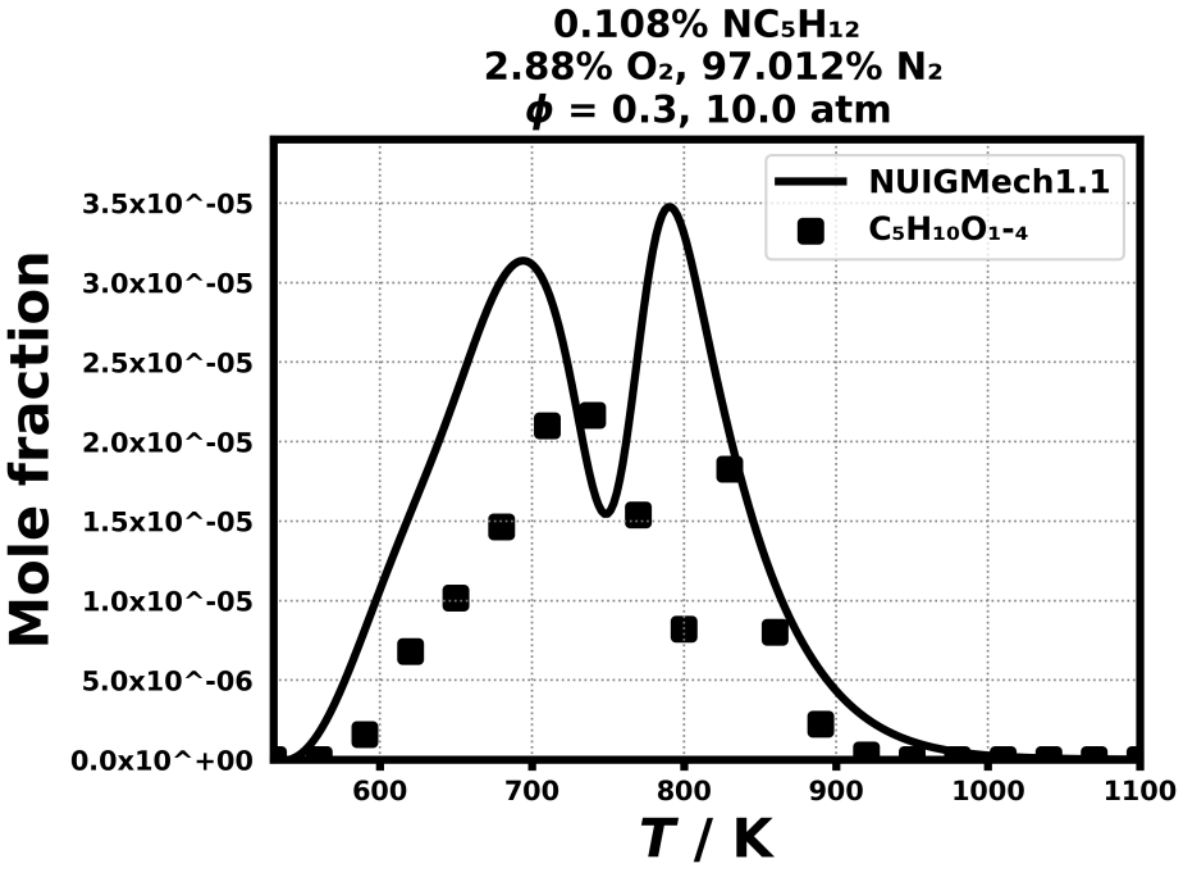

Figure 182: Dataset: 10_ATM_PHI_0.3

1.3.153 Case: n-C5H12/JSR/BUGLER/10_ATM_PHI_0.3

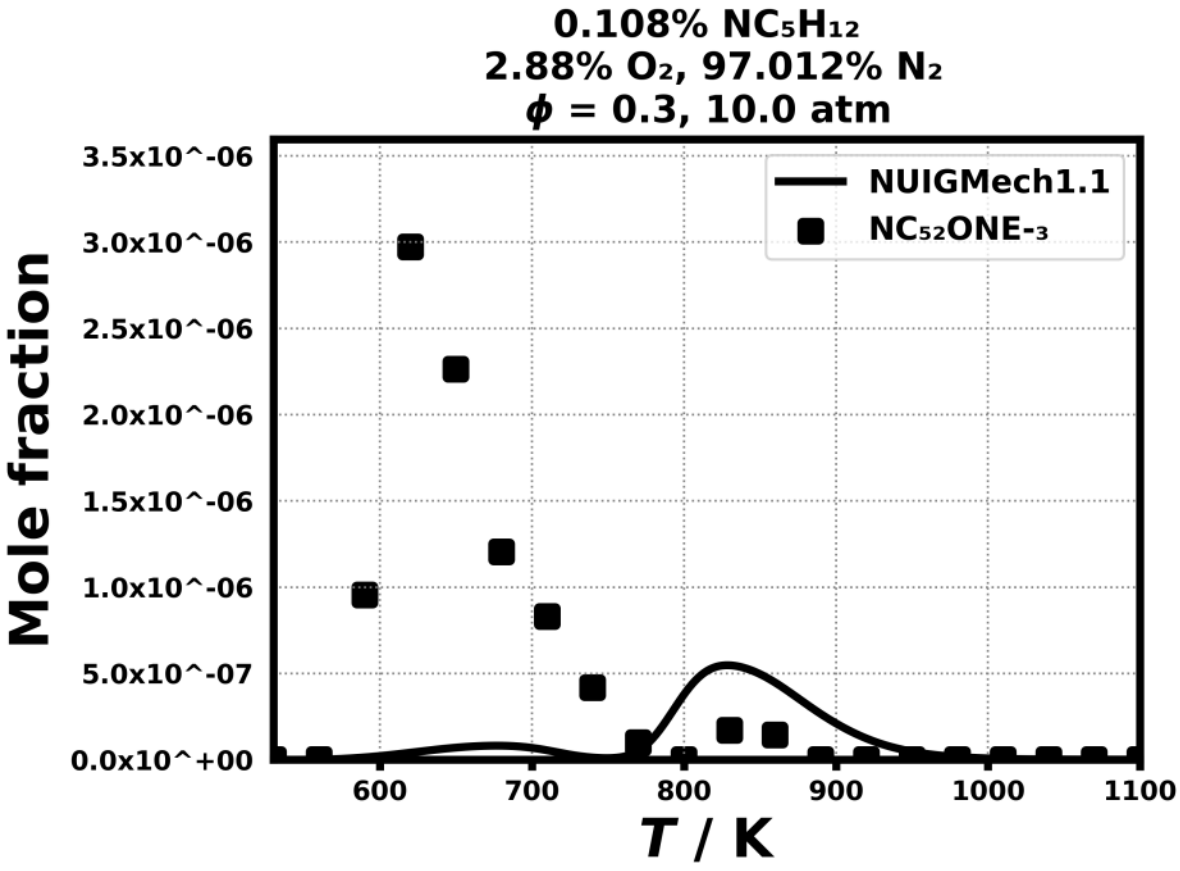

Figure 183: Dataset: 10_ATM_PHI_0.3

1.3.154 Case: n-C5H12/JSR/BUGLER/10_ATM_PHI_0.3

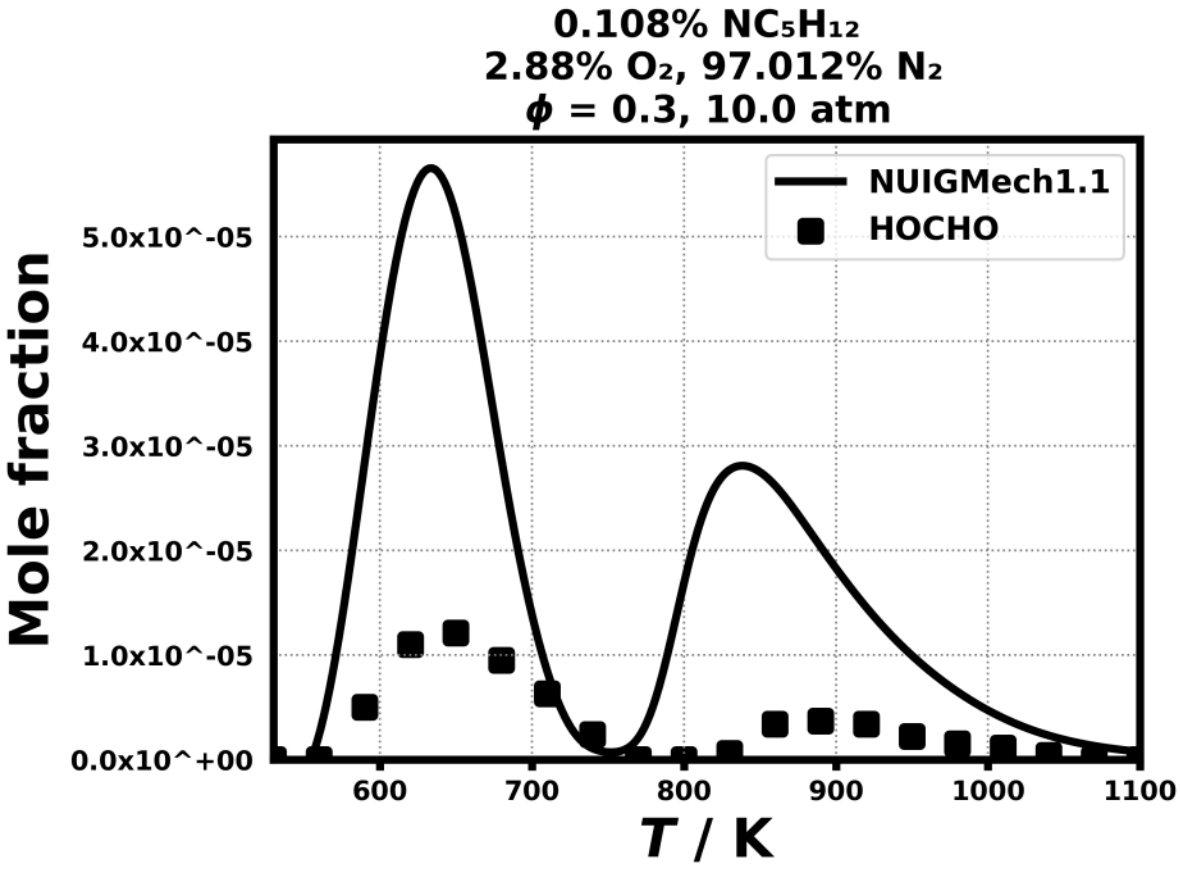

Figure 184: Dataset: 10_ATM_PHI_0.3

1.3.155 Case: n-C5H12/JSR/BUGLER/10_ATM_PHI_0.3

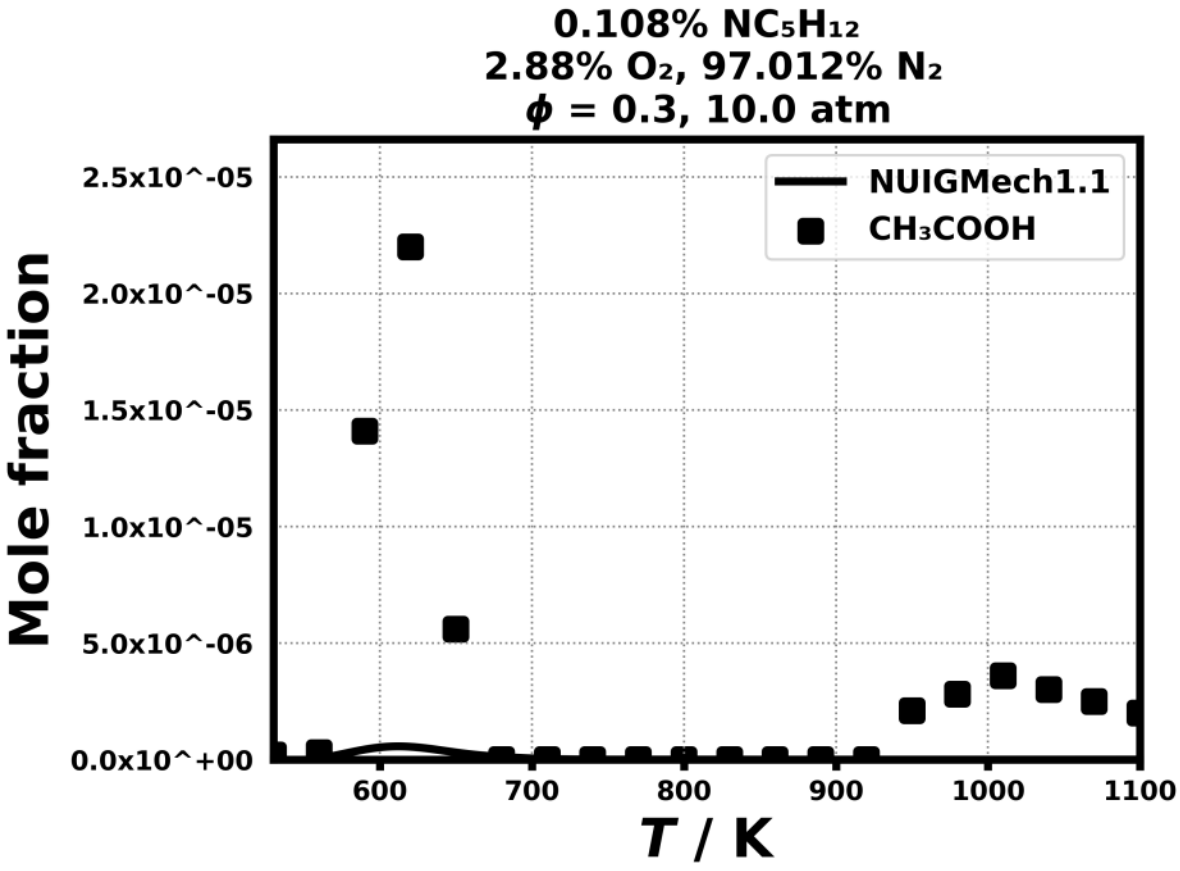

Figure 185: Dataset: 10_ATM_PHI_0.3

1.3.156 Case: n-C5H12/JSR/BUGLER/10_ATM_PHI_0.5

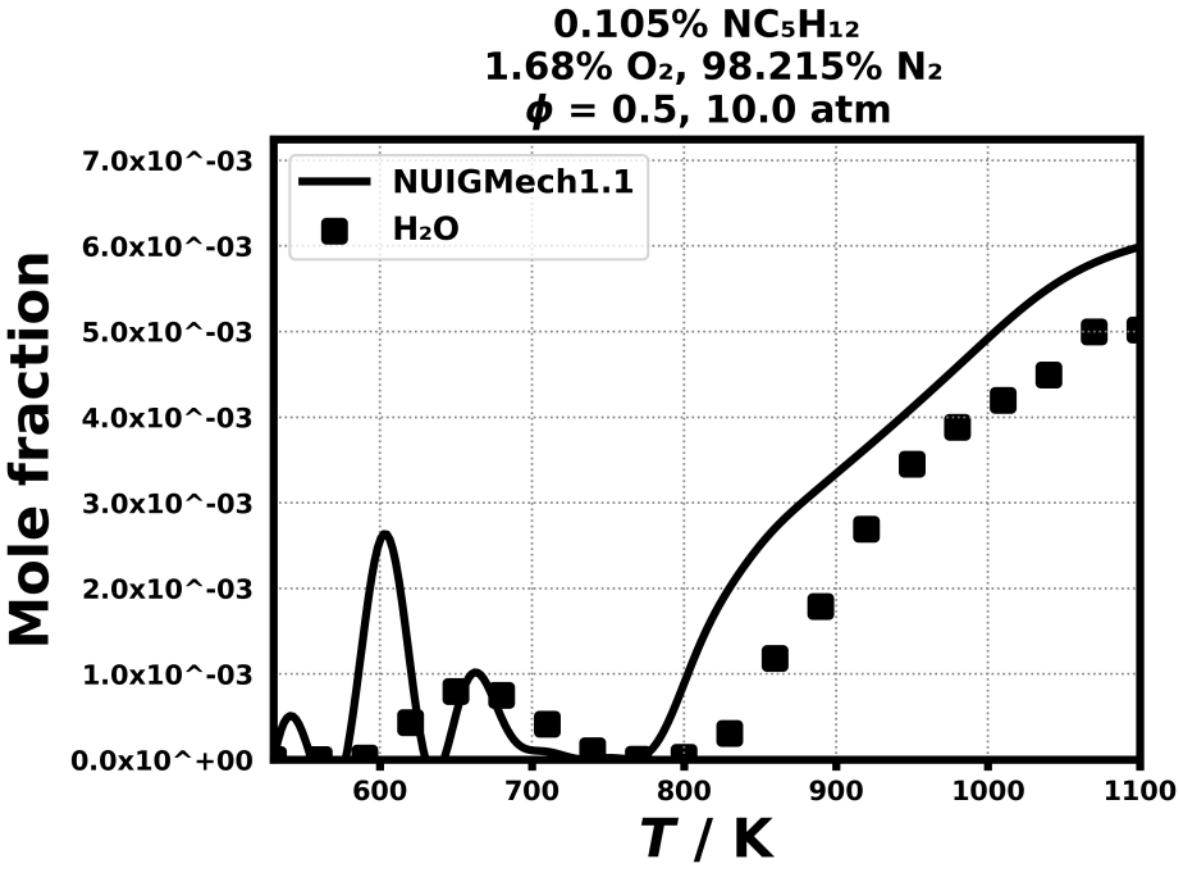

Figure 186: Dataset: 10_ATM_PHI_0.5

1.3.157 Case: n-C5H12/JSR/BUGLER/10_ATM_PHI_0.5

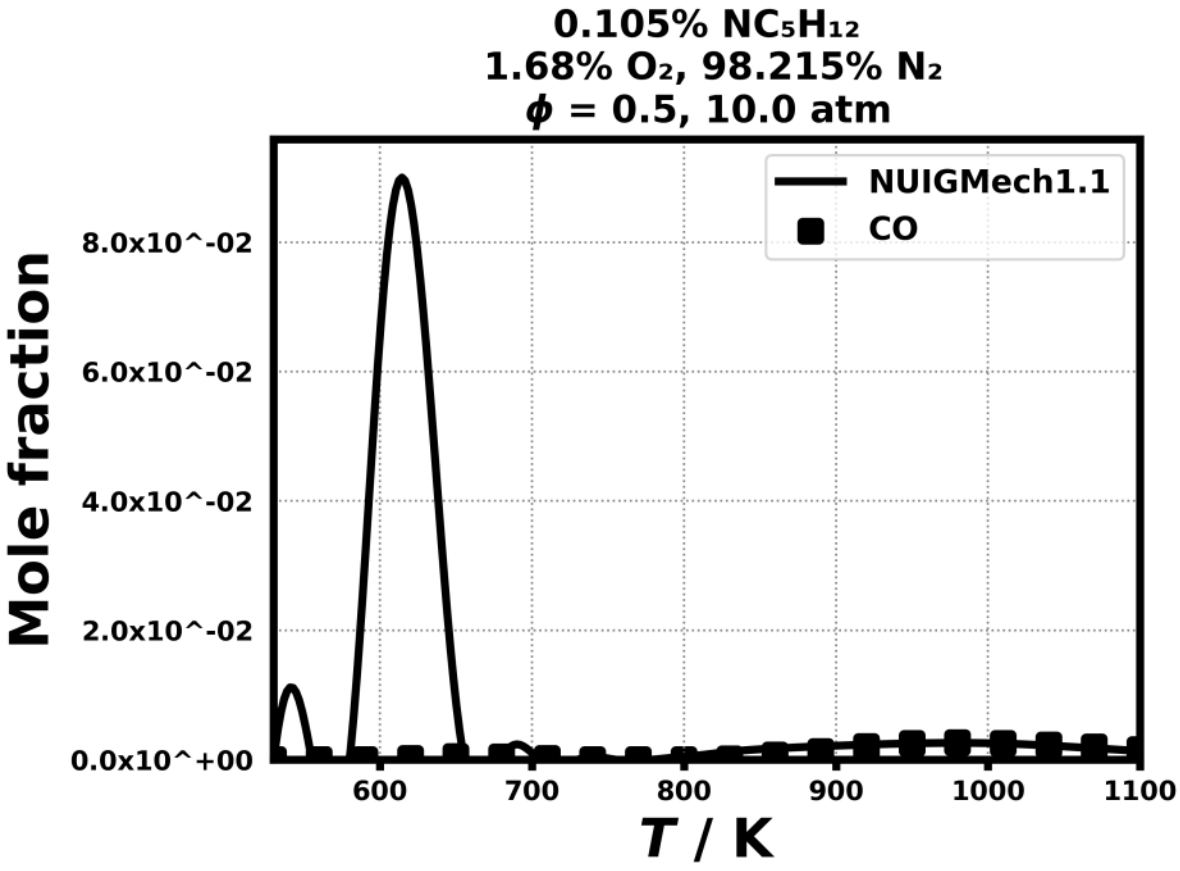

Figure 187: Dataset: 10_ATM_PHI_0.5

1.3.158 Case: n-C5H12/JSR/BUGLER/10_ATM_PHI_0.5

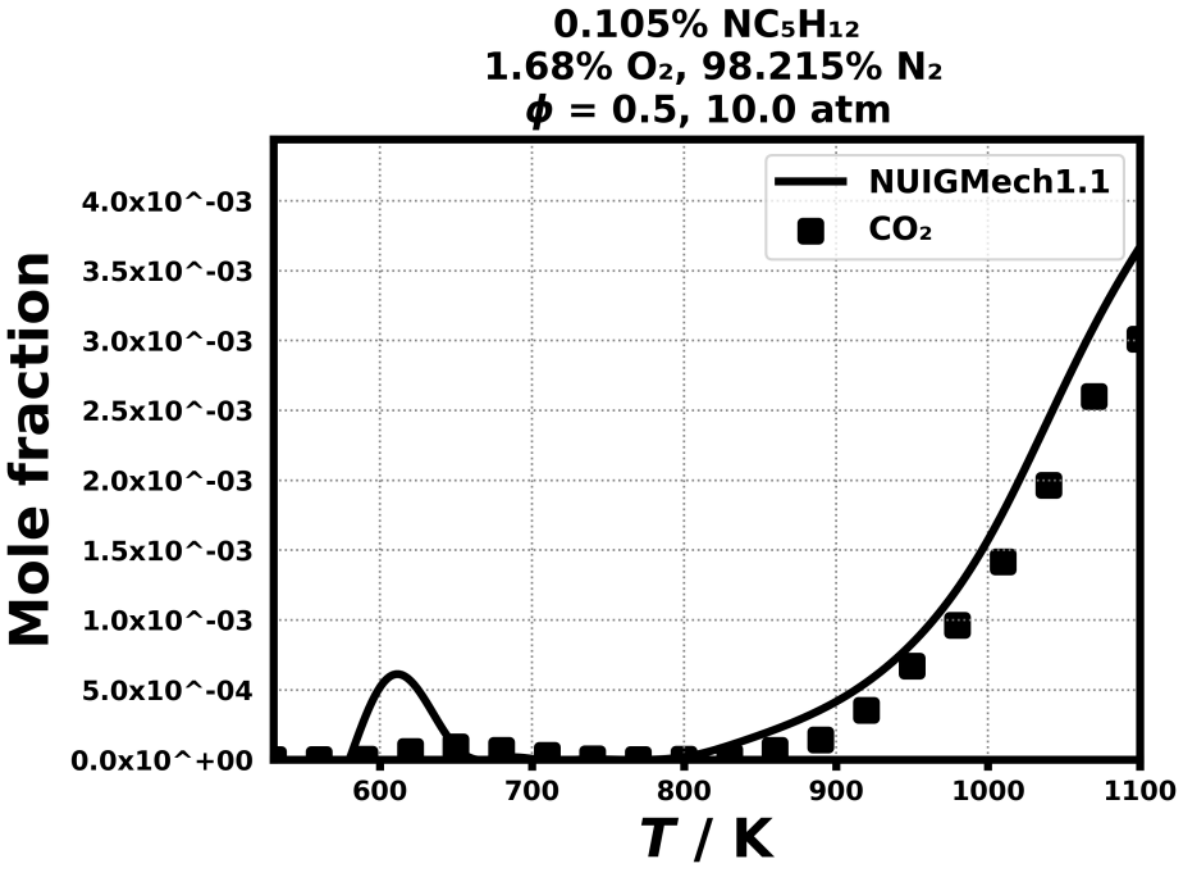

Figure 188: Dataset: 10_ATM_PHI_0.5

1.3.159 Case: n-C5H12/JSR/BUGLER/10_ATM_PHI_0.5

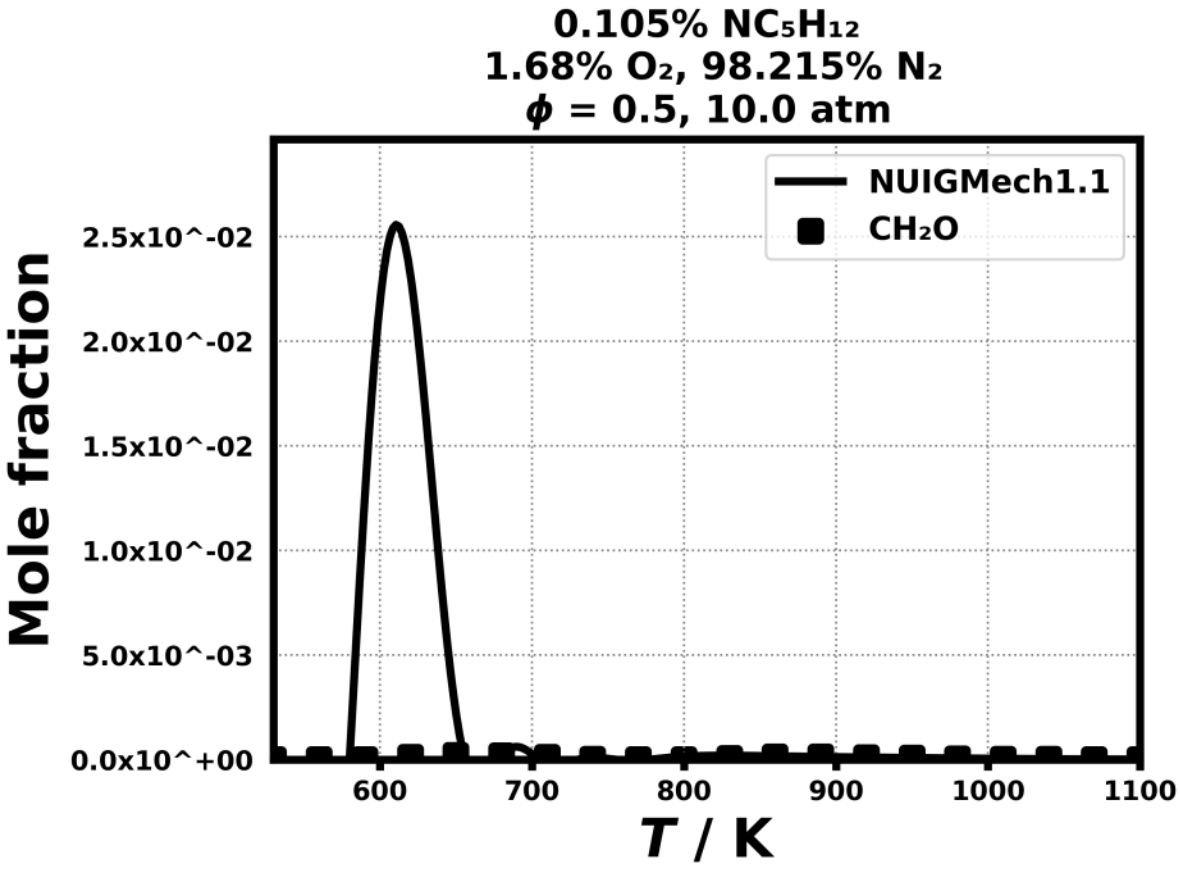

Figure 189: Dataset: 10_ATM_PHI_0.5

1.3.160 Case: n-C5H12/JSR/BUGLER/10_ATM_PHI_0.5

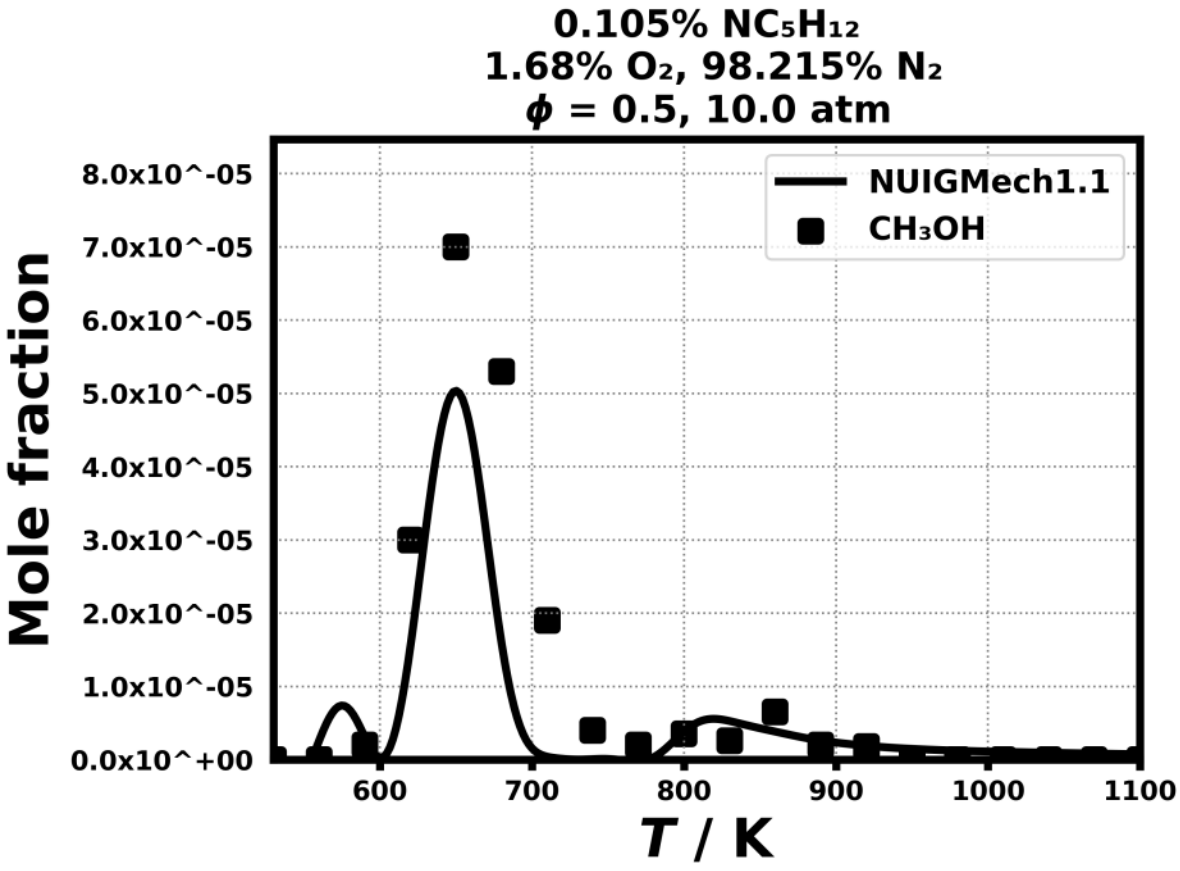

Figure 190: Dataset: 10_ATM_PHI_0.5

1.3.161 Case: n-C5H12/JSR/BUGLER/10_ATM_PHI_0.5

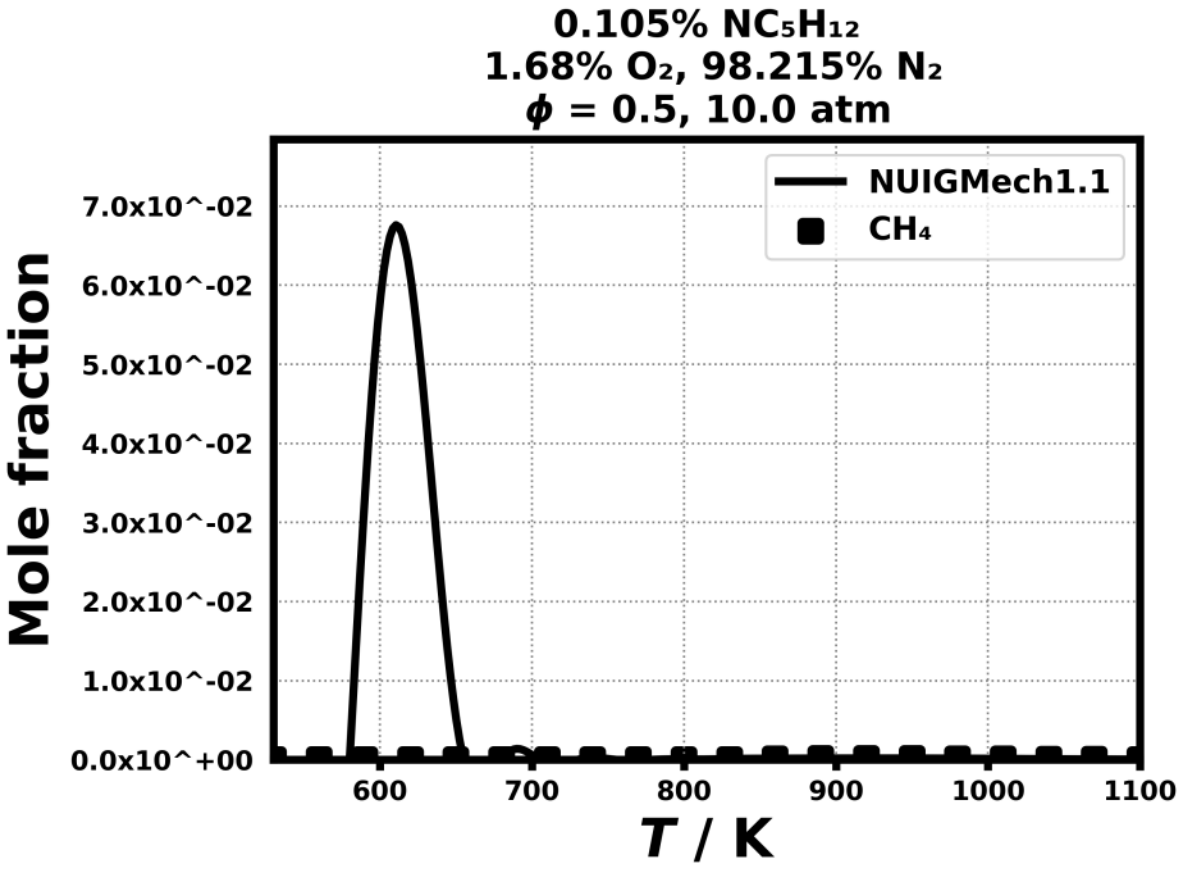

Figure 191: Dataset: 10_ATM_PHI_0.5

1.3.162 Case: n-C5H12/JSR/BUGLER/10_ATM_PHI_0.5

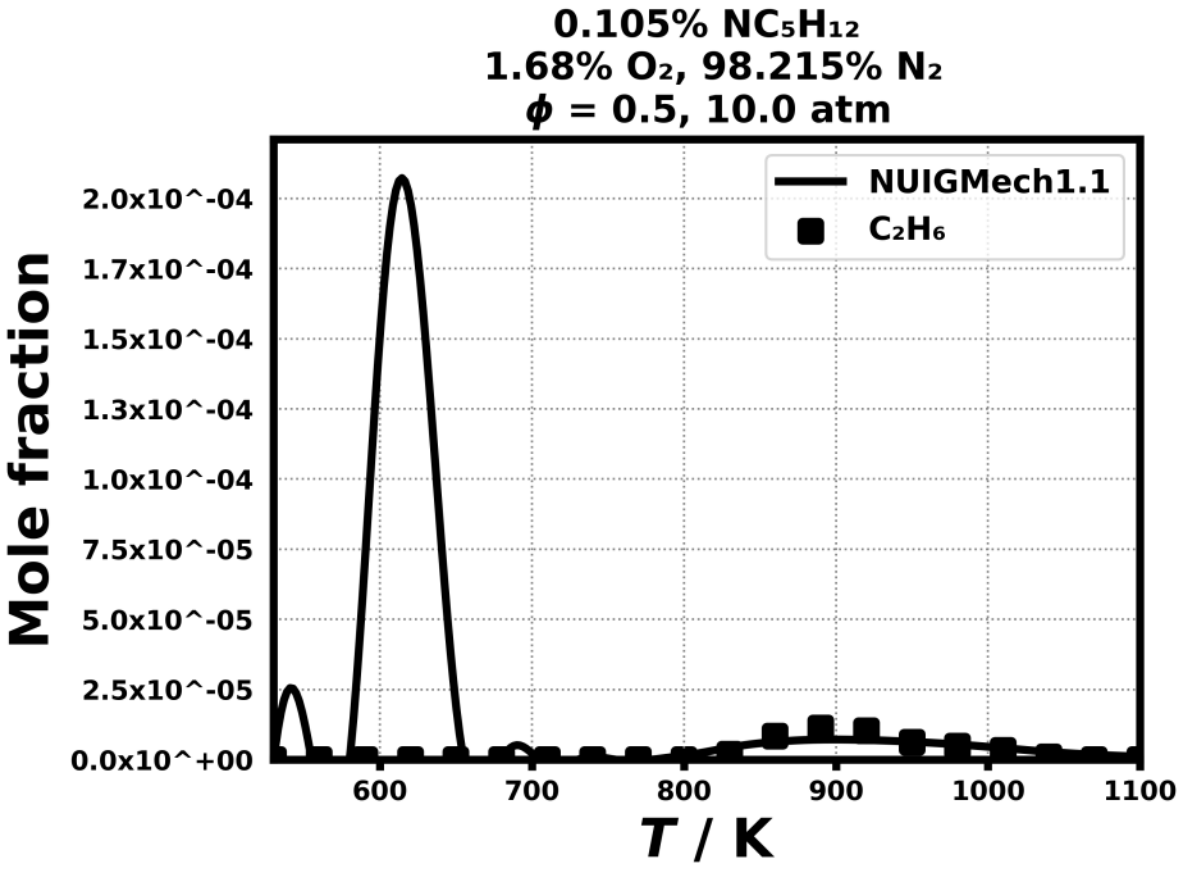

Figure 192: Dataset: 10_ATM_PHI_0.5

1.3.163 Case: n-C5H12/JSR/BUGLER/10_ATM_PHI_0.5

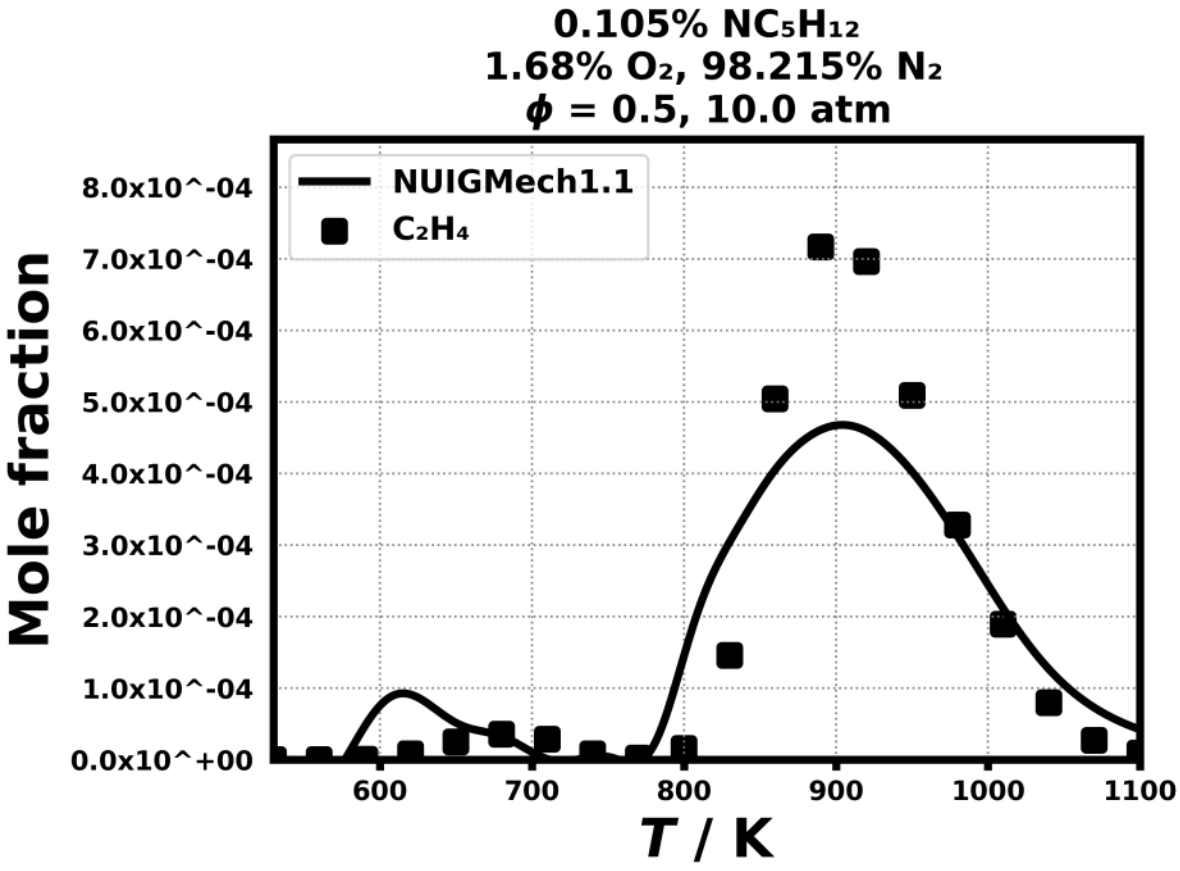

Figure 193: Dataset: 10_ATM_PHI_0.5

1.3.164 Case: n-C5H12/JSR/BUGLER/10_ATM_PHI_0.5

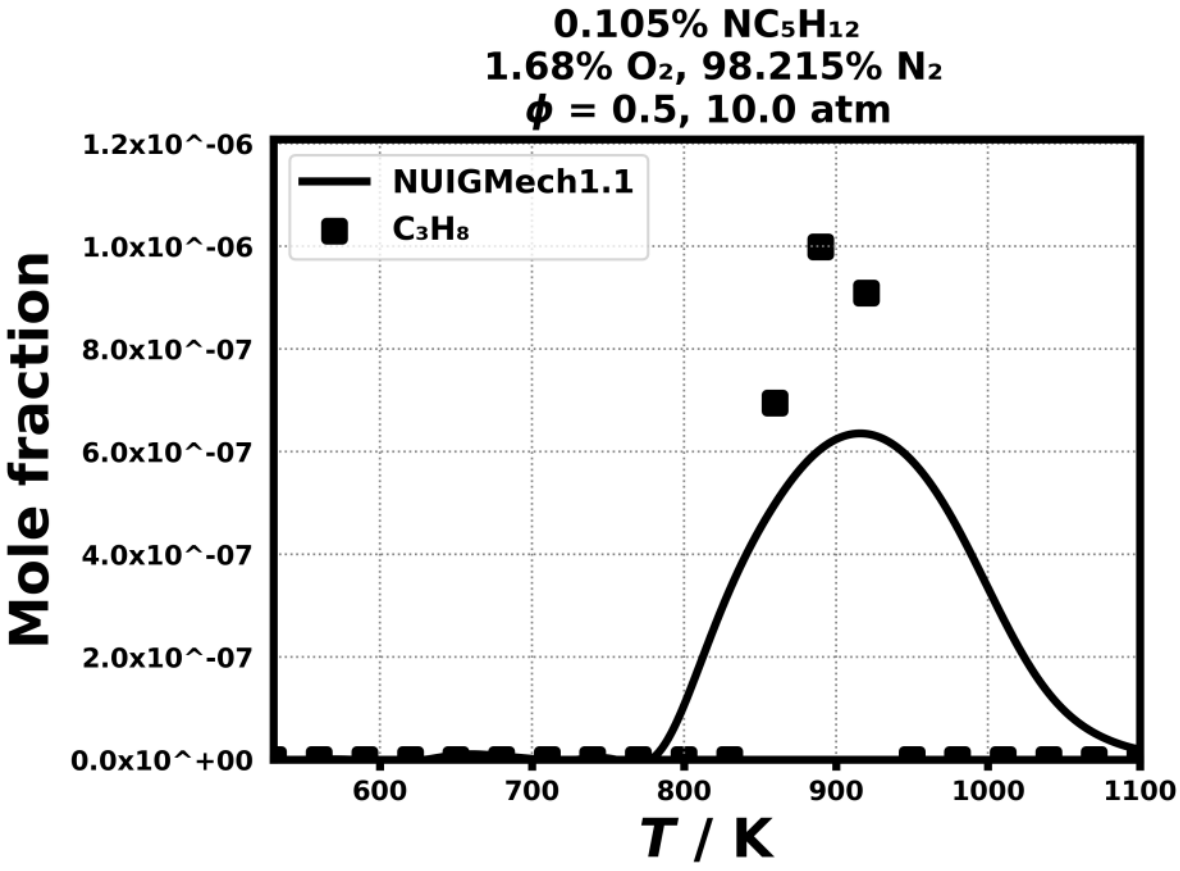

Figure 194: Dataset: 10_ATM_PHI_0.5

1.3.165 Case: n-C5H12/JSR/BUGLER/10_ATM_PHI_0.5

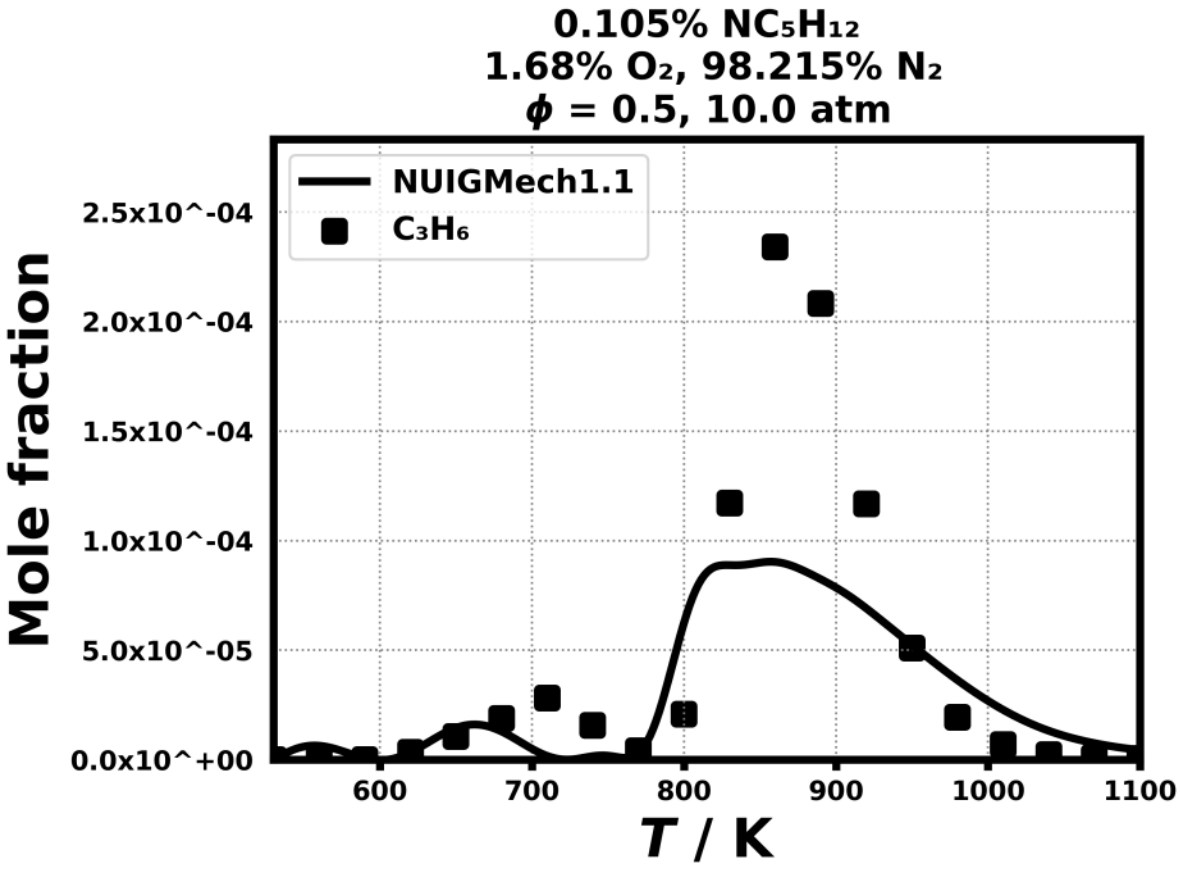

Figure 195: Dataset: 10_ATM_PHI_0.5

1.3.166 Case: n-C5H12/JSR/BUGLER/10_ATM_PHI_0.5

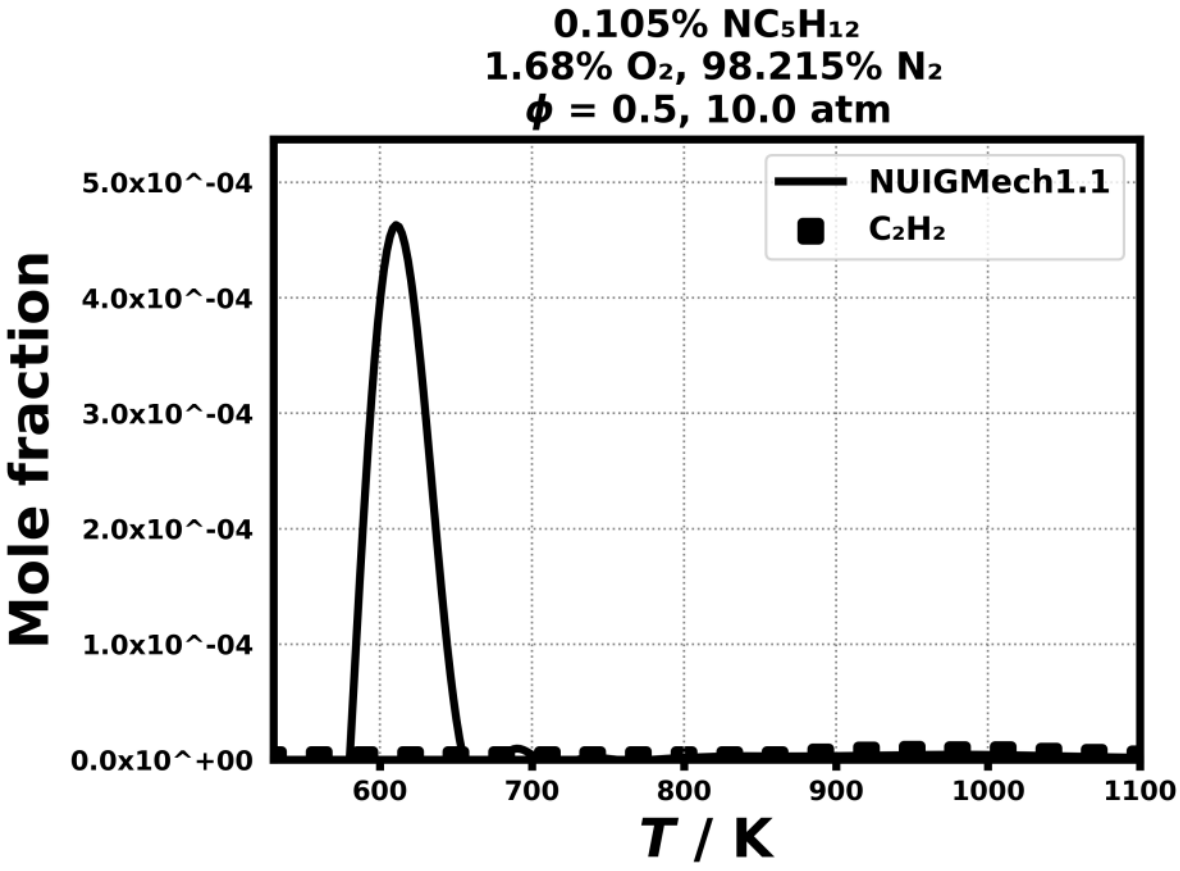

Figure 196: Dataset: 10_ATM_PHI_0.5

1.3.167 Case: n-C5H12/JSR/BUGLER/10_ATM_PHI_0.5

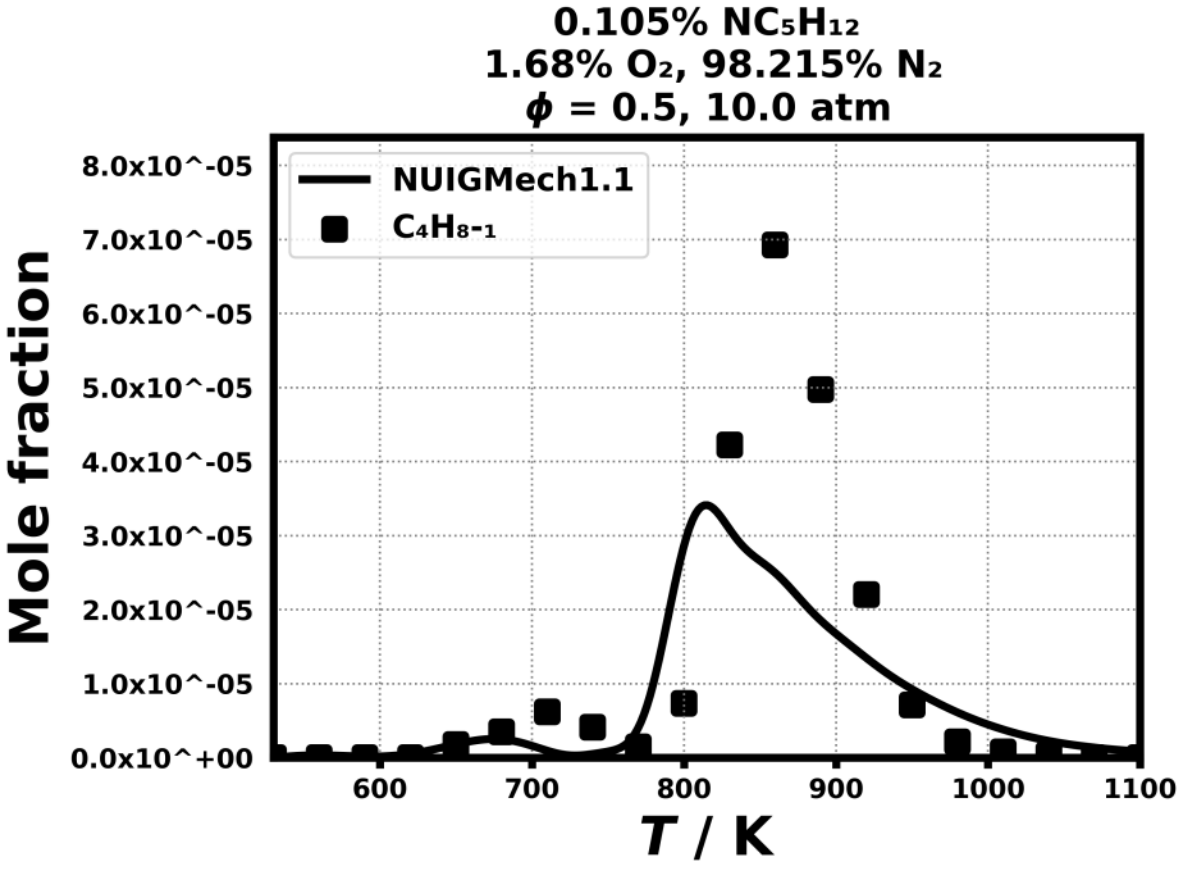

Figure 197: Dataset: 10_ATM_PHI_0.5

1.3.168 Case: n-C5H12/JSR/BUGLER/10_ATM_PHI_0.5

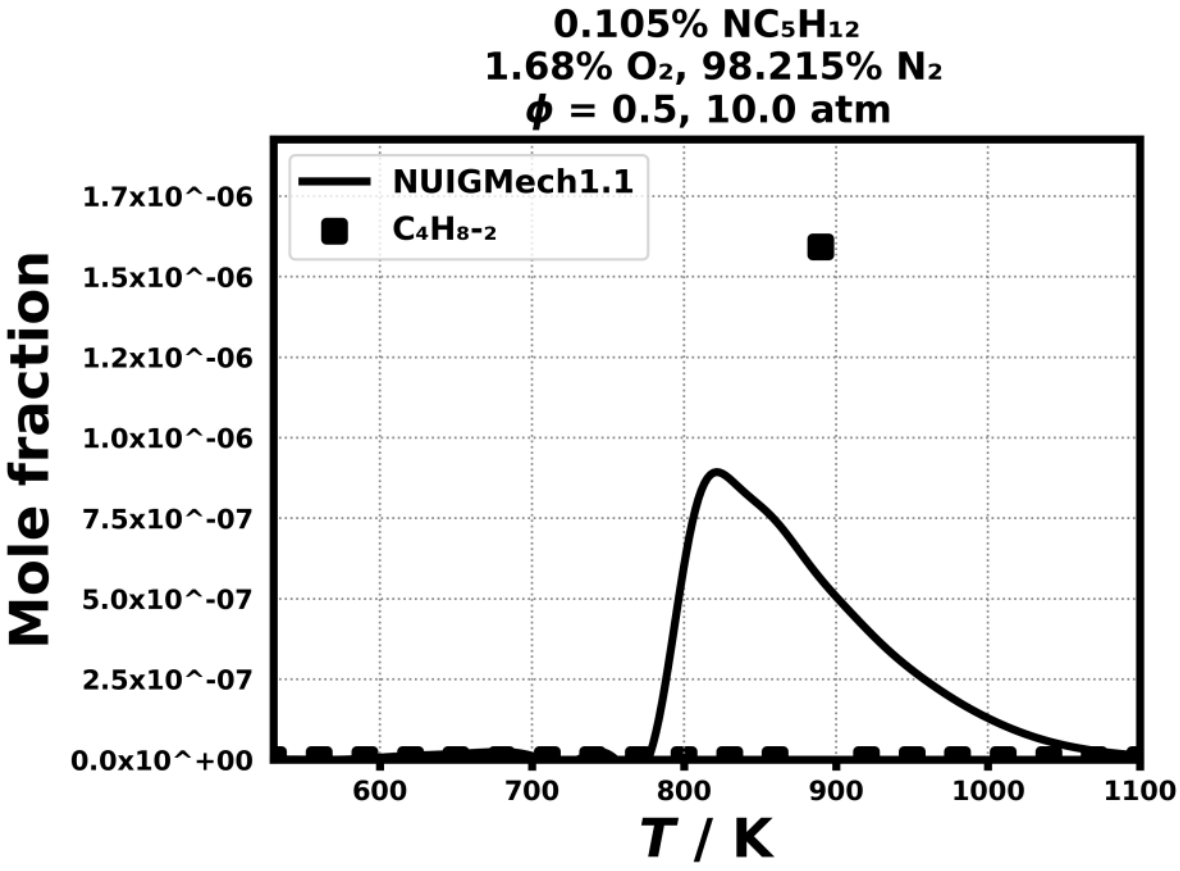

Figure 198: Dataset: 10_ATM_PHI_0.5

1.3.169 Case: n-C5H12/JSR/BUGLER/10_ATM_PHI_0.5

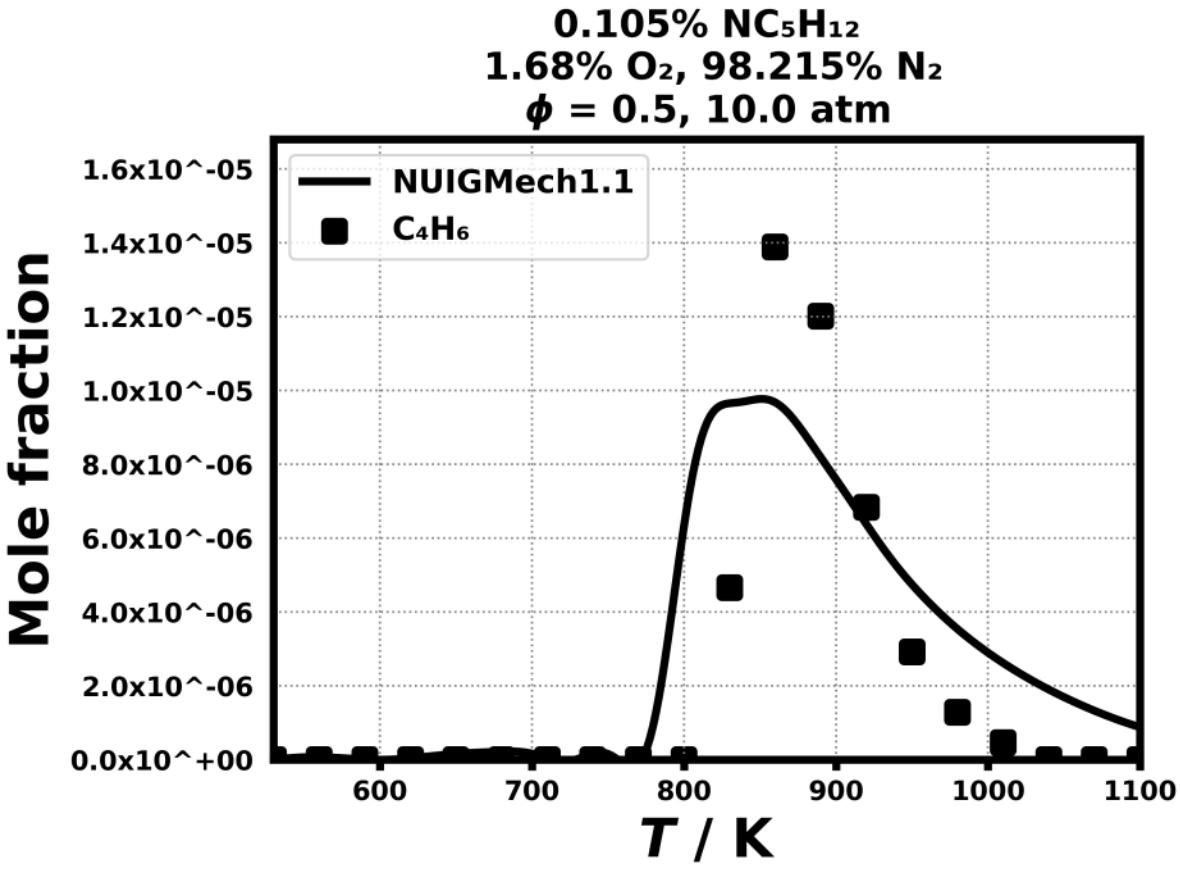

Figure 199: Dataset: 10_ATM_PHI_0.5

1.3.170 Case: n-C5H12/JSR/BUGLER/10_ATM_PHI_0.5

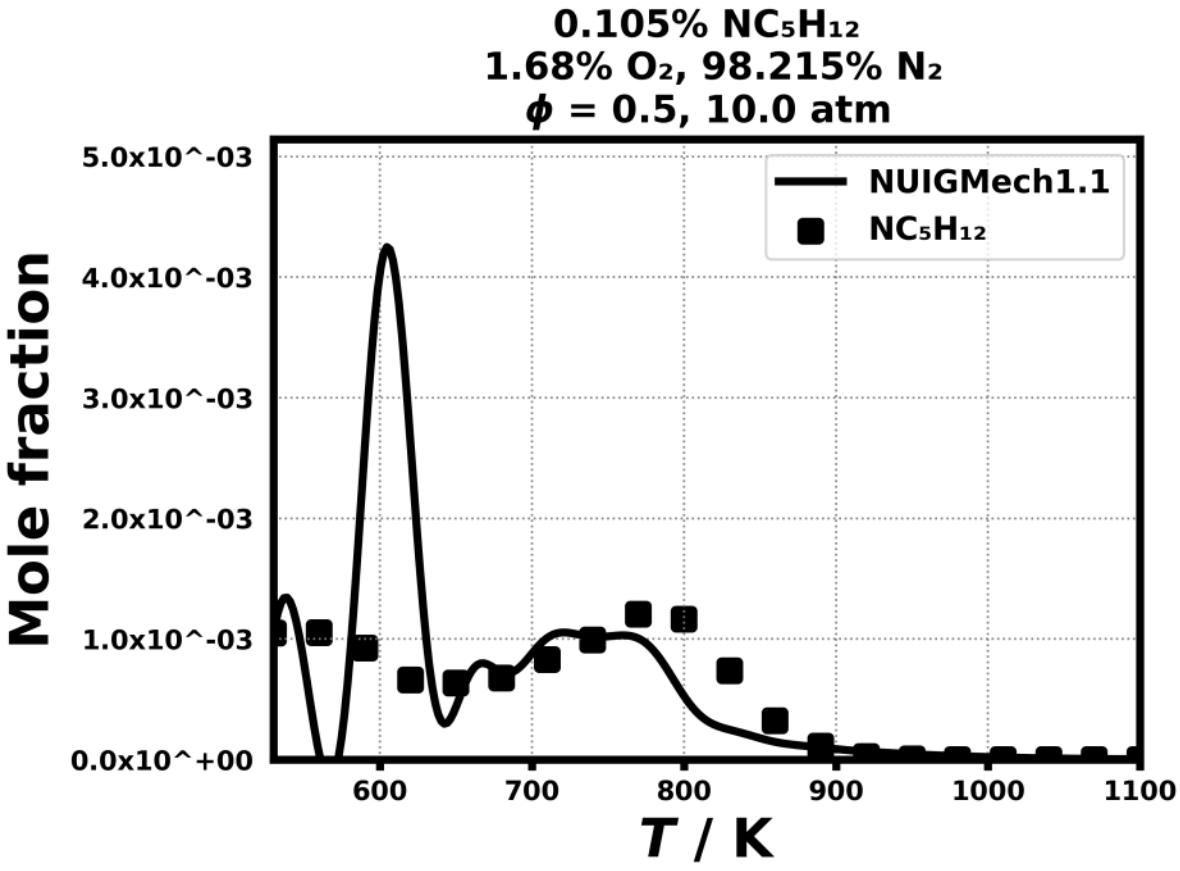

Figure 200: Dataset: 10_ATM_PHI_0.5

1.3.171 Case: n-C5H12/JSR/BUGLER/10_ATM_PHI_0.5

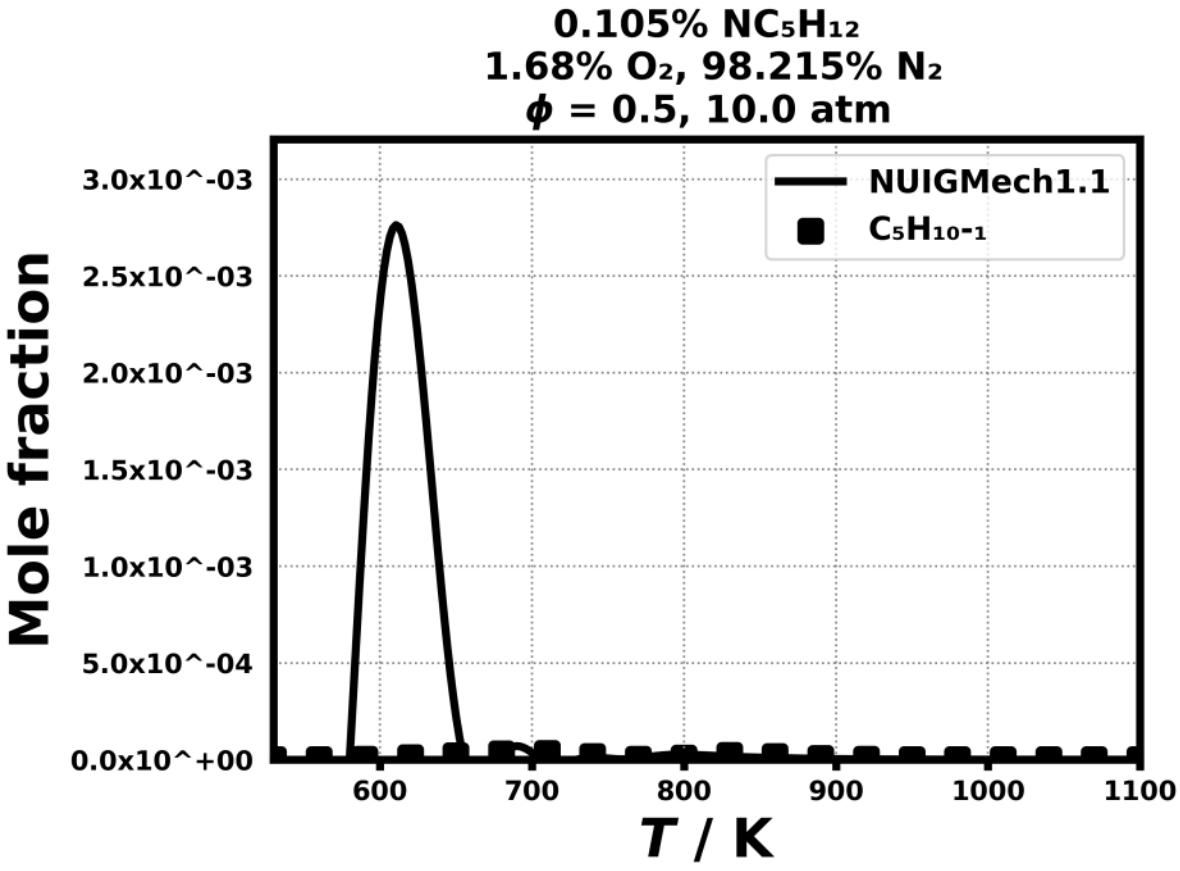

Figure 201: Dataset: 10_ATM_PHI_0.5

1.3.172 Case: n-C5H12/JSR/BUGLER/10_ATM_PHI_0.5

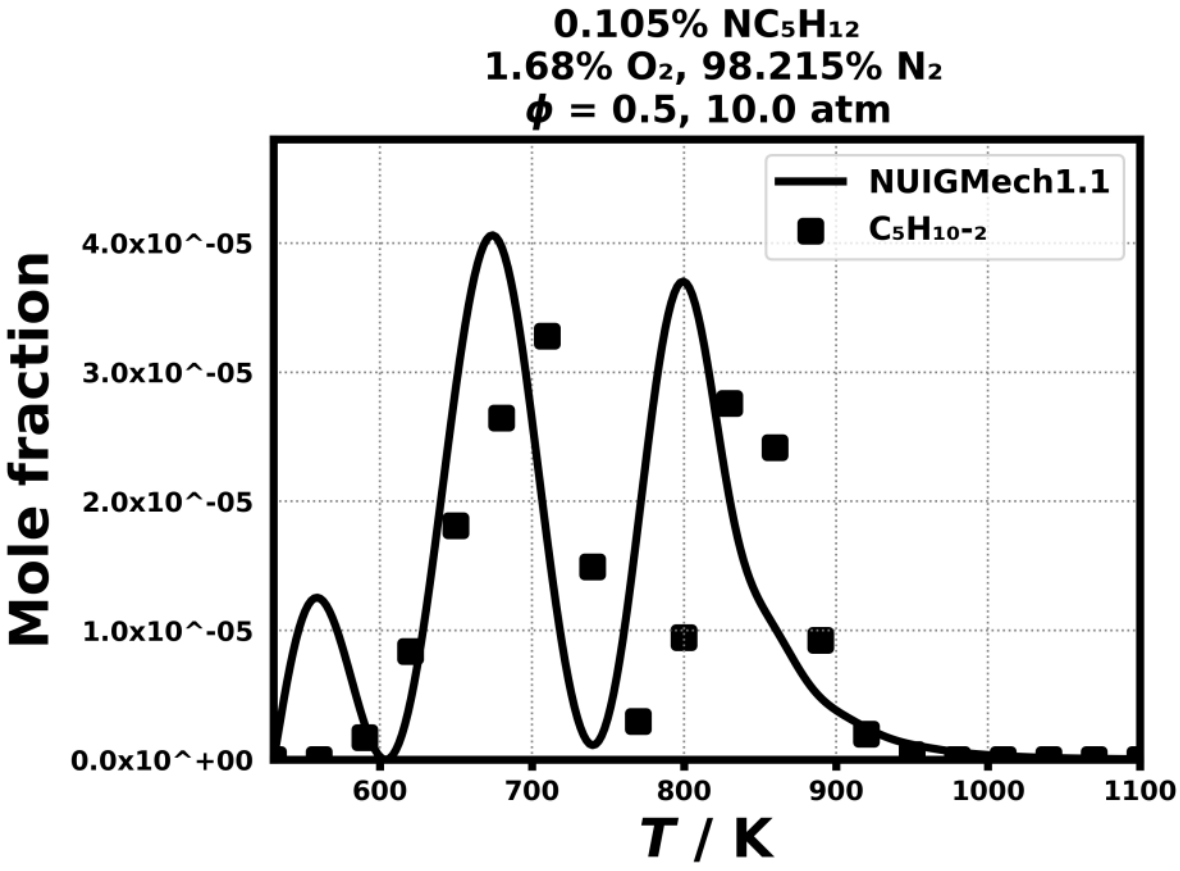

Figure 202: Dataset: 10_ATM_PHI_0.5

1.3.173 Case: n-C5H12/JSR/BUGLER/10_ATM_PHI_0.5

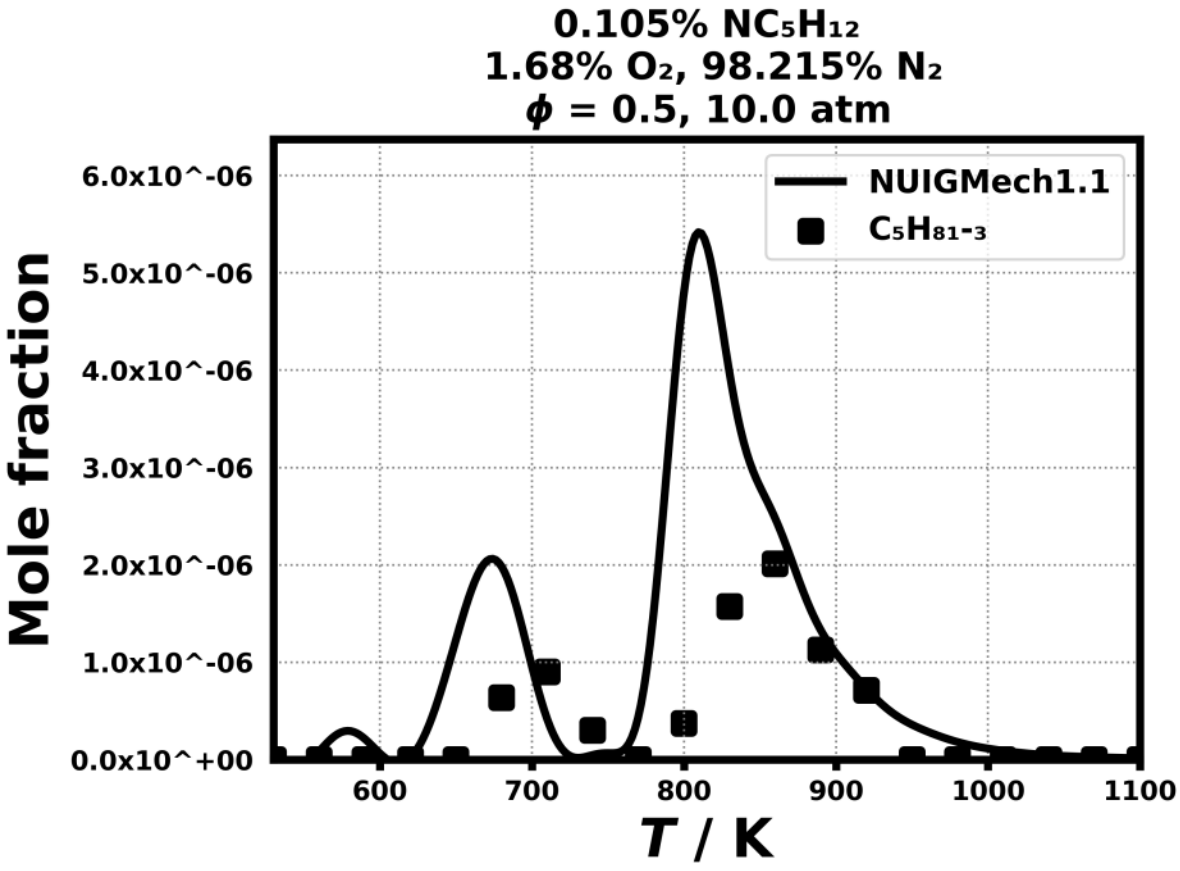

Figure 203: Dataset: 10_ATM_PHI_0.5

1.3.174 Case: n-C5H12/JSR/BUGLER/10_ATM_PHI_0.5

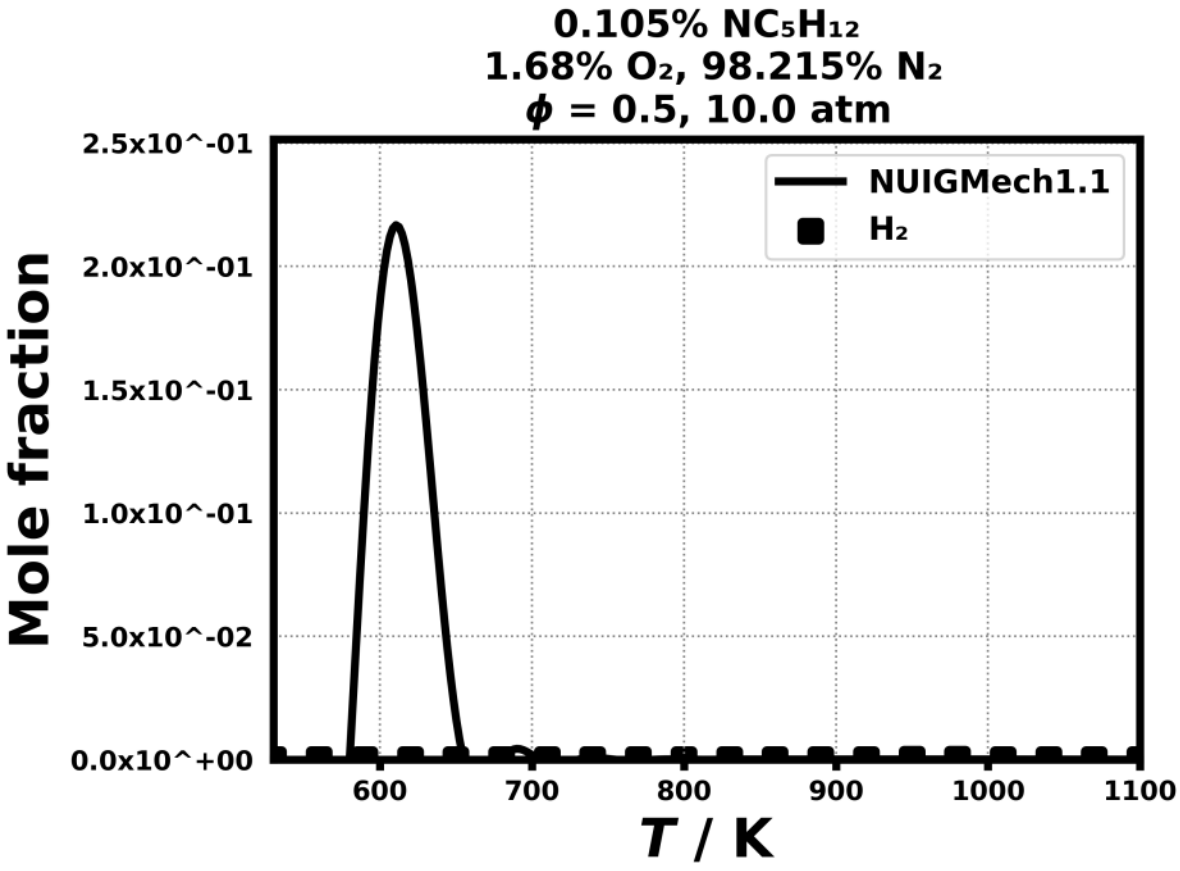

Figure 204: Dataset: 10_ATM_PHI_0.5

1.3.175 Case: n-C5H12/JSR/BUGLER/10_ATM_PHI_0.5

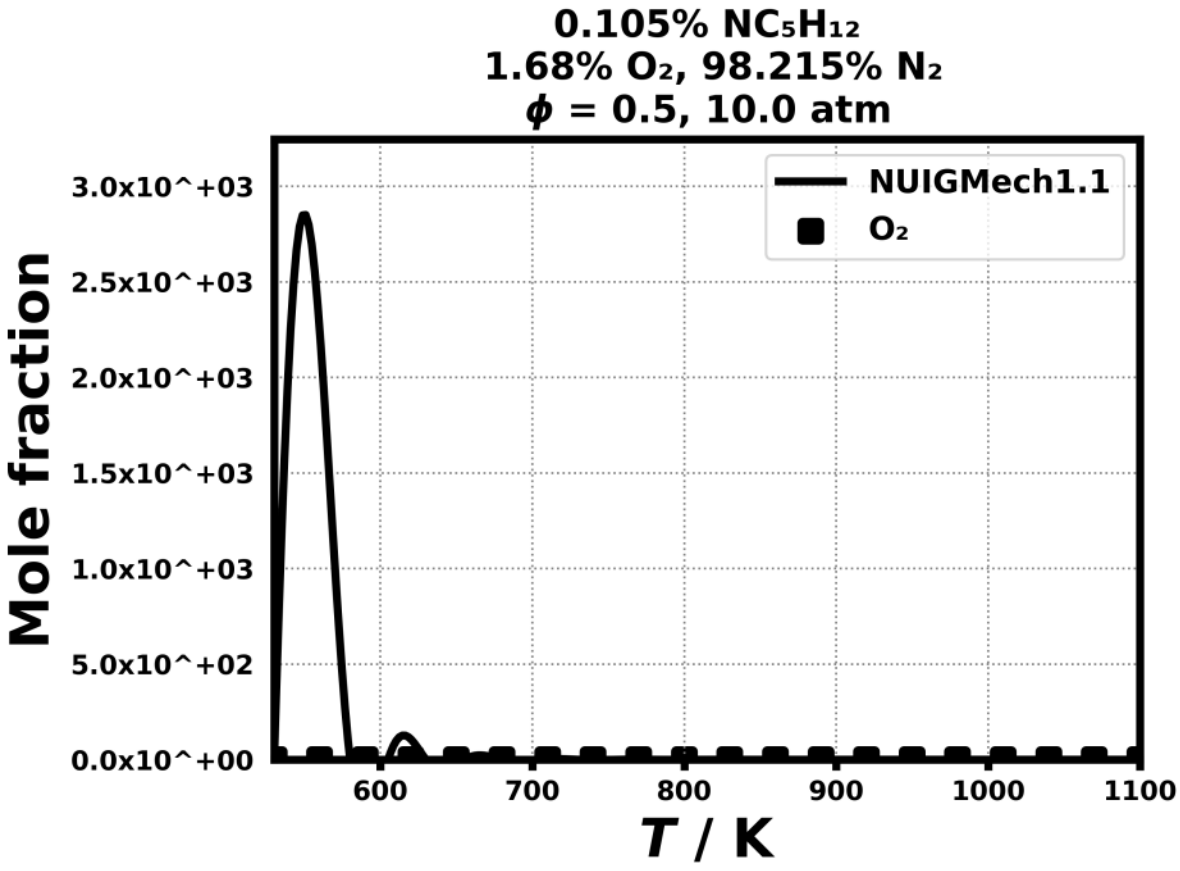

Figure 205: Dataset: 10_ATM_PHI_0.5

1.3.176 Case: n-C5H12/JSR/BUGLER/10_ATM_PHI_0.5

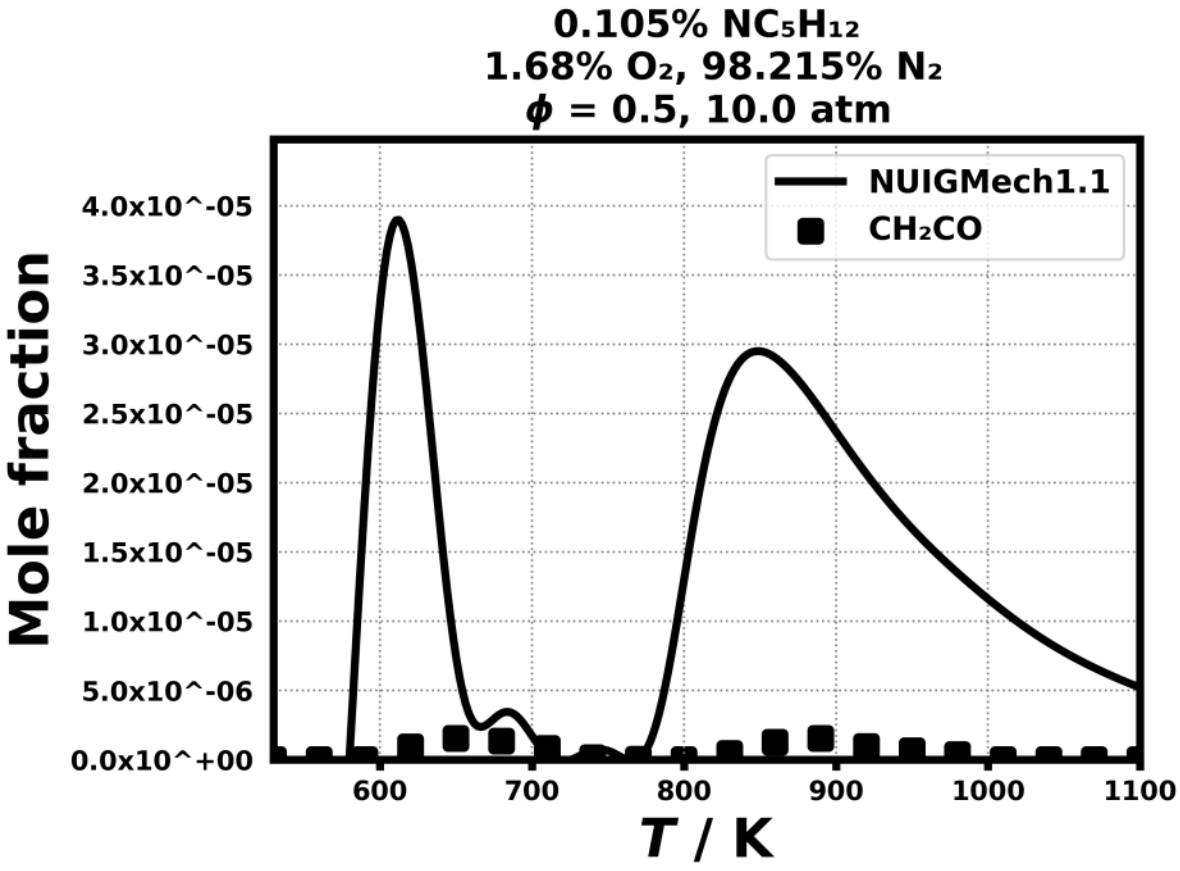

Figure 206: Dataset: 10_ATM_PHI_0.5

1.3.177 Case: n-C5H12/JSR/BUGLER/10_ATM_PHI_0.5

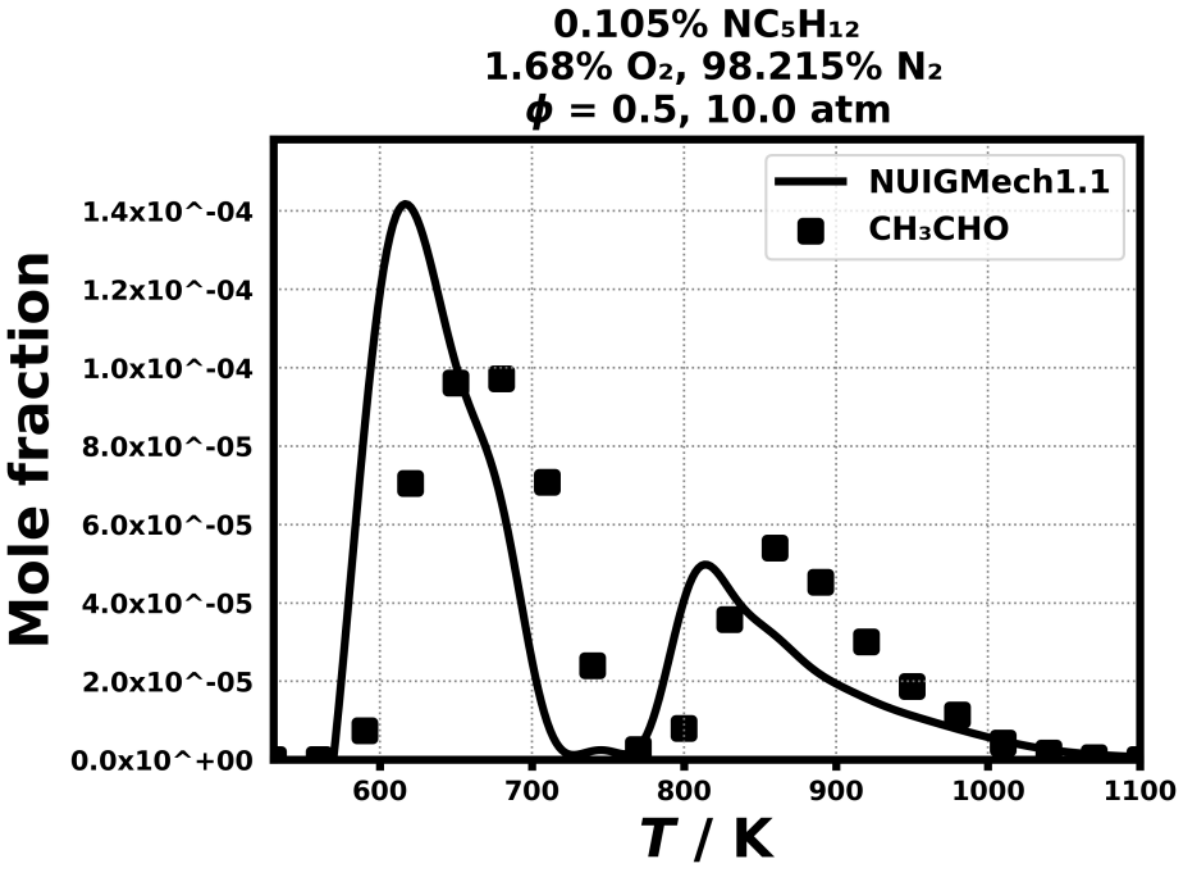

Figure 207: Dataset: 10_ATM_PHI_0.5

1.3.178 Case: n-C5H12/JSR/BUGLER/10_ATM_PHI_0.5

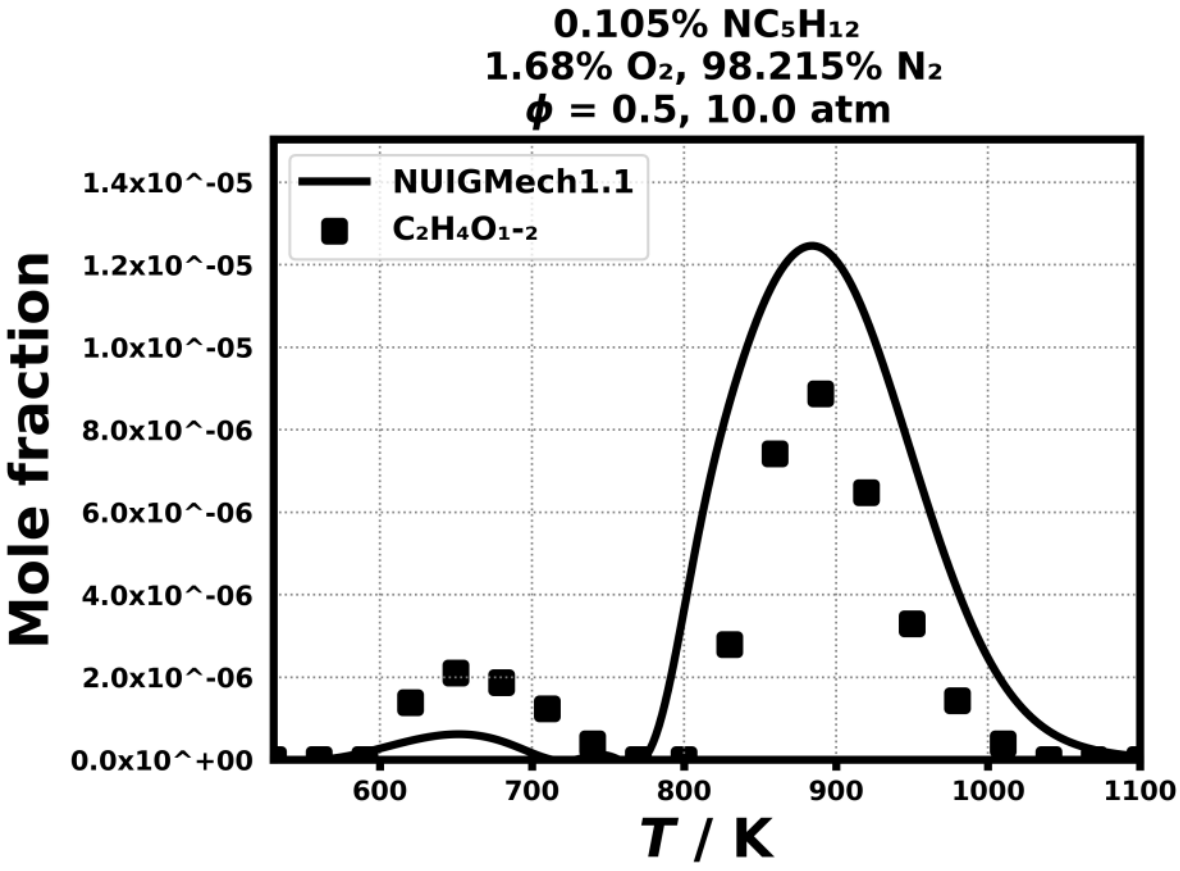

Figure 208: Dataset: 10_ATM_PHI_0.5

1.3.179 Case: n-C5H12/JSR/BUGLER/10_ATM_PHI_0.5

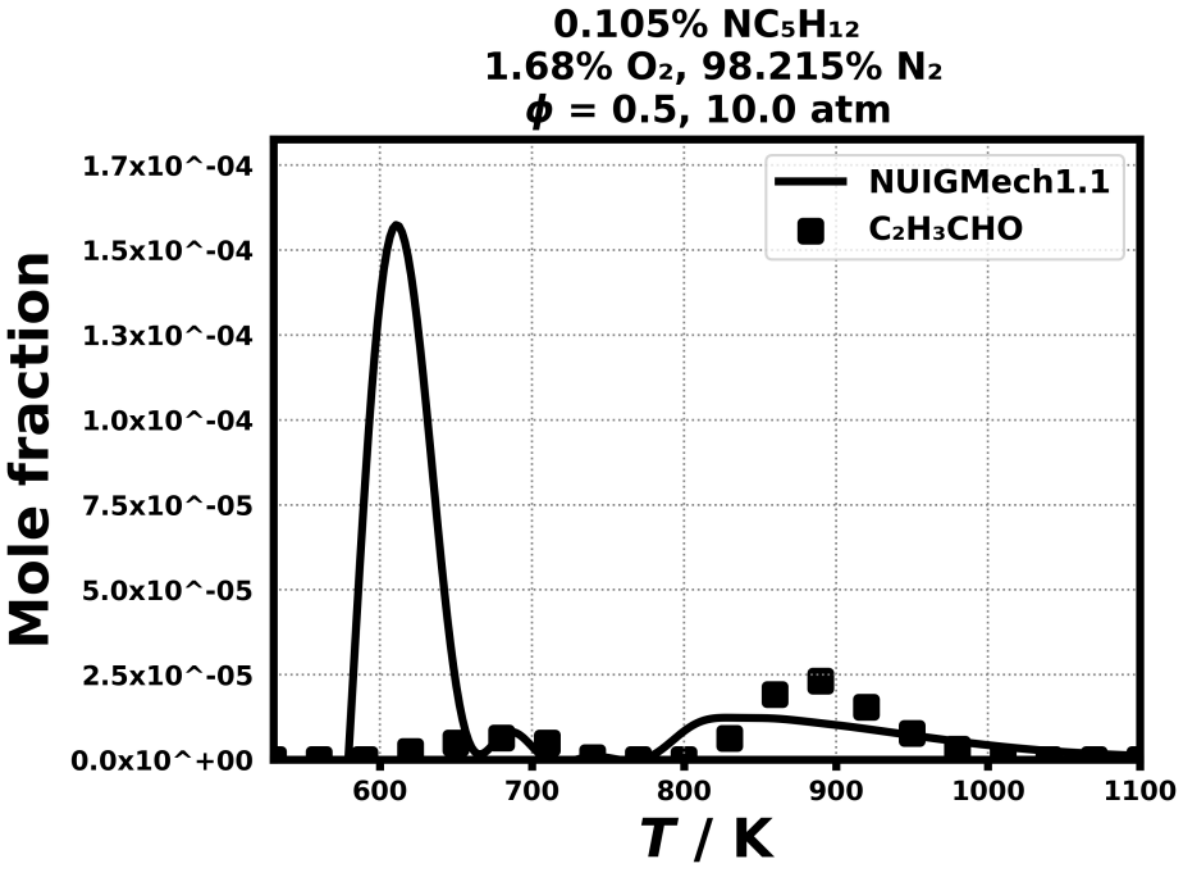

Figure 209: Dataset: 10_ATM_PHI_0.5

1.3.180 Case: n-C5H12/JSR/BUGLER/10_ATM_PHI_0.5

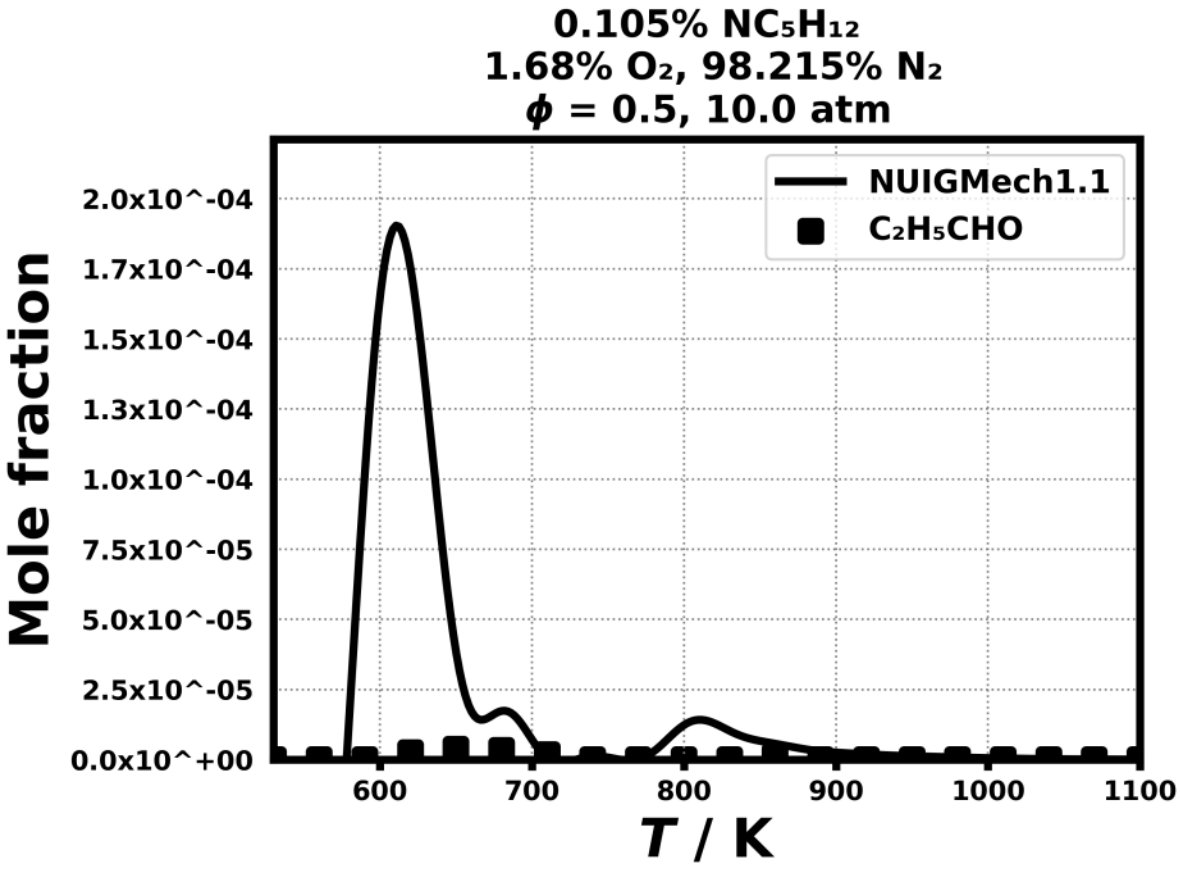

Figure 210: Dataset: 10_ATM_PHI_0.5

1.3.181 Case: n-C5H12/JSR/BUGLER/10_ATM_PHI_0.5

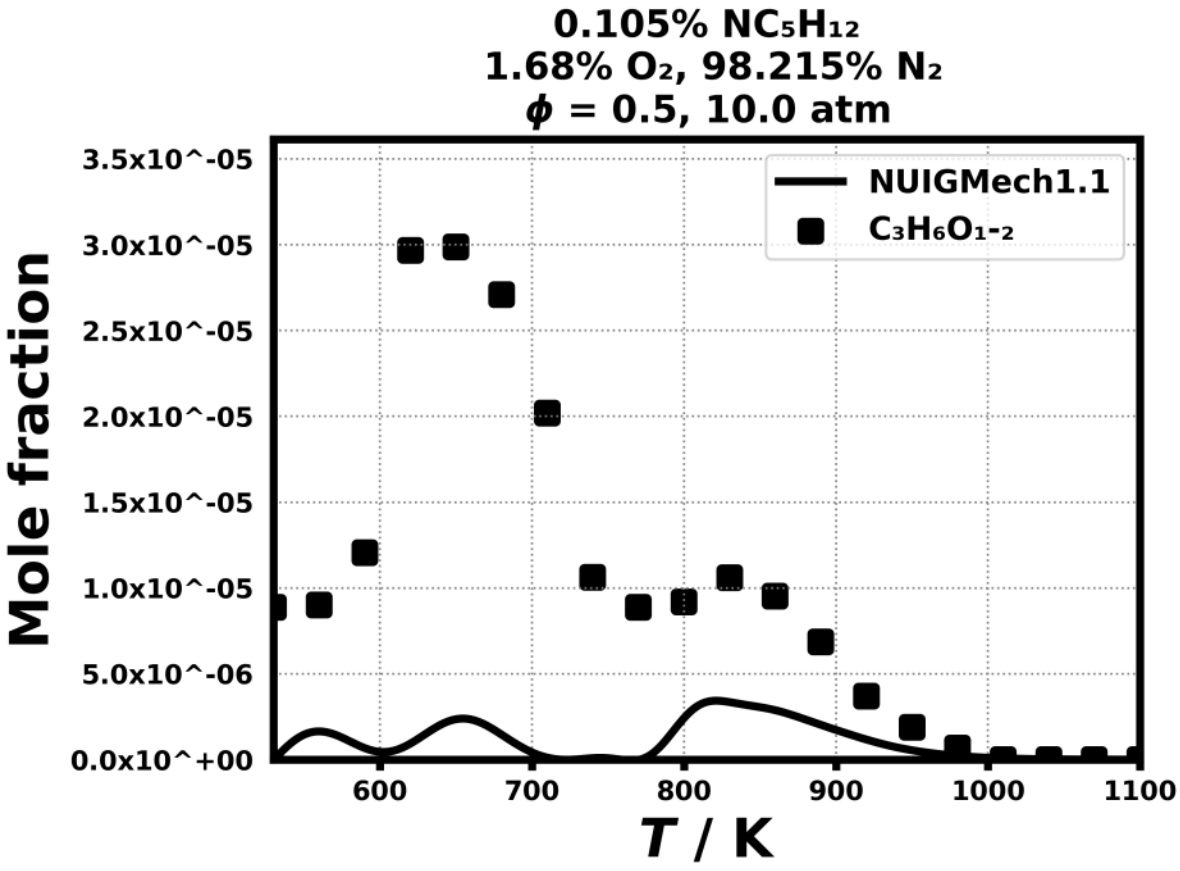

Figure 211: Dataset: 10_ATM_PHI_0.5

1.3.182 Case: n-C5H12/JSR/BUGLER/10_ATM_PHI_0.5

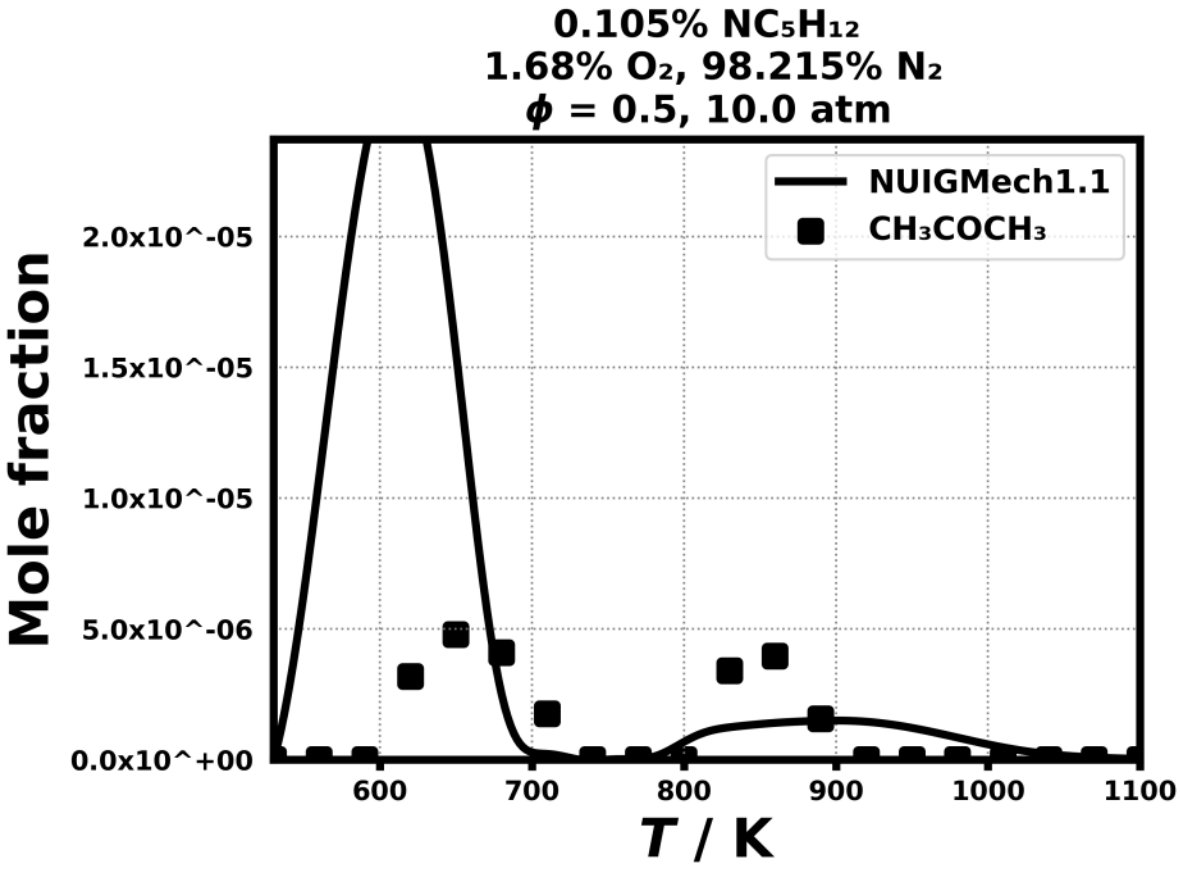

Figure 212: Dataset: 10_ATM_PHI_0.5

1.3.183 Case: n-C5H12/JSR/BUGLER/10_ATM_PHI_0.5

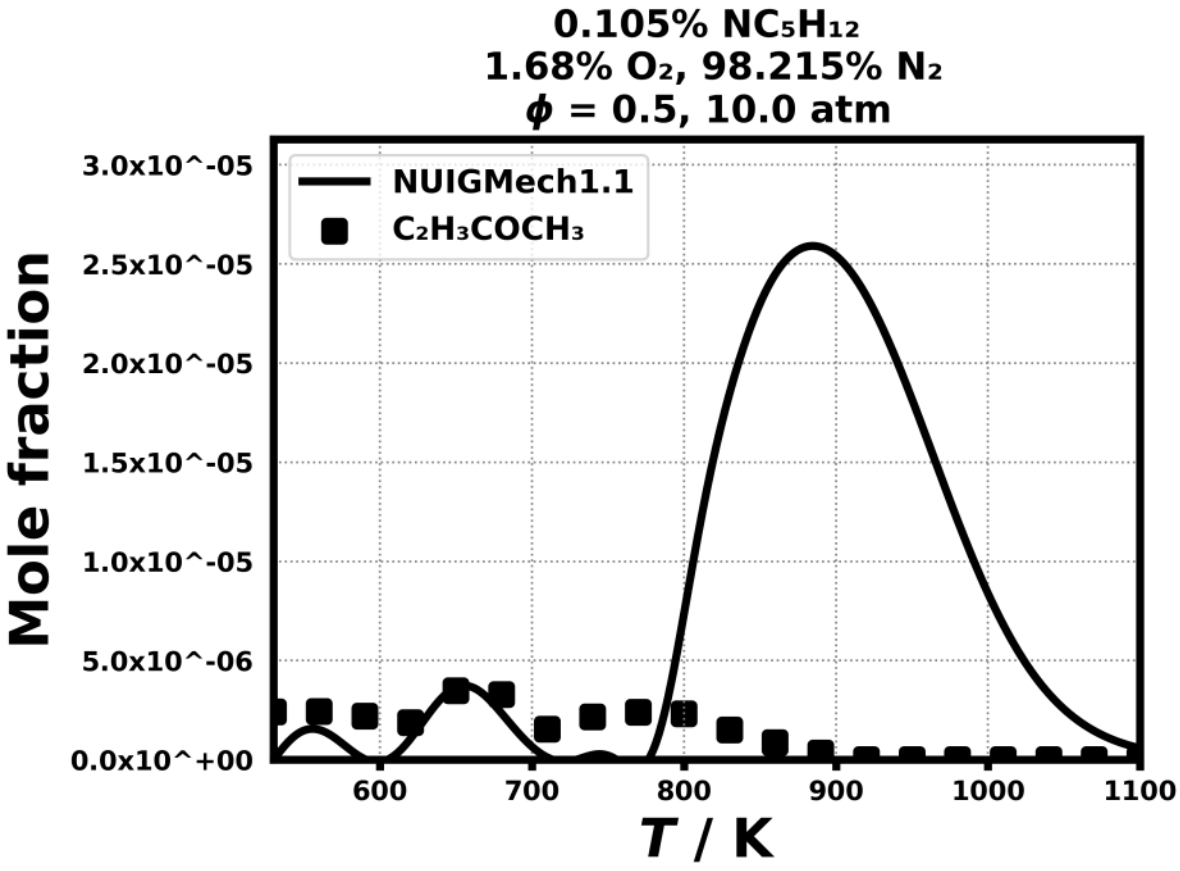

Figure 213: Dataset: 10_ATM_PHI_0.5

1.3.184 Case: n-C5H12/JSR/BUGLER/10_ATM_PHI_0.5

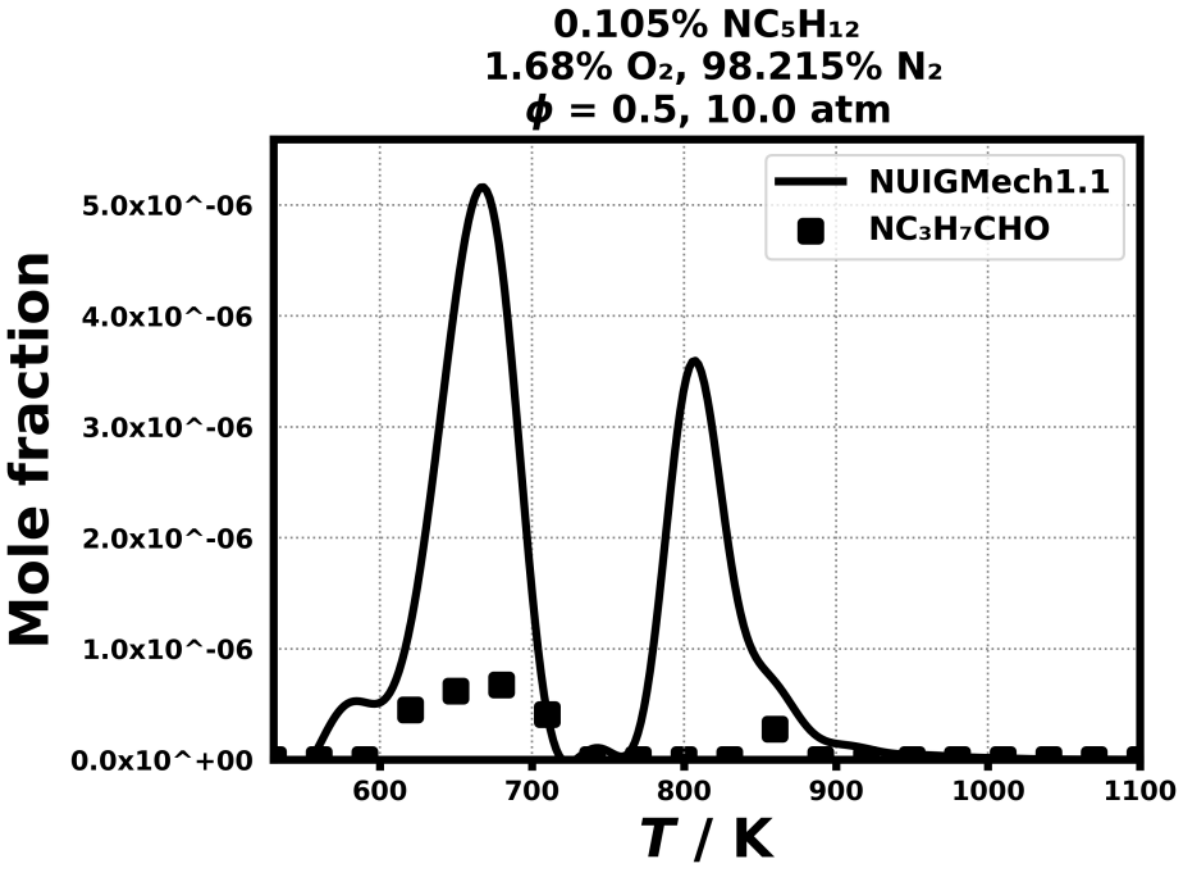

Figure 214: Dataset: 10_ATM_PHI_0.5

1.3.185 Case: n-C5H12/JSR/BUGLER/10_ATM_PHI_0.5

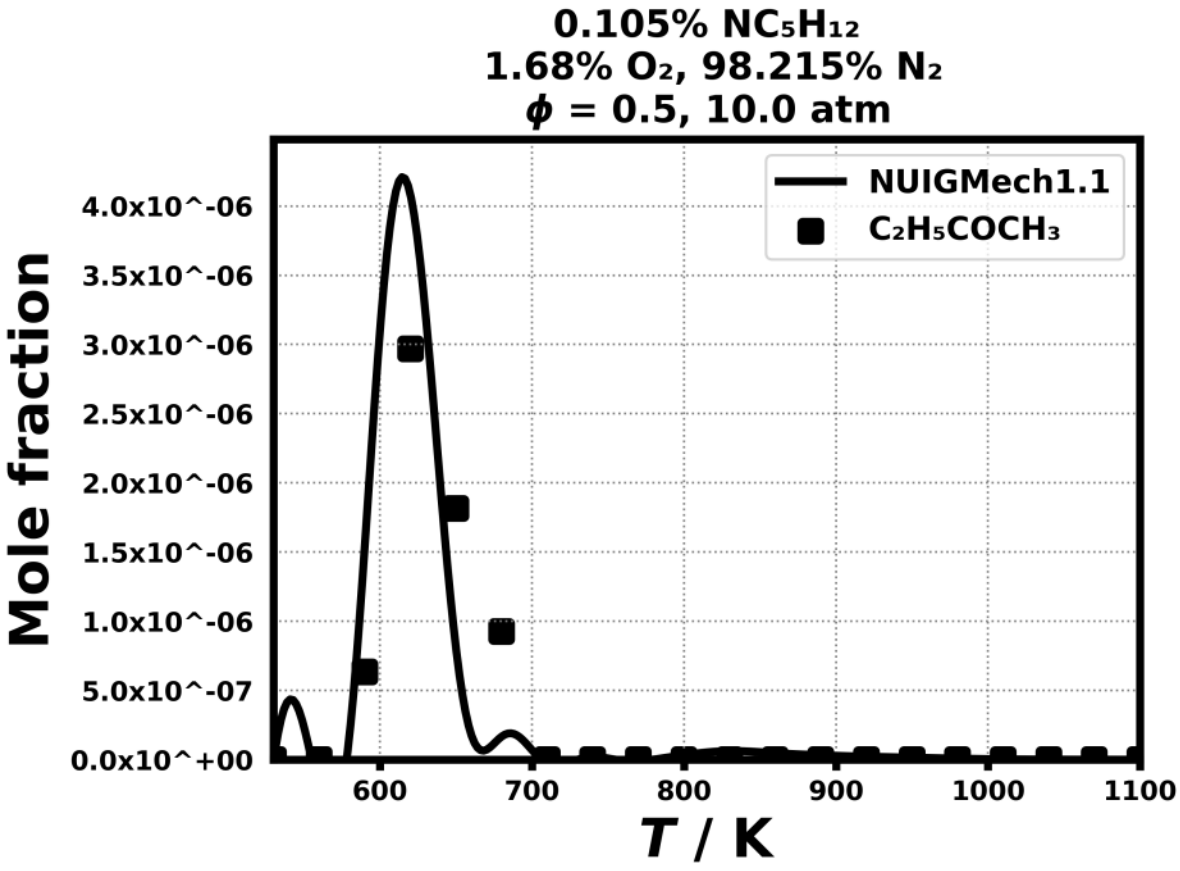

Figure 215: Dataset: 10_ATM_PHI_0.5

1.3.186 Case: n-C5H12/JSR/BUGLER/10_ATM_PHI_0.5

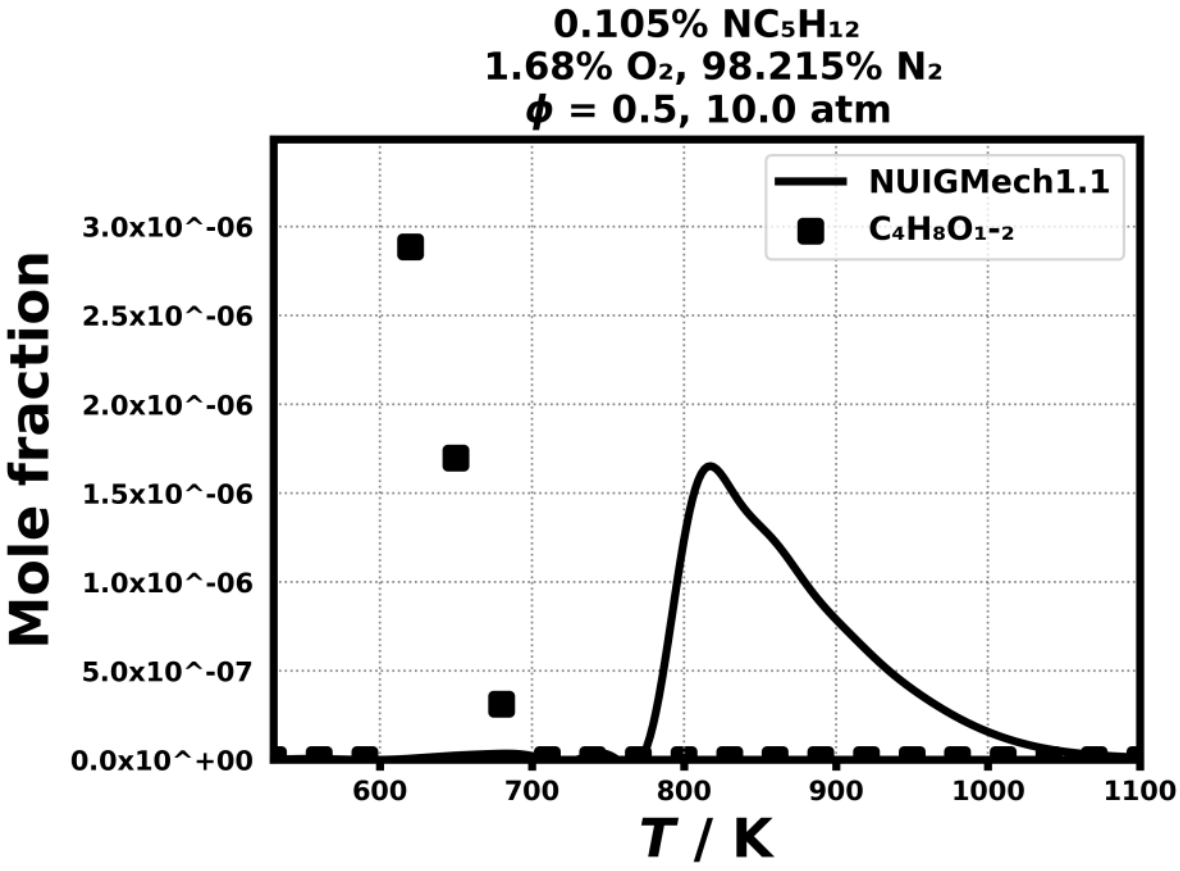

Figure 216: Dataset: 10_ATM_PHI_0.5

1.3.187 Case: n-C5H12/JSR/BUGLER/10_ATM_PHI_0.5

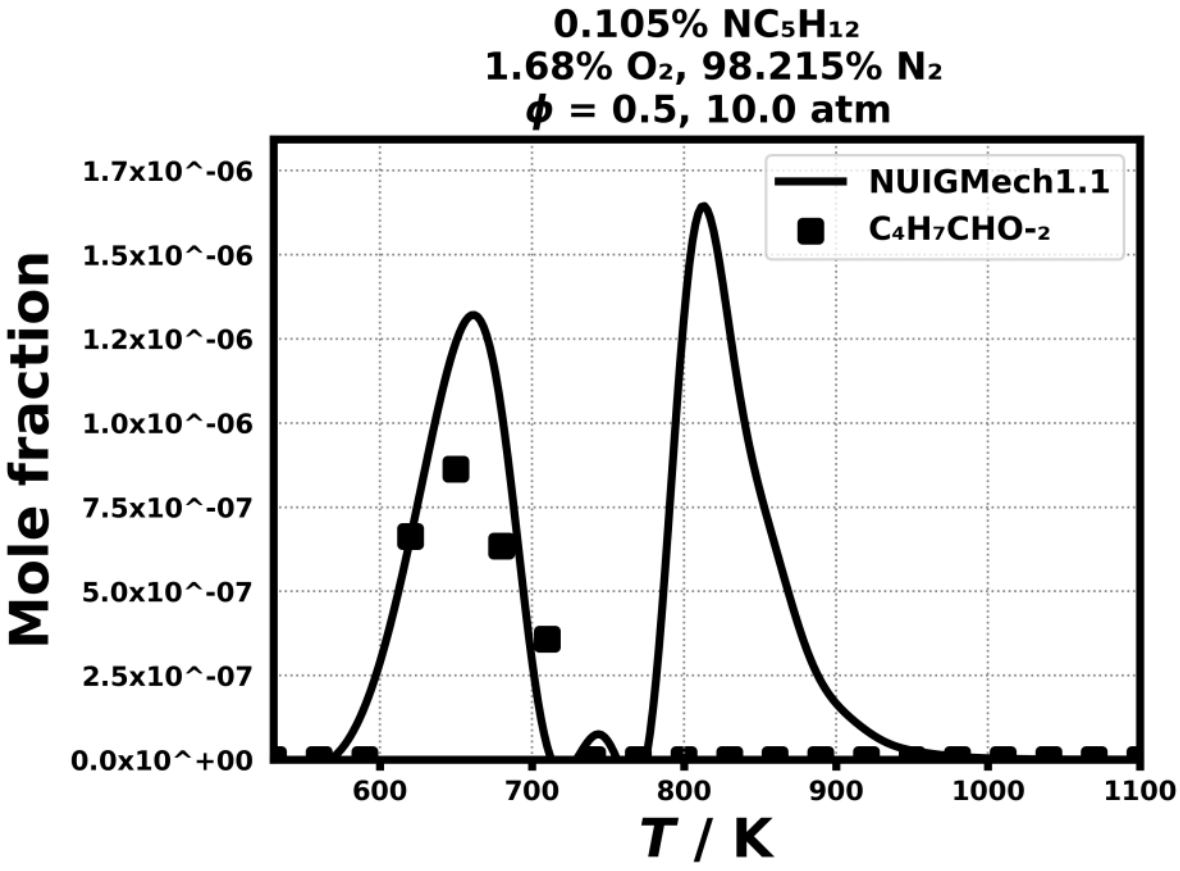

Figure 217: Dataset: 10_ATM_PHI_0.5

1.3.188 Case: n-C5H12/JSR/BUGLER/10_ATM_PHI_0.5

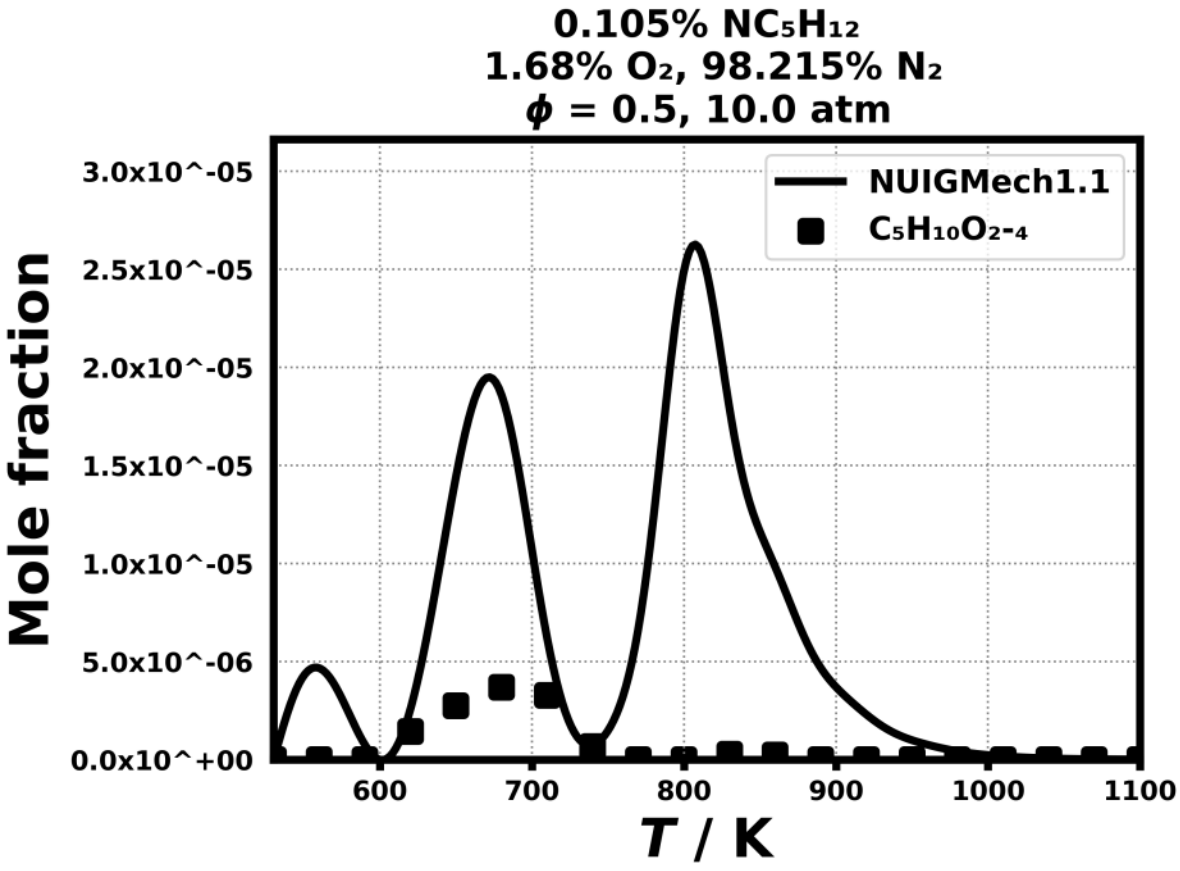

Figure 218: Dataset: 10_ATM_PHI_0.5

1.3.189 Case: n-C5H12/JSR/BUGLER/10_ATM_PHI_0.5

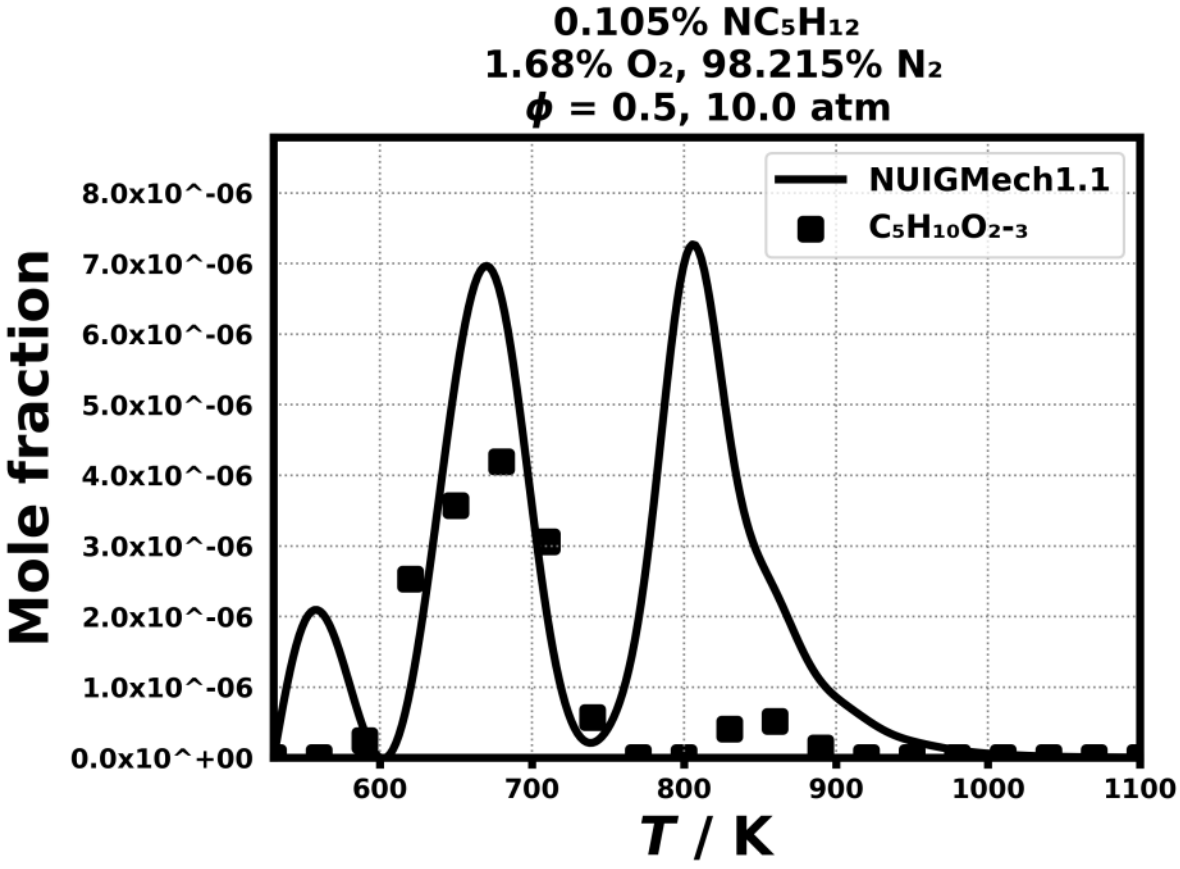

Figure 219: Dataset: 10_ATM_PHI_0.5

1.3.190 Case: n-C5H12/JSR/BUGLER/10_ATM_PHI_0.5

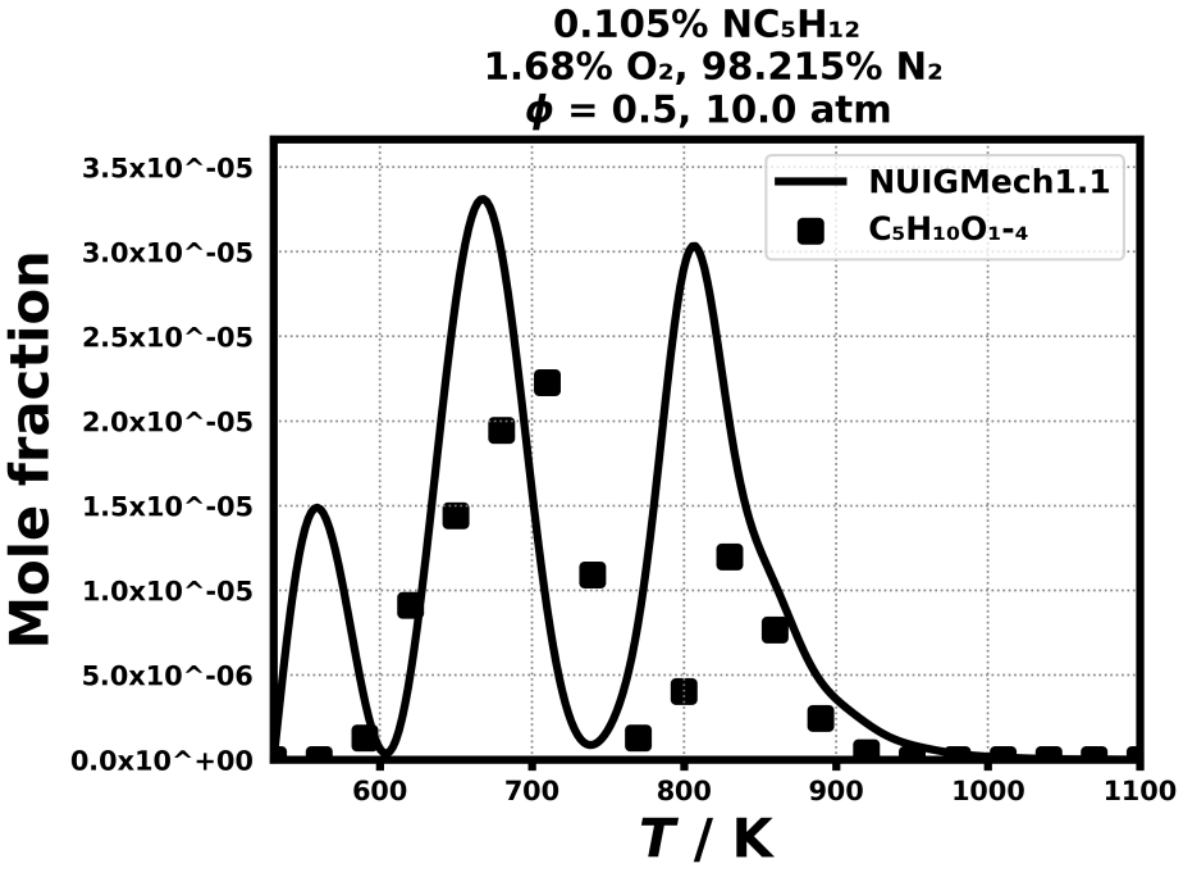

Figure 220: Dataset: 10_ATM_PHI_0.5

1.3.191 Case: n-C5H12/JSR/BUGLER/10_ATM_PHI_0.5

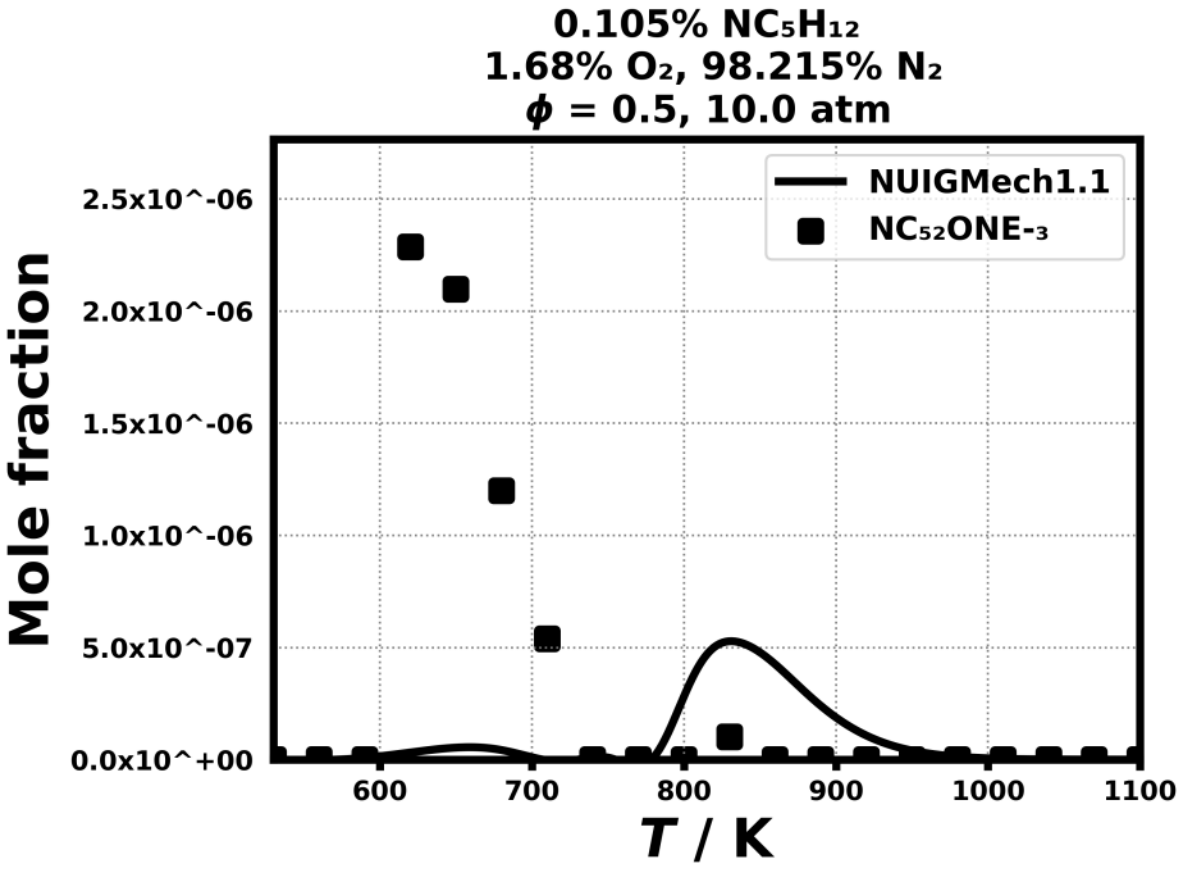

Figure 221: Dataset: 10_ATM_PHI_0.5

1.3.192 Case: n-C5H12/JSR/BUGLER/10_ATM_PHI_0.5

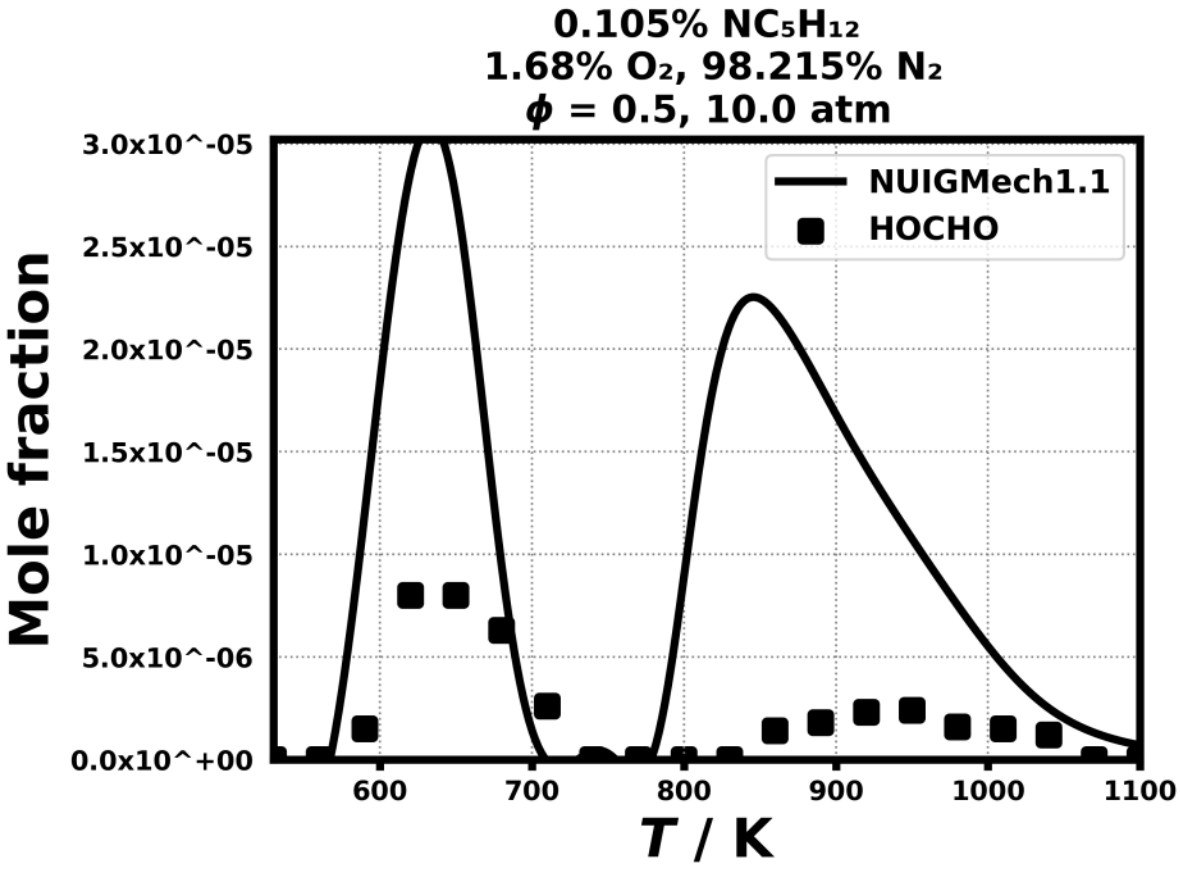

Figure 222: Dataset: 10_ATM_PHI_0.5

1.3.193 Case: n-C5H12/JSR/BUGLER/10_ATM_PHI_0.5

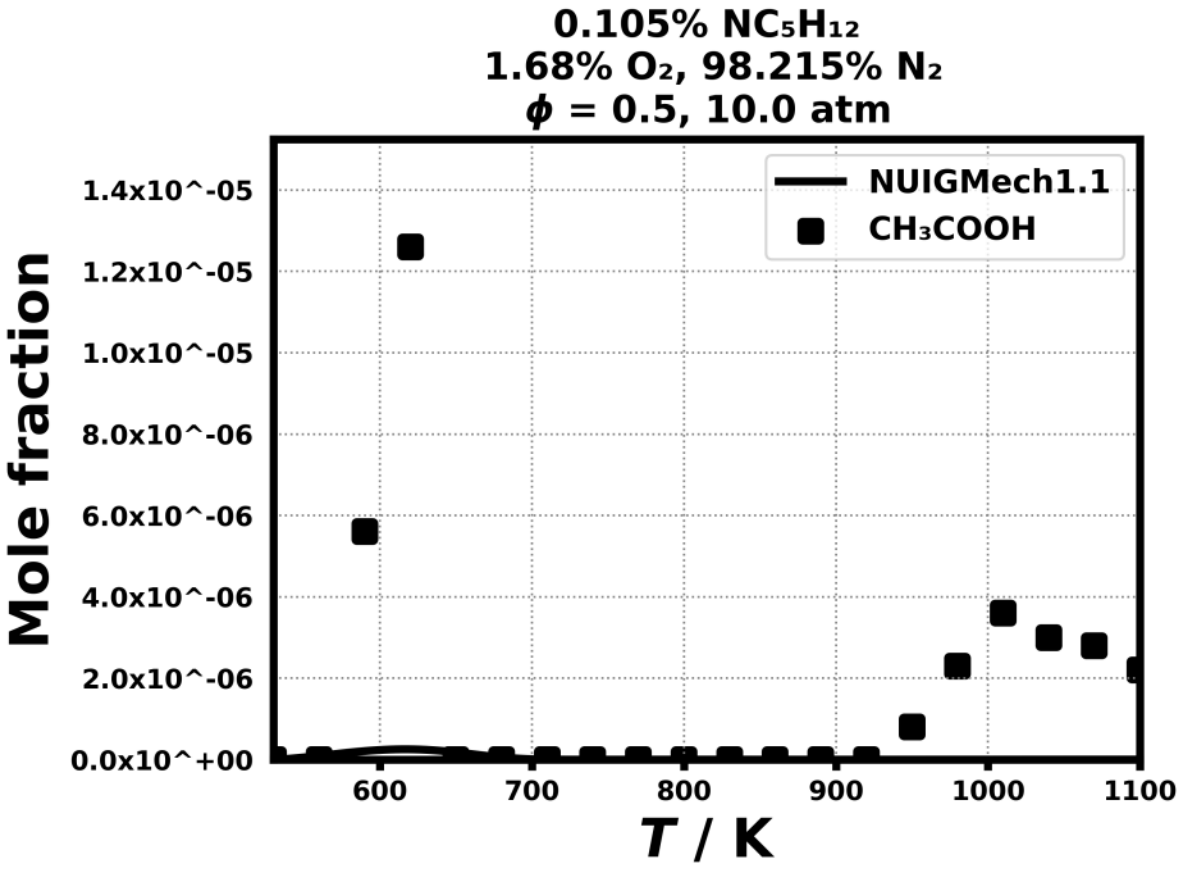

Figure 223: Dataset: 10_ATM_PHI_0.5

1.3.194 Case: n-C5H12/JSR/BUGLER/10_ATM_PHI_1.0

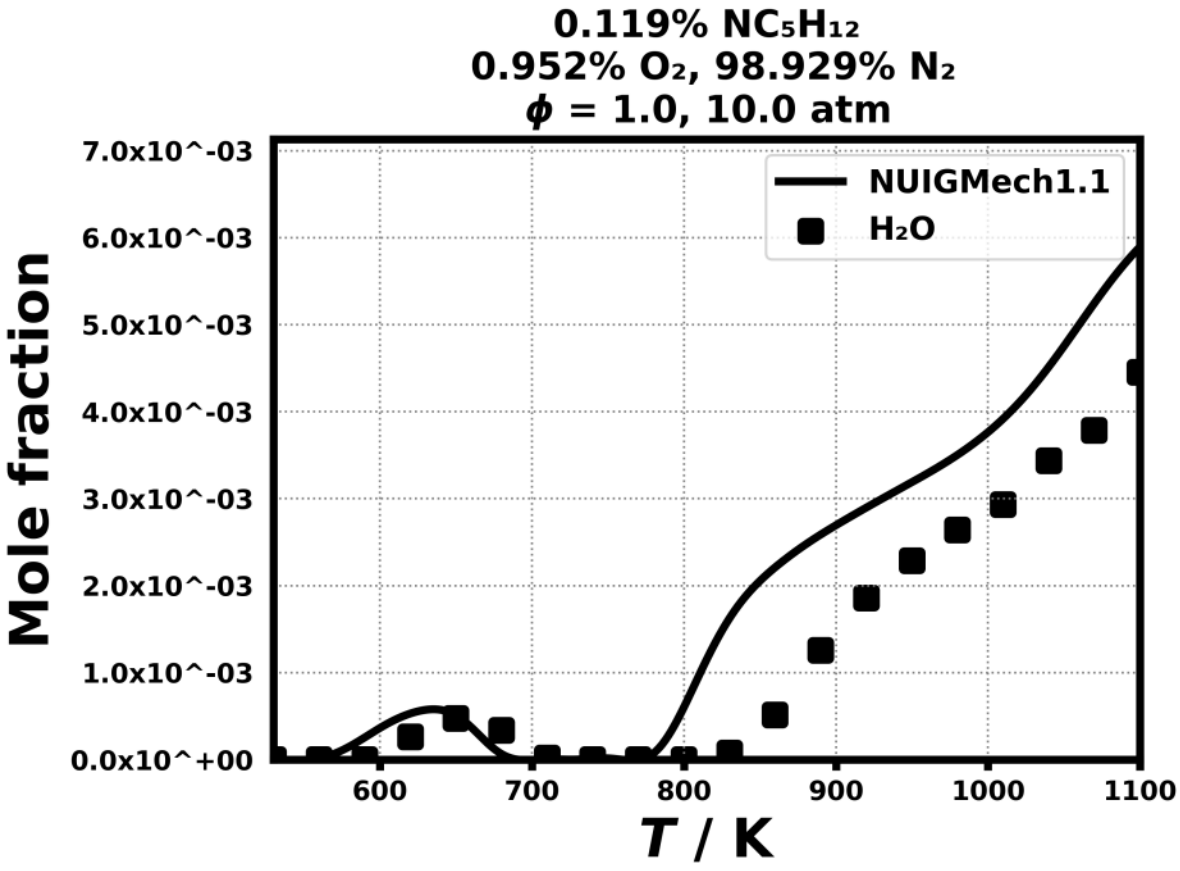

Figure 224: Dataset: 10_ATM_PHI_1.0

1.3.195 Case: n-C5H12/JSR/BUGLER/10_ATM_PHI_1.0

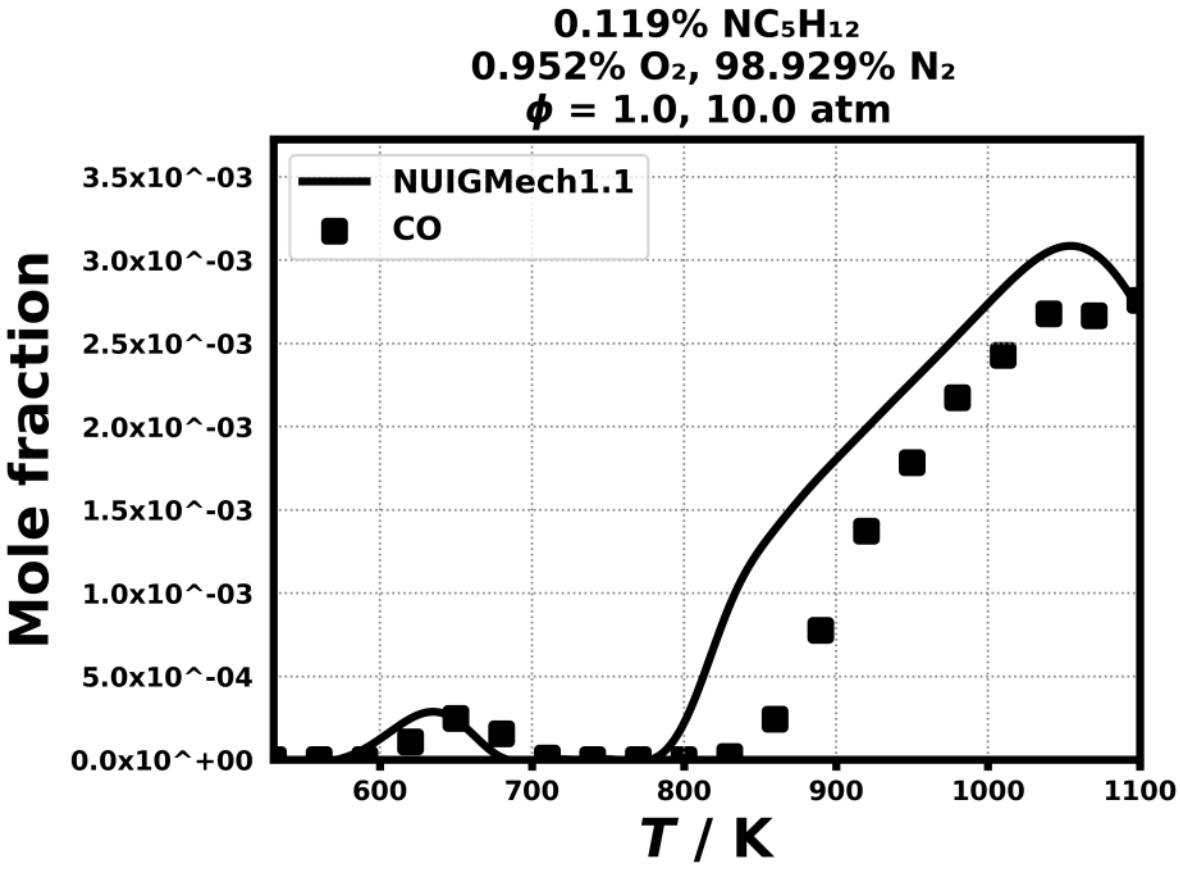

Figure 225: Dataset: 10_ATM_PHI_1.0

1.3.196 Case: n-C5H12/JSR/BUGLER/10_ATM_PHI_1.0

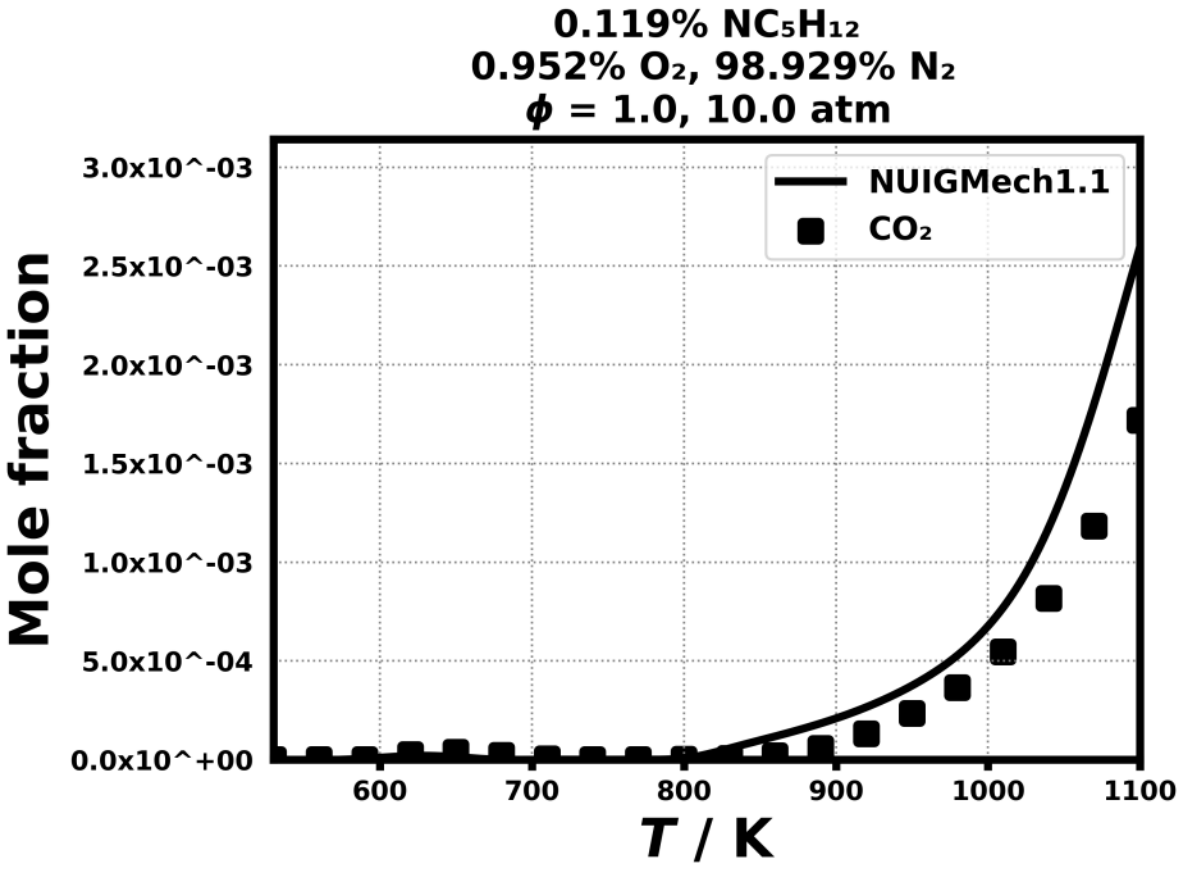

Figure 226: Dataset: 10_ATM_PHI_1.0

1.3.197 Case: n-C5H12/JSR/BUGLER/10_ATM_PHI_1.0

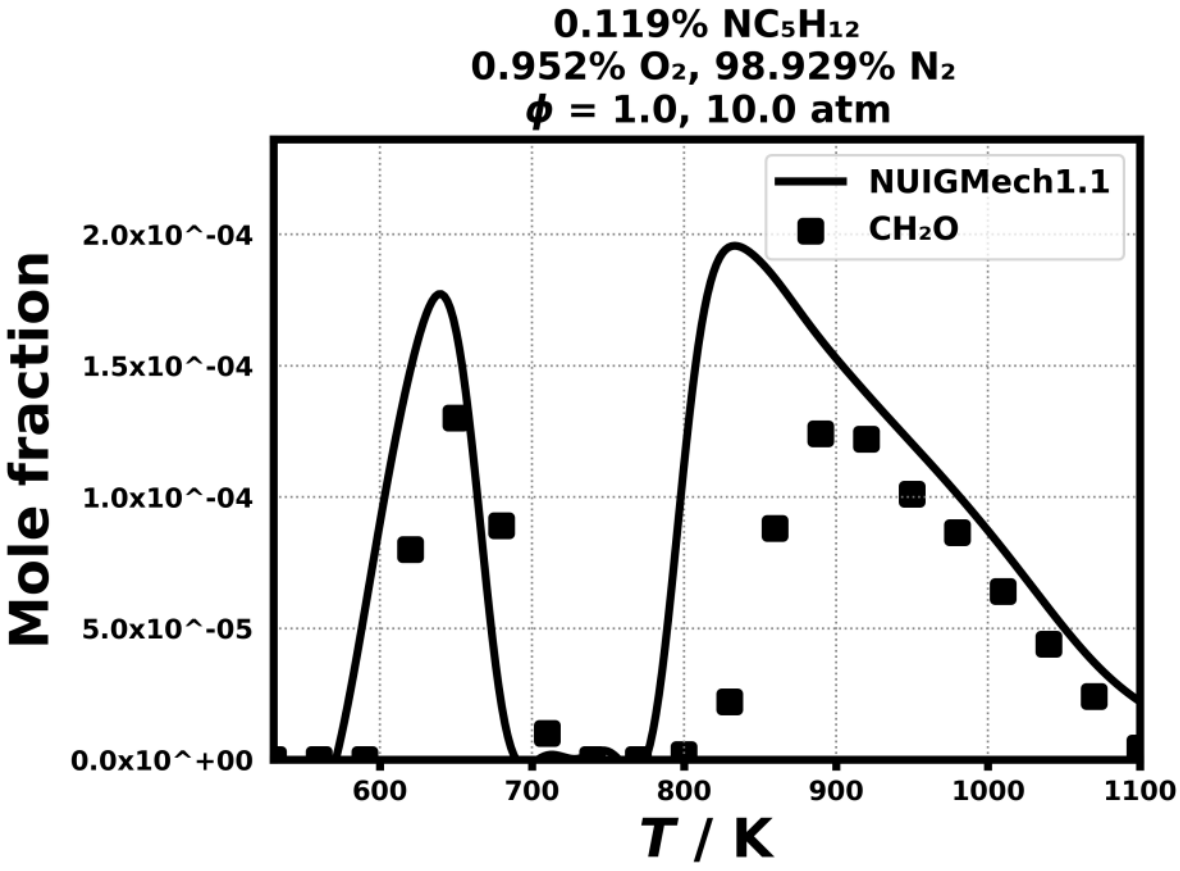

Figure 227: Dataset: 10_ATM_PHI_1.0

1.3.198 Case: n-C5H12/JSR/BUGLER/10_ATM_PHI_1.0

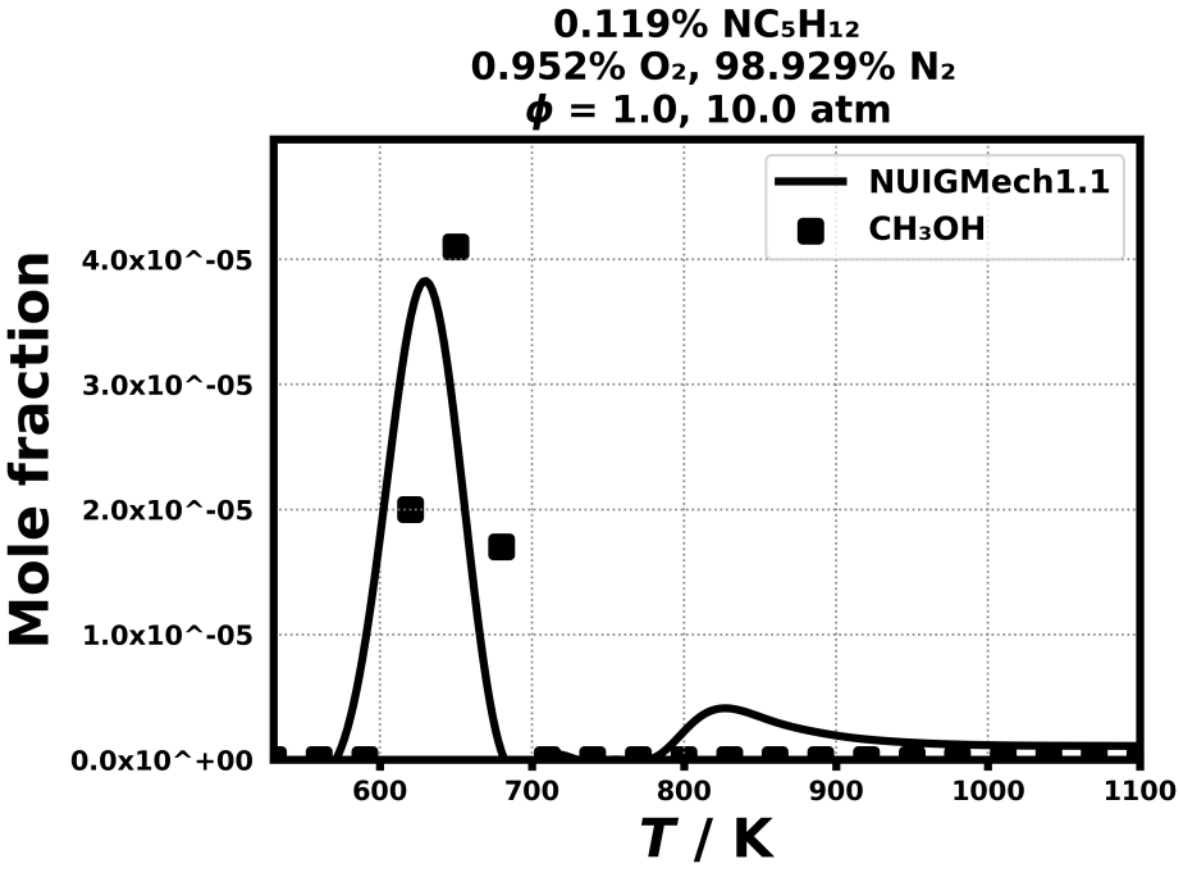

Figure 228: Dataset: 10_ATM_PHI_1.0

1.3.199 Case: n-C5H12/JSR/BUGLER/10_ATM_PHI_1.0

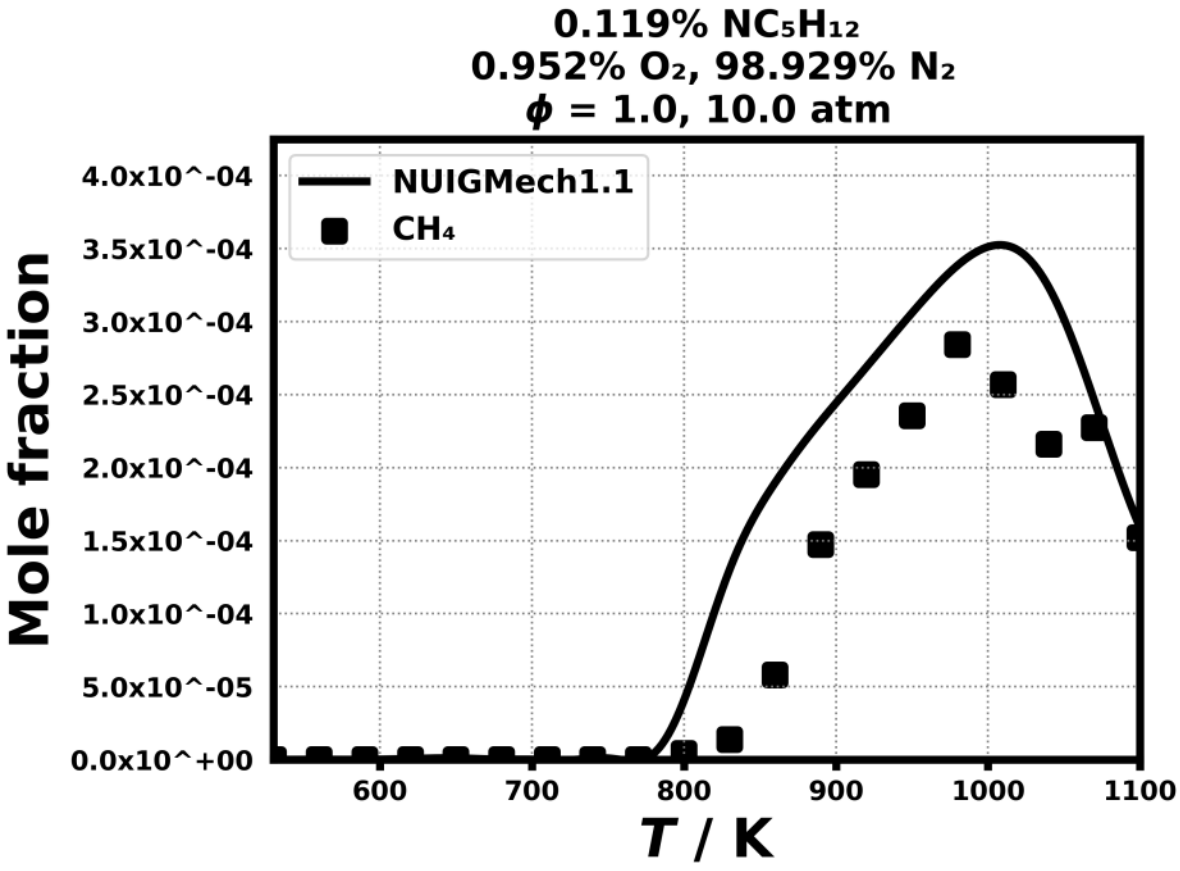

Figure 229: Dataset: 10_ATM_PHI_1.0

1.3.200 Case: n-C5H12/JSR/BUGLER/10_ATM_PHI_1.0

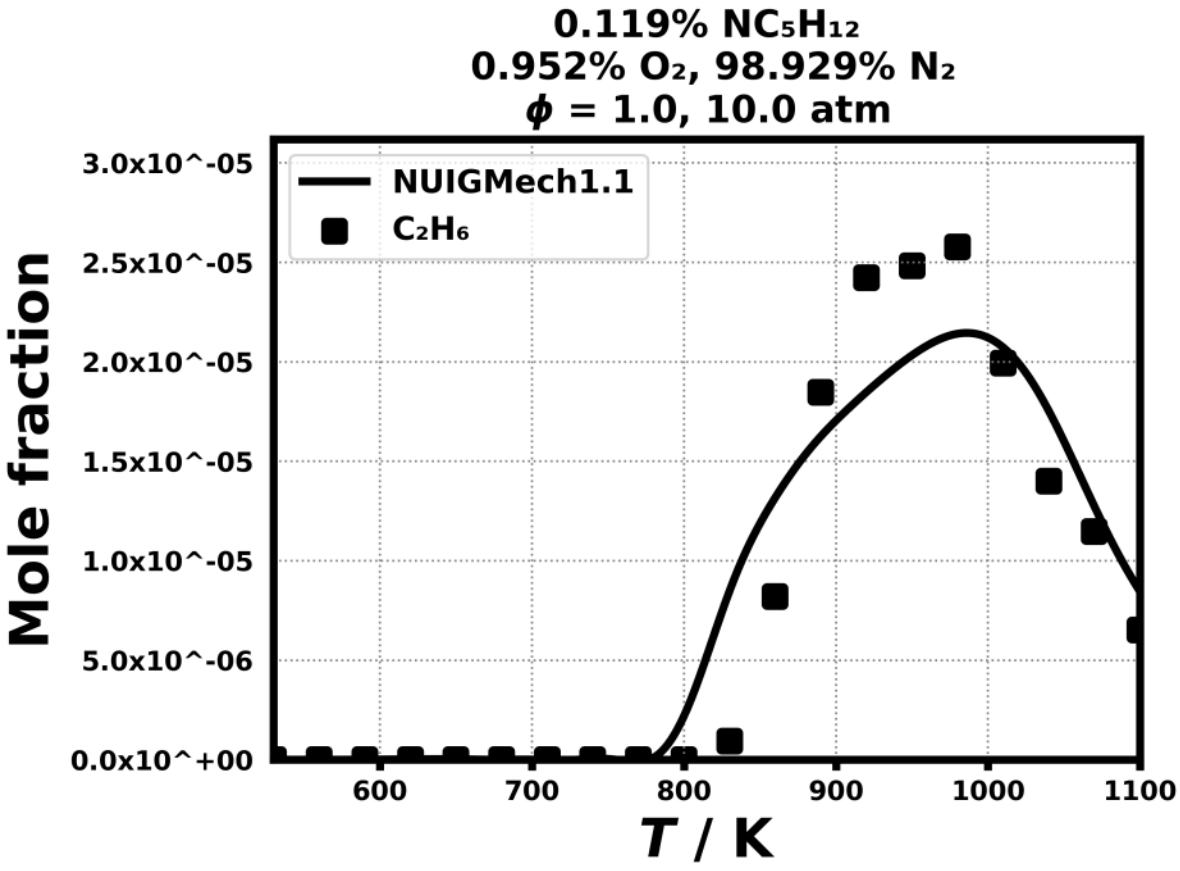

Figure 230: Dataset: 10_ATM_PHI_1.0

1.3.201 Case: n-C5H12/JSR/BUGLER/10_ATM_PHI_1.0

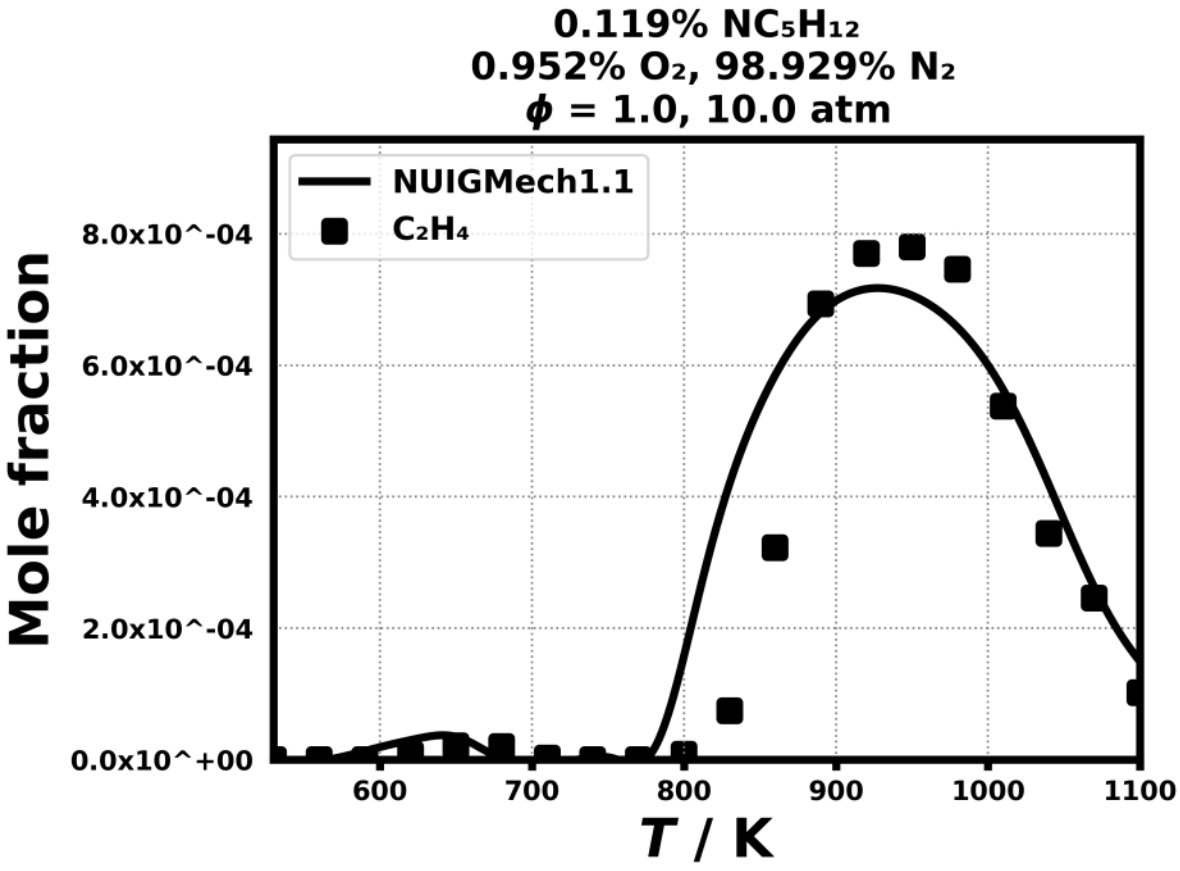

Figure 231: Dataset: 10_ATM_PHI_1.0

1.3.202 Case: n-C5H12/JSR/BUGLER/10_ATM_PHI_1.0

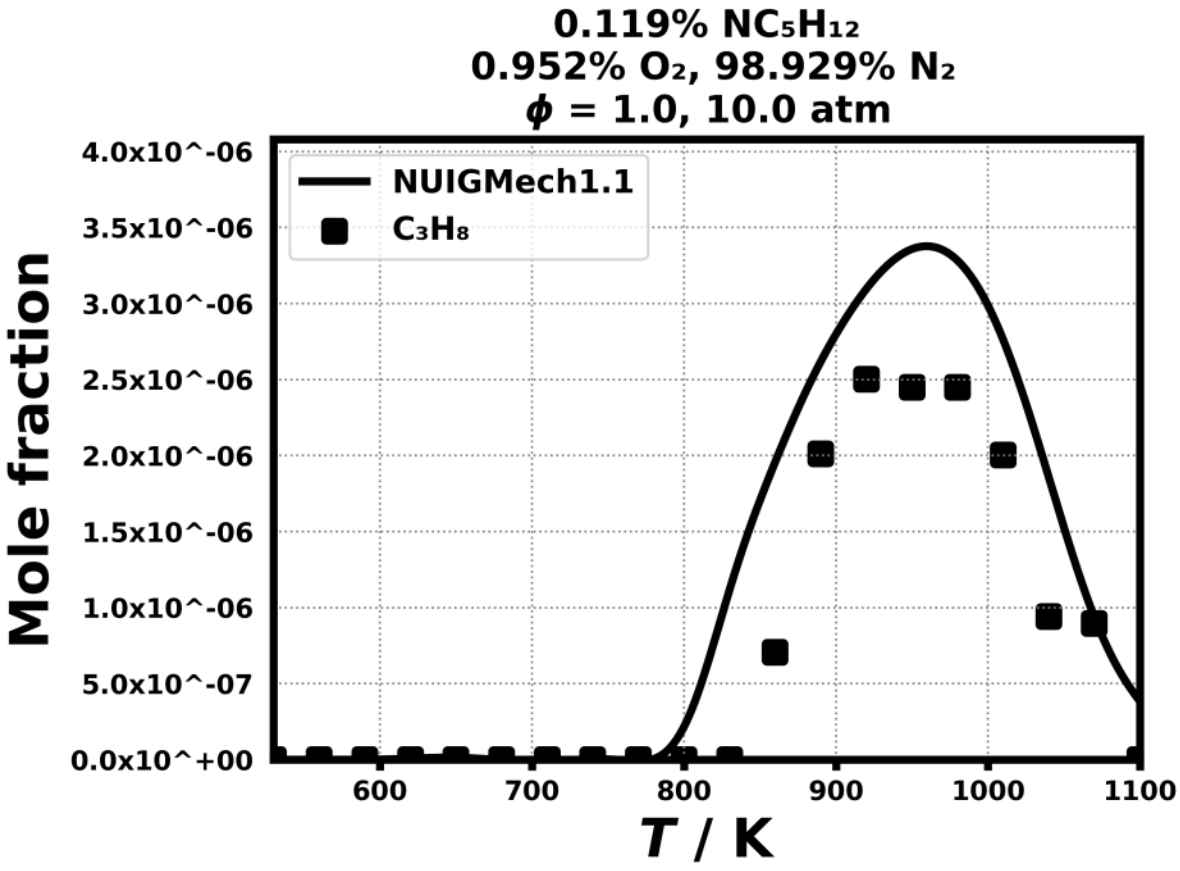

Figure 232: Dataset: 10_ATM_PHI_1.0

1.3.203 Case: n-C5H12/JSR/BUGLER/10_ATM_PHI_1.0

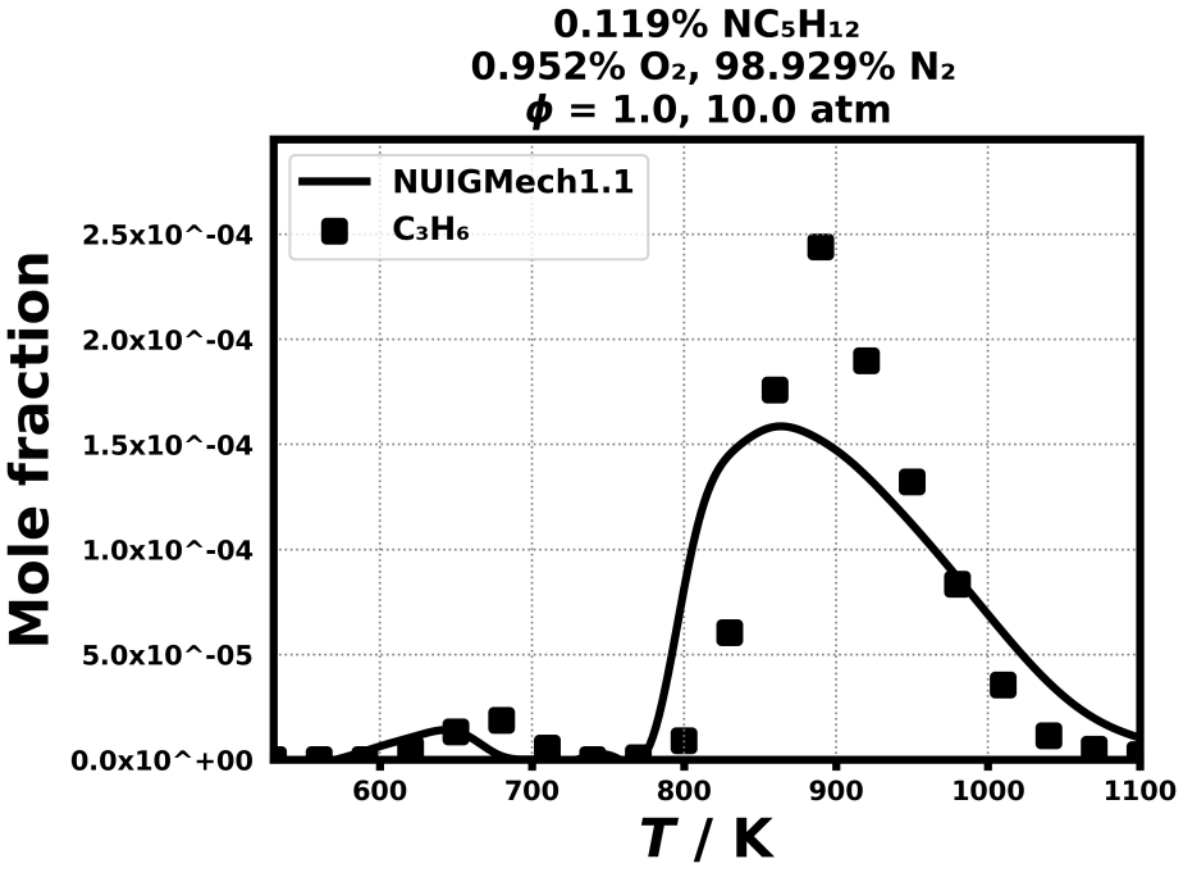

Figure 233: Dataset: 10_ATM_PHI_1.0

1.3.204 Case: n-C5H12/JSR/BUGLER/10_ATM_PHI_1.0

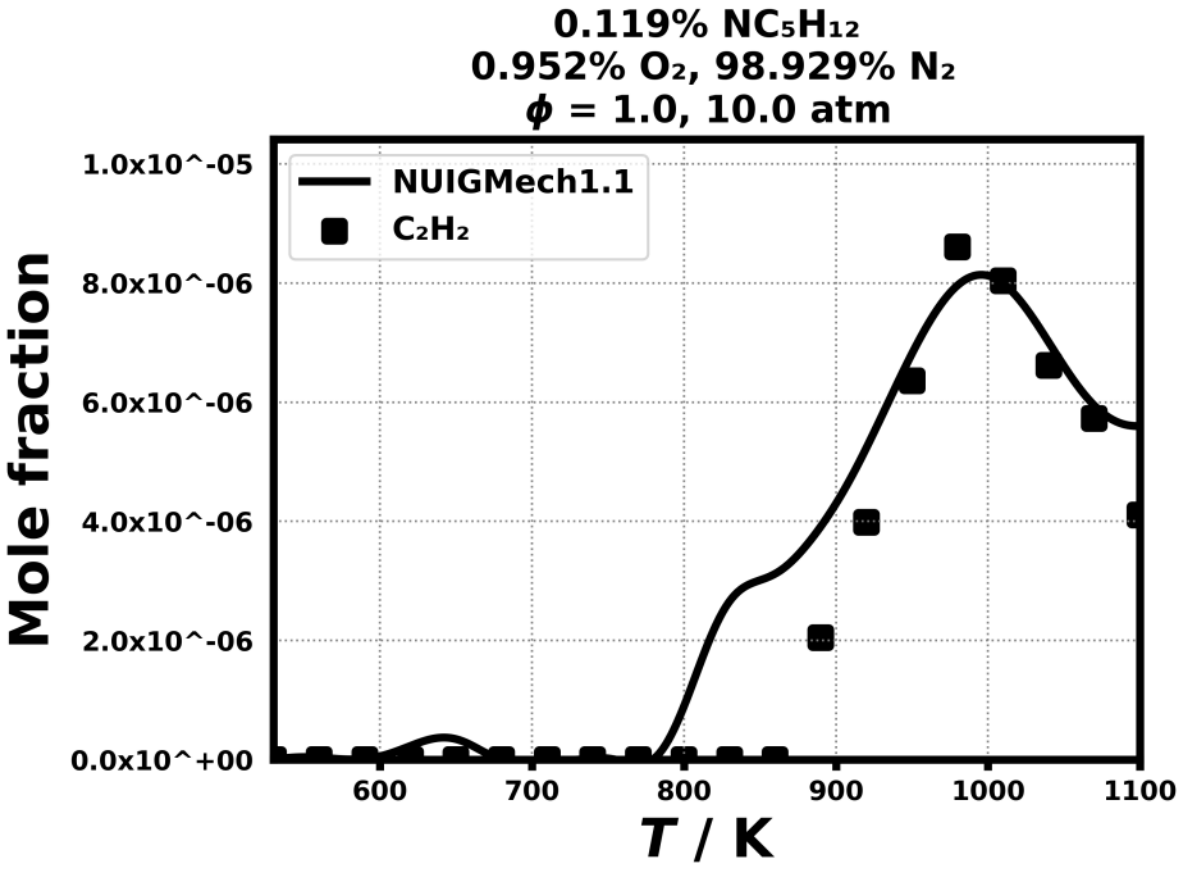

Figure 234: Dataset: 10_ATM_PHI_1.0

1.3.205 Case: n-C5H12/JSR/BUGLER/10_ATM_PHI_1.0

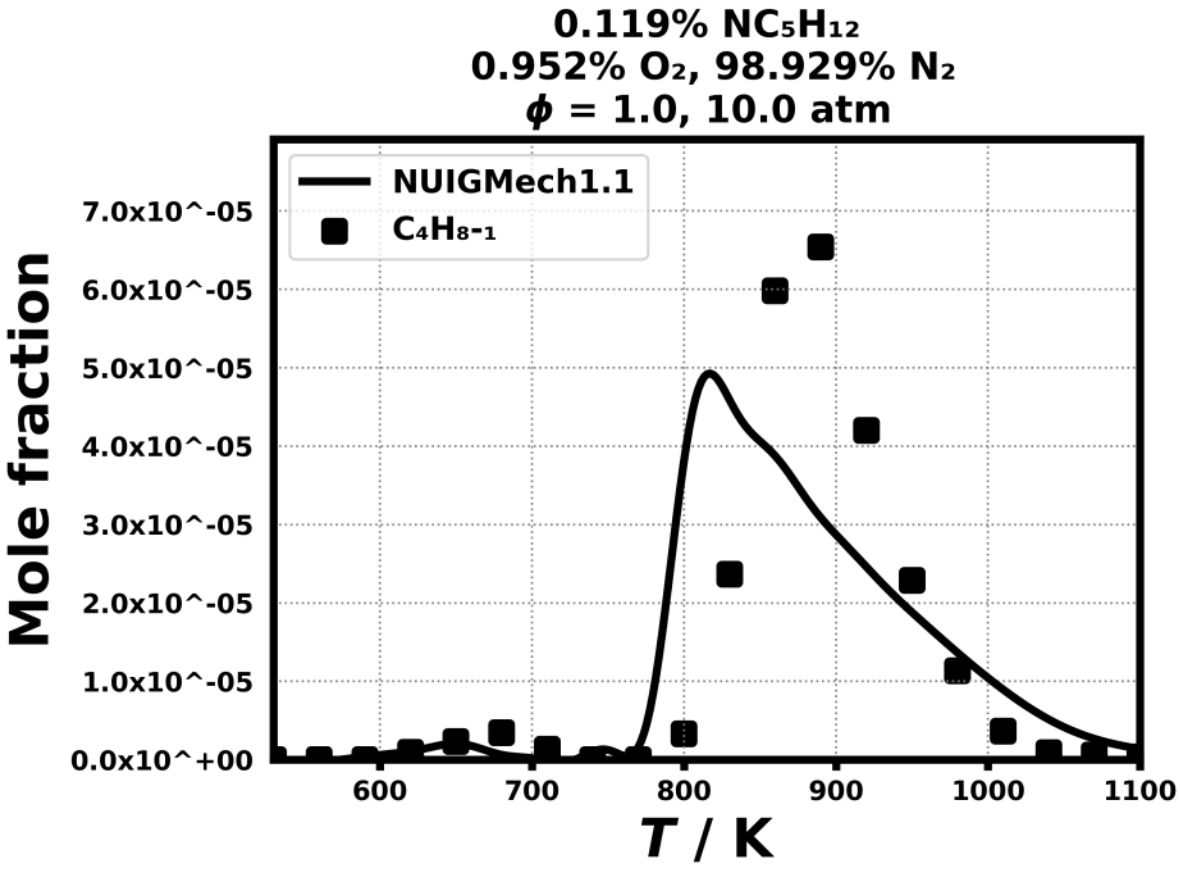

Figure 235: Dataset: 10_ATM_PHI_1.0

1.3.206 Case: n-C5H12/JSR/BUGLER/10_ATM_PHI_1.0

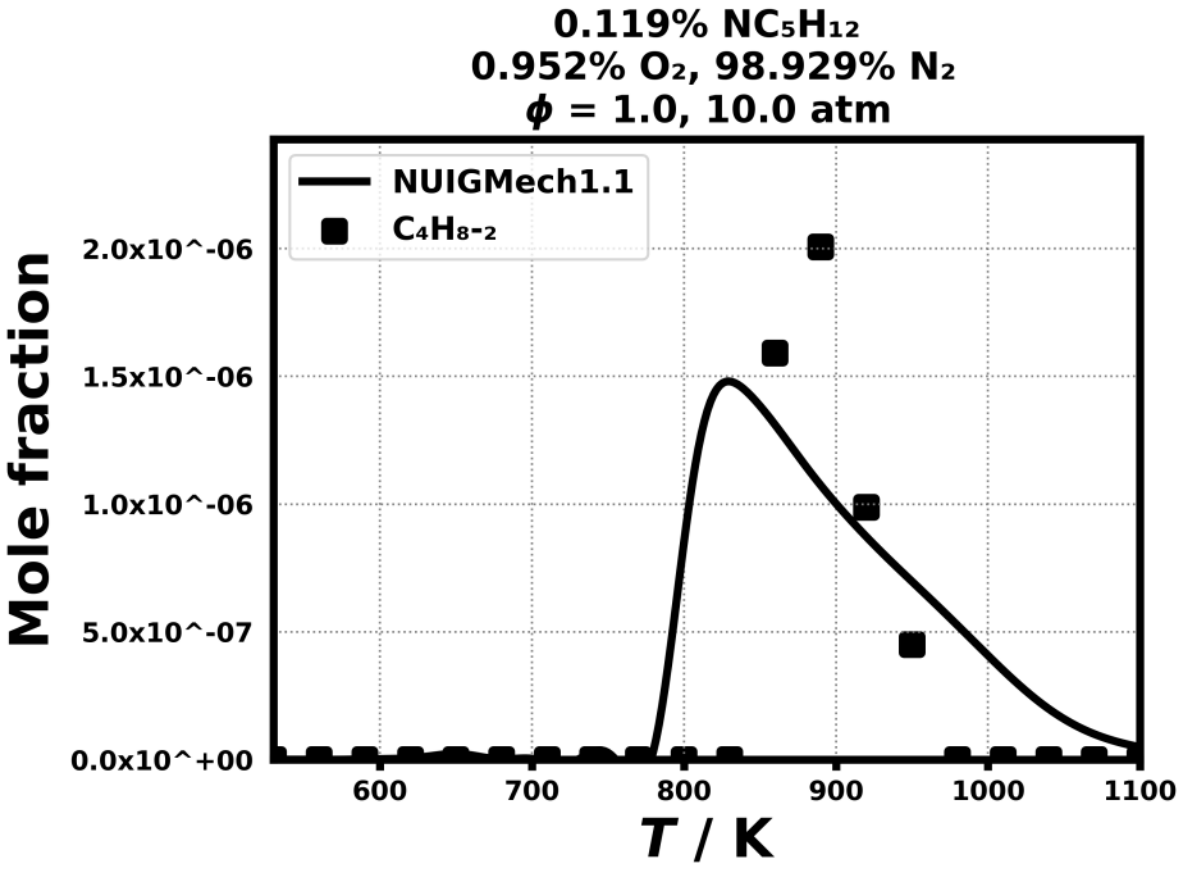

Figure 236: Dataset: 10_ATM_PHI_1.0

1.3.207 Case: n-C5H12/JSR/BUGLER/10_ATM_PHI_1.0

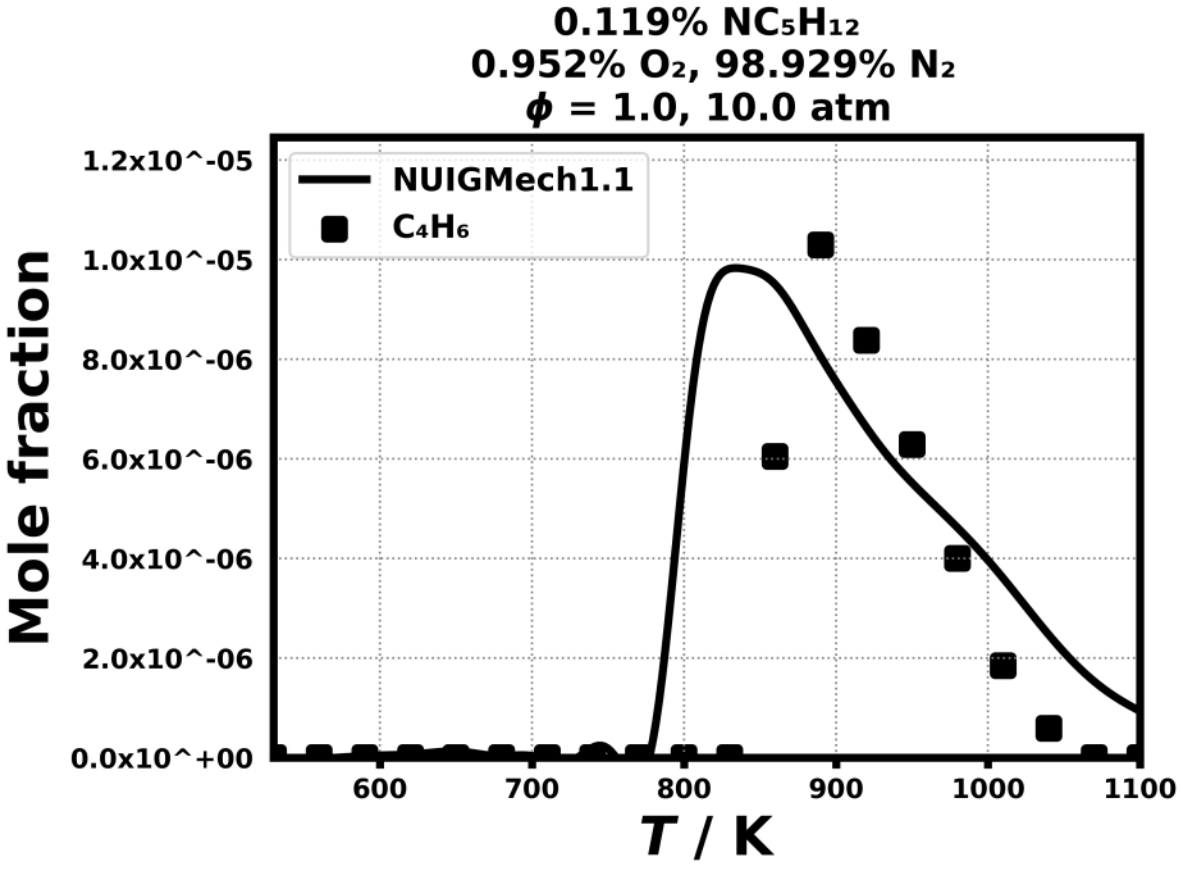

Figure 237: Dataset: 10_ATM_PHI_1.0

1.3.208 Case: n-C5H12/JSR/BUGLER/10_ATM_PHI_1.0

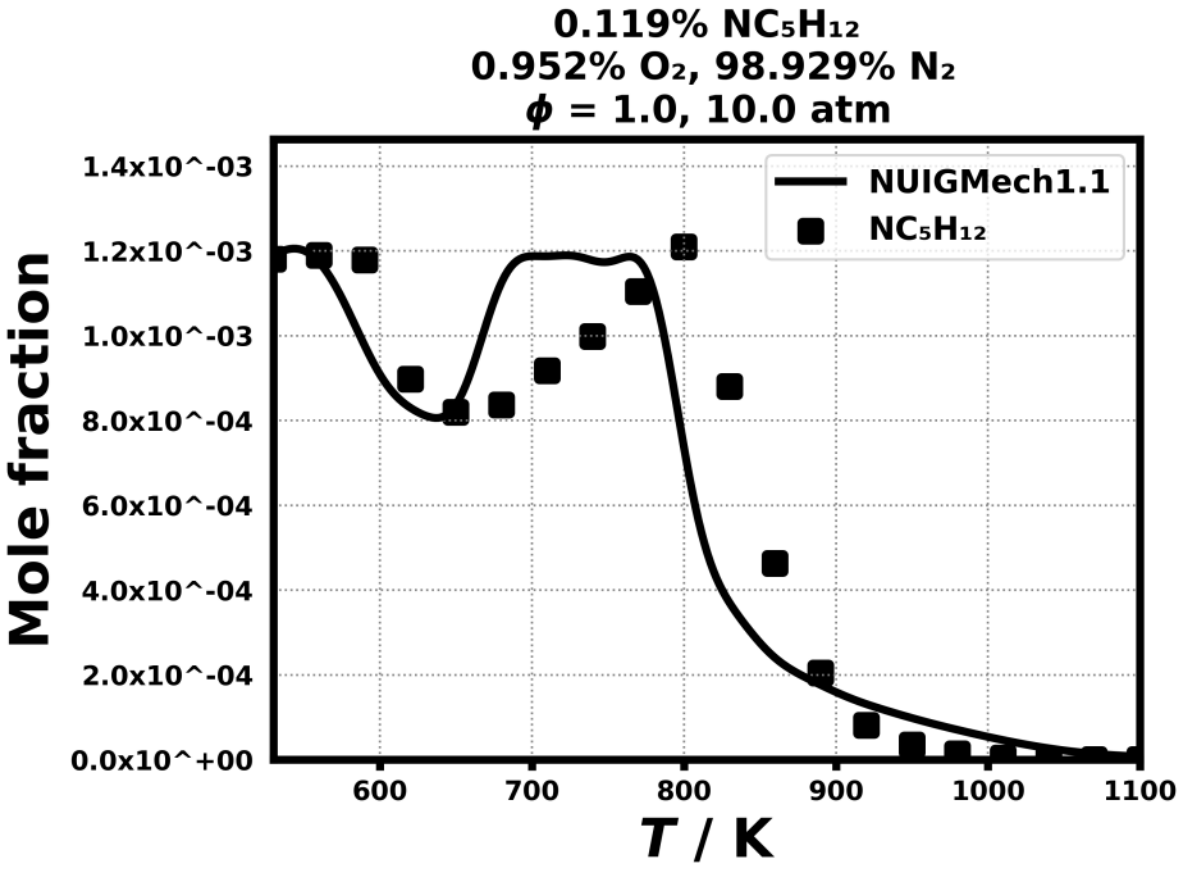

Figure 238: Dataset: 10_ATM_PHI_1.0

1.3.209 Case: n-C5H12/JSR/BUGLER/10_ATM_PHI_1.0

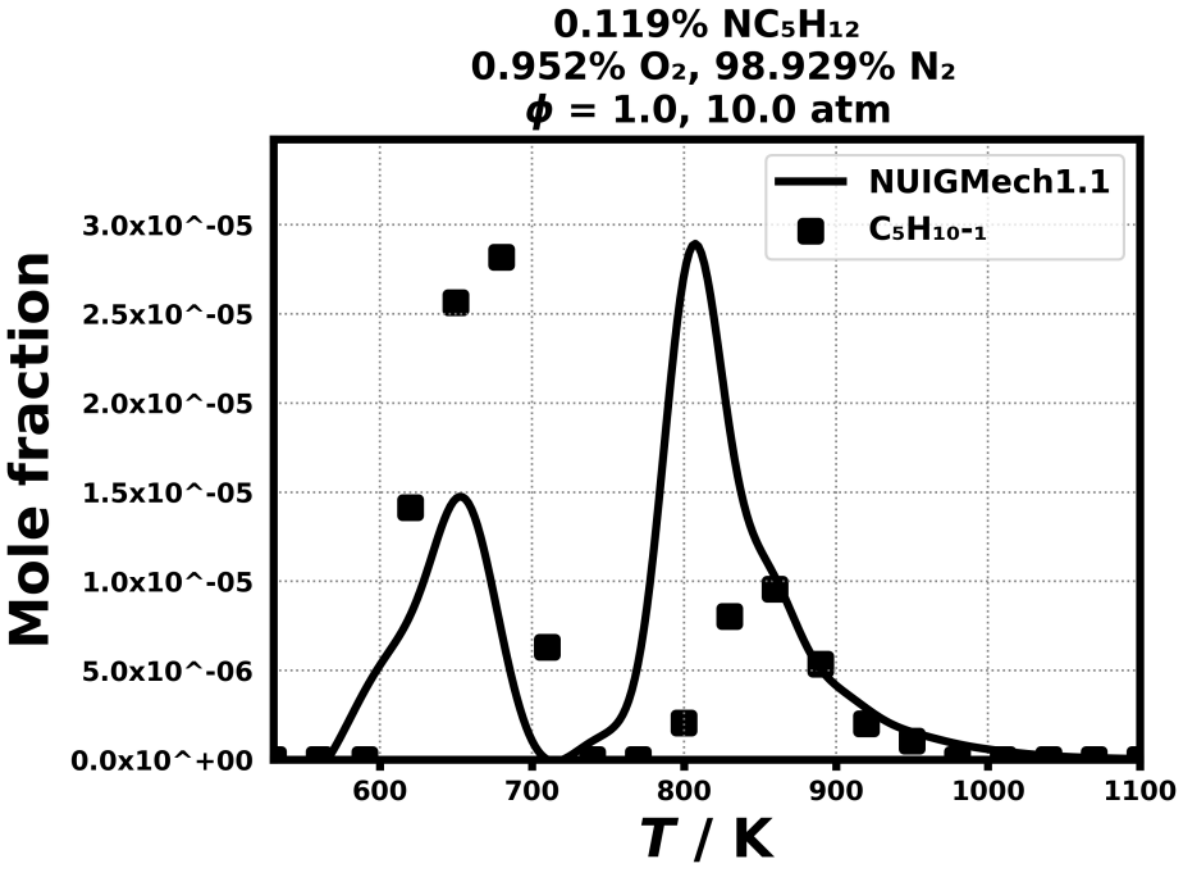

Figure 239: Dataset: 10_ATM_PHI_1.0

1.3.210 Case: n-C5H12/JSR/BUGLER/10_ATM_PHI_1.0

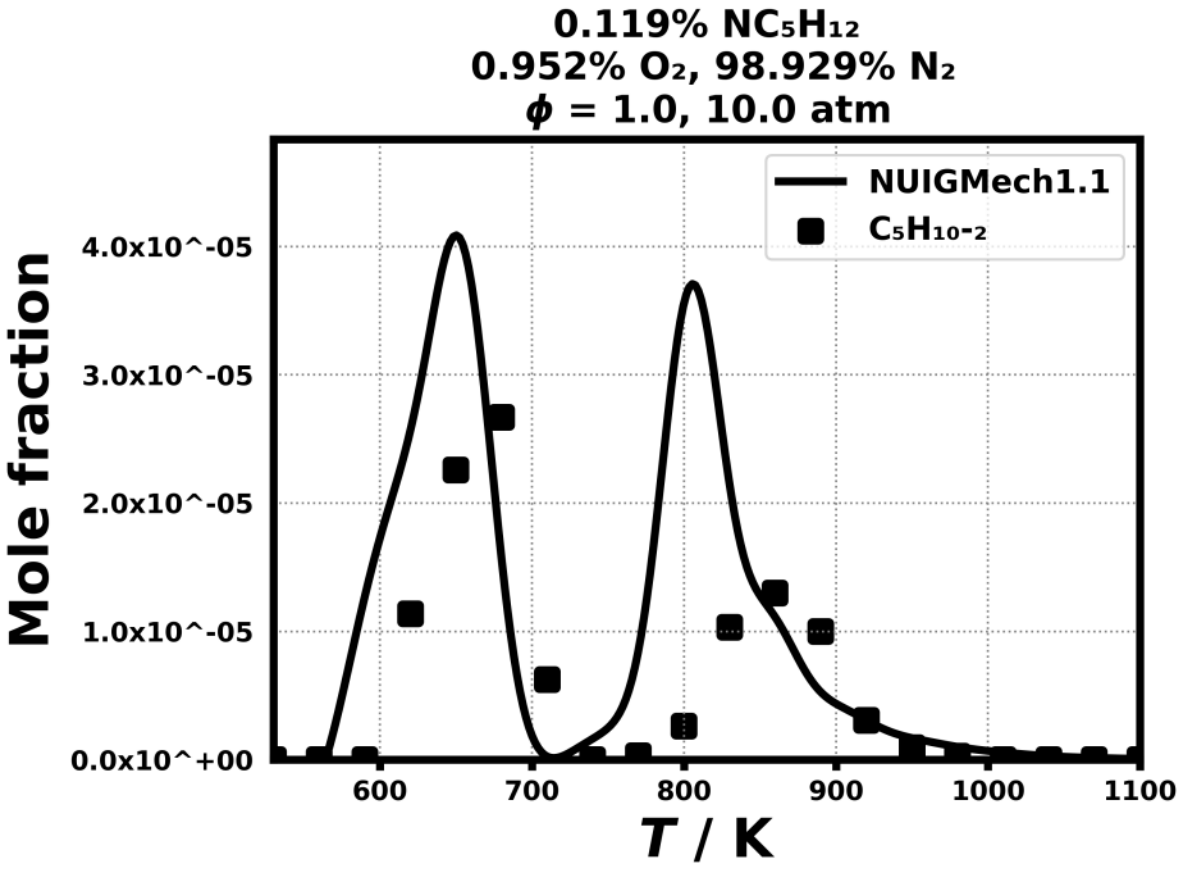

Figure 240: Dataset: 10_ATM_PHI_1.0

1.3.211 Case: n-C5H12/JSR/BUGLER/10_ATM_PHI_1.0

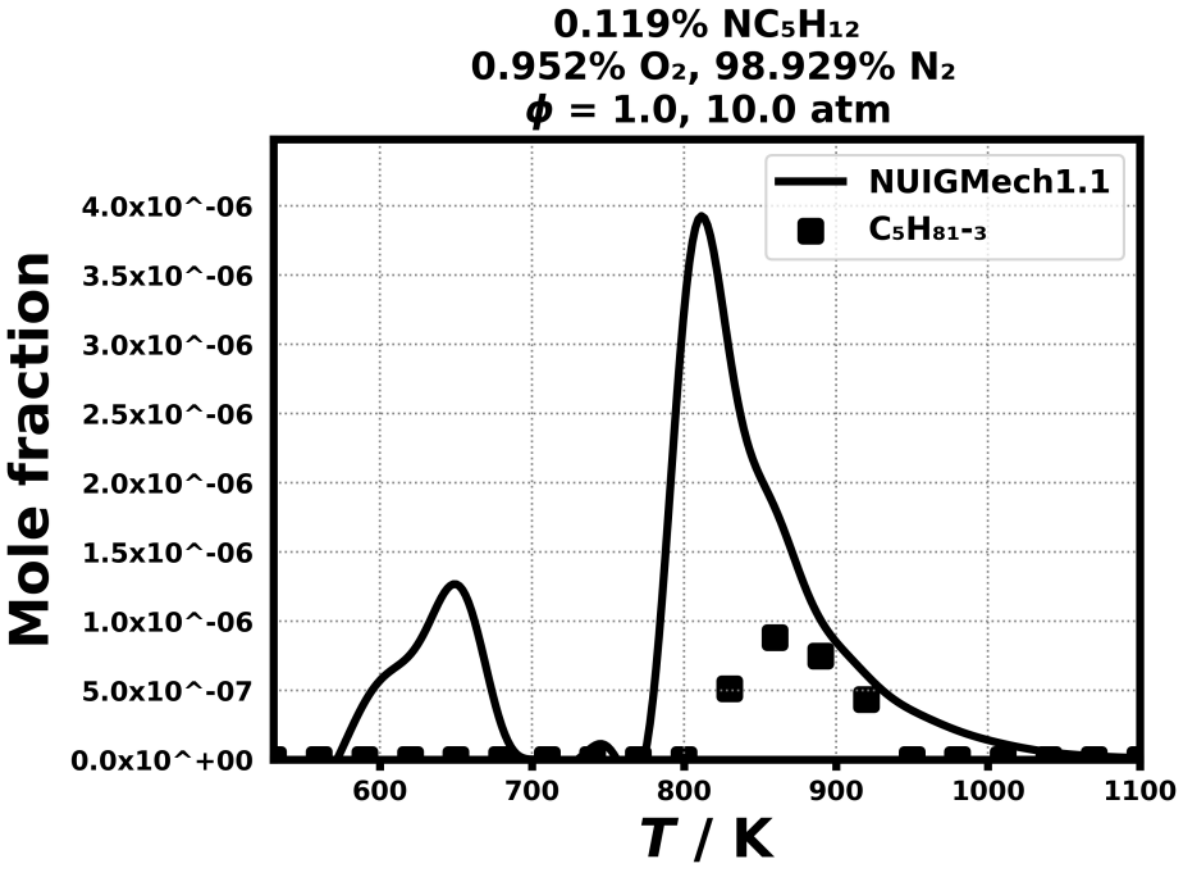

Figure 241: Dataset: 10_ATM_PHI_1.0

1.3.212 Case: n-C5H12/JSR/BUGLER/10_ATM_PHI_1.0

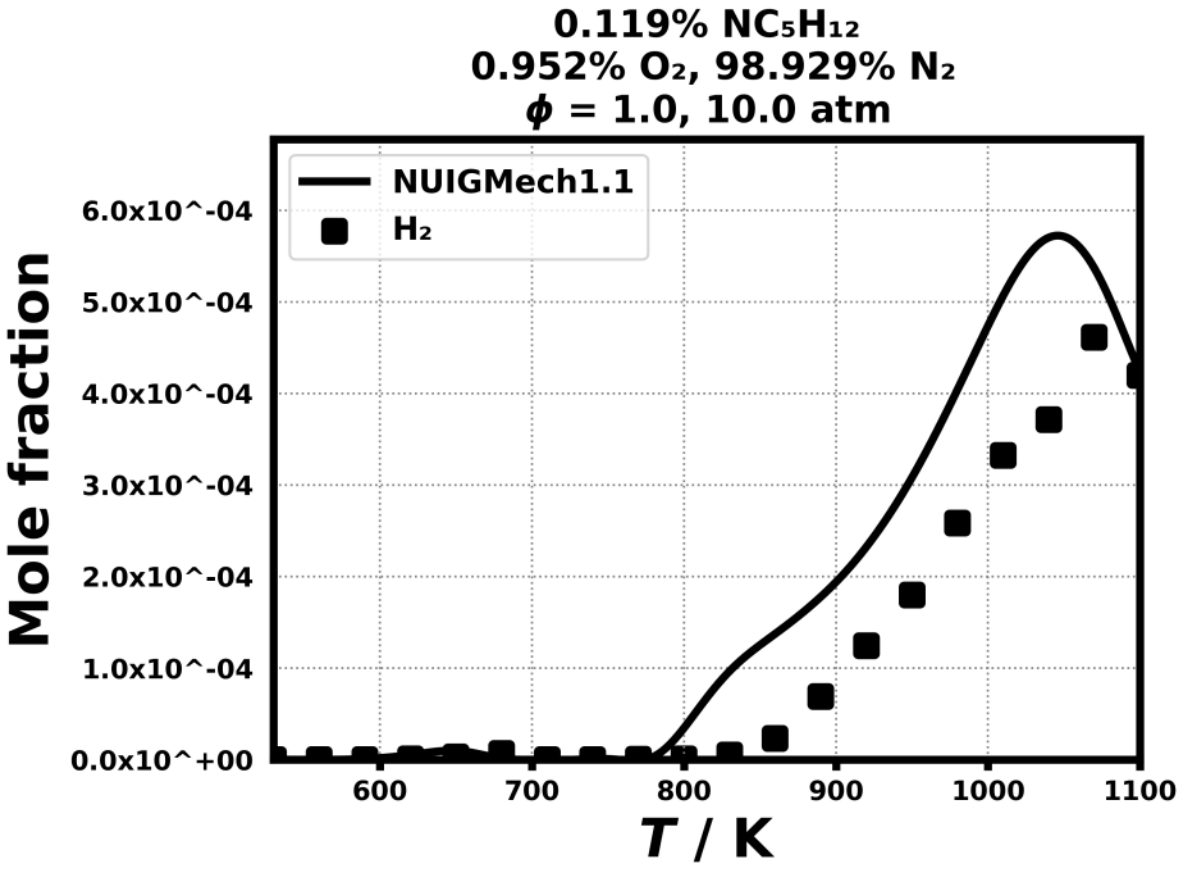

Figure 242: Dataset: 10_ATM_PHI_1.0

1.3.213 Case: n-C5H12/JSR/BUGLER/10_ATM_PHI_1.0

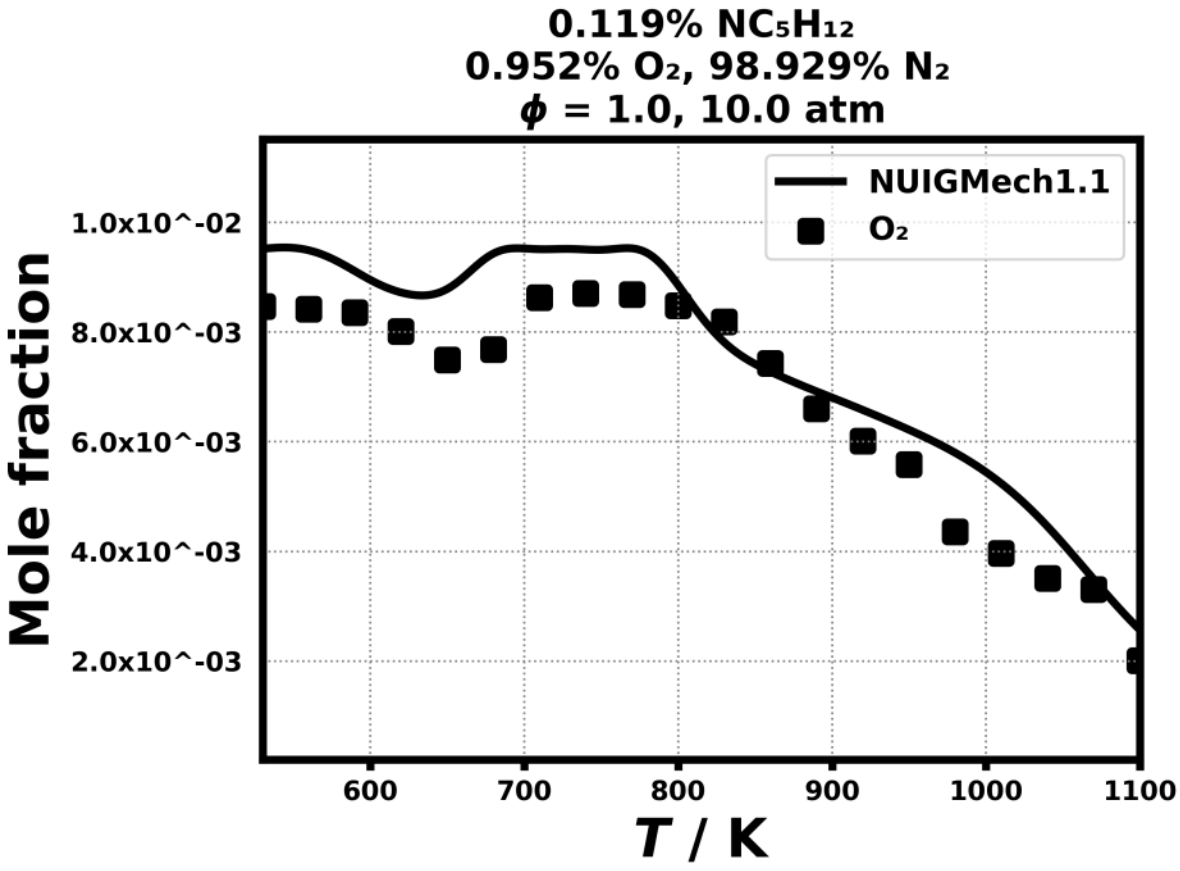

Figure 243: Dataset: 10_ATM_PHI_1.0

1.3.214 Case: n-C5H12/JSR/BUGLER/10_ATM_PHI_1.0

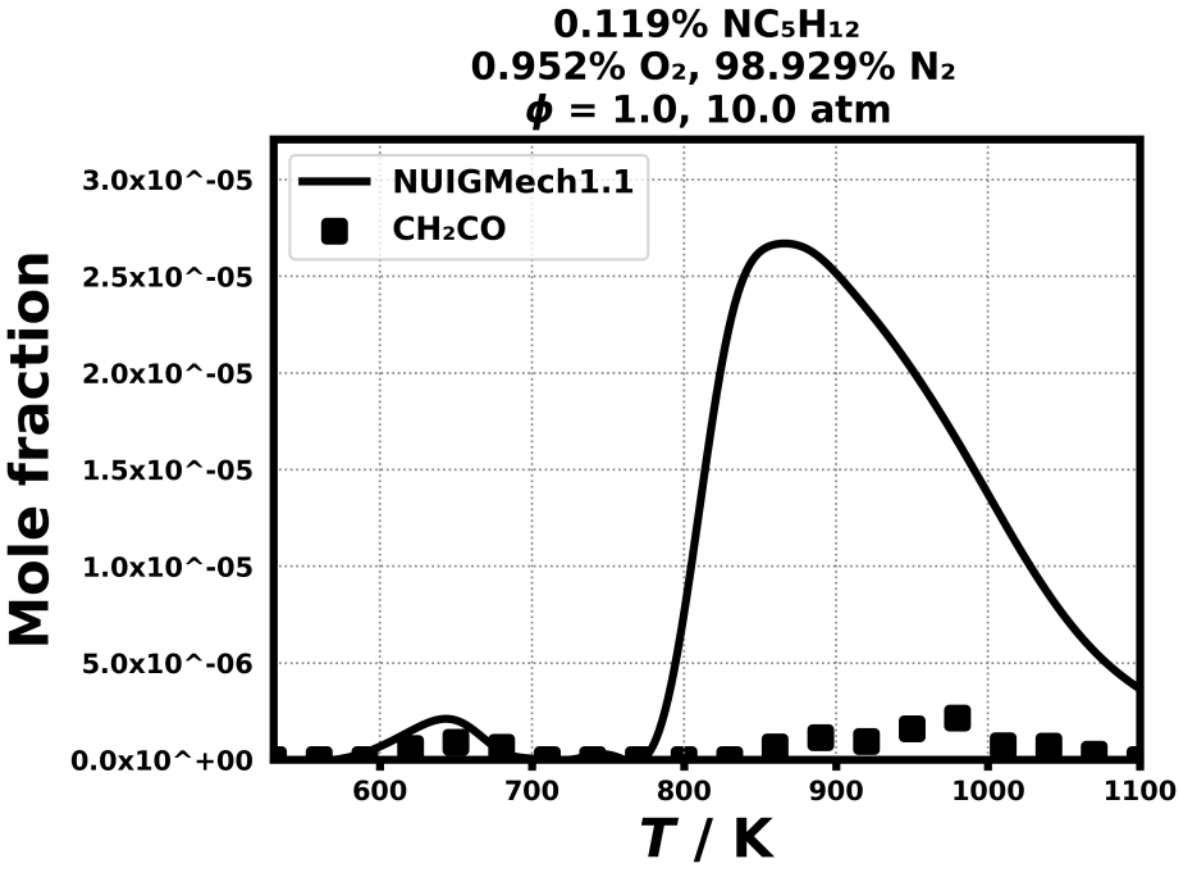

Figure 244: Dataset: 10_ATM_PHI_1.0

1.3.215 Case: n-C5H12/JSR/BUGLER/10_ATM_PHI_1.0

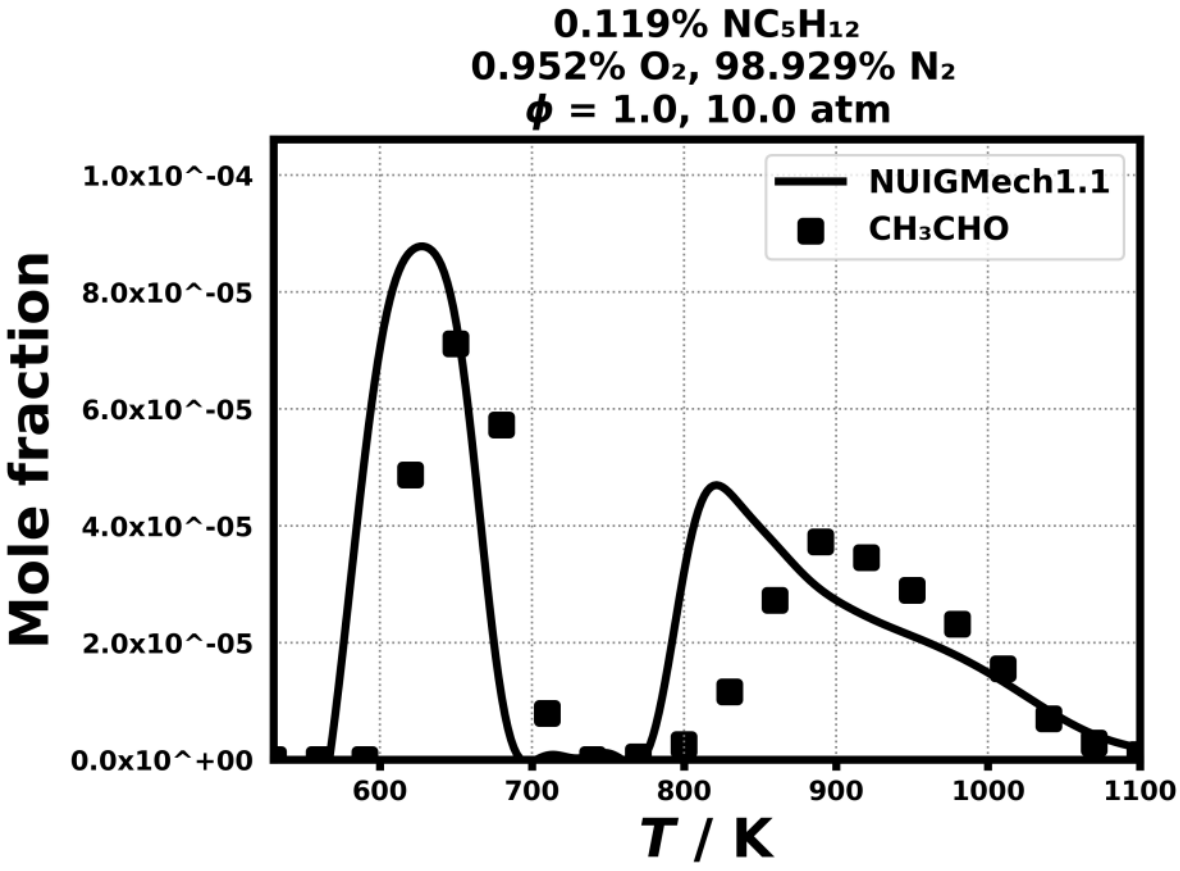

Figure 245: Dataset: 10_ATM_PHI_1.0

1.3.216 Case: n-C5H12/JSR/BUGLER/10_ATM_PHI_1.0

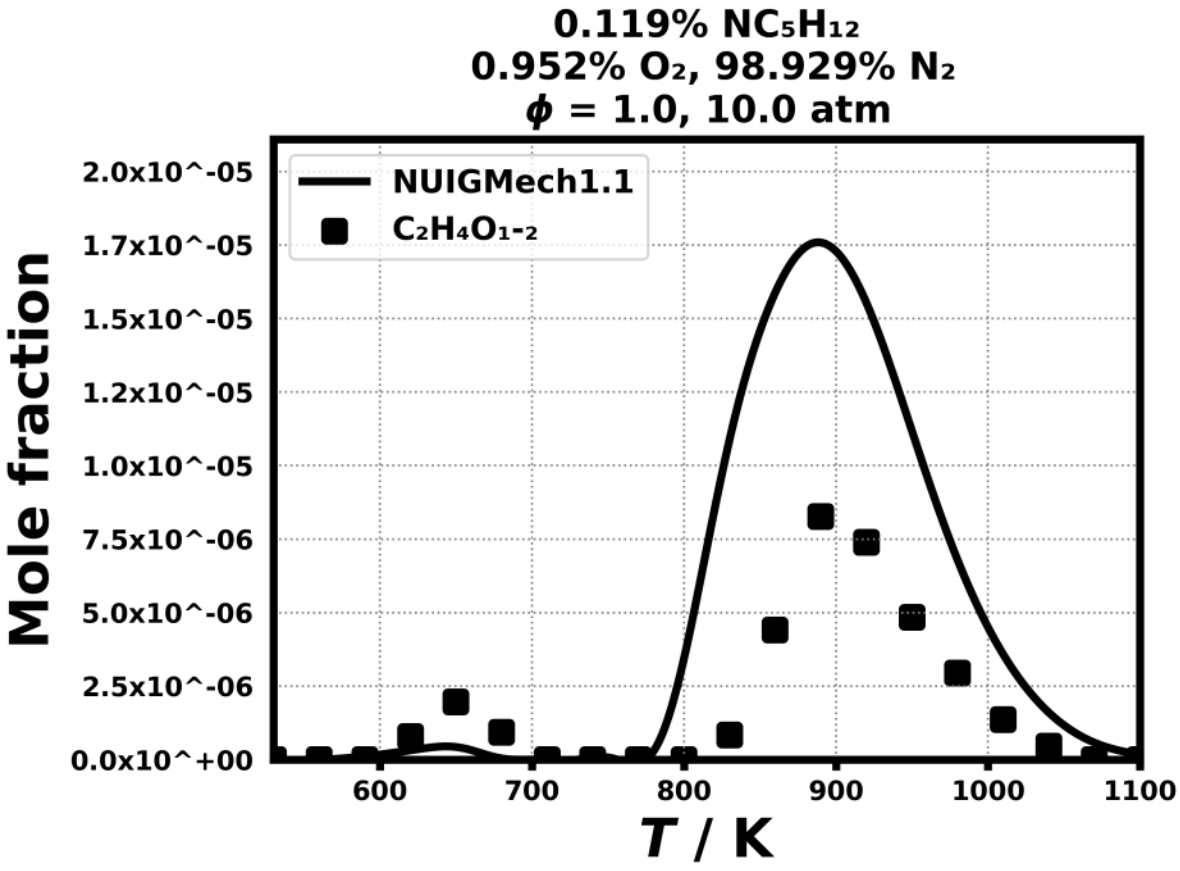

Figure 246: Dataset: 10_ATM_PHI_1.0

1.3.217 Case: n-C5H12/JSR/BUGLER/10_ATM_PHI_1.0

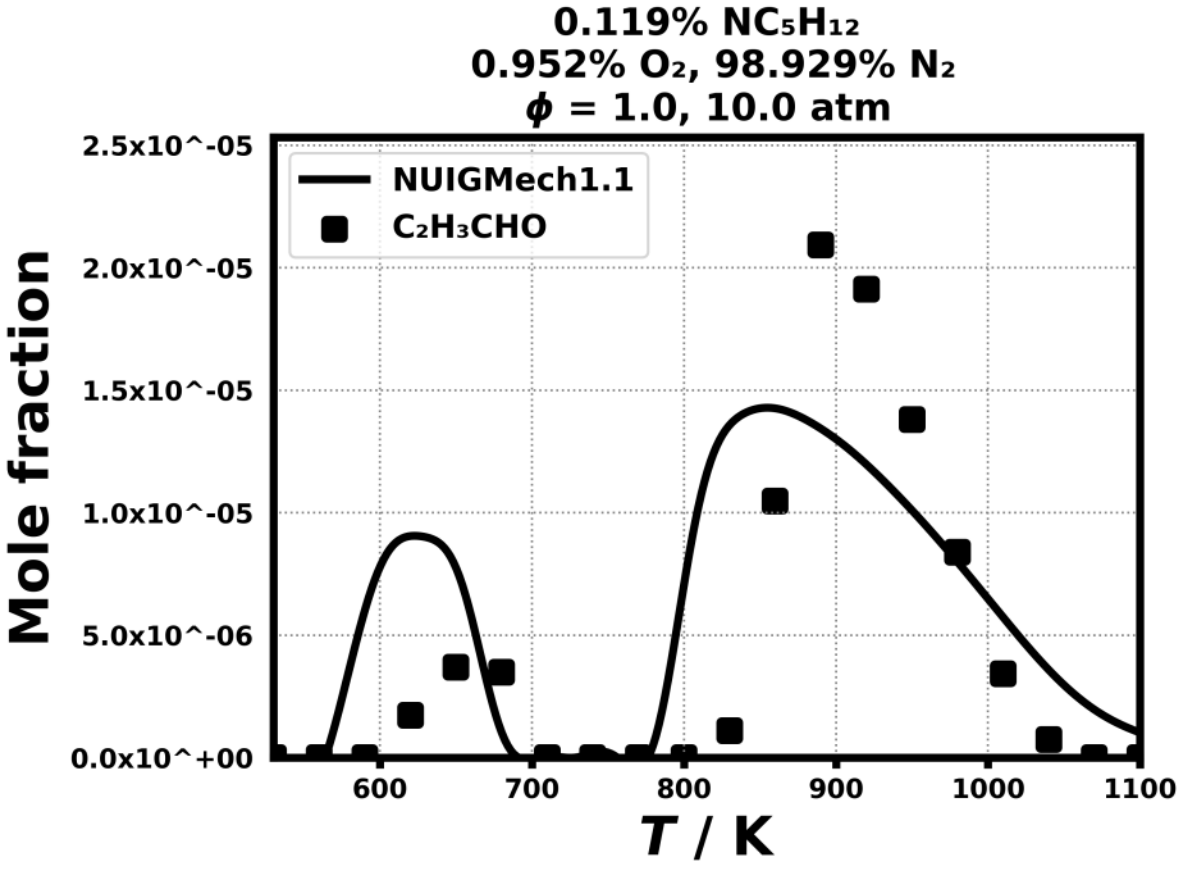

Figure 247: Dataset: 10_ATM_PHI_1.0

1.3.218 Case: n-C5H12/JSR/BUGLER/10_ATM_PHI_1.0

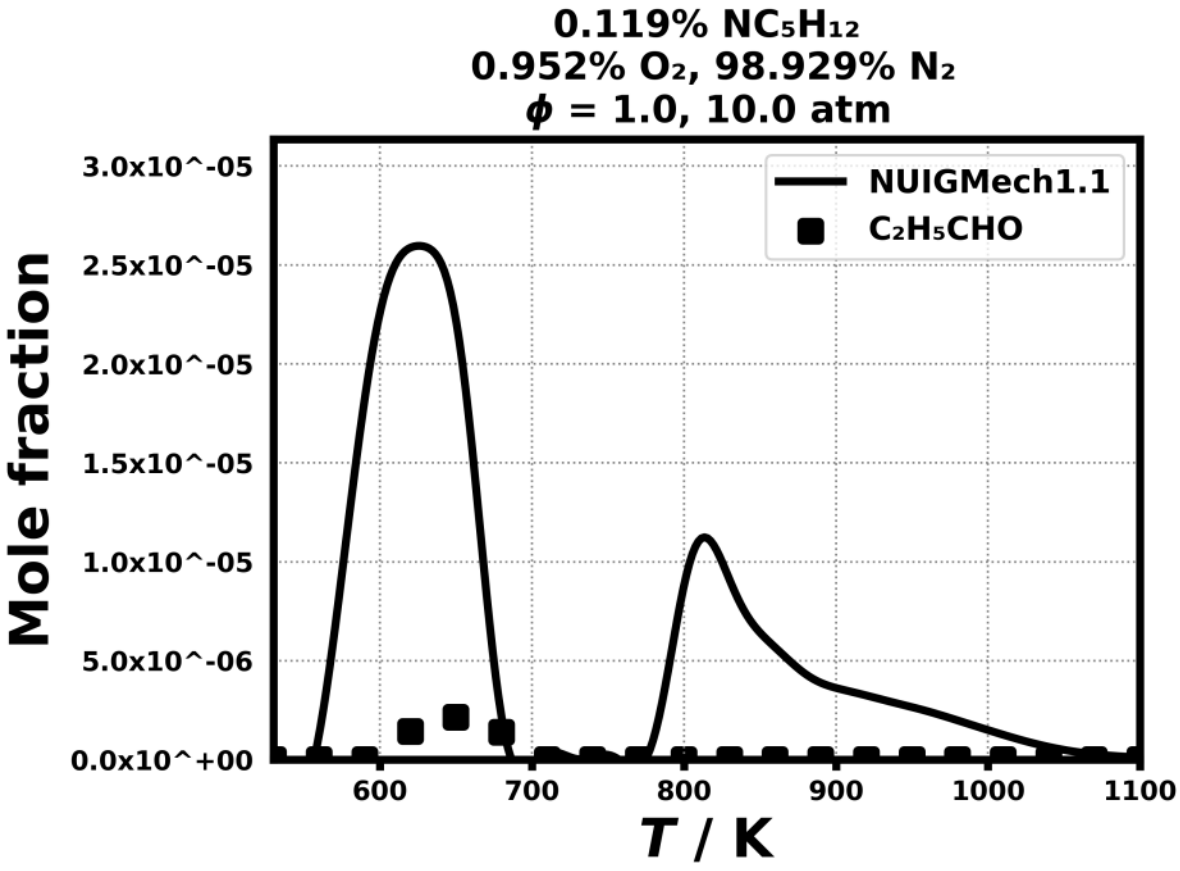

Figure 248: Dataset: 10_ATM_PHI_1.0

1.3.219 Case: n-C5H12/JSR/BUGLER/10_ATM_PHI_1.0

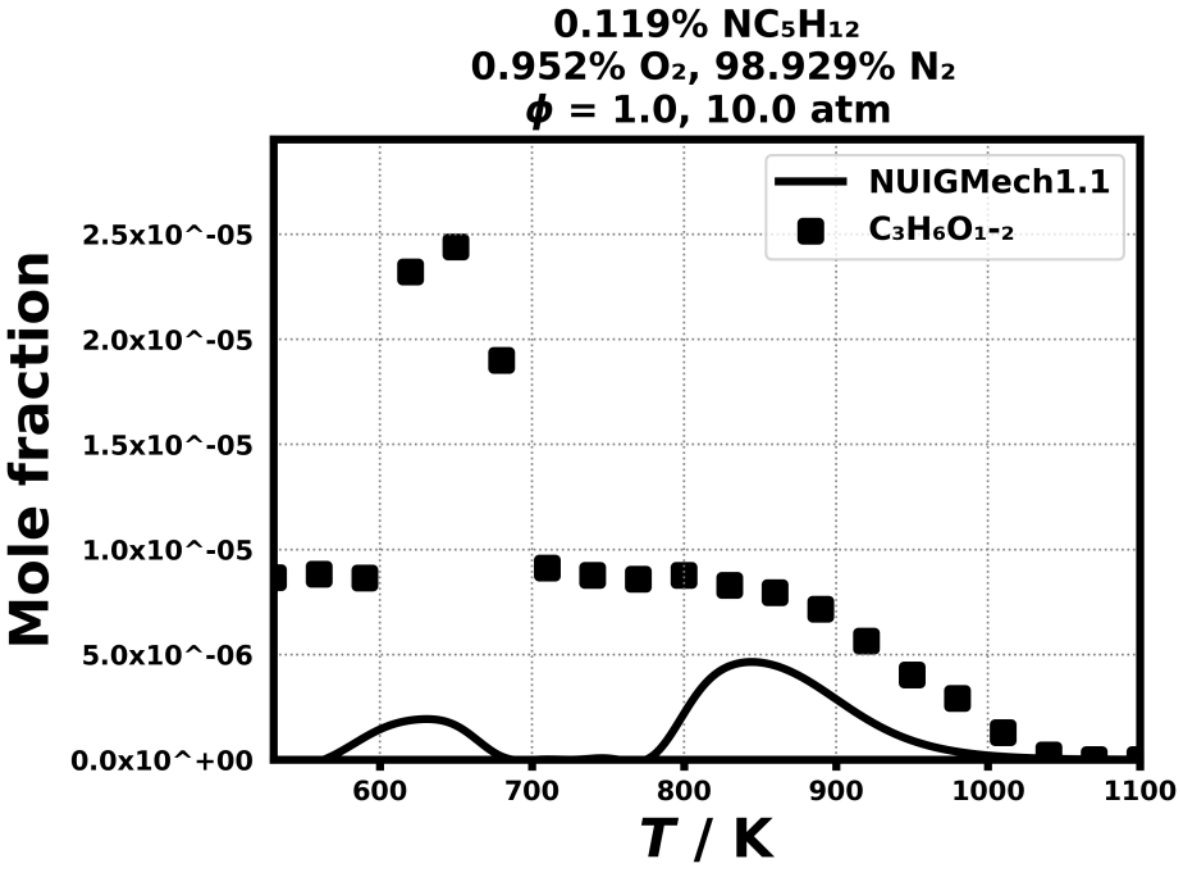

Figure 249: Dataset: 10_ATM_PHI_1.0

1.3.220 Case: n-C5H12/JSR/BUGLER/10_ATM_PHI_1.0

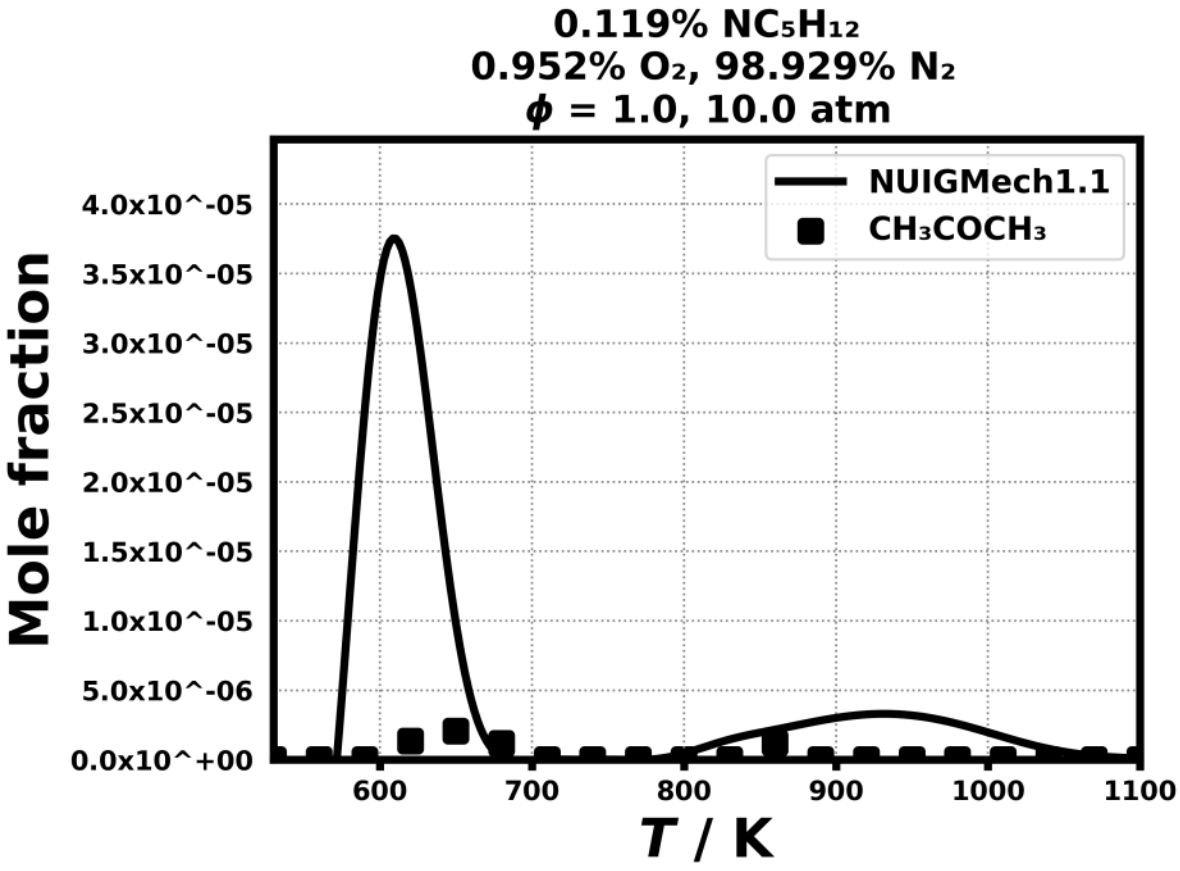

Figure 250: Dataset: 10_ATM_PHI_1.0

1.3.221 Case: n-C5H12/JSR/BUGLER/10_ATM_PHI_1.0

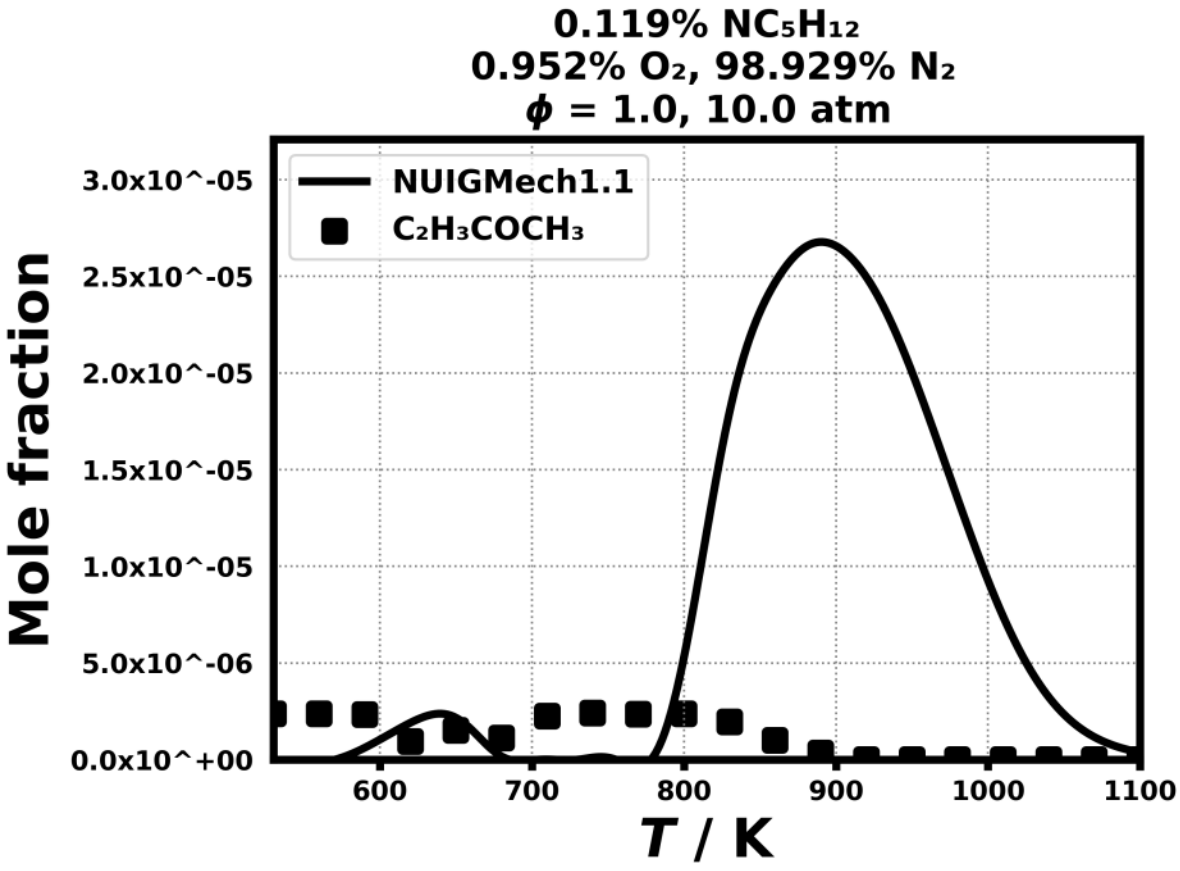

Figure 251: Dataset: 10_ATM_PHI_1.0

1.3.222 Case: n-C5H12/JSR/BUGLER/10_ATM_PHI_1.0

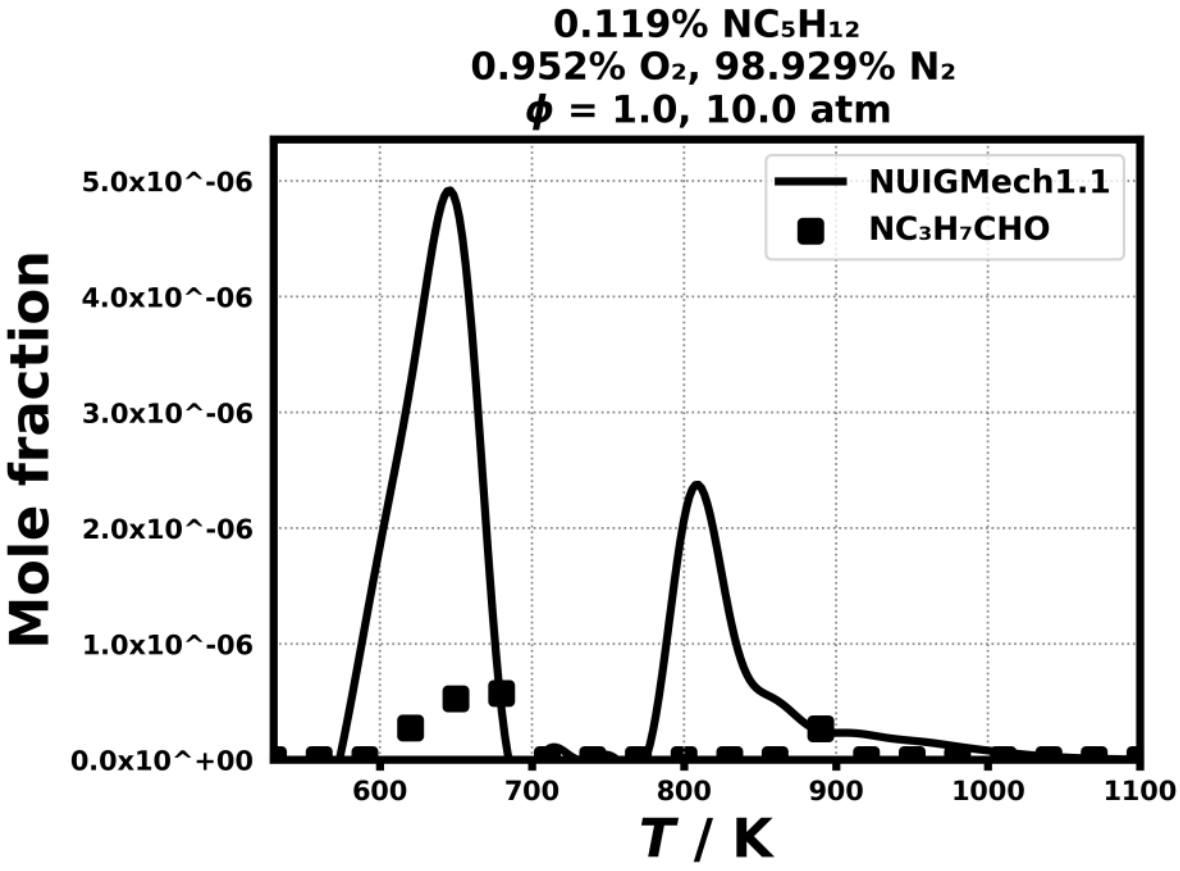

Figure 252: Dataset: 10_ATM_PHI_1.0

1.3.223 Case: n-C5H12/JSR/BUGLER/10_ATM_PHI_1.0

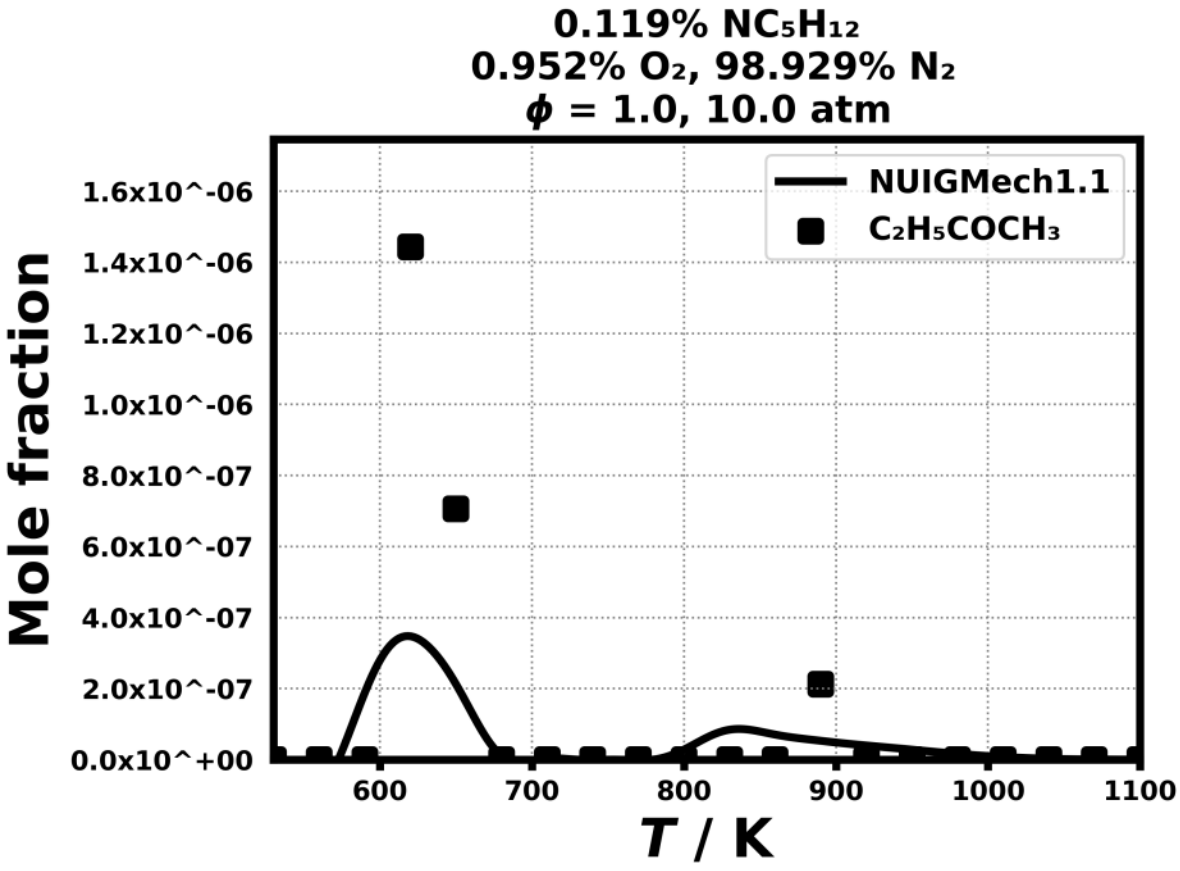

Figure 253: Dataset: 10_ATM_PHI_1.0

1.3.224 Case: n-C5H12/JSR/BUGLER/10_ATM_PHI_1.0

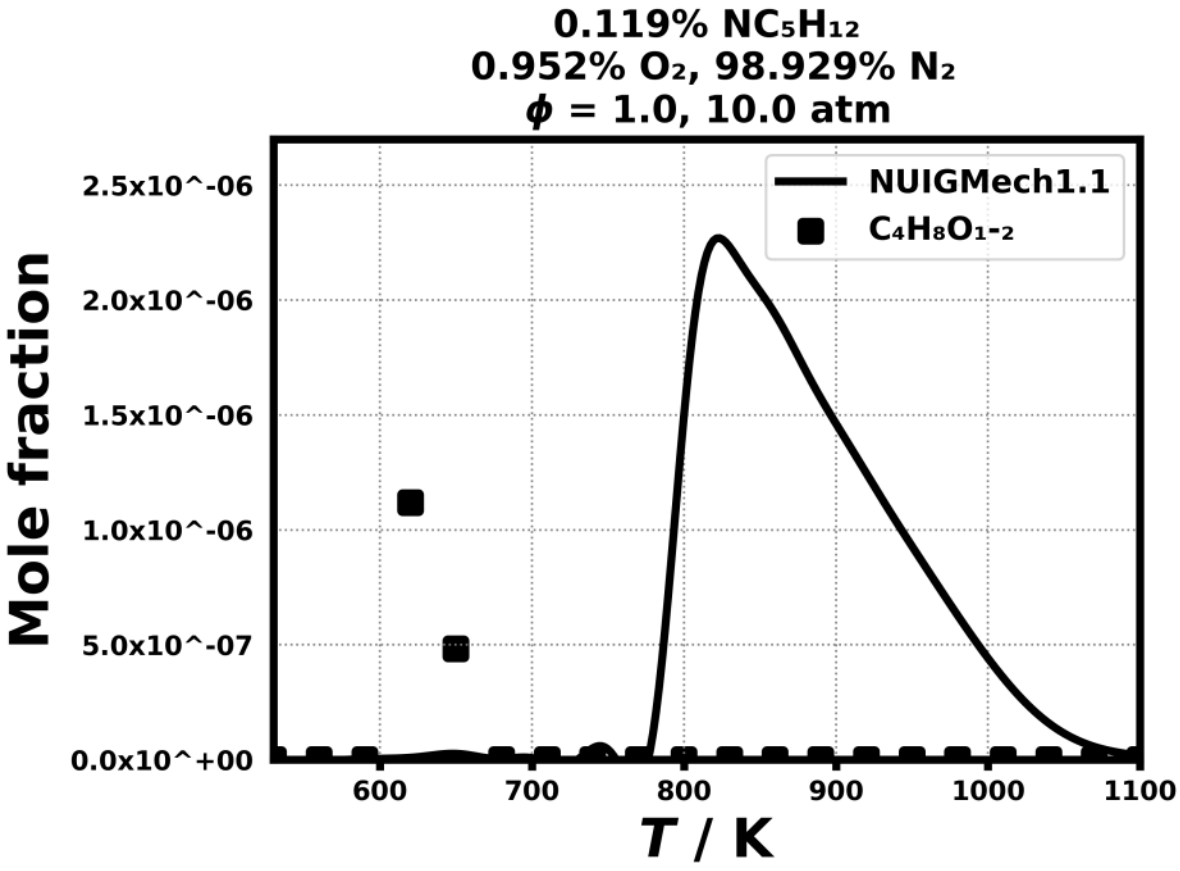

Figure 254: Dataset: 10_ATM_PHI_1.0

1.3.225 Case: n-C5H12/JSR/BUGLER/10_ATM_PHI_1.0

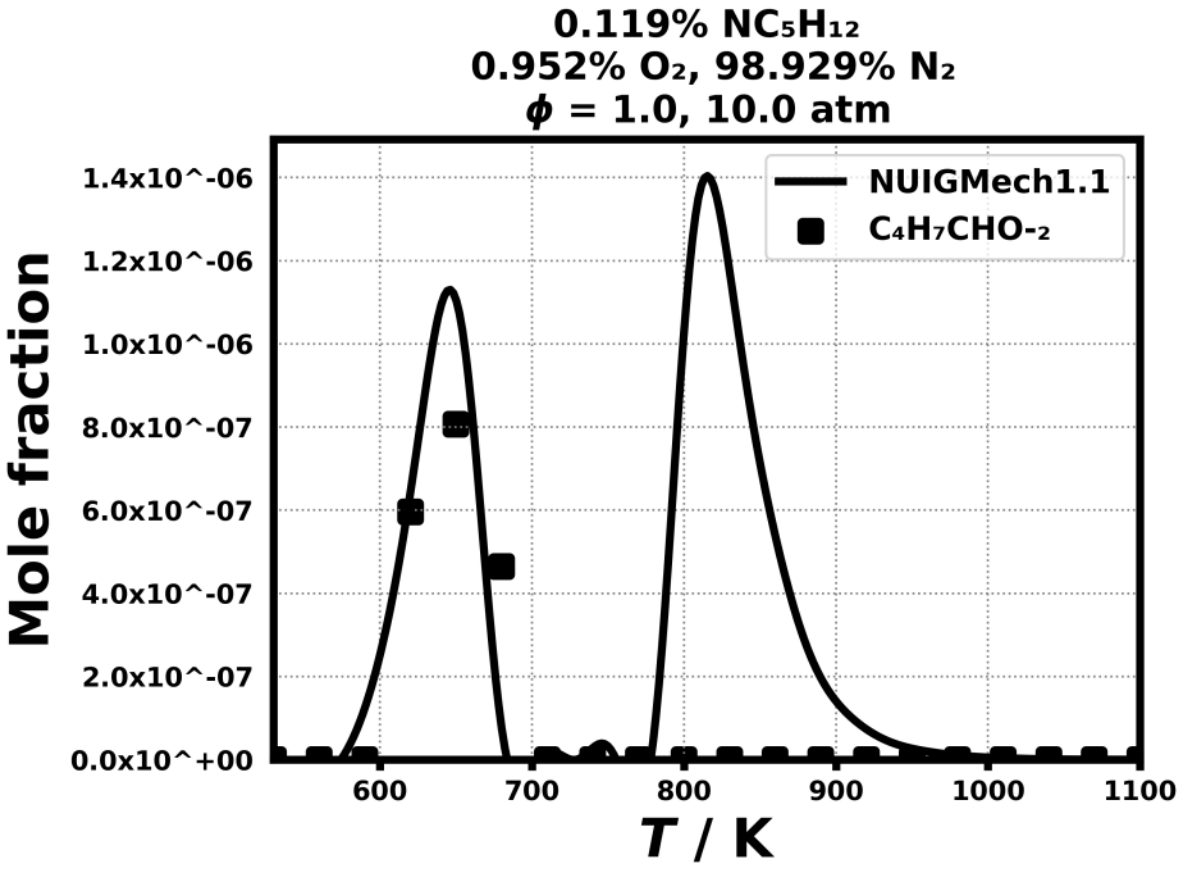

Figure 255: Dataset: 10_ATM_PHI_1.0

1.3.226 Case: n-C5H12/JSR/BUGLER/10_ATM_PHI_1.0

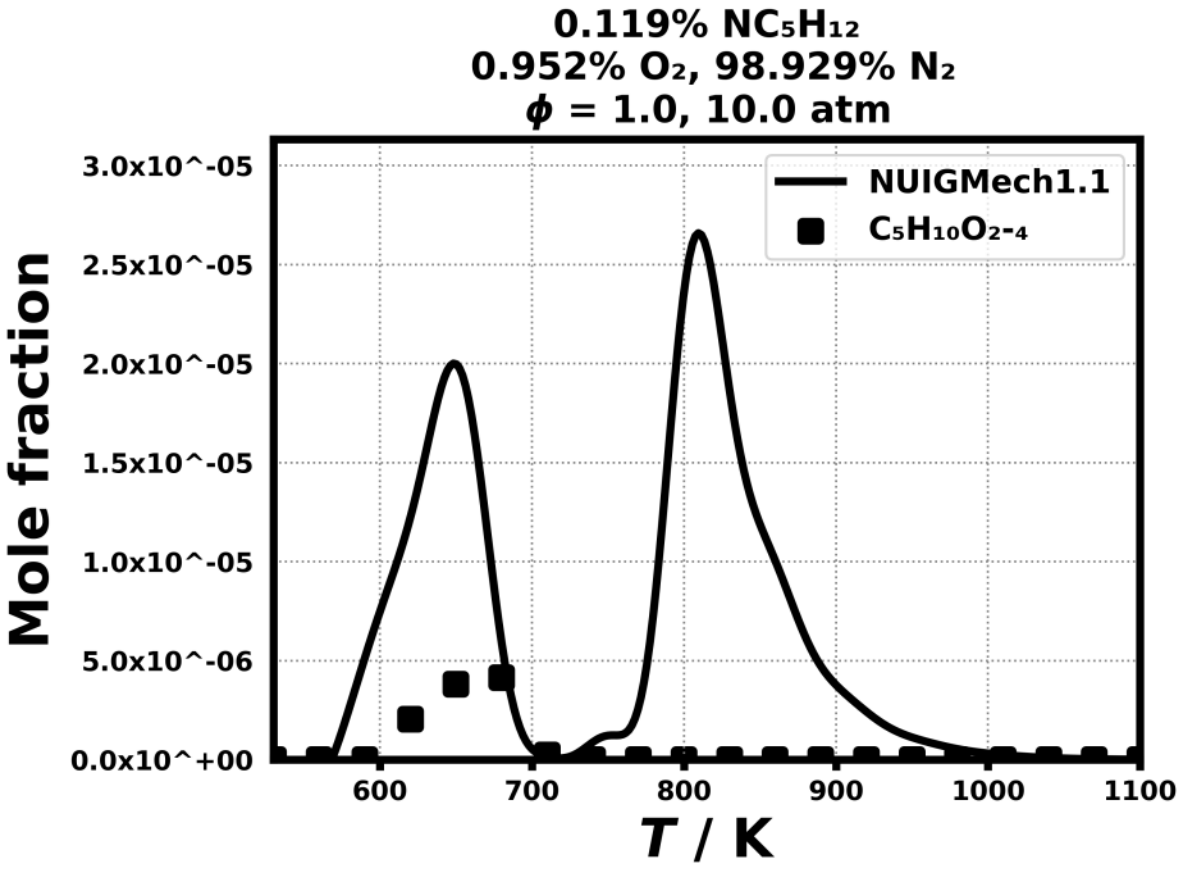

Figure 256: Dataset: 10_ATM_PHI_1.0

1.3.227 Case: n-C5H12/JSR/BUGLER/10_ATM_PHI_1.0

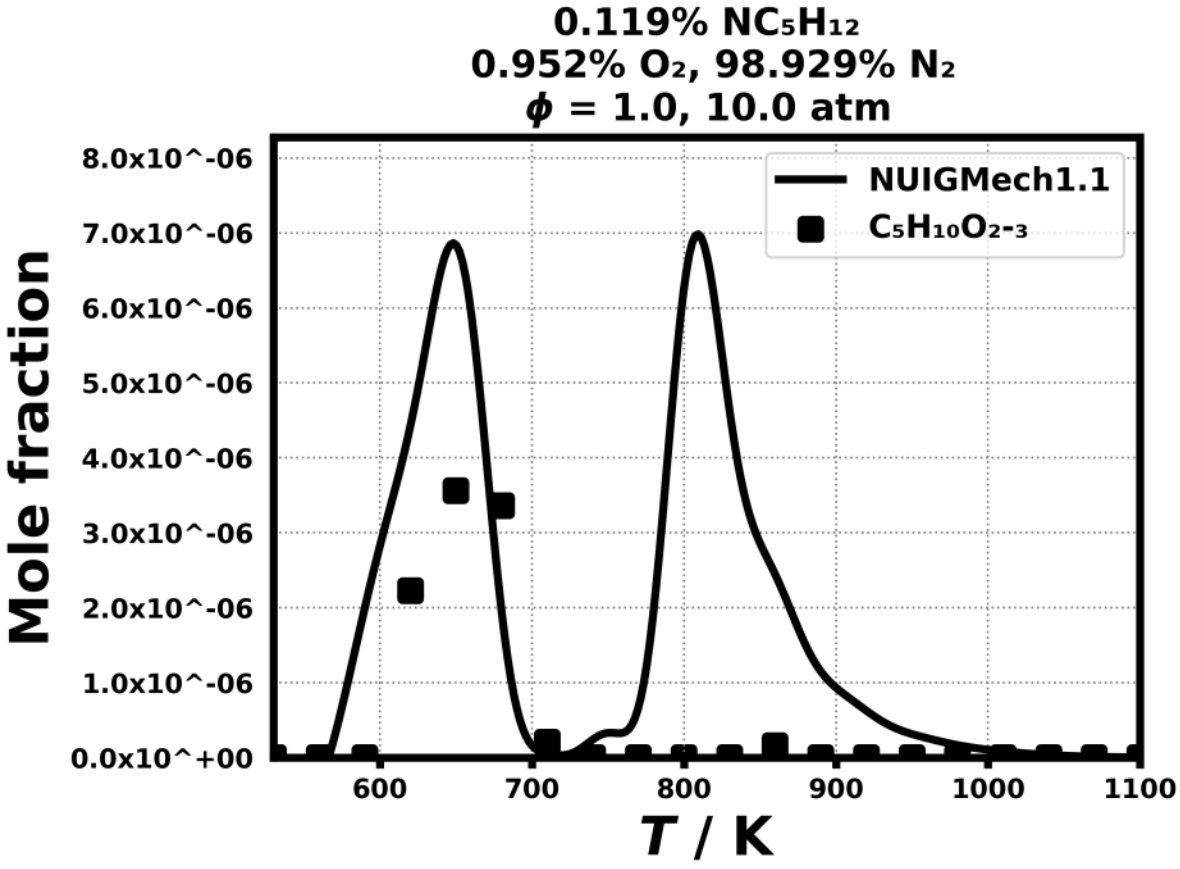

Figure 257: Dataset: 10_ATM_PHI_1.0

1.3.228 Case: n-C5H12/JSR/BUGLER/10_ATM_PHI_1.0

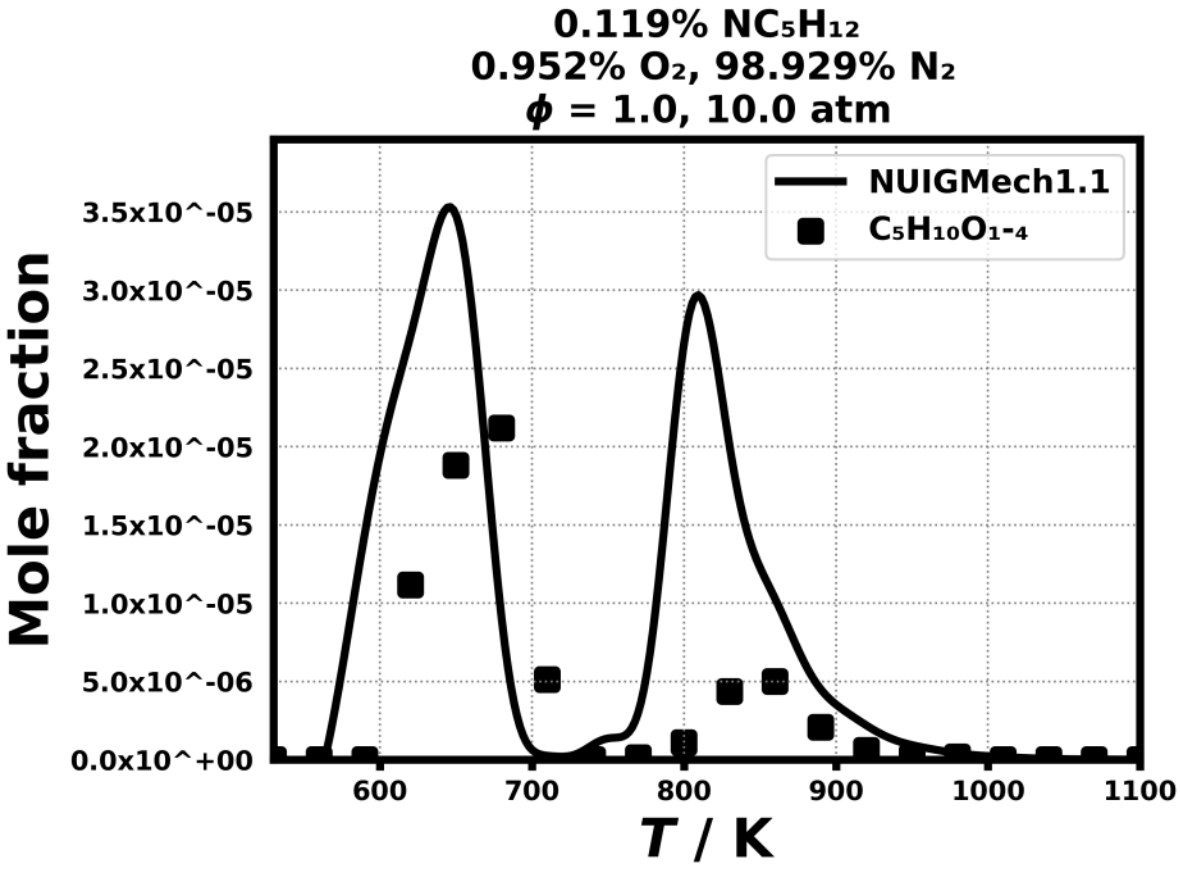

Figure 258: Dataset: 10_ATM_PHI_1.0

1.3.229 Case: n-C5H12/JSR/BUGLER/10_ATM_PHI_1.0

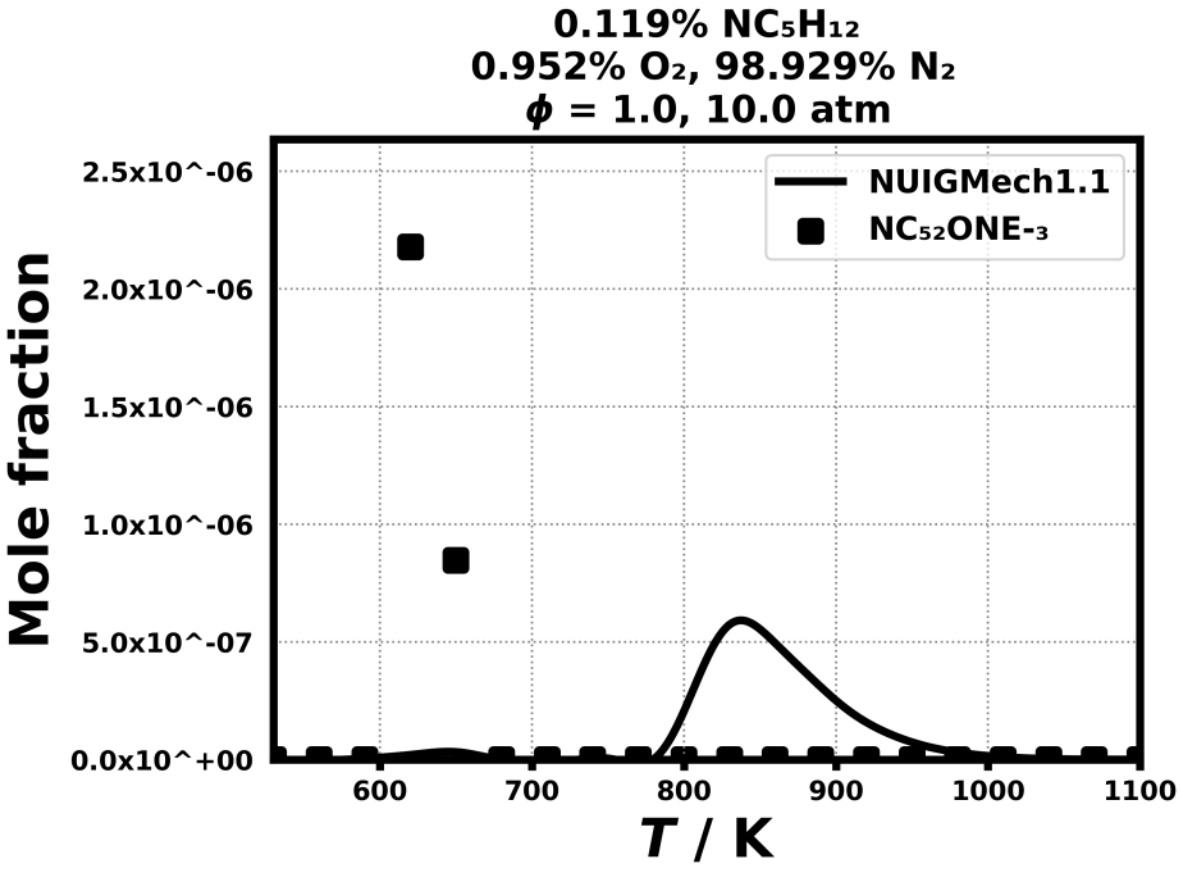

Figure 259: Dataset: 10_ATM_PHI_1.0

1.3.230 Case: n-C5H12/JSR/BUGLER/10_ATM_PHI_1.0

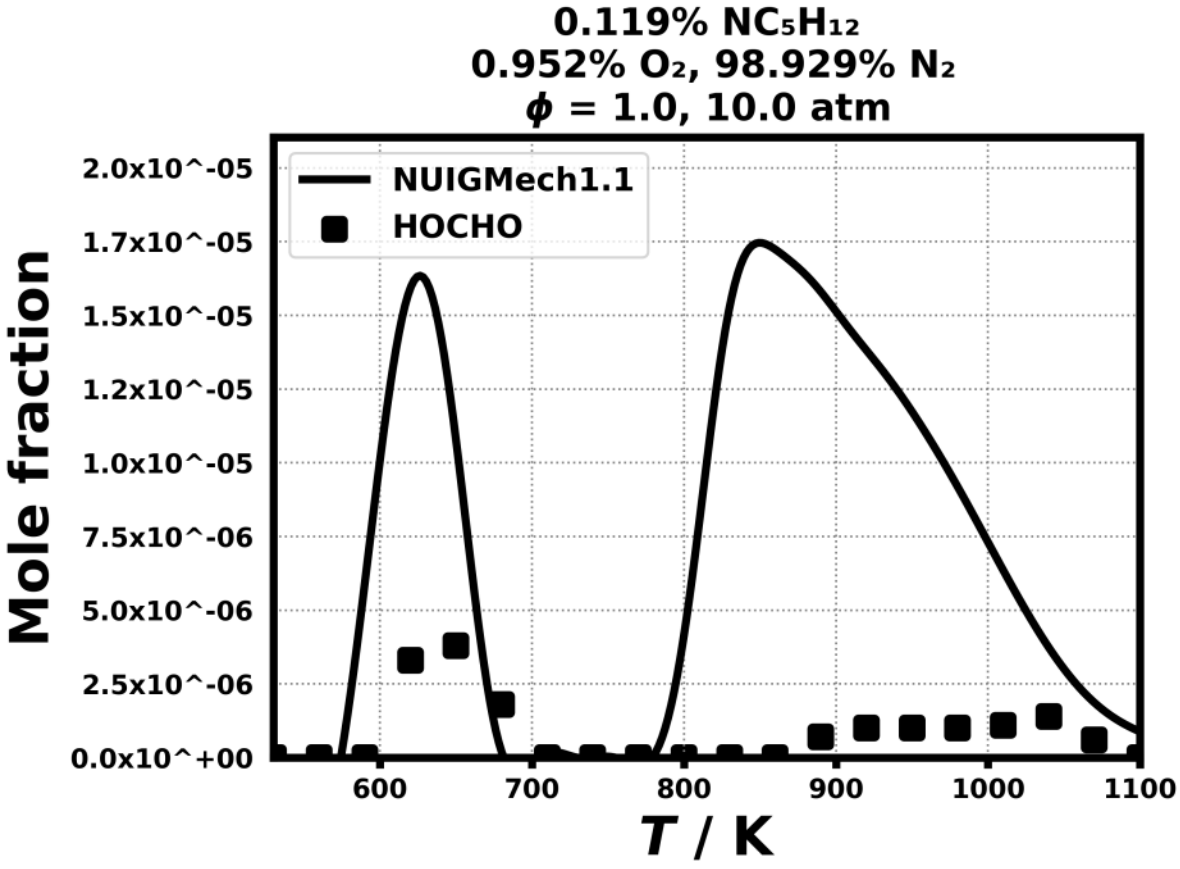

Figure 260: Dataset: 10_ATM_PHI_1.0

1.3.231 Case: n-C5H12/JSR/BUGLER/10_ATM_PHI_1.0

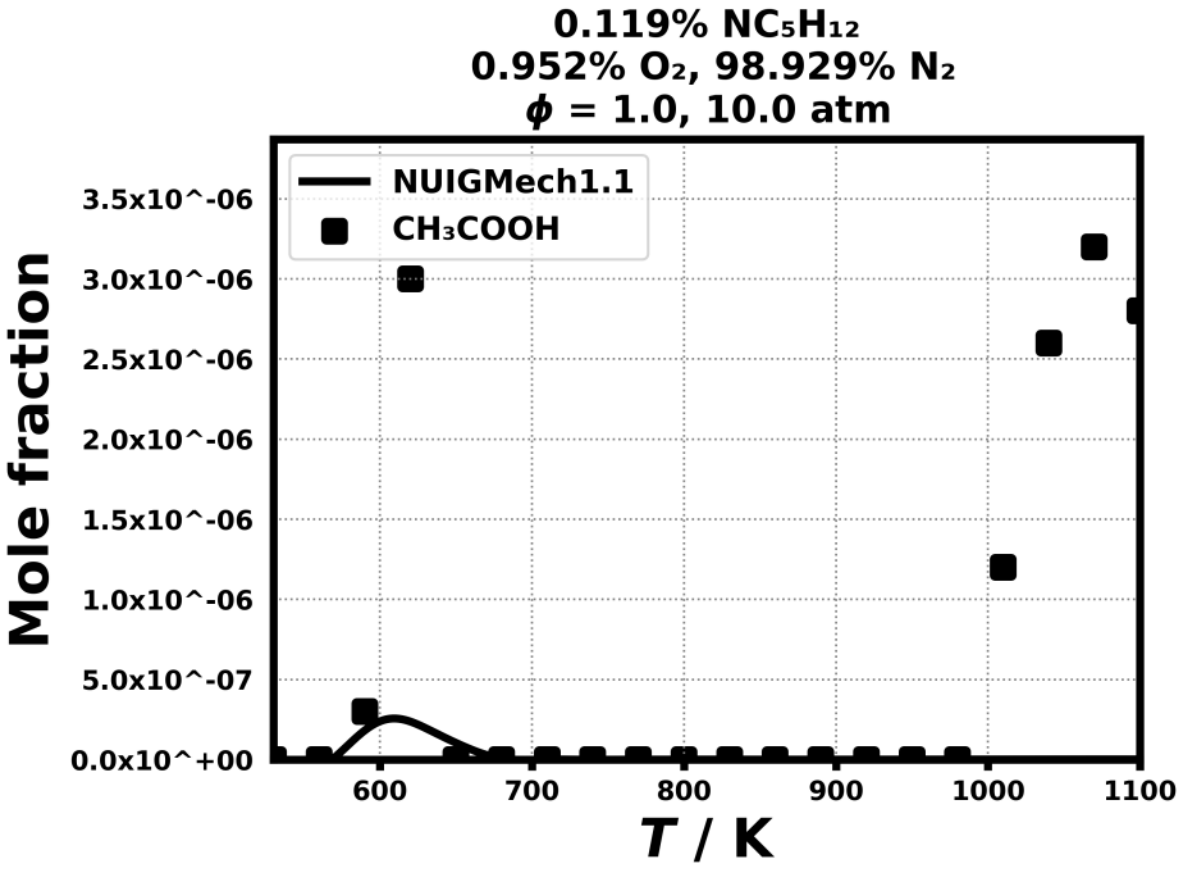

Figure 261: Dataset: 10_ATM_PHI_1.0

1.3.232 Case: n-C5H12/JSR/BUGLER/10_ATM_PHI_2.0

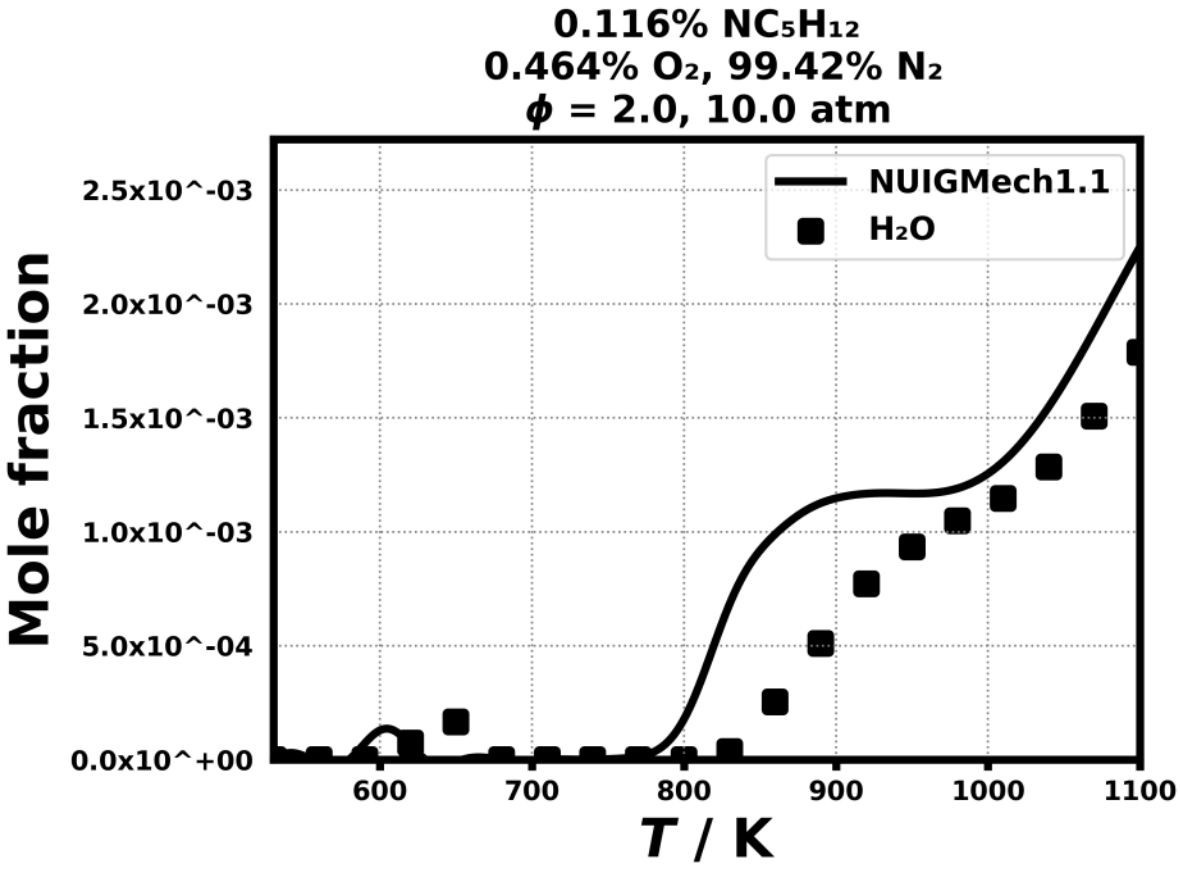

Figure 262: Dataset: 10_ATM_PHI_2.0

1.3.233 Case: n-C5H12/JSR/BUGLER/10_ATM_PHI_2.0

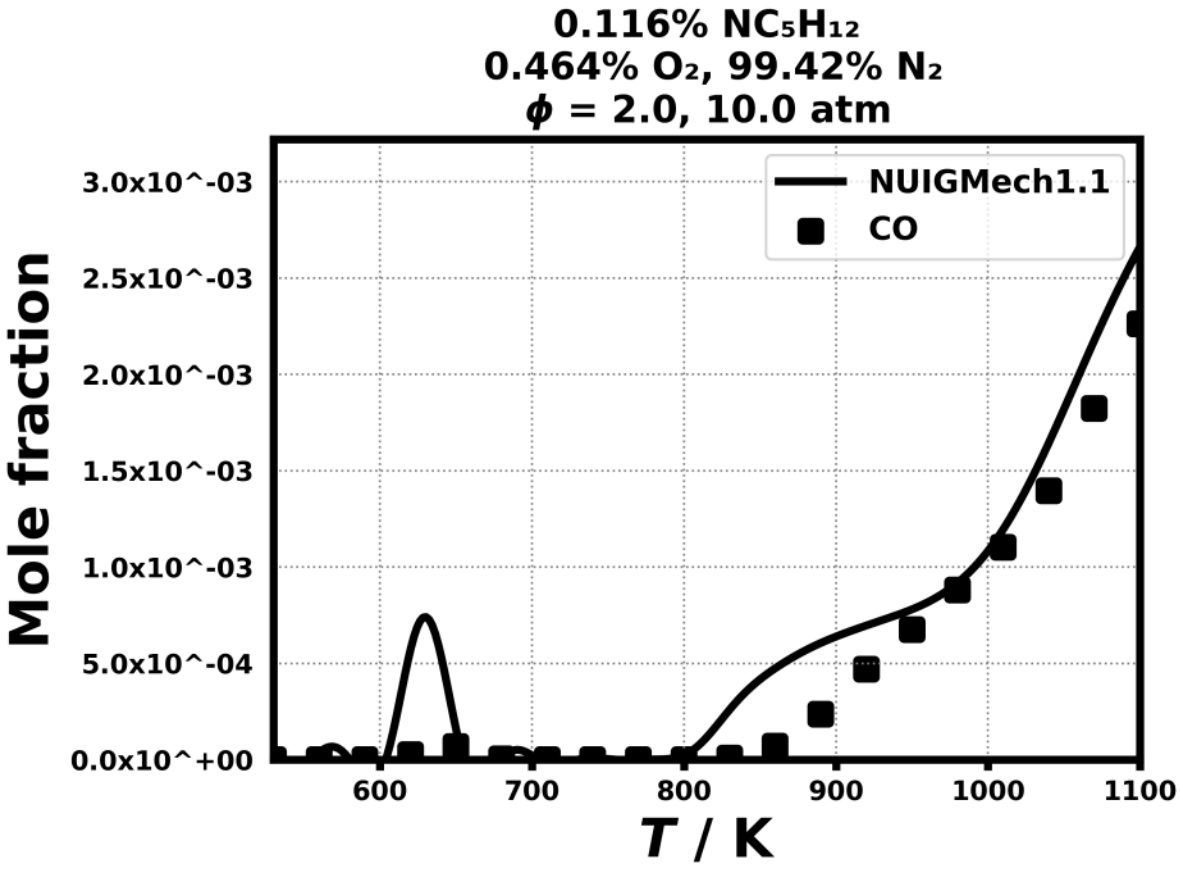

Figure 263: Dataset: 10_ATM_PHI_2.0

1.3.234 Case: n-C5H12/JSR/BUGLER/10_ATM_PHI_2.0

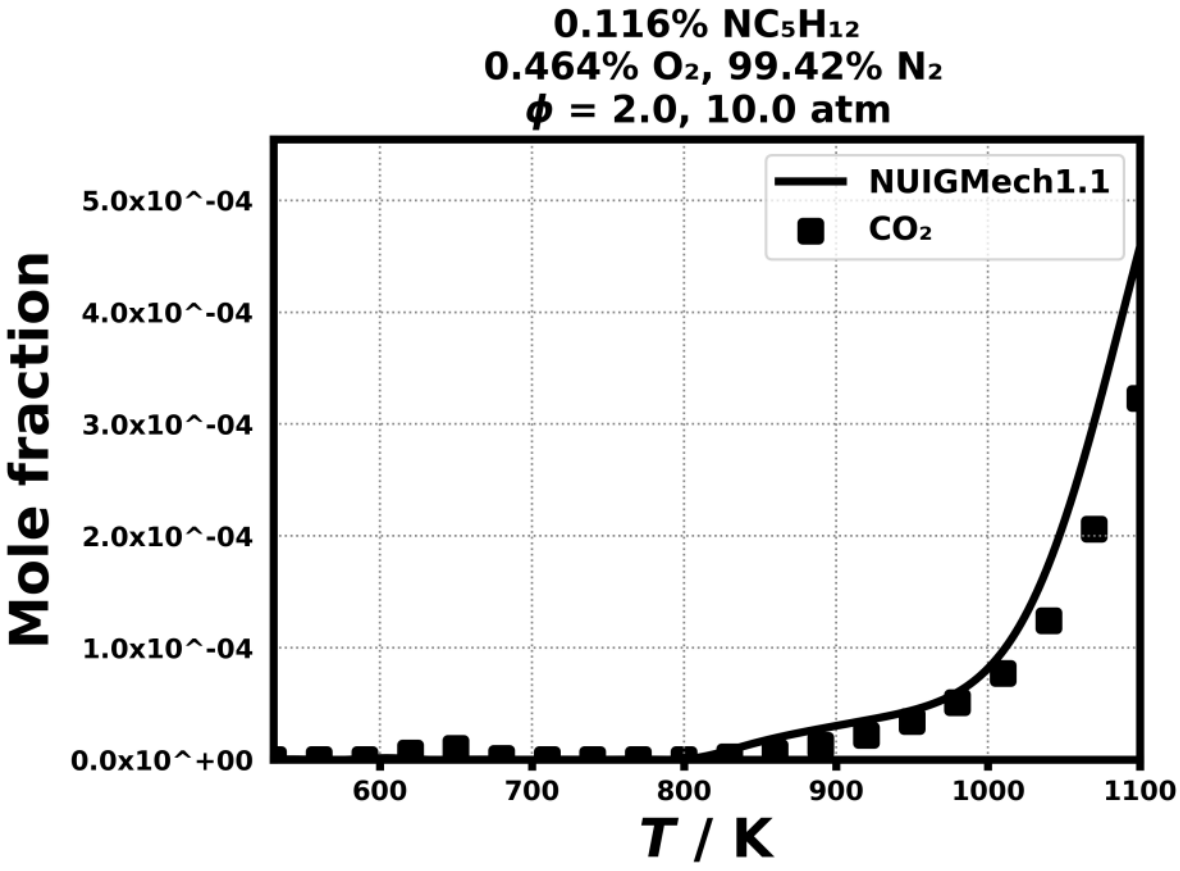

Figure 264: Dataset: 10_ATM_PHI_2.0

1.3.235 Case: n-C5H12/JSR/BUGLER/10_ATM_PHI_2.0

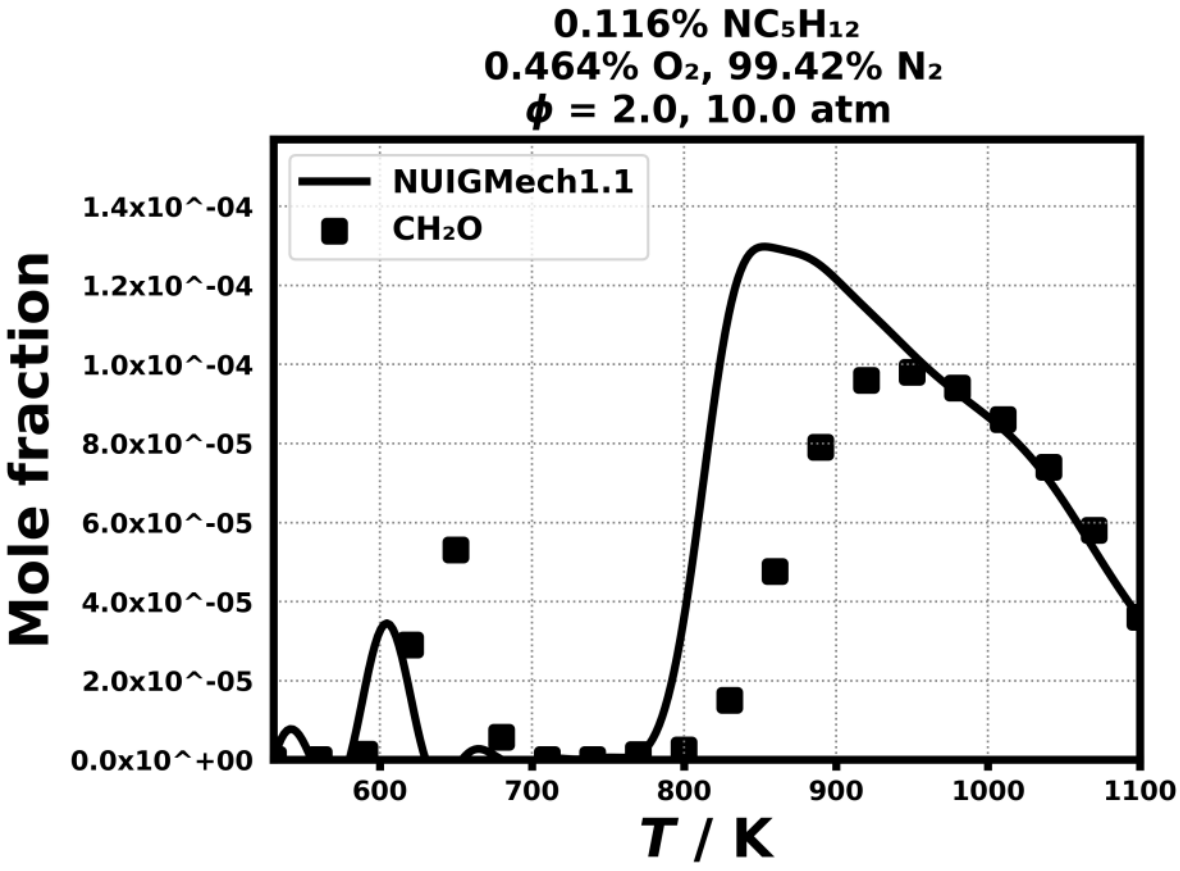

Figure 265: Dataset: 10_ATM_PHI_2.0

1.3.236 Case: n-C5H12/JSR/BUGLER/10_ATM_PHI_2.0

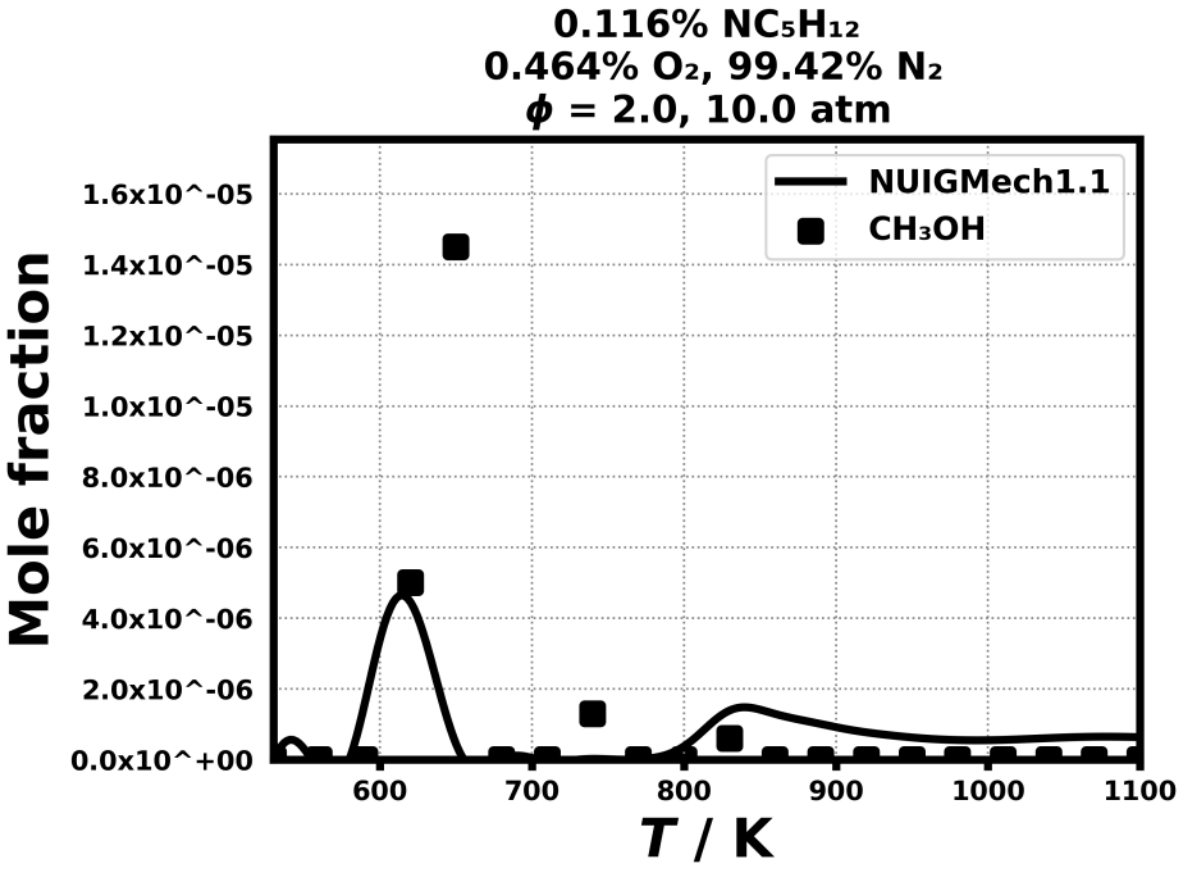

Figure 266: Dataset: 10_ATM_PHI_2.0

1.3.237 Case: n-C5H12/JSR/BUGLER/10_ATM_PHI_2.0

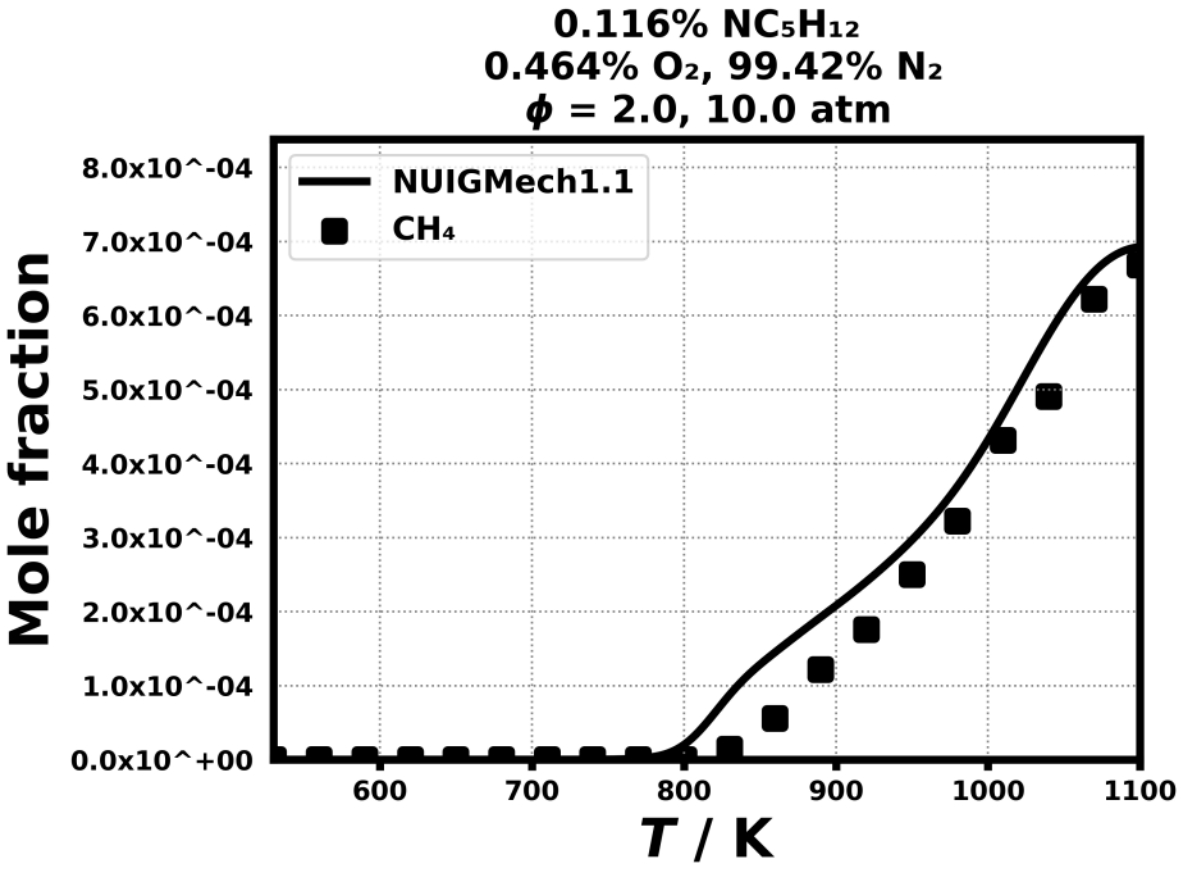

Figure 267: Dataset: 10_ATM_PHI_2.0

1.3.238 Case: n-C5H12/JSR/BUGLER/10_ATM_PHI_2.0

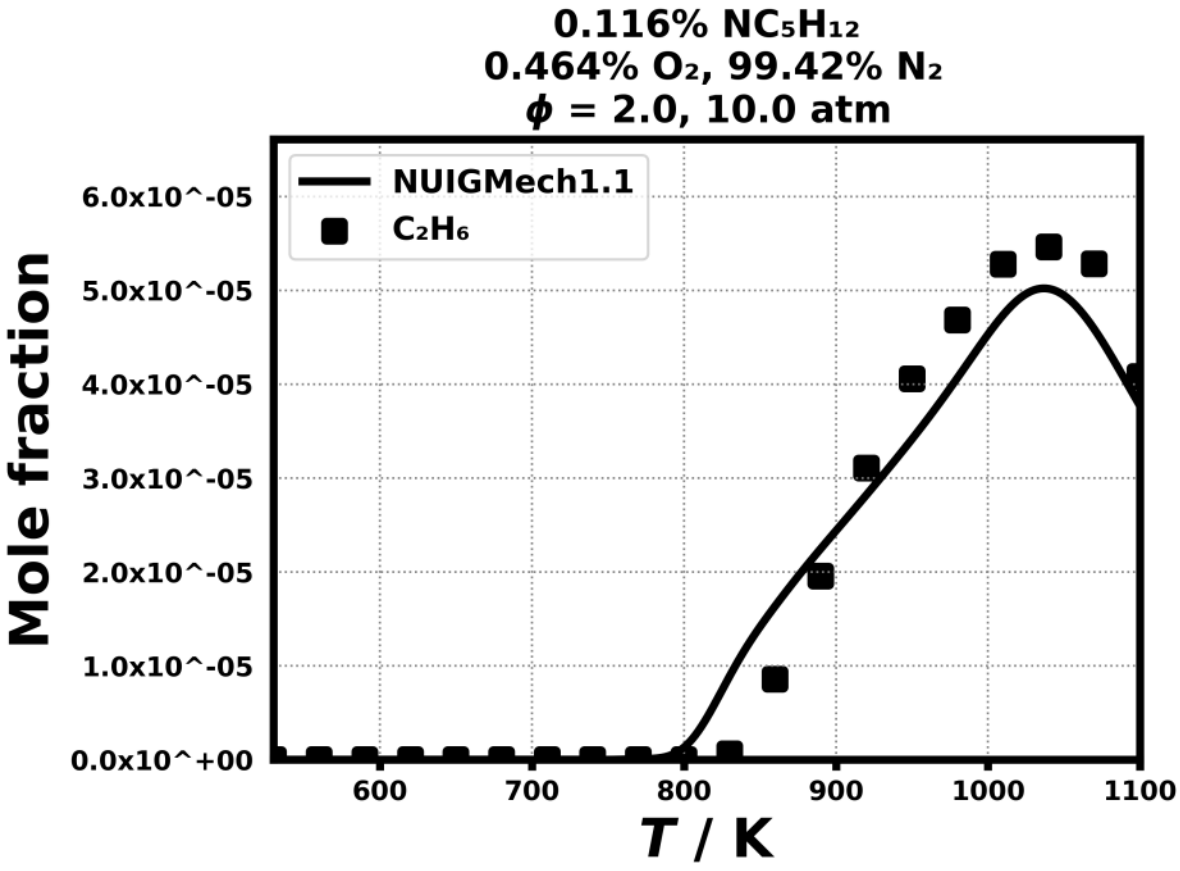

Figure 268: Dataset: 10_ATM_PHI_2.0

1.3.239 Case: n-C5H12/JSR/BUGLER/10_ATM_PHI_2.0

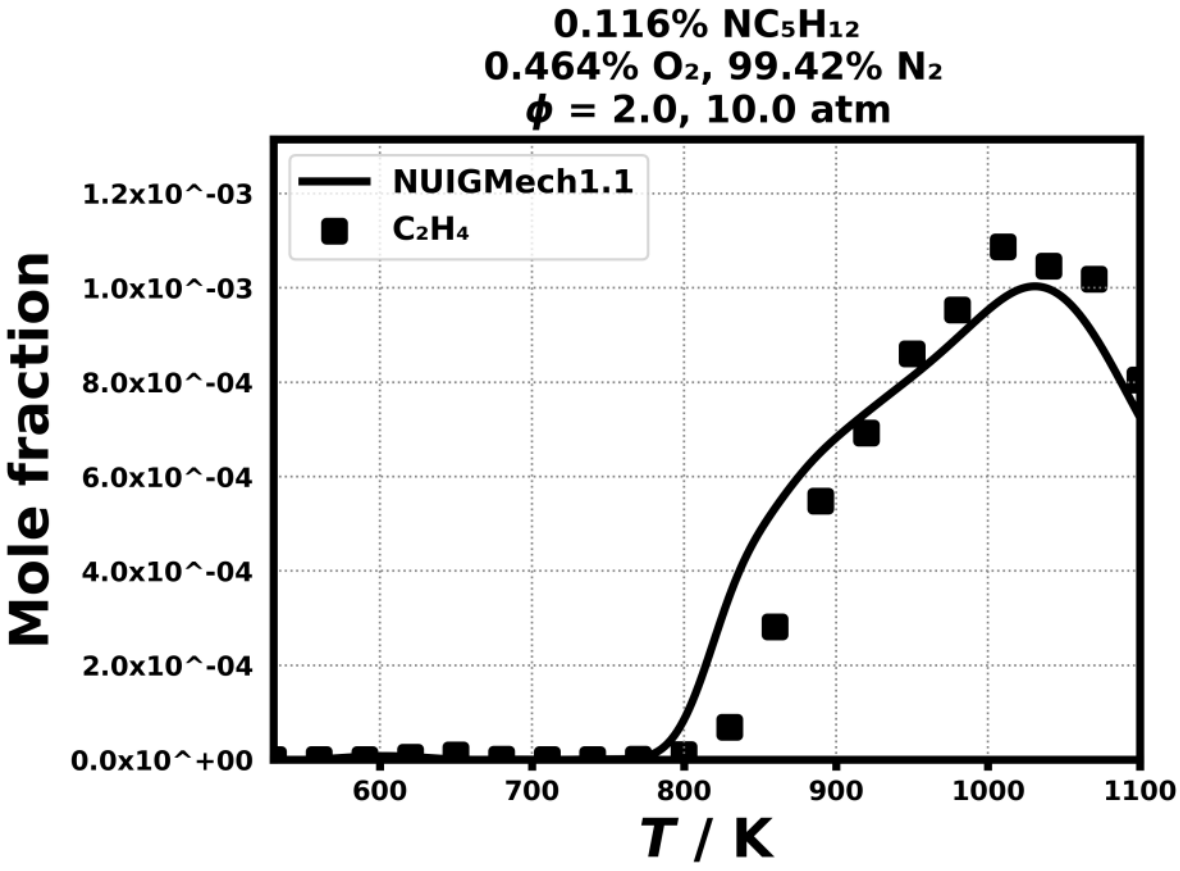

Figure 269: Dataset: 10_ATM_PHI_2.0

1.3.240 Case: n-C5H12/JSR/BUGLER/10_ATM_PHI_2.0

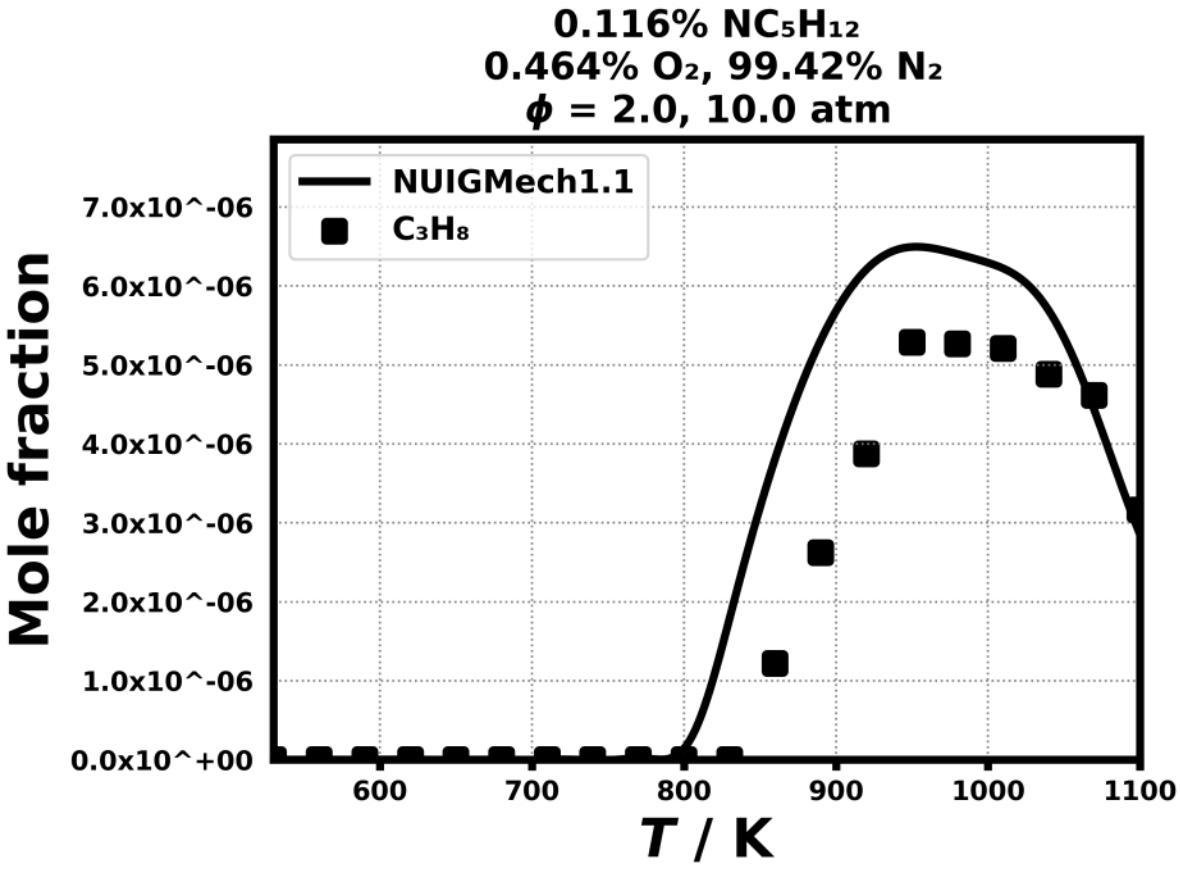

Figure 270: Dataset: 10_ATM_PHI_2.0

1.3.241 Case: n-C5H12/JSR/BUGLER/10_ATM_PHI_2.0

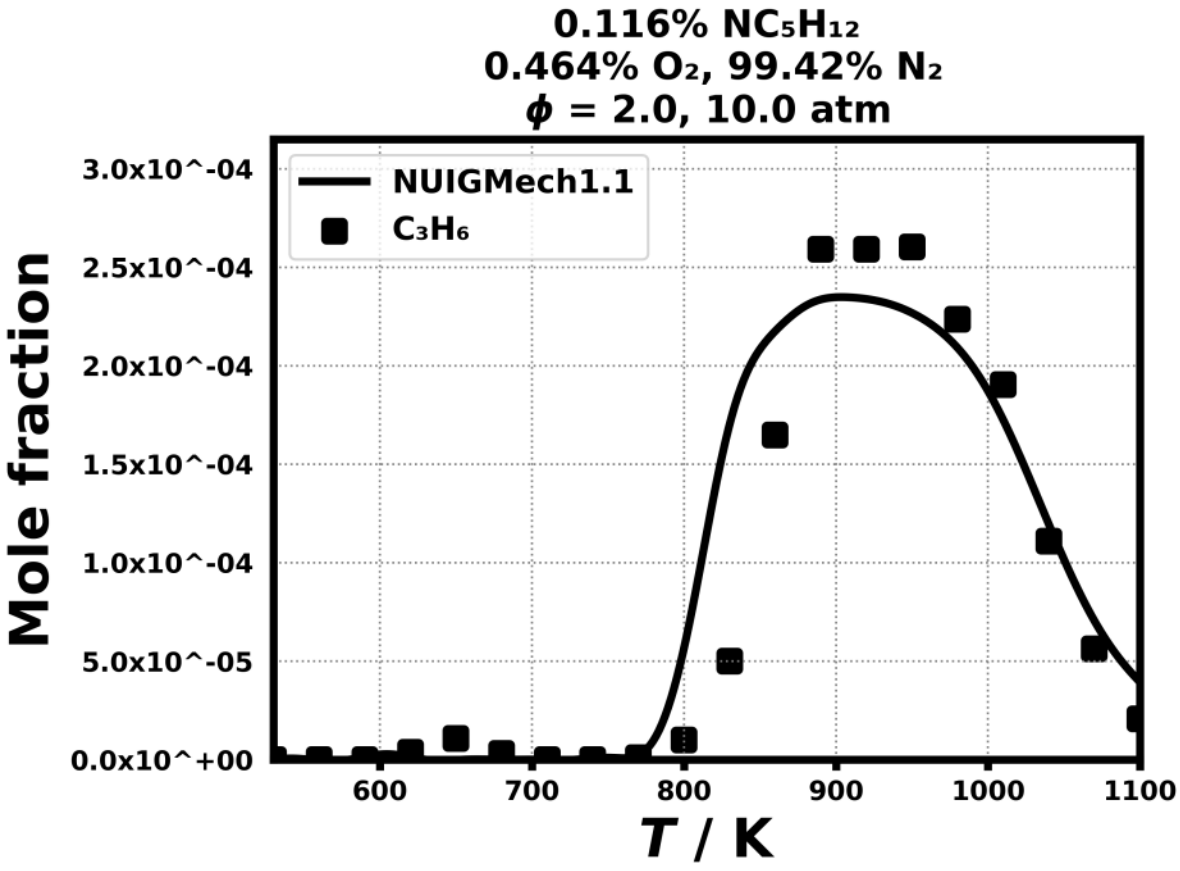

Figure 271: Dataset: 10_ATM_PHI_2.0

1.3.242 Case: n-C5H12/JSR/BUGLER/10_ATM_PHI_2.0

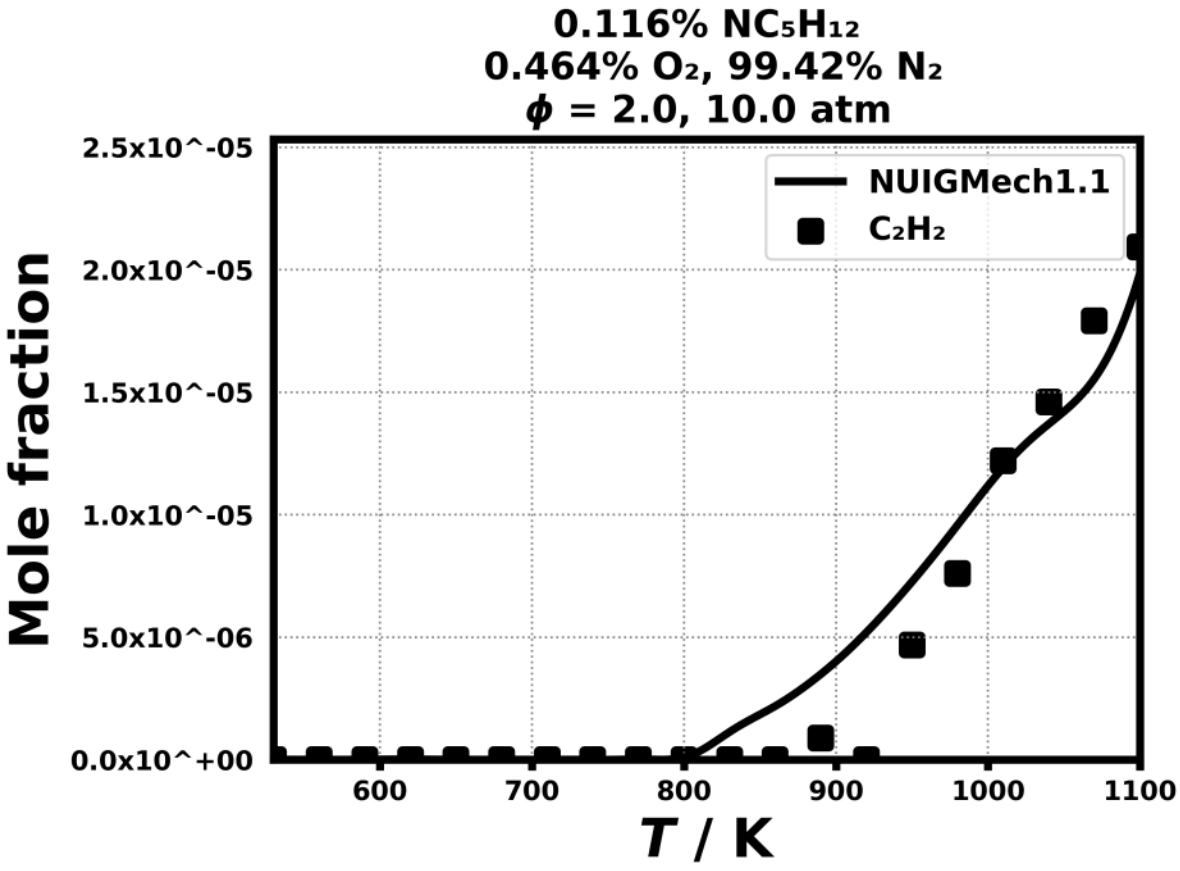

Figure 272: Dataset: 10_ATM_PHI_2.0

1.3.243 Case: n-C5H12/JSR/BUGLER/10_ATM_PHI_2.0

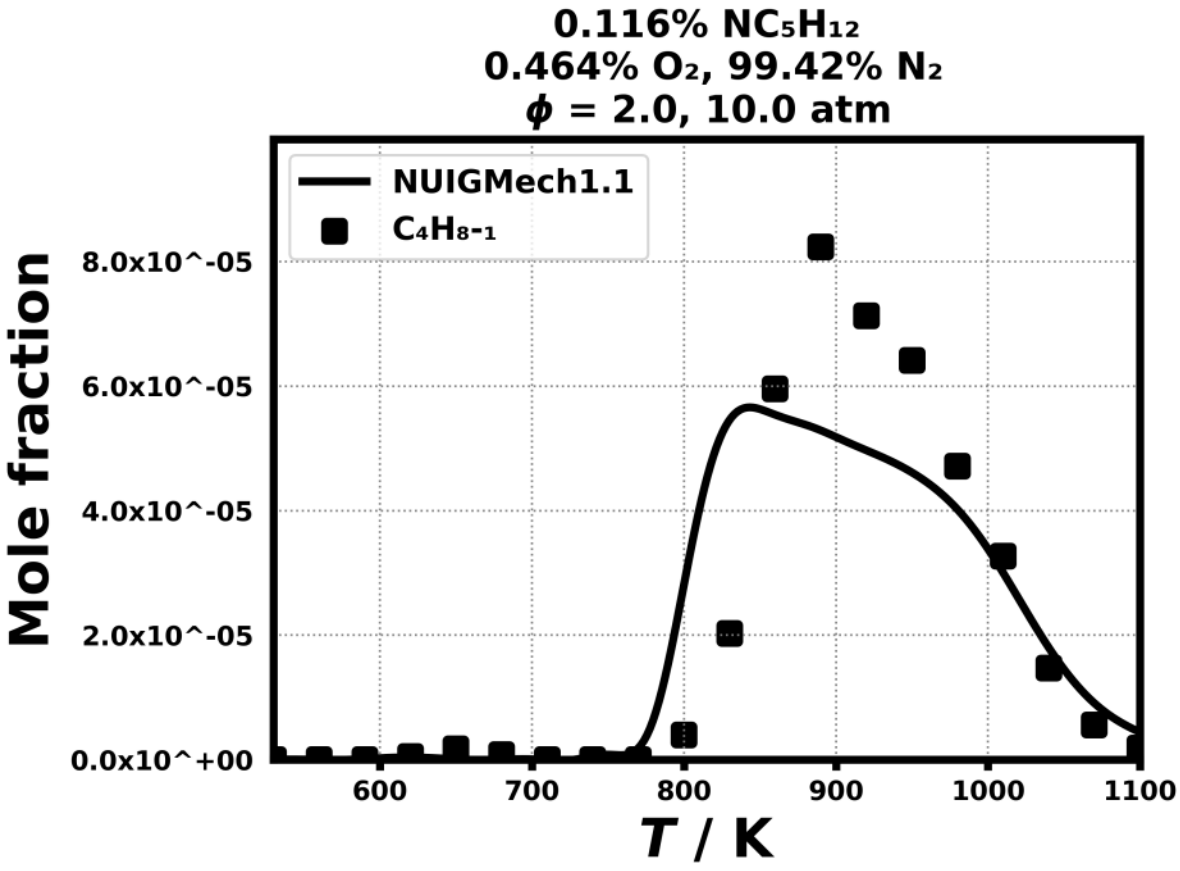

Figure 273: Dataset: 10_ATM_PHI_2.0

1.3.244 Case: n-C5H12/JSR/BUGLER/10_ATM_PHI_2.0

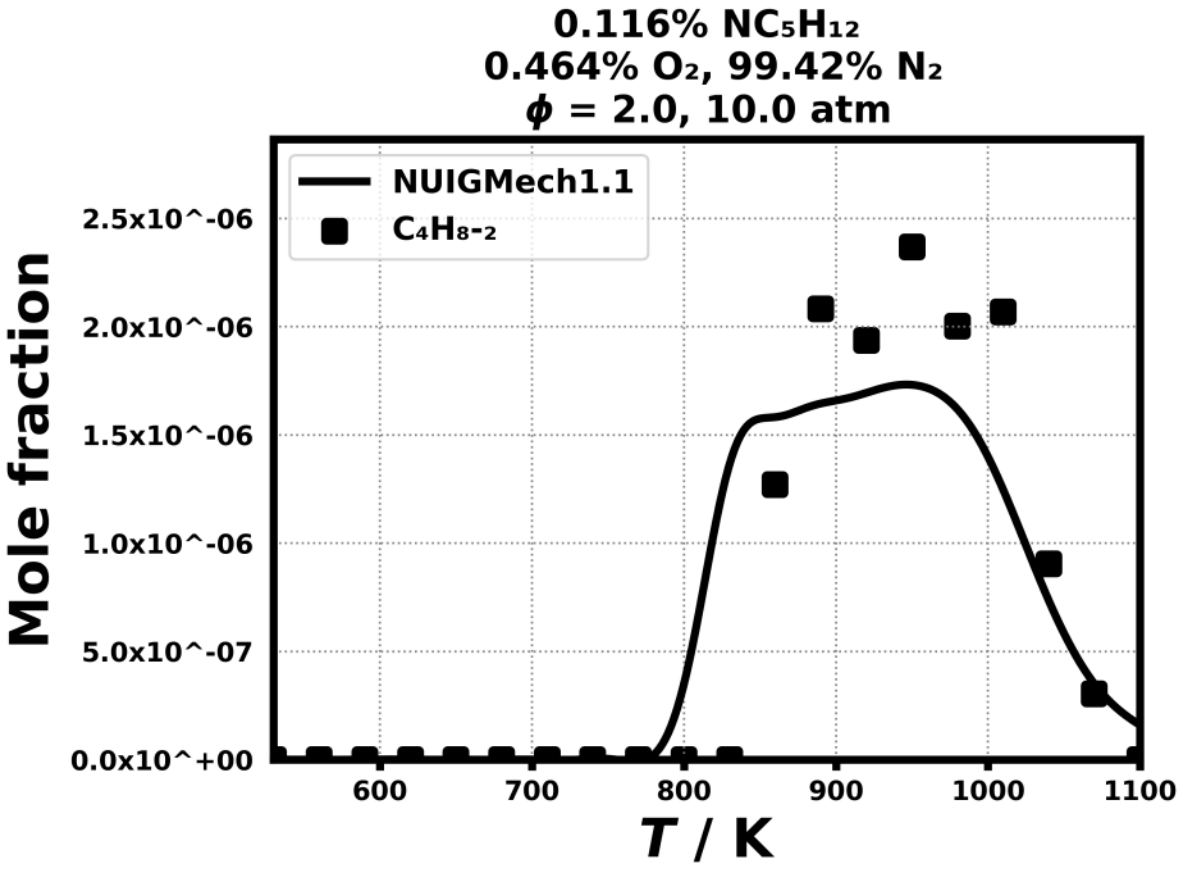

Figure 274: Dataset: 10_ATM_PHI_2.0

1.3.245 Case: n-C5H12/JSR/BUGLER/10_ATM_PHI_2.0

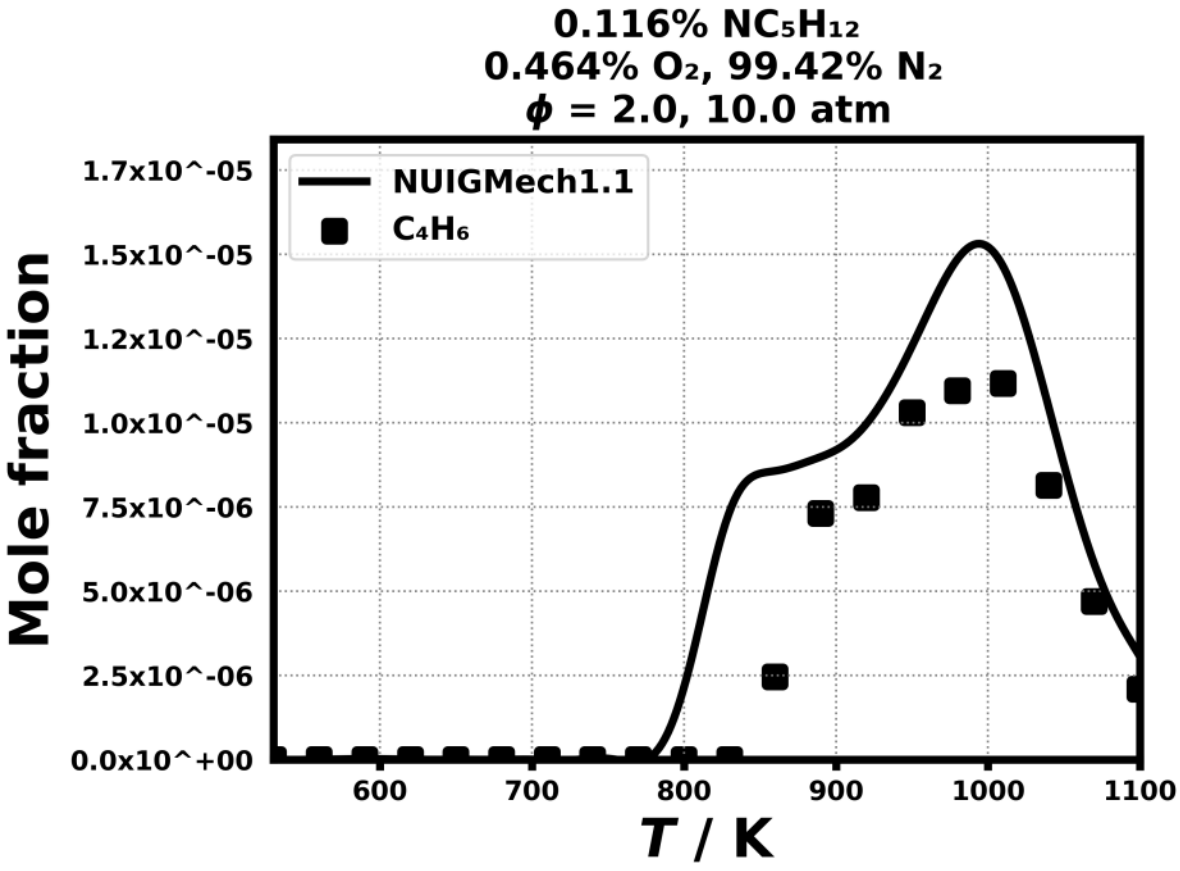

Figure 275: Dataset: 10_ATM_PHI_2.0

1.3.246 Case: n-C5H12/JSR/BUGLER/10_ATM_PHI_2.0

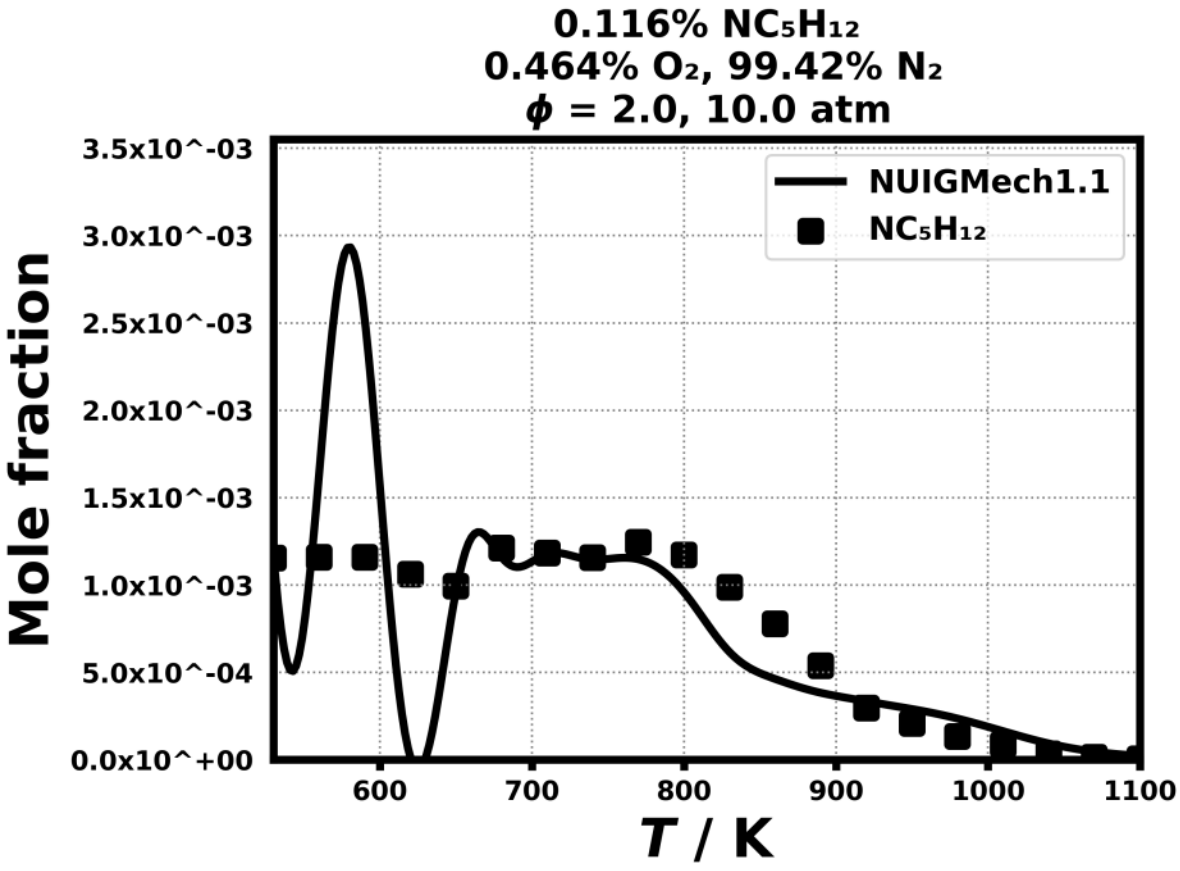

Figure 276: Dataset: 10_ATM_PHI_2.0

1.3.247 Case: n-C5H12/JSR/BUGLER/10_ATM_PHI_2.0

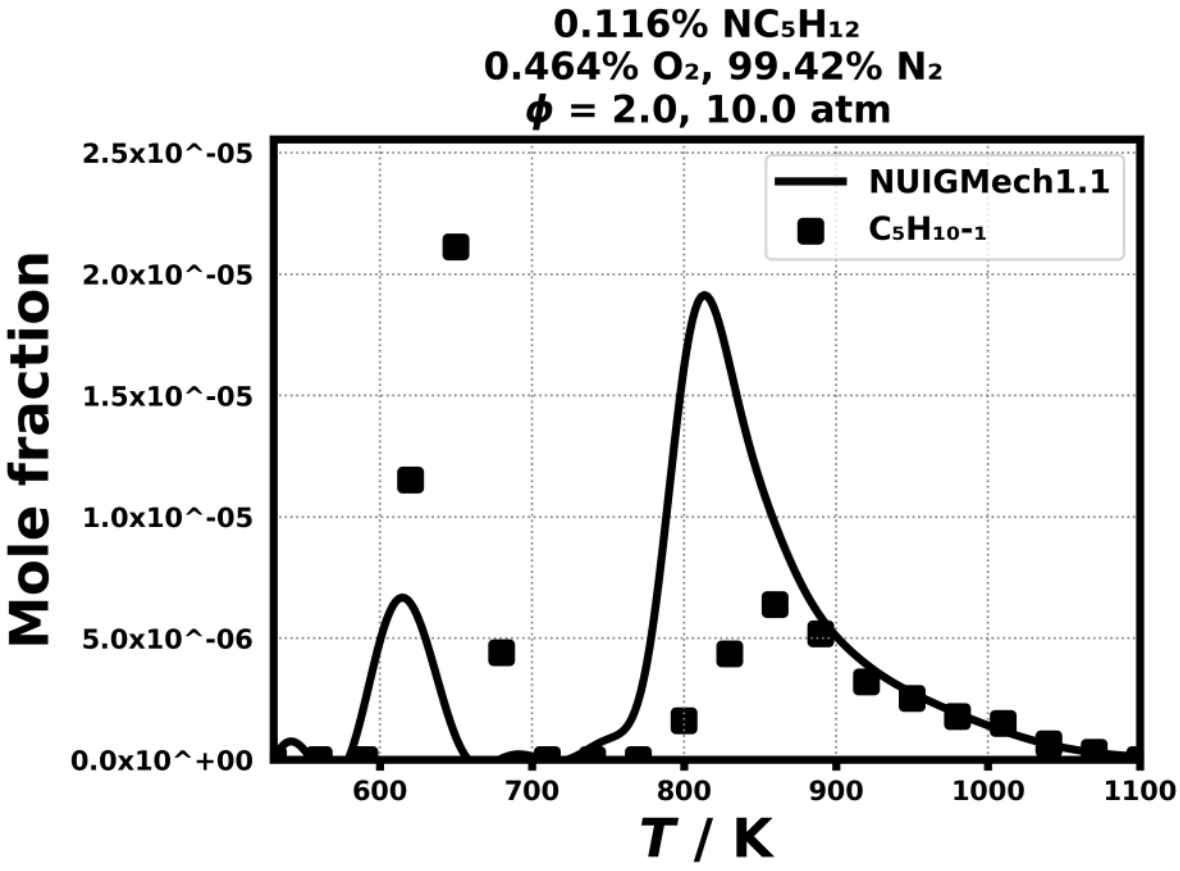

Figure 277: Dataset: 10_ATM_PHI_2.0

1.3.248 Case: n-C5H12/JSR/BUGLER/10_ATM_PHI_2.0

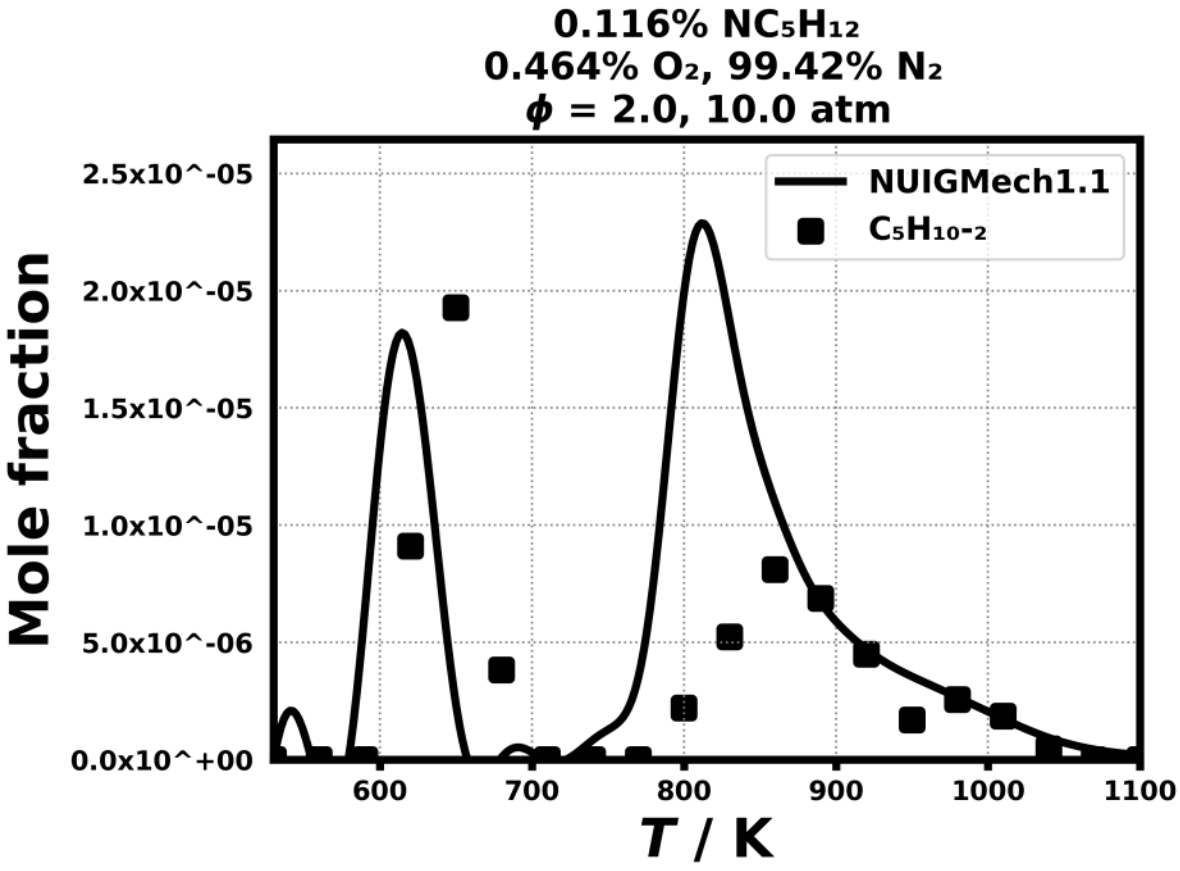

Figure 278: Dataset: 10_ATM_PHI_2.0

1.3.249 Case: n-C5H12/JSR/BUGLER/10_ATM_PHI_2.0

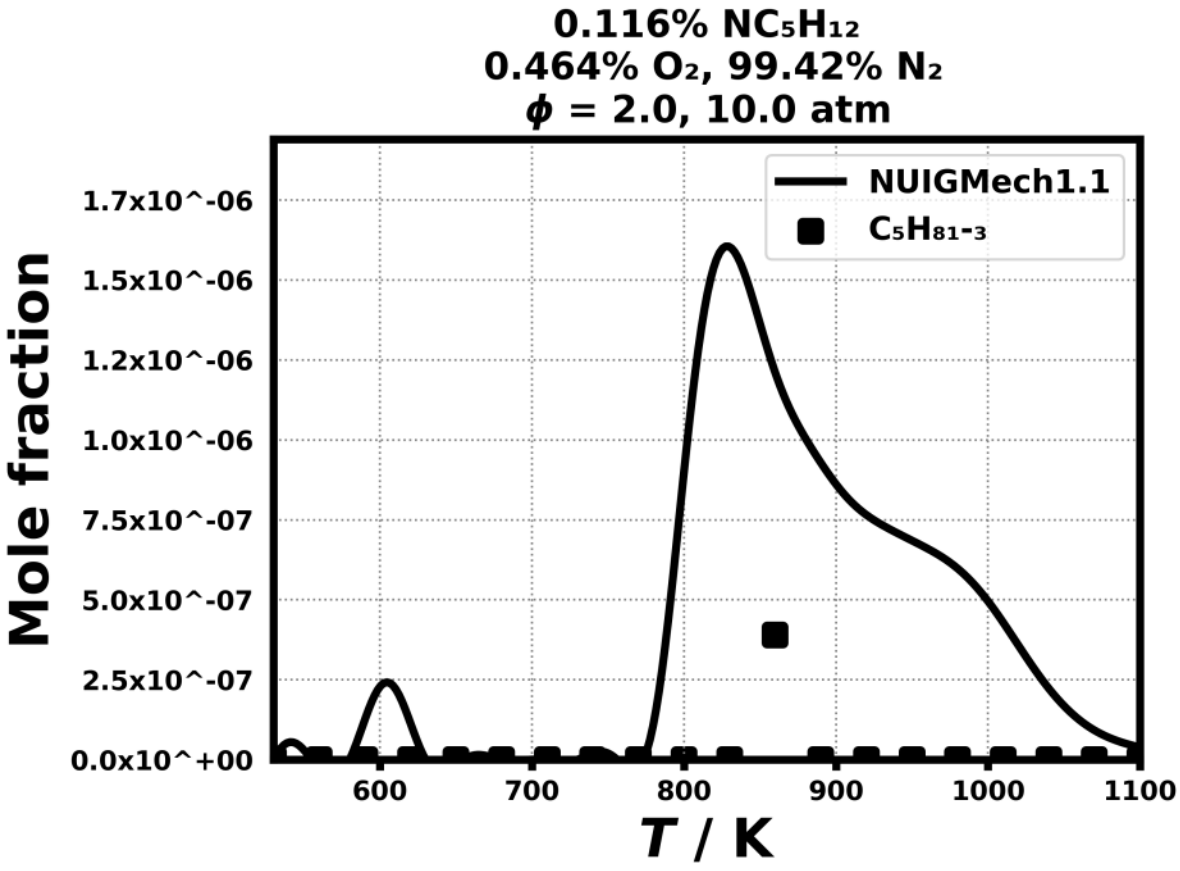

Figure 279: Dataset: 10_ATM_PHI_2.0

1.3.250 Case: n-C5H12/JSR/BUGLER/10_ATM_PHI_2.0

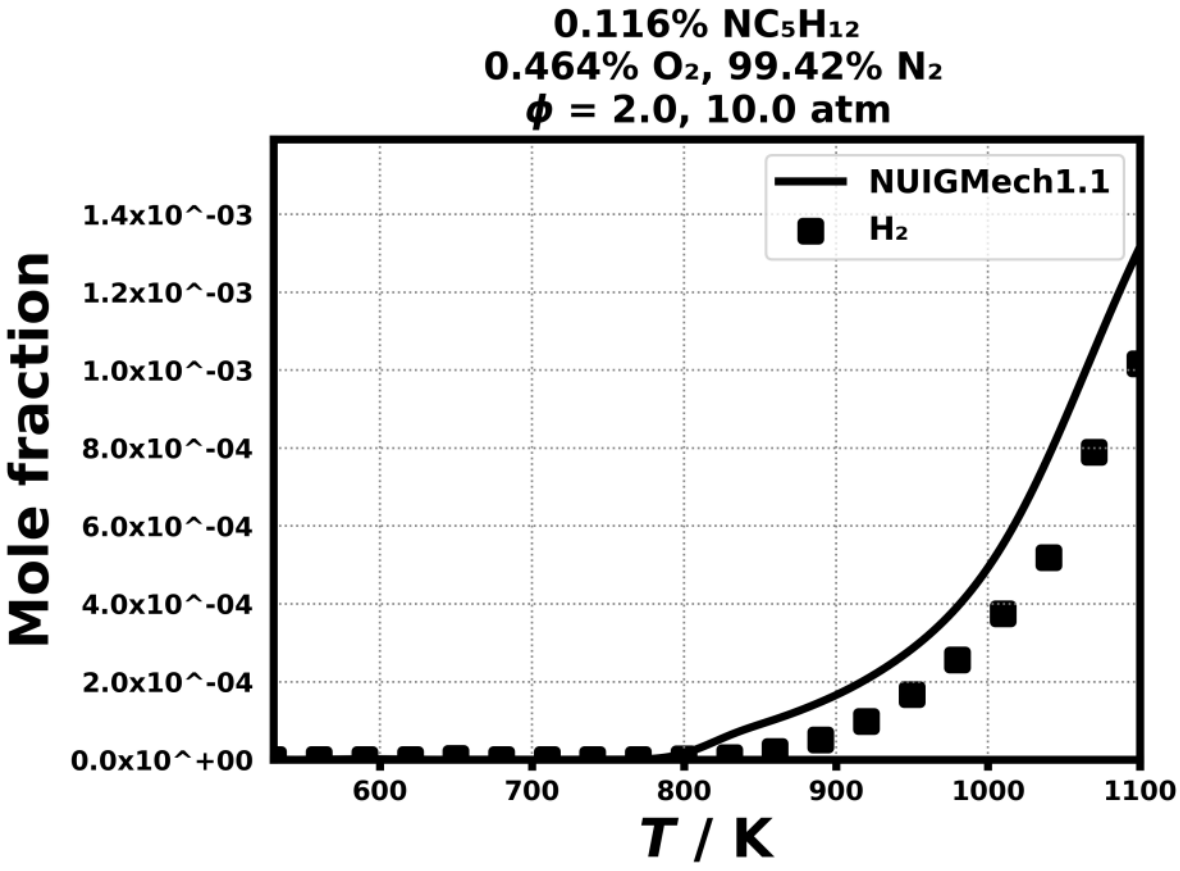

Figure 280: Dataset: 10_ATM_PHI_2.0

1.3.251 Case: n-C5H12/JSR/BUGLER/10_ATM_PHI_2.0

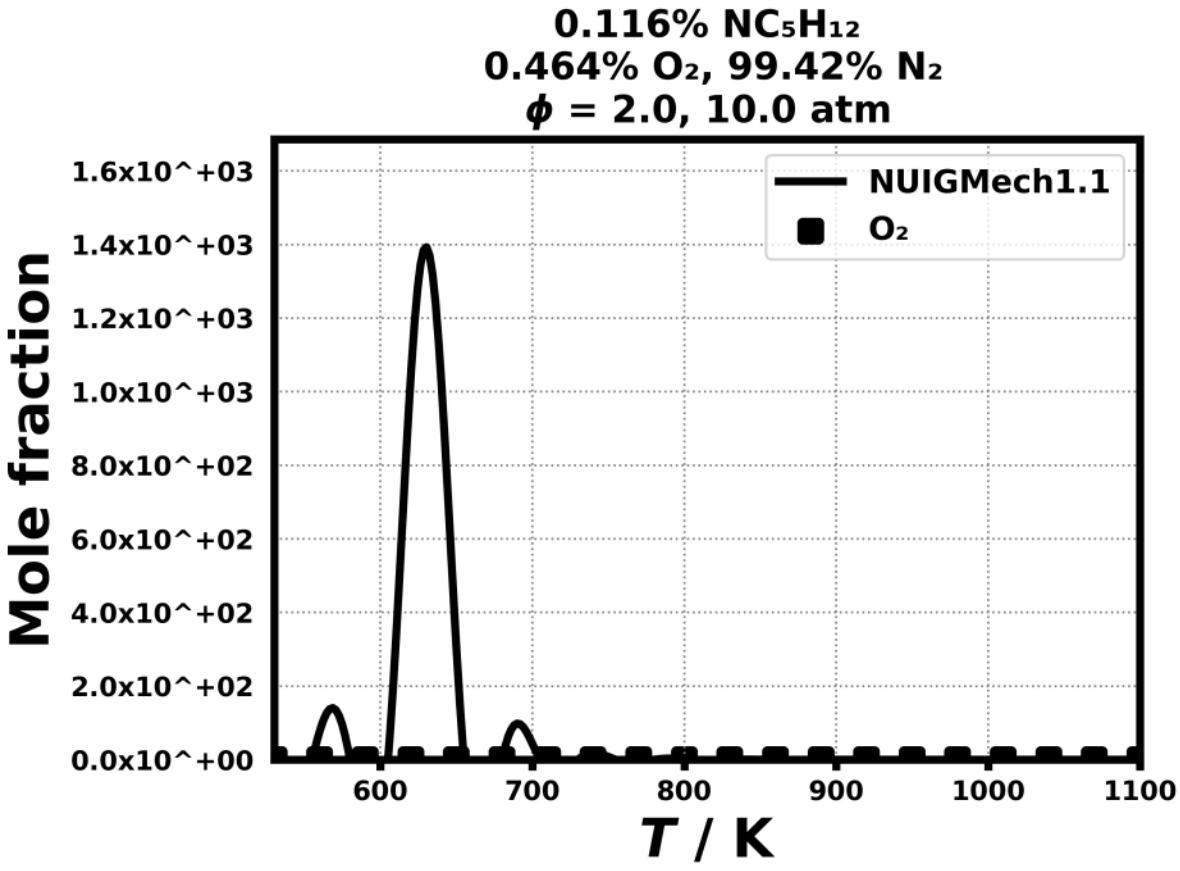

Figure 281: Dataset: 10_ATM_PHI_2.0

1.3.252 Case: n-C5H12/JSR/BUGLER/10_ATM_PHI_2.0

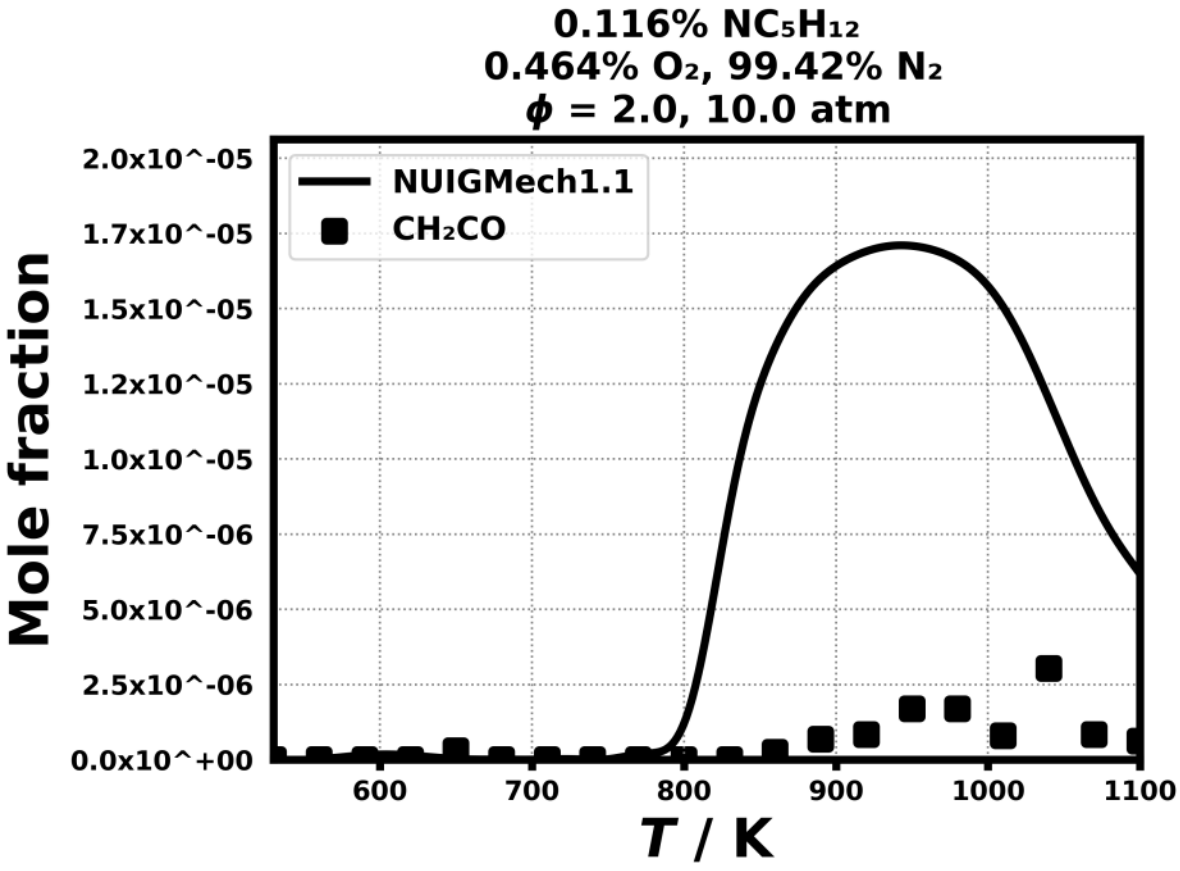

Figure 282: Dataset: 10_ATM_PHI_2.0

1.3.253 Case: n-C5H12/JSR/BUGLER/10_ATM_PHI_2.0

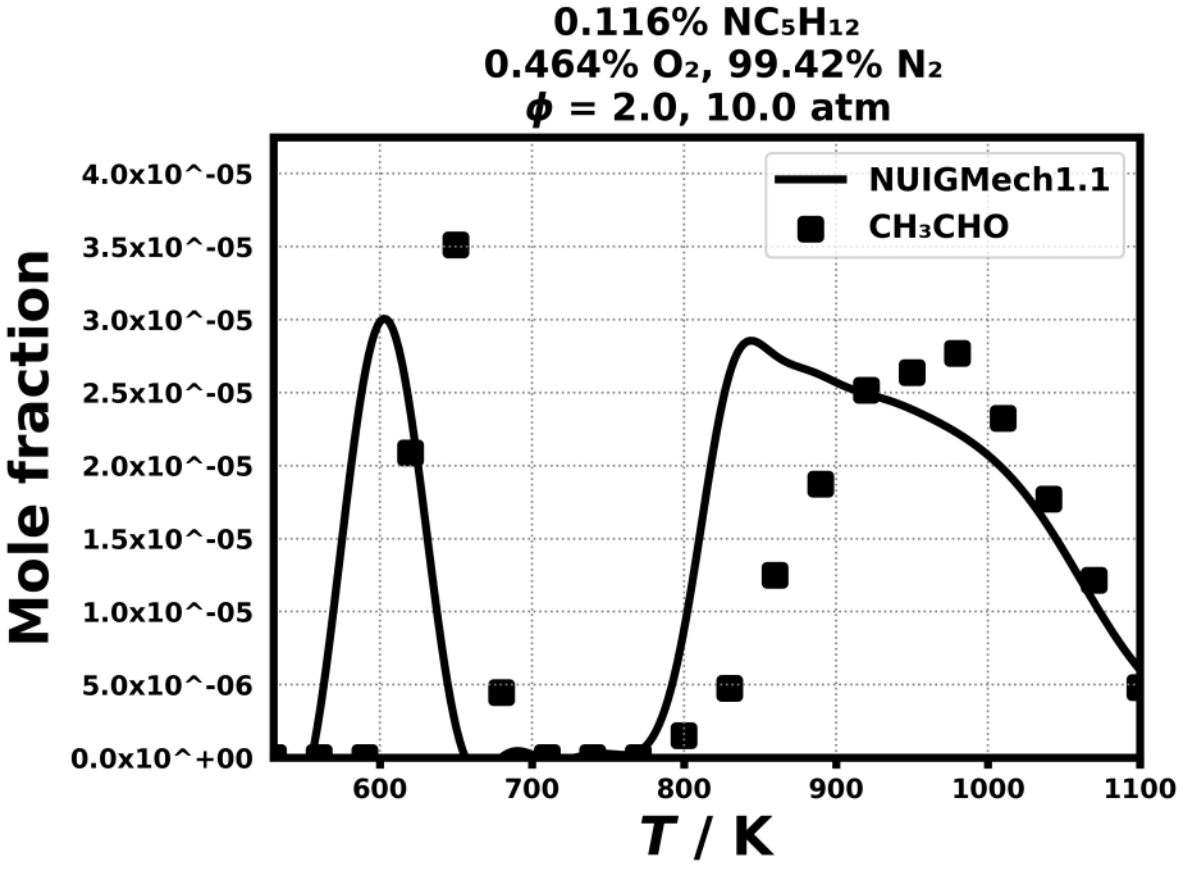

Figure 283: Dataset: 10_ATM_PHI_2.0

1.3.254 Case: n-C5H12/JSR/BUGLER/10_ATM_PHI_2.0

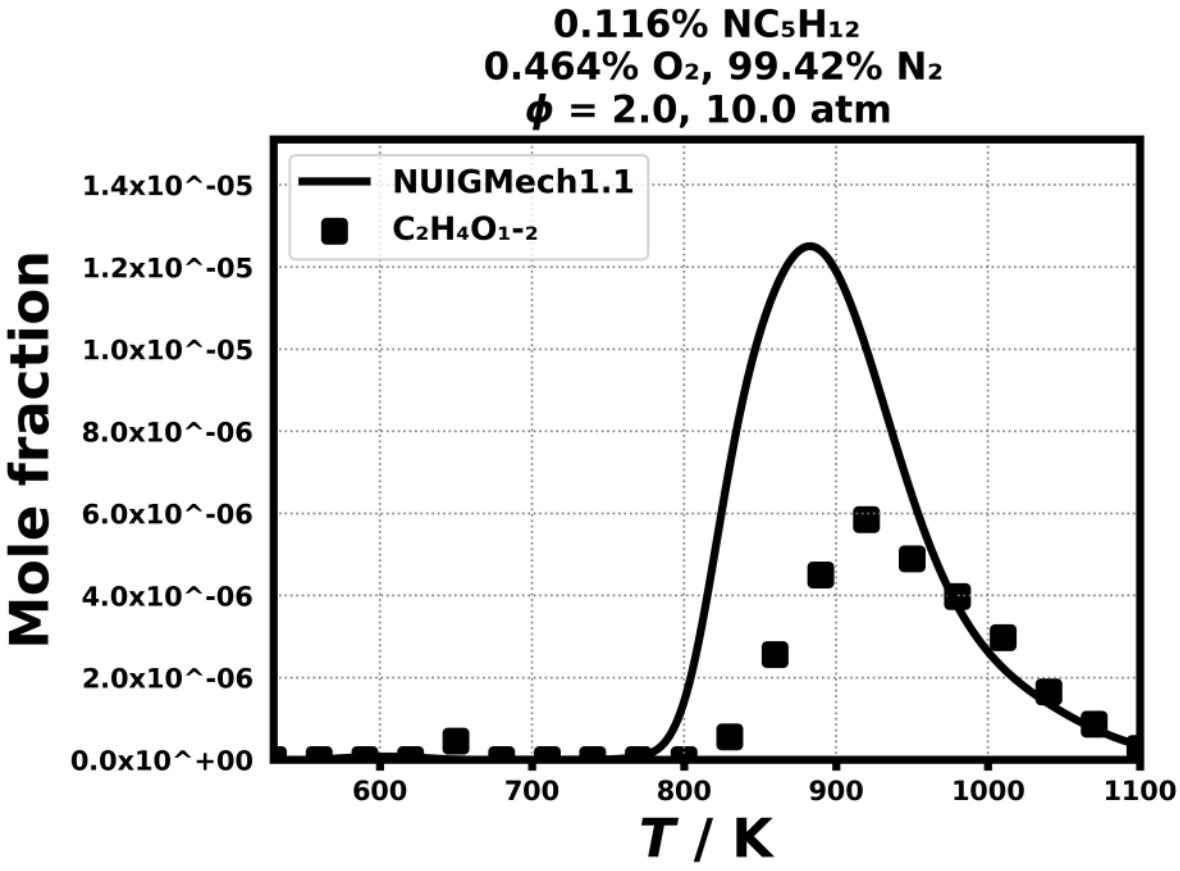

Figure 284: Dataset: 10_ATM_PHI_2.0

1.3.255 Case: n-C5H12/JSR/BUGLER/10_ATM_PHI_2.0

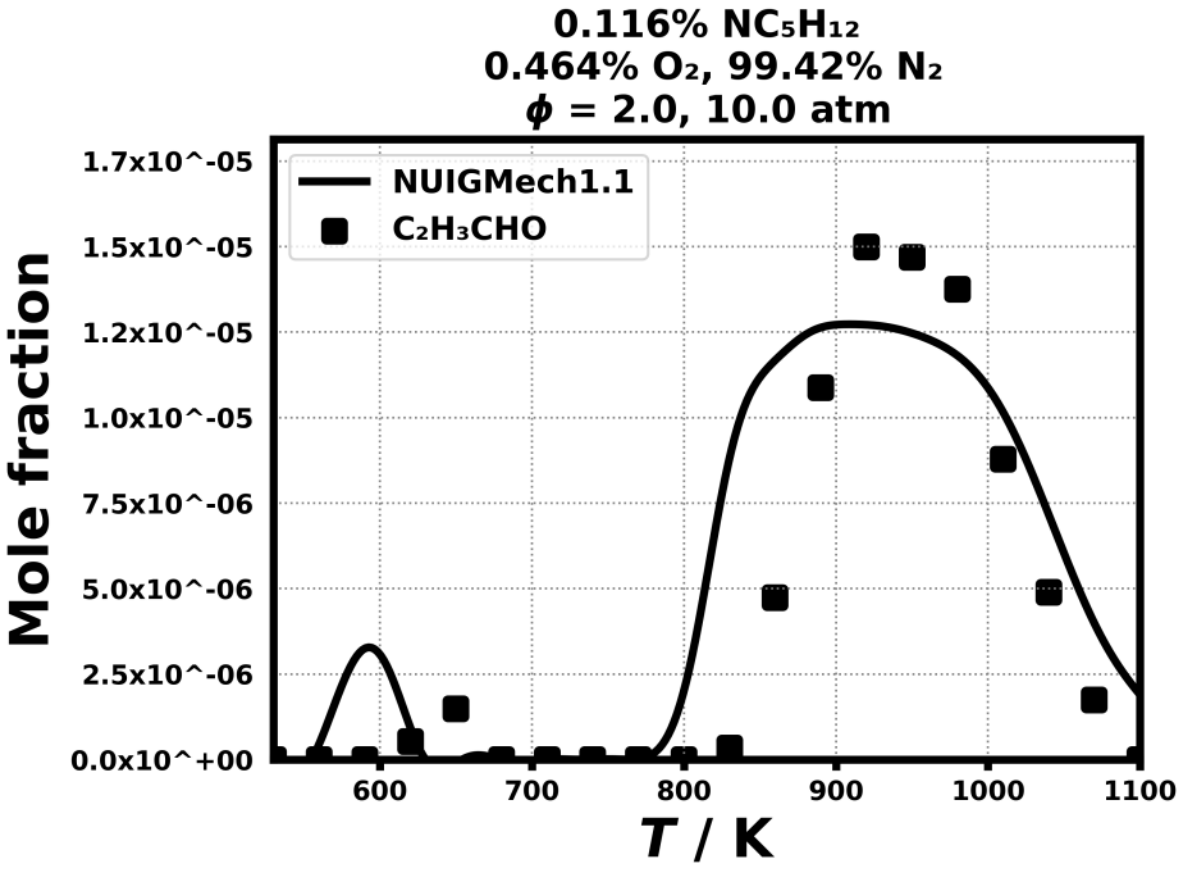

Figure 285: Dataset: 10_ATM_PHI_2.0

1.3.256 Case: n-C5H12/JSR/BUGLER/10_ATM_PHI_2.0

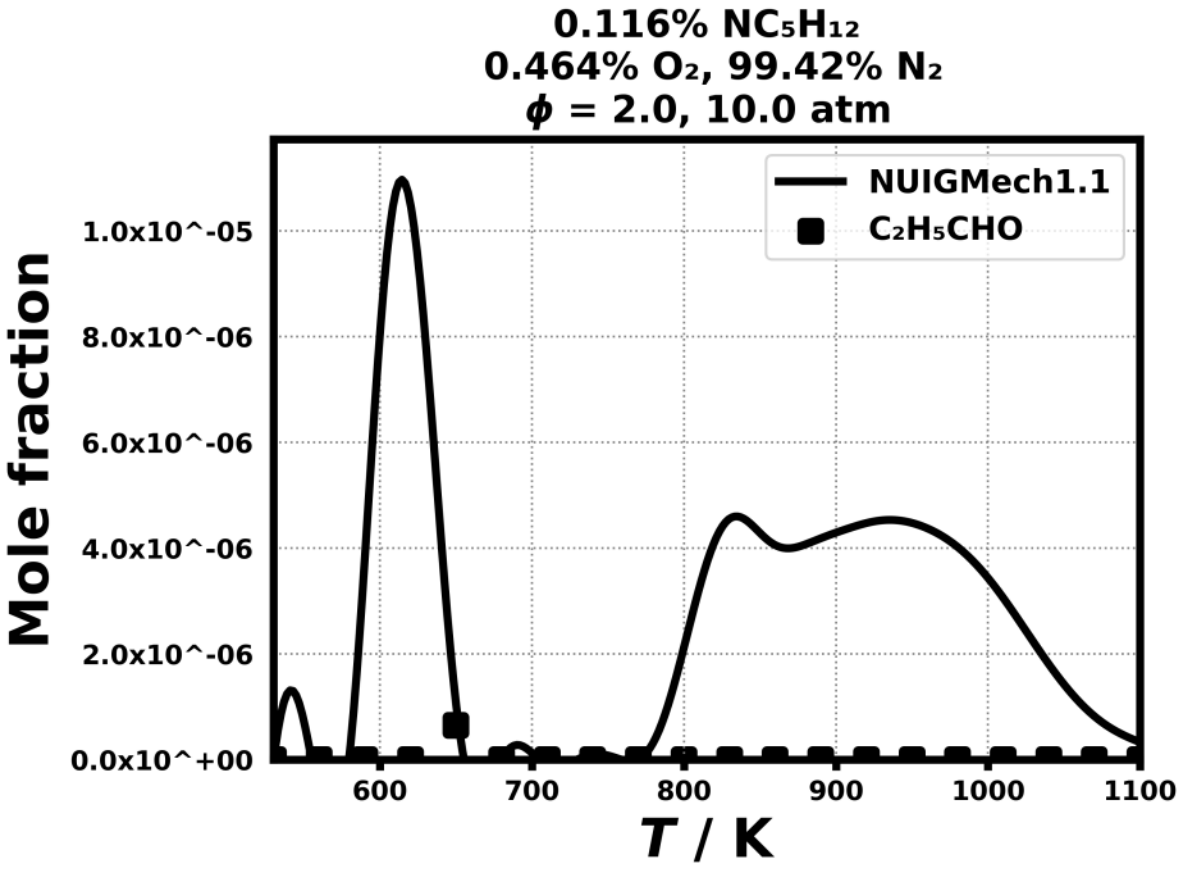

Figure 286: Dataset: 10_ATM_PHI_2.0

1.3.257 Case: n-C5H12/JSR/BUGLER/10_ATM_PHI_2.0

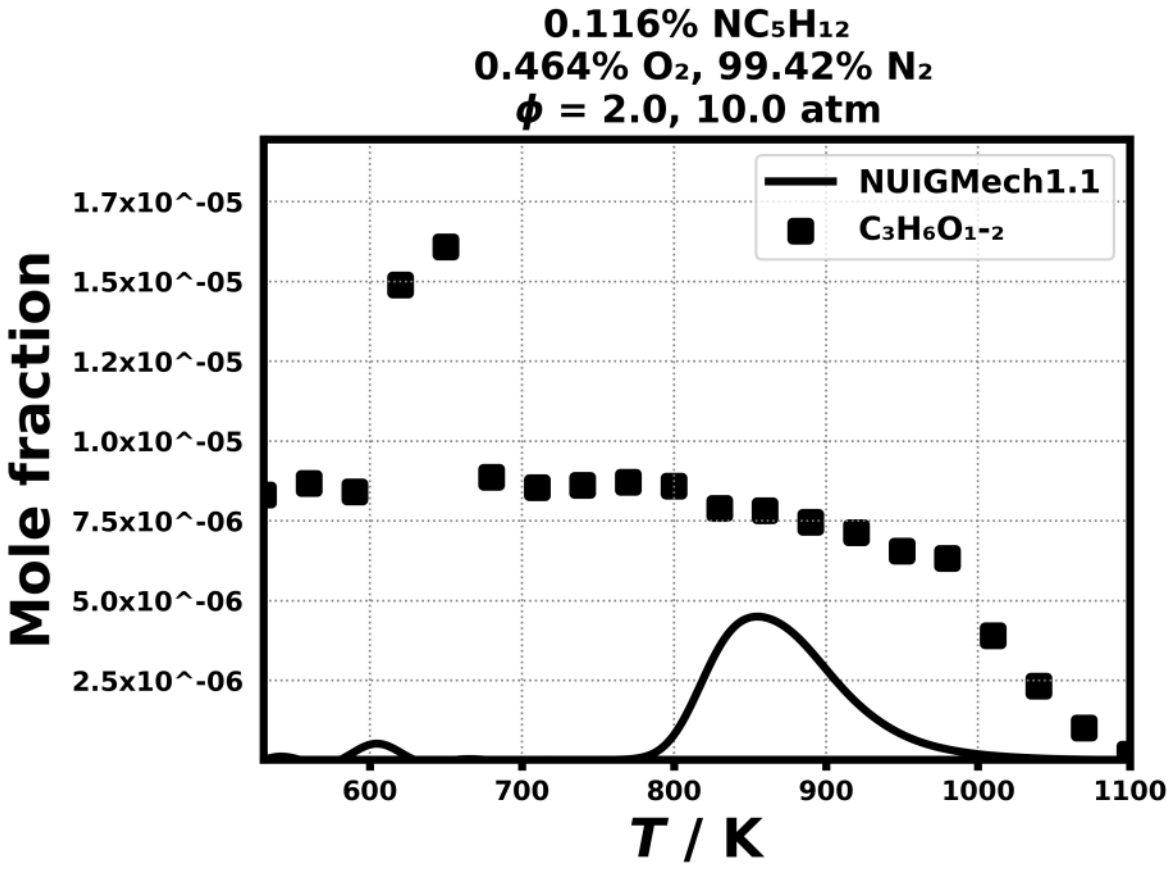

Figure 287: Dataset: 10_ATM_PHI_2.0

1.3.258 Case: n-C5H12/JSR/BUGLER/10_ATM_PHI_2.0

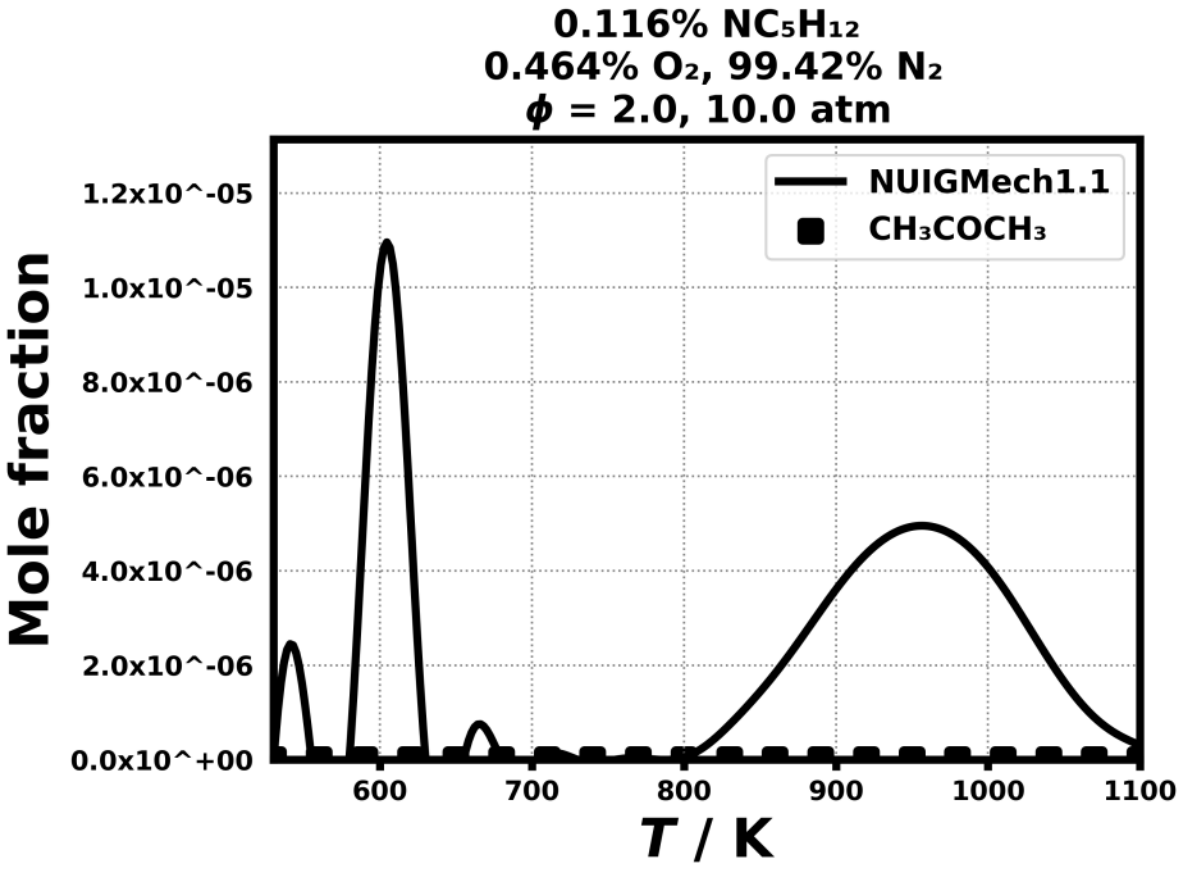

Figure 288: Dataset: 10_ATM_PHI_2.0

1.3.259 Case: n-C5H12/JSR/BUGLER/10_ATM_PHI_2.0

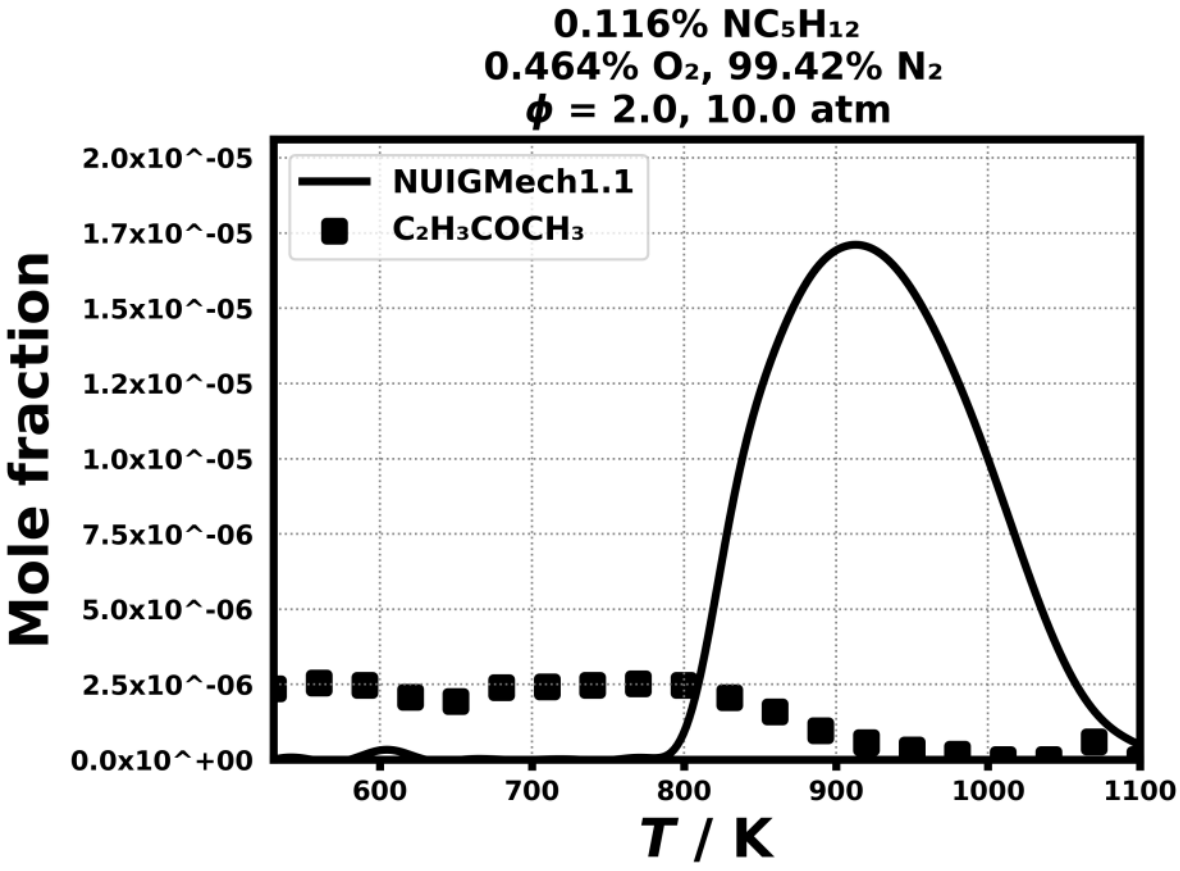

Figure 289: Dataset: 10_ATM_PHI_2.0

1.3.260 Case: n-C5H12/JSR/BUGLER/10_ATM_PHI_2.0

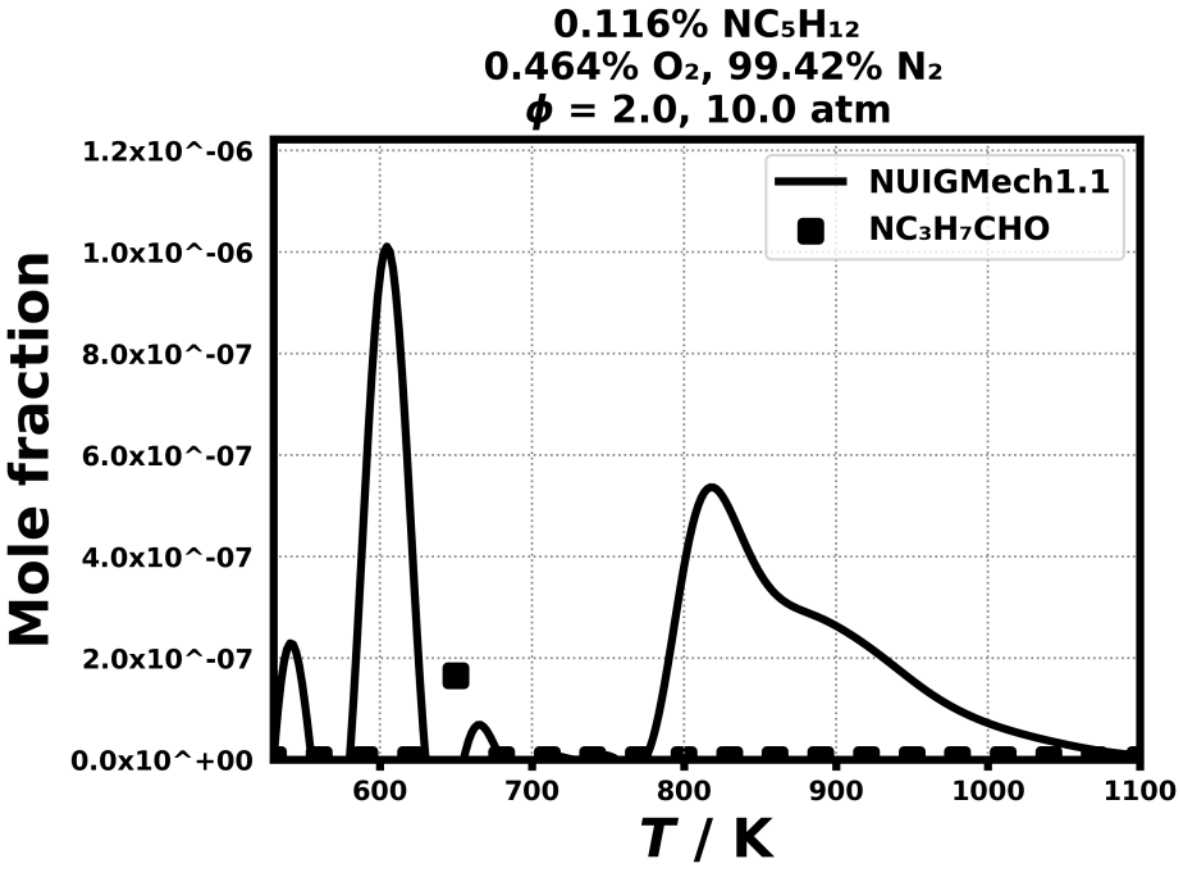

Figure 290: Dataset: 10_ATM_PHI_2.0

1.3.261 Case: n-C5H12/JSR/BUGLER/10_ATM_PHI_2.0

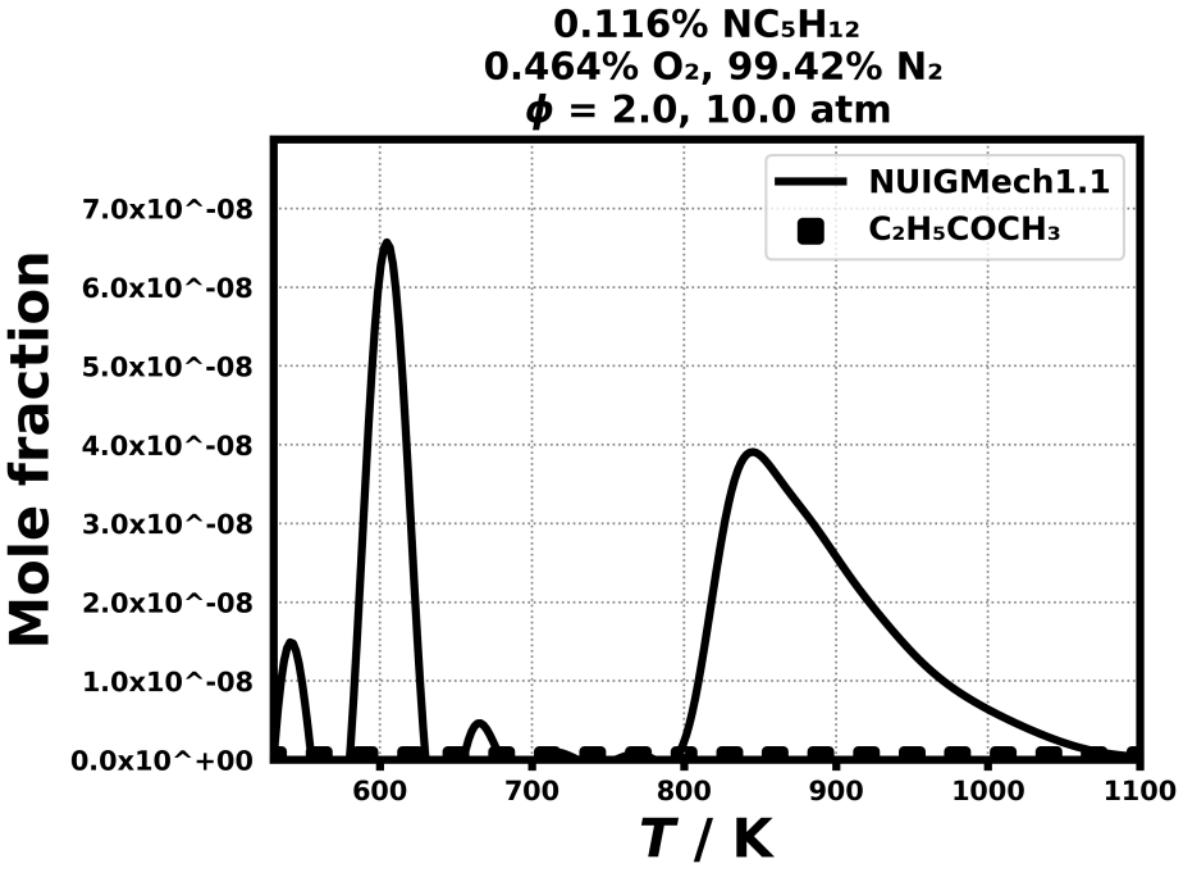

Figure 291: Dataset: 10_ATM_PHI_2.0

1.3.262 Case: n-C5H12/JSR/BUGLER/10_ATM_PHI_2.0

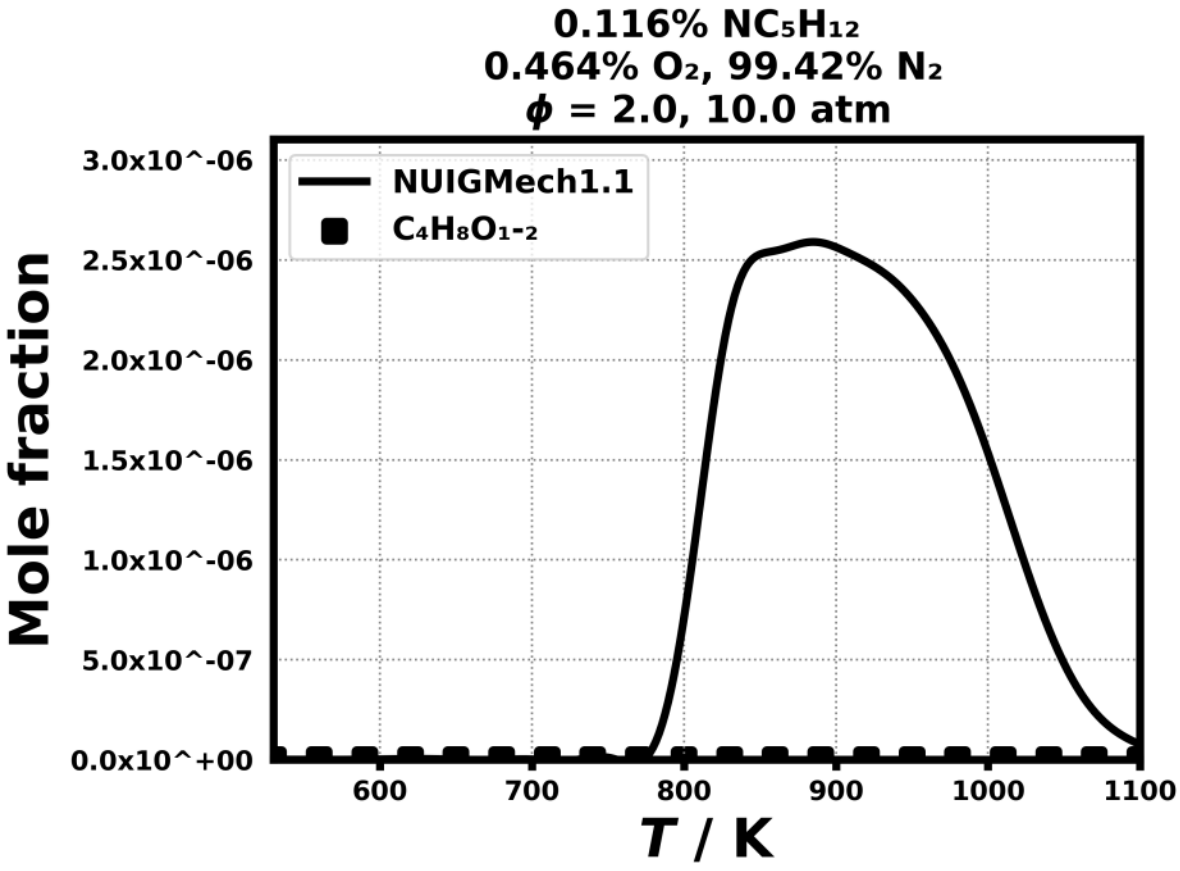

Figure 292: Dataset: 10_ATM_PHI_2.0

1.3.263 Case: n-C5H12/JSR/BUGLER/10_ATM_PHI_2.0

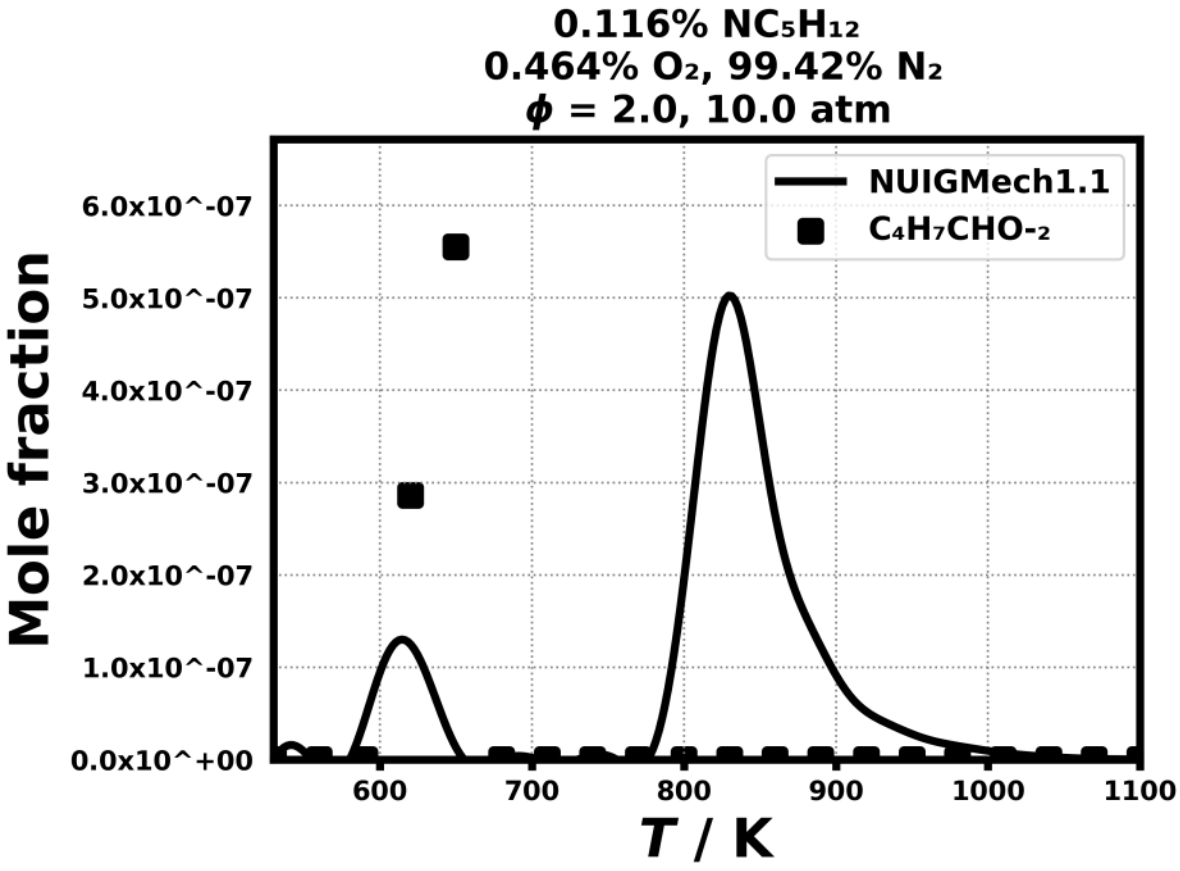

Figure 293: Dataset: 10_ATM_PHI_2.0

1.3.264 Case: n-C5H12/JSR/BUGLER/10_ATM_PHI_2.0

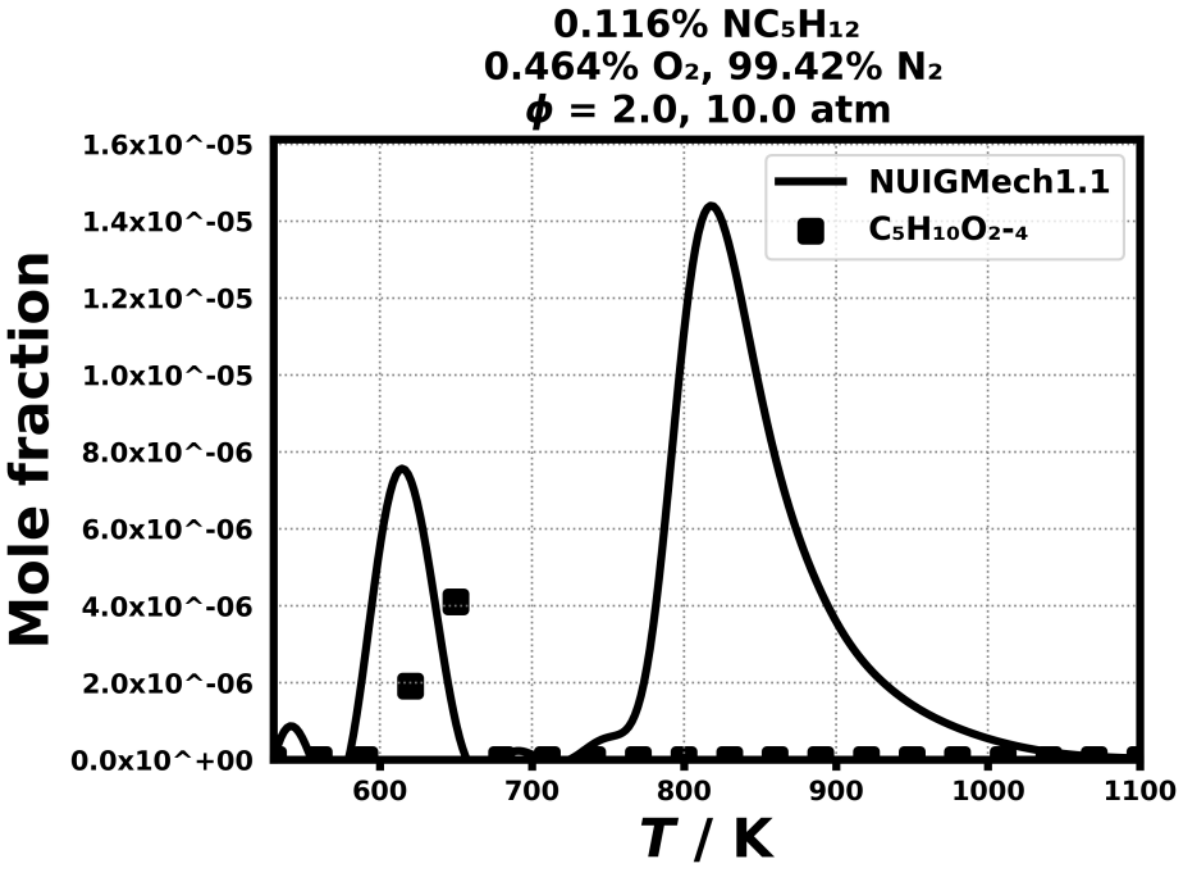

Figure 294: Dataset: 10_ATM_PHI_2.0

1.3.265 Case: n-C5H12/JSR/BUGLER/10_ATM_PHI_2.0

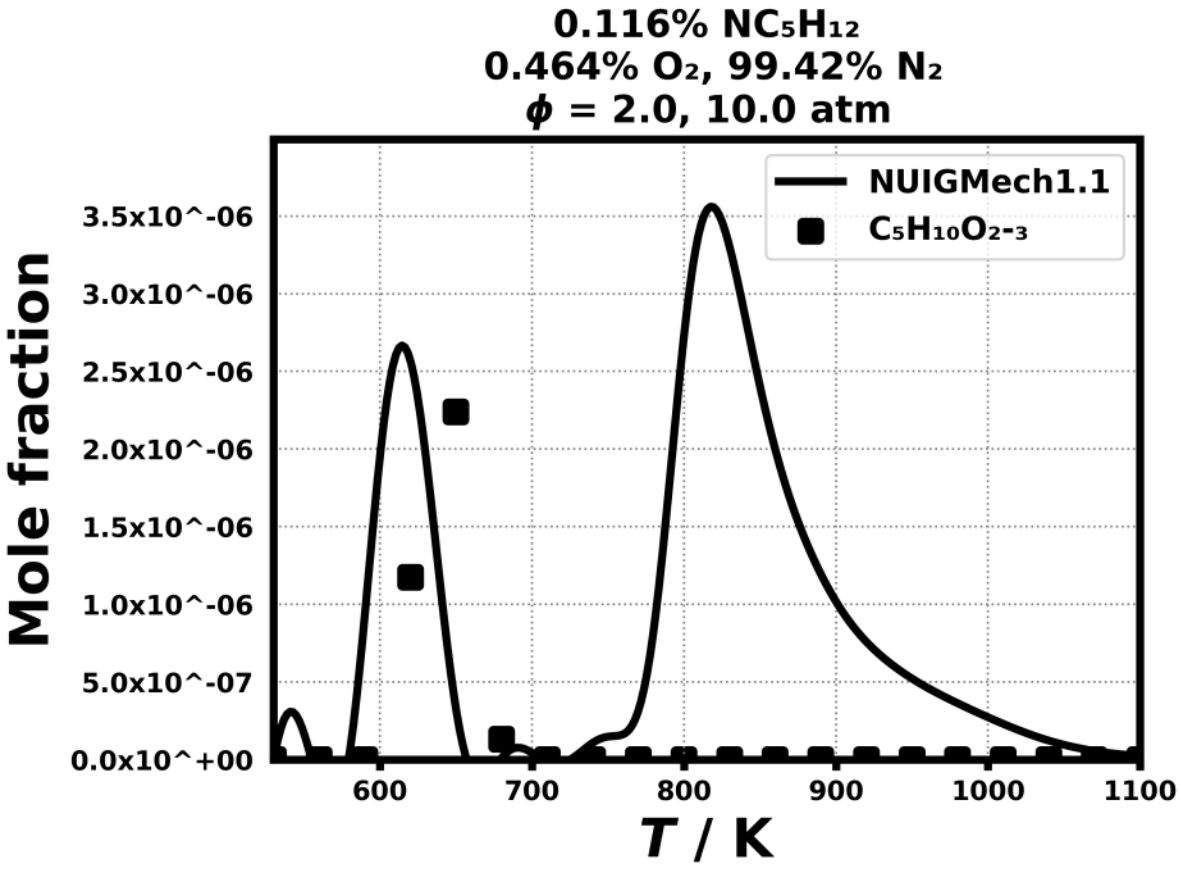

Figure 295: Dataset: 10_ATM_PHI_2.0

1.3.266 Case: n-C5H12/JSR/BUGLER/10_ATM_PHI_2.0

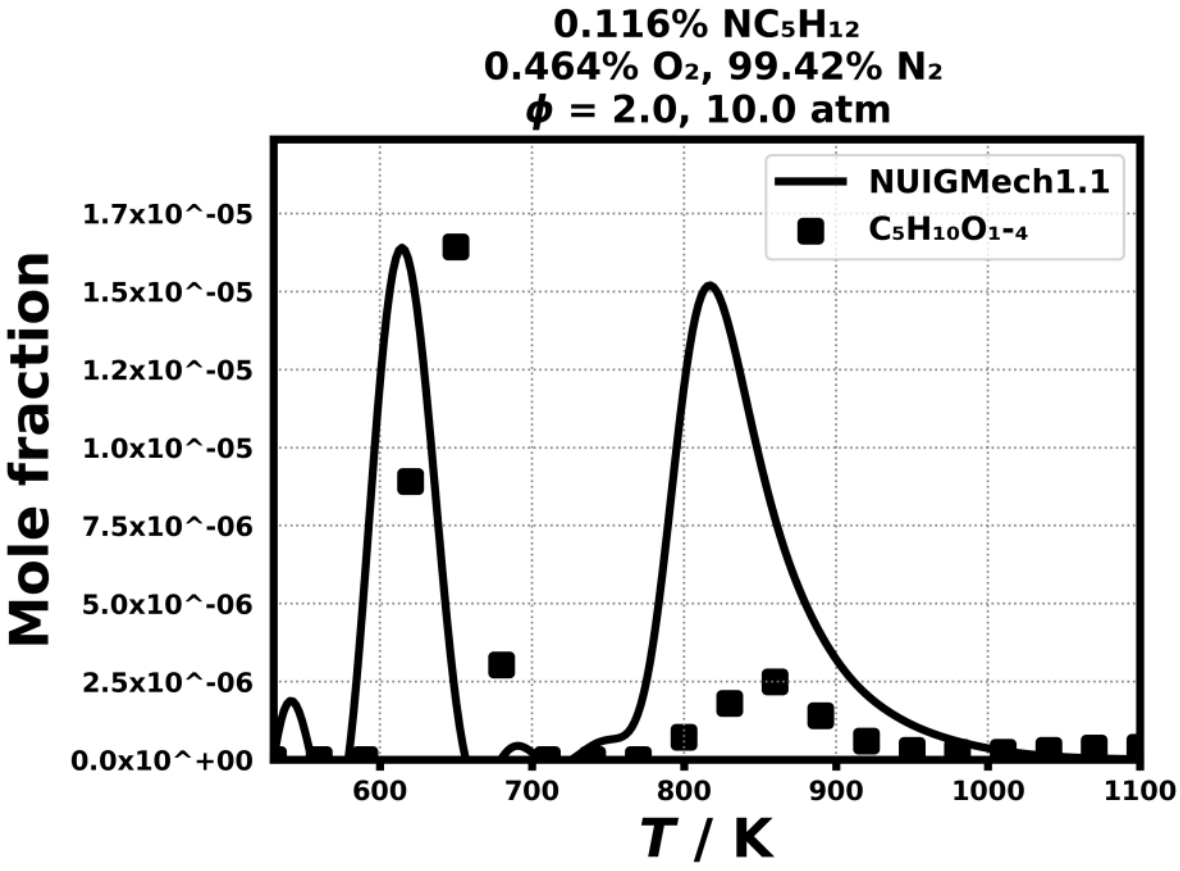

Figure 296: Dataset: 10_ATM_PHI_2.0

1.3.267 Case: n-C5H12/JSR/BUGLER/10_ATM_PHI_2.0

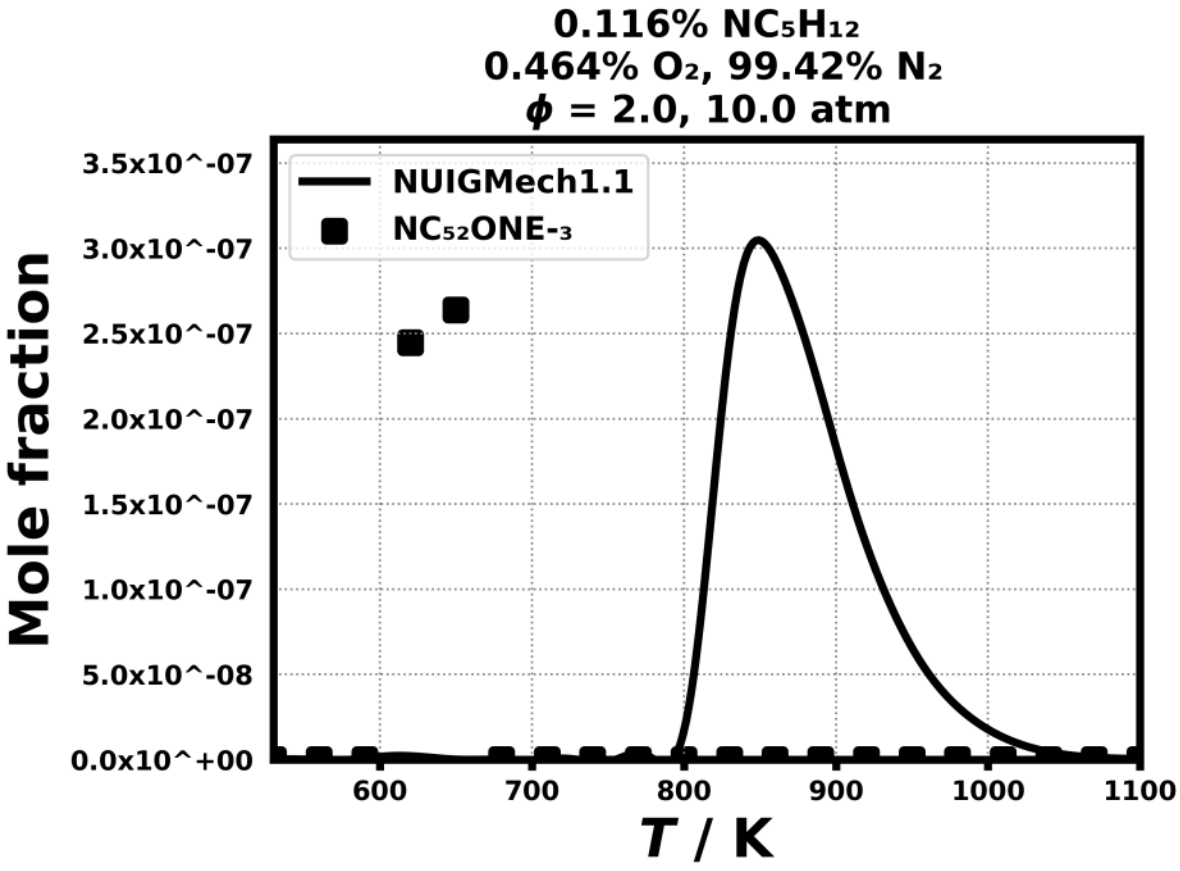

Figure 297: Dataset: 10_ATM_PHI_2.0

1.3.268 Case: n-C5H12/JSR/BUGLER/10_ATM_PHI_2.0

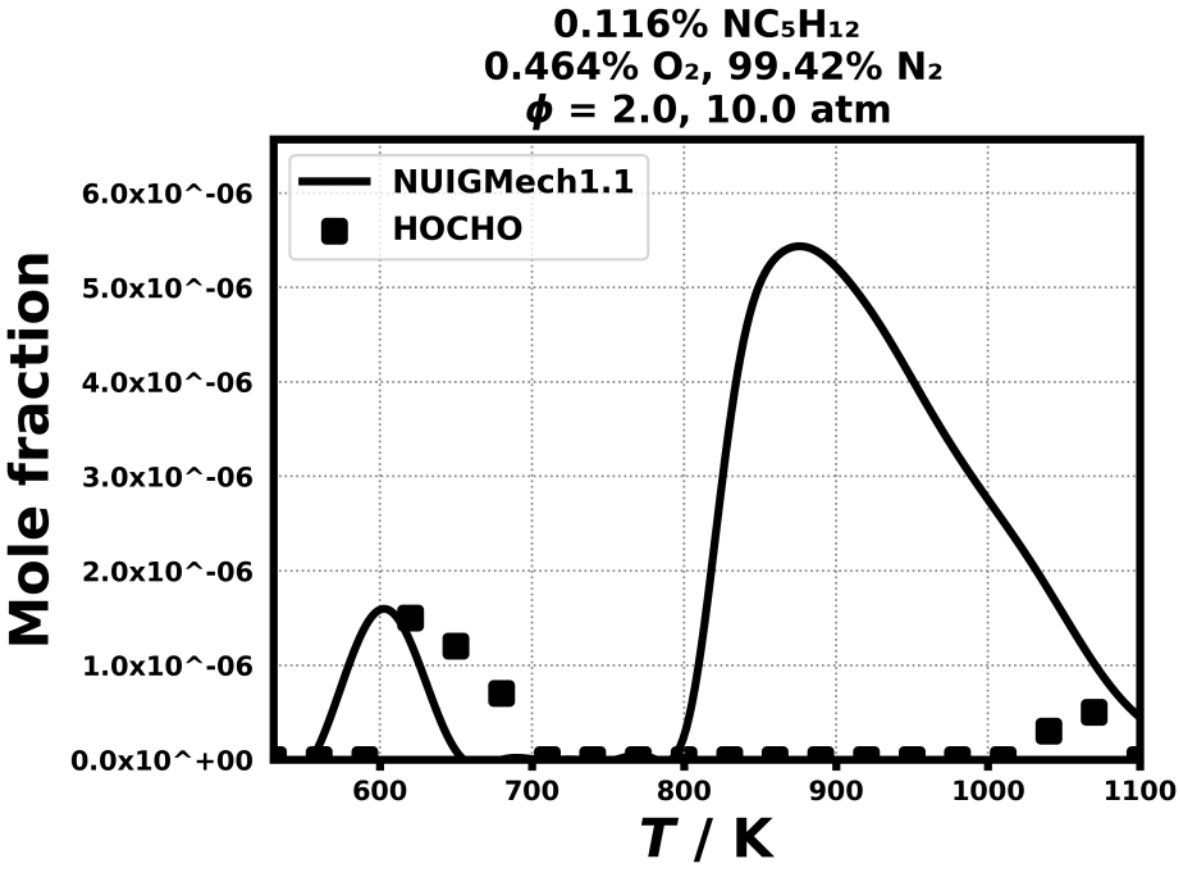

Figure 298: Dataset: 10_ATM_PHI_2.0

1.3.269 Case: n-C5H12/JSR/BUGLER/10_ATM_PHI_2.0

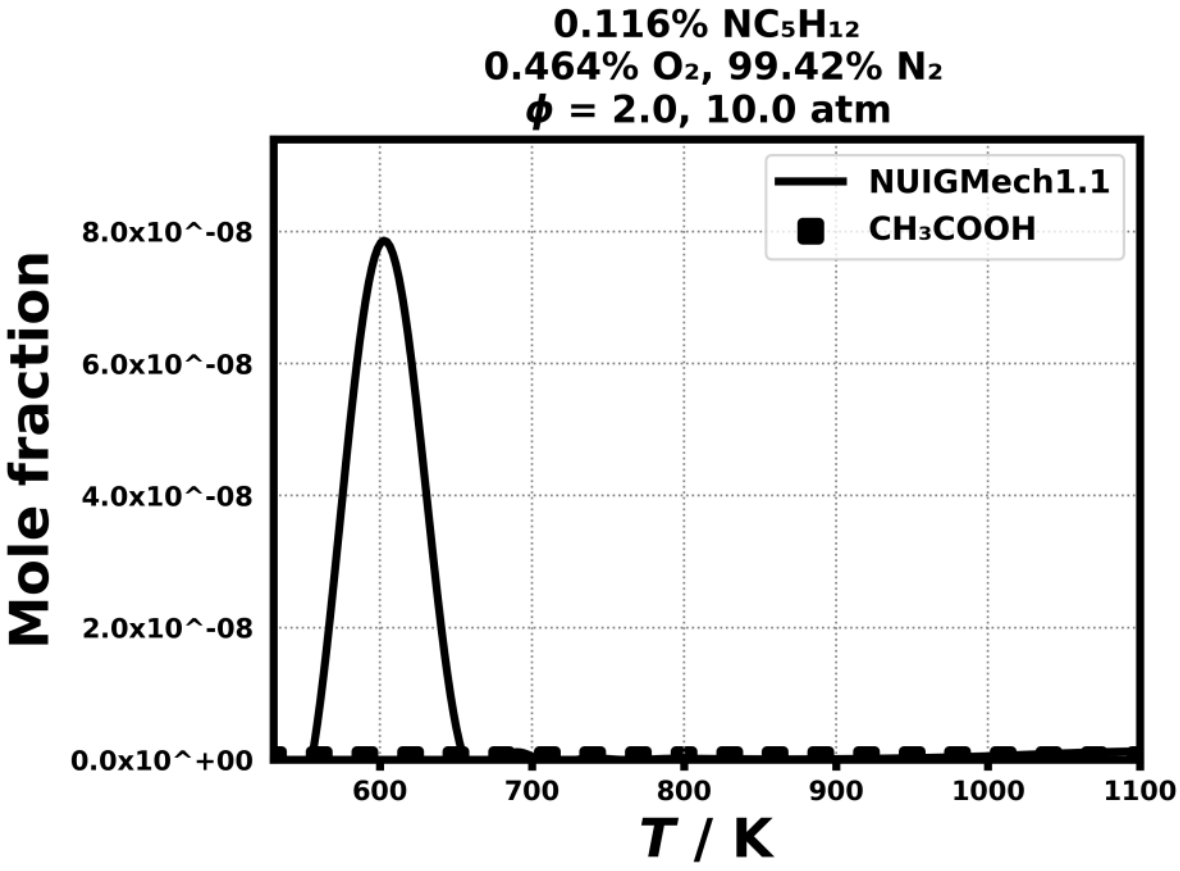

Figure 299: Dataset: 10_ATM_PHI_2.0

Bugler, John, et al. "An ignition delay time and chemical kinetic modeling study of the pentane isomers." Combustion and Flame 163 (2016): 138-156.

Validation for iC_5H_{12}

Shock tube ignition delay time

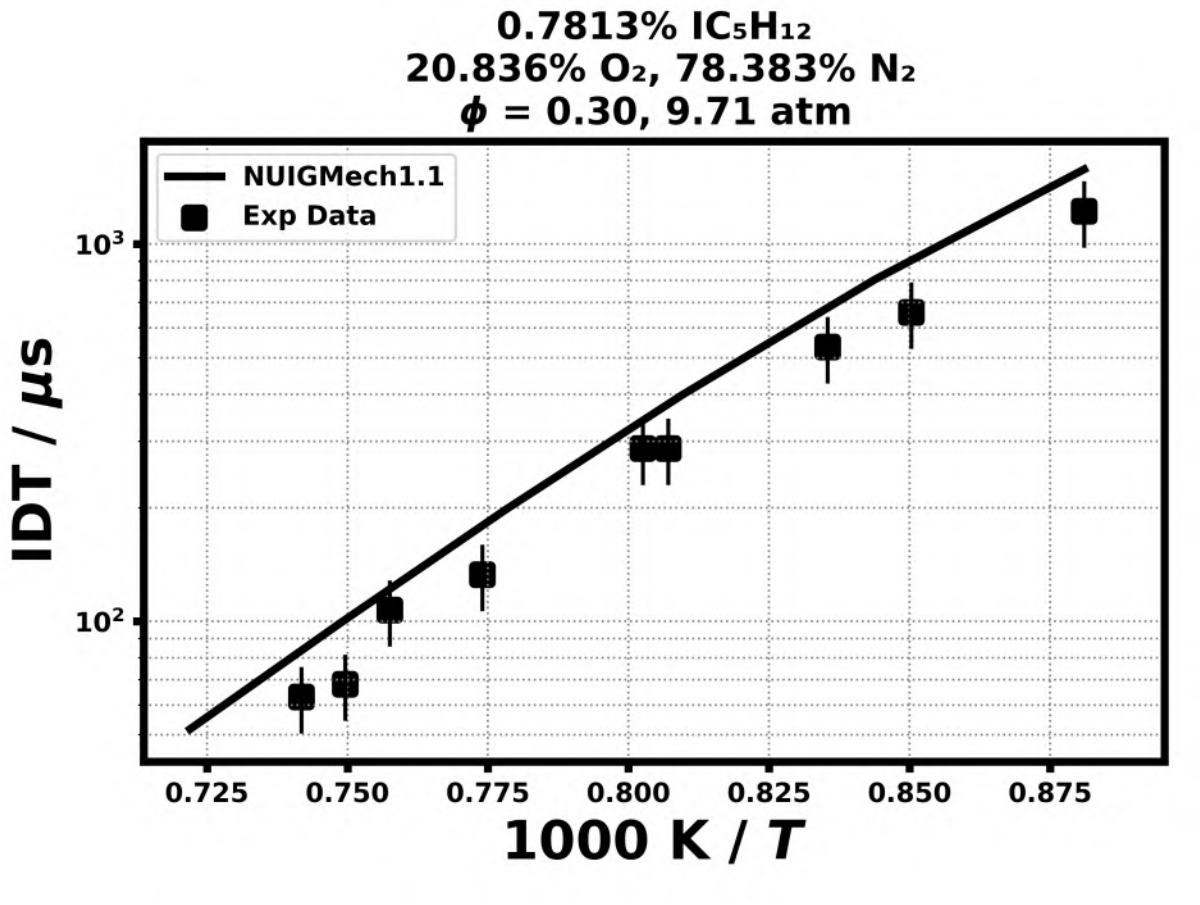

Figure 300: Dataset: 10_ATM_0.8_IC5H12_PHI_0.3

2.1.2 Case: iso-C5H12/ST/BUGLER/10_ATM_1.3_IC5H12_PHI_0.5

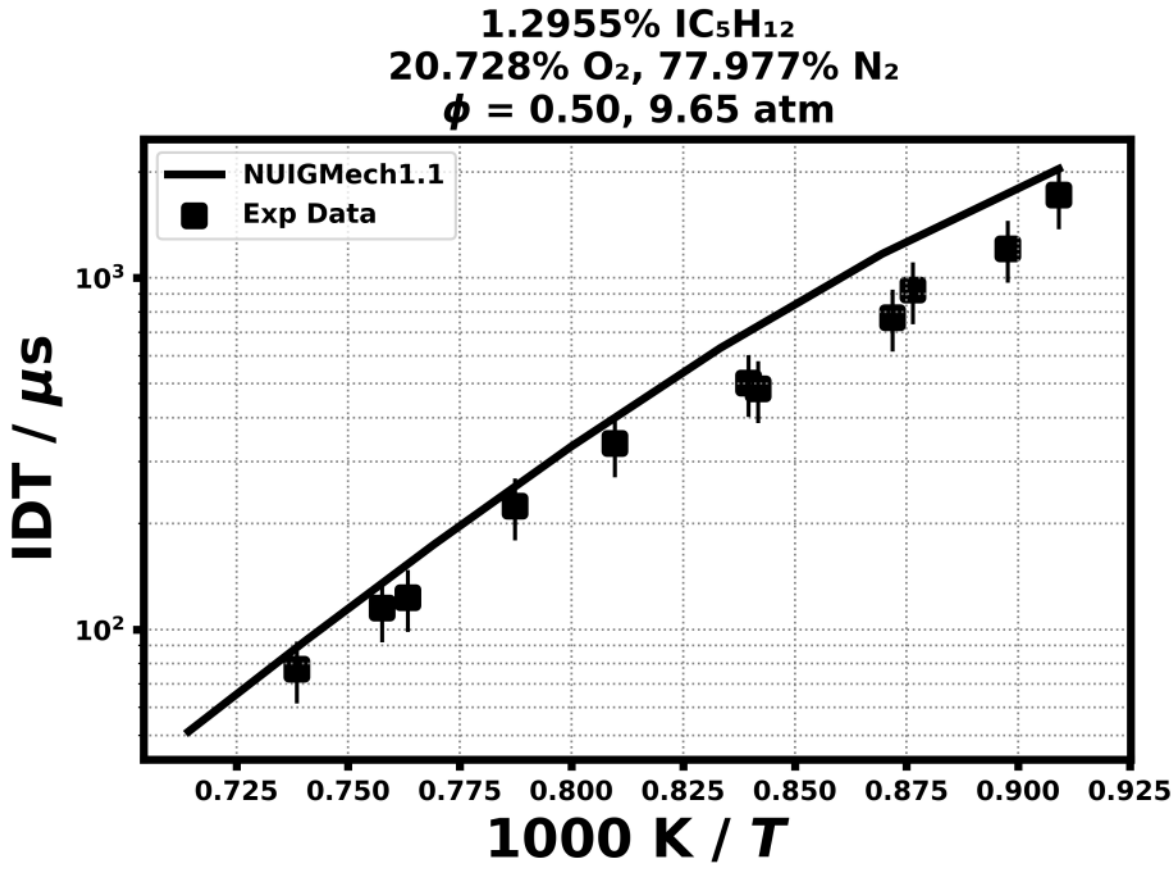

Figure 301: Dataset: 10_ATM_1.3_IC5H12_PHI_0.5

2.1.3 Case: iso-C5H12/ST/BUGLER/10_ATM_2.6_IC5H12_PHI_1.0

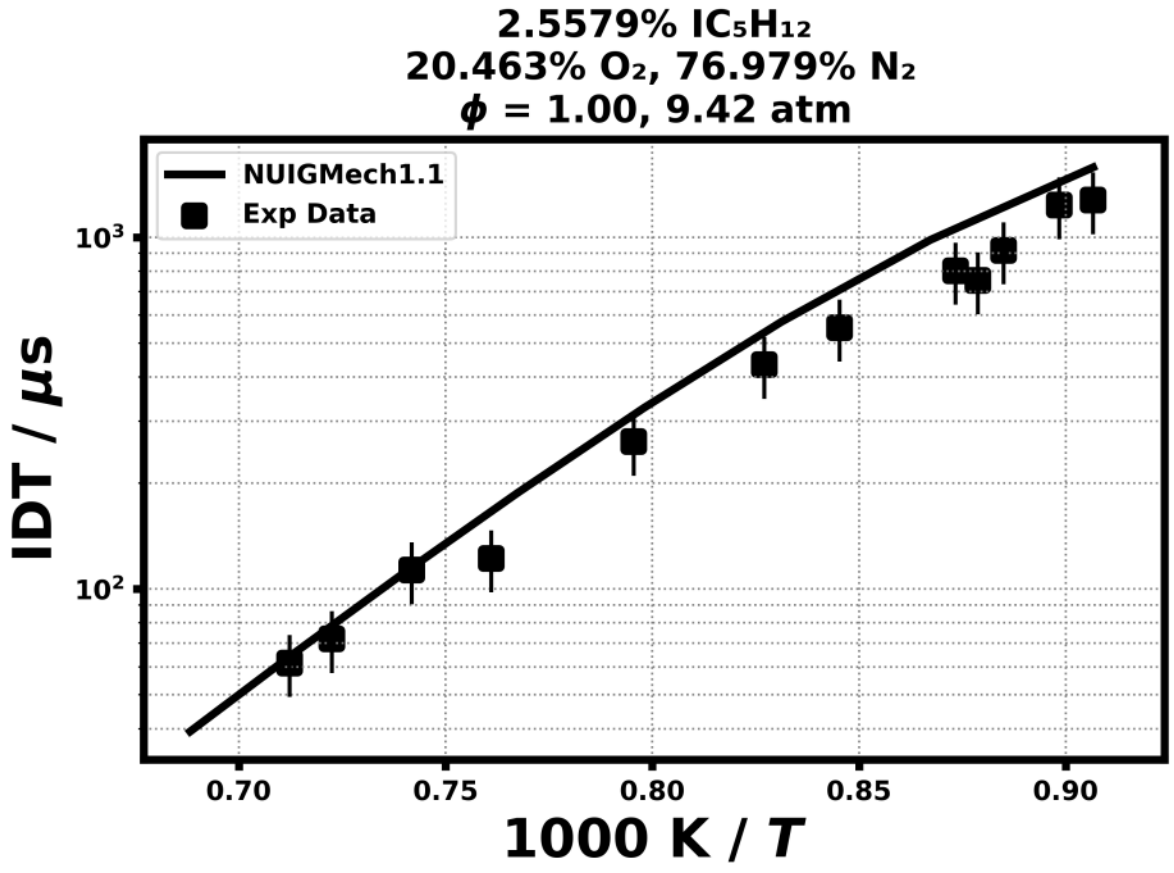

Figure 302: Dataset: 10_ATM_2.6_IC5H12_PHI_1.0

2.1.4 Case: iso-C5H12/ST/BUGLER/10_ATM_5.0_IC5H12_PHI_2.0

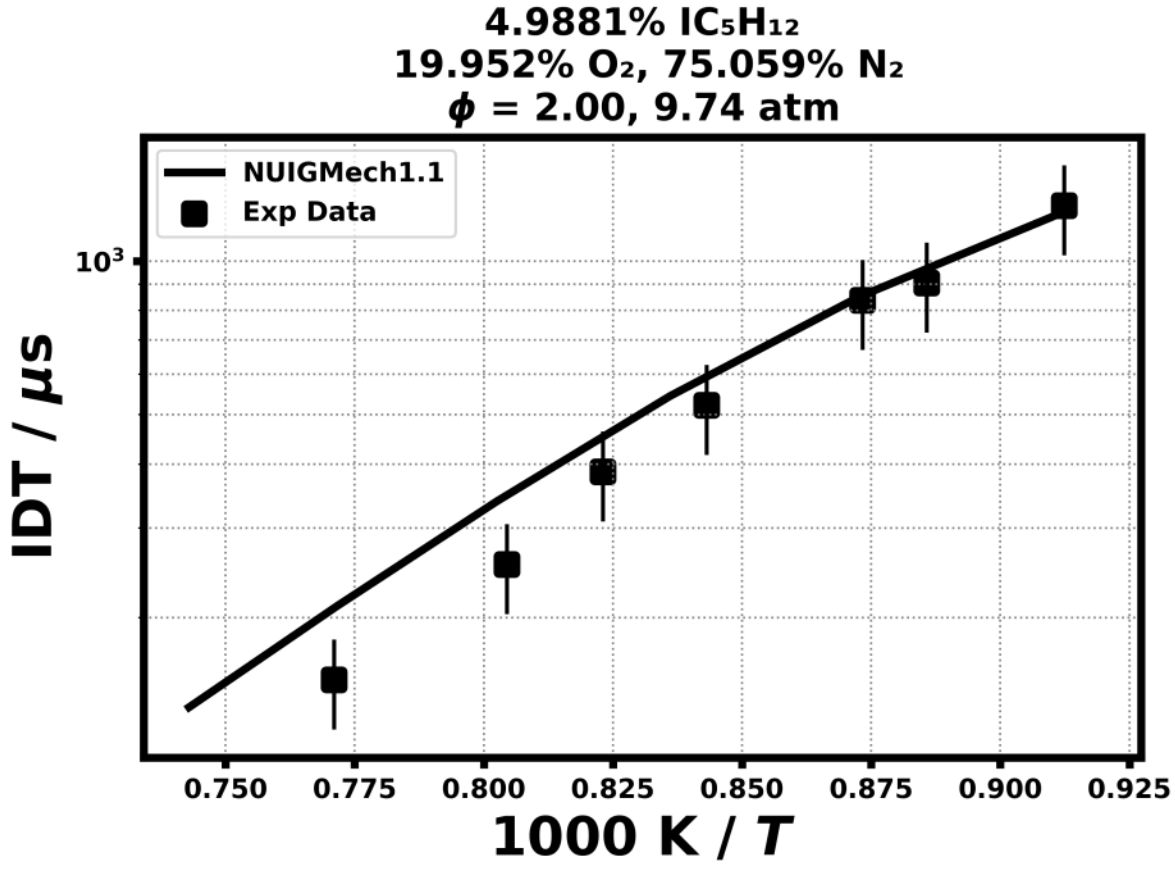

Figure 303: Dataset: 10_ATM_5.0_IC5H12_PHI_2.0

2.1.5 Case: iso-C5H12/ST/BUGLER/20_ATM_0.8_IC5H12_PHI_0.3

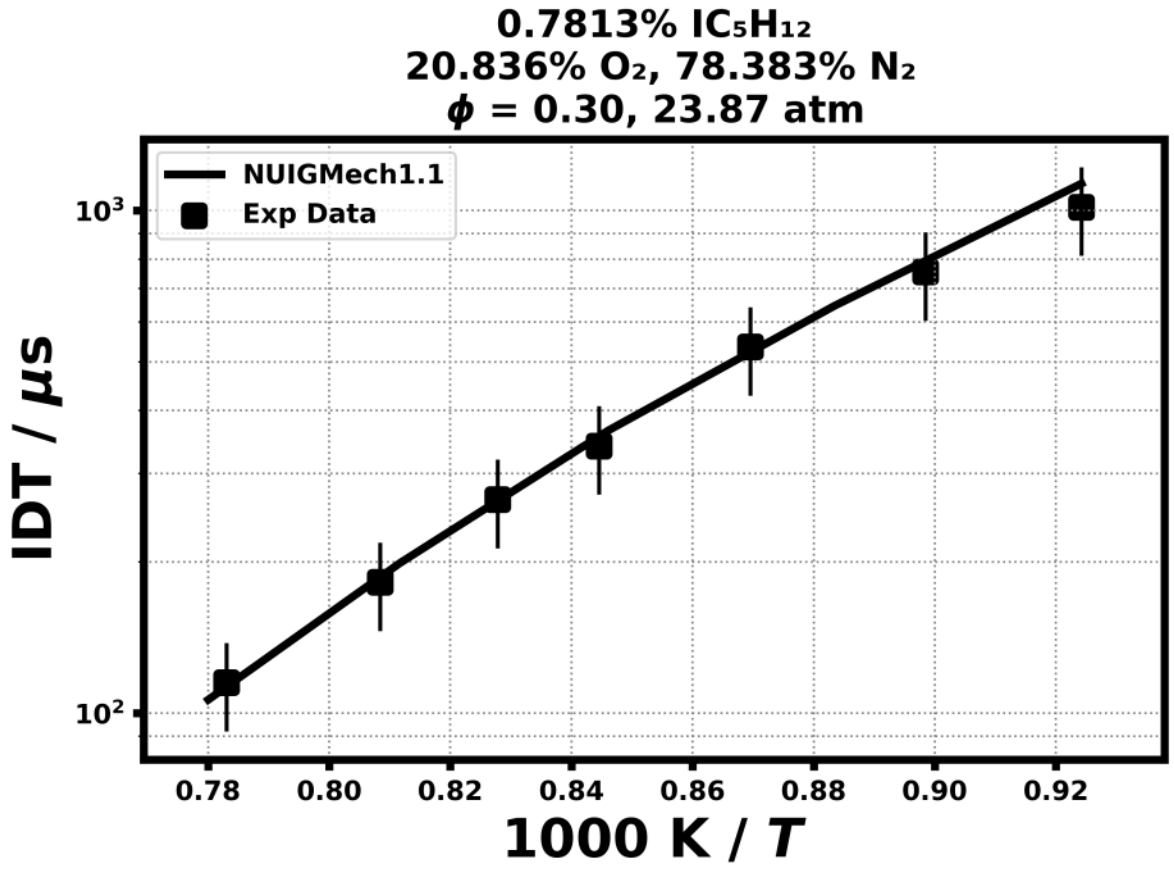

Figure 304: Dataset: 20_ATM_0.8_IC5H12_PHI_0.3

2.1.6 Case: iso-C5H12/ST/BUGLER/20_ATM_1.3_IC5H12_PHI_0.5

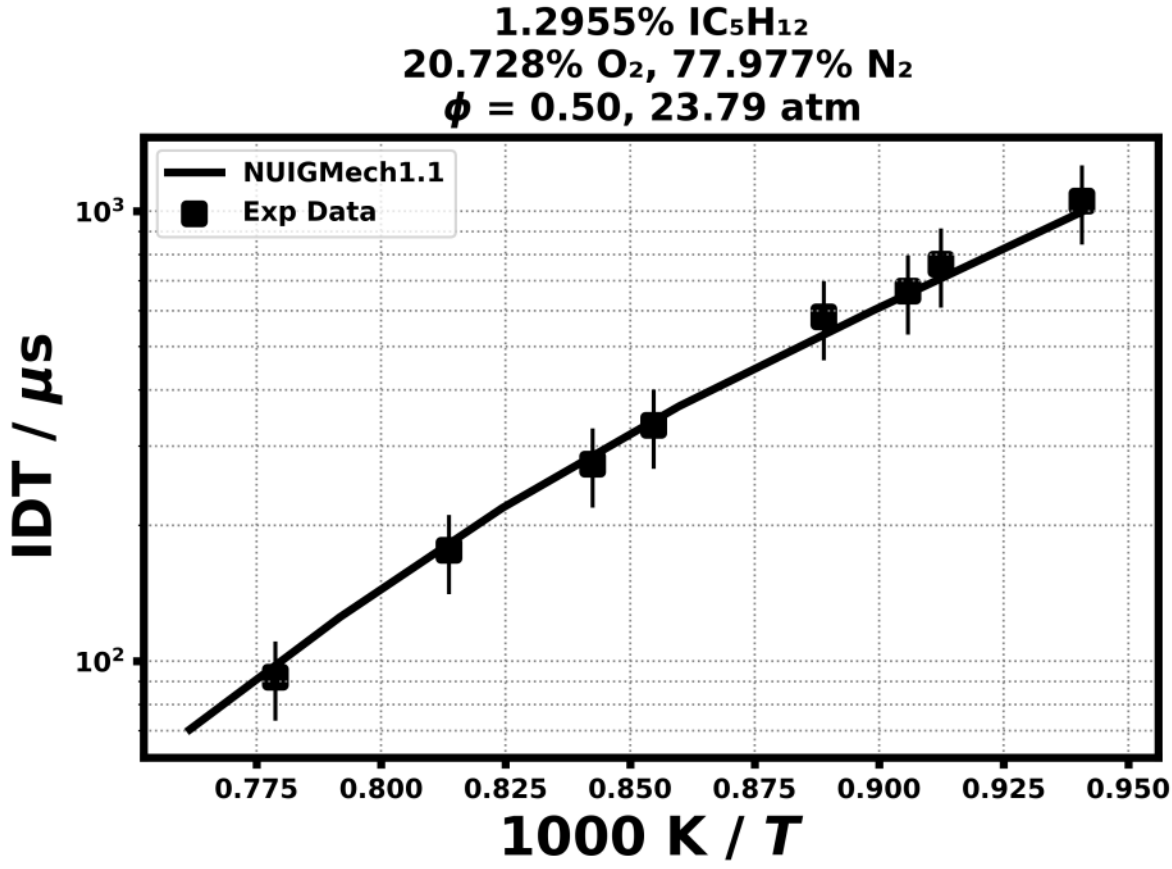

Figure 305: Dataset: 20_ATM_1.3_IC5H12_PHI_0.5

2.1.7 Case: iso-C5H12/ST/BUGLER/20_ATM_2.6_IC5H12_PHI_1.0

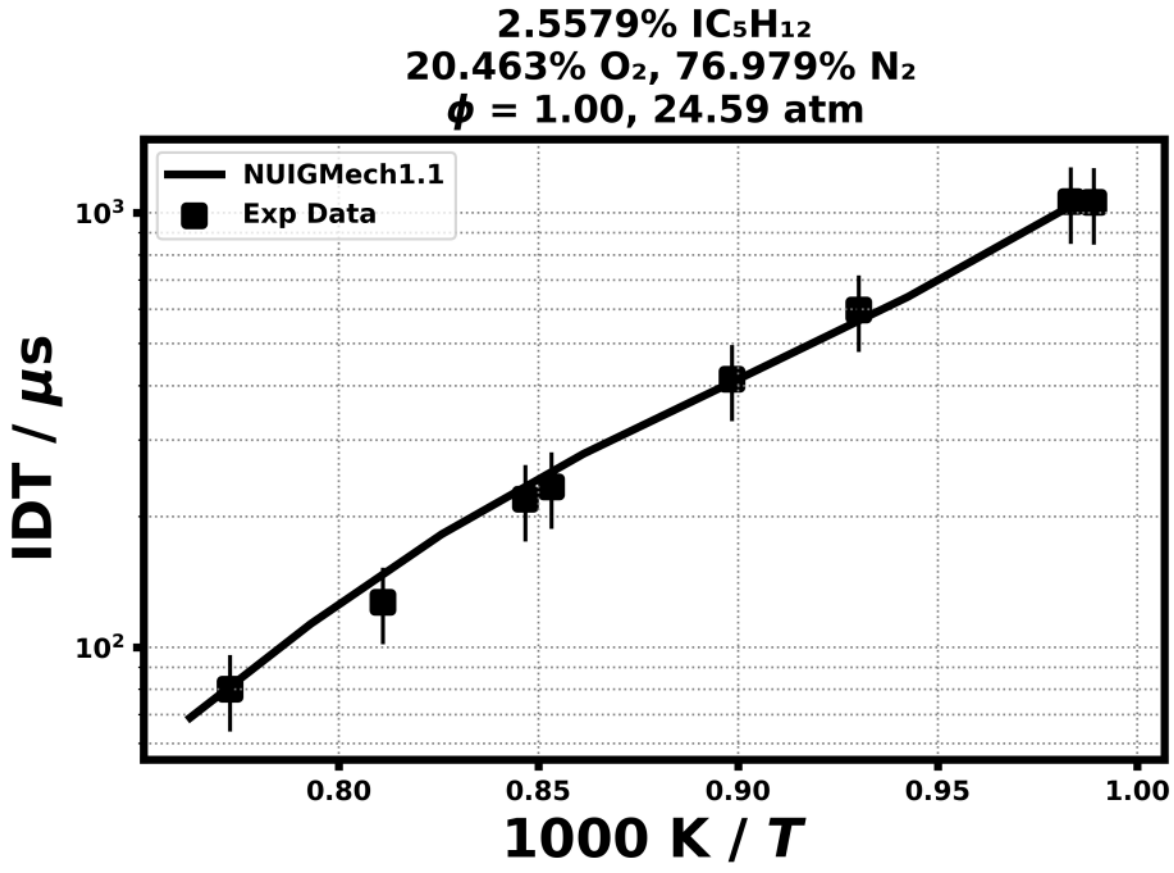

Figure 306: Dataset: 20_ATM_2.6_IC5H12_PHI_1.0

1.1.1 Case: iso-C5H12/ST/BUGLER/20_ATM_5.0_IC5H12_PHI_2.0

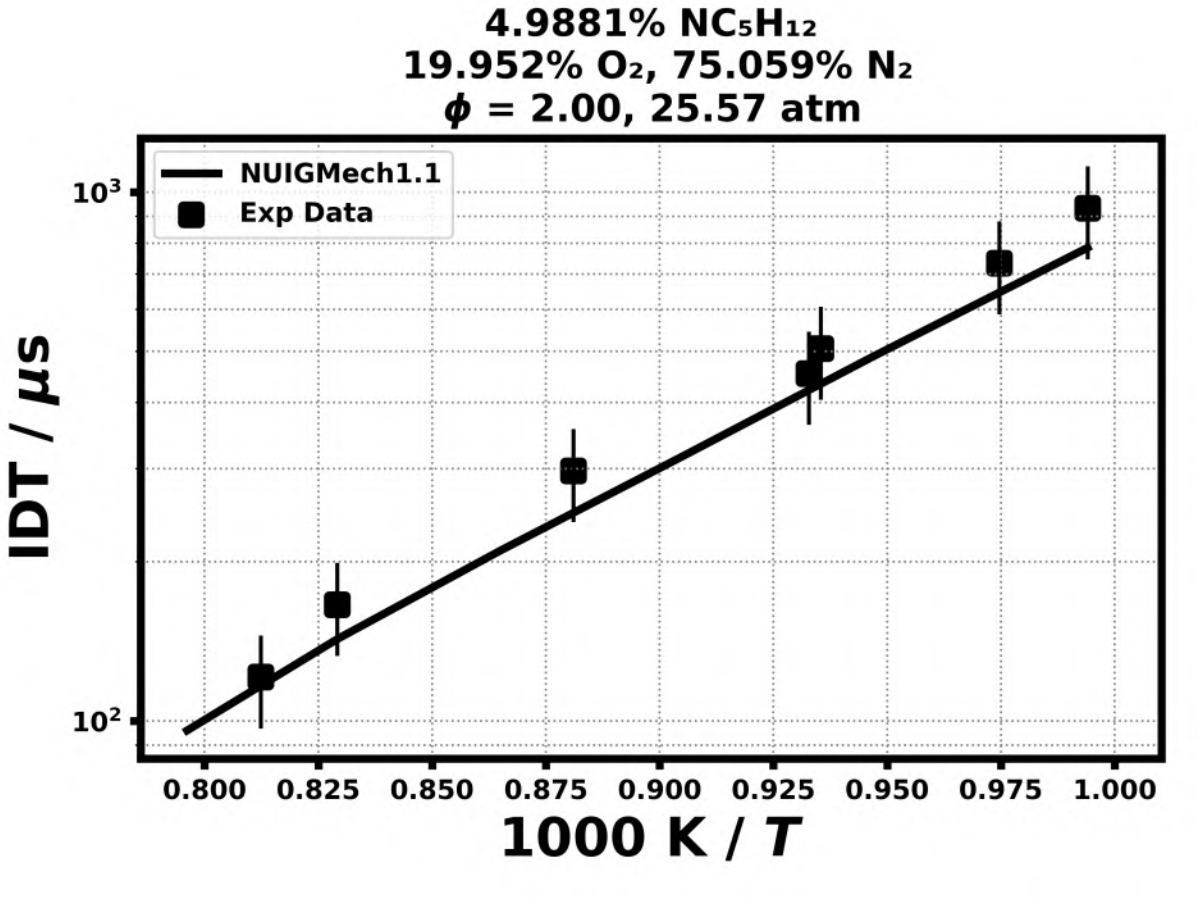

Figure 1: Dataset: 20_ATM_5.0_IC5H12_PHI_2.0

Bugler, John, et al. "An ignition delay time and chemical kinetic modeling study of the pentane isomers." Combustion and Flame 163 (2016): 138-156.

RCM Ignition delay time

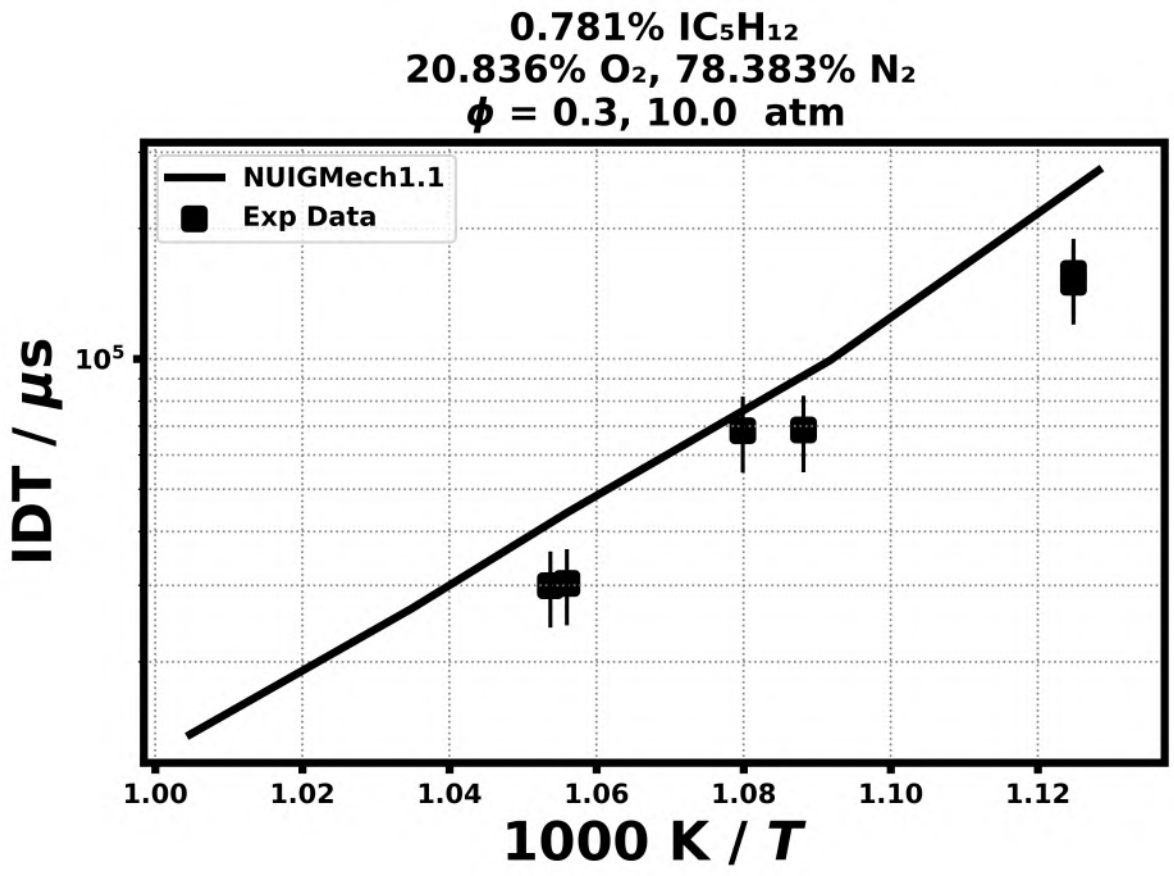

Figure 307: Dataset: F030_10ATM_100_N2

2.2.2 Case: iso-C5H12/RCM/BUGLER/F030_20ATM_100_N2

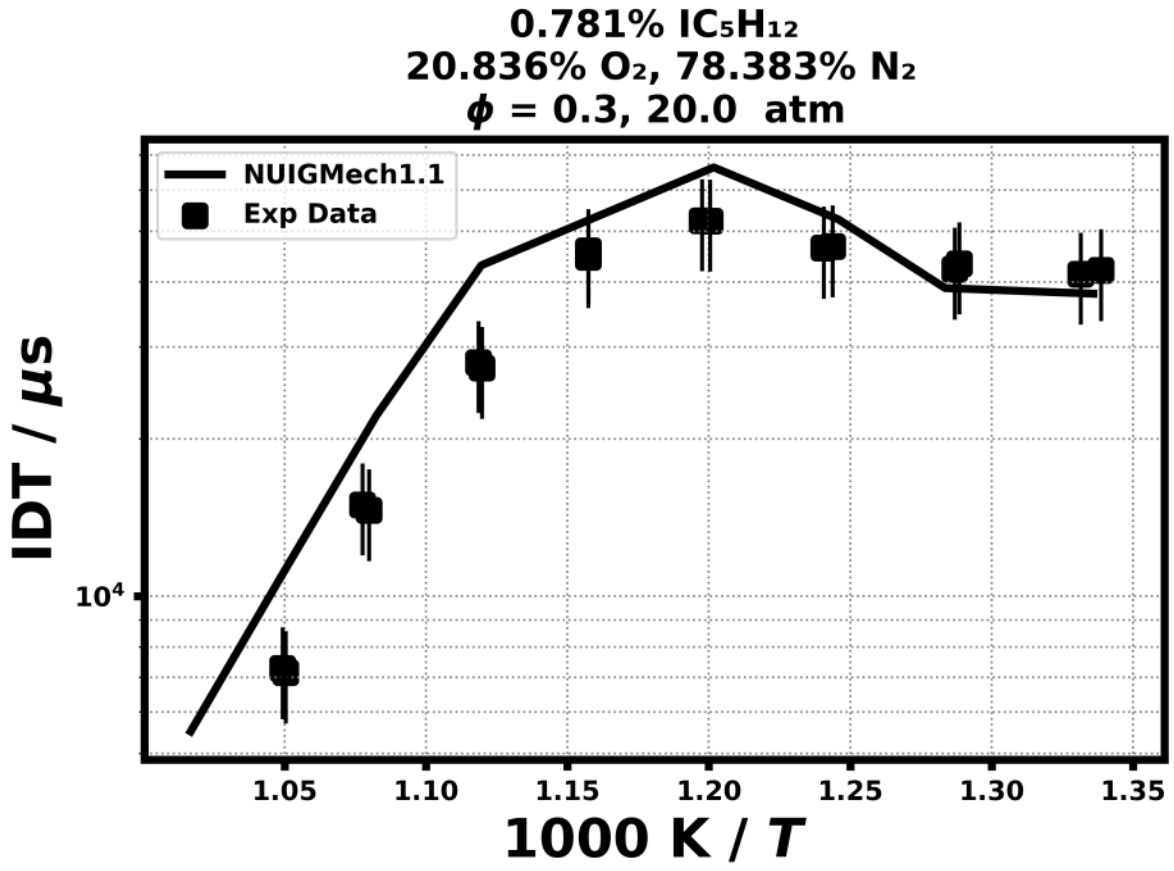

Figure 308: Dataset: F030_20ATM_100_N2

2.2.3 Case: iso-C5H12/RCM/BUGLER/F050_10ATM_100_N2

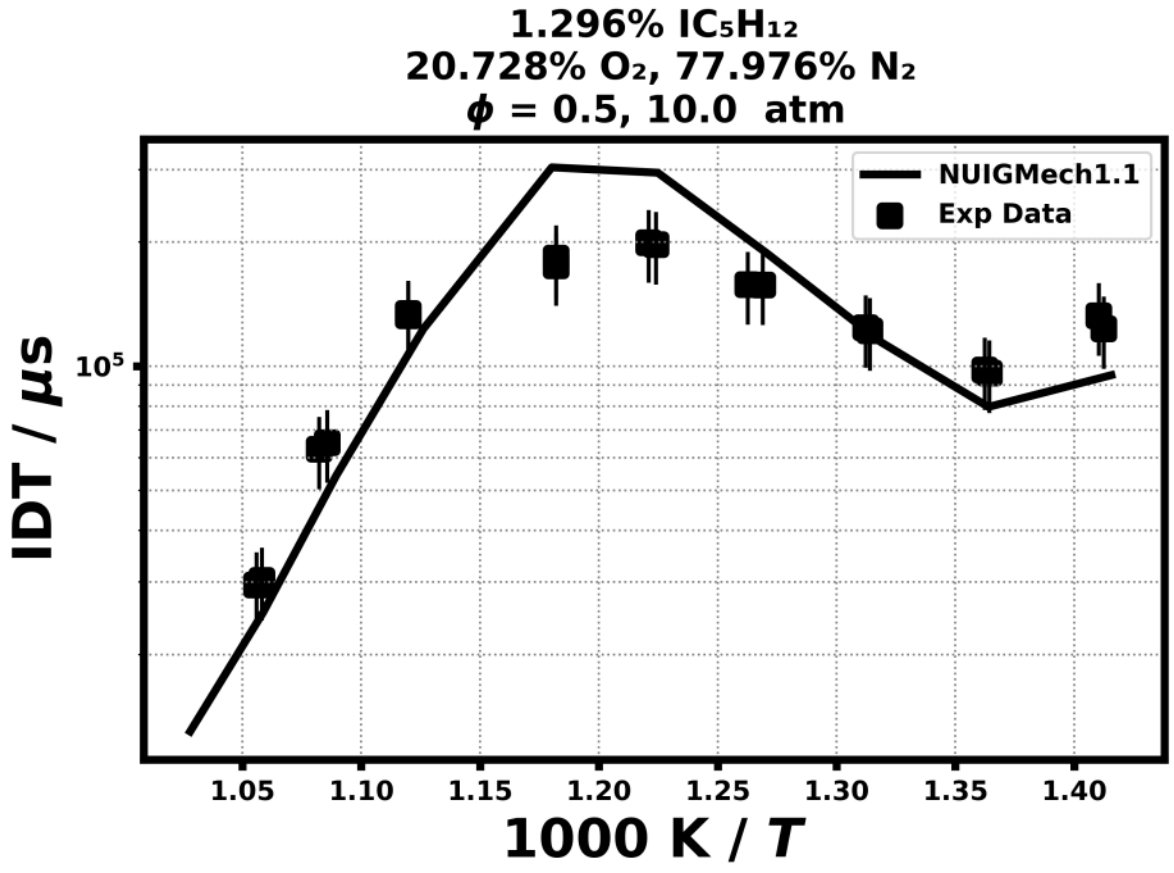

Figure 309: Dataset: F050_10ATM_100_N2

2.2.4 Case: iso-C5H12/RCM/BUGLER/F050_20ATM_100_N2

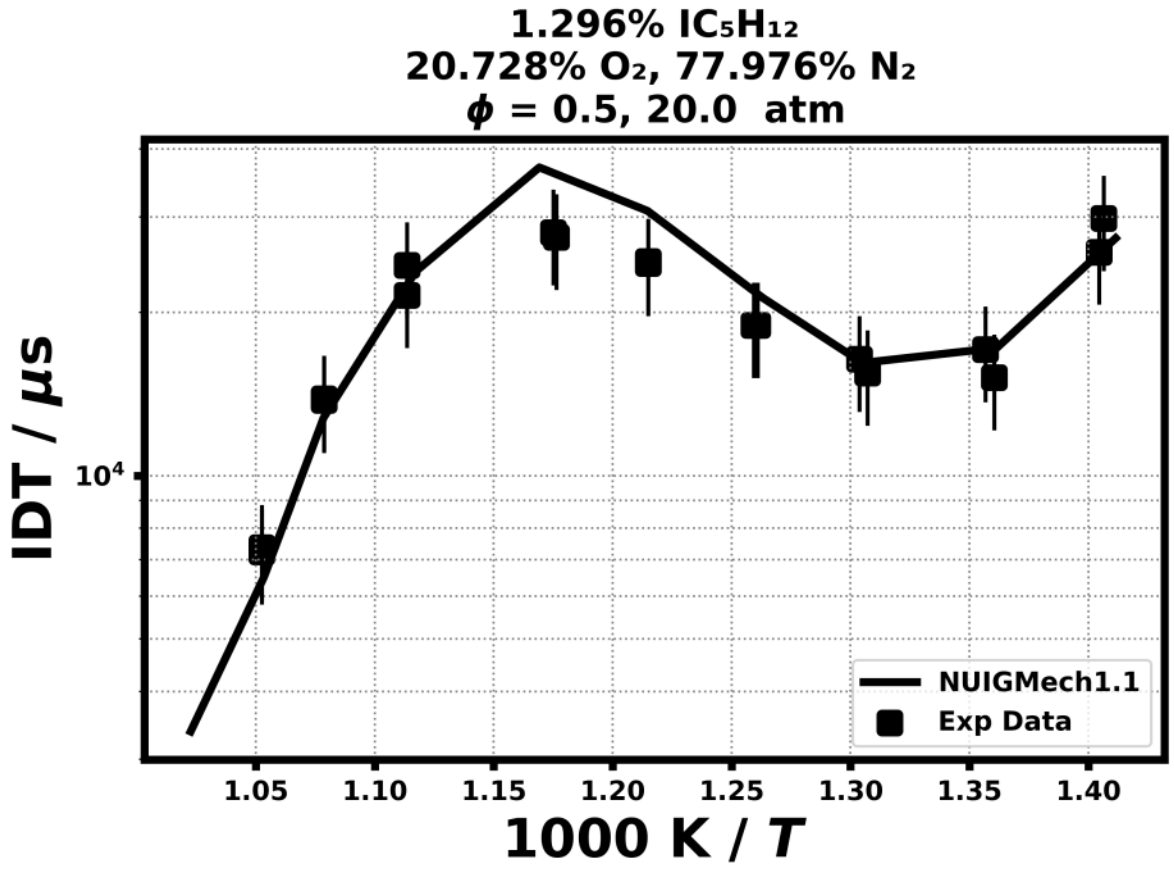

Figure 310: Dataset: F050_20ATM_100_N2

Bugler, John, et al. "An ignition delay time and chemical kinetic modeling study of the pentane isomers." Combustion and Flame 163 (2016): 138-156.

Validation for neo-C_5H_{12}

Shock tube ignition delay time

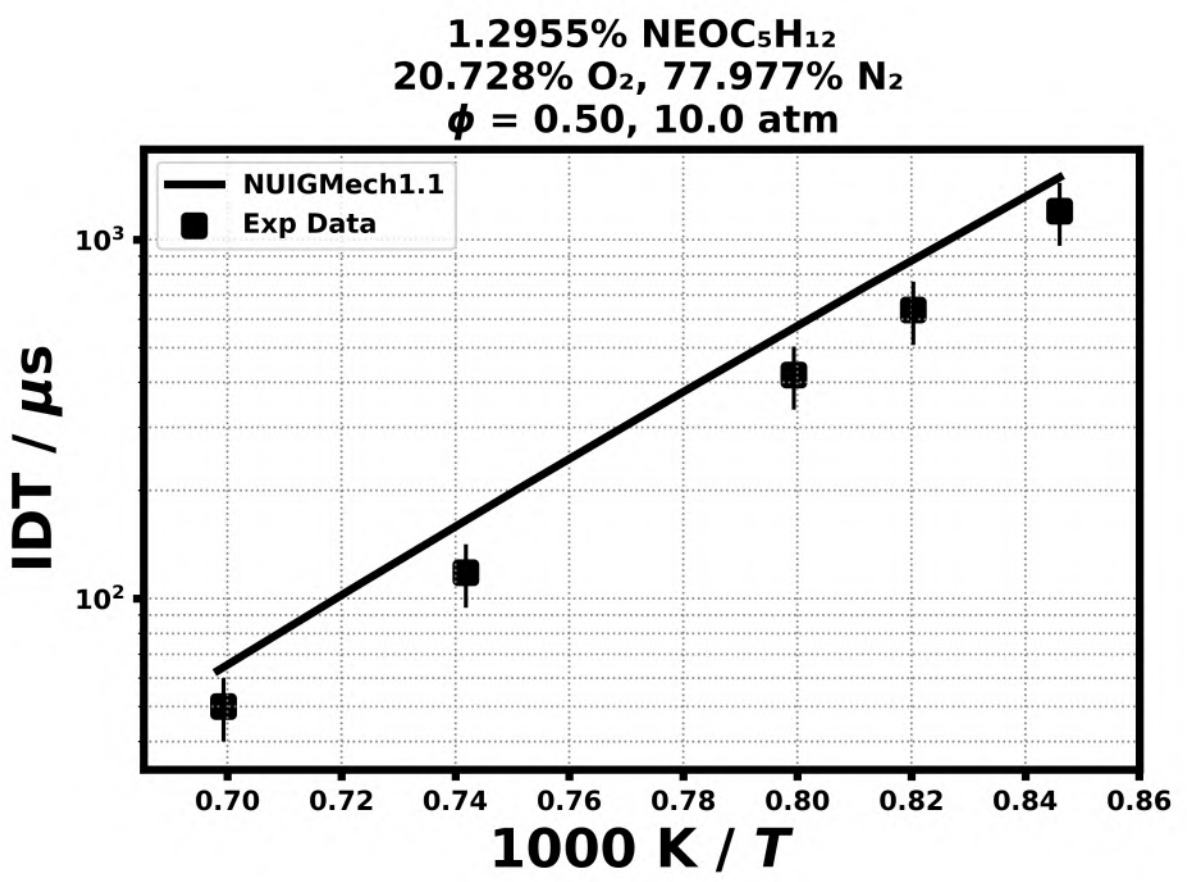

Figure 319: Dataset: 10_ATM_1.3_NEOC5H12_PHI_0.5

3.1.2 Case: neo-C5H12/ST/BUGLER/10_ATM_2.6_NEOC5H12_PHI_1.0

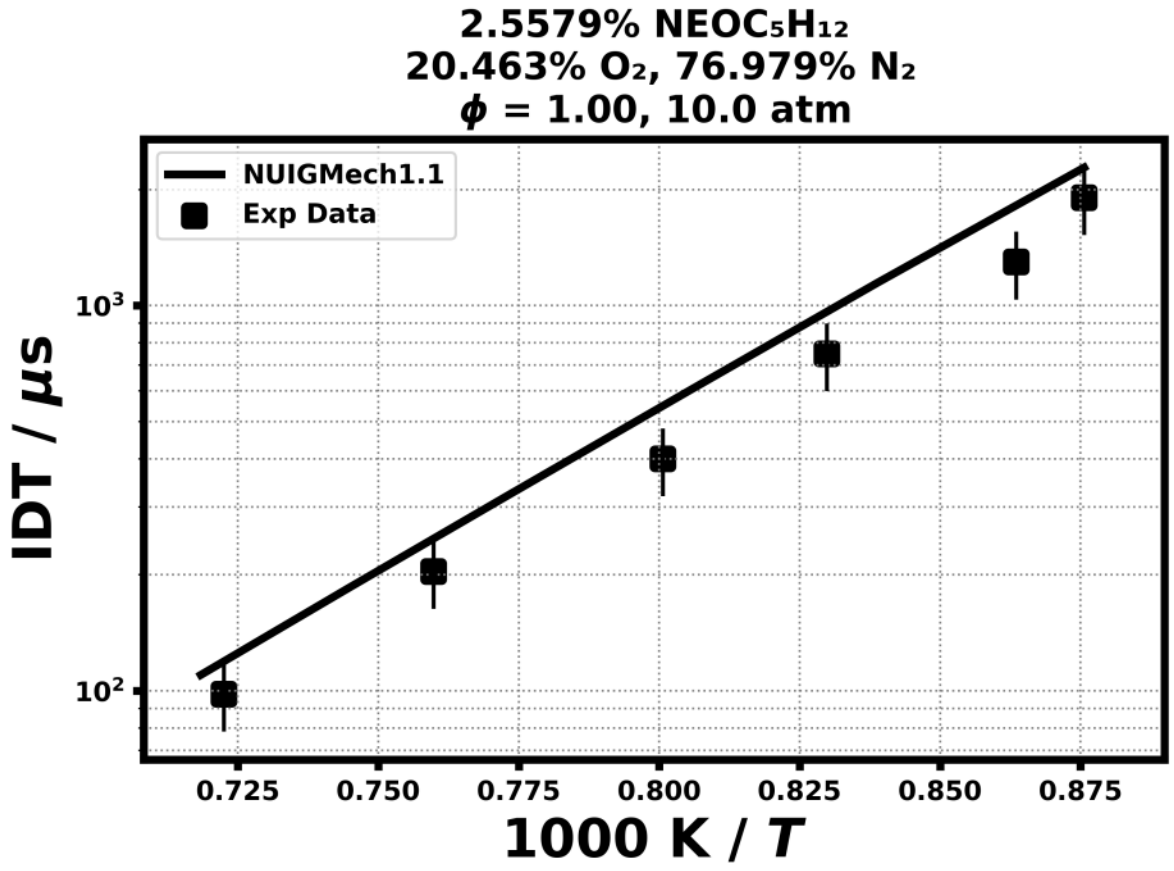

Figure 320: Dataset: 10_ATM_2.6_NEOC5H12_PHI_1.0

3.1.3 Case: neo-C5H12/ST/BUGLER/10_ATM_5.0_NEOC5H12_PHI_2.0

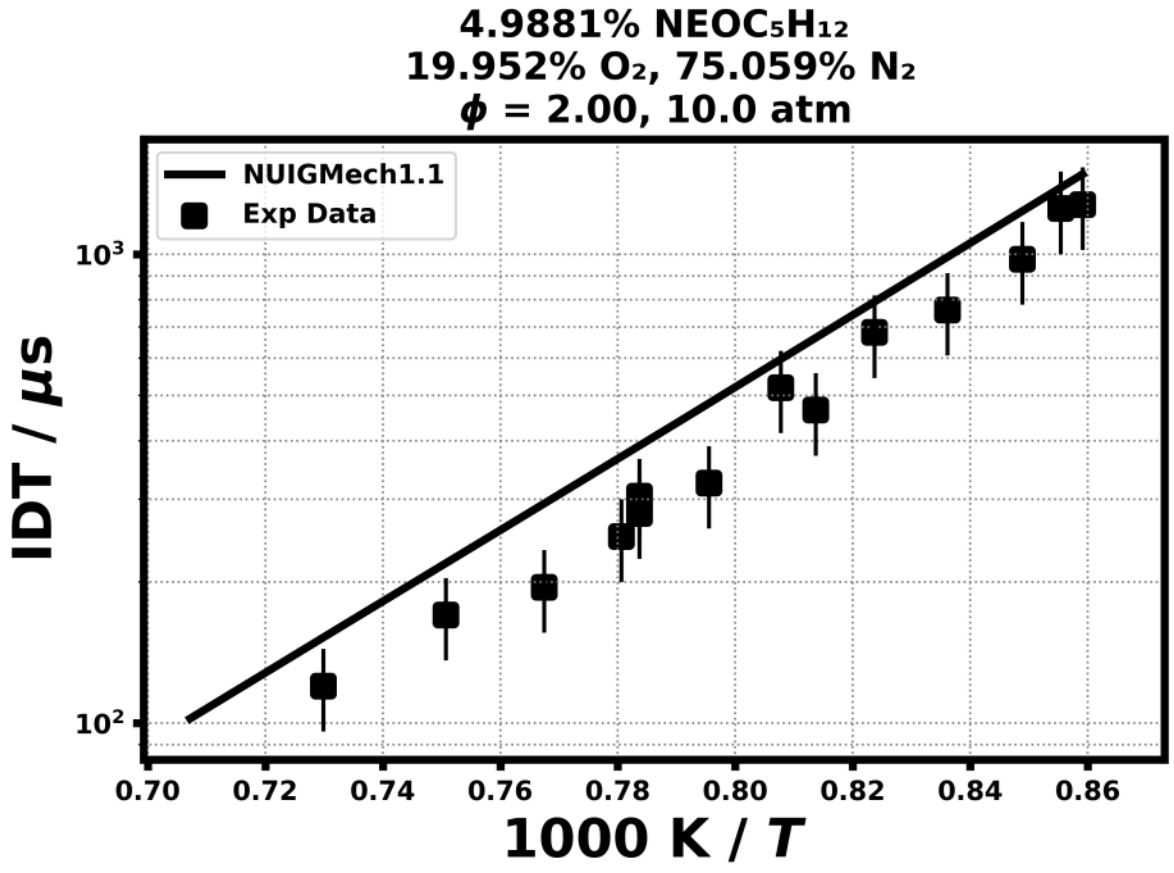

Figure 321: Dataset: 10_ATM_5.0_NEOC5H12_PHI_2.0

3.1.4 Case: neo-C5H12/ST/BUGLER/20_ATM_1.3_NEOC5H12_PHI_0.5

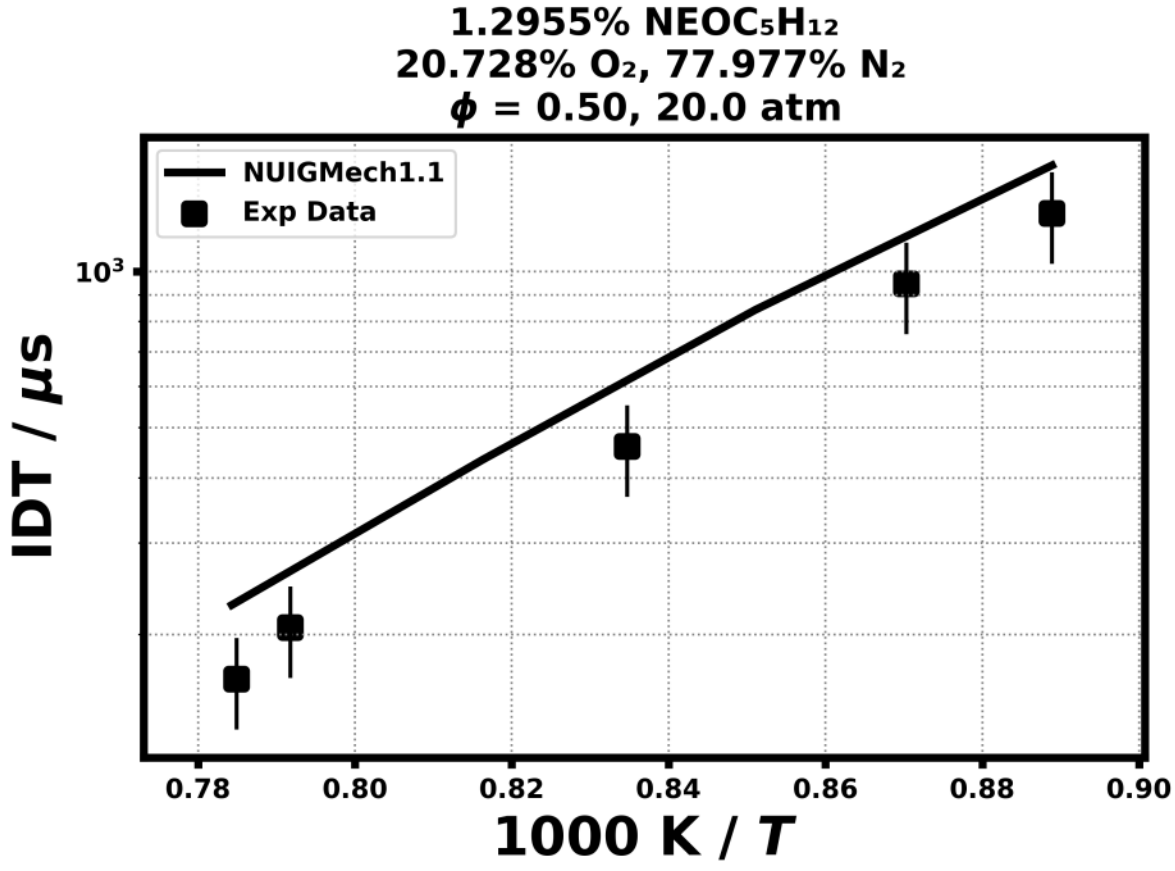

Figure 322: Dataset: 20_ATM_1.3_NEOC5H12_PHI_0.5

3.1.5 Case: neo-C5H12/ST/BUGLER/20_ATM_2.6_NEOC5H12_PHI_1.0

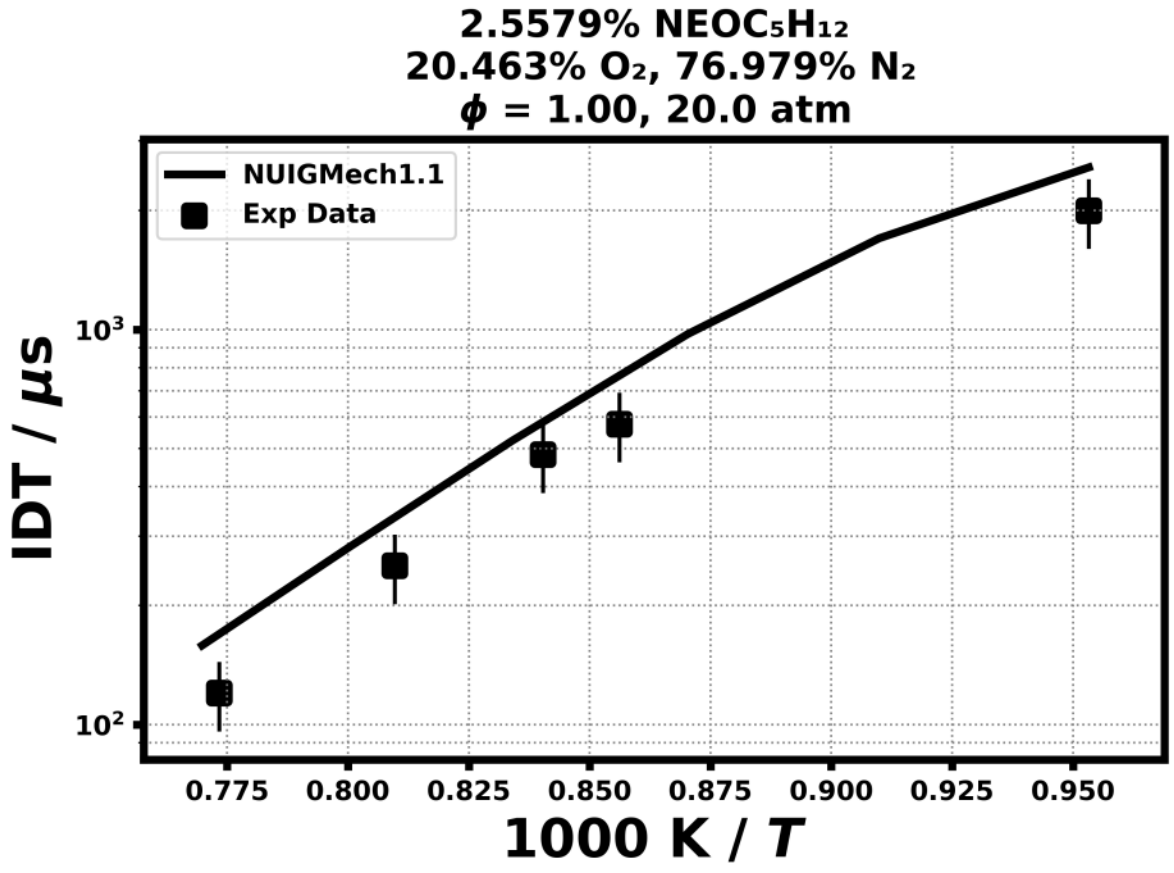

Figure 323: Dataset: 20_ATM_2.6_NEOC5H12_PHI_1.0

3.1.6 Case: neo-C5H12/ST/BUGLER/20_ATM_5.0_NEOC5H12_PHI_2.0

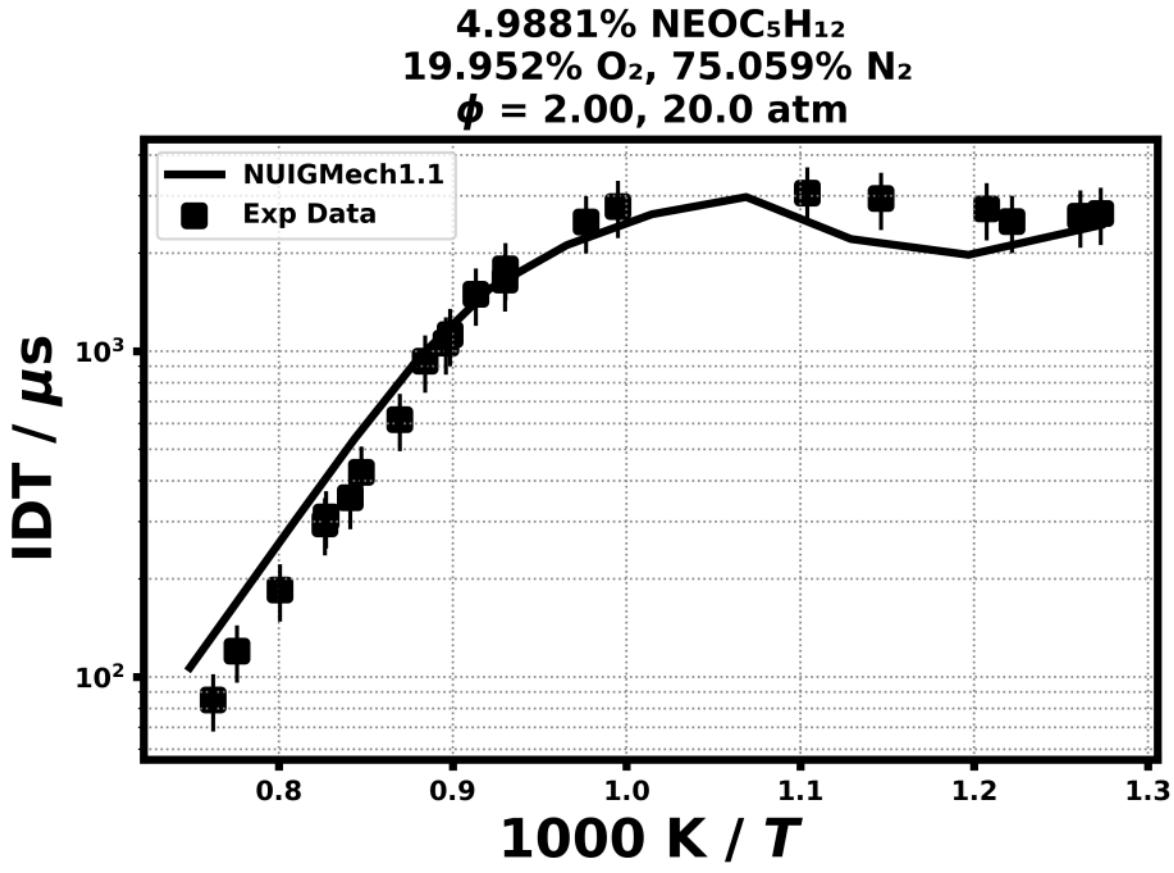

Figure 324: Dataset: 20_ATM_5.0_NEOC5H12_PHI_2.0

RCM Ignition delay time

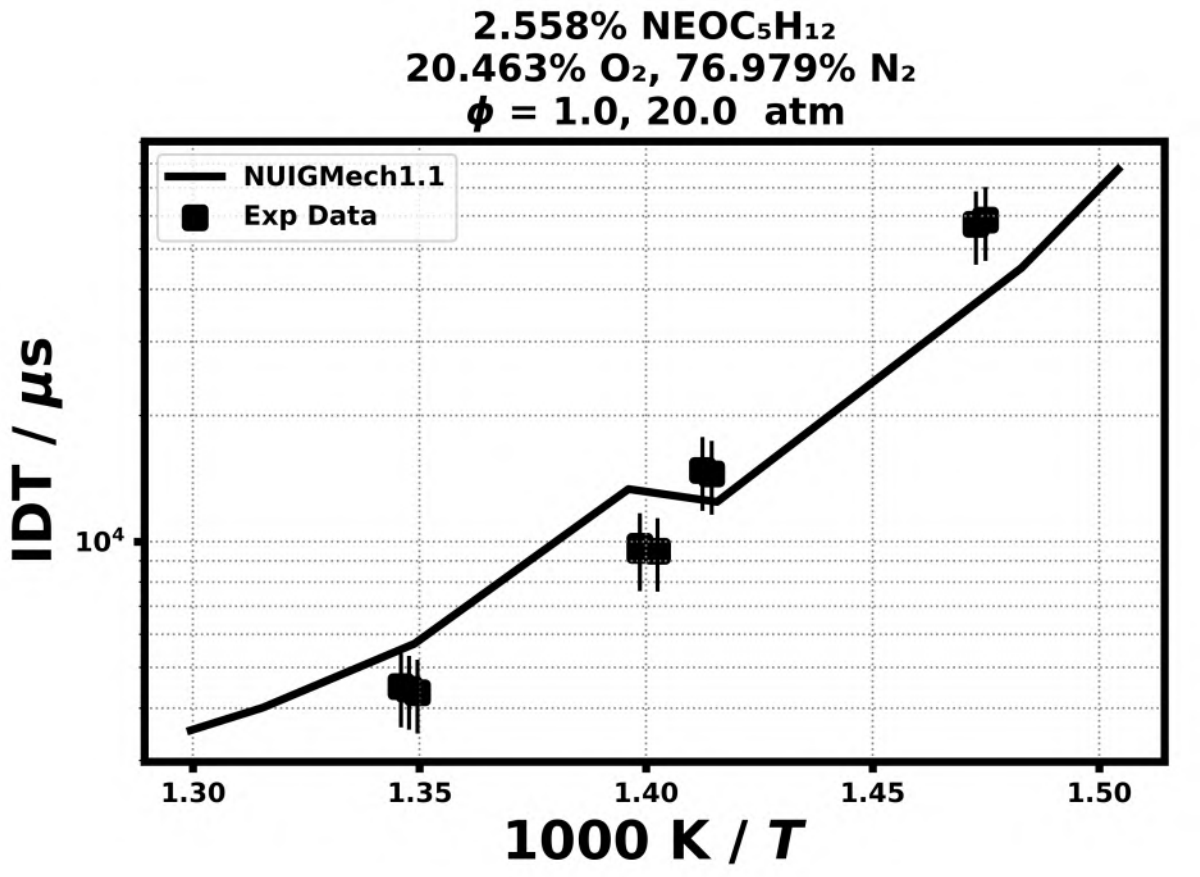

Figure 329: Dataset: F100_20ATM_100_N2

3.2.8 Case: neo-C5H12/RCM/BUGLER/F200_20ATM_100_N2

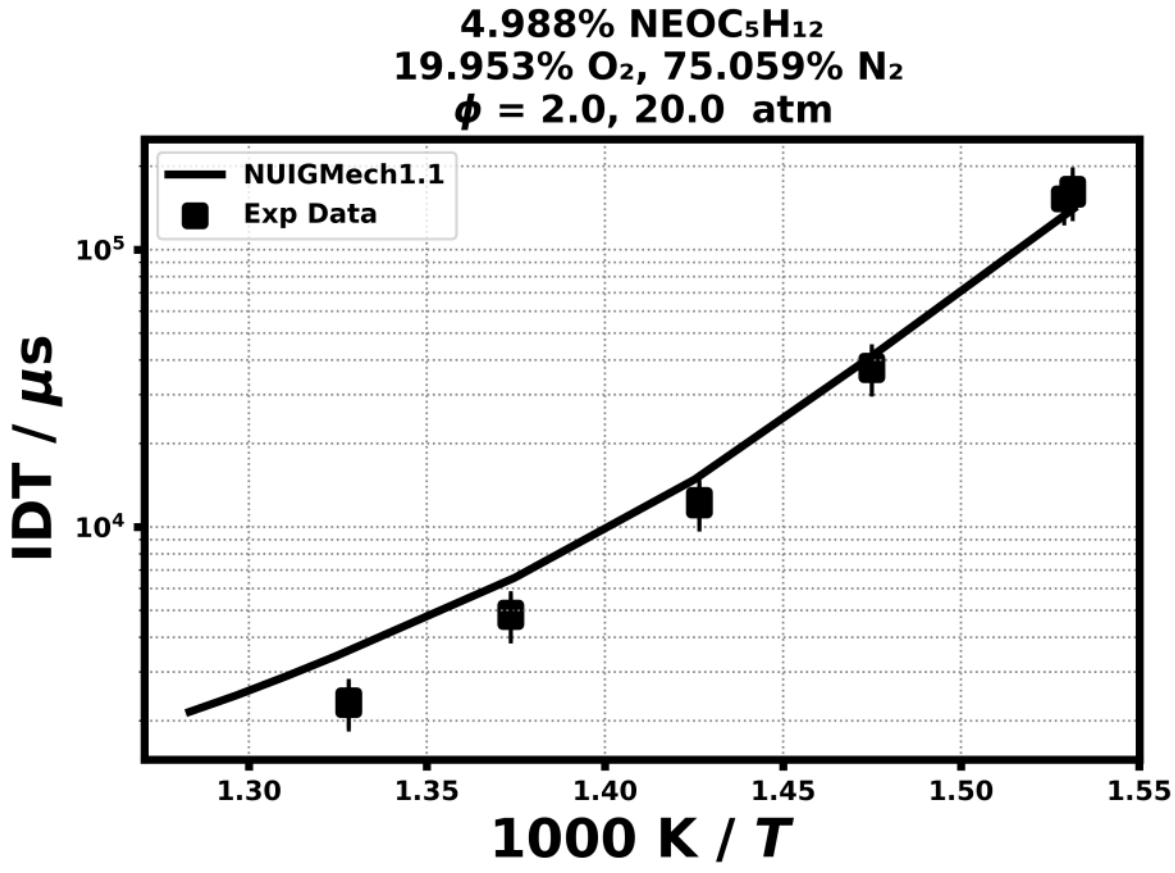

Figure 332: Dataset: F200_20ATM_100_N2

24. Validation for C_5H_{10}-1/C_5H_{10}-2

1. IDT data

S. Dong, K. Zhang, E.M. Ninnemann, A. Najjar, G. Kukkadapu, J. Baker, F. Arafin, Z. Wang, W.J. Pitz, S.S. Vasu, S.M. Sarathy, P.K. Senecal, H.J. Curran A comprehensive experimental and kinetic modeling study of 1- and 2-pentene Combustion and Flame 223 (2021) 166–180.

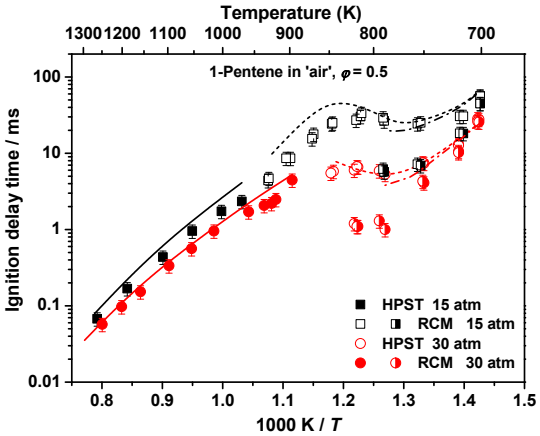

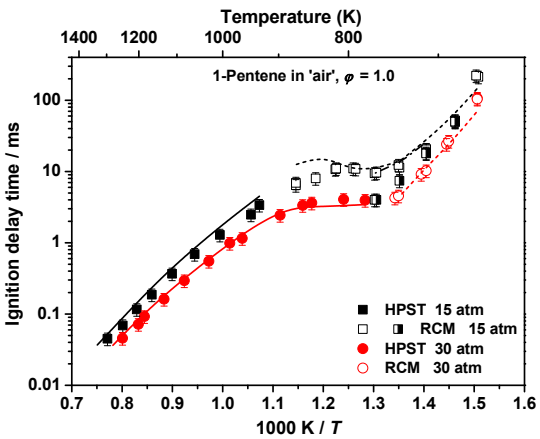

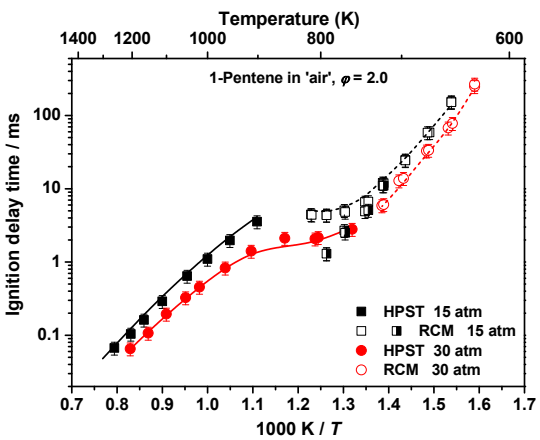

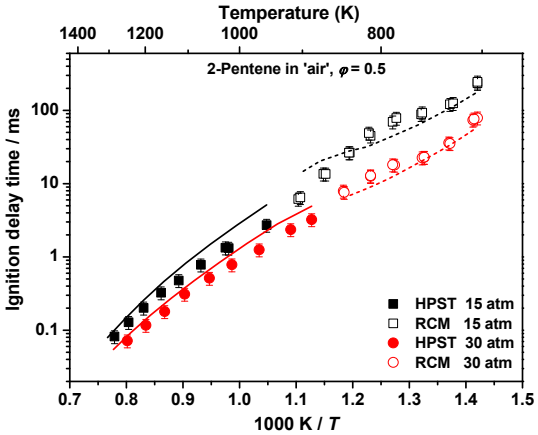
Temperature (K)
1400
1200
1000
800
2-Pentene in 'air', φ = 0.5
Ignition delay time / ms
100
10
1
0.1
HPST 15 atm
RCM 15 atm
HPST 30 atm
RCM 30 atm
0.7
0.8
0.9
1.0
1.1
1.2
1.3
1.4
1.5
1000 K / T

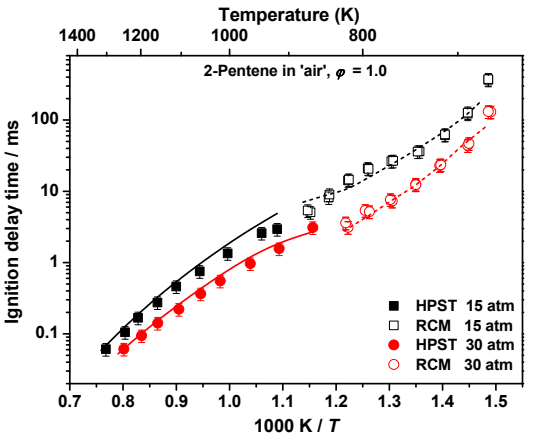
Temperature (K)
1400
1200
1000
800
2-Pentene in 'air', φ = 1.0
Ignition delay time / ms
100
10
1
0.1
HPST 15 atm
RCM 15 atm
HPST 30 atm
RCM 30 atm
0.7
0.8
0.9
1.0
1.1
1.2
1.3
1.4
1.5
1000 K / T

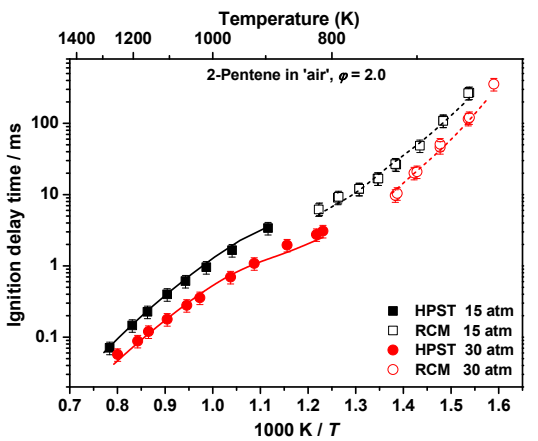
Temperature (K)
1400
1200
1000
800
2-Pentene in 'air', φ = 2.0
Ignition delay time / ms
100
10
1
0.1
HPST 15 atm
RCM 15 atm
HPST 30 atm
RCM 30 atm
0.7
0.8
0.9
1.0
1.1
1.2
1.3
1.4
1.5
1.6
1000 K / T

Cheng Y, Hu E, Deng F, Yang F, Zhang Y, Tang C, et al. Experimental and kinetic comparative study on ignition characteristics of 1-pentene and n-pentane. Fuel 2016;172:263–72.

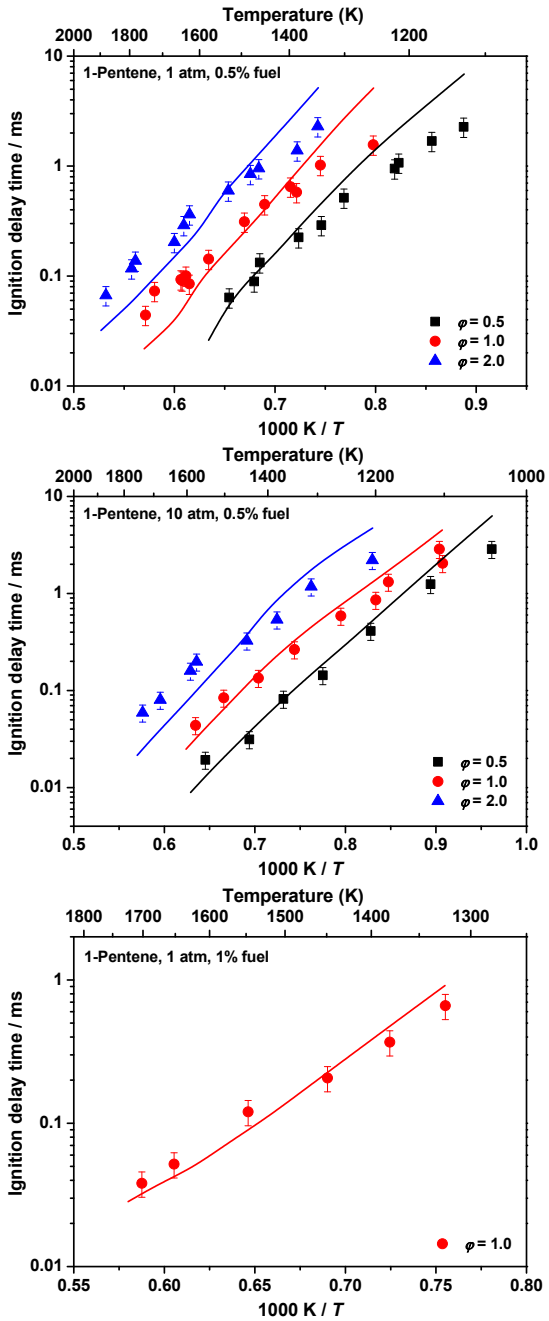

Mehl M, Pitz WJ, Westbrook CK, Yasunaga K, Conroy C, Curran HJ. Autoignition behavior of unsaturated hydrocarbons in the low and high temperature regions. Proc Combust Inst 2011;33:201–8.

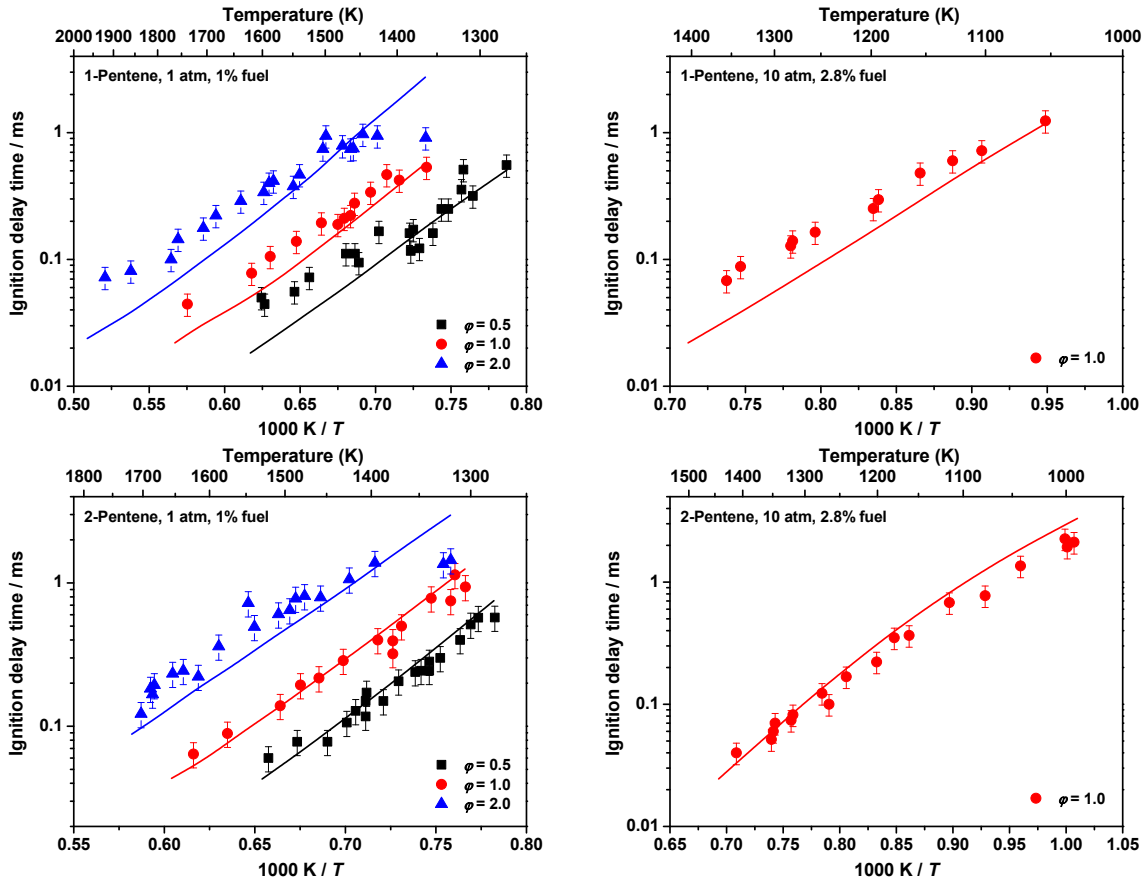

2. Shock-tube CO time-histories

S. Dong, K. Zhang, E.M. Ninnemann, A. Najjar, G. Kukkadapu, J. Baker, F. Arafin, Z. Wang, W.J. Pitz, S.S. Vasu, S.M. Sarathy, P.K. Senecal, H.J. Curran A comprehensive experimental and kinetic modeling study of 1- and 2-pentene Combustion and Flame 223 (2021) 166–180.

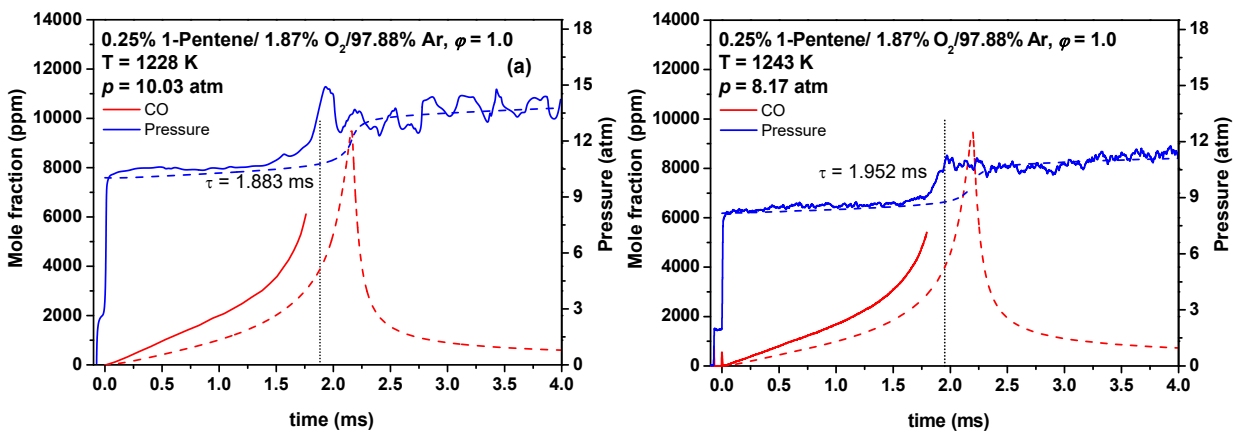

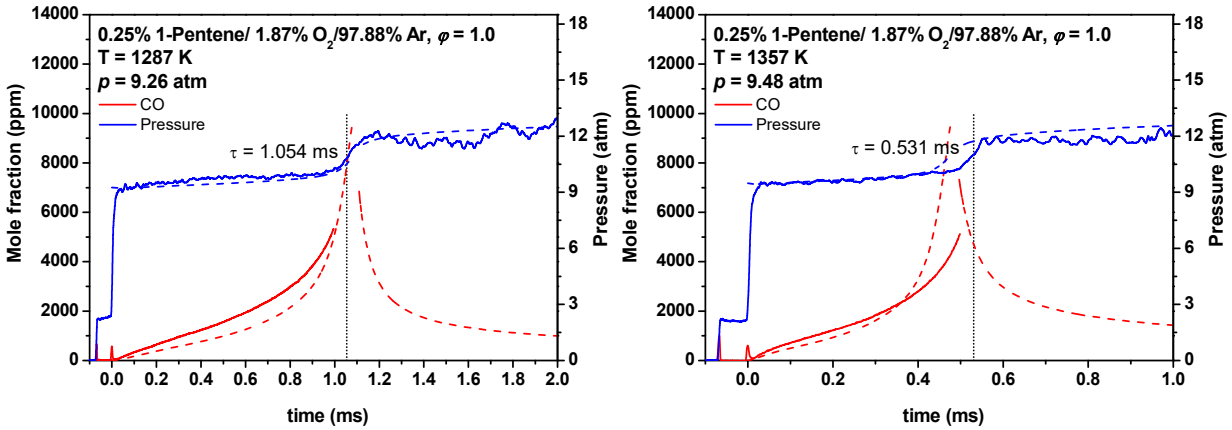
0.25% 1-Pentene/ 1.87% O2/97.88% Ar, φ = 1.0
T = 1287 K
p = 9.26 atm
CO
Pressure
τ = 1.054 ms
Mole fraction (ppm)
Pressure (atm)
time (ms)
0.25% 1-Pentene/ 1.87% O2/97.88% Ar, φ = 1.0
T = 1357 K
p = 9.48 atm
CO
Pressure
τ = 0.531 ms
Mole fraction (ppm)
Pressure (atm)
time (ms)

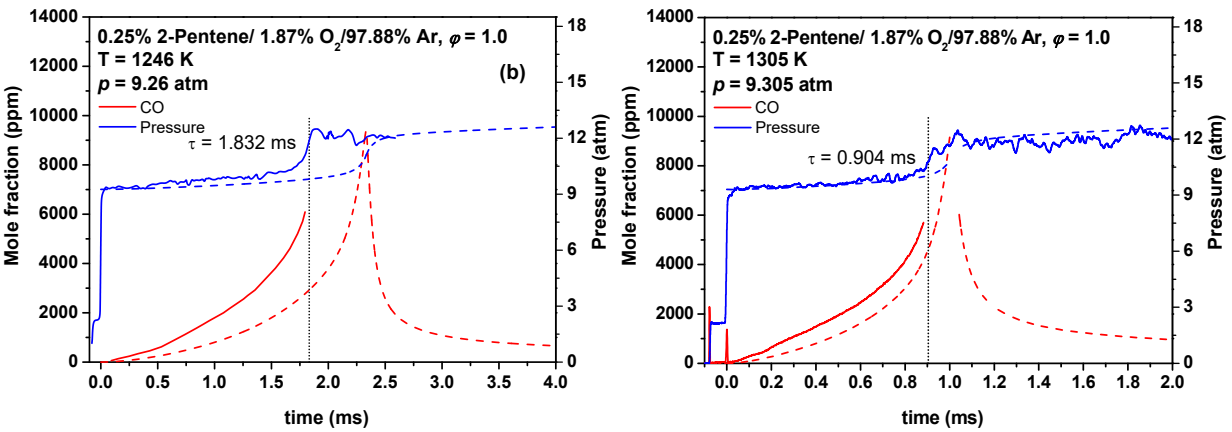
0.25% 2-Pentene/ 1.87% O2/97.88% Ar, φ = 1.0
T = 1246 K
p = 9.26 atm
(b)
CO
Pressure
τ = 1.832 ms
Mole fraction (ppm)
Pressure (atm)
time (ms)
0.25% 2-Pentene/ 1.87% O2/97.88% Ar, φ = 1.0
T = 1305 K
p = 9.305 atm
CO
Pressure
τ = 0.904 ms
Mole fraction (ppm)
Pressure (atm)
time (ms)

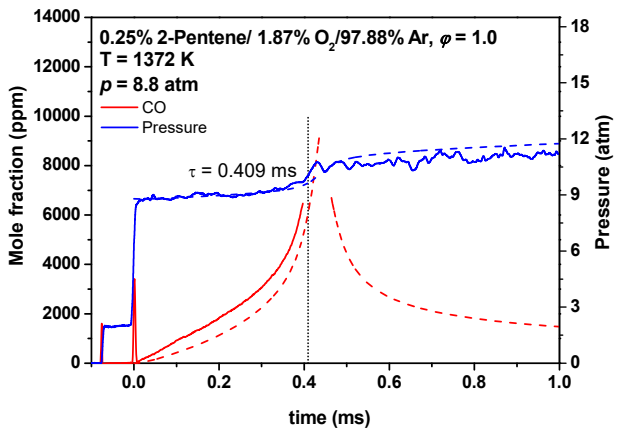
0.25% 2-Pentene/ 1.87% O2/97.88% Ar, φ = 1.0
T = 1372 K
p = 8.8 atm
CO
Pressure
τ = 0.409 ms
Mole fraction (ppm)
Pressure (atm)
time (ms)

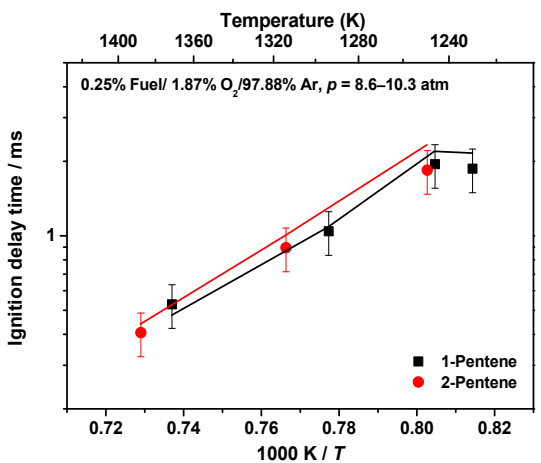
Temperature (K)
1400
1360
1320
1280
1240
0.25% Fuel/ 1.87% O2/97.88% Ar, p = 8.6–10.3 atm
Ignition delay time / ms
1-Pentene
2-Pentene
1000 K / T

3. JSR data

S. Dong, K. Zhang, E.M. Ninnemann, A. Najjar, G. Kukkadapu, J. Baker, F. Arafin, Z. Wang, W.J. Pitz, S.S. Vasu, S.M. Sarathy, P.K. Senecal, H.J. Curran A comprehensive experimental and kinetic modeling study of 1- and 2-pentene Combustion and Flame 223 (2021) 166–180.

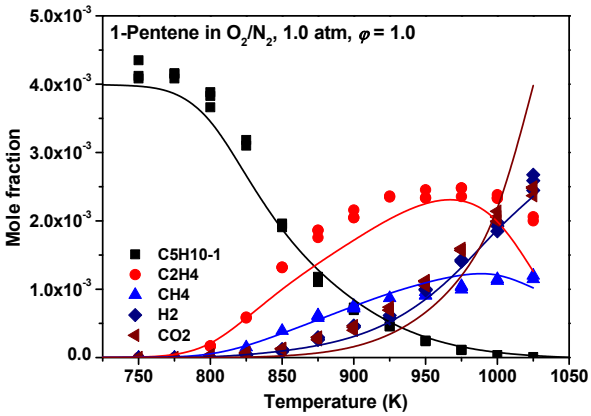

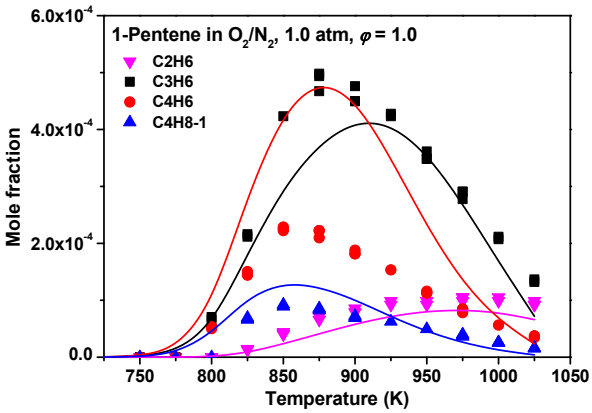

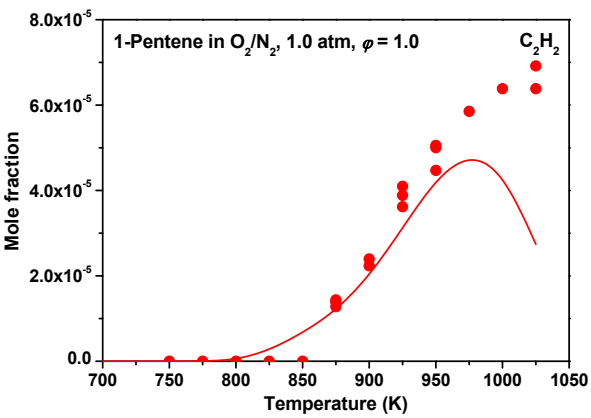

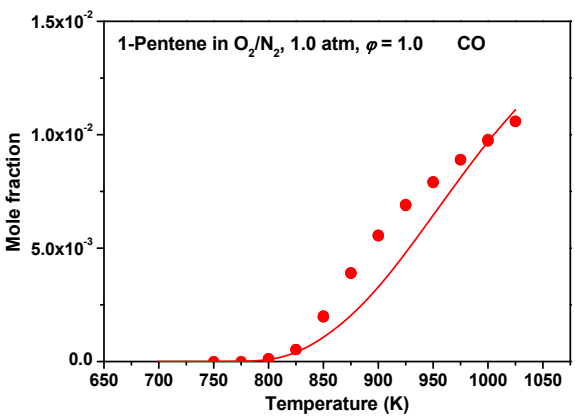

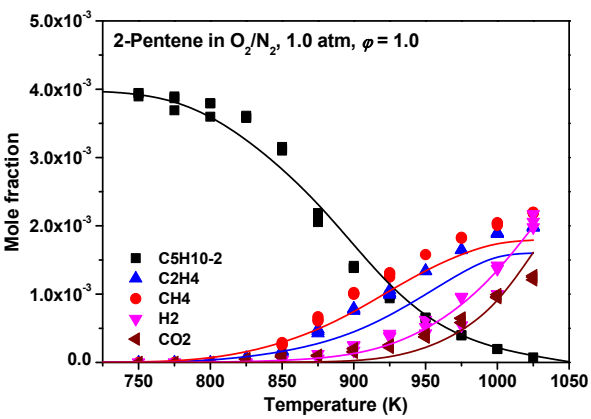

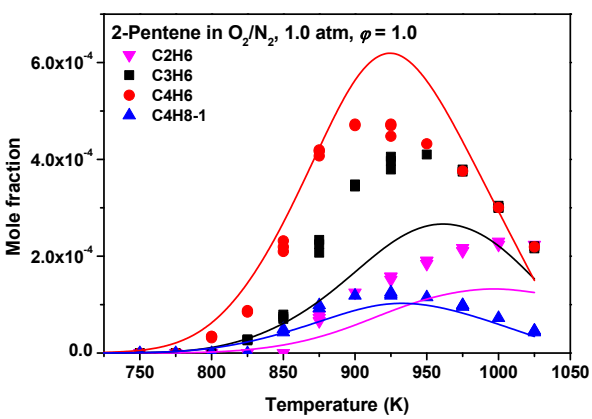

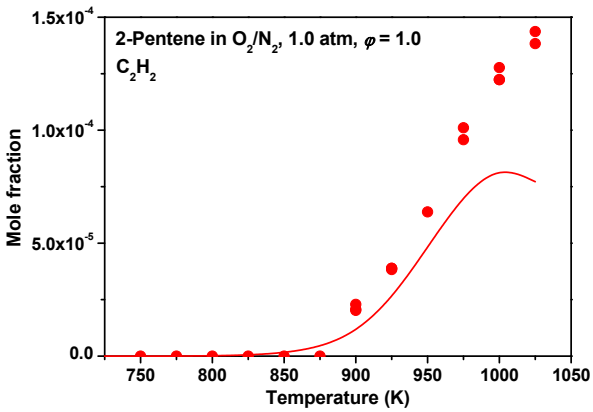

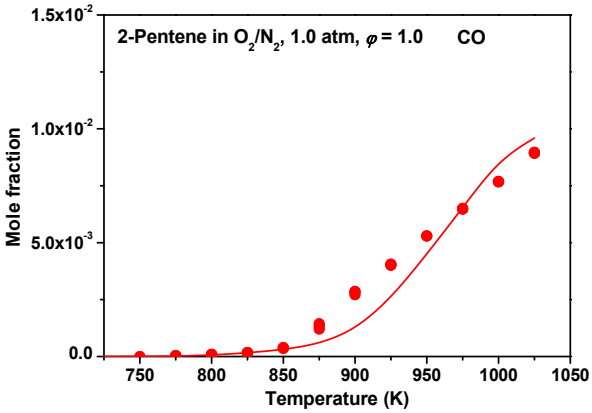

4. LBV data

Cheng Y, Hu E, Lu X, Li X, Gong J, Li Q, et al. Experimental and kinetic study of pentene isomers and n-pentane in laminar flames. Proc Combust Inst 2017;36:1279–86.